UNIFIED MODEL DOCUMENTATION PAPER

No 15

JOY OF U.M. 5.5 - MODEL FORMULATION

A. Staniforth, A. White, N. Wood, J. Thuburn, M. Zerroukat, E. Cordero, T. Davies

and a cast of hundreds (well ... dozens at least)

7th July 2003

Model version 5.5

Dynamics Research
Numerical Weather Prediction
Met Office
London Road
Bracknell
Berkshire
RG12 2SZ
United Kingdom

Modification record		
Document version	Authors	Description
5.1	A. Staniforth, A. White, N. Wood, J. Thuburn, M. Zerroukat + ...	Original document
5.2	A. Staniforth, A. White, N. Wood, J. Thuburn, M. Zerroukat, E. Cordero + ...	Formulation of U.M. 5.2
5.3	A. Staniforth, A. White, N. Wood, J. Thuburn, M. Zerroukat, E. Cordero + ...	Formulation of U.M. 5.3 + Moisture mods
5.4	A. Staniforth, A. White, N. Wood, J. Thuburn, M. Zerroukat, E. Cordero + ...	Formulation of U.M. 5.4 + Moisture mods
5.5	A. Staniforth, A. White, N. Wood, J. Thuburn, M. Zerroukat, E. Cordero, T. Davies + ...	Formulation of U.M. 5.5

Abstract

This is the documentation of the model formulation for UM5.5, the 5th version of the "New Dynamics" for the UM system.

Changes from UM 5.4 formulation

1. Convection option 1 removed from the first physics correctors in the horizontal momentum (Section 6), thermodynamic (Section 9) and moisture (Section 10) equations.

2. A simple correction to the semi-Lagrangian advection of moisture and tracer variables is now applied in the event of the Priestley algorithm failing to converge (Section 10).

3. A conserving option has been introduced into the horizontal diffusion scheme (Section 12).

4. A "targeted" horizontal diffusion scheme is now available (Section 12), motivated by the need to control gridpoint storms.

Contents

1 The governing equations in conventional spherical polar coordinates

The first three sections of these notes present the *continuous equations* that are the basis of the New Dynamics for the Unified Model, together with some of their properties. Sections 4-17 describe the *finite difference schemes* and *methods* that are used in numerical integration.

The present section covers the momentum, continuity, thermodynamic and state equations for dry air (Sections 1.1 to 1.4) and the modifications made to represent moisture and its effects (Section 1.5). The equations - listed in Section 1.6 - are written in forms appropriate for a conventional spherical polar (SP) coordinate system in which the polar axis coincides with the Earth's rotation axis. Section 2 covers the transformation of the equations to the co-ordinate systems actually used by the New Dynamics: the rotated SP system used in limited area versions, and the terrain-following co-ordinate system used in all versions.

It might be thought that the basic equations of meteorological dynamics were decided upon long ago. However, authoritative texts such as those of Lorenz (1967), Phillips (1973), Gill (1982), and Emanuel (1994) indicate a number of areas in which uncertainty exists, either about the validity of certain assumptions and approximations or about which physical processes may be neglected. Mainly in "Asides", we shall note several such areas which we believe deserve further study. In order of currently perceived importance (most important first) these are:

1. representation of moisture [1.5];
2. rotation vector issues and tidal effects [1.1];
3. replacement of spheroidal geopotential surfaces by spheres [1.1];
4. horizontal variations of apparent gravity [1.1];
5. issues of reversibility and irreversibility[1.3];
6. electromagnetic effects at high levels [1.1].

For most of these areas we shall note results and developments which cast light on the issues involved.

It should be emphasised that the main objective of this section (and of the next) is to give an account of the governing equations as seen at present by the New Dynamics; possible future improvements are an important, but secondary, issue.

1.1 Momentum equation

In this section it is assumed that the atmosphere consists of **dry** air. Modifications to represent moisture in its various phases are discussed in Section 1.5.

In terms of velocities $\hat{\mathbf{u}} = \hat{\mathbf{u}}(\mathbf{r}, t)$ measured or defined relative to an inertial frame, the Navier-Stokes equation may be written as

$$\frac{\hat{D}\hat{\mathbf{u}}}{Dt} = -\frac{1}{\rho}\mathbf{grad}p + \mathbf{G}. \tag{1.1}$$

In (1.1), $\rho = \rho(\mathbf{r}, t)$ is density, $p = p(\mathbf{r}, t)$ is pressure,

$$\frac{\hat{D}}{Dt} \equiv \frac{\partial}{\partial t} + (\hat{\mathbf{u}} \cdot \mathbf{grad}), \tag{1.2}$$

and $\mathbf{G}$ includes all forces (per unit mass) except the pressure gradient force. The pressure gradient force per unit mass is represented by the first r.h.s. term in (1.1). **grad** is the usual spatial gradient operator of mathematical physics.

The operator $\hat{D}/Dt$ defined by (1.2) indicates the material rate of change (of the operand) as seen by an observer in an inertial frame. If the operand is a scalar quantity, the material rate of change (i.e. the time rate of change applying to a material particle of fluid) is the same in inertial and rotating frames. If the operand is a vector quantity, then its material rate of change seen in a rotating frame is not the same as that seen in an inertial frame because different rates of change of direction are perceived in the two frames.

To convert (1.1) to a form dealing with velocities $\mathbf{u} = \mathbf{u}(\mathbf{r}, t)$ measured or defined relative to the rotating Earth, use is made of the relation between the rates of change of vectors seen in inertial and rotating frames:

$$\frac{\hat{D}\mathbf{a}}{Dt} = \frac{D\mathbf{a}}{Dt} + \boldsymbol{\Omega} \times \mathbf{a}. \tag{1.3}$$

Here D/Dt indicates the material rate of change seen by an observer in a frame rotating relative to the "fixed stars" with angular velocity $\boldsymbol{\Omega}$. With $\mathbf{a} = \mathbf{r} =$ position vector relative to a point on the axis of rotation, (1.3) gives [since $\hat{\mathbf{u}} \equiv \hat{D}\mathbf{r}/Dt$ and $\mathbf{u} \equiv D\mathbf{r}/Dt$]

$$\hat{\mathbf{u}} = \mathbf{u} + \boldsymbol{\Omega} \times \mathbf{r}. \tag{1.4}$$

Eq (1.4) is virtually obvious (and therefore mnemonic for (1.3)) since $\boldsymbol{\Omega} \times \mathbf{r}$ is the velocity relative to the inertial frame of a point fixed in the rotating frame; see Figure 1.1.

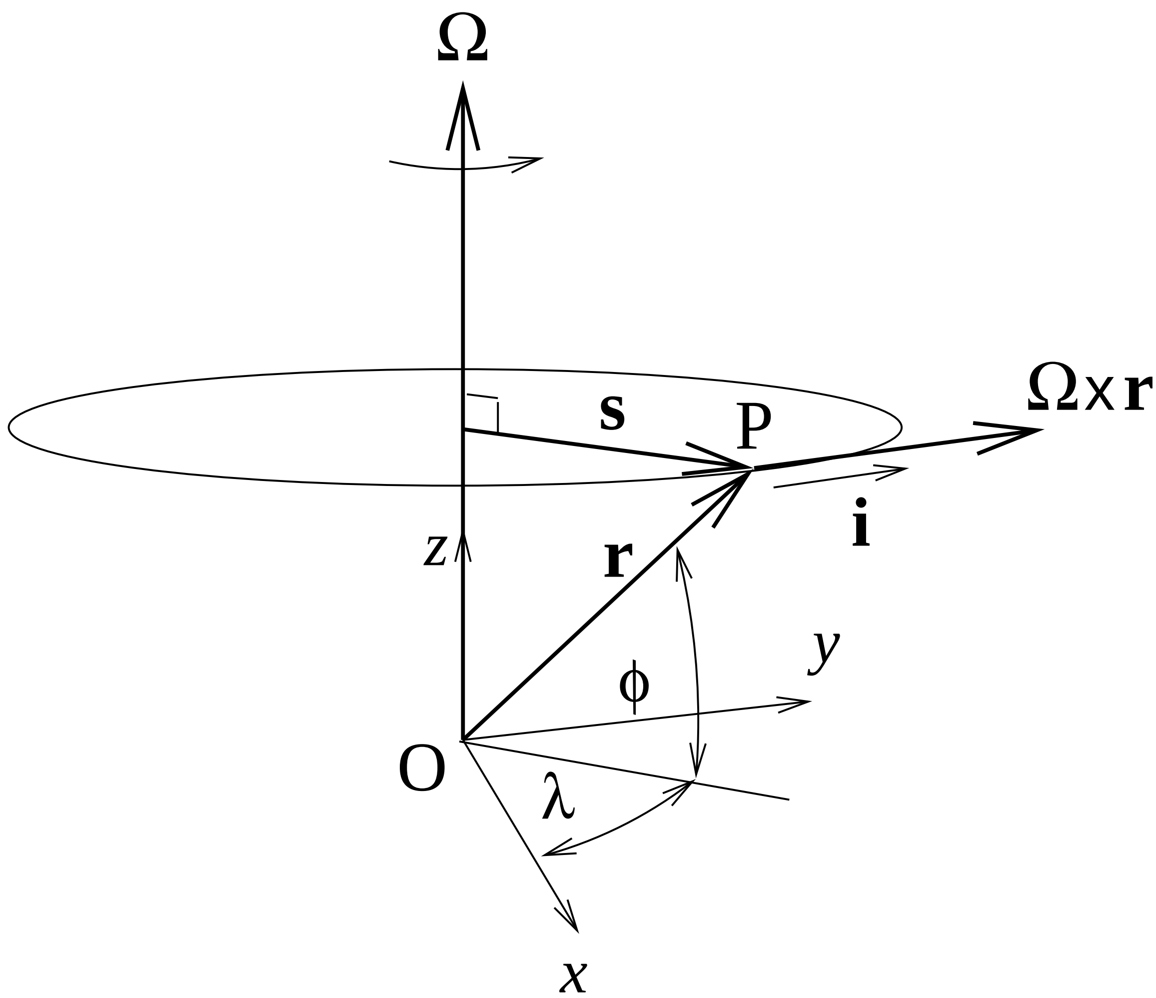

Figure 1.1: Frame $Oxyz$ rotates with angular velocity $\mathbf{\Omega}$ about its z axis. Point P is fixed in $Oxyz$ and has position vector $\mathbf{r}$ relative to O. Vector $\mathbf{s}$ represents the perpendicular from the rotation axis Oz to P; $\mathbf{i}$ is unit vector in the zonal direction at P (i.e. perpendicular to the plane containing $\mathbf{\Omega}$, $\mathbf{r}$ and $\mathbf{s}$). The velocity of point P relative to the inertial frame in which $Oxyz$ is rotating is $\mathbf{\Omega} \times \mathbf{s} = \mathbf{i}\,|\mathbf{\Omega}|\,|\mathbf{s}| = \mathbf{i}\,|\mathbf{\Omega}|\,|\mathbf{r}|\cos\phi = \mathbf{\Omega} \times \mathbf{r}$. [$\phi$ is the latitude of P in a spherical polar system in which Oz is the polar axis; the diagram also shows the longitude, λ, of P relative to Ox as zero.] A unit mass instantaneously at P and moving relative to $Oxyz$ with zonal velocity u has absolute angular momentum $(u + \Omega r\cos\phi)\, r\cos\phi$ about Oz.

Application of (1.3) with $\mathbf{a} = \hat{\mathbf{u}}$ and use of (1.4) gives

$$\frac{\hat{D}\hat{\mathbf{u}}}{Dt} = \frac{D\mathbf{u}}{Dt} + 2\boldsymbol{\Omega} \times \mathbf{u} + \boldsymbol{\Omega} \times (\boldsymbol{\Omega} \times \mathbf{r}) + \dot{\boldsymbol{\Omega}} \times \mathbf{r}, \tag{1.5}$$

where $\dot{\boldsymbol{\Omega}} \equiv D\boldsymbol{\Omega}/Dt$ is the rate of change of $\boldsymbol{\Omega}$.

Astronomically detectable changes in magnitude and direction of the Earth's rotation vector do occur (see Barnes, Hide, White & Wilson (1983)), but they are sufficiently small and slow to make the term $\dot{\boldsymbol{\Omega}} \times \mathbf{r}$ negligible in (1.5). Eq. (1.1) is thus written as:

$$\frac{D\mathbf{u}}{Dt} = -2\boldsymbol{\Omega} \times \mathbf{u} - \boldsymbol{\Omega} \times (\boldsymbol{\Omega} \times \mathbf{r}) - \frac{1}{\rho}\mathbf{grad}p + \mathbf{G}. \tag{1.6}$$

In (1.6):

$-2\boldsymbol{\Omega} \times \mathbf{u}$ is the Coriolis force per unit mass;

$-\boldsymbol{\Omega} \times (\boldsymbol{\Omega} \times \mathbf{r})$ is the centrifugal force per unit mass.

How should $\boldsymbol{\Omega}$ be interpreted?

Aside :

It is usually considered that $\boldsymbol{\Omega}$ represents the angular velocity of rotation of the Earth about its polar axis, and this idealisation is probably a good approximation. Commonly, the magnitude of $\boldsymbol{\Omega}$ is defined by the sidereal day, but the assumption of polar axial coincidence is retained. A more detailed treatment would take account of the component of $\boldsymbol{\Omega}$ that represents the 28-day rotation about the centre of mass, C_{EM}, of the Earth-Moon system; C_{EM} is about 4700 km from the centre of the Earth. The total rotation (in the sense of Chasles' theorem) occurs about an axis which is 4700/[28days/1day] $\approx$ 170 km from the polar axis. An alternative treatment would consider the motion of the Earth as a compound rotation: the diurnal rotation about the polar axis, combined with motion in a circle of radius 4700 km (about C_{EM} and in the plane of the moon's orbit) with period 28 days. The kinematic problem thus posed is straightforward if the moon's orbit is assumed to lie in the equatorial plane of the Earth (which seems an acceptable idealization for an order of magnitude calculation). As well as the main centrifugal force (seen in (1.6)) arising from the diurnal rotation about the polar axis, one finds a secondary centrifugal force arising from the circular motion *about C_{EM} ; this is typically* $(4700/6360)/(28)^2 \approx 0.1\%$ *of the magnitude of the main centrifugal force, and is evidently negligible. There is no secondary Coriolis force in this co-planar problem. Other centrifugal forces arise from the rotation of the Earth about the Sun, and from the rotation of the Galaxy; these contributions are mentioned in classical mechanics texts such as Goldstein (1959), where they are uneasily considered to be negligible in their dynamical effects. All these forces, and their relation to tidal effects, deserve further study; see Phillips (1973) and in particular the Appendix to Chapter VIII of Lamb (1932) .*

For current purposes, usual practice in dynamical meteorology will be followed: $\mathbf{\Omega}$ will be assumed to lie along the polar axis and to have a magnitude equal to the sidereal rotation rate. Secondary rotations will be neglected. The force per unit mass, $\mathbf{G}$, in (1.6), includes the contributions of gravity, friction and electromagnetic forces. Only gravity and friction will be represented.

Aside :

Electromagnetic effects are usually considered to be negligible below altitudes of 80 km, although some sources quote a threshold of 50km. At great heights the continuum model of fluid motion breaks down. Both aspects deserve clarification.

Thus we write

$$\mathbf{G} = -\mathbf{grad}\Phi + \mathbf{S^u}, \tag{1.7}$$

where $\mathbf{S^u}$ is the frictional force per unit mass and Φ is the true gravitational potential (the negative of the gradient of which gives the acceleration due to the distribution of mass; see Munk & Macdonald (1960)). Eq. (1.6) becomes

$$\frac{D\mathbf{u}}{Dt} = -2\mathbf{\Omega} \times \mathbf{u} - \frac{1}{\rho}\mathbf{grad}p - \mathbf{grad}\Phi - \mathbf{\Omega} \times (\mathbf{\Omega} \times \mathbf{r}) + \mathbf{S^u}. \tag{1.8}$$

As is well known, the centrifugal term $-\mathbf{\Omega} \times (\mathbf{\Omega} \times \mathbf{r})$ can be written as the gradient of a centrifugal potential $\Omega^2 s^2/2$, where $\mathbf{s}$ (see Figure 1.1) points perpendicularly outwards from the axis of $\mathbf{\Omega}$ and has magnitude equal to distance from it:

$$\mathbf{\Omega} \times (\mathbf{\Omega} \times \mathbf{r}) = \mathbf{\Omega} \times (\mathbf{\Omega} \times \mathbf{s}) = -\Omega^2\mathbf{s} = -\mathbf{grad}\left(\Omega^2 s^2/2\right). \tag{1.9}$$

Hence, in terms of

$$\Phi_a = \Phi + \frac{1}{2}\Omega^2 s^2, \tag{1.10}$$

(1.8) becomes

$$\frac{D\mathbf{u}}{Dt} = -2\mathbf{\Omega} \times \mathbf{u} - \frac{1}{\rho}\mathbf{grad}p - \mathbf{grad}\Phi_a + \mathbf{S}^{\mathbf{u}}. \tag{1.11}$$

The direction normal to surfaces of constant Φ_a (i.e. the direction of $\mathbf{grad}\Phi_a$) defines the direction of *apparent vertical*. It is the vertical as revealed by a plumb-line at rest relative to the rotating Earth; see Figure 1.2. Unit vector in the upward (apparent) vertical direction, $\mathbf{k}$, and the magnitude of *apparent gravity*, g, are given by

$$\mathbf{grad}\Phi_a = g\mathbf{k}. \tag{1.12}$$

Φ_a is called the *apparent gravitational potential*. Surfaces of constant Φ_a are often referred to (somewhat imprecisely) as *geopotentials*.

Aside :

> *Surfaces of constant Φ_a have radically different shapes close to and far distant from the Earth. Close to the Earth, where Newtonian gravity is dominant, they take the form of closed surfaces of oblate spheroidal type. Far distant from the Earth's rotation axis, since $\Omega^2 s^2/2$ then dominates Φ (i.e. the centrifugal term dominates Newtonian gravity), they are infinite cylinders coaxial with $\mathbf{\Omega}$. The relevant behaviour for a numerical model of the Earth's atmosphere is the oblate spheroidal regime (see Figure 1.2, and below).*

Decomposition of (1.11) into components within and perpendicular to geopotentials has the obvious advantage that (apparent) gravity appears in only one component equation; the components in the (apparent) horizontal plane have contributions only from the relative acceleration $[D\mathbf{u}/Dt]$, Coriolis $[-2\mathbf{\Omega} \times \mathbf{u}]$, pressure gradient $[-(1/\rho)\,\mathbf{grad}p]$ and friction $[\mathbf{F}]$ terms. In more immediate physical terms, of course, such a resolution corresponds to the conventional definition of vertical direction and horizontal plane.

A disadvantage of the decomposition is that the geopotentials are not precisely spherical. Customarily, however, this effect is neglected: when the horizontal and vertical components of (1.11) are isolated, it is assumed that the oblate spheroidal geopotentials (whose local tangent planes and normals define the horizontal and vertical) may be treated **as if they were spheres**. This is justified by the smallness of the contribution of the centrifugal term to apparent gravity (except far distant from the Earth's rotation axis): $C \equiv \Omega^2 r/g << 1$; tropospheric parameter values give $C \approx 3 \times 10^{-3}$. See Figure 1.2.

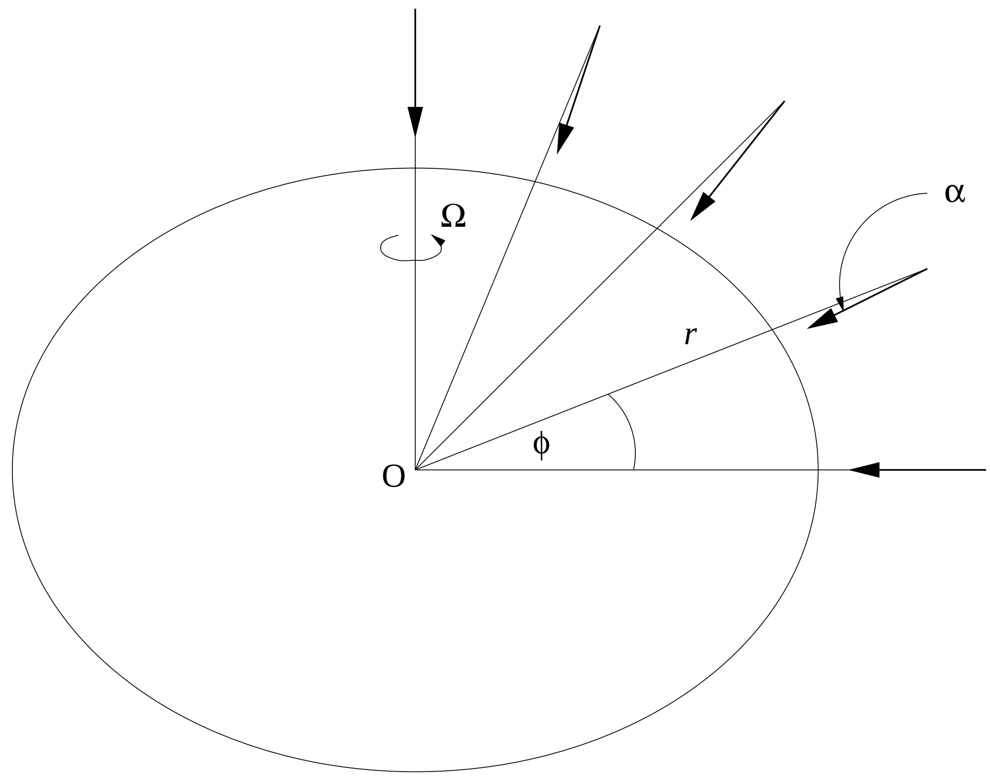

Figure 1.2: A polar section of an oblately spheroidal Earth (centre O); for clarity, the eccentricity of the ellipse defining the figure of the Earth is exaggerated. The ellipse is a geopotential surface, and *apparent gravity* acts at right angles to it, and hence towards the centre of the Earth only at the equator and poles. The arrows indicate the direction of apparent gravity - which defines *apparent vertical* - at various latitudes. The angle α (in radians) between apparent vertical and the radius from O at latitude ϕ is well approximated by $\Omega^2 r \cos\phi \sin\phi/\mathrm{g}$, where Ω is the Earth's rotation rate and r is distance from O. α achieves its maximum absolute value $\alpha_{max} = \Omega^2 r/2g$ at latitudes $\phi = \pm 45^o$. Tropospheric parameter values give $\alpha_{max} \approx 1.7 \times 10^{-3}$, so the difference between "real" and apparent vertical is 0.1^o at most, and the oblately spheroidal geopotentials are reasonably represented as spheres. [It may be observed, however, that 0.1^o is not negligibly small compared with a typical 1 in 100 (0.6^o) slope of isentropic surfaces in the free atmosphere.] The notions of apparent vertical and the implied apparent horizontal are important because the balance of forces in the apparent horizontal plane contains no centrifugal contribution. This is *not* the case if we consider the meridional force balance in tangent planes to a perfect sphere centred at O: a centrifugal term $-\Omega^2 r \cos\phi \sin\phi$ occurs, and it is numerically much larger than the Coriolis term $-2\Omega u \sin\phi$ so long as $|u|/\Omega r \cos\phi \ll 1$ (which, away from the poles, is satisfied for virtually all motion in the atmosphere). The situation is summarised by the order-of-magnitude inequalities $|u| \ll \Omega r \ll 1\sqrt{gr}$, the first of which expresses the smallness of relative compared to absolute velocities in the atmosphere, and the second the dominance of Newtonian gravity over centrifugal effects.

On this basis it might be considered that the distinction between the apparent vertical and the radial direction is of academic interest only. However, if we decompose (1.8) into its components in a **true** spherical polar system, we find that the meridional component of the centrifugal term is a key contributor to the meridional force balance; see Figure 1.2. We conclude that:

1. the apparent vertical / apparent horizontal decomposition is necessary in order to separate the Coriolis force from the centrifugal force; **but**
2. g is so much larger than $\Omega^2 r$ (about 300:1; see above) that geopotentials may be represented as (concentric) spheres to a very good approximation.

Aside :

Gill (1982) gives a more detailed account of this argument. It would be conceptually helpful to follow through the decomposition of the components of (1.11) *in an oblate spheroidal system, as indicated by Gill, to verify conclusion 2, above. Separating the components of* (1.11) *in any curvilinear coordinate system may be accomplished by using the (lengthy) expressions given in Appendix 2 of Batchelor (1967). It is perhaps worth noting that a substantial part (about 1 in 3) of the departure of real geopotentials from sphericity is a true gravitational consequence of the deviation of the Earth's mass distribution from spherical symmetry; see Munk & Macdonald (1960).*

In the current treatment we simply decompose (1.11) into its spherical polar (λ, ϕ, r) components, whilst recognising that our spherical polar system is an approximate representation of the oblate spheroidal geopotential system. Here λ = longitude, ϕ = latitude, clearly enough; but what is r? It is no longer distance from the centre of the Earth. Rather, if a is the Earth's mean radius and z = distance above mean sea level (considered to be a geopotential surface) then we define

$$r \equiv a + z. \tag{1.13}$$

The zonal, meridional and vertical components of (1.11) are

$$\frac{Du}{Dt} = -\frac{uw}{r} - 2\Omega w \cos\phi + \frac{uv\tan\phi}{r} + 2\Omega v \sin\phi - \frac{1}{\rho r\cos\phi}\frac{\partial p}{\partial \lambda} + S^u, \tag{1.14}$$

$$\frac{Dv}{Dt} = -\frac{vw}{r} - \frac{u^2 \tan\phi}{r} - 2\Omega u \sin\phi - \frac{1}{\rho r}\frac{\partial p}{\partial \phi} + S^v, \qquad (1.15)$$

$$\frac{Dw}{Dt} = \frac{(u^2+v^2)}{r} + 2\Omega u \cos\phi - g - \frac{1}{\rho}\frac{\partial p}{\partial r} + S^w. \qquad (1.16)$$

The material derivative in (1.14) - (1.16) is given by

$$\frac{D}{Dt} \equiv \frac{\partial}{\partial t} + \frac{u}{r\cos\phi}\frac{\partial}{\partial \lambda} + \frac{v}{r}\frac{\partial}{\partial \phi} + w\frac{\partial}{\partial r}. \qquad (1.17)$$

The quadratic velocity component terms in $1/r$ in (1.14) - (1.16) (called *metric* terms) arise because of the intrinsic curvature of the spherical polar coordinate system; the directions of the unit vectors $\mathbf{i}, \mathbf{j}, \mathbf{k}$ in the local zonal, meridional, and radial directions change as one moves zonally or meridionally within a surface of constant r. Eqs. (1.14) - (1.16) may be derived by obtaining expressions for $D\mathbf{i}/Dt$, $D\mathbf{j}/Dt$, $D\mathbf{k}/Dt$ by geometric arguments and then isolating the components of $D\mathbf{u}/Dt = D(u\mathbf{i} + v\mathbf{j} + w\mathbf{k})/Dt$. This is the method used in most textbooks on dynamical meteorology. (As already noted, the components of $D\mathbf{u}/Dt$ in any orthogonal curvilinear coordinate system may be obtained by using expressions given in Appendix 2 of Batchelor (1967)). An alternative approach, which we shall outline, highlights conservation properties and reveals some key aspects of (1.14) - (1.16) that might otherwise not be noticed.

- Eq. (1.14) follows in a few lines from the axial absolute angular momentum conservation law for a parcel of fluid of density ρ and volume $\delta\tau = r^2 \cos\phi \delta\lambda\delta\phi\delta r$ located at (λ, ϕ, r) - see Figure 1.1:

$$\frac{D}{Dt}\left[\rho\delta\tau\left(u + \Omega r\cos\phi\right) r\cos\phi\right] = \text{axial torque acting on parcel.} \qquad (1.18)$$

  The axial torque acting on the parcel of fluid consists of contributions from the pressure gradient force and other forces (except gravity, which exerts no torque about the polar axis of the Earth). Of greater interest is the l.h.s. Since $D(\rho\delta\tau)/Dt = 0$ (by mass conservation) and $Dr/Dt = w$, it is clear that the terms containing w on the r.h.s. of (1.14) arise from the r factors in the definition of the axial absolute angular momentum (see (1.18)); and since $rD\phi/Dt = v$, it is clear that the terms containing v on the r.h.s. of (1.14) arise from the $\cos\phi$ factors in (1.18). Explicitly,

$$\frac{D}{Dt}\left\{\rho\delta\tau\left(u + \Omega r\cos\phi\right) r\cos\phi\right\} = \rho\delta\tau\frac{D}{Dt}\left\{ur\cos\phi + \Omega r^2\cos^2\phi\right\}$$

$$= \rho\delta\tau \left\{ r\cos\phi \frac{Du}{Dt} + uw\cos\phi - uv\sin\phi + 2\Omega wr\cos^2\phi - 2\Omega rv\sin\phi\cos\phi \right\}$$
$$= \rho\delta\tau \left\{ r\cos\phi \left[\frac{Du}{Dt} + \frac{uw}{r} - \frac{uv\tan\phi}{r} + 2\Omega w\cos\phi - 2\Omega v\sin\phi \right] \right\}. \qquad (1.19)$$

- A kinetic energy equation may be formed in the usual way by taking the scalar product of the velocity vector $\mathbf{u}$ with (1.11):

$$\frac{D}{Dt}\left(\frac{1}{2}\mathbf{u}^2\right) = \mathbf{u} \cdot \left(\mathbf{S}^\mathbf{u} - \frac{1}{\rho}\mathbf{grad}p - \mathbf{grad}\Phi_a\right). \qquad (1.20)$$

Neither metric nor Coriolis terms appear. This places major constraints on the possible forms of the meridional and vertical components of (1.11), given that the zonal component takes the form (1.14). Indeed, the $\tan\phi$ metric term in (1.15) must have its sign and form in order that it will cancel with the $\tan\phi$ metric term in (1.14) when a kinetic energy equation is formed; a similar argument accounts for the sign and form of the Coriolis terms (both $\sin\phi$ and $\cos\phi$) in (1.15) and (1.16). Similarly, the presence of the term $-uw/r$ on the r.h.s. of (1.14) suggests that a term $+u^2/r$ must occur on the r.h.s. of (1.16). Such a term on its own would imply anisotropy with respect to horizontal velocity, so we should expect a companion term $+v^2/r$ on the r.h.s. of (1.16); when $\Omega = 0$, the combined term $+\left(u^2+v^2\right)/r$ represents simply the centripetal acceleration of particles moving along great circles. Finally, the presence of the term $+v^2/r$ on the r.h.s of (1.16) means that a term $-vw/r$ must appear on the r.h.s. of (1.15) in order to make the energetics consistent.

<u>Aside :</u>

If we set $r = a =$ Earth's mean radius in (1.18) - a shallow atmosphere approximation - then neither of the terms containing w on the r.h.s. of (1.19) will remain:

$$\frac{D}{Dt}\left\{\rho\delta\tau\left(u + \Omega a\cos\phi\right)a\cos\phi\right\} = \rho\delta\tau\frac{D}{Dt}\left\{ua\cos\phi + \Omega a^2\cos^2\phi\right\}$$
$$= \rho\delta\tau\left\{a\cos\phi\left[\frac{Du}{Dt} - \frac{uv\tan\phi}{a} - 2\Omega v\sin\phi\right]\right\}. \qquad (1.21)$$

The material derivative is now given by

$$\frac{D}{Dt} \equiv \frac{\partial}{\partial t} + \frac{u}{a\cos\phi}\frac{\partial}{\partial\lambda} + \frac{v}{a}\frac{\partial}{\partial\phi} + w\frac{\partial}{\partial z}, \qquad (1.22)$$

where z = height above mean sea level. This procedure leads to the zonal component of the momentum equation in the Hydrostatic Primitive Equations (HPE) model. Application of the energy argument then makes clear that the term $-vw/r$ on the r.h.s. of (1.15) and the terms $(u^2 + v^2)/r$ and $2\Omega u \cos\phi$ on the r.h.s. of (1.16) must be omitted if the shallow atmosphere approximation is made in (1.18), and hence in (1.14). In this way the other two components of the HPE momentum equation may be derived.Note that a consistent application of the shallow atmosphere approximation, as outlined here, involves the actual omission of some terms - the Coriolis terms that vary as $\cos\phi$ and all metric terms except those invoving $\tan\phi$. Conservation of angular momentum and energy demands this. The same results may be obtained by shallow atmosphere approximation of variational formulations of the equations of motion; see Müller (1989) and Roulstone & Brice (1995), who also discuss approximations less severe than the HPEs but more severe than the basic New Dynamics equations.

A remaining aspect is the spatial variation of g. The observed latitude variation amounts to about 0.5% between equator and poles. If the geopotentials are represented as (concentric) spheres, then it seems inconsistent to include the latitude variation of g (since g is numerically equal to the gradient of the geopotential, and the perpendicular distance between concentric spheres is constant, of course).

The latitude variation of g, although it is a systematic effect, is sufficiently small that one has few qualms about neglecting it. The height variation of g might be considered more significant: g decreases by about 1% between the Earth's surface and an elevation of 30 km. If the shallow atmosphere approximation is made, then *inclusion* of the height variation of g is an inconsistent step; if the shallow atmosphere approximation is *not* made, then *neglect* of the height variation of g is an inconsistent step. The reasoning in each case is the same: by Gauss's theorem, the total flux of the gravitational field vector across a sphere enclosing the Earth must be proportional to the mass of the Earth and independent of the radius of the sphere. In the shallow atmosphere case that can only be achieved by requiring $g =$ constant, since all spheres have the same radius in this idealisation. Without the shallow atmosphere approximation, constancy of the total gravitational flux requires g to decrease inversely as the square of the radius of the sphere. (Only the gravitational contribution to

g is considered here.) The radial variation of g should be represented in the New Dynamics because the shallow atmosphere approximation is not made.

Aside :

Apparent gravity contains small lunar and solar contributions which are responsible for the generation of tidal motion in the atmosphere and ocean. There is also a self-gravitating contribution due to the uneven distribution of mass in the atmosphere itself. In the theory of ocean tides (see Lamb (1932)) it is found that the effect of self-gravitation is not negligible. The key non-dimensional quantity is the ratio of the density of the fluid to the mean density of the Earth. [In broad terms, the Earth/ fluid gravitational attraction varies as $\rho_{Earth}\rho_{Fluid}$ *, and the self-gravitating effect of the fluid as* ρ^2_{Fluid} *, so the ratio* ρ_{Fluid} *:* ρ_{Earth} *measures the relative importance of self-gravitation and Earth/fluid gravitation.] Self-gravitation effects in the atmosphere are negligible because* ρ_{Fluid} *:* ρ_{Earth} $\approx 2 \times 10^{-4}$*. Finally, we note that gravity exhibits small subglobal-scale variations because the distribution of mass within the Earth is not radially symmetric. Such variations are customarily neglected in meteorological models, and we consider this to be a quantitatively good approximation.*

1.2 Continuity equation

In this section it is assumed that the atmosphere consists of **dry** air. Modifications to represent moisture in its various phases are discussed in Section 1.5.

If mass sources are neglected (see Section 1.5), elementary considerations of the mass budget lead to the continuity equation in the equivalent forms

$$\frac{\partial \rho}{\partial t} + \mathrm{div}\,(\rho \mathbf{u}) = 0, \tag{1.23}$$

$$\frac{D\rho}{Dt} + \rho \mathrm{div}\mathbf{u} = 0. \tag{1.24}$$

Eq (1.24) is perhaps the more fundamental form, since it involves the material derivative of a scalar, which is a frame-independent derivative (unlike the local derivative of a scalar). As in Section 1.1, $\mathbf{u}$ is the velocity in the rotating frame (although in (1.24) it could just as well be the velocity $\widehat{\mathbf{u}}$ in an inertial frame, since $\widehat{\mathbf{u}} = \mathbf{u} + \mathbf{\Omega} \times \mathbf{r}$, and $\mathbf{\Omega} \times \mathbf{r}$ is a non-divergent vector: $\mathrm{div}(\mathbf{\Omega} \times \mathbf{r}) = \mathbf{r} \cdot \mathrm{curl}\mathbf{\Omega} - \mathbf{\Omega} \cdot \mathrm{curl}\mathbf{r} = 0$).

The spherical polar form of (1.24) is

$$\frac{D\rho}{Dt} + \rho\left(\frac{1}{r\cos\phi}\left[\frac{\partial u}{\partial\lambda} + \frac{\partial}{\partial\phi}(v\cos\phi)\right] + \frac{1}{r^2}\frac{\partial}{\partial r}\left[r^2 w\right]\right) = 0, \tag{1.25}$$

in which D/Dt is given by (1.17). An alternative form, which is convenient as a starting point for transformation to a terrain-following coordinate system (see Section 2.2), is

$$\frac{D}{Dt}\left(\rho r^2\cos\phi\right) + \rho r^2\cos\phi\left(\frac{\partial}{\partial\lambda}\left[\frac{u}{r\cos\phi}\right] + \frac{\partial}{\partial\phi}\left[\frac{v}{r}\right] + \frac{\partial w}{\partial r}\right) = 0. \tag{1.26}$$

Since $u = r\cos\phi D\lambda/Dt = \dot\lambda r\cos\phi$, $v = rD\phi/Dt = r\dot\phi$ and $w = Dr/Dt = \dot r$, (1.26) can be written as

$$\frac{D}{Dt}\left(\rho r^2\cos\phi\right) + \rho r^2\cos\phi\left(\frac{\partial\dot\lambda}{\partial\lambda} + \frac{\partial\dot\phi}{\partial\phi} + \frac{\partial\dot r}{\partial r}\right) = 0. \tag{1.27}$$

Aside :

In Section 1.1 we noted that the components of $\frac{D\mathbf{u}}{Dt}$ in a general orthogonal curvilinear system (GOCS) may be written down from expressions given in Appendix 2 of Batchelor (1967), but we did not quote them because of their length. The GOCS versions of the scalar equations are much shorter, and we give the necessary ingredients here, using the continuity equation as an example. Suppose that $(\xi_1,\ \xi_2,\ \xi_3)$ are orthogonal curvilinear coordinates related to Cartesian coordinates $(x_1,\ x_2,\ x_3)$ by invertible, differentiable relations of the form $x_i = x_i(\xi_j)$, $\quad i,j = 1,2,3$. Then the distance element δs given by $\delta s^2 = \delta x_1^2 + \delta x_2^2 + \delta x_3^2$ may be expressed as

$$\delta s^2 = h_1^2\delta\xi_1^2 + h_2^2\delta\xi_2^2 + h_3^2\delta\xi_3^2, \tag{1.28}$$

$$\textit{where} \quad h_i^2 = \left(\frac{\partial x_1}{\partial\xi_i}\right)^2 + \left(\frac{\partial x_2}{\partial\xi_i}\right)^2 + \left(\frac{\partial x_3}{\partial\xi_i}\right)^2. \tag{1.29}$$

As is well known, the expressions for gradient and divergence are

$$\nabla\Phi = \left(\frac{1}{h_1}\frac{\partial\Phi}{\partial\xi_1},\ \frac{1}{h_2}\frac{\partial\Phi}{\partial\xi_2},\ \frac{1}{h_3}\frac{\partial\Phi}{\partial\xi_3}\right), \tag{1.30}$$

$$\nabla\cdot\mathbf{u} = \frac{1}{h_1h_2h_3}\left\{\frac{\partial}{\partial\xi_1}\left(u_1h_2h_3\right) + \frac{\partial}{\partial\xi_2}\left(u_2h_3h_1\right) + \frac{\partial}{\partial\xi_3}\left(u_3h_1h_2\right)\right\}. \tag{1.31}$$

Since, by definition, $u_1 = h_1 D\xi_1/Dt = h_1\dot{\xi}_1$*,* $u_2 = h_2 D\xi_2/Dt = h_2\dot{\xi}_2$ *and* $u_3 = h_3 D\xi_3/Dt = h_3\dot{\xi}_3$*, we can write* (1.31) *as*

$$\nabla\cdot\mathbf{u} = \frac{1}{h_1h_2h_3}\left\{\frac{\partial}{\partial\xi_1}\left(h_1h_2h_3\dot{\xi}_1\right) + \frac{\partial}{\partial\xi_2}\left(h_1h_2h_3\dot{\xi}_2\right) + \frac{\partial}{\partial\xi_3}\left(h_1h_2h_3\dot{\xi}_3\right)\right\}, \quad (1.32)$$

and, from (1.30) *(or first principles),*

$$\frac{D}{Dt} \equiv \frac{\partial}{\partial t} + \dot{\xi}_1\frac{\partial}{\partial\xi_1} + \dot{\xi}_2\frac{\partial}{\partial\xi_2} + \dot{\xi}_3\frac{\partial}{\partial\xi_3}. \quad (1.33)$$

Hence (noting that $\partial/\partial t\,[h_1h_2h_3] = 0$*) we derive the continuity equation as*

$$\frac{D}{Dt}\left(\rho h_1h_2h_3\right) + \rho h_1h_2h_3\left\{\frac{\partial\dot{\xi}_1}{\partial\xi_1} + \frac{\partial\dot{\xi}_2}{\partial\xi_2} + \frac{\partial\dot{\xi}_3}{\partial\xi_3}\right\} = 0. \quad (1.34)$$

The quantity $J \equiv h_1h_2h_3$ *is the Jacobian of the transformation from* x_1*,* x_2*,* x_3 *to* ξ_1*,* ξ_2*,* ξ_3*. In the case of spherical polar coordinates,* $\xi_1 = \lambda$*,* $\xi_2 = \phi$*,* $\xi_3 = r$ *and* $h_1 = r\cos\phi$*,* $h_2 = r$*,* $h_3 = 1$*; from the GOCS form we recover the spherical polar form already given [*(1.27)*]. [Gill (1982), p92, gives* h_1*,* h_2*,* h_3 *for oblate spheroidal coordinates.] The expression* (1.33) *for* D/Dt *may be used to write the thermodynamic and moisture budget equations (see later sections) in GOCS form.*

1.3 Thermodynamic equation

In this section it is assumed that the atmosphere consists of **dry** air. Modifications to represent moisture in its various phases are discussed in Section 1.5.

The First Law of Thermodynamics relates the change δU in the internal energy of a mass of fluid to the heating δQ and the work δW done *by* the mass of fluid:

$$\delta U = \delta Q - \delta W. \quad (1.35)$$

δQ is considered to be the total heating, including the (irreversible) contribution of frictional dissipation. If the mass of fluid has pressure p, and its volume changes (reversibly) by δV, then $\delta W = p\delta V$ and (1.35) becomes

$$\delta U + p\delta V = \delta Q. \quad (1.36)$$

In terms of quantities per unit mass, (1.36) may be written

$$c_v\delta T + p\delta\alpha = \delta Q. \quad (1.37)$$

Here c_v is the specific heat at constant volume and α $(= 1/\rho)$ is the specific volume. Hence

$$c_v \frac{DT}{Dt} + p \frac{D\alpha}{Dt} = \dot{Q}, \tag{1.38}$$

in which $\dot{Q}$ is the *rate* of heating, per unit mass, to which the element of fluid is subject.

Particularising to a perfect gas, we have $p\alpha = RT$ (see Section 1.4) and $c_p - c_v = R$, where c_p is the specific heat at constant pressure; (1.38) becomes

$$c_p \frac{DT}{Dt} - \alpha \frac{Dp}{Dt} = \dot{Q}. \tag{1.39}$$

In terms of potential temperature θ defined by

$$\theta = T \left(\frac{p_0}{p} \right)^{\frac{R}{c_p}}, \tag{1.40}$$

[where p_o is a reference pressure; conventionally $p_o = 1000$hPa], (1.39) simplifies to

$$\frac{D\theta}{Dt} = \left(\frac{\theta}{T} \right) \frac{\dot{Q}}{c_p}. \tag{1.41}$$

The source term in the potential temperature equation (1.41) is thus (θ/T) multiplied by the heating rate divided by c_p. The non-dimensional factor (θ/T) is worth noting, lying as it does on the parish boundary between adiabatic and diabatic thermodynamics.

Aside :

With two parenthetic exceptions, this simple treatment ((1.36)-(1.41)*) avoids mention of reversibility and irreversibility, and we believe it is adequate for the description of a numerical model based on the full equations of motion - given also that the heating (or heating rate) in* (1.36)-(1.41) *includes the contribution of frictional dissipation. The reversibility/irreversibility issue deserves further attention, however. A related issue which also warrants further study is whether a general statement of the Conservation of Energy (taking into account all forms of energy, macroscopic and microscopic, and all forces acting) should be used as the axiomatic starting point, rather than the First Law of Thermodynamics in the familiar form* (1.36)*. Holton (1992), pp.47-51, finds that the choice between these two starting points does not affect conclusions, but his treatment explicitly omits the effects of friction (including frictional dissipation, which is a fundamental process in the themodynamics of real fluids).*

1.4 Equation of state and the Exner function

In this section it is assumed that the atmosphere consists of **dry** air. Modifications to represent moisture in its various phases are discussed in Section 1.5.

The perfect gas law is adopted. In terms of density, ρ $(= 1/\alpha)$:

$$p = \rho R T. \tag{1.42}$$

Here R is the gas constant for unit mass of dry air. Eq (1.42) is a good approximation under conditions typical of the atmosphere.

Aside :

How good? Gill (1982) says "better than 1 in 1000" for tropospheric conditions. Emanuel (1994) notes that water vapour (see Section 1.5 below) is less well behaved.

Rather than retaining p as a dependent variable, it is convenient for many purposes to work in terms of the Exner function Π defined by

$$\Pi = \left(\frac{p}{p_0}\right)^{\frac{R}{c_p}}, \tag{1.43}$$

The relationship between temperature and potential temperature becomes simply

$$\theta = T/\Pi, \tag{1.44}$$

and the pressure gradient terms in the components of the momentum equation may be written in terms of θ rather than ρ (which varies far more rapidly with height):

$$\frac{1}{\rho}\frac{\partial p}{\partial X} = \frac{RT}{p}\frac{\partial p}{\partial X} = \frac{R\theta\Pi}{p}\frac{\partial p}{\partial X} = c_p\theta\frac{\partial \Pi}{\partial X}, \tag{1.45}$$

where $X = \lambda, \phi$ or r .

Aside :

The same qualitative effect regarding the pressure gradient terms could be achieved by working in terms of $\ln p$*:*

$$\frac{1}{\rho}\frac{\partial p}{\partial X} = \frac{RT}{p}\frac{\partial p}{\partial X} = RT\frac{\partial}{\partial X}(\ln p). \tag{1.46}$$

The multiplying factor in this case, RT, also varies much more slowly with height than does $1/\rho$. The use of the quantity $\ln p$ as an independent variable facilitated application of a semi-implicit time integration scheme in the nonhydrostatic, shallow atmosphere model described by Tanguay, Robert & Laprise (1990), and the use of $\ln p$ was suggested by Richardson (1922).

In terms of Π, and $\kappa \equiv R/c_p$, the perfect gas law (1.42) may be written as

$$\Pi^{\frac{\kappa-1}{\kappa}}\rho\theta = \frac{p_0}{\kappa c_p}. \tag{1.47}$$

1.5 Representation of moisture

Attention must first be drawn to a potential problem of notation. We wish to distinguish between dry-air quantities and moist-air quantities, and will introduce a subscript notation (see below) for this purpose. It seems natural to use unqualified symbols (such as p, ρ, κ, c_p) for the moist air, since the moist air (i.e. dry air + various phases of water) is the multi-component system that we wish to describe. So far, however, we have used unqualified symbols to represent the properties of dry air - for the very good reason that dry air has been the single-component system that we have wished to describe! We shall note where the new subscript notation must be applied to earlier equations.

Moisture -"water substance" if we want to be pedantic - is explicitly represented in the New Dynamics in three forms: water vapour, cloud liquid water and cloud frozen water. The main reasons for representing them are: (i) they are important in their own right (customers of the Met. Office are naturally interested in humidity, cloud cover and cloud type) and (ii) they are responsible for radiative feedbacks which are important even on short timescales and absolutely crucial on climatological timescales. Precipitation (i.e. water substance that is not moving with the flow) is not explicitly treated.

The basic requirement is that the model should have a budget equation of the form

$$\frac{Dm_X}{Dt} = S^{m_X}, \tag{1.48}$$

for each type of moisture. Here m_X is the amount of water substance of type X associated with unit mass of dry air, D/Dt is the material derivative (1.17) [as used in the momentum, continuity and thermodynamic equations], and S^{m_X} represents the source of water substance of type X. (The precise sense in which S^{m_X} represents a source of X is considered in the next **Aside)** . From (1.48), m_X may be forecast so long as the current m_X, S^{m_X} and velocity $\mathbf{u}$ are known.

It should be noted that m_X is the amount of water substance of type X associated with unit mass of *dry* air. If the mass of water substance of type X per unit volume of *moist* air is ρ_X, then

$$m_X \equiv \rho_X \,/\rho_y \ , \tag{1.49}$$

where ρ_y is the mass of dry air per unit volume of moist air. So m_X is the *mixing ratio of water substance of type X* with respect to dry air. The rationale for the seemingly bizarre notation ρ_y for dry-air density is that subscript y is a covert abbreviation of subscript *dry*: subscript d is used in later sections to indicate evaluation at the departure point (in semi-Lagrangian schemes). Note however that there are four exceptions to this convention, viz. R_d, c_{pd}, c_{vd} and κ_d are used, without ambiguity, to denote the dry-air values of R, c_p, c_v and κ respectively. Let subscripts v, cl , cf refer to vapour, cloud liquid water and cloud frozen water respectively. Thus

$$m_v \equiv \rho_v \,/\rho_y \ = \text{mixing ratio of water vapour,} \tag{1.50}$$

$$m_{cl} \equiv \rho_{cl} \,/\rho_y \ = \text{mixing ratio of cloud liquid water,} \tag{1.51}$$

$$m_{cf} \equiv \rho_{cf} \,/\rho_y \ = \text{mixing ratio of cloud frozen water.} \tag{1.52}$$

The mass of the moist air in unit volume, including all water substance, is simply the sum of the individual component masses

$$\rho = \rho_y + \rho_v + \rho_{cl} + \rho_{cf}. \tag{1.53}$$

Notice (from (1.49)) that the quantity m_y, which might whimsically be called the mixing ratio of dry air, is trivially given by

$$m_y \equiv \rho_y \,/\rho_y \ = 1. \tag{1.54}$$

The respective *specific humidities*, q_X, which are **not** used in the New Dynamics, are defined by

$$q_X = \rho_X \,/\rho \ . \tag{1.55}$$

Hence

$$q_X = m_X \bigg/ \left(1 + \sum_{X=(v,cl,cf)} m_X\right) , \tag{1.56}$$

$$m_X = q_X \bigg/ \left(1 - \sum_{X=(v,cl,cf)} q_X\right) . \tag{1.57}$$

These relations permit conversions between m_X and q_X if required, e.g. for parametrisation purposes.

Having set up the budget equations and defined notation, we now consider what modifications the presence of water substance requires in the momentum, continuity, thermodynamic and state equations. This is where the fun begins. Not only does water vapour have a different gas constant per unit mass from that of dry air, it is a triatomic gas. The specific heat of liquid water is much greater ($\times 3$ for c_v) than that of water vapour - which in turn is different from that of dry air. Fortunately, m_v, m_{cl} and m_{cf} are in reality always small quantities ($\ll 1$), so there is scope for approximation (and survival).

Aside :

Clarification is needed of the sense in which S^{m_X} *in* (1.48) *represents a source of water substance of type* X. *If a source of mass* S^ρ *per unit volume is present, then the generic continuity equation* (1.24) *becomes*

$$\frac{D\rho}{Dt} + \rho div\mathbf{u} = S^\rho. \tag{1.58}$$

This equation may be applied to each type X *of water substance that is advected with the flow* **u***:*

$$\frac{D\rho_X}{Dt} + \rho_X div\mathbf{u} = S^{\rho_X}. \tag{1.59}$$

The source terms S^{ρ_X} *represent changes of state, precipitation formation (and evaporation) and unresolved transports by turbulence and convection. For the* dry-air *fraction it is assumed that no sources are present:*

$$\frac{D\rho_y}{Dt} + \rho_y div\mathbf{u} = 0. \tag{1.60}$$

From (1.59), (1.60) *and* (1.53) *it follows easily that the total density* ρ *obeys*

$$\frac{D\rho}{Dt} + \rho div\mathbf{u} = \sum_{X=(v,cl,cf)} S^{\rho_X}. \tag{1.61}$$

Also, from (1.49)*,* (1.59) *and* (1.60)*:*

$$\frac{Dm_X}{Dt} = \frac{S^{\rho_X}}{\rho_y}. \tag{1.62}$$

Eq. (1.62) *relates the source term in* (1.48) *to the mass sources in* (1.59)*, i.e.*

$$S^{m_X} \equiv S^{\rho_X}/\rho_y. \tag{1.63}$$

From (1.59) *and* (1.61)*, the specific humidities* $q_X \equiv \rho_X/\rho$ *(which are* ***not*** *used in the New Dynamics) obey*

$$\frac{Dq_X}{Dt} = \frac{S^{\rho_X}}{\rho} - \frac{q_X}{\rho}\sum_{X=(v,cl,cf)} S^{\rho_X} \equiv S^{q_X}, \tag{1.64}$$

which is considerably more complicated than (1.62)*.*

The budget equations for m_v, m_{cl}, and m_{cf} are

$$\frac{Dm_v}{Dt} = S^{m_v}, \tag{1.65}$$

$$\frac{Dm_{cl}}{Dt} = S^{m_{cl}}, \tag{1.66}$$

$$\frac{Dm_{cf}}{Dt} = S^{m_{cf}}. \tag{1.67}$$

Note that only dry air and water vapour exert a pressure; cloud liquid and frozen water do not. According to Dalton's Law of Partial Pressures (which is consistent with the perfect gas assumption as expressed in (1.42)), the pressure exerted by a mixture of dry air and water vapour is equal to the sum of the pressures which would be exerted by the dry air and water vapour fractions separately. If R_d and R_v are the gas constants (per unit mass) for dry air and water vapour, and $\epsilon \equiv R_d/R_v$ ($\cong 0.622$), we find (using (1.50)-(1.52))

$$p = p_y + p_v = (\rho_y R_d + \rho_v R_v)\, T = \rho R_d T \left(\frac{\rho_y}{\rho} + \frac{\rho_v R_v}{\rho R_d} \right), \tag{1.68}$$

$$\text{or} \quad p = \rho R_d T_v, \tag{1.69}$$

$$\text{where} \quad T_v = T \left(\frac{1 + \frac{1}{\epsilon} m_v}{1 + m_v + m_{cl} + m_{cf}} \right). \tag{1.70}$$

Note that R_d, the gas constant per unit mass for *dry* air, appears in (1.69). T_v is called the *virtual temperature*; it is the temperature that *dry* air would have to have, at a given density, in order to exert the same pressure as the mixture of dry air and water substance at temperature T. [The subscript v has now accumulated 3 different meanings : "virtual" (as in T_v), "vapour" (as in R_v), and "constant volume" (as in c_v). No ambiguity should arise so long as the possibility of it is appreciated.]

Aside :

The physical volume occupied by the cloud liquid and frozen water has been neglected in writing (1.68) *and* (1.70). *Let* $\widehat{\alpha}_{cl}$ *and* $\widehat{\alpha}_{cf}$ *be the true specific volumes of cloud liquid water and cloud frozen water, i.e. the volumes occupied by unit mass of water and by unit mass of ice. If* $\widehat{\alpha}_g$ *is the volume occupied by unit mass of the gaseous component (dry air + water vapour) of the moist air, then the specific volume* α *of the moist air obeys*

$$(1 + m_v + m_{cl} + m_{cf})\,\alpha = (1 + m_v)\,\widehat{\alpha}_g + m_{cl}\widehat{\alpha}_{cl} + m_{cf}\widehat{\alpha}_{cf}; \tag{1.71}$$

i.e. the volume occupied by the moist air is the sum of the volumes occupied by the gaseous, liquid and frozen components individually. The perfect gas law for the gaseous component is

$$p\widehat{\alpha}_g = \frac{(R_d + m_v R_v)}{(1 + m_v)} T = \frac{R_d\left(1 + \frac{1}{\epsilon} m_v\right)}{(1 + m_v)} T. \tag{1.72}$$

Use of (1.71) *to eliminate* $\widehat{\alpha}_g$ *from* (1.72), *and* $\rho = \frac{1}{\alpha}$, *gives* (1.69) *with*

$$T_v = T\left(\frac{1 + \frac{1}{\epsilon} m_v}{1 + m_v + m_{cl}\left(1 - \frac{\widehat{\alpha}_{cl}}{\alpha}\right) + m_{cf}\left(1 - \frac{\widehat{\alpha}_{cf}}{\alpha}\right)}\right) \tag{1.73}$$

The terms in $\frac{\widehat{\alpha}_{cl}}{\alpha}$ *and* $\frac{\widehat{\alpha}_{cf}}{\alpha}$ *in the denominator of* (1.73) *do not appear in* (1.70). *Since* $\frac{\widehat{\alpha}_{cl}}{\alpha}$ *and* $\frac{\widehat{\alpha}_{cf}}{\alpha}$ *are of order* 10^{-3} *or less (the ratio of the density of air to the density of water or ice) the approximation involved in using* (1.70) *is negligible.*

Eq. (1.69) may be used to modify the pressure gradient term in the **components of the momentum equation**. Instead of terms of the form $c_p\theta\partial\Pi/\partial X$ [which is the right side of (1.45) in the current notation], we put $c_{pd}\theta_v\partial\Pi/\partial X$, where

$$\theta_v \equiv \frac{T_v}{\Pi} = T_v\left(\frac{p_0}{p}\right)^{\frac{R_d}{c_{pd}}}, \tag{1.74}$$

is the *virtual potential temperature* [see Emanuel (1994)]. Notice that the definition (1.43) of the Exner function Π, in terms of dry-air quantities, has been retained (though expressed in the current subscript notation). By virtue of (1.44) and (1.70), (1.74) may be written alternatively as

$$\theta_v = \theta \left(\frac{1 + \frac{1}{\epsilon} m_v}{1 + m_v + m_{cl} + m_{cf}} \right). \tag{1.75}$$

In terms of the dry-air Exner function Π, the **equation of state** (the perfect gas law) becomes

$$\Pi^{\frac{\kappa_d - 1}{\kappa_d}} \rho \theta_v = \frac{p_0}{\kappa_d c_{pd}}, \tag{1.76}$$

where $\kappa_d = R_d / c_{pd}$.

The **continuity equation** is modified to allow for the fact that the dry air (which still obeys (1.25)) contributes only a fraction $1/\left(1 + m_v + m_{cl} + m_{cf}\right)$ of the (total) air density ρ. Hence ρ is replaced by $\rho_y = \rho / \left(1 + m_v + m_{cl} + m_{cf}\right)$ in (1.24). By treating dry air alone, we avoid the complication of a continuity equation which has source/sink terms. [See the first **Aside** of this subsection.]

The **thermodynamic equation** requires lengthier consideration. In the current notation, (1.41) for *dry* air is

$$\frac{D\theta}{Dt} = \left(\frac{\theta}{T} \right) \frac{\dot{Q}}{c_{pd}}, \tag{1.77}$$

where ((1.40))

$$\theta = T \left(\frac{p_0}{p} \right)^{\frac{R_d}{c_{pd}}}. \tag{1.78}$$

Subject to certain provisos (see next **Aside)** the moist-air versions of (1.77) and (1.78) have similar forms, but with R_d and c_{pd} replaced by suitably modified values of R and c_p:

$$R = \frac{\left(R_d + R_v m_v\right)}{\left(1 + m_v + m_{cl} + m_{cf}\right)} = R_d \frac{\left(1 + \frac{1}{\epsilon} m_v\right)}{\left(1 + m_v + m_{cl} + m_{cf}\right)}; \tag{1.79}$$

$$c_p = \frac{\left(c_{pd} + m_v c_{pv} + m_{cl} c_{cl} + m_{cf} c_{cf}\right)}{\left(1 + m_v + m_{cl} + m_{cf}\right)}. \tag{1.80}$$

In (1.80), c_{pv} is the value of c_p for water vapour, c_{cl} is the specific heat of liquid water and c_{cf} is the specific heat of ice. Elementary kinetic theory of gases gives $c_{pd} = \frac{7}{2} R_d$ (diatomic gas) and $c_{pv} = 4 R_v$ (triatomic gas); hence, from (1.80):

$$c_p = \frac{7}{2} R_d \frac{\left(1 + \frac{8}{7\epsilon} m_v + m_{cl} \frac{c_{cl}}{c_{pd}} + m_{cf} \frac{c_{cf}}{c_{pd}}\right)}{\left(1 + m_v + m_{cl} + m_{cf}\right)}. \tag{1.81}$$

[Gill (1982) and Emanuel (1994) give equivalent expressions valid for the case $m_{cl} = m_{cf} = 0$.] From (1.79) and (1.81),

$$\frac{R}{c_p} = \frac{2}{7} \frac{\left(1 + \frac{1}{\epsilon} m_v\right)}{\left(1 + \frac{8}{7\epsilon} m_v + m_{cl} \frac{c_{cl}}{c_{pd}} + m_{cf} \frac{c_{cf}}{c_{pd}}\right)}. \tag{1.82}$$

Now $\epsilon = 0.622$ gives $\frac{1}{7\epsilon} \cong 0.23$ and $\left(\frac{8}{7\epsilon} - 1\right) \cong 0.84$; thus (given m_v, m_{cl}, $m_{cf} \ll 1$),

$$c_p \cong \frac{7}{2} R_d \left[1 + 0.84 m_v + m_{cl} \left(\frac{c_{cl}}{c_{pd}} - 1\right) + m_{cf} \left(\frac{c_{cf}}{c_{pd}} - 1\right)\right], \tag{1.83}$$

and

$$\frac{R}{c_p} \cong \frac{2}{7} \left[1 - 0.23 m_v - m_{cl} \frac{c_{cl}}{c_{pd}} - m_{cf} \frac{c_{cf}}{c_{pd}}\right]. \tag{1.84}$$

Although the specific heats of water and ice are about 4 times c_{pd}, values of m_{cl} and m_{cf} are so small ($\simeq 10^{-3}$; P R A Brown, private communication) that the terms in m_{cl} and m_{cf} in (1.83) and (1.84) may be neglected. The mixing ratio of water vapour m_v, however, may range up to 0.04 in the tropics, so the terms in m_v in (1.83) and (1.84) are generally much more important. The dependence of c_p on m_v (1.83) is between 3 and 4 times more rapid than that of R/c_p on m_v (1.84). Given that $m_v = 0.04$ is a large value for the atmosphere, errors of less than 1% in R/c_p are made by adopting the dry-air value $2/7$. Larger errors (over 3% for high tropical humidities) in c_p are made by adopting the dry-air value $\frac{7}{2} R_d$. Both approximations are made in the New Dynamics; the thermodynamic equation is written in the dry air form (1.77), with potential temperature defined by the dry air form (1.78).

Aside :

Given the use of the dry-air form (1.77) *of the thermodynamic equation, it seems strictly inconsistent that the virtual temperature adjustment defined by* (1.70) *is applied to the pressure gradient terms in the momentum equation; the error made by ignoring that adjustment would be, at most, only 2.5%. Note, however, that the r.h.s. of* (1.77) *vanishes if* $Q = 0$, *so* in adiabatic motion *the virtual temperature adjustment may be worthwhile whatever approximation is applied to the factor multiplying* Q. *The best way of addressing the inconsistency would be to use*

$$\frac{D\theta}{Dt} = \left(\frac{\theta}{T}\right) \frac{\dot{Q}}{c_{pd}\left(1 + 0.84 m_v\right)} \tag{1.85}$$

instead of (1.77).

Aside :

Our discussion from (1.77) *onwards has assumed that the First Law of Thermodynamics for a mixture of dry air, water vapour, cloud liquid water and cloud frozen water may be written in a potential temperature form (of which* (1.77) *and* (1.85) *are particular examples). This may be justified as follows. If an amount of heat δQ per unit mass is supplied reversibly to the mixture, and its temperature and specific volume change by δT and $\delta\alpha$, then the First Law of Thermodynamics requires that*

$$\frac{(c_{vd} + m_v c_{vv} + m_{cl} c_{cl} + m_{cf} c_{cf})}{(1 + m_v + m_{cl} + m_{cf})} \delta T + p\delta\alpha = \delta Q. \tag{1.86}$$

Here c_{vv} is the value of c_v for the water vapour. Assuming that m_v, m_{cl} and m_{cf} remain constant, and that the cloud liquid water and cloud frozen water are incompressible, it follows from (1.71) *and* (1.72) *that*

$$(1 + m_v + m_{cl} + m_{cf})\, p\delta\alpha = (1 + m_v)\, p\delta\widehat{\alpha}_g = (R_d + m_v R_v)\, T \left(\frac{\delta T}{T} - \frac{\delta p}{p} \right). \tag{1.87}$$

Use of (1.87) *in* (1.86)*, and application of*

$$c_{pd} - c_{vd} = R_d \quad \textit{and} \quad c_{pv} - c_{vv} = R_v,$$

gives

$$\frac{\delta T}{T} - \frac{(R_d + m_v R_v)}{(c_{pd} + m_v c_{pv} + m_{cl} c_{cl} + m_{cf} c_{cf})} \frac{\delta p}{p} = \frac{(1 + m_v + m_{cl} + m_{cf})}{(c_{pd} + m_v c_{pv} + m_{cl} c_{cl} + m_{cf} c_{cf})} \frac{\delta Q}{T}. \tag{1.88}$$

Hence

$$\frac{D}{Dt} \ln T - \frac{R}{c_p} \frac{D}{Dt} \ln p = \frac{Q}{T c_p} \tag{1.89}$$

where R and c_p are defined by (1.79) *and* (1.80)*. If m_v, m_{cl} and m_{cf} remain constant, then the factor $\frac{R}{c_p}$ may be taken inside the second material derivative in* (1.89) *to give*

$$\frac{D\theta}{Dt} = \left(\frac{\theta}{T} \right) \frac{Q}{c_p}, \tag{1.90}$$

with

$$\theta = T \left(\frac{p_0}{p} \right)^{\frac{R}{c_p}}, \tag{1.91}$$

R and c_p being defined by (1.79) *and* (1.80). *The quantities m_v, m_{cl} and m_{cf} do not, of course, remain constant: the model has dynamical equations (*(1.65) - (1.67)*) for each. The justification for the use of* (1.90) *is that m_v, m_{cl} and m_{cf} are each very small (especially m_{cl} and m_{cf}), so the neglect of their Lagrangian time variations is acceptable so long as the relevant time scale is comparable with (or longer than) that of the Lagrangian time variations of θ.*

1.6 The story so far

After the manoeuvres described in Sections 1.4 and 1.5, the governing equations have undergone various changes, and it is convenient to draw up a list of final forms.

Horizontal momentum components

$$\frac{Du}{Dt} = -\frac{uw}{r} - 2\Omega w \cos\phi + \frac{uv\tan\phi}{r} + 2\Omega v \sin\phi - \frac{c_{pd}\theta_v}{r\cos\phi}\frac{\partial\Pi}{\partial\lambda} + S^u, \tag{1.92}$$

$$\frac{Dv}{Dt} = -\frac{vw}{r} \qquad - \frac{u^2\tan\phi}{r} - 2\Omega u \sin\phi - \frac{c_{pd}\theta_v}{r}\frac{\partial\Pi}{\partial\phi} + S^v, \tag{1.93}$$

where

$$\frac{D}{Dt} \equiv \frac{\partial}{\partial t} + \frac{u}{r\cos\phi}\frac{\partial}{\partial\lambda} + \frac{v}{r}\frac{\partial}{\partial\phi} + w\frac{\partial}{\partial r}, \tag{1.94}$$

$$\Pi = \left(\frac{p}{p_0}\right)^{\frac{R_d}{c_{pd}}}, \qquad \text{[Exner function; } p_0 = 1000hPa\text{]} \tag{1.95}$$

$$\theta_v = \frac{T}{\Pi}\left(\frac{1 + \frac{1}{\epsilon}m_v}{1 + m_v + m_{cl} + m_{cf}}\right). \quad \text{[Virtual potential temperature; } \epsilon = \frac{R_d}{R_v} \cong 0.622\text{]} \tag{1.96}$$

Vertical momentum component

$$\frac{Dw}{Dt} = \frac{(u^2 + v^2)}{r} + 2\Omega u \cos\phi \; - \; g \; - c_{pd}\theta_v\frac{\partial\Pi}{\partial r} + S^w. \tag{1.97}$$

Continuity

$$\frac{D}{Dt}\left(\rho_y r^2 \cos\phi\right) + \rho_y r^2 \cos\phi\left(\frac{\partial}{\partial\lambda}\left[\frac{u}{r\cos\phi}\right] + \frac{\partial}{\partial\phi}\left[\frac{v}{r}\right] + \frac{\partial w}{\partial r}\right) = 0, \tag{1.98}$$

where

$$\rho = \rho_y\left(1 + m_v + m_{cl} + m_{cf}\right). \tag{1.99}$$

Thermodynamics

$$\frac{D\theta}{Dt} = S^\theta = \left(\frac{\theta}{T}\right)\frac{\dot{Q}}{c_{pd}}, \tag{1.100}$$

where

$$\theta = \frac{T}{\Pi} = T\left(\frac{p_0}{p}\right)^{\frac{R_d}{c_{pd}}}. \quad \text{[Potential temperature; } \; p_0 = 1000hPa\text{]} \tag{1.101}$$

State

$$\Pi^{\frac{\kappa_d-1}{\kappa_d}}\rho\theta_v = \frac{p_0}{\kappa_d c_{pd}}. \quad [\kappa_d \equiv \frac{R_d}{c_{pd}}] \tag{1.102}$$

Moisture

$$\frac{Dm_v}{Dt} = S^{m_v}, \tag{1.103}$$

$$\frac{Dm_{cl}}{Dt} = S^{m_{cl}}, \tag{1.104}$$

$$\frac{Dm_{cf}}{Dt} = S^{m_{cf}}. \tag{1.105}$$

In a sense, (1.92)-(1.105) are the equations on which the New Dynamics are based, since the transformations described in Section 2 are exact, and no terms are neglected.

2 The governing equations in the model's transformed coordinates

Chapter 1 of this documentation culminated in a list of the New Dynamics governing equations written in conventional spherical polar form ((1.92)-(1.105)). The present chapter deals with the horizontal coordinate transforms which are the basis of limited area versions of the model (Section 2.1) and with the vertical coordinate transforms which are applied in all versions (Section 2.2). The equations under both transformations are listed in Section 2.3.

2.1 Transformation to a rotated latitude/longitude system

Mesoscale versions of the current UM and of the New Dynamics use a "rotated" latitude/longitude system that is not coincident with the usual geographical system. There are two good reasons for what might seem at first sight a perverse manoeuvre:

(a) use of a regular latitude/longitude grid always leads to numerical complications close to the poles (where meridians converge and the actual zonal separation of gridpoints becomes small), so it is desirable to move the poles far away from the mesoscale domain;

(b) the actual separation of grid points on a regular latitude/longitude grid varies most slowly with latitude at its equator, so a quasi-uniform gridding may be achieved by ensuring that the equator of the latitude/longitude system passes through the mesoscale domain.

A key attribute of a rotated latitude/longitude system is the geographical or "true" location of its North Pole, but this is not a complete specification: we also have to locate the latitude/longitude origin of the rotated system. Section 2.1.1 is devoted to an elementary discussion of this issue. In Section 2.1.2, the governing equations are written in terms of latitude and longitude in the rotated system; this is a fairly straightforward operation in itself, since the Earth's rotation axis is the only "preferred direction" in the problem. Section 2.1.3 deals with the rather more challenging issue of transforming coordinates and velocity components between the geographical and rotated systems.

2.1.1 Specification of rotated latitude/longitude grids

Figures 2.1-2.3 illustrate in two simple cases the ambiguities that can arise if the location of the latitude/longitude origin of a rotated system is not specified. Each diagram is a view from over the North (geographical) Pole, and panel (a) of each shows (small open circle) where we wish to place the North Pole of the rotated system. The arrows indicate the axes of various Cartesian systems having their origin O at the centre of the Earth. The outer circle in each diagram represents the geographical equator, and arrows extending to it represent axes lying in the equatorial plane. Shorter arrows represent axes which intersect the Earth's surface away from the equator; the extreme case of an axis lying through the North Pole is denoted by a solid circle.

In Fig 2.1(a) the arrows indicate 0^o and 90^oE, and are labelled x and y; the z axis is imagined to lie along the polar axis and so to point towards the North Pole (and hence towards the reader). The desired location of the North Pole of the rotated system in this case lies in the meridian having true longitude 180^o and has true latitude $(90-\alpha)^o$, say. One obvious way of achieving this location is to rotate the x and z axes about the y axis until the z axis passes through the desired point; see Fig 2.1(b). According to the usual conventions, this rotation (through an angle α^o) is a negative rotation - the x and z axes have been rotated clockwise as seen by an observer looking along the y axis towards the origin. To achieve the desired North Pole re-location in a single positive rotation one could carry out the complementary rotation through an angle $(360-\alpha)^o$. Alternatively, it could be achieved in two positive rotations - as Fig 2.1(c) and (d) show. First, rotate x and y through 180^o anticlockwise about the (true) polar axis z (Fig 2.1(c)). Second, rotate the z and x axes through an angle α^o anticlockwise about y so that z achieves the required orientation (Fig 2.1(d)). It will be observed that the x axis finally points into the (true) Southern Hemisphere, whereas in the single-step rotation (Fig 2.1(b)) it points towards the antipodean point in the Northern Hemisphere. (The y axis also points in the opposite direction.)

<u>Aside :</u>

> *Rotated latitude/longitude specification has a lot in common with specifying the orientation of a rigid body in motion, such as a top, projectile or spacecraft. The two-stage rotation illustrated in Figs 2.1(c) and 2.1(d) can be broadly identified with the specification of the first two* Euler angles *in rigid-body dynamics (see Goldstein (1959)), and the choice of longitude origin is broadly analogous to identification of the third Euler angle. There are many ways of describing rotations, and of defining sign conventions within individual descriptions. Goldstein*

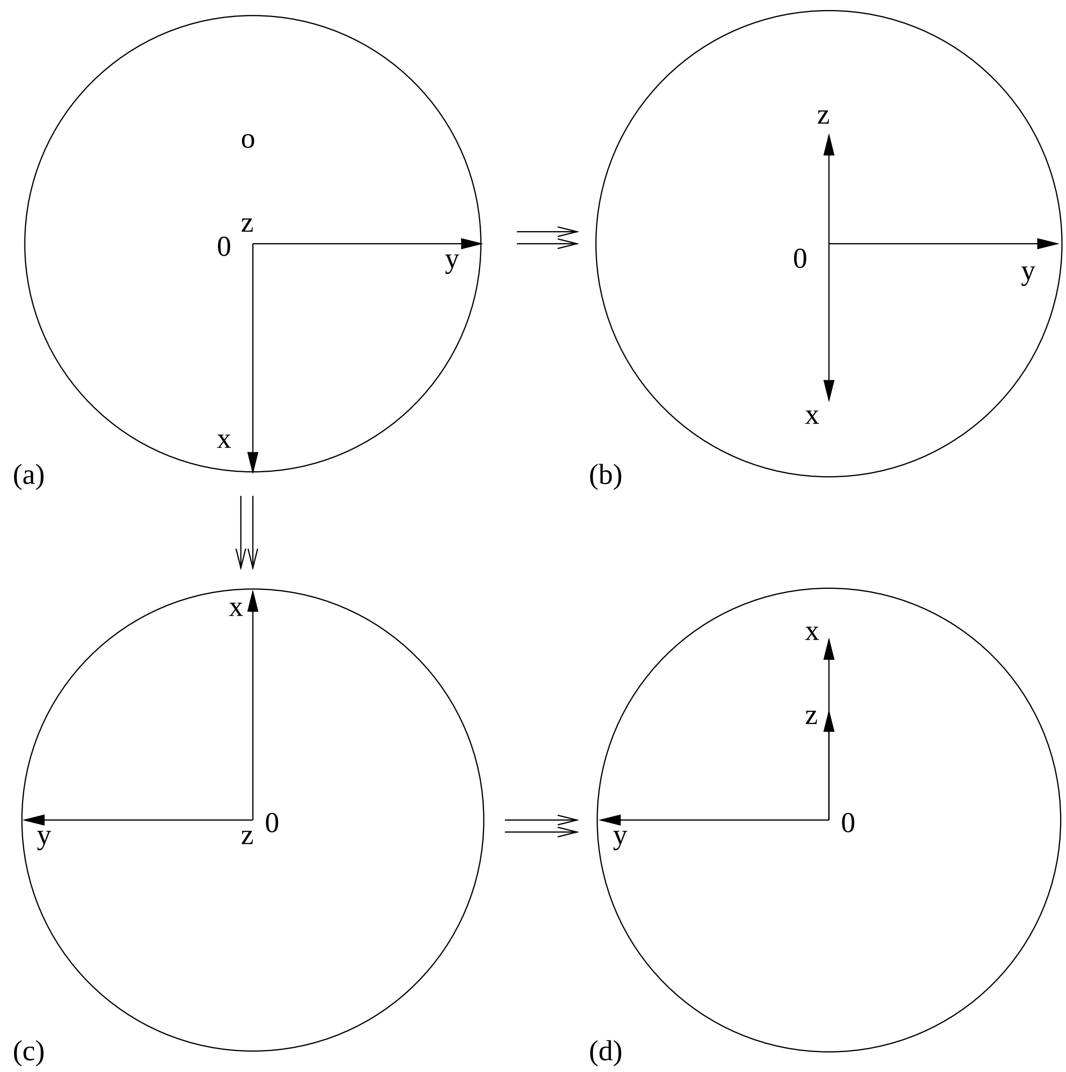

Figure 2.1: Illustrating transformations of coordinate system on the sphere. Each diagram is a view from over the North (geographical) Pole, and (a) shows (small open circle) where we wish to place the North Pole of a rotated longitude/latitude system. Two ways of achieving the desired North Pole location are shown: a single rotation (a)→(b), and a two-stage rotation (a)→(c)→(d). See text for further details.

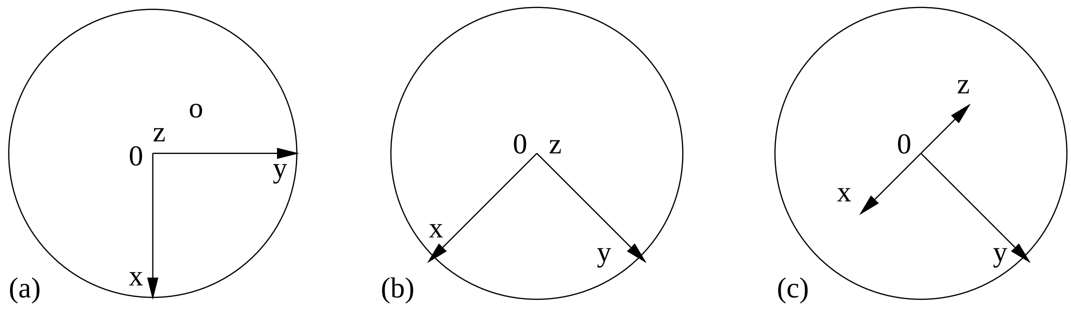

Figure 2.2: One way of moving the North Pole to 135^oE in the geographical system by two rotations. See text for discussion.

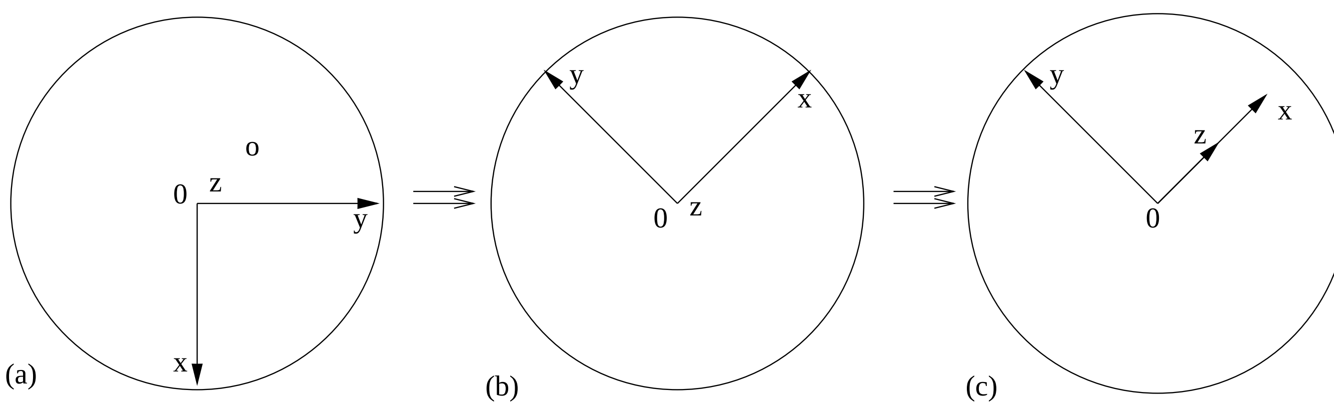

Figure 2.3: Another way of moving the North Pole to 135^oE in the geographical system by two rotations. See text for discussion.

(1959) includes a fraught footnote (p108) about the use of lefthanded coordinate systems, non-standard definitions of Euler angles, and even (in some "quantum-mechanical discussions") "clockwise ... rather than anticlockwise" rotations! Although one must distinguish carefully between a sign convention for rotations and an exclusion of negative rotations once a convention has been adopted, it is clear that meteorological dynamics is not the only branch of physics in which rotations in three dimensions sometimes cause distress.

Another case is shown in Figures 2.2 and 2.3. This time the desired location of the rotated pole lies in the $135^o E$ meridian. Clearly, the z axis could be immediately rotated to the required direction, but the axis of rotation would not coincide with either the x or the y axes (and the geographical pole would not lie on longitude 0^o or 180^o in the rotated system). Fig 2.2 shows one way in which the desired pole re-location may be achieved by two successive rotations. In the first, the x and y axes are rotated through 45^o about the z axis; this is a negative rotation according to the usual convention. In the second, the z and x axes are rotated about the y axis until the z axis is pointing in the desired direction; this is another negative rotation. Another way is shown in Fig 2.3: the first rotation is of the x and y axes through 135^o about the z axis; the second is of the z and x axes about the y axis, until the z axis coincides with the desired direction. Both rotations are in this case positive. The x axis finally points in the opposite direction to that found in the previous case (Fig 2.3), as indeed does the y axis.

These examples emphasise that the new North Pole can always be reached in one rotation, but that one then has the freedom to choose the new origin of latitude and longitude. This is usually done so that the geographic pole has longitude 0^o or some other major value - such as 180^o. The key point is that we have freedom to place the origin of latitude and longitude: so long as we make a choice, and stick to it - and use the correct transformation formulae! - then the choice does not really matter.

2.1.2 The governing equations in terms of latitude and longitude in a rotated system

The rotation of the Earth is the only influence that gives a special (or "preferred") direction in a spherical polar description. If the Earth were not rotating, we could orientate a latitude/longitude system how we liked, and the governing equations would be *formally* the same. [Transformation between different latitude/longitude systems is another matter; see Section 2.1.3.] The only equations that are *formally* changed when written in terms of rotated latitude and longitude are therefore the components of the momentum equation, and the Coriolis and centrifugal terms are the only terms that require attention. Furthermore, the centrifugal terms have been absorbed into apparent gravity, and the spherical geopotential approximation applied (see Section 1.1); hence only the Coriolis terms have to be considered.

Aside :

> *We argued in Section 1.1 that - for reasons of geometric consistency - the* horizontal *variation of apparent gravity should* ***not*** *be allowed for when the spherical*

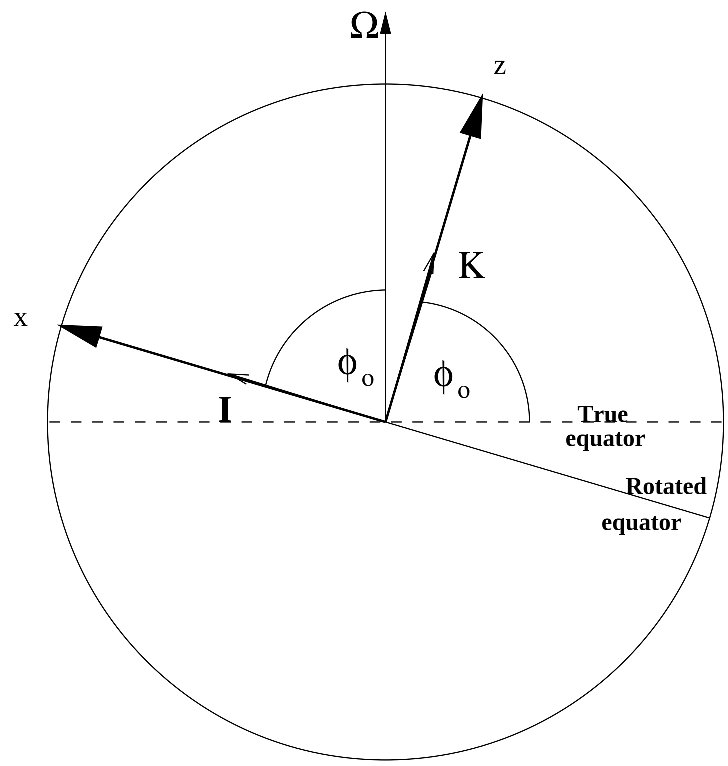

Figure 2.4: Meridional section of the sphere showing the polar axis Oz of a rotated longitude/latitude system, the Earth's rotation vector Ω, and the axis Ox which represents the zero of longitude in the rotated system. Compare Figure 2.2. See text for discussion

> *geopotential approximation is applied. It is this aspect, strictly, which enables us to conclude that only the Coriolis terms need be considered. If a spheroidal geopotential coordinate system were to be employed (again see Section 1.1), then the horizontal variation of apparent gravity would be allowable, but the scope for choice of convenient rotated systems would clearly be much reduced.*

Our problem, then, is simply to isolate the zonal, meridional and radial components of the Coriolis force $-2\mathbf{\Omega} \times \mathbf{u}$ in the chosen rotated system.

Suppose we choose to place both the rotated North Pole and the origin of latitude and longitude in the geographical Northern Hemisphere; in the terms of Section 2.1.2, this amounts to making a choice of the type shown in Figure 2.2. If the *geographical* latitude of the rotated pole is ϕ_0, then the Earth's rotation vector has latitude ϕ_0 and longitude zero (rather than π) in the rotated system; see Figure 2.4, which shows the rotated x and z axes in their (meridional) plane.

Let $\mathbf{I}$, $\mathbf{J}$, $\mathbf{K}$ be unit vectors in the directions Ox, Oy, Oz in the rotated system, as shown in Figure 2.4 - which gives the view of an observer looking along the y axis *towards* the origin O. Then

$$\mathbf{\Omega} = \mathbf{I}\Omega\cos\phi_0 + \mathbf{K}\Omega\sin\phi_0. \tag{2.1}$$

Now the velocity vector $\mathbf{u}$ may be expressed in terms of its zonal, meridional and radial components in the rotated system as

$$\mathbf{u} = (u,\ v,\ w) = u\mathbf{i} + v\mathbf{j} + w\mathbf{k}, \tag{2.2}$$

where $\mathbf{i}$, $\mathbf{j}$, $\mathbf{k}$ are unit vectors in the zonal (λ), meridional (ϕ) and radial (r) directions in the rotated system. By reference to Figure 2.5, which depicts the relative orientations of $\mathbf{i}$, $\mathbf{j}$, $\mathbf{k}$ and $\mathbf{I}$, $\mathbf{J}$, $\mathbf{K}$, it is straightforward to express $\mathbf{i}$, $\mathbf{j}$ and $\mathbf{k}$ in terms of $\mathbf{I}$, $\mathbf{J}$ and $\mathbf{K}$:

$$\mathbf{i} = -\mathbf{I}\sin\lambda + \mathbf{J}\cos\lambda, \tag{2.3}$$

$$\mathbf{j} = -\mathbf{I}\sin\phi\cos\lambda - \mathbf{J}\sin\phi\sin\lambda + \mathbf{K}\cos\phi, \tag{2.4}$$

$$\mathbf{k} = \ \ \mathbf{I}\cos\phi\cos\lambda + \mathbf{J}\cos\phi\sin\lambda + \mathbf{K}\sin\phi. \tag{2.5}$$

Also,

$$\mathbf{\Omega} = (\Omega_\lambda,\ \Omega_\phi,\ \Omega_r) = \Omega_\lambda\mathbf{i} + \Omega_\phi\mathbf{j} + \Omega_r\mathbf{k}, \tag{2.6}$$

in which, from (2.1), (2.3), (2.4) and (2.5),

$$\Omega_\lambda = \mathbf{\Omega}.\mathbf{i} = -\Omega\sin\lambda\cos\phi_0 \equiv \frac{1}{2}f_1\ , \tag{2.7}$$

$$\Omega_\phi = \mathbf{\Omega}.\mathbf{j} = \Omega\left(\cos\phi\sin\phi_0 - \sin\phi\cos\lambda\cos\phi_0\right) \equiv \frac{1}{2}f_2\ , \tag{2.8}$$

$$\Omega_z = \mathbf{\Omega}.\mathbf{k} = \Omega\left(\sin\phi\sin\phi_0 + \cos\phi\cos\lambda\cos\phi_0\right) \equiv \frac{1}{2}f_3\ . \tag{2.9}$$

Hence

$$-2\mathbf{\Omega}\times\mathbf{u} = (u\mathbf{i} + v\mathbf{j} + w\mathbf{k})\times(f_1\mathbf{i} + f_2\mathbf{j} + f_3\mathbf{k}) = (f_3v - f_2w)\,\mathbf{i} + (f_1w - f_3u)\,\mathbf{j} + (f_2u - f_1v)\,\mathbf{k}. \tag{2.10}$$

With this resolution of the Coriolis force (per unit mass), the zonal, meridional and radial components of the momentum equation in the rotated system, written in terms of λ, ϕ, r and u, v, w also defined in the rotated system, are [cf. (1.92), (1.93) and (1.97)]:

$$\frac{Du}{Dt} = -\frac{uw}{r} + \frac{uv\tan\phi}{r} + f_3v - f_2w - \frac{c_{pd}\theta_v}{r\cos\phi}\frac{\partial\Pi}{\partial\lambda} + S^u\ , \tag{2.11}$$

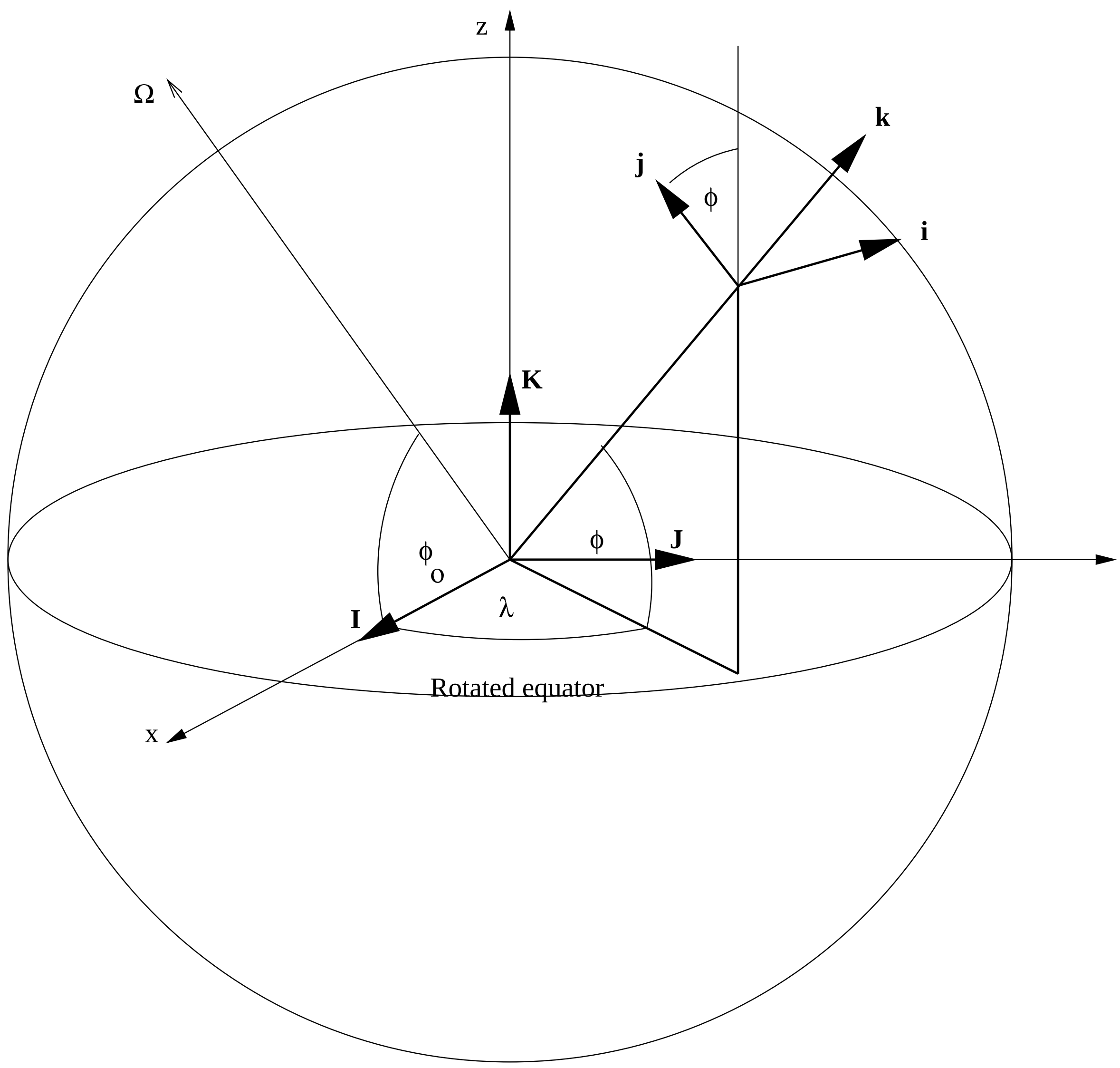

Figure 2.5: Depicting the unit vectors **I**, **J**, **K** associated with the directions Ox, Oy, Oz in the rotated system, and the unit vectors **i**, **j**, **k** associated with the zonal, meridional and radial directions at a point P having longitude λ and latitude ϕ in the rotated system.

$$\frac{Dv}{Dt} = -\frac{vw}{r} - \frac{u^2 \tan\phi}{r} + f_1 w - f_3 u - \frac{c_{pd}\theta_v}{r}\frac{\partial \Pi}{\partial \phi} + S^v \, , \tag{2.12}$$

$$\frac{Dw}{Dt} = \frac{(u^2+v^2)}{r} + f_2 u - f_1 v - g\left(1 + q_{cl} + q_{cf}\right) - c_{pd}\theta_v \frac{\partial \Pi}{\partial r} + S^w \, . \tag{2.13}$$

Here (from (2.7) - (2.9)):

$$f_1 = -2\Omega \sin\lambda \cos\phi_0 \, , \tag{2.14}$$

$$f_2 = 2\Omega\left(\cos\phi \sin\phi_0 - \sin\phi\cos\lambda\cos\phi_0\right) \, , \tag{2.15}$$

$$f_3 = 2\Omega\left(\sin\phi \sin\phi_0 + \cos\phi\cos\lambda\cos\phi_0\right) \, . \tag{2.16}$$

[Notice that, as expected, $f_1 = 0$, $f_2 = 2\Omega\cos\phi$, $f_3 = 2\Omega\sin\phi$ when $\phi_o = 90^o$.]

Aside :

It is straightforward to repeat this analysis for the choice of rotated system in which the North Pole remains in the Northern Hemisphere but the origin of latitude and longitude is in the Southern Hemisphere at the antipodean point to that chosen above. This corresponds to a choice of the type illustrated in Figure 2.3; see also Figure 2.6, which depicts the second rotation in the Oxz plane as seen by an observer looking along the rotated y axis towards O. *The Earth's rotation vector still has latitude ϕ_0 in the rotated system, but its longitude is now π (see Figure 2.6), and in terms of this system's unit vectors*

$$\Omega = -\mathbf{I}\Omega\cos\phi_0 + \mathbf{K}\Omega\sin\phi_0. \tag{2.17}$$

The expressions for the unit vectors $\boldsymbol{i}$, $\boldsymbol{j}$, $\boldsymbol{k}$ *are formally unchanged, and we find*

$$f_1 = 2\Omega \sin\lambda \cos\phi_0 \, , \tag{2.18}$$

$$f_2 = 2\Omega\left(\cos\phi \sin\phi_0 + \sin\phi\cos\lambda\cos\phi_0\right) \, , \tag{2.19}$$

$$f_3 = 2\Omega\left(\sin\phi \sin\phi_0 - \cos\phi\cos\lambda\cos\phi_0\right) \, . \tag{2.20}$$

Eqs (2.18) - (2.20) *are slightly more convenient than* (2.14) - (2.16) *in that each leading r.h.s. term has positive sign. The relationship of* (2.18) - (2.20) *to* (2.14) - (2.16) *is immediately obvious if we note that the two systems transform into one another as $\phi \leftrightarrow \phi$, $\lambda \leftrightarrow \lambda + \pi$, which corresponds to a sign change of both* $\sin\lambda$ *and* $\cos\lambda$ *but to no other modification.*

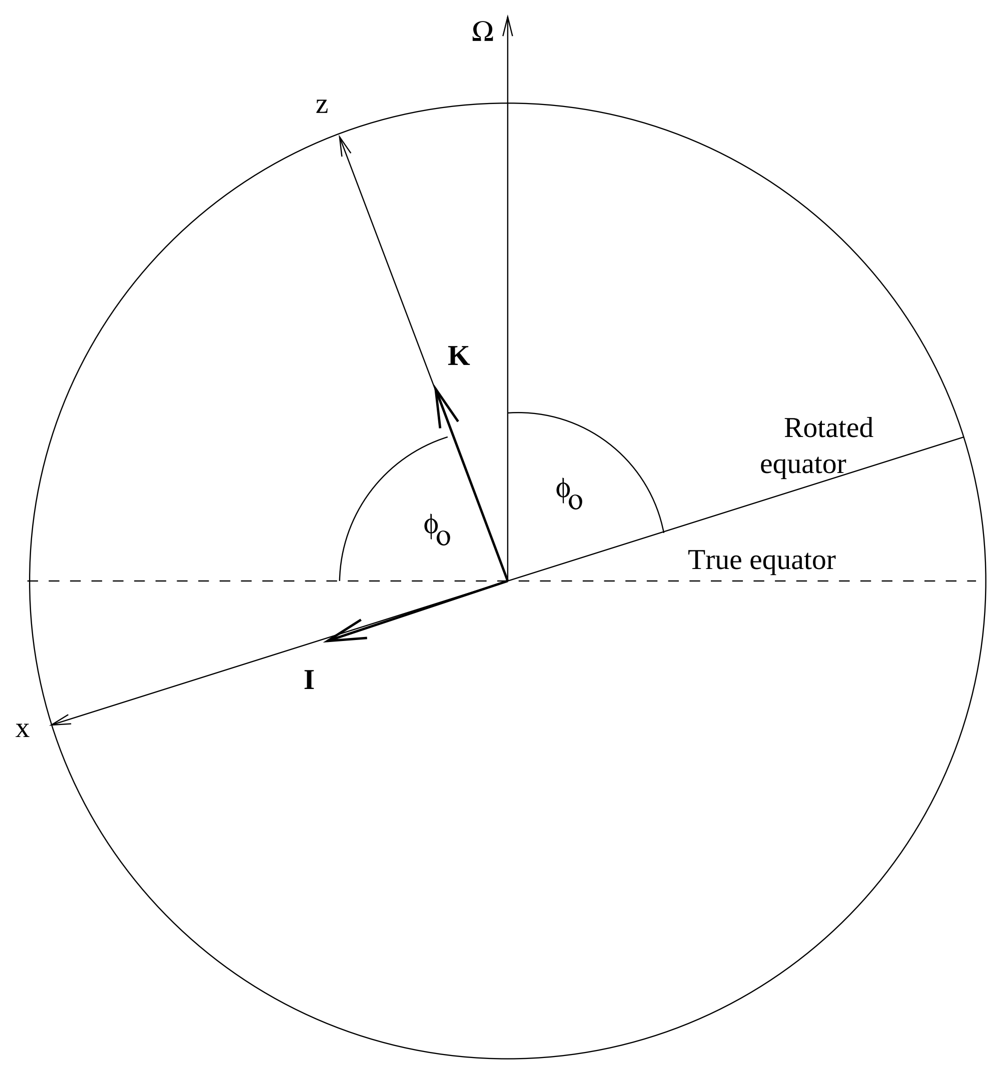

Figure 2.6: Meridional section of the sphere showing the polar axis Oz of a rotated longitude/latitude system, the Earth's rotation vector Ω and the axis Ox which represents the zero of longitude in the rotated system. Compare Figure 2.3. See text for discussion.

2.1.3 Transformation between the geographical and rotated systems

To derive the transformation formulae we follow at first the method of McDonald & Bates (1989), who introduced an "auxiliary spherical coordinate system" to resolve difficulties which occurred near the poles in the primary spherical coordinate system of a semi-Lagrangian, shallow water model. [Rotated spherical systems have been used for various purposes in several meteorological studies over the past two decades; the paper by McDonald & Bates (1989) is one of the few which gives a detailed analytical account of the procedure used.]

Consider an arbitrary point P whose geographical longitude and latitude are $(\lambda_A,\ \phi_A)$ - the subscripts $_A$ may be construed as indicating "actual" longitude and latitude. Suppose that the longitude and latitude of P in the rotated system are $(\lambda,\ \phi)$, and that the rotated system is defined by: (i) the location $(\lambda_I,\ \phi_J)$ in the "actual" system of its *origin* of longitude and latitude $(\lambda,\ \phi)\ =\ (0,\ 0)$; and (ii) the decision that its polar axis should lie in the meridian plane $\lambda\ = \lambda_I$ of the "actual" longitude/latitude system. See Figure 2.7. The decision (ii) simplifies things a lot. If we associate Cartesian coordinate systems with the actual and rotated systems in the usual way, we can obtain the latter from the former by two elementary rotations, as indicated by the arrows on Figure 2.7: first, a rotation through λ_I about the z axis; second, a rotation through ϕ_J about the y axis. [For current purposes we take λ_I and ϕ_J to be positive when the associated rotations are in the directions shown by the arrows on Figure 2.7. This unconventional choice is convenient because it means that $\phi_J > 0$ corresponds to the origin of the rotated longitude/latitude system being in the Northern Hemisphere of the geographical system.]

We must be more precise about the associated Cartesian coordinate systems in order to proceed. Their origins lie at O, the centre of the Earth. With the geographical system $(\lambda_A,\ \phi_A)$ we associate the Cartesian system $Ox_Ay_Az_A$ having unit vectors $(\mathbf{I}_A,\ \mathbf{J}_A,\ \mathbf{K}_A)$, where $\mathbf{I}_A$ points from O towards $(\lambda_A,\ \phi_A) = (0,\ 0)$, $\mathbf{J}_A$ from O towards $(\lambda_A,\ \phi_A) = \left(\frac{\pi}{2},\ 0\right)$, and $\mathbf{K}_A$ towards the North Pole $\left(\phi_A = \frac{\pi}{2}\right)$. The corresponding Cartesian system $Oxyz$ associated with the rotated coordinates $(\lambda,\ \phi)$ is obtained by carrying out two rotations of the $Ox_Ay_Az_A$ system: first, the system $Ox_Ay_Az_A$ is rotated through the angle λ_I about $\mathbf{K}_A$, giving an intermediate system $O\widehat{x}\widehat{y}\widehat{z}$ having unit vectors $\left(\widehat{\mathbf{I}},\ \widehat{\mathbf{J}},\ \widehat{\mathbf{K}}\right)$; second, the intermediate system is rotated about $\widehat{\mathbf{J}}$ through the angle ϕ_J (as shown in Figure 2.7) giving the new system $(\mathbf{I},\ \mathbf{J},\ \mathbf{K})$.

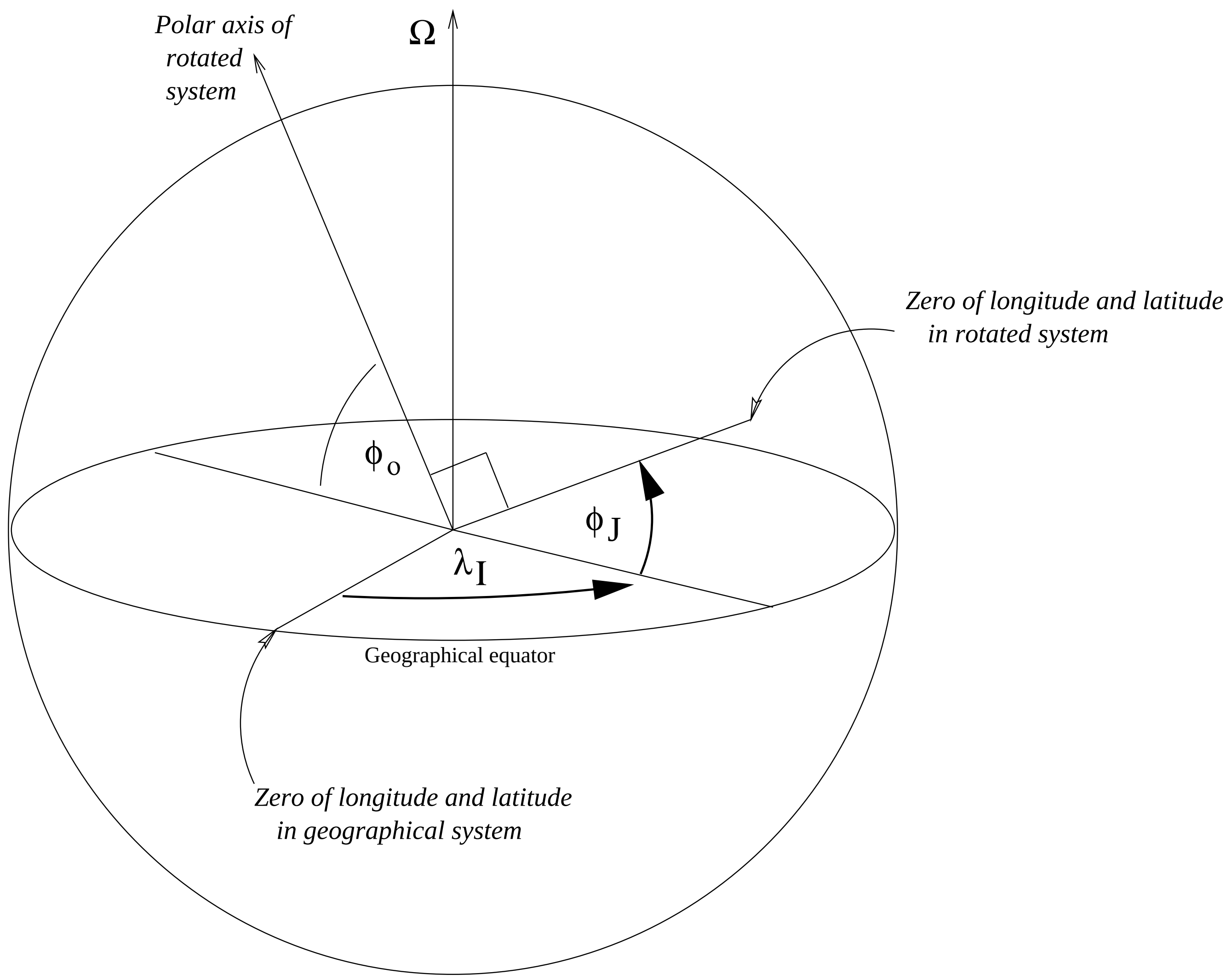

Figure 2.7: The rotated coordinate system is obtained by two successive rotations of the geographical system: the origin of longitude and latitude is moved to geographical longitude λ_I in the first rotation, and then to geographical latitude ϕ_J (with no change of geographical longitude) in the second rotation. In the case shown, $\phi_J > 0$, the geographical longitude of the rotated polar axis is $\lambda_o = \lambda_I + \pi$, and its geographical latitude is $\phi_o = \frac{\pi}{2} - \phi_J$; but in cases having $\phi_J < 0$ (rotated origin in the Southern geographical hemisphere), $\lambda_o = \lambda_I$ and $\phi_o = \frac{\pi}{2} + \phi_J$.

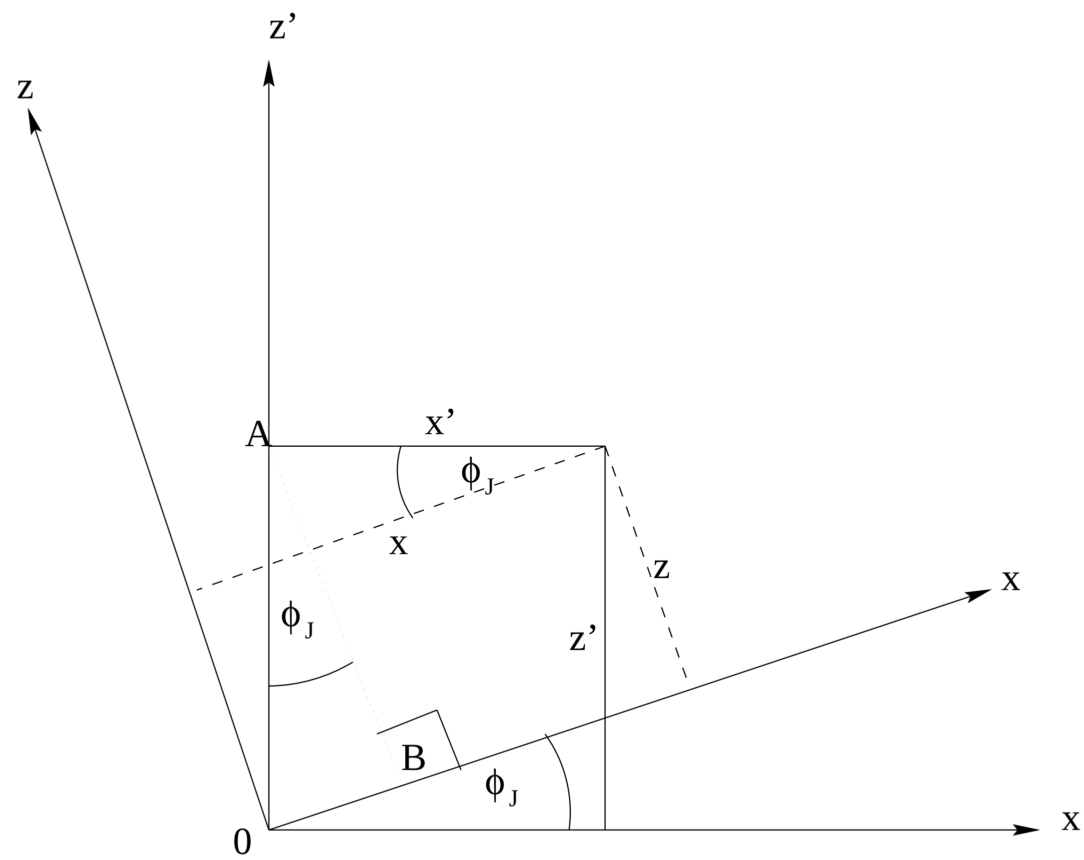

Figure 2.8: Construct AB perpendicular to Ox as shown. Then, immediately:
$x = \widehat{x}\cos\phi_J + \widehat{z}\sin\phi_J$; and $z = \widehat{z}\cos\phi_J - \widehat{x}\sin\phi_J$.
[The quantities shown as x' and z' in the diagram are to be understood as $\widehat{x}$ and $\widehat{z}$ as in the text and caption.]

The associated Cartesian coordinates of P are related to its longitude and latitude in the geographical system by

$$x_A = a\cos\phi_A\cos\lambda_A\,, \qquad y_A = a\cos\phi_A\sin\lambda_A\,, \qquad z_A = a\sin\phi_A. \tag{2.21}$$

Similar expressions, for $\widehat{x}$, $\widehat{y}$, $\widehat{z}$ in terms of $\widehat{\lambda}$,$\widehat{\phi}$ apply in the intermediate system; and since $\left(\widehat{\lambda},\,\widehat{\phi}\right) = (\lambda_A - \lambda_I,\,\phi_A)$ we can immediately write

$$\widehat{x} = a\cos\phi_A\cos\left(\lambda_A - \lambda_I\right)\,, \qquad \widehat{y} = a\cos\phi_A\sin\left(\lambda_A - \lambda_I\right)\,, \qquad \widehat{z} = a\sin\phi_A. \tag{2.22}$$

The second rotation is made in the $O\widehat{x}\widehat{z}$ plane, and gives (see Figure 2.8)

$$x = \widehat{x}\cos\phi_J + \widehat{z}\sin\phi_J\,, \qquad y = \widehat{y}\,, \qquad z = \widehat{z}\cos\phi_J - \widehat{x}\sin\phi_J. \tag{2.23}$$

Now x, y and z are related to λ and ϕ by expressions having the same form as that of (2.21); and (2.22) enables us to substitute in (2.23) for the intermediate coordinates $\widehat{x}$, $\widehat{y}$, $\widehat{z}$

in terms of the geographical longitude (λ_A) and latitude (ϕ_A). Hence we arrive at the transformation formulae giving the latitude and longitude in the rotated system in terms of the geographical latitude and longitude:

$$\left(\frac{x}{a}=\right) \qquad \cos\phi\cos\lambda = \cos\phi_A\cos\left(\lambda_A-\lambda_I\right)\cos\phi_J + \sin\phi_A\sin\phi_J, \tag{2.24}$$

$$\left(\frac{y}{a}=\right) \qquad \cos\phi\sin\lambda = \cos\phi_A\sin\left(\lambda_A-\lambda_I\right), \tag{2.25}$$

$$\left(\frac{z}{a}=\right) \qquad \sin\phi = \sin\phi_A\cos\phi_J - \cos\phi_A\cos\left(\lambda_A-\lambda_I\right)\sin\phi_J. \tag{2.26}$$

The reverse formulae, readily obtained from (2.24) - (2.26), are:

$$\left(\frac{x_A}{a}=\right) \qquad \cos\phi_A\cos\left(\lambda_A-\lambda_I\right) = \cos\phi\cos\lambda\cos\phi_J - \sin\phi\sin\phi_J, \tag{2.27}$$

$$\left(\frac{y_A}{a}=\right) \qquad \cos\phi_A\sin\left(\lambda_A-\lambda_I\right) = \cos\phi\sin\lambda, \tag{2.28}$$

$$\left(\frac{z_A}{a}=\right) \qquad \sin\phi_A = \sin\phi\cos\phi_J + \cos\phi\cos\lambda\sin\phi_J. \tag{2.29}$$

Both the forward formulae (2.24) - (2.26) and thereverseformulae (2.27) - (2.29) must be used with care. Equation (2.26) gives ϕ unambiguously in terms of ϕ_A and λ_A; then (2.24) and (2.25) give $\cos\lambda$ and $\sin\lambda$, from which λ may be evaluated in the correct quadrant. Similar remarks apply to (2.27) - (2.29).

Relationships between the horizontal velocity components in our two systems may be derived by taking the material derivatives of (2.24) and (2.25). Upon noting that

$$u_A = a\cos\phi_A\frac{D\lambda_A}{Dt}, \quad v_A = a\frac{D\phi_A}{Dt}, \tag{2.30}$$

$$u\ = a\cos\phi\,\frac{D\lambda}{Dt}, \quad v\ =\ a\frac{D\phi}{Dt} \tag{2.31}$$

material differentiation of (2.26) leads in a few lines of algebra to

$$v\cos\phi = u_A\sin\left(\lambda_A-\lambda_I\right)\sin\phi_J + v_A\left[\cos\phi_A\cos\phi_J + \sin\phi_A\cos\left(\lambda_A-\lambda_I\right)\sin\phi_J\right]. \tag{2.32}$$

Finding an expression for $u\cos\phi$ is harder. Material differentiation of (2.24) and (2.25) gives

$$u\sin\lambda + v\sin\phi\cos\lambda = u_A\sin\left(\lambda_A-\lambda_I\right)\cos\phi_J + v_A\left[\sin\phi_A\cos\left(\lambda_A-\lambda_I\right)\cos\phi_J - \cos\phi_A\sin\phi_J\right], \tag{2.33}$$

$$u\cos\lambda - v\sin\phi\sin\lambda = u_A\cos\left(\lambda_A-\lambda_I\right) - v_A\sin\phi_A\sin\left(\lambda_A-\lambda_I\right). \tag{2.34}$$

By multiplying (2.33) by $\cos\phi\sin\lambda$, (2.34) by $\cos\phi\cos\lambda$, adding the results and using (2.24) and (2.25) to re-express $\cos\phi\cos\lambda$, and $\cos\phi\sin\lambda$, one obtains

$$u\cos\phi = u_A\left[\cos\phi_A\cos\phi_J + \sin\phi_A\cos\left(\lambda_A - \lambda_I\right)\sin\phi_J\right] - v_A\sin\left(\lambda_A - \lambda_I\right)\sin\phi_J. \tag{2.35}$$

Equations (2.35) and (2.32) may be writtenconcisely as

$$u = u_A\cos\left(ROT\right) + v_A\sin\left(ROT\right), \tag{2.36}$$

$$v = v_A\cos\left(ROT\right) - u_A\sin\left(ROT\right), \tag{2.37}$$

in which

$$\cos\left(ROT\right)\cos\phi = \cos\phi_A\cos\phi_J + \sin\phi_A\cos\left(\lambda_A - \lambda_I\right)\sin\phi_J, \tag{2.38}$$

$$\sin\left(ROT\right)\cos\phi = -\sin\left(\lambda_A - \lambda_I\right)\sin\phi_J. \tag{2.39}$$

From the form of (2.36) and (2.37), it is clear that, at each location $(\lambda,\ \phi)$, ROT is the angle between lines of latitude in the geographical and rotated systems; see (2.23) and Figure 2.8. ROT is positive when lines of constant latitude in the λ, ϕ system are orientated anticlockwise with respect to those in the $\lambda_A,\ \phi_A$ system.

Aside :

Strictly, it is not quite clear that ROT is the angle between lines of latitude in the two systems. All we have done in writing (2.35) *and* (2.32) *as* (2.36) *and* (2.37) *is to* define *quantities* $\cos\left(ROT\right)$ *and* $\sin\left(ROT\right)$ *by* (2.38) *and* (2.39)*, but we have not demonstrated that they are the cosine and sine of a real angle. In other words, we have noted that* $(u_A,\ v_A)$ *is transformed to* $(u,\ v)$ *by the operation of a matrix having equal diagonal elements and off-diagonal elements of equal magnitude and opposite sign, but we have not shown that this matrix represents a real rotation. Given the physical context, it would be astonishing if it did not, but some work is needed to demonstrate the point analytically: form* $\left(\cos^2\left(ROT\right) + \sin^2\left(ROT\right)\right)\cos^2\phi$ *from* (2.38) *and* (2.39) *and manipulate (using* (2.27) - (2.29)*) to show that - as the notation correctly but presumptuously suggests -* $\cos^2\left(ROT\right) + \sin^2\left(ROT\right) = 1$*; observe from their definitions* (2.38) *and* (2.39) *that both* $\cos\left(ROT\right)$ *and* $\sin\left(ROT\right)$ *are real quantities, and deduce that both* $\cos\left(ROT\right)$ *and* $\sin\left(ROT\right)$ *must have absolute value unity at most; the conclusion that* $\cos\left(ROT\right)$ *and* $\sin\left(ROT\right)$ *are indeed the functions they pretend to be is then almost unavoidable.*

Equations (2.36) and (2.37) give the velocity components in the rotated coordinate system in terms of the velocity components in the geographical system, and may be regarded as forward formulae. The reverse formulae are simply

$$u_A = u\cos(ROT) - v\sin(ROT)\,, \tag{2.40}$$

$$v_A = v\cos(ROT) + u\sin(ROT)\,. \tag{2.41}$$

Various alternative forms of (2.38) and (2.39) may be derived. Versions featuring "actual" latitude on the left sides and rotated longitude and latitude on the right sides are

$$\cos(ROT)\cos\phi_A = \cos\phi\cos\phi_J - \sin\phi\cos\lambda\sin\phi_J, \tag{2.42}$$

$$\sin(ROT)\cos\phi_A = -\sin\lambda\sin\phi_J. \tag{2.43}$$

[Equation (2.43) follows immediately from (2.39) and (2.25). Derivation of (2.42) from (2.38) involves multiplication by $\cos\phi_A$, use of the reverse relations (2.28) and (2.29) , and a considerable amount of manipulation.] A further version of (2.38) may be obtained by noting that (from $\cos(\lambda_A - \lambda_I)\times$(2.24) + $\sin(\lambda_A - \lambda_I)\times$(2.25))

$$\cos\phi\,[\cos\lambda\cos(\lambda_A - \lambda_I) + \sin\lambda\sin(\lambda_A - \lambda_I)\cos\phi_J] = \cos\phi_A\cos\phi_J + \sin\phi_A\cos(\lambda_A - \lambda_I)\sin\phi_J. \tag{2.44}$$

Hence (2.38) may be written as

$$\cos(ROT) = \cos\lambda\cos(\lambda_A - \lambda_I) + \sin\lambda\sin(\lambda_A - \lambda_I)\cos\phi_J. \tag{2.45}$$

Although (2.45) features both geographical and rotated longitude on its right side, it has the advantage of giving $\cos(ROT)$ as the sum of two product terms (whereas (2.38) and (2.42) bothgive $\cos(ROT)$ only after a division).

Aside :

> *In view of the "forward" and "reverse" formulae previously obtained for the coordinates and velocity components, one might seek expressions for* $\cos(ROT)$ *and* $\sin(ROT)$ *which do not involve the rotated longitude and latitude, and alternative forms which do not involve the geographical longitude and latitude. It appears, however, that* (2.45) *and* (2.39) *or* (2.43)*, which are all mixed forms, are the simplest. This may reflect the fact that* ROT *describes the local physical disposition*

of the rotated and geographical systems with respect to one another, rather than relating components evaluated in one system to the corresponding values in the other; it expresses a mutual relationship, not a transformation. Expressions for $\cos(ROT)$ *and* $\sin(ROT)$ *solely in terms of one set of coordinates can be derived by use of the appropriate forward or reverse formulae to eliminate the other set, but they are complicated. Some simplification may be achieved by working in terms of* $u_A \cos\phi_A$, $v_A \cos\phi_A$, $u\cos\phi$, *and* $v\cos\phi$ *rather than in terms of* u_A, v_A, u *and* v*; the former are well known to have better transformation properties than the latter. Further investigation of these issues is desirable.*

Our chosen expressions for $\cos(ROT)$ and $\sin(ROT)$ are (2.45) and a form of (2.39):

$$\cos(ROT) = \cos\lambda\cos(\lambda_A - \lambda_I) + \sin\lambda\sin(\lambda_A - \lambda_I)\cos\phi_J, \tag{2.46}$$

$$\sin(ROT) = -\frac{\sin(\lambda_A - \lambda_I)\sin\phi_J}{\cos\phi}. \tag{2.47}$$

We now apply these results in our rotated pole problem, noting two possible choices of relationship between the location of the pole and the systems discussed above. In each case the longitude and latitude of the rotated pole are λ_0 and ϕ_0.

Choice 1

This follows Figure 2.7 as drawn.

◇ The first rotation puts the new pole in longitude π; thus $\lambda_I = \lambda_0 - \pi$.

◇ The second rotation is through an angle $\phi_J = \left(\frac{\pi}{2} - \phi_0\right)$.

Hence $\cos(\lambda_A - \lambda_I) \rightarrow -\cos(\lambda_A - \lambda_0)$, $\sin(\lambda_A - \lambda_I) \rightarrow -\sin(\lambda_A - \lambda_0)$, $\cos\phi_J \rightarrow \sin\phi_0$, $\sin\phi_J \rightarrow \cos\phi_0$, and (2.46), (2.47) become

$$\cos(ROT) = -\cos\lambda\cos(\lambda_A - \lambda_0) - \sin\lambda\sin(\lambda_A - \lambda_0)\sin\phi_0, \tag{2.48}$$

$$\sin(ROT) = \frac{\sin(\lambda_A - \lambda_0)\cos\phi_0}{\cos\phi}. \tag{2.49}$$

Choice 2

This does not follow Figure 2.7 as drawn. Rather, ϕ_J is negative; i.e. the origin of rotated longitude and latitude lies in the Southern hemisphere of the geographical system.

◇ The first rotation puts the new pole in longitude 0; thus $\lambda_I = \lambda_0$.

◇ The second rotation is through an angle $\phi_J = \phi_0 - \frac{\pi}{2}$ (so that the new North Pole is at geographical latitude ϕ_0).

Hence $\cos\phi_J \;\rightarrow \sin\phi_0$, $\sin\phi_J \;\rightarrow -\cos\phi_0$ and (2.46), (2.47) become

$$\cos(ROT) = \cos\lambda\cos(\lambda_A - \lambda_0) + \sin\lambda\sin(\lambda_A - \lambda_0)\sin\phi_0, \tag{2.50}$$

$$\sin(ROT) = \frac{\sin(\lambda_A - \lambda_0)\cos\phi_0}{\cos\phi}. \tag{2.51}$$

In conclusion it should be emphasised that the question of transformation between the geographical and rotated systems does not affect the operation of the model during time integration. As we showed in Section 2.1.2, the equations may be written solely in terms of velocity components, latitude and longitude in the rotated system, with the geographical latitude of the rotated pole appearing as a parameter in the Coriolis terms; it is only necessary to transform between the geographical and rotated systems at the start of an integration and when output fields are required.

2.2 Transformation to the terrain-following η system

The vertical coordinate η is chosen so that it is zero at the Earth's surface $r_S = r_S(\lambda,\phi)$ and unity at $r_T = r_T(\lambda,\phi)$ $(> r_S(\lambda,\phi))$. (Currently r_T = constant in the New Dynamics.) The simplest choice which satisfies these requirements is

$$\eta \equiv \frac{r - r_S}{r_T - r_S} = \frac{z - z_S}{z_T - z_S}, \tag{2.52}$$

where z represents height above mean sea level and, in terms of the Earth's mean radius, a, the radius $r = a + z$. Other choices are discussed in Appendix B, including the current preferred one (see Section B.4). In the treatment here, we assume only that η is a smooth, differentiable function of r and that

$$\eta(z_S) = 0, \quad \eta(z_T) = 1, \quad \frac{\partial\eta}{\partial r} > 0. \tag{2.53}$$

The third requirement in (2.53) ensures that the transformation $r \leftrightarrow \eta$ is 1:1. [Note that we do not assume $\left.\frac{\partial r}{\partial t}\right|_\eta = 0$, although this condition is obeyed by (2.52) and in the New Dynamics; our treatment covers $\left.\frac{\partial r}{\partial t}\right|_\eta = 0$ as a particular case.]

The transformation of the governing equations from r to η coordinates is accomplished by applying two elementary results:

$$\left.\frac{\partial}{\partial r}\right|_{\lambda,\phi,t} = \frac{\partial\eta}{\partial r}\left.\frac{\partial}{\partial\eta}\right|_{\lambda,\phi,t}, \tag{2.54}$$

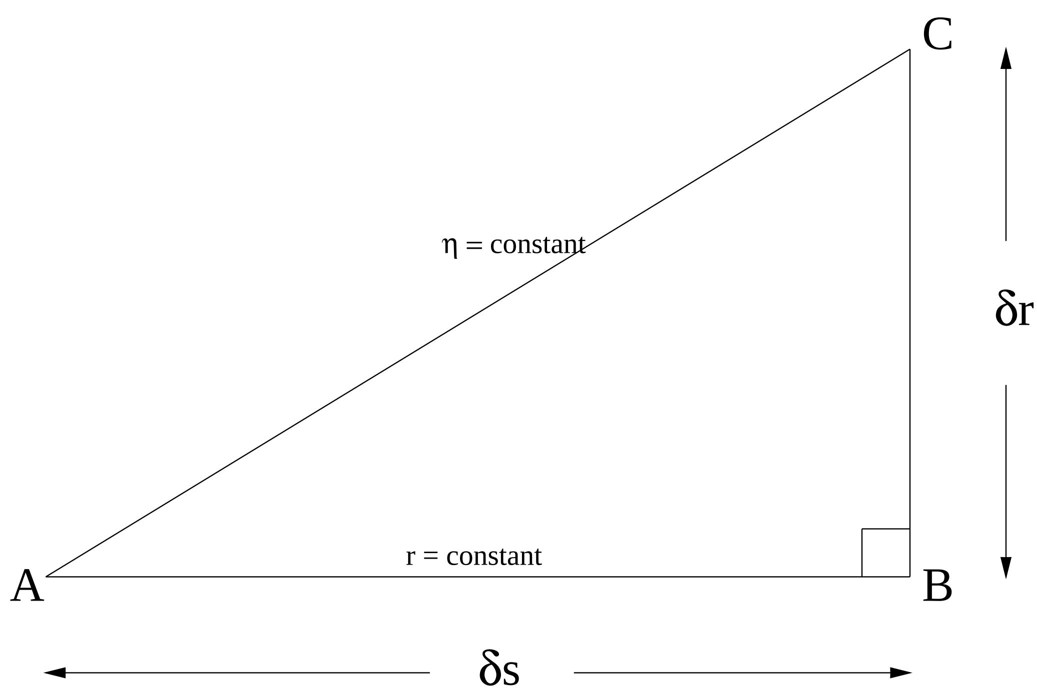

Figure 2.9: Showing a local vertical section (containing the direction s): BC is vertical, AB is horizontal (r =constant) and η = constant on AC.

and, for $s = \lambda$, ϕ or t :

$$\left.\frac{\partial}{\partial s}\right|_r = \left.\frac{\partial}{\partial s}\right|_\eta - \left.\frac{\partial r}{\partial s}\right|_\eta \left.\frac{\partial}{\partial r}\right|_{\lambda,\phi,t} . \tag{2.55}$$

Result (2.54) represents a simple change of variable in the vertical. Result (2.55) is readily derived by considering the change of some (differentiable) quantity Q along a surface of constant η in the direction s ; referring to Figure 2.9,

$$\delta Q_{AC} = \delta Q_{AB} + \delta Q_{BC} = \delta s \left.\frac{\partial Q}{\partial s}\right|_r + \delta r \left.\frac{\partial Q}{\partial r}\right|_{\lambda,\phi,t} \Rightarrow \left.\frac{\partial Q}{\partial s}\right|_\eta = \left.\frac{\partial Q}{\partial s}\right|_r + \left.\frac{\partial r}{\partial s}\right|_\eta \left.\frac{\partial Q}{\partial r}\right|_{\lambda,\phi,t} . \tag{2.56}$$

For brevity, the explicit statements of constant λ, ϕ, t in the r and η derivatives will be omitted when (2.54) and (2.55) are used.

Since $Q = Q(\lambda, \phi, \eta, t)$ in the η system, the material derivative can be written as

$$\frac{DQ}{Dt} = \left.\frac{\partial Q}{\partial t}\right|_\eta + \frac{u}{r\cos\phi}\left.\frac{\partial Q}{\partial \lambda}\right|_\eta + \frac{v}{r}\left.\frac{\partial Q}{\partial \phi}\right|_\eta + \dot{\eta}\frac{\partial Q}{\partial \eta}. \tag{2.57}$$

Aside :

Any doubt about the validity of (2.57) *and the interpretation of its individual terms may be dispelled by a direct proof using* (2.54) *and* (2.55), *starting with* *expression (1.84) for the material derivative in* r *coordinates:*

$$\frac{DQ}{Dt} = \left.\frac{\partial Q}{\partial t}\right|_r + \frac{u}{r\cos\phi}\left.\frac{\partial Q}{\partial \lambda}\right|_r + \frac{v}{r}\left.\frac{\partial Q}{\partial \phi}\right|_r + w\frac{\partial Q}{\partial r}. \tag{2.58}$$

Use of (2.55) *enables* (2.58) *to be cast as*

$$\frac{DQ}{Dt} = \left.\frac{\partial Q}{\partial t}\right|_\eta + \frac{u}{r\cos\phi}\left.\frac{\partial Q}{\partial \lambda}\right|_\eta + \frac{v}{r}\left.\frac{\partial Q}{\partial \phi}\right|_\eta \tag{2.59}$$

$$+\frac{\partial Q}{\partial r}\left[w - \left.\frac{\partial r}{\partial t}\right|_\eta - \frac{u}{r\cos\phi}\left.\frac{\partial r}{\partial \lambda}\right|_\eta - \frac{v}{r}\left.\frac{\partial r}{\partial \phi}\right|_\eta\right]. \tag{2.60}$$

Setting $Q = \eta$ *in* (2.60) *shows that*

$$\dot{\eta} \equiv \frac{D\eta}{Dt} = \frac{\partial \eta}{\partial r}\left[w - \left.\frac{\partial r}{\partial t}\right|_\eta - \frac{u}{r\cos\phi}\left.\frac{\partial r}{\partial \lambda}\right|_\eta - \frac{v}{r}\left.\frac{\partial r}{\partial \phi}\right|_\eta\right]. \tag{2.61}$$

Hence(noting that $\partial\eta/\partial r \neq 0$*),* (2.60) *can be written as*

$$\frac{DQ}{Dt} = \left.\frac{\partial Q}{\partial t}\right|_\eta + \frac{u}{r\cos\phi}\left.\frac{\partial Q}{\partial \lambda}\right|_\eta + \frac{v}{r}\left.\frac{\partial Q}{\partial \phi}\right|_\eta + \dot{\eta}\frac{\partial Q}{\partial r}\frac{\partial r}{\partial \eta}. \tag{2.62}$$

But, from (2.54), $\frac{\partial Q}{\partial r} = \frac{\partial \eta}{\partial r}\frac{\partial Q}{\partial \eta}$ *, so* (2.62) *reduces to* (2.57).

The velocity components u and v in (2.57) are the usual horizontal components; they are *not* the components of the velocity parallel to constant η surfaces. The derivatives w.r.t. t, λ and ϕ in (2.57) are taken in constant η surfaces, so that the increments of Q are those seen as one moves in the relevant direction whilst constrained to remain on a constant η surface; the relevant distances are those in the horizontal, *not* those measured within η surfaces. Also, $\partial/\partial\eta$ represents differentiation in the vertical, *not* perpendicular to surfaces of constant η. Representations in terms of velocity components and gradients within and perpendicular to η surfaces can of course be developed (see, for example, Gal-Chen & Somerville (1975)), but they are generally more complicated, and consequently more difficult to handle.

We now have all the results needed to transform the momentum component equations, the thermodynamic equation and the moisture equations to η coordinates. The material derivatives are written as in (2.57), and the pressure (Exner function) gradient terms in the momentum component equations are transformed using (2.54) and (2.55). For example:

$$\left.\frac{\partial \Pi}{\partial \lambda}\right|_r = \left.\frac{\partial \Pi}{\partial \lambda}\right|_\eta - \frac{\partial \Pi}{\partial r}\left.\frac{\partial r}{\partial \lambda}\right|_\eta .$$

Section 2.3 gives the relevant equations in an abbreviated notation in which all local time and "horizontal" derivatives are assumed to be taken at constant η.

The continuity equation remains to be considered. It is convenient to start with the form

$$\frac{D}{Dt}\left(\rho_y r^2 \cos\phi\right) + \rho_y r^2 \cos\phi \left\{ \left.\frac{\partial\dot\lambda}{\partial\lambda}\right|_r + \left.\frac{\partial\dot\phi}{\partial\phi}\right|_r + \frac{\partial\dot r}{\partial r} \right\} = 0. \tag{2.63}$$

Eq (2.63) is (1.98) written in terms of $\dot\lambda = u/r\cos\phi$ and $\dot\phi = v/r$; it corresponds to (1.27) with $\rho \to \rho_y$ (the dry-air adjustment described in Section 1.5). From (2.54) and (2.55) we have

$$\left.\frac{\partial\dot\lambda}{\partial\lambda}\right|_r = \left.\frac{\partial\dot\lambda}{\partial\lambda}\right|_\eta - \left.\frac{\partial r}{\partial\lambda}\right|_\eta \left.\frac{\partial\dot\lambda}{\partial r}\right|, \tag{2.64}$$

$$\left.\frac{\partial\dot\phi}{\partial\phi}\right|_r = \left.\frac{\partial\dot\phi}{\partial\phi}\right|_\eta - \left.\frac{\partial r}{\partial\phi}\right|_\eta \left.\frac{\partial\dot\phi}{\partial r}\right|, \tag{2.65}$$

and

$$\frac{\partial\dot r}{\partial r} = \frac{\partial w}{\partial\eta}\frac{\partial\eta}{\partial r} = \frac{\partial\eta}{\partial r}\frac{\partial}{\partial\eta}\left[\left.\frac{\partial r}{\partial t}\right|_\eta + \dot\lambda\left.\frac{\partial r}{\partial\lambda}\right|_\eta + \dot\phi\left.\frac{\partial r}{\partial\phi}\right|_\eta + \dot\eta\frac{\partial r}{\partial\eta}\right],$$

i.e.

$$\frac{\partial\dot r}{\partial r} = \frac{\partial\eta}{\partial r}\frac{D}{Dt}\left(\frac{\partial r}{\partial\eta}\right) + \frac{\partial\dot\lambda}{\partial r}\left.\frac{\partial r}{\partial\lambda}\right|_\eta + \frac{\partial\dot\phi}{\partial r}\left.\frac{\partial r}{\partial\phi}\right|_\eta + \left.\frac{\partial\dot\eta}{\partial\eta}\right|. \tag{2.66}$$

Add (2.64), (2.65) and (2.66):

$$\left.\frac{\partial\dot\lambda}{\partial\lambda}\right|_r + \left.\frac{\partial\dot\phi}{\partial\phi}\right|_r + \frac{\partial\dot r}{\partial r} = \frac{\partial\eta}{\partial r}\frac{D}{Dt}\left(\frac{\partial r}{\partial\eta}\right) + \left.\frac{\partial\dot\lambda}{\partial\lambda}\right|_\eta + \left.\frac{\partial\dot\phi}{\partial\phi}\right|_\eta + \frac{\partial\dot\eta}{\partial\eta}. \tag{2.67}$$

Put (2.67) in (2.63) to obtain

$$\frac{D}{Dt}\left(\rho_y r^2 \cos\phi\right) + \rho_y r^2 \cos\phi \left\{ \frac{\partial\eta}{\partial r}\frac{D}{Dt}\left(\frac{\partial r}{\partial\eta}\right) + \left.\frac{\partial\dot\lambda}{\partial\lambda}\right|_\eta + \left.\frac{\partial\dot\phi}{\partial\phi}\right|_\eta + \frac{\partial\dot\eta}{\partial\eta} \right\} = 0. \tag{2.68}$$

Multiply (2.68) by $\partial r/\partial\eta$, re-arrange, and restore u and v:

$$\frac{D}{Dt}\left(\rho_y r^2 \cos\phi\frac{\partial r}{\partial\eta}\right) + \rho_y r^2 \cos\phi\frac{\partial r}{\partial\eta} \left\{ \left.\frac{\partial}{\partial\lambda}\left(\frac{u}{r\cos\phi}\right)\right|_\eta + \left.\frac{\partial}{\partial\phi}\left(\frac{v}{r}\right)\right|_\eta + \frac{\partial\dot\eta}{\partial\eta} \right\} = 0. \tag{2.69}$$

This is the η-coordinate continuity equation in perhaps its most compact form (see the discussion in Section 1.2 and cf. (2.63)). An alternative form is

$$\frac{D}{Dt}\left(\rho_y r^2 \frac{\partial r}{\partial\eta}\right) + \rho_y r^2 \frac{\partial r}{\partial\eta} \left\{ \frac{1}{\cos\phi}\left.\frac{\partial}{\partial\lambda}\left(\frac{u}{r}\right)\right|_\eta + \frac{1}{\cos\phi}\left.\frac{\partial}{\partial\phi}\left(\frac{v\cos\phi}{r}\right)\right|_\eta + \frac{\partial\dot\eta}{\partial\eta} \right\} = 0. \tag{2.70}$$

It will be observed that r occurs in various geometric factors even after the equations have been transformed to η coordinates. The transformation $r \leftrightarrow \eta$ is used in the reverse direction to evaluate these factors in the η-coordinate forms.

2.3 Summary of the governing equations in the model's transformed coordinates

In the following, local time derivatives and all horizontal derivatives are taken at constant η.

Horizontal momentum components

$$\frac{Du}{Dt} = \frac{uv\tan\phi}{r} - \frac{uw}{r} + f_3 v - f_2 w - \frac{c_{pd}\theta_v}{r\cos\phi}\left(\frac{\partial\Pi}{\partial\lambda} - \frac{\partial\Pi}{\partial r}\frac{\partial r}{\partial\lambda}\right) + S^u, \tag{2.71}$$

$$\frac{Dv}{Dt} = -\frac{u^2\tan\phi}{r} - \frac{vw}{r} + f_1 w - f_3 u - \frac{c_{pd}\theta_v}{r}\left(\frac{\partial\Pi}{\partial\phi} - \frac{\partial\Pi}{\partial r}\frac{\partial r}{\partial\phi}\right) + S^v, \tag{2.72}$$

where

$$\frac{D}{Dt} \equiv \frac{\partial}{\partial t} + \frac{u}{r\cos\phi}\frac{\partial}{\partial\lambda} + \frac{v}{r}\frac{\partial}{\partial\phi} + \dot{\eta}\frac{\partial}{\partial\eta}, \tag{2.73}$$

$$\Pi = \left(\frac{p}{p_0}\right)^{\frac{R_d}{c_{pd}}}, \qquad [Exner\ function;\ \ p_0 = 1000hPa] \tag{2.74}$$

$$\theta_v = \frac{T}{\Pi}\left(\frac{1+\frac{1}{\epsilon}m_v}{1+m_v+m_{cl}+m_{cf}}\right),\ [Virtual\ potential\ temperature;\ \ \epsilon = \frac{R_d}{R_v} \cong 0.622] \tag{2.75}$$

See (2.77) - (2.79) for definitions of f_1, f_2, f_3.

Vertical momentum component

$$\frac{Dw}{Dt} = \frac{(u^2+v^2)}{r} + f_2 u - f_1 v - g - c_{pd}\theta_v\frac{\partial\Pi}{\partial r} + S^w. \tag{2.76}$$

In (2.71),(2.72) and (2.76),

$$f_1 = 2\Omega\sin\lambda\cos\phi_0\ , \tag{2.77}$$

$$f_2 = 2\Omega\left(\cos\phi\sin\phi_0 + \sin\phi\cos\lambda\cos\phi_0\right)\ , \tag{2.78}$$

$$f_3 = 2\Omega\left(\sin\phi\sin\phi_0 - \cos\phi\cos\lambda\cos\phi_0\right)\ . \tag{2.79}$$

ϕ_0 is the geographical latitude of the North Pole of the model's rotated latitude/longitude system. The geographical North Pole is assigned longitude $\lambda = 0$ in the rotated system. If the model uses the geographical latitude/longitude system (i.e. a rotated system is not introduced) then $\phi_0 = 90^o$ and we find $f_1 = 0$, $f_2 = 2\Omega\cos\phi$ and $f_3 = 2\Omega\sin\phi$, which are the non-rotated forms; cf. the Coriolisterms in (1.92), (1.93) and (1.97).

Continuity

$$\frac{D}{Dt}\left(r^2\rho_y\frac{\partial r}{\partial \eta}\right)+\left(r^2\rho_y\frac{\partial r}{\partial \eta}\right)\left[\frac{1}{\cos\phi}\frac{\partial}{\partial\lambda}\left(\frac{u}{r}\right)+\frac{1}{\cos\phi}\frac{\partial}{\partial\phi}\left(\frac{v\cos\phi}{r}\right)+\frac{\partial\dot{\eta}}{\partial\eta}\right]=0, \tag{2.80}$$

where

$$\rho_y=\rho/\left(1+m_v+m_{cl}+m_{cf}\right), \tag{2.81}$$

Thermodynamics

$$\frac{D\theta}{Dt}=\left(\frac{\theta}{T}\right)\frac{\dot{Q}}{c_{pd}}\equiv S^{\theta}, \tag{2.82}$$

where

$$\theta=\frac{T}{\Pi}=T\left(\frac{p_0}{p}\right)^{\frac{R_d}{c_{pd}}}, \qquad [Potential\ temperature;\ \ p_0=1000hPa] \tag{2.83}$$

State

$$\Pi^{\frac{\kappa_d-1}{\kappa_d}}\rho\theta_v=\frac{p_o}{\kappa_d c_{pd}}, \qquad [\kappa_d\equiv\frac{R_d}{c_{pd}}] \tag{2.84}$$

Moisture

$$\frac{Dm_v}{Dt}=S^{m_v}, \tag{2.85}$$

$$\frac{Dm_{cl}}{Dt}=S^{m_{cl}}, \tag{2.86}$$

$$\frac{Dm_{cf}}{Dt}=S^{m_{cf}}, \tag{2.87}$$

Vertical motion

$$\dot{\eta}\frac{\partial r}{\partial\eta}=w-\frac{u}{r\cos\phi}\frac{\partial r}{\partial\lambda}-\frac{v}{r}\frac{\partial r}{\partial\phi}. \tag{2.88}$$

2.4 Conservation properties of the governing equations in the model's transformed coordinates

Various conservation properties of the governing equations in the model's transformed coordinates are derived in Appendix A.

3 Normal modes of the compressible Euler equations for a deep spherical rotating atmosphere.

3.1 Prelude and overview

This section is an amalgam of the Thuburn, Wood & Staniforth (2002*a*) and Thuburn, Wood & Staniforth (2002*b*) papers on the normal modes of the compressible Euler equations for a deep spherical rotating atmosphere. The rest of this prelude is an overview summary of the remainder of the section.

Numerical weather and climate prediction models have traditionally applied the hydrostatic approximation and also, in particular, the shallow-atmosphere approximation. In addition, and probably as a result, studies of the normal modes of the atmosphere too have made the shallow-atmosphere approximation. The approximation appears to be based on simple scaling arguments. Here, the forms of the unforced, linear normal modes for the deep atmosphere on a sphere are considered and compared with those of the shallow atmosphere. Also the impact of ignoring the vertical variation of gravity is investigated. For terrestrial parameters, it is found that relaxing either or both of these approximations has very little impact on the spatial form of the energetically significant components of most normal modes. In nearly all cases the normal mode frequencies are smaller in magnitude when the shallow-atmosphere approximation is relaxed, but only slightly smaller. However, relaxing the shallow-atmosphere approximation does lead to significant changes in the tropical structure of long-zonal-wavelength internal acoustic modes. Relaxing the shallow-atmosphere approximation also leads to nonzero vertical velocity and potential temperature fields for external acoustic and Rossby modes; these fields are identically zero when the shallow-atmosphere approximation is made.

These results are particularly surprising in the tropics where the inclusion of the $F = 2\Omega\cos\phi$ Coriolis terms (which are dropped in the shallow-atmosphere approximation) might be expected to dominate the usual $f = 2\Omega\sin\phi$ Coriolis terms. The complexity of the full equations, however, prevents analysis of why this insensitivity to the extra terms arises. Normal modes under the f-F-plane approximation are therefore examined and compared with those on the more usual f-plane. The resulting equations are more amenable to analysis than the full equation set, and analytic expressions for the dispersion relation and for the normal mode structures are obtained for the particular case of an isothermal reference profile. This simplified geometry allows the effects of the F Coriolis terms to be examined while eliminating the geometrical effects of relaxing the shallow-atmosphere approximation, giving some insight into the relative importance of the two types of effect as well as the physical mechanisms at work. The F Coriolis terms are found to be responsible for the structural changes to long-zonal-wavelength internal acoustic modes, and can also affect extremely shallow and extremely deep gravity modes. However, these terms are found to have only a small effect on normal mode frequencies, and geometrical effects, rather than these Coriolis terms, are responsible for the systematic reduction in the magnitude of normal mode frequencies in a deep spherical atmosphere.

In Cartesian geometry the inclusion of the F terms gives rise to a new kind of normal mode in addition to the usual Rossby, gravity, and acoustic modes. The new modes are inertial in character, have frequency very close to f, and have extremely strong vertical tilt.

For a finite difference numerical model to be able to represent well the behaviour of the free atmosphere it must be able to capture accurately the structures of the normal modes. Therefore, the structures of normal modes can have implications for the choice of prognostic variables and grid staggering. In particular, the vertical structure of normal modes suggests that density and temperature should be analytically eliminated in favour of pressure and potential temperature as the prognostic thermodynamic variables, and that potential temperature and vertical velocity should be staggered in the vertical with respect to the other dynamic prognostic variables, the so-called Charney-Phillips grid.

3.2 Introduction

Studies of normal modes are useful for a number of reasons. They provide elementary solutions that isolate different aspects of the dynamics and, in particular, allow the effects of different approximations to the governing equations to be quantified. They provide valuable test cases for numerical models and are useful tools for analysing stability properties of numerical schemes. Understanding the properties of normal modes is important for initialization of numerical models, since initialization often means suppressing or filtering some subset of the possible modes. Finally, as will be discussed below, the vertical structure of normal modes can indicate a preferred choice for numerical model predicted variables and vertical grid staggering.

Global numerical weather and climate prediction models have traditionally applied the hydrostatic (or quasi-hydrostatic) approximation, in which vertical accelerations are neglected. For the increasing horizontal resolutions that are now affordable in global numerical weather prediction models, the hydrostatic approximation is approaching its limit of validity. Motivated by this, Daley (1988) and Kasahara & Qian (2000) have studied the normal modes of a non-hydrostatic atmosphere.

Global numerical weather and climate prediction models have also traditionally applied the shallow-atmosphere approximation, in which r the distance from the centre of the Earth is replaced by a constant a the Earth's radius, and the "traditional approximation", in which the Coriolis terms involving $2\Omega\cos\phi$ and some other small terms are dropped. It is now well understood (e.g. Phillips (1966), White & Bromley (1995)) that the shallow-atmosphere and traditional approximations must be made together if the resulting equations are to retain angular momentum and potential vorticity conservation principles. In this section both of these approximations made together are referred to as the shallow-atmosphere approximation and making them separately is not considered, except on a non-rotating planet (Section 3.4) or in Cartesian geometry (Section 3.5) where one or other of the approximations becomes irrelevant.

The rationale for the shallow-atmosphere approximation appears to be based on simple scaling arguments or on the claim that the neglected terms have only a small effect on the frequency of linear normal modes (e.g. Phillips (1968), Phillips (1990)). However, its weaknesses include the fact that the direction of the Earth's rotation, and hence the direction of the Coriolis force, are misrepresented, and the fact that vertical variations in the planetary contribution to angular momentum are neglected (e.g. Newton (1971)). More detailed scaling arguments for both the atmosphere and the ocean (Draghici (1987), Beckmann & Diebels (1994), Colin de Verdière & Schopp (1994), White & Bromley (1995), Marshall, Hill, Perelman & Adcroft (1997)) suggest that for many scales of motion the shallow-atmosphere approximation is more problematic than the hydrostatic approximation. For example, the $2\Omega\cos\phi$ terms can significantly modify both hydrostatic and geostrophic balance in the deep tropics (Colin de Verdière & Schopp (1994)). Deep diabatic circulations in the tropics can also be affected (e.g. White & Bromley (1995)). For example, air ascending from the surface at the equator to a height of 10 km, conserving its full angular momentum on the way, would experience a westward change in velocity of about $1.5\,\mathrm{ms}^{-1}$; this effect is neglected under the shallow-atmosphere approximation. The $2\Omega\cos\phi$ terms might also be important when stratification is weak so that an important constraint on vertical motions is removed, for example in a near neutrally stratified ocean mixed layer (Garwood, Gallacher & Muller 1985) or planetary boundary layer (Mason & Thompson 1987). These considerations have resulted in the shallow-atmosphere approximation being dropped from some recent global numerical models of the atmosphere (Cullen (1993), Cullen, Davies, Mawson, James, Coulter & Malcolm (1997)) and ocean (Marshall et al. 1997).

The studies of normal modes by Daley (1988) and Kasahara & Qian (2000), although non-hydrostatic, still made the shallow-atmosphere approximation. In the present work some properties are presented of the linear normal modes of oscillation about a state of rest for the dry governing equations for a deep rotating spherical non-hydrostatic atmosphere, that is, without the shallow-atmosphere approximation. The normal modes for such an atmosphere do not appear to have been previously documented. There is no analytic solution for these normal modes; they must be found numerically. Moreover, the problem for the latitude-height structure does not separate into simpler problems for the latitudinal structure and the height structure, as it does in the shallow-atmosphere case (e.g. Daley (1988), Kasahara & Qian (2000)). Therefore, the full two-dimensional structure problem must be solved numerically. By comparing normal modes with and without the shallow-atmosphere approximation the importance can be assessed of the terms neglected under the shallow-atmosphere approximation, including the terms involving $2\Omega\cos\phi$, for the various kinds of normal mode. This comparison will help to determine the importance of retaining the full governing equations in numerical weather prediction and climate models, which is currently an unresolved issue.

Another approximation made in most, if not all, numerical weather prediction and climate models is to approximate g, the acceleration due to gravity (plus the centrifugal force due to the Earth's rotation), as a constant equal to its surface value. However, g actually decreases by about 3% between the surface and 100 km altitude and it is important to know whether this effect can be neglected, especially for middle atmosphere modelling. The normal mode calculations presented herein have also been extended to assess the impact of realistic variations in g on the structure and frequency of normal modes.

The governing equations of the linear normal modes for a deep rotating non-hydrostatic atmosphere are developed in Section 3.3. Some solutions are evaluated numerically and the most significant differences in mode structure from the shallow-atmosphere case are described. The effects on mode frequency of relaxing the shallow-atmosphere approximation and of allowing realistic vertical variations in g are presented.

Because of the mathematical complexity of the problem, the normal mode solutions presented in Section 3.3 had to be obtained numerically. This makes it difficult to obtain insight into the physical mechanisms at work, for example by examining limiting cases of small or large parameters. In particular, it is useful to attempt to understand the extent to which the differences between the deep- and shallow-atmosphere cases are due to (i) the effects of the $2\Omega \cos\phi$ Coriolis terms and (ii) geometrical effects. The case of a non-rotating atmosphere is considered in Section 3.4. Neglecting rotation allows further progress to be made analytically and allows some of the geometrical effects of relaxing the shallow-atmosphere approximation to be considered in isolation from the effects of the $2\Omega \cos\phi$ Coriolis terms.

In Section 3.5 normal modes are derived in a simpler, Cartesian, geometry, neglecting latitudinal variations in the Coriolis parameters $f \equiv 2\Omega \sin\phi$ and $F \equiv 2\Omega \cos\phi$: the f-F-plane. In this simpler geometry the structures of the normal modes can be derived analytically for a given frequency σ, and the dispersion relation for σ can also be derived analytically, though it must be solved numerically. The f-F-plane framework helps to separate the effects of the F terms from the geometrical effects of relaxing the shallow-atmosphere approximation. Moreover, because analytic solutions are available it is possible to explore the parameter regimes under which the F terms might have a significant effect on normal mode structure and to understand why their effect on normal mode frequency is so small.

A curious property of the f-F-plane framework with the rigid upper and lower boundary conditions used herein is that, in addition to the usual Rossby, gravity, and acoustic modes, another kind of normal mode solution exists. The properties of these modes are discussed in Section 3.5.

The separability and vertical structure of normal modes in the shallow-atmosphere case are briefly reviewed in Section 3.6 to prepare for the discussion in Section 3.7 of their implications for vertical grid staggering and the choice of thermodynamic variables used in finite-difference numerical models of the atmosphere.

3.3 Normal modes of a deep non-hydrostatic rotating spherical atmosphere

3.3.1 Continuous governing equations

The derivation begins from the governing equations for a deep rotating spherical atmosphere ((1.14)-(1.16), (1.25), and (1.41) of Section 1, see also Daley (1988)). Only the dry unforced equations are analysed; the effects of moisture, diabatic processes and friction are neglected. In standard notation, these equations are:

$$\frac{Du}{Dt} + 2\Omega w \cos\phi - 2\Omega v \sin\phi + \frac{1}{\rho r \cos\phi}\frac{\partial p}{\partial \lambda} + \frac{uw}{r} - \frac{uv\tan\phi}{r} = 0, \tag{3.1}$$

$$\frac{Dv}{Dt} + 2\Omega u \sin\phi + \frac{1}{\rho r}\frac{\partial p}{\partial \phi} + \frac{vw}{r} + \frac{u^2\tan\phi}{r} = 0, \tag{3.2}$$

$$\frac{Dw}{Dt} - 2\Omega u \cos\phi + g + \frac{1}{\rho}\frac{\partial p}{\partial r} - \frac{(u^2+v^2)}{r} = 0, \tag{3.3}$$

$$\frac{D\theta}{Dt} = 0, \tag{3.4}$$

$$\frac{D\rho}{Dt} + \rho\left\{\frac{1}{r\cos\phi}\frac{\partial u}{\partial \lambda} + \frac{1}{r\cos\phi}\frac{\partial}{\partial \phi}\left(v\cos\phi\right) + \frac{1}{r^2}\frac{\partial}{\partial r}\left(r^2 w\right)\right\} = 0, \tag{3.5}$$

$$p = \rho R T, \tag{3.6}$$

where

$$\frac{D}{Dt} \equiv \frac{\partial}{\partial t} + \frac{u}{r\cos\phi}\frac{\partial}{\partial \lambda} + \frac{v}{r}\frac{\partial}{\partial \phi} + w\frac{\partial}{\partial r}, \tag{3.7}$$

$$\theta = T\left(\frac{p_0}{p}\right)^{\frac{R}{c_p}}. \tag{3.8}$$

Eqs. (3.1)-(3.6) are respectively the three components of the momentum equation, the thermodynamic equation, the continuity equation and the equation of state. In writing these equations a number of simplifying assumptions, e.g. approximation of the geoid by a sphere, have been made - see e.g. Phillips (1973) for discussion and justification.

Combining (3.5) with (3.4), (3.6), and (3.8) to obtain an equation for the pressure

$$\frac{Dp}{Dt} + \gamma p\left\{\frac{1}{r\cos\phi}\frac{\partial u}{\partial \lambda} + \frac{1}{r\cos\phi}\frac{\partial}{\partial \phi}\left(v\cos\phi\right) + \frac{1}{r^2}\frac{\partial}{\partial r}\left(r^2 w\right)\right\} = 0, \tag{3.9}$$

where $\gamma = c_p/c_v$, eases the subsequent analysis (Daley 1988).

These equations are linearised about a reference state (indicated by subscript s), which is at rest and for which the thermodynamic variables are in hydrostatic balance and are functions only of r. Following Daley (1988), the perturbed quantities are defined by $u' = \rho_s u$, $v' = \rho_s v$, $w' = \rho_s w$, $p' = p - p_s$, and $\theta' = g\rho_s(\theta - \theta_s)/\theta_s$, and the reference state sound speed and buoyancy frequency are respectively defined by $c_s^2(r) = \gamma R T_s(r)$ and $N_s^2(r) = (g/\theta_s)\, d\theta_s/dr$. To keep the notation compact, $2\Omega \sin\phi$ and $2\Omega\cos\phi$ are written as f and F respectively, and subscripts t, λ, ϕ, and r indicate partial derivatives. The linearised equations are:

$$u'_t + Fw' - fv' + \frac{1}{r\cos\phi} p'_\lambda = 0, \tag{3.10}$$

$$v'_t + fu' + \frac{1}{r} p'_\phi = 0, \tag{3.11}$$

$$w'_t - Fu' + p'_r + \frac{g}{c_s^2} p' - \theta' = 0, \tag{3.12}$$

$$\theta'_t + N_s^2 w' = 0, \tag{3.13}$$

$$p'_t + c_s^2 \left[\frac{1}{r\cos\phi} \left\{ u'_\lambda + (v'\cos\phi)_\phi \right\} + \frac{1}{r^2} \left(r^2 w' \right)_r + \frac{N_s^2}{g} w' \right] = 0. \tag{3.14}$$

Note that the linearisation has removed the so-called metric terms proportional to $1/r$ in the three momentum equations.

Because all coefficients in the linearised equations are independent of time and longitude, the time and longitude dependence of the solution can be separated:

$$\left.\begin{array}{ccc} u' & & \widehat{u}\,(\phi, r) \\ v' & & i\widehat{v}\,(\phi, r) \\ w' & = & i\widehat{w}\,(\phi, r) \\ \theta' & & \widehat{\theta}\,(\phi, r) \\ p' & & \widehat{p}\,(\phi, r) \end{array}\right\} \exp\left(im\lambda - i\sigma t\right). \tag{3.15}$$

Here the factors of i have been judiciously inserted so that, as long as the reference state is statically stable so that σ is real (see below), the structure functions $\widehat{u}$, $\widehat{v}$, $\widehat{w}$, $\widehat{\theta}$, and $\widehat{p}$ can all be taken to be real. The linearised equations then become:

$$-\sigma\widehat{u} + F\widehat{w} - f\widehat{v} + \frac{m}{r\cos\phi}\widehat{p} = 0, \tag{3.16}$$

$$\sigma\widehat{v} + f\widehat{u} + \frac{1}{r}\widehat{p}_\phi = 0, \tag{3.17}$$

$$\sigma\widehat{w} - F\widehat{u} + \left(\frac{\partial}{\partial r} + \frac{g}{c_s^2}\right)\widehat{p} - \widehat{\theta} = 0, \tag{3.18}$$

$$-\sigma\widehat{\theta} + N_s^2\widehat{w} = 0, \tag{3.19}$$

$$-\sigma\widehat{p} + c_s^2\left[\frac{1}{r\cos\phi}\left\{m\widehat{u} + (\widehat{v}\cos\phi)_\phi\right\} + \frac{1}{r^2}\left(\frac{\partial}{\partial r} + \frac{N_s^2}{g}\right)\left(r^2\widehat{w}\right)\right] = 0. \tag{3.20}$$

Together with the appropriate boundary conditions, these equations constitute an eigenvalue problem for the frequency σ and the structure of the normal modes. Boundary conditions that are relevant to numerical weather prediction and climate models are assumed, namely that $\widehat{w}$ should vanish at the rigid, spherical top and bottom boundaries. Since the equations are written in spherical polar coordinates, the solution is required to be nonsingular at the poles; this must be taken into account when computing numerical solutions.

Only a little further progress can be made analytically. $\widehat{u}$, $\widehat{v}$, and $\widehat{w}$ can be eliminated to leave two equations relating $\widehat{p}$ and $\widehat{\theta}$:

$$\left(\sigma^2 - N_s^2 + \frac{F^2\sigma^2}{f^2-\sigma^2}\right)\frac{\widehat{\theta}}{N_s^2} + \frac{F}{f^2-\sigma^2}\left(\frac{m\sigma}{r\cos\phi}\widehat{p} + \frac{f}{r}\widehat{p}_\phi\right) + \left(\frac{\partial}{\partial r} + \frac{g}{c_s^2}\right)\widehat{p} = 0, \tag{3.21}$$

$$\begin{aligned}
&-\sigma\widehat{p} \\
&+c_s^2\left[\frac{\sigma}{r^2}\left(\frac{\partial}{\partial r} + \frac{N_s^2}{g}\right)\left(\frac{r^2\widehat{\theta}}{N_s^2}\right)\right. \\
&-\frac{m}{(f^2-\sigma^2)\,r\cos\phi}\left(\frac{F\sigma^2}{N_s^2}\widehat{\theta} + \frac{m\sigma}{r\cos\phi}\widehat{p} + \frac{f}{r}\widehat{p}_\phi\right) \\
&\left.+\frac{1}{r\cos\phi}\left\{\frac{1}{(f^2-\sigma^2)}\left(\frac{fF\sigma\cos\phi}{N_s^2}\widehat{\theta} + \frac{mf}{r}\widehat{p} + \frac{\sigma\cos\phi}{r}\widehat{p}_\phi\right)\right\}_\phi\right] \quad = \quad 0.
\end{aligned} \tag{3.22}$$

(In fact it is possible to go further and eliminate $\widehat{\theta}/N_s^2$.) However, this pair of equations is not straightforward to solve numerically because the eigenvalue σ appears in several places in both equations.

One useful analytical result can be obtained by forming the energy equation. By taking $-\widehat{u}^*\times$ (3.16) $+\widehat{v}^*\times$ (3.17) $+\widehat{w}^*\times$(3.18) $-\widehat{\theta}^*/N_s^2\times$(3.19) $-\widehat{p}^*/c_s^2\times$(3.20) (superscript * means complex conjugate), dividing by ρ_s to obtain the appropriate density weighting, and integrating globally, by parts where necessary using the upper and lower boundary conditions $\widehat{w} = 0$, an energy equation is obtained, of the form

$$\int \{\sigma E + (\mathrm{real})\}\, r^2\cos\phi\, dr\, d\lambda\, d\phi = 0, \tag{3.23}$$

where

$$E = \frac{1}{2}\left(\frac{|\widehat{u}|^2 + |\widehat{v}|^2 + |\widehat{w}|^2}{\rho_s}\right) + \frac{1}{2}\left(\frac{\left|\widehat{\theta}\right|^2}{\rho_s N_s^2}\right) + \frac{1}{2}\left(\frac{|\widehat{p}|^2}{\rho_s c_s^2}\right), \tag{3.24}$$

and (real) means terms whose imaginary part is zero. The terms on the right hand side of (3.24), are respectively the perturbation kinetic, thermobaric and elastic energies (e.g. Phillips (1990)). Subtracting the complex conjugate of (3.23) from (3.23) itself then gives

$$(\sigma - \sigma^*) \int Er^2 \cos\phi dr d\lambda d\phi = 0. \tag{3.25}$$

Provided the reference state is statically stable so that $N_s^2 > 0$, E is positive definite; then the only way to satisfy (3.25) is to have σ real, that is, there are no growing (unstable) or decaying modes.

3.3.2 Numerical solutions for normal modes

To obtain numerical solutions for the frequencies and eigenmodes it is most straightforward to work directly with (3.16)-(3.20). The method of numerical solution is described in Section 3.9.

Figures 3.1 and 3.2 show examples of an external Rossby mode and an eastward-propagating internal acoustic mode for a deep, rotating, isothermal atmosphere. Figure 3.3 shows the shallow-atmosphere counterpart of the eastward-propagating internal acoustic mode. (See Section 3.6 for the shallow-atmosphere perturbation equations.) The variables displayed in the figures are $\rho_s^{-1/2}\widehat{u}$, $\rho_s^{-1/2}\widehat{v}$, $\rho_s^{-1/2}\widehat{p}/c_s$, $\rho_s^{-1/2}\widehat{\theta}/N_s$, and $\rho_s^{-1/2}\widehat{w}$. These are convenient variables for plotting the mode structures since they are proportional to the square root of the corresponding contribution to the perturbation energy - see (3.24) - and these contributions have similar amplitude at all altitudes. The parameters used are $g = 9.80616\,\mathrm{ms}^{-2}$,$\Omega = 7.292\times10^{-5}\mathrm{s}^{-1}$, $R = 287.05\,\mathrm{Jkg}^{-1}\mathrm{K}^{-1}$, $c_p = 1005.0\,\mathrm{Jkg}^{-1}\mathrm{K}^{-1}$, Earth's mean radius $a = 6371.22\,\mathrm{km}$, domain depth 80 km, reference temperature $T_s = 250\,\mathrm{K}$ implying $N_s^2 = 3.83\times10^{-4}\,\mathrm{s}^{-2}$, and zonal wavenumber $m = 1$. The numerical solution used 40 latitudes per hemisphere and 20 levels in the vertical.

The amplitudes of the modes are normalised so that the maximum value of $\rho_s^{-1}\left(\widehat{u}^2 + \widehat{v}^2\right)$ is 1. For any given mode, the relative amplitudes of the different variables help to identify the physical mechanism of the mode. For example, for the Rossby mode (Fig. 3.1) the

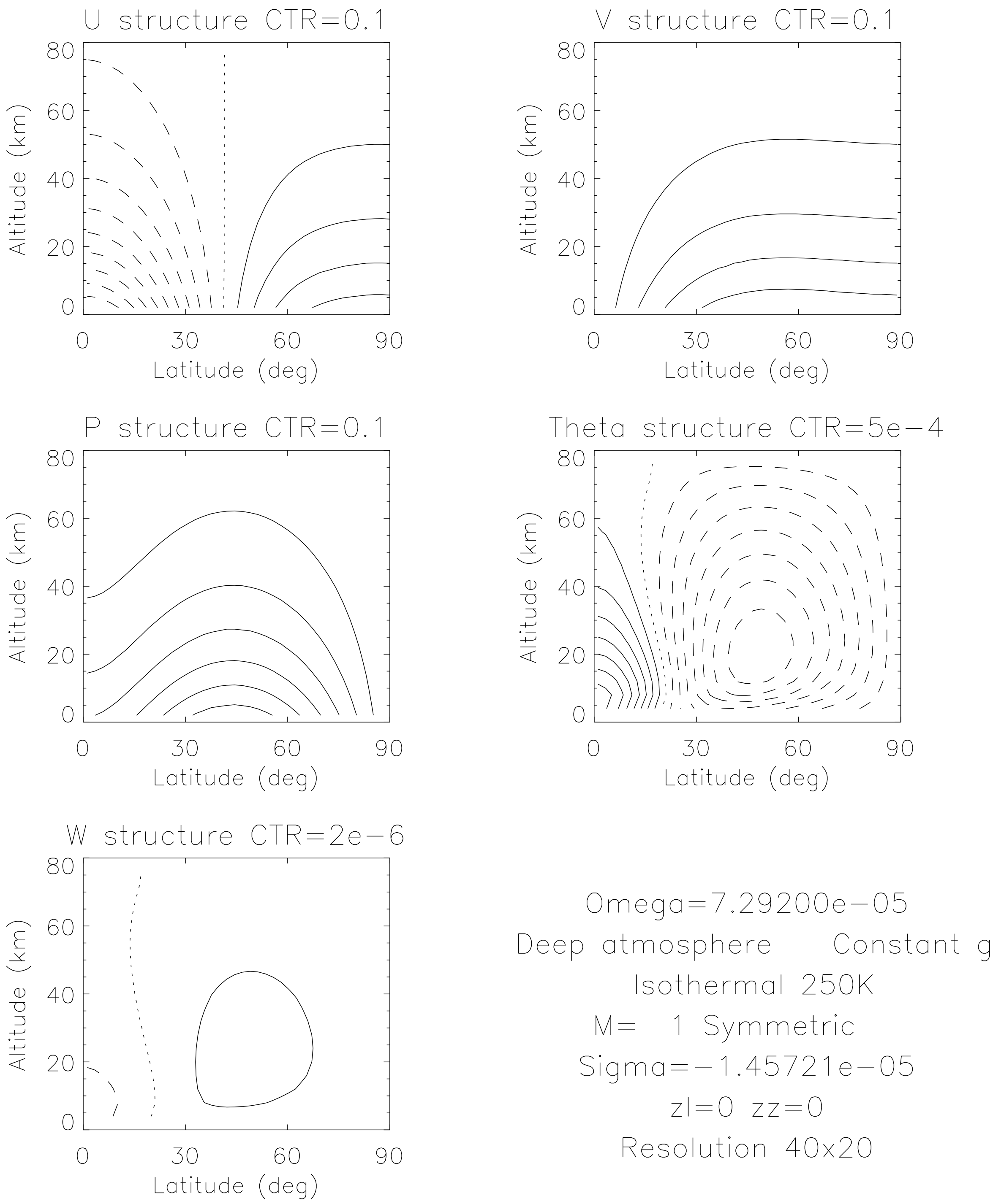

Figure 3.1: Latitude-height structure of the longest meridional wavelength external Rossby mode for a deep atmosphere. The parameters used are given in the text. Note that the vertical velocity and potential temperature are nonzero, in contrast to the shallow-atmosphere case. zl and zz indicate the number of zeros in the pressure structure in the latitudinal and vertical directions respectively.

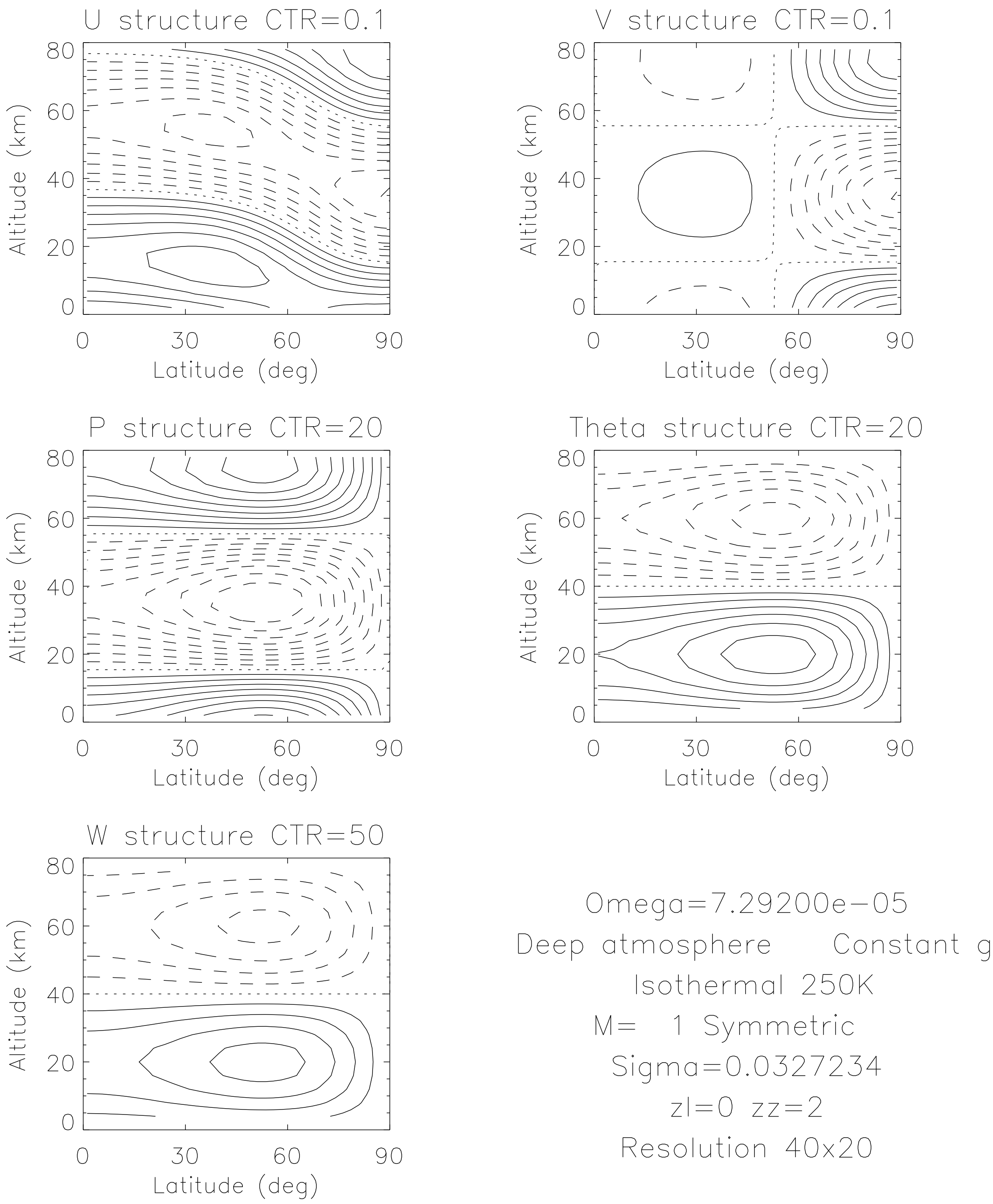

Figure 3.2: Latitude-height structure of the longest meridional wavelength 2nd internal eastward propagating acoustic mode for a deep atmosphere. The parameters used are as in Fig. 3.1 and are given in the text. Note the tilted zonal wind structure, the extra zero in the meridional wind structure, and the suppressed tropical amplitude compared to the shallow-atmosphere counterpart (Fig. 3.3).

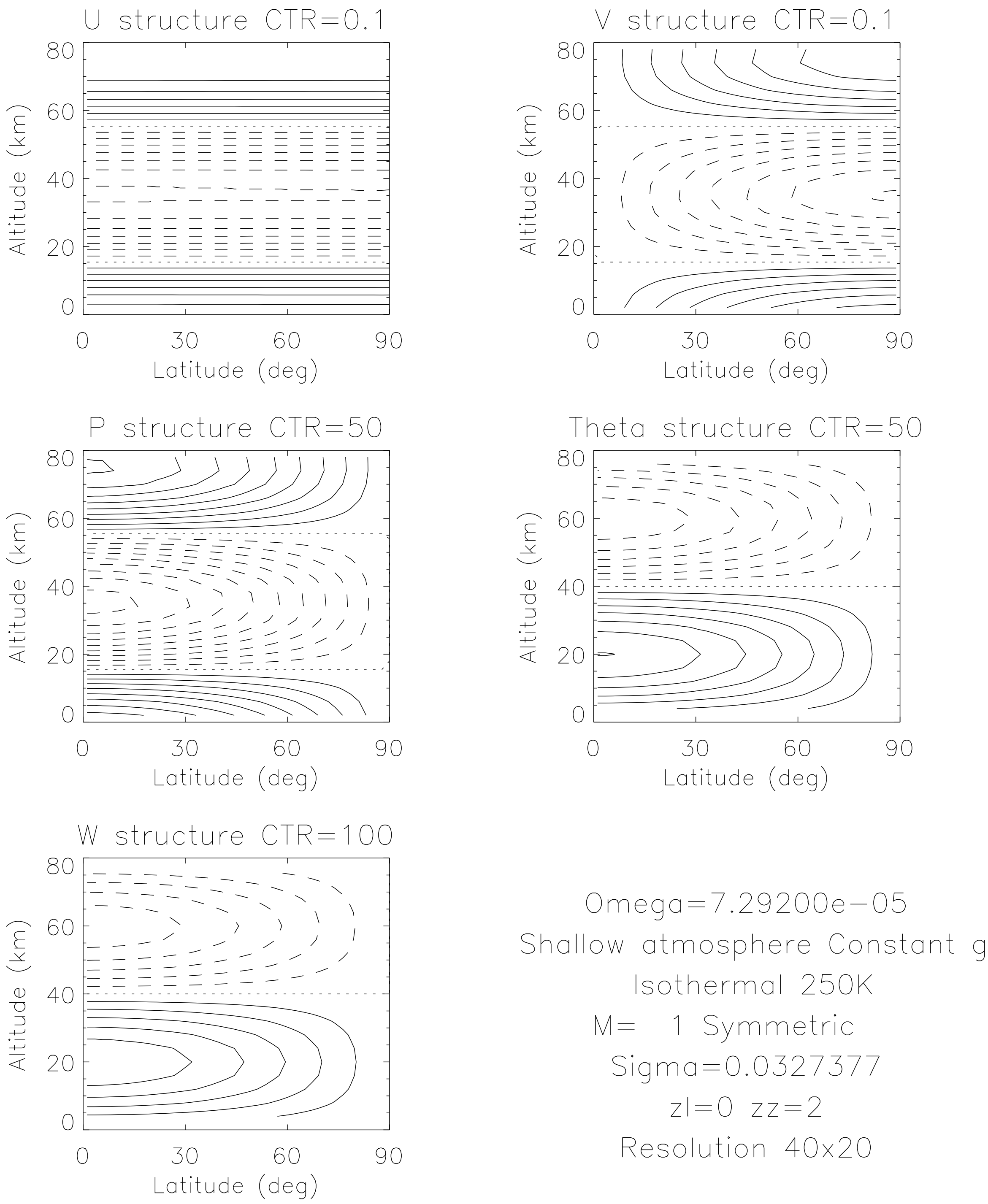

Figure 3.3: Latitude-height structure of the longest meridional wavelength 2nd internal eastward propagating acoustic mode for a shallow atmosphere. The parameters used are as in Fig. 3.1 and are given in the text.

mode energy is dominated by the horizontal velocity and pressure perturbations, while for the internal acoustic modes (Figs. 3.2, 3.3), the mode energy is dominated by the vertical velocity, pressure, and potential temperature perturbations.

The differences between the deep-atmosphere modes and their shallow-atmosphere counterparts give an indication of the importance of retaining the more complete dynamical equations. In the shallow-atmosphere case the latitude-height structures of the normal modes can be written as products of separate latitudinal and vertical structure functions (Daley (1988), Kasahara & Qian (2000), Section 3.6 below). Moreover, the external modes have vertical velocity and potential temperature perturbations identically zero. Figure 3.1 shows that for a deep atmosphere the external Rossby mode has small but essentially nonzero vertical velocity and potential temperature perturbations. The other deep-atmosphere external Rossby modes with different meridional structures and the deep-atmosphere external acoustic modes (not shown) also have small but nonzero vertical velocity and potential temperature perturbations. The corresponding shallow-atmosphere external Rossby and acoustic modes (not shown) do indeed have zero vertical velocity and potential temperature perturbations (except for numerical roundoff error, which is at least four orders of magnitude smaller than the physical values found for the deep-atmosphere case), while their pressure and horizontal velocity perturbations are almost identical to the deep-atmosphere case. The nonzero vertical velocity of the deep-atmosphere external modes appears to be attributable to the spherical geometry rather than the F terms: it is noted in Section 3.4 that deep-atmosphere external acoustic modes must have nonzero vertical velocity even for a non-rotating atmosphere, while in Section 3.5 it is shown that in Cartesian geometry the external modes do have zero vertical velocity even in the presence of the F terms.

The other characteristic of the deep-atmosphere normal modes that is clear from Fig. 3.1 is that the mode structure does not separate into a product of separate latitudinal and vertical structure functions. The zero contours (dotted) are not all strictly vertical or horizontal. This nonseparability was anticipated because of the inability to find analytically separable solutions and is confirmed by the numerical results.

The differences in structure between the deep-atmosphere and shallow-atmosphere external modes are conspicuous but energetically small. For the internal acoustic modes, however, the differences are energetically more significant. Figure 3.2 shows that the horizontal velocity structure of the deep-atmosphere internal eastward acoustic mode is significantly different from its shallow-atmosphere counterpart (Fig. 3.3). The nonseparability is again clear from the tilt of the zero contours. The $\widehat{v}$ structure has an extra latitudinal zero, and the $\widehat{u}$ structure tilts upwards and equatorwards. Near the pole the $\widehat{u}$ structure is similar to the shallow-atmosphere case and the vertical coincidence of the $\widehat{u}$ and $\widehat{p}$ peaks is consistent with the expected structure of an eastward propagating acoustic mode. Near the equator, however, the $\widehat{u}$ peaks are shifted upwards and are consistent with the $\widehat{u}$ field being driven by the F terms acting on the much stronger $\widehat{w}$ field. This vertical shift of the $\widehat{u}$ structure as a result of the F terms is predicted by an analysis of the normal mode structures in Cartesian geometry (Section 3.5). More importantly, there are significant differences in the tropical structure of the energetically dominant $\widehat{p}$, $\widehat{\theta}$ and $\widehat{w}$ components of the mode. The change in the $\widehat{v}$ structure is consistent with the change in the $\widehat{p}$ structure and the prediction (again see Section 3.5) that $\widehat{v}$ should be roughly proportional to the northward gradient of $\widehat{p}$.

In the shallow-atmosphere case the corresponding westward-propagating internal acoustic mode is, to a very close approximation, a mirror image of the eastward-propagating mode shown in Fig. 3.3. In the deep-atmosphere case this symmetry is destroyed; the $\widehat{u}$ structure then tilts downwards and equatorwards, again consistent with the $\widehat{u}$ field being driven by the F terms acting on the $\widehat{w}$ field in the tropics.

These differences in internal acoustic mode structure between deep- and shallow-atmosphere cases are most significant for the largest zonal wavelengths (smallest m). The differences rapidly become less noticeable for m greater than about 5 because the zonal pressure gradient in the zonal momentum equation increases in significance compared to the $2\Omega w \cos\phi$ term. Again, this result is consistent with the predictions of a Cartesian geometry analysis (Section 3.5). These long-zonal-wavelength acoustic modes are not thought to be meteorologically important for the Earth's atmosphere. However, they might be spuriously generated in numerical models by parametrized processes or assimilation of observations.

For other kinds of modes, namely internal Rossby modes and inertia-gravity modes (not shown), the structures of the deep-atmosphere modes are virtually identical to their shallow-atmosphere counterparts.

The differences in mode frequency between deep atmosphere and shallow atmosphere are small, always less than 1% for the cases examined. Table 3.1 shows frequencies of some

Mode type	Meridional mode	Vertical mode	Frequency shallow constant g	Frequency deep constant g	Frequency deep variable g
Acoustic	0	0 (external)	-1.32896×10^{-4}	5.44156×10^{-5}	5.44145×10^{-5}
			-1.32896×10^{-4}	-1.32748×10^{-4}	-1.32747×10^{-4}
Acoustic	2	0 (external)	2.87183×10^{-4}	2.86538×10^{-4}	2.86533×10^{-4}
			-2.92754×10^{-4}	-2.92117×10^{-4}	-2.92112×10^{-4}
Acoustic	0	2	3.27377×10^{-2}	3.27234×10^{-2}	3.25373×10^{-2}
			-3.27377×10^{-2}	-3.27235×10^{-2}	-3.25374×10^{-2}
Gravity	0 (Kelvin)	2	3.14113×10^{-5}	3.12593×10^{-5}	3.10370×10^{-5}
Gravity	2	2	1.87932×10^{-4}	1.87105×10^{-4}	1.86170×10^{-4}
			-1.95262×10^{-4}	-1.94349×10^{-4}	-1.93459×10^{-4}
Rossby	0	0 (external)	-1.45975×10^{-5}	-1.45721×10^{-5}	-1.45719×10^{-5}
Rossby	2	0 (external)	-3.06824×10^{-6}	-3.06671×10^{-6}	-3.06671×10^{-6}
Rossby	0	2	-9.58848×10^{-6}	-9.52404×10^{-6}	-9.46493×10^{-6}

Table 3.1: Frequencies (s^{-1}) of selected modes for shallow and deep rotating atmospheres with constant and variable$g$. All modes are symmetric about the equator with zonal wavenumber $m = 1$. Where two values are shown these are for an eastward and westward propagating pair of modes.

selected modes. The largest differences were found for gravity modes and the longest vertical wavelength internal Rossby modes. For gravity and Rossby modes the frequencies for a deep atmosphere with surface at $r = a$ and top at $r = a + 80000\,\mathrm{m}$ were found to be smaller in magnitude than those for a shallow atmosphere of radius a and greater in magnitude than those for a shallow atmosphere of radius $a + 80000\,\mathrm{m}$. Taken in isolation, the geometrical effects of relaxing the shallow-atmosphere approximation (see Section 3.4 below) tend to change the gravity mode frequencies in the sense found here. On the other hand, inclusion of the F terms in isolation from geometrical effects does not systematically decrease the magnitude of the normal mode frequencies (Section 3.5). Evidently the geometrical effects dominate the effects of the F terms.

The behaviour of the internal acoustic modes is rather different. Their frequencies for a deep atmosphere with surface at $r = a$ and top at $r = a + 80000\,\mathrm{m}$ were found to be smaller in magnitude than those for a shallow atmosphere of radius either a or $a + 80000\,\mathrm{m}$. A similar reduction in acoustic mode frequency for a deep atmosphere is seen in the non-rotating case, except at very short horizontal wavelengths (Section 3.4). For a pair of eastward and westward propagating acoustic modes, just as for gravity modes, the leading order effect of the F terms in isolation from geometrical effects is to increase the frequency of one member of the pair and decrease the frequency of the other (Section 3.5). Again, geometrical effects evidently dominate the effect of the F terms.

Although g is usually taken as constant in numerical models of the atmosphere, in reality it decreases with distance from the Earth's centre according to the inverse square law. Strictly speaking, inclusion of the height variation of g for a deep atmosphere is necessary for consistency, since the total flux of the gravitational field vector across a sphere enclosing the Earth should be proportional to the mass of the Earth and independent of the radius of the enclosing sphere (see Section 1.1 for further discussion of this point). It would be useful to assess whether including realistic variations in g would make a significant difference to numerical model behaviour. Although g has been taken as constant to compute the results shown in Figs. 3.1 to 3.3, the mathematical derivation carries through even for variable g. When the deep-atmosphere normal modes are recomputed with $g \propto 1/r^2$ (neglecting the smaller variations in the effective g due to the centrifugal contribution), and taking $9.80616\,\mathrm{ms}^{-2}$ as the surface value, the frequencies of the modes become systematically smaller in magnitude. See Table 3.1 for some selected results. Giving g a constant value appropriate for an altitude of 80000 m reduces the mode frequencies even further. The most obvious physical explanation for these results is that reducing g, locally or globally, reduces the strength of one of the wave restoring mechanisms and hence reduces the mode frequencies. However, for a given reference temperature profile $T_s(r)$, the reference hydrostatically balanced pressure, potential temperature, and buoyancy frequency profiles are all dependent on the profile of g, so that these changes in frequency probably result from a combination of changes in gravitational restoring force and changes in the reference state p_s, θ_s, and N_s^2. The largest effects of including realistic variations in g occur for gravity modes, low vertical wavenumber internal acoustic modes, and high vertical wavenumber internal Rossby modes, but were found to be always less than 1.5%. In all cases examined, using variable g rather than constant g has no noticeable effect on the mode structures.

3.4 Normal modes of a deep non-hydrostatic non-rotating spherical atmosphere

For a non-rotating planet further progress can be made analytically, and the resulting numerical problem is simpler to solve than in the rotating case. Analysing the non-rotating case allows us to separate some of the geometrical effects of relaxing the shallow-atmosphere approximation from the effects of the F terms. Setting $f = 0$ and $F = 0$ in (3.21) and (3.22) and eliminating $\widehat{\theta}/N_s^2$ gives

$$-\widehat{p} + c_s^2 \left[\frac{1}{r^2} \left(\frac{\partial}{\partial r} + \frac{N_s^2}{g} \right) \left\{ \frac{r^2}{N_s^2 - \sigma^2} \left(\frac{\partial}{\partial r} + \frac{g}{c_s^2} \right) \right\} \widehat{p} - \frac{1}{r^2 \sigma^2} \nabla_m^2 \widehat{p} \right] = 0, \tag{3.26}$$

where ∇_m^2 is shorthand for the operator $\left\{ - \left(m / \cos\phi \right)^2 + \left(1/\cos\phi \right) \left(\partial / \partial\phi \right) \left(\cos\phi \partial / \partial\phi \right) \right\}$. Since the frequency now appears only as σ^2, the nonzero eigenvalues must occur in pairs differing only in sign. This happens because there is no preferred horizontal direction on a non-rotating sphere so that acoustic and gravity modes each occur in eastward and westward propagating pairs with the eastward propagating modes being mirror images of their westward propagating counterparts. The "Rossby modes" all have zero frequency since there is no background potential vorticity gradient to provide a propagation mechanism.

The structure function $\widehat{p}$ can be written as a product of a horizontal structure function and a vertical structure function

$$\widehat{p} = \Phi(\phi) R_1(r). \tag{3.27}$$

Substituting this expression in (3.26) gives

$$-\frac{r^2}{c_s^2} + \frac{1}{R_1} \left(\frac{d}{dr} + \frac{N_s^2}{g} \right) \left\{ \frac{r^2}{N_s^2 - \sigma^2} \left(\frac{d}{dr} + \frac{g}{c_s^2} \right) \right\} R_1 - \frac{1}{\sigma^2} \frac{1}{\Phi} \nabla_m^2 \Phi = 0. \tag{3.28}$$

All dependence on r is in the first two terms while all horizontal dependence is in the last term. Therefore the last term must equal a constant, implying that the solutions for Φ are associated Legendre functions and the complete horizontal structures are spherical harmonics, again reflecting the fact that there is no preferred horizontal direction on a non-rotating sphere. The constant in question is of the form $n(n+1)/\sigma^2$ for non-negative integer n. Replacing the last term by this constant gives the eigenvalue problem for σ and the vertical structure:

$$\left(\frac{d}{dr}+\frac{N_s^2}{g}\right)\left\{\frac{r^2}{N_s^2-\sigma^2}\left(\frac{d}{dr}+\frac{g}{c_s^2}\right)\right\}R_1-\frac{r^2}{c_s^2}R_1+\frac{n(n+1)}{\sigma^2}R_1=0. \tag{3.29}$$

In general this one-dimensional eigenvalue problem must still be solved numerically. Further progress can be made analytically in a couple of special cases. One case is for steady solutions, i.e. $\sigma = 0$, which includes the "Rossby modes". Putting $\sigma = f = F = 0$ in (3.21) and (3.22) shows that $\nabla_m^2 \widehat{p} = 0$, i.e. m must equal zero and $\widehat{p}$ must be independent of latitude but may be an arbitrary function of r. Also

$$\widehat{\theta} = \left(\frac{d}{dr}+\frac{g}{c_s^2}\right)\widehat{p}, \tag{3.30}$$

i.e. the perturbed state must be in hydrostatic balance. Returning to (3.16) - (3.20) and putting $\sigma = f = F = 0$ shows that $w = 0$ while u and v can be any steady horizontally nondivergent velocity field, again with arbitrary dependence on r.

Another special case is for an isothermal reference state (and constant g) implying N_s^2 and c_s^2 are constant. Then (3.29) can be recast as a confluent hypergeometric equation whose solution is composed of confluent hypergeometric functions. The requirement to satisfy both the upper and lower boundary conditions determines the allowed values of σ. However, since all of the parameters of the confluent hypergeometric functions depend on σ, this leads to a complicated nonlinear problem for the eigenvalues (analogous to that studied by Staniforth, Williams & Neta (1993)) that must be solved numerically. In practice it is more straightforward to discretise and solve (3.29) directly.

One final analytical result concerns the external modes. If $f = F = 0$ then solutions with $\widehat{w} = 0$ are possible only if $\sigma = 0$ i.e. the Rossby modes discussed above, or for special reference temperature profiles $T_s \propto r^2$. In other words, external acoustic modes must in general have $\widehat{w}$ nonzero.

Returning then to the general case, (3.29) can be rewritten in self-adjoint form. Let

$$\widetilde{R}_1 = \rho_s^{-1/2} R_1, \tag{3.31}$$

and note that

$$\frac{(\rho_s)_r}{\rho_s} = -\left(\frac{g}{c_s^2}+\frac{N_s^2}{g}\right). \tag{3.32}$$

Then (3.29) becomes

$$\left(\frac{d}{dr}-\Gamma\right)\left\{\frac{r^2}{N_s^2-\sigma^2}\left(\frac{d}{dr}+\Gamma\right)\right\}\widetilde{R}_1-\left(\frac{r^2}{c_s^2}-\frac{n(n+1)}{\sigma^2}\right)\widetilde{R}_1=0, \tag{3.33}$$

where $\Gamma = \frac{1}{2}\left\{(g/c_s^2) - (N_s^2/g)\right\}$. The boundary condition $w = 0$ becomes

$$\left(\frac{d}{dr} + \Gamma\right)\widetilde{R}_1 = 0, \tag{3.34}$$

at the top and bottom boundaries, which can be taken to be at r_T and r_S respectively.

Because of the way σ^2 appears in (3.33), discretizing the equation directly does not lead to a straightforward matrix eigenvalue problem that can be solved numerically. To overcome this a second flow variable is introduced

$$Q = \frac{r^2/a^2}{N_s^2 - \sigma^2}\left(\frac{d}{dr} + \Gamma\right)\widetilde{R}_1. \tag{3.35}$$

(In fact Q is proportional to the vertical velocity perturbation, while $\widetilde{R}_1$, recall, is proportional to the pressure perturbation.) The eigenvalue problem then becomes

$$\frac{r^2}{a^2}\left(\frac{d}{dr} + \Gamma\right)\widetilde{R}_1 - N_s^2 Q = -\sigma^2 Q, \tag{3.36}$$

$$\frac{n(n+1)}{a^2}\widetilde{R}_1 = \sigma^2\left\{\frac{r^2}{a^2 c_s^2}\widetilde{R}_1 - \left(\frac{d}{dr} - \Gamma\right)Q\right\}, \tag{3.37}$$

with $Q = 0$ at $r = r_S$ and $r = r_T$. A straightforward discretization, using a staggered grid for Q and $\widetilde{R}_1$ and centred differences and averages, leads to a generalised matrix eigenvalue problem

$$\mathbf{Ax} = \sigma^2\mathbf{Bx}, \tag{3.38}$$

which can be solved using standard packages.

This problem has been solved, using the same parameters as in Section 3.3 except that $\Omega = 0$, for both deep and shallow atmospheres and for both constant and variable g. A staggered grid with 80 vertical levels was used. For some of the longest vertical wavelength modes and for horizontal wavenumbers $n = 1$ and $n = 1000$, the effects on the frequencies of relaxing the shallow atmosphere and constant g approximations are summarised in the tables in Section 3.10.

Retaining the deep-atmosphere terms systematically reduces the mode frequencies, though always by less than 1%. For long horizontal wavelength the internal gravity waves are most strongly affected. For short horizontal wavelengths the internal acoustic modes are most strongly affected.

Including realistic vertical variations in g makes virtually no difference to the external mode frequencies but decreases the internal mode frequencies, with the largest changes of order 1%. As in the rotating atmosphere case, the decrease in gravity mode frequencies is probably associated with a combination of the reduction in the gravitational restoring force and modifications to the reference state.

To help understand the effects of relaxing the shallow-atmosphere approximation an analytical result for a "slightly deep" non-rotating atmosphere, derived in Section 3.11, can be applied. For a deep atmosphere extending from r_S to r_T, the gravity modes have frequencies lying between those for a shallow atmosphere with $a = r_S$ and those for a shallow atmosphere with $a = r_T$, i.e. (from (3.114))

$$\sigma^2_{a=r_T} < \sigma^2_{deep} < \sigma^2_{a=r_S}. \tag{3.39}$$

This pattern was indeed found to hold for the gravity mode frequencies computed numerically, and, moreover, was found to hold for the gravity mode frequencies computed for a rotating atmosphere too (Section 3.3). The most obvious geometrical effect of relaxing the shallow-atmosphere approximation is to modify the horizontal pressure gradient terms. For a given horizontal mode structure, and hence given p'_λ and p'_ϕ, $|(1/r)\, p'_\lambda|$ will be smaller than $|(1/r_s)\, p'_\lambda|$, etc., leading to slower accelerations and smaller frequencies. This simple physical picture is consistent with (3.39).

For acoustic modes the result (3.39) does not hold because $N_s^2 - \sigma_0^2 < 0$ so that the numerator in (3.113) is not of definite sign. The numerical results show that acoustic mode frequencies for a deep atmosphere extending from r_S to r_T are smaller in magnitude than those for a shallow atmosphere with either $a = r_S$ or $a = r_T$ as long as the vertical wavelength is much smaller than the horizontal wavelength. The simple physical picture described above for gravity waves is not relevant for these internal acoustic modes because other aspects of the dynamics dominate the horizontal pressure gradients. A similar tendency for the frequencies of long horizontal wavelength internal acoustic modes to be reduced in a deep atmosphere was found for a rotating atmosphere (Section 3.3). However, when the vertical and horizontal wavelengths become comparable the simple physical picture described for gravity waves becomes relevant for acoustic modes too, and the frequencies were found to follow the pattern implied by (3.39).

3.5 Normal modes of a deep non-hydrostatic rotating Cartesian-geometry atmosphere

Because of the mathematical complexity of the problem, the normal mode solutions presented in Section 3.3 had to be obtained numerically. This makes it difficult to obtain insight into the physical mechanisms at work, for example by examining limiting cases of small or large parameters. In this and the following sections normal modes are derived in a simpler, Cartesian, geometry, neglecting latitudinal variations in the Coriolis parameters f and F. The domain is assumed to be a tangent plane to the sphere at a particular latitude, and the Coriolis parameters are fixed at values appropriate to that latitude. Because the Coriolis parameters have no spatial variation there is no Rossby restoring mechanism so that the Rossby modes have zero frequency. It is usual to retain only the $2\Omega \sin\phi$ Coriolis terms; the geometry is then referred to as the f-plane. In fact it is possible to retain the $2\Omega \cos\phi$ terms too. This geometry will be referred to as the f-F-plane.

3.5.1 The f-F-plane equations

Consider small perturbations to a stationary, hydrostatically balanced reference state indicated by subscript s. Eqs. (3.10) - (3.14) then become

$$u'_t + Fw' - fv' + p'_x = 0, \tag{3.40}$$

$$v'_t + fu' + p'_y = 0, \tag{3.41}$$

$$\delta_H w'_t - Fu' + p'_z + \frac{g}{c_s^2}p' - \theta' = 0, \tag{3.42}$$

$$\theta'_t + N_s^2 w' = 0, \tag{3.43}$$

$$p'_t + c_s^2\left(u'_x + v'_y + w'_z + \frac{N_s^2}{g}w'\right) = 0. \tag{3.44}$$

A hydrostatic switch δ_H is included to allow normal modes of the quasi-hydrostatic equations to be considered too; setting $\delta_H = 1$ gives the full equation set while setting $\delta_H = 0$ approximates the vertical momentum equation by one of quasi-hydrostatic balance. As is well known, making the quasi-hydrostatic approximation suppresses the internal acoustic mode solutions. These equations are to be solved subject to the boundary condition $w = 0$ at the bottom and top boundaries $z = 0$ and $z = z_T$, respectively. The flow is assumed periodic in the x and y directions.

Note that, unlike the f-plane, the f-F-plane is not isotropic in the horizontal because the planetary rotation vector $(0, F/2, f/2)$ is tilted away from the vertical. (See, e.g. Beckmann & Diebels (1994), who refer to the geometry as the f-$\widetilde{f}$-plane.) Results for the f-plane can be recovered by setting $F = 0$ in what follows. Results for an equatorial F-plane can be recovered by setting $f = 0$.

In spherical geometry it is important (e.g. Phillips (1973)) when neglecting or approximating terms to do so in such a way as to retain proper analogues of the conservation laws on which the full equations are based. It has been verified that the f-F-plane equations do indeed have appropriate analogues to the conservation laws for mass, angular momentum, energy and potential vorticity. In particular, the full nonlinear equation for the Lagrangian conservation of potential vorticity takes its usual form

$$\frac{D}{Dt}\left(\frac{\underline{\zeta}\cdot\nabla\theta}{\rho}\right) = 0, \tag{3.45}$$

where here the absolute vorticity vector $\underline{\zeta}$ includes a constant contribution $(0, F, f)$ from the planetary rotation, and the full nonlinear conservation law for angular momentum is

$$m_t + \nabla.\,(um + p, vm, wm) = 0, \tag{3.46}$$

where $m = \rho\,(u - fy + Fz)$. The linearised forms in terms of scaled variables may be obtained either by linearising these equations or directly from the linear governing equations (3.40) - (3.44), though they are algebraically rather cumbersome.

3.5.2 Normal mode structures

In the f-F-plane geometry the x, y, and t dependences of the normal modes all separate, allowing the following to be written:

$$\left.\begin{array}{ccc} u' & & \widehat{u}(z) \\ v' & & i\widehat{v}(z) \\ w' & = & i\widehat{w}(z) \\ p' & & \widehat{p}(z) \\ \theta' & & \widehat{\theta}(z) \end{array}\right\} \exp(ikx + ily - i\sigma t). \tag{3.47}$$

(A form similar to (3.15) has been used in order to facilitate the derivations below and allow comparison with Section 3.3; however, because of the assumed y dependence, $\widehat{u}$ etc. are no longer necessarily real.)

Consider first Rossby mode solutions, which here have zero frequency, so as to eliminate them from further consideration later. Substituting (3.47) into (3.40) - (3.44) and setting $\sigma = 0$ implies that $\widehat{w} = 0$. (It may be verified that this remains true even for the neutrally stratified case $N_s^2 = 0$ because of the lower and upper boundary conditions.) Hence

$$-f\widehat{v} + k\widehat{p} = 0, \tag{3.48}$$

$$f\widehat{u} + il\widehat{p} = 0, \tag{3.49}$$

$$-F\widehat{u} + \left(\frac{d}{dz} + \frac{g}{c_s^2}\right)\widehat{p} - \widehat{\theta} = 0, \tag{3.50}$$

$$k\widehat{u} + il\widehat{v} = 0. \tag{3.51}$$

The hydrostatic switch δ_H does not appear in these equations so Rossby modes are not affected by making the quasi-hydrostatic approximation. Now (3.51) is automatically satisfied for any $\widehat{u}$ and $\widehat{v}$ that satisfy (3.48) and (3.49). Hence solutions of (3.48) - (3.51) can be obtained by choosing an arbitrary $\widehat{p}(z)$, then defining $\widehat{u}$ and $\widehat{v}$ through (3.48) and (3.49), and defining $\widehat{\theta}$ through (3.50). The only effect of the F terms is to modify the phase relationship between θ and the other variables. Eliminating $\widehat{u}$ from (3.50) suggests that the effect could be significant when lF/f is comparable to the inverse of the vertical length scale, e.g. near the equator or for extremely short meridional wavelengths.

Now proceed to look for other mode solutions, which have nonzero frequency. Substituting (3.47) into (3.40)-(3.44), leads to a set of equations for the vertical structure functions $\widehat{u}$ etc. Incidentally, these equations can be shown to imply an equation for the perturbation energy analogous to (3.23) and (3.24), confirming that there are no growing modes provided $N_s^2 > 0$. Eliminating $\widehat{u}$, $\widehat{v}$, $\widehat{w}$ and $\widehat{\theta}$, and dividing by σ (which is permissible since, by assumption, $\sigma \neq 0$), finally leaves

$$\begin{aligned} &\left(\frac{d}{dz} + \frac{N_s^2}{g} + \frac{(-k\sigma + ilf)\,F}{f^2 - \sigma^2}\right) \times \\ &\left\{\left(\delta_H\sigma^2 - N_s^2 + \frac{F^2\sigma^2}{f^2-\sigma^2}\right)^{-1}\left(\frac{d}{dz} + \frac{g}{c_s^2} + \frac{(k\sigma + ilf)\,F}{f^2-\sigma^2}\right)\right\}\widehat{p} \\ &+ \left(\frac{1}{c_s^2} + \frac{K^2}{f^2-\sigma^2}\right)\widehat{p} = \quad 0, \end{aligned} \tag{3.52}$$

where $K^2 = k^2 + l^2$. It is also assumed here that $\sigma^2 \neq f^2$ to avoid division by zero. The solutions of the dispersion relation derived below confirm that this condition does indeed hold except when f itself vanishes or in the limit $K \to 0$.

For an arbitrary reference temperature profile this one-dimensional eigenvalue problem must be solved numerically. However, for an isothermal profile (and assuming constant g) c_s^2 and N_s^2 are constants and further progress can be made analytically. Eq. (3.52) can then be written as

$$\left(\frac{d}{dz}+A\right)\left(\frac{d}{dz}+B\right)\widehat{p}+C\widehat{p}=0, \tag{3.53}$$

where

$$A=\frac{N_s^2}{g}+\frac{(-k\sigma+ilf)\,F}{f^2-\sigma^2}, \tag{3.54}$$

$$B=\frac{g}{c_s^2}+\frac{(k\sigma+ilf)\,F}{f^2-\sigma^2}, \tag{3.55}$$

$$C=\left(\frac{1}{c_s^2}+\frac{K^2}{f^2-\sigma^2}\right)\left(\delta_H\sigma^2-N_s^2+\frac{F^2\sigma^2}{f^2-\sigma^2}\right). \tag{3.56}$$

The boundary condition $w=0$ becomes, from (3.40)-(3.44) and (3.47),

$$\left(\frac{d}{dz}+B\right)\widehat{p}=0, \tag{3.57}$$

at the bottom and top boundaries $z=0$ and $z=z_T$, respectively.

Now make the change of variable

$$\widehat{p}=\widetilde{p}\exp\left\{-\left(\frac{A+B}{2}\right)z\right\}. \tag{3.58}$$

Note that $(A+B)/2=1/(2H)+ilfF/(f^2-\sigma^2)$, where H is the scale depth of the atmosphere, given by $1/H\equiv-(1/\rho_s)d\rho_s/dz=g/\{(1-\kappa)c_s^2\}$ for an isothermal atmosphere. With this change of variable the problem becomes

$$\left(\frac{d^2}{dz^2}+k_z^2\right)\widetilde{p}=0, \tag{3.59}$$

where

$$k_z^2=C-\frac{(B-A)^2}{4}, \tag{3.60}$$

subject to boundary conditions

$$\left\{\frac{d}{dz}+\frac{(B-A)}{2}\right\}\widetilde{p}=0 \tag{3.61}$$

at $z=0$ and $z=z_T$. Note that both C and $B-A$ are real, so that k_z^2 is real. Also, note that

$$(B-A)/2=\Gamma+\sigma kF/\left(f^2-\sigma^2\right), \tag{3.62}$$

where

$$\Gamma = \frac{1}{2}\left\{\left(g/c_s^2\right) - \left(N_s^2/g\right)\right\}. \tag{3.63}$$

There are two types of solution to (3.59) that satisfy these boundary conditions: external modes and internal modes.

External modes

First, for $k_z^2 < 0$ the boundary conditions can be satisfied only if $k_z^2 = -\left\{(B-A)/2\right\}^2$, which, from (3.60), implies $C = 0$. This is the external mode solution

$$\widetilde{p} = \widehat{p}(0)\exp\left\{-\left(\frac{B-A}{2}\right)z\right\}, \tag{3.64}$$

where $\widehat{p}(0)$ is an arbitrary constant with dimensions of pressure that gives the amplitude of the pressure perturbation at the ground. The corresponding perturbations in the physical variables are

$$p - p_s = \widehat{p}(0)\exp\left\{-\frac{(1-\kappa)z}{H} - \frac{(k\sigma + ilf)F}{f^2-\sigma^2}z\right\}\exp i\left(kx+ly-\sigma t\right), \tag{3.65}$$

$$u = -\frac{\widehat{p}(0)}{\rho_s(0)}\left(\frac{k\sigma+ilf}{f^2-\sigma^2}\right)\exp\left\{\frac{\kappa z}{H} - \frac{(k\sigma+ilf)F}{f^2-\sigma^2}z\right\}\exp i\left(kx+ly-\sigma t\right), \tag{3.66}$$

$$v = i\frac{\widehat{p}(0)}{\rho_s(0)}\left(\frac{kf+il\sigma}{f^2-\sigma^2}\right)\exp\left\{\frac{\kappa z}{H} - \frac{(k\sigma+ilf)F}{f^2-\sigma^2}z\right\}\exp i\left(kx+ly-\sigma t\right), \tag{3.67}$$

$$w = 0, \tag{3.68}$$

$$\theta - \theta_s = 0. \tag{3.69}$$

If it is assumed that the effect of the F terms on σ is small (in fact for external modes they have no effect—see below) then (3.65)-(3.69) can be used to determine how the F terms will modify the external mode structures and for what parameter ranges the modifications will be significant. Even with the inclusion of the F terms the external mode has $w = 0$ at all altitudes, not just at the lower and upper boundaries. This is in contrast to the full spherical geometry results of Sections 3.3 and 3.4, where w is nonzero for the deep-atmosphere external modes, with or without planetary rotation. The nonzero vertical velocity for deep spherical atmosphere external modes must therefore be attributable primarily to the geometrical effects of relaxing the shallow-atmosphere approximation, in particular the form of the vertical divergence term in the continuity equation (compare the w' terms in (3.14) and (3.44) above), rather than the inclusion of the F terms. The F terms do introduce extra vertical structure in both amplitude and phase in the pressure and horizontal velocity. Whether the effect is significant will depend on whether $(k\sigma + ilf)\,F/\left(f^2 - \sigma^2\right)$ is significant compared to $1/H$. Substituting from the external mode dispersion relation ((3.81) below) shows that the F terms could become significant only for horizontal wavelengths greater than the Earth's circumference, and so they will not be significant in practice.

Internal modes

For $k_z^2 > 0$ there are infinitely many independent solutions of the form

$$\widetilde{p} = k_z \cos\left(k_z z\right) - \left(\frac{B-A}{2}\right) \sin\left(k_z z\right), \tag{3.70}$$

where $k_z = m\pi/z_T$ with m a positive integer. These are the internal modes. Analytic solutions for the perturbations to the physical variables may be recovered from their scaled vertical structure functions:

$$\widehat{p} = \left\{k_z \cos\left(k_z z\right) - \left(\frac{B-A}{2}\right) \sin\left(k_z z\right)\right\} \exp\left(-\frac{z}{2H} - \frac{ilfF}{f^2-\sigma^2} z\right), \tag{3.71}$$

$$\widehat{\theta} = N_s^2 \left(\delta_H \sigma^2 - N_s^2 + \frac{F^2\sigma^2}{f^2-\sigma^2}\right)^{-1} \left\{k_z^2 + \left(\frac{B-A}{2}\right)^2\right\} \sin k_z z \exp\left(-\frac{z}{2H} - \frac{ilfF}{f^2-\sigma^2} z\right), \tag{3.72}$$

$$\widehat{w} = \frac{\sigma}{N_s^2}\widehat{\theta}, \tag{3.73}$$

$$\widehat{u} = -\left(f^2 - \sigma^2\right)^{-1} \left\{(\sigma k + ilf)\,\widehat{p} + \sigma F \widehat{w}\right\}, \tag{3.74}$$

$$\widehat{v} = \left(f^2 - \sigma^2\right)^{-1} \left\{(fk + il\sigma)\,\widehat{p} + fF \widehat{w}\right\}. \tag{3.75}$$

Again it is assumed that the effect of the F terms on σ is small (this will be confirmed below) and their effect on the mode structures is examined. There are several ways that the F terms might affect the mode structure.

1. If $Fk\sigma/\left(f^2-\sigma^2\right)$ were significant compared to Γ and k_z then $(B-A)/2$ would differ significantly from Γ (see (3.62)) and the nodes in the $\widehat{p}$ vertical structure would be shifted.

2. If $lfF/\left(f^2-\sigma^2\right)$ were significant compared to k_z then the F terms could introduce a significant vertical phase tilt through the exponential term.

3. The vertical phase structure of $\widehat{u}$ could be significantly modified if the $\widehat{w}$ term in (3.74) were significant compared to the $\widehat{p}$ term. This would require
$$\sigma^2 F \left(\delta_H \sigma^2 - N_s^2 + \frac{F^2\sigma^2}{f^2 - \sigma^2} \right)^{-1} \max(k_z, \Gamma)$$
to be comparable to $\sigma k + ilf$.

4. The vertical phase structure of $\widehat{v}$ could be significantly modified if the $\widehat{w}$ term in (3.75) were significant compared to the $\widehat{p}$ term. This would require
$$\sigma f F \left(\delta_H \sigma^2 - N_s^2 + \frac{F^2\sigma^2}{f^2 - \sigma^2} \right)^{-1} \max(k_z, \Gamma)$$
to be comparable to $fk + il\sigma$.

A careful analysis of when these conditions can be satisfied, using the approximate dispersion relations for very shallow gravity modes $(K/k_z \ll 1)$,

$$\sigma^2 \approx f^2 + \frac{N_s^2 K^2}{k_z^2}, \tag{3.76}$$

and very deep non-hydrostatic gravity modes $(K/k_z \gg 1)$,

$$\sigma^2 \approx N^2 \left(1 - \frac{k_z^2 + \Gamma^2}{K^2} \right), \tag{3.77}$$

shows that there are essentially three situations in which the F terms can have a significant effect on normal mode structure. The first is for very shallow gravity modes with K/k_z comparable to Ω^2/N_s^2. In this situation all four conditions above can be satisfied and the node distribution, tilt, and $\widehat{u}$ and $\widehat{v}$ structures can all be affected. The second and third situations can occur only for non-hydrostatic flow. The second is for very deep non-hydrostatic gravity modes with K/k_z comparable to N_s/Ω. In this situation conditions (1), (3), and (4) can be satisfied and the node distribution and $\widehat{u}$ and $\widehat{v}$ structures can be affected. The third situation is for internal acoustic modes with long, planetary scale, zonal wavelength. Then condition (3) can be satisfied and the $\widehat{u}$ phase structure can be shifted in the vertical relative to the $\widehat{p}$ structure. Figures 3.4-3.9 show examples of these three situations. The variables plotted are $\rho_s^{-1/2}\mathrm{Re}(\widehat{u})$ and $\rho_s^{-1/2}\mathrm{Re}(\widehat{p})/c_s$. These are proportional to the contributions to the wave energy density from the u and p fields respectively. These are useful variables for displaying the mode structures because their amplitude does not have a systematic variation

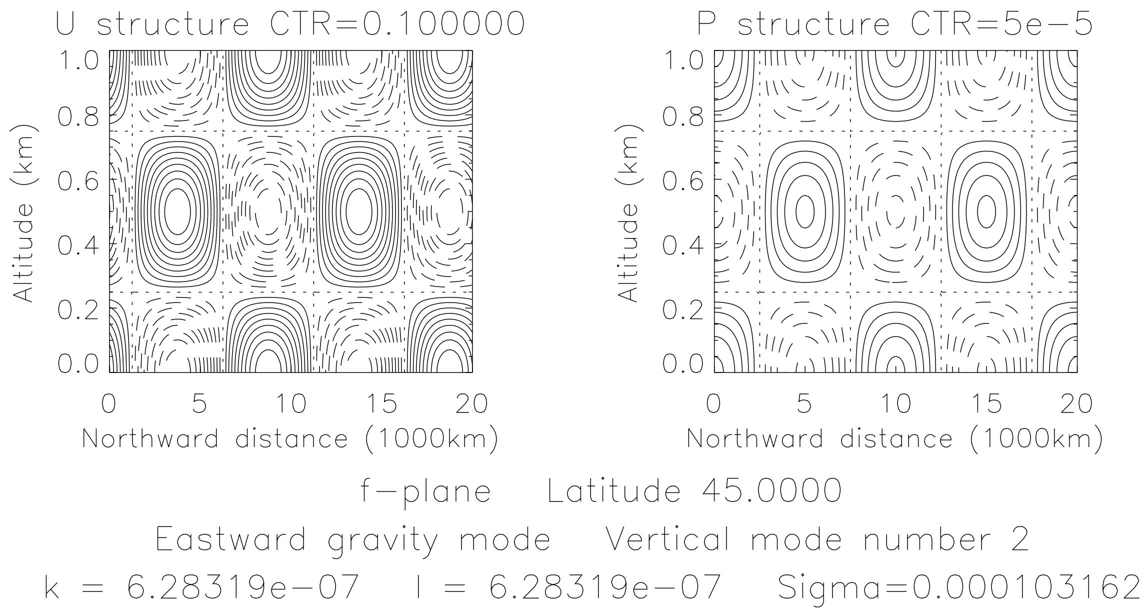

Figure 3.4: Latitude-height u and p structure of an eastward propagating shallow gravity mode on an f-plane at 45°N. The reference state is isothermal with $T_s = 250$K. (A shallow domain with a top at 1 km has been chosen to illustrate clearly the structure of this shallow mode. However, similar modes with the same k, l, k_z, and σ are clearly possible on deeper domains since these parameters imply $w = 0$ at $z = M/2\,\text{km}$ for all integers M.)

with altitude and because they allow the wave energy contributions from different variables to be compared. Figures 3.2 and 3.3 illustrate the third situation for a long-zonal-wavelength acoustic mode in a deep rotating spherical atmosphere. In that case the effect of the F terms is latitudinally dependent, leading to a conspicuous tilting of the u structure.

3.5.3 Dispersion relations

Eq. (3.60) gives the following polynomial equation for σ,

$$\begin{aligned} &\left\{\sigma^2 - f^2 - c_s^2 K^2\right\}\left\{\left(\delta_H \sigma^2 - N_s^2\right)\left(\sigma^2 - f^2\right) - F^2\sigma^2\right\} \\ &\quad - c_s^2\left[k_z^2\left(\sigma^2 - f^2\right)^2 + \left\{\Gamma\left(\sigma^2 - f^2\right) - Fk\sigma\right\}^2\right] = 0. \end{aligned} \tag{3.78}$$

To simplify the following discussion, analysis is presented only for non-hydrostatic flow: $\delta_H = 1$. Two cases need to be considered, one for the external modes and one for the

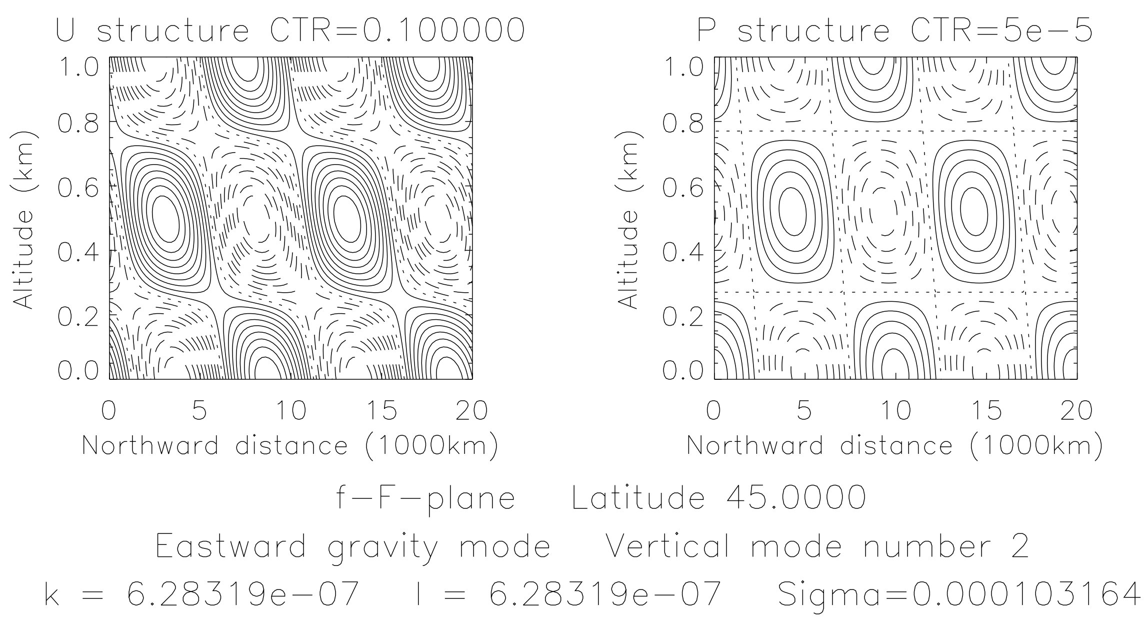

Figure 3.5: Latitude-height u and p structure of an eastward propagating shallow gravity mode on an f-F-plane at 45°N. Compare Fig. 3.4 and note the tilt introduced by the F terms.

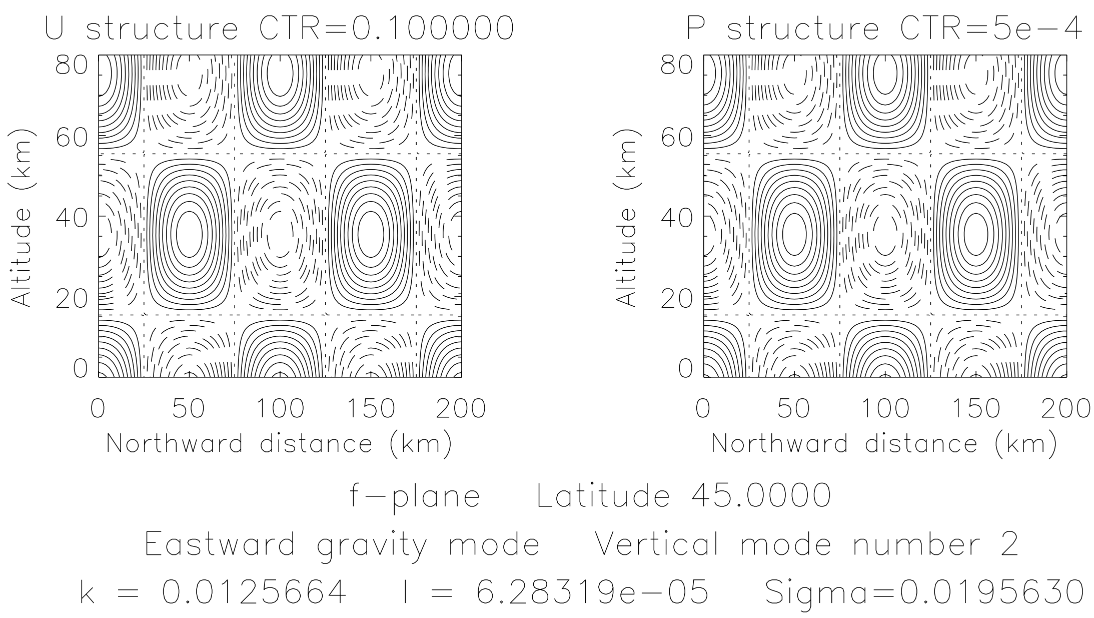

Figure 3.6: Latitude-height u and p structure of an eastward propagating deep gravity mode (zonal wavelength 500 m) on an f-plane at 45°N.

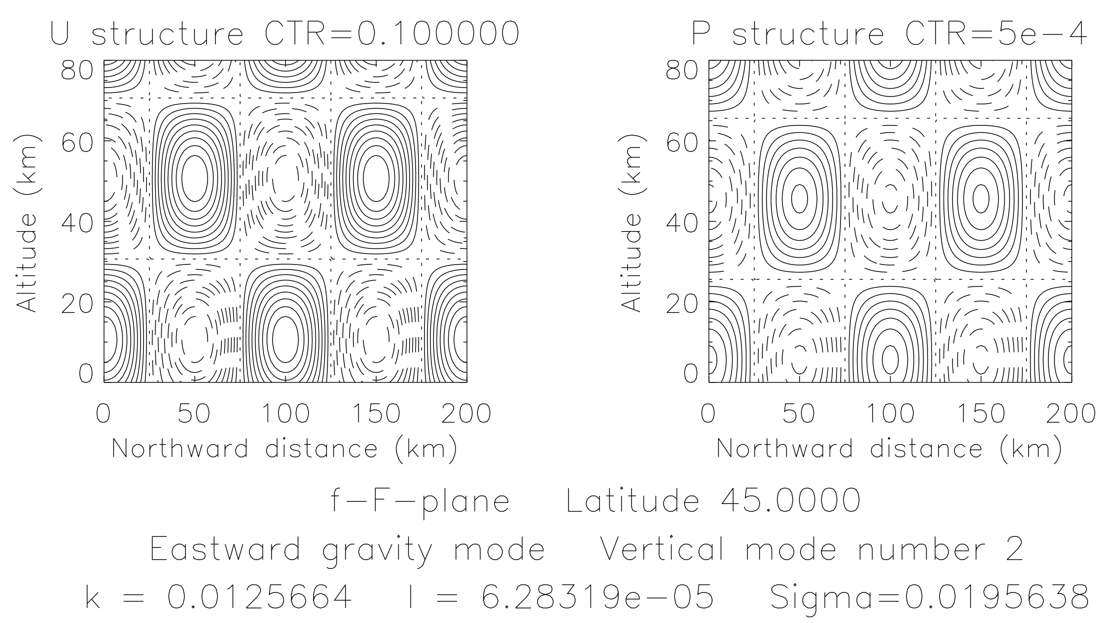

Figure 3.7: Latitude-height u and p structure of an eastward propagating deep gravity mode on an f-F-plane at 45°N. Compare Fig. 3.6 and note the vertical shift in the p structure nodes, and the vertical shift of the u structure relative to the p structure, introduced by the F terms.

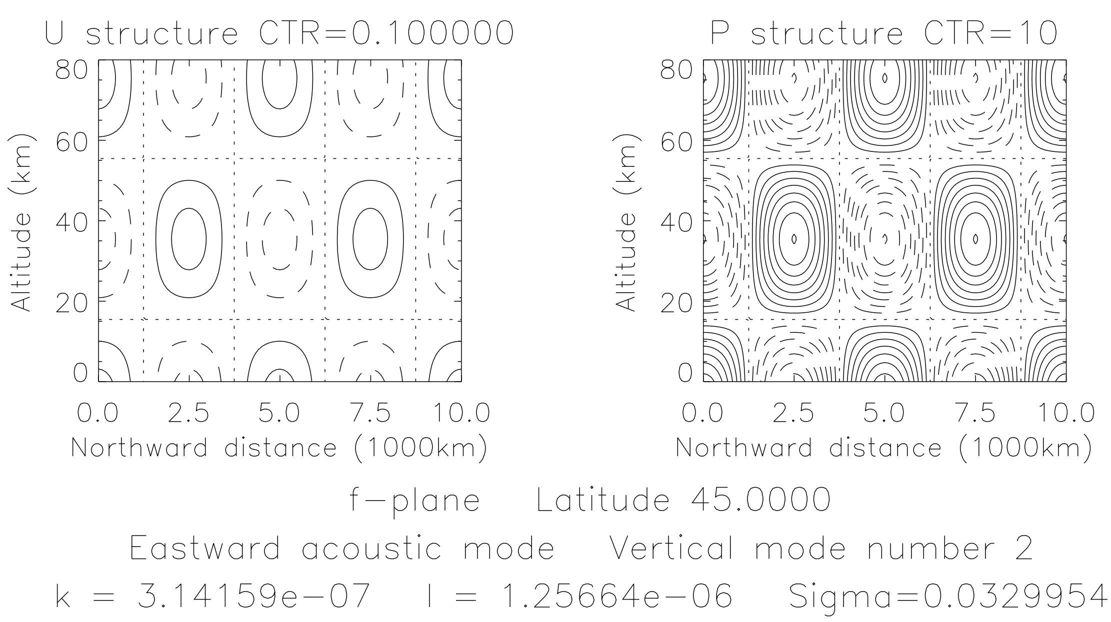

Figure 3.8: Latitude-height u and p structure of an eastward propagating long-zonal-wavelength (20000 km) acoustic mode on an f-plane at 45^oN.

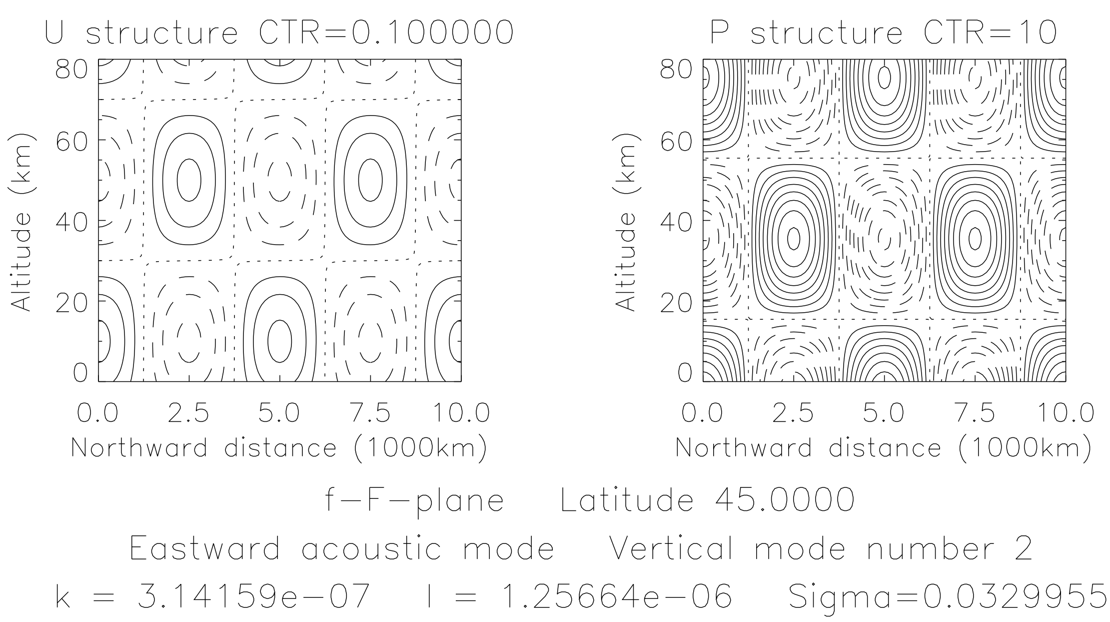

Figure 3.9: Latitude-height u and p structure of an eastward propagating long-zonal-wavelength acoustic mode on an f-F-plane at 45°N. Compare Fig. 3.8 and note the vertical shift of the u structure relative to the p structure introduced by the F terms.

internal modes.

External modes

For the external modes it has been shown that $k_z^2 = -\left\{(B-A)/2\right\}^2$ so that (3.60) reduces to $C = 0$ and the dispersion relation becomes

$$\left\{\sigma^2 - f^2 - c_s^2 K^2\right\}\left\{\left(\sigma^2 - N_s^2\right)\left(\sigma^2 - f^2\right) - F^2\sigma^2\right\} = 0. \tag{3.79}$$

There are six roots to (3.79). However, four of these, given by

$$\left(\sigma^2 - N_s^2\right)\left(\sigma^2 - f^2\right) - F^2\sigma^2 = 0, \tag{3.80}$$

are in fact spurious and the resulting "solutions" do not satisfy (3.40)-(3.44). These roots are a consequence of the singular term $\left\{\sigma^2 - N_s^2 + F^2\sigma^2/\left(f^2 - \sigma^2\right)\right\}^{-1}$ appearing in (3.52). The remaining two roots are genuine and correspond to the external acoustic modes. Their frequencies are the solutions to

$$\sigma^2 = f^2 + c_s^2 K^2. \tag{3.81}$$

The roots for σ are independent of F, and in fact this is exactly the dispersion relation that would be derived on an f-plane. In other words, the frequencies of the external modes are not affected at all by the inclusion of the F terms, even though their vertical structures are affected. It may be verified that the external mode frequencies are also unaffected by making the quasi-hydrostatic approximation.

A further external normal mode is the external Rossby mode given by $\sigma = 0$. This is not a solution of (3.79) as it was eliminated in obtaining (3.52). As noted already, its frequency remains zero and so is also not affected by the F terms.

Internal modes

For the internal modes the dispersion relation is the full sixth degree polynomial (3.78) and so there are six roots for σ. Four of these roots correspond to the familiar eastward and westward propagating internal acoustic and gravity modes. It is shown below that their frequencies are only slightly perturbed from their f-plane values by the inclusion of the F terms. The other two modes also form an eastward and westward propagating pair, and are new in the sense that no corresponding modes exist on the f-plane. These new modes will be discussed in detail in the next subsection.

On an f-plane the frequencies σ_0 of the internal acoustic and gravity modes satisfy the f-plane dispersion relation

$$\left(\sigma_0^2 - f^2 - c_s^2 K^2\right)\left(\sigma_0^2 - N_s^2\right) - c_s^2\left(k_z^2 + \Gamma^2\right)\left(\sigma_0^2 - f^2\right) = 0. \tag{3.82}$$

This is a quadratic equation for σ_0^2, so the modes occur in eastward and westward propagating pairs with frequencies of exactly the same magnitude. This eastward-westward symmetry is perturbed by the inclusion of the F terms, which introduces odd powers of σ in the dispersion relation.

If it is assumed that the F terms perturb the mode frequencies only slightly from their f-plane values then $\sigma = \sigma_0 + \sigma'$ can be put in (3.78), terms neglected in σ'^2 and $F\sigma'$, and (3.82) subtracted to obtain

$$\frac{\sigma'}{\sigma_0} \approx \frac{\left\{\frac{c_s^2 F\Gamma k}{\sigma_0} - \frac{F^2}{2}\left(1 - \frac{c_s^2 l^2}{\sigma_0^2 - f^2}\right)\right\}}{\left\{f^2 + N_s^2 + c_s^2\left(K^2 + k_z^2 + \Gamma^2\right) - 2\sigma_0^2\right\}}. \tag{3.83}$$

Note that, although F is considered here to be small in some sense, all terms involving F have been retained, not just those linear in F, since it is not obvious *a priori* which will dominate. It is now confirmed that σ'/σ_0 is indeed small, so that the approximation leading to (3.83) is indeed consistent.

First note that the denominator in (3.83) can never approach zero. This follows from solving the quadratic equation (3.82) to obtain

$$\begin{aligned} 2\sigma_0^2 \;=\;& f^2 + N_s^2 + c_s^2\left(K^2 + k_z^2 + \Gamma^2\right) \\ & \pm\left[\left\{f^2 + N_s^2 + c_s^2\left(K^2 + k_z^2 + \Gamma^2\right)\right\}^2 - 4\left(f^2 + c_s^2 K^2\right)N_s^2 - 4c_s^2\left(k_z^2 + \Gamma^2\right)f^2\right]^{1/2}, \end{aligned} \tag{3.84}$$

and hence

$$\begin{aligned} & 2\sigma_0^2 - \left\{f^2 + N_s^2 + c_s^2\left(K^2 + k_z^2 + \Gamma^2\right)\right\} \\ & = \pm\left[\left\{N_s^2 + c_s^2\left(k_z^2 + \Gamma^2\right) - \left(f^2 + c_s^2 K^2\right)\right\}^2 + 2c_s^4\left(k_z^2 + \Gamma^2\right)K^2\right]^{1/2}. \end{aligned} \tag{3.85}$$

The right hand side is clearly bounded away from zero, by at least $c_s^2\Gamma^2$, and therefore so is the denominator in (3.83).

Next consider under what circumstances the numerator in (3.83) can be large enough to make σ'/σ_0 significant. For gravity waves with small enough aspect ratio ($K \ll k_z, f/c_s$), which have $\sigma_0 \approx f$, the first term in the numerator could make σ'/σ_0 significant provided $Fk/\Gamma f$ were of order 1. However, combining these conditions shows that it would require $F/\Gamma c_s$ to be of order 1, which does not hold for realistic terrestrial parameters. The second term in the numerator in (3.83) might conceivably be significant when σ_0^2 is close to f^2. However, substituting the approximate expression for the frequency of shallow gravity modes (3.76) shows that this term too is always much smaller than the denominator. Therefore, in all circumstances the F terms lead to only small perturbations to the f-plane frequencies.

A similar analysis for the quasi-hydrostatic case leads to an equation like (3.83) except that the denominator is replaced by $\{N_s^2 + c_s^2\,(k_z^2 + \Gamma^2)\}$. Again, in all circumstances the F terms lead to only small perturbations to the f-plane frequencies.

Frequencies calculated numerically for normal modes of a deep atmosphere in spherical geometry (Section 3.3) were found to be always slightly smaller in magnitude than those of the corresponding shallow-atmosphere modes. It would be interesting to know whether this tendency can be explained by the F terms alone rather than the geometrical effects of relaxing the shallow-atmosphere approximation. The denominator in (3.83) is positive for gravity modes and negative for acoustic modes. However, the numerator can be either positive or negative depending on which term dominates there. Roots of (3.78) computed numerically show that inclusion of the F terms can indeed either increase or decrease the magnitude of the mode frequency for realistic parameter values. Therefore the F terms alone cannot explain the spherical atmosphere results. Results for a non-rotating spherical atmosphere discussed in Section 3.4 suggest that the geometrical effects of relaxing the shallow-atmosphere approximation are responsible for the general decrease in magnitude of frequencies in the deep-atmosphere case.

The above theoretical predictions have been confirmed by computing roots of the dispersion relation numerically for a range of horizontal wavenumbers. The parameters used were as in Section 3.3: $g = 9.80616\,\mathrm{ms}^{-2}$, $\Omega = 7.292 \times 10^{-5}\mathrm{s}^{-1}$, $R = 287.05\,\mathrm{Jkg}^{-1}\mathrm{K}^{-1}$, $c_p = 1005.0\,\mathrm{Jkg}^{-1}\mathrm{K}^{-1}$, domain depth $z_T = 80\,\mathrm{km}$, and reference temperature $T_s = 250\,\mathrm{K}$, implying $N_s^2 = 3.83 \times 10^{-4}\,\mathrm{s}^{-2}$. In all cases examined the effect on σ of including the F terms is extremely small. For example, for an f-F-plane at 45°N, implying $f = F = 1.03 \times 10^{-4}\,\mathrm{s}^{-1}$, the percentage difference between the f-F-plane frequency and the f-plane frequency is always less than 1%. It is largest for the longest vertical wavelength internal modes, essentially because vertical parcel displacements are largest for these modes, for a given mode energy. For the first internal mode the greatest change in gravity mode frequency is 0.22% and the greatest change in acoustic mode frequency is 0.10%. For the 50^{th} internal mode the greatest change in gravity mode frequency is about 0.01% while the greatest change in acoustic mode frequency is 10^{-4}%. The effect of retaining the F terms is only slightly larger near the equator.

3.5.4 New modes

For internal modes the dispersion relation (3.78) has six roots, but only four of those correspond to the familiar eastward and westward propagating acoustic and gravity modes. The other two do not correspond to any solutions that exist on the f-plane. In contrast to the external mode case, in which four of the roots are spurious, the two new roots here do correspond to solutions of (3.40)-(3.44). They are therefore new modes that exist only when the F terms are included.

The new modes depend crucially on the top and bottom boundary conditions for their existence. For example, if the top and bottom boundary conditions are ignored and solutions sought for $\widehat{p}$ etc. proportional to $\exp\left(-z/2H + ikx + ily + ik_z z\right)$ then a fifth degree polynomial dispersion relation is obtained whose roots correspond to a pair of acoustic modes, a pair of gravity modes, and a Rossby mode (e.g. Phillips (1990)). However, this dispersion relation involves terms in k_z as well as k_z^2, so that a mode proportional to $\exp\left(ik_z z\right)$ will have a different frequency from a mode proportional to $\exp\left(-ik_z z\right)$; it is therefore not possible to satisfy the top and bottom boundary conditions by superposing such modes, as it would be in the f-plane case. The extra powers of σ in the dispersion relation (3.78) that give rise to the two new roots arise ultimately, though in a rather subtle way, through the need to satisfy the top and bottom boundary conditions.

The new modes have frequencies very close to $\pm f$, and in fact the magnitude of the frequencies is slightly smaller than f. This can be seen, for example, by putting $\sigma = f + \sigma'$ in (3.78) and dropping terms in σ'^2 and $F\sigma'$ to obtain

$$\sigma' \approx -\frac{l^2 F^2 f}{2K^2\left(N_s^2 - f^2\right)}. \tag{3.86}$$

The deviation of σ from f is indeed small because of the smallness of F^2/N_s^2.

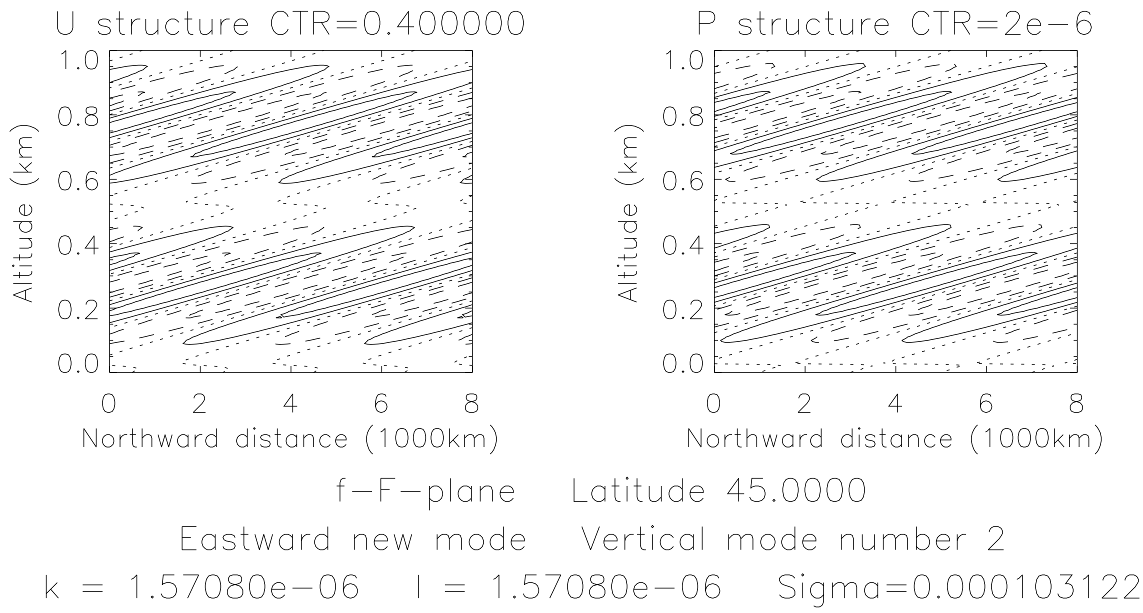

Figure 3.10: Latitude-height u and p structure of an eastward propagating new mode.

The closeness of σ to f has important consequences for the structure of the new modes because the terms in (3.71)-(3.75) involving $\left(f^2-\sigma^2\right)^{-1}$ become large. For example, the mode energy is dominated by the horizontal wind components while the pressure field is particularly weak. Thus these modes might justifiably be called a kind of inertial mode. Also, these modes acquire a very strongly tilted structure associated with the $\exp\left\{-ilfFz/\left(f^2-\sigma^2\right)\right\}$ term and modulated by the $\sin k_z z$ term. The vertical scale associated with this tilt is extremely short, typically a few metres to a few hundred metres. Figure 3.10 shows an example of the structure of one of these new modes. Note that the domain is only 1 km deep in order to make the strongly tilted structure visible.

In the f-plane limit, as $F \to 0$, the $\left(f^2-\sigma^2\right)^{-1}$ terms become unboundedly large and the vertical scale of the tilted structure approaches zero: the new modes become singular and cease to exist, as might have been expected from their absence in the f-plane case. The modes also become singular and cease to exist in the limit of an equatorial f-F-plane where $f \to 0$, because σ also approaches zero and the $\left(f^2-\sigma^2\right)^{-1}$ terms again blow up.

The existence of the new modes does not depend on using the full non-hydrostatic equations. When the quasi-hydrostatic approximation is made by setting $\delta_H = 0$ in (3.78) the dispersion relation for internal modes becomes a quartic polynomial equation; its four roots correspond to a pair of eastward and westward propagating gravity modes and a pair of the new modes.

3.6 Normal modes of a shallow non-hydrostatic rotating spherical atmosphere

In Section 3.4 the complete normal mode calculation of Section 3.3 was simplified by neglecting the Earth's rotation. In this Section the calculation is simplified in another way by making the shallow-atmosphere approximation. This is done to highlight some properties of the normal mode structures that were referred to in Section 3.3 and others that will be used in Section 3.7 below. The derivation essentially follows Daley (1988), except that here, in order to allow for the possibility of setting $\Omega = 0$, the problem has not been non-dimensionalised. In (3.16)-(3.20), the distance r is replaced by the constant a, $\partial/\partial r$ is replaced by $\partial/\partial z$, and the terms involving $2\Omega\cos\phi$ are dropped. This simplification allows further progress to be made analytically and, in contrast to the deep-atmosphere case, the latitude-height structure functions can be written as products of separate latitudinal and vertical structure functions. Moreover, because of the way u' and v' were originally defined, $\widehat{u}$, $\widehat{v}$ and $\widehat{p}$ all have the same vertical structure function, and $\widehat{\theta}/N_s^2$ and $\widehat{w}$ have the same vertical structure function. Thus

$$\widehat{u}(\phi, z) = \widetilde{u}(\phi)Z_1(z), \tag{3.87}$$

$$\widehat{v}(\phi, z) = \widetilde{v}(\phi)Z_1(z), \tag{3.88}$$

$$\widehat{p}(\phi, z) = \widetilde{p}(\phi)Z_1(z), \tag{3.89}$$

$$\widehat{\theta}(\phi, z) = (\widetilde{\theta}(\phi)/N_s^2(z))Z_2(z), \tag{3.90}$$

$$\widehat{w}(\phi, z) = \widetilde{w}(\phi)Z_2(z). \tag{3.91}$$

Following Daley (1988)'s notation, substitution of these forms into the (simplified forms of) (3.16)-(3.20) then leads to the vertical structure equation

$$c_s^2\left(\frac{d}{dz} + \frac{N_s^2}{g}\right)\left\{\frac{1}{(N_s^2 - \sigma^2)}\left(\frac{d}{dz} + \frac{g}{c_s^2}\right)Z_1\right\} = \left(1 - \frac{c_s^2}{b_m}\right)Z_1, \tag{3.92}$$

and to the horizontal structure equation

$$H_m^\sigma\left(\widetilde{p}\right) = -\frac{a^2}{b_m}\widetilde{p}, \tag{3.93}$$

where

$$H_m^\sigma \equiv \frac{1}{\cos\phi}\frac{d}{d\phi}\left\{\frac{1}{(\sigma^2 - f^2)}\left(\frac{mf}{\sigma} + \cos\phi\frac{d}{d\phi}\right)\right\} - \frac{m}{\cos\phi\left(\sigma^2 - f^2\right)}\left(\frac{m}{\cos\phi} + \frac{f}{\sigma}\frac{d}{d\phi}\right), \tag{3.94}$$

is, to within a multiplicative factor, the Laplace tidal operator.

Eqs. (3.92) - (3.93) constitute a coupled pair of eigenvalue problems, one for the vertical structure and one for the horizontal structure. Note that the Earth's rotation rate directly enters only the horizontal structure problem, not the vertical structure one. However, both (3.92) and (3.93) each involve both eigenvalues (i.e. σ and b_m), suggesting that an iterative solution might be necessary. This is in fact the approach adopted by Kasahara & Qian (2000). However, as Daley (1988) noticed, for an *isothermal* reference state and constant g, implying both N_s^2 and c_s^2 are constant, (3.92) simplifies to

$$c_s^2\left(\frac{d}{dz} + \frac{N_s^2}{g}\right)\left(\frac{d}{dz} + \frac{g}{c_s^2}\right)Z_1 = \left(N_s^2 - \sigma^2\right)\left(1 - \frac{c_s^2}{b_m}\right)Z_1. \tag{3.95}$$

This means that the vertical structure equation can now be solved, independently of the horizontal structure equation, to determine the eigenvalue

$$\widetilde{\gamma} = \left(N_s^2 - \sigma^2\right)\left(\frac{1}{c_s^2} - \frac{1}{b_m}\right). \tag{3.96}$$

The horizontal structure equation (3.93) then becomes

$$H_m^\sigma\left(\widetilde{p}\right) + \frac{a^2}{c_s^2}\left(1 - \frac{\widetilde{\gamma}c_s^2}{\left(N_s^2 - \sigma^2\right)}\right)\widetilde{p} = 0, \tag{3.97}$$

which is a "straightforward" eigen problem for $\widetilde{p}$ and σ that defines the Hough functions (see e.g. Longuet-Higgins (1968)).

For an isothermal shallow atmosphere the vertical structure equation (3.95) can be solved analytically subject to the boundary conditions

$$\left(\frac{d}{dz} + \frac{g}{c_s^2}\right)Z_1 = 0, \tag{3.98}$$

at $z = 0$ and $z = z_T$. These conditions follow from $w = 0$ at $z = 0$ and $z = z_T$, via (3.18) - (3.20) with F set to zero. There are two types of solution.

The first corresponds to the "external" mode and

$$Z_1 \propto \exp\left\{-\left(1-\kappa\right)z/H\right\}, \tag{3.99}$$

$$Z_2 = 0, \tag{3.100}$$

where $\kappa = R/c_p$, and H is the scale depth of the atmosphere, given by $1/H \equiv -(1/\rho_s)d\rho_s/dz = g/\{(1-\kappa)c_s^2\}$ for an isothermal atmosphere. Thus the pressure perturbation is proportional to $\exp\left\{-\left(1-\kappa\right)z/H\right\}$, the horizontal velocity perturbation is proportional to $\exp\left\{\kappa z/H\right\}$ (recall that the velocity was scaled early in Section 3.3 by the basic state density $\rho_s\left(z\right)$), and the vertical velocity and potential temperature perturbations for these modes are identically zero.

The second corresponds to the "internal" modes, and for these

$$Z_1 \propto \left\{\Gamma\sin\left(k_z z\right) - k_z\cos\left(k_z z\right)\right\}\exp\left(-z/2H\right), \tag{3.101}$$

$$Z_2 \propto \left(\Gamma^2 + k_z^2\right)\sin k_z z \exp\left(-z/2H\right), \tag{3.102}$$

where $k_z = m\pi/z_T$ with m a positive integer. The corresponding perturbations in the physical variables (after appropriate re-introduction of the density scaling) have the following vertical structures:

$$\text{pressure perturbation} \propto \left\{\Gamma\sin\left(k_z z\right) - k_z\cos\left(k_z z\right)\right\}\exp\left(-z/2H\right), \tag{3.103}$$

$$\text{horizontal velocity perturbation} \propto \left\{\Gamma\sin\left(k_z z\right) - k_z\cos\left(k_z z\right)\right\}\exp\left(z/2H\right), \tag{3.104}$$

$$\text{vertical velocity perturbation} \propto \left(\Gamma^2 + k_z^2\right)\sin k_z z \exp\left(z/2H\right), \tag{3.105}$$

$$\text{potential temperature perturbation} \propto \left(\Gamma^2 + k_z^2\right)\sin k_z z \exp\left\{\left(1+2\kappa\right)z/2H\right\}. \tag{3.106}$$

3.7 Implications for choice of model variables and for vertical grid staggering

There is ongoing debate about what vertical arrangement of model variables is most appropriate for NWP and climate models, e.g. different versions of the Lorenz and Charney-Phillips grids. Of course the answer might depend on exactly which variables are chosen as model prognostic variables, and there is a related ongoing debate over which two thermodynamic variables from pressure (or a related variable such as logarithm of pressure or Exner function), density, temperature, and potential temperature are the most appropriate. The analysis of Section 3.6 above suggests a rational way to approach these questions.

The analysis of Daley (1988), on which Section 3.6 is based, implies that essentially only two vertical structure functions are needed to describe any normal mode of a shallow atmosphere at rest on a rotating planet: one for pressure and horizontal velocity, and one for potential temperature and vertical velocity. Although the vertical structure for horizontal velocity is not proportional to that for pressure (recall that the variables used in (3.87) - (3.91) have been scaled by a function of z) the two are related by a factor that does not change sign with z, so that they have the same zeros. Similar remarks apply to potential temperature and vertical velocity. Moreover, each zero of potential temperature lies between two zeros of pressure (except at the boundary), and each zero of pressure lies between two zeros of potential temperature. Density or temperature, on the other hand, would require a separate vertical structure function (see e.g .Kasahara & Qian (2000), who use density as one of their prognostic variables in their normal mode analysis). This follows from the linearized forms of the ideal gas equation and the definition of potential temperature in terms of temperature and pressure, which imply that the vertical structure functions for density and temperature are appropriately weighted combinations of those for pressure and potential temperature. Consequently the zeros of density or temperature do not coincide with those of either pressure or potential temperature.

This result suggests that numerical modelling of normal modes might be achieved most economically and accurately by using pressure and potential temperature as thermodynamic variables, and using a vertically staggered grid with pressure and horizontal velocity on one set of levels and potential temperature and vertical velocity on the intermediate levels (i.e. the Charney & Phillips (1953) grid staggering). Density or temperature should not be used since their structure for high vertical wavenumbers would not be accurately captured on either the horizontal velocity levels or the vertical velocity levels. As noted in Section 3.3 above, the extension to a deep atmosphere makes only small modifications to the energetically significant components of the normal modes, so this conclusion will remain valid for the deep-atmosphere case too.

This conclusion, however, has only been shown to be valid for free linear normal modes of a resting atmosphere. It would be valuable to know whether a similar conclusion holds for nonzero background flow and for forced modes (either diabatically or orographically forced). It should be possible to address these questions using linear analytic models. It would also be valuable to know whether a similar conclusion holds for strongly nonlinear (but near balance) flows typical of real weather systems. Yet another related issue is whether the choice of pressure and potential temperature as thermodynamic prognostic variables is also appropriate for the physical processes that must be parametrised.

3.8 Conclusions and discussion

Normal modes of a deep, rotating, spherical terrestrial atmosphere have structures and frequencies that are mostly very close to those of their shallow-atmosphere counterparts. Exceptions are the external Rossby and acoustic modes, which have weak but non-zero vertical velocity and potential temperature perturbations in a deep atmosphere, and long-zonal-wavelength internal acoustic modes, whose tropical structure is significantly modified by the $F \equiv 2\Omega \cos\phi$ Coriolis terms in a deep atmosphere. Differences in frequency between deep- and shallow-atmosphere modes were found to be less than 1%, and appear to be dominated by the geometrical differences between the deep- and shallow-atmosphere cases.

Inclusion of realistic vertical variation in the gravitational acceleration leads to a small but systematic decrease in the magnitude of normal mode frequencies, with the largest differences found being less than 1.5%.

For the Cartesian geometry case, the effects of retaining or omitting the F Coriolis terms (for which analytic solutions can be found) have been further explored. It has been confirmed, using both a perturbation analysis and numerical solution of the dispersion relation, that the F terms do indeed have only a small effect on normal mode frequencies. The F terms also have only a small effect on normal mode structures, except in three situations: very shallow gravity modes; very deep gravity modes; and long-zonal-wavelength acoustic modes. The long-zonal-wavelength acoustic mode case helps to explain some of the differences seen in full spherical geometry between between deep- and shallow-atmosphere normal modes (Section 3.3).

Another effect of retaining the F terms is that they give rise to a pair of new modes, dominated by inertia, with frequencies very close to f and with very strong vertical tilt. No evidence has been found for analogous new modes in the full spherical geometry deep-atmosphere case among the numerical solutions computed in Section 3.3. It is possible that such modes, if they do exist, have strongly tilted vertical structure or short vertical scales, at least locally like those in Fig. 3.10, putting them far beyond the resolution of our numerical solutions. On the other hand, the new modes appear to depend crucially on having frequency close to f; this could only hold locally on the sphere, which suggests that analogues of the new modes might not be possible on the sphere. The existence of such new modes on the sphere must remain, for the moment, an open question.

Although the inclusion of the F terms has only a small effect on the structure and frequency of adiabatic linear normal modes in large-scale flow, this does not rule out the possibility that they might be important for other kinds of flow. The F terms are related to the conservation of angular momentum, where angular momentum is defined using the full distance from the centre of the earth, not just the radius of the earth. Therefore they are likely to be most important when parcel vertical displacements are large. For example, the scale analysis of White & Bromley (1995) implies that the F terms are likely to be significant for tropical diabatic circulations. An air parcel raised from rest on the surface at the equator to a height of 10 km, conserving its full angular momentum on the way, would attain a westward velocity of about $1.5\,\mathrm{ms}^{-1}$. Convective mass fluxes from the cloud resolving model of Tompkins & Craig (1998) imply a convective transport timescale of about 10 days or less. If this timescale is appropriate for momentum transport too then this suggests a contribution to the upper tropospheric momentum budget of the order $0.1\,\mathrm{ms}^{-1}\mathrm{day}^{-1}$. This contribution is large enough to suggest that parametrisations of convection should attempt to take into account convective fluxes of the full angular momentum (notwithstanding the great difficulties that already exist in parametrising convective momentum fluxes), that is, to include the effects of the F terms acting on unresolved motions.

The F terms might be important when stratification is weak so that a major restriction on vertical motions is removed, for example in a near neutrally-stratified planetary boundary layer. As part of their large-eddy simulation (LES) study of the neutrally-stratified boundary layer, Mason & Thompson (1987) considered the impact of making the more complete f-F-plane approximation compared with the more usual f-plane approximation (though they did not use this terminology). Potential numerical issues aside, they found that retention of the extra Coriolis terms did lead to significant differences, in particular to an increased boundary-layer depth. The increased importance of the F terms when N_s^2 is small is consistent with the scale analysis of Phillips (1968) and with the conditions derived in Section 3.5 above for normal mode structures to be affected. Moreover, an LES is a strongly forced and strongly nonlinear flow, suggesting that the criteria for the F terms to be significant or negligible derived above for linear adiabatic normal modes might also have some value for forced, nonlinear flow.

The vertical structure of normal modes suggests that numerical models should be able to represent them most economically and accurately by using pressure and potential temperature as thermodynamic variables, and using a vertically staggered grid with pressure and horizontal velocity on one set of levels and potential temperature and vertical velocity on the intermediate levels. Density and temperature should be eliminated analytically since their structure for high vertical wavenumbers would not be accurately captured on either the horizontal velocity levels or the vertical velocity levels.

Finally, the following three sections give details of the numerical calculations and their results, as well as the derivation of (3.114), referred to previously.

3.9 Numerical solution for a deep rotating spherical atmosphere

The dynamical and thermodynamic variables are represented on a staggered grid as illustrated in Fig. 3.11. This allows straightforward centred differences and centred averages to be used to discretise equations (3.16)-(3.20). This problem can be converted to a matrix eigenvalue problem of the form

$$\mathbf{A}\mathbf{x} = \sigma\mathbf{x}, \tag{3.107}$$

where $\mathbf{x}$ consists of all of the values of $\widehat{u}$, $\widehat{v}$, $\widehat{w}$, $\widehat{p}$, and $\widehat{\theta}$.

Particular care must be taken with the boundary conditions. Values of $\widehat{w}$ and $\widehat{\theta}$ at the top and bottom boundaries are not included in the vector $\mathbf{x}$. When these values are needed to compute tendencies they are taken to be zero. To reduce the computational size of the problem only one hemisphere is considered. Eigenmodes are either symmetric or antisymmetric about the equator. To find symmetric modes, $\widehat{p}$ at a point immediately south of the equator is set equal to $\widehat{p}$ at its mirror image point north of the equator when computing $\widehat{p}_\phi$ in the $\widehat{v}$ equation on the equator. To find antisymmetric modes, $\widehat{p}$ south of the equator is set equal to $-\widehat{p}$ north of the equator.

At the pole fields must remain nonsingular. Different zonal wavenumbers require separate consideration. For $m = 0$, $\widehat{u}$ and $\widehat{v}$ must vanish at the pole but $\widehat{w}$, $\widehat{p}$, and $\widehat{\theta}$ can be finite and nonzero. The $\widehat{u}$ tendency is set to zero and the $\widehat{p}$ tendency equation needs to be modified to compute the latitudinal derivative of $\widehat{v}\cos\phi$ appropriately. For $m = 1$, $\widehat{w}$, $\widehat{p}$, and $\widehat{\theta}$ must vanish at the pole but $\widehat{u}$ and $\widehat{v}$ can be nonzero provided $\widehat{u} = \widehat{v}$ there. The $\widehat{u}$ tendency at the pole is set equal to an appropriately extrapolated $\widehat{v}$ tendency. The $\widehat{w}$, $\widehat{p}$, and $\widehat{\theta}$ tendencies are set to zero. For $m > 1$ all fields must vanish at the pole. The $\widehat{u}$, $\widehat{w}$, $\widehat{p}$, and $\widehat{\theta}$ tendencies are set to zero. In all cases no modification is needed to the $\widehat{v}$ tendency equation since $\widehat{v}$ is not stored at the pole.

Some numerical solutions were computed with $\Omega = 0$ and compared with those obtained for the one-dimensional non-rotating atmosphere problem (Section 3.4) to check the correctness of the code.

3.10 Mode frequencies for non-rotating atmosphere

Tables 3.2 and 3.3 show the numerically evaluated frequencies for a selection of modes in the shallow-atmosphere constant g case and the percentage change in frequency upon relaxing the constant g and shallow-atmosphere approximations. Table 3.2 is for global horizontal wavenumber $n = 1$; Table 3.3 is for $n = 1000$. An isothermal reference temperature profile of 250 K was used; the results for a US standard atmosphere (not shown) are very similar.

3.11 Gravity mode frequency bounds for "slightly deep" non-rotating atmospheres

The shallow-atmosphere version of (3.33) is

$$\left(\frac{\partial}{\partial r} - \Gamma\right)\left\{\frac{a^2}{N_s^2 - \sigma_0^2}\left(\frac{\partial}{\partial r} + \Gamma\right)\right\} R_0 - \left\{\frac{a^2}{c_s^2} - \frac{n(n+1)}{\sigma_0^2}\right\} R_0 = 0, \tag{3.108}$$

where a is the Earth's radius, and σ_0 and R_0 are the corresponding eigenvalue and eigenmode solutions for the shallow-atmosphere case. It can be determined how the frequency and structure of any shallow-atmosphere mode are perturbed in the deep-atmosphere case for a non-rotating atmosphere that is not very deep compared to the Earth's radius.

Write

$$r = a + z, \tag{3.109}$$

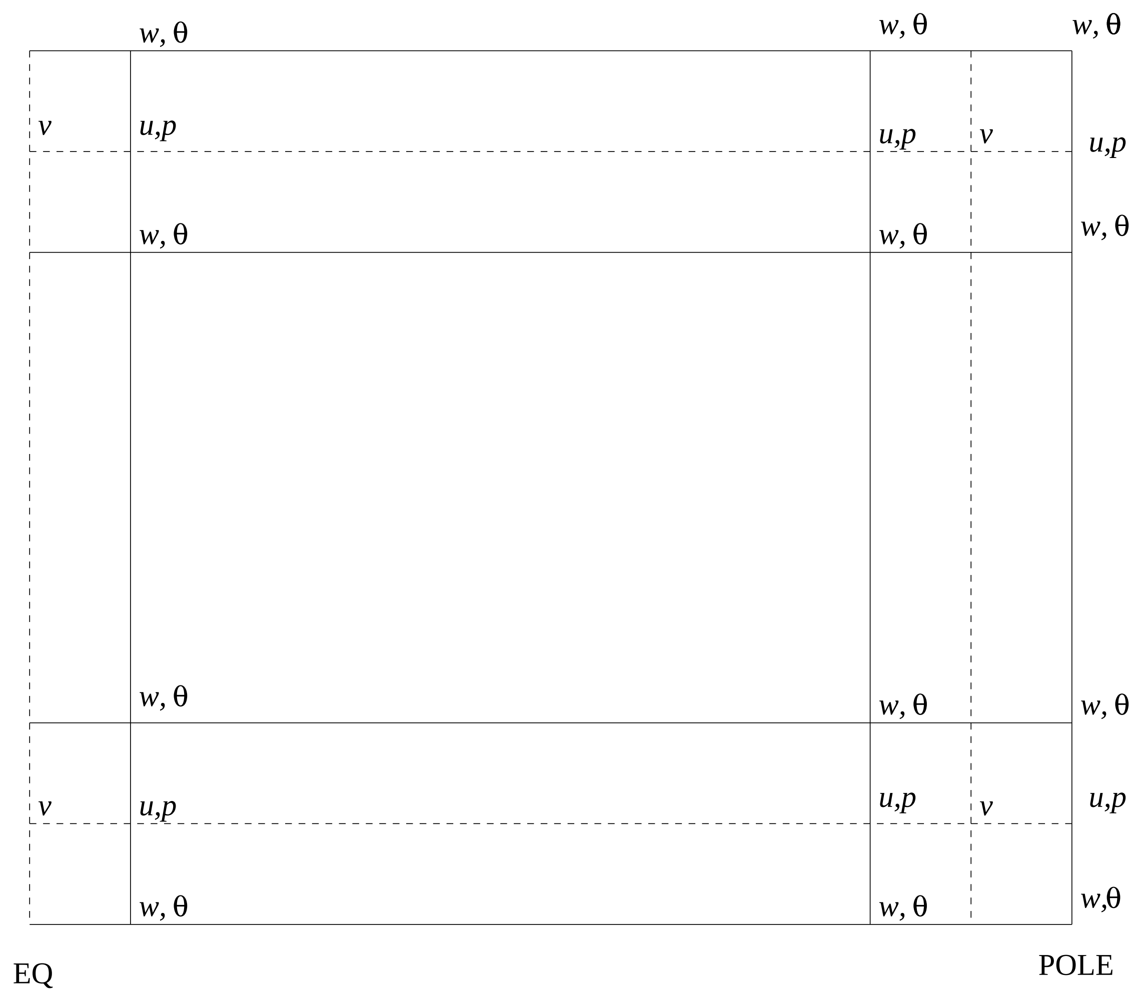

Figure 3.11: Distribution of variables on the staggered grid used to find normal modes of the deep-atmosphere equations.

	Shallow Constant g Frequency s^{-1}	Shallow Variable g % Change	Deep Constant g % Change	Deep Variable g % Change
External mode	0.7035E-04	0.00	-0.26	-0.26
1st internal GW	0.5511E-04	-0.24	-0.74	-0.98
2nd internal GW	0.4172E-04	-0.67	-0.65	-1.29
3rd internal GW	0.3190E-04	-0.91	-0.63	-1.50
1st internal AC	0.2498E-01	-1.04	-0.08	-1.08
2nd internal AC	0.3299E-01	-0.58	-0.06	-0.64
3rd internal AC	0.4314E-01	-0.32	-0.02	-0.35

Table 3.2: Horizontal wavenumber $n = 1$.

	Shallow Constant g Frequency s^{-1}	Shallow Variable g % Change	Deep Constant g % Change	Deep Variable g % Change
External mode	0.4977E-01	0.00	-0.26	-0.26
1st internal GW	0.1854E-01	-1.13	-0.05	-1.19
2nd internal GW	0.1701E-01	-1.12	-0.18	-1.29
3rd internal GW	0.1519E-01	-1.12	-0.26	-1.38
1st internal AC	0.5251E-01	-0.10	-0.74	-0.82
2nd internal AC	0.5724E-01	-0.10	-0.52	-0.61
3rd internal AC	0.6409E-01	-0.09	-0.39	-0.47

Table 3.3: Horizontal wavenumber $n = 1000$.

$$\widetilde{R}_1 = R_0 + R', \tag{3.110}$$

$$\sigma^2 = \sigma_0^2 + \varepsilon, \tag{3.111}$$

where z, R', and ε are considered to be small compared to a, R_0, and σ_0^2 respectively. Substituting in (3.33), subtracting (3.108), and dropping terms that are products of small quantities gives

$$\begin{aligned}\left(\frac{\partial}{\partial r} - \Gamma\right)\left\{\frac{a^2}{N_s^2 - \sigma_0^2}\left(\frac{\partial}{\partial r} + \Gamma\right)\right\} R' - \left\{\frac{a^2}{c_s^2} - \frac{n(n+1)}{\sigma_0^2}\right\} R' & \\ + \left(\frac{\partial}{\partial r} - \Gamma\right)\left\{\frac{a^2\varepsilon}{\left(N_s^2 - \sigma_0^2\right)^2}\left(\frac{\partial}{\partial r} + \Gamma\right)\right\} R_0 - \frac{n(n+1)\varepsilon}{\sigma_0^4} R_0 & \\ + \left(\frac{\partial}{\partial r} - \Gamma\right)\left\{\frac{2az}{N_s^2 - \sigma_0^2}\left(\frac{\partial}{\partial r} + \Gamma\right)\right\} R_0 - \frac{2az}{c_s^2} R_0 &= 0.\end{aligned} \tag{3.112}$$

Multiplying by R_0 and integrating from r_S to r_T, by parts where necessary using the boundary conditions $(\partial/\partial r + \Gamma)\, R_0 = 0$ and $(\partial/\partial r + \Gamma)\, R' = 0$, leads to

$$\varepsilon = -\frac{\int_{r_S}^{r_T} 2az \left[\frac{1}{\left(N_s^2 - \sigma_0^2\right)}\left\{\left(\frac{\partial}{\partial r} + \Gamma\right) R_0\right\}^2 + \frac{1}{c_s^2} R_0^2\right] dr}{\int_{r_S}^{r_T} \left[\frac{a^2}{\left(N_s^2 - \sigma_0^2\right)^2}\left\{\left(\frac{\partial}{\partial r} + \Gamma\right) R_0\right\}^2 + \frac{n(n+1)}{\sigma_0^4} R_0^2\right] dr}. \tag{3.113}$$

First consider the case in which a is set equal to r_S. Then, for the gravity modes, for which $N_s^2 - \sigma_0^2 > 0$, all terms in both the numerator and denominator are positive, implying that $\varepsilon < 0$. Then consider the case in which a is set equal to r_T; then z will be negative while all other terms will remain positive, so that $\varepsilon > 0$ for gravity modes. Thus for a deep atmosphere extending from r_S to r_T, the gravity modes have frequencies lying between those for a shallow atmosphere with $a = r_S$ and those for a shallow atmosphere with $a = r_T$, i.e.

$$\sigma_{a=r_T}^2 < \sigma_{deep}^2 < \sigma_{a=r_S}^2. \tag{3.114}$$

4 The grid structure

4.1 The co-ordinate system

As discussed in Section 1 the model is formulated in terms of the three independent spatial co-ordinates (λ, ϕ, r). The definition of these spherical polar co-ordinates is given in Fig. 4.1.

Aside :

Note that whilst the direction of rotation of the Earth has been indicated in this figure as if the Z-axis represents the rotational axis of the Earth, in general (λ, ϕ) are defined relative to an arbitrary co-ordinate pole.

In terms of these variables, the approximation to the mean sea level surface employed in the model is given by $r = a$ where a is the mean radius of this surface. A transformation of the vertical co-ordinate, r, is made into a generalised "terrain-following" vertical co-ordinate, η (see Appendix B for details). This transformation can be written in the form:

$$\eta = \eta(r, r_S, r_T), \tag{4.1}$$

where $\eta = 0$ on $r = r_S(\lambda, \phi)$ and $\eta = 1$ on $r = r_T$ =constant. Here $r_S(\lambda, \phi)$ is the height of the Earth's local surface which is assumed to depart from the mean sea level value, a, due only to local, orographic features, and r_T is the top of the model domain. Thus, in η-co-ordinates the integration domain is $0 \le \eta \le 1$. Since r_T is a constant and $r_S = r_S(\lambda, \phi)$, $\eta = \eta(r, \lambda, \phi)$ and therefore

$$r = r(\lambda, \phi, \eta). \tag{4.2}$$

Various possibilities for defining the precise functional forms of (4.1) and (4.2) are described and discussed in Appendix B, and Figs. 4.2 and 4.3 show schematics of these two vertical co-ordinates (see below for details of the index notation K applied to the vertical levels). Note that whilst depicted here as flat surfaces, in reality the surfaces of constant r are spherical, reflecting the approximate sphericity of the Earth (see Section 1 for further discussion of the definition of r).

Aside :

In the model code the three independent spatial co-ordinates are (λ, ϕ, η). Therefore, as (4.2) indicates, the value of r depends on all three spatial co-ordinates.

For example, for fixed η, its value will in general vary with λ and ϕ. Thus, in the code the variable r is stored as a three-dimensional array .

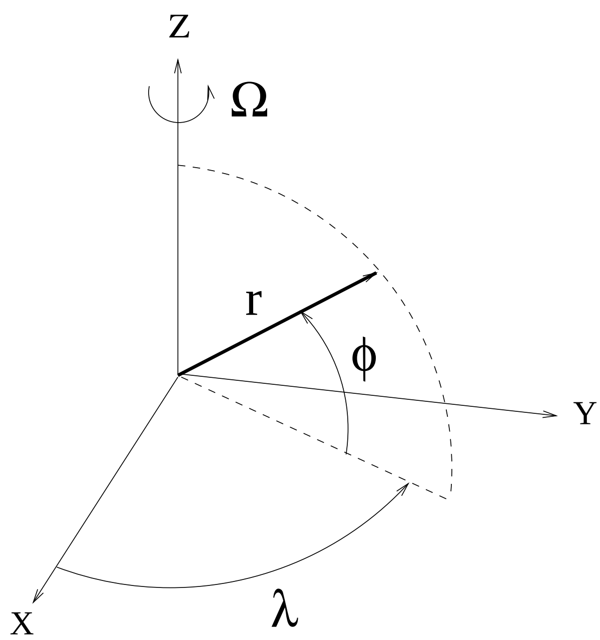

Figure 4.1: Definition of the spherical polar co-ordinates, (λ, ϕ, r), employed in the model.

4.2 The grid arrangement and storage of variables

The continuous equations summarised in Section 2 are discretized on grids defined independently in each of the three model co-ordinate directions (λ, ϕ, η). Since each of the grids is independent of the others, the position of any point on this discrete mesh of grid points can be identified by three unique indices (i, j, k). Each of these indices identifies a particular model co-ordinate plane in which one of the model co-ordinates is held constant (note that in physical space these model planes are in general non-planar surfaces). These are respectively the $\phi - \eta$, $\lambda - \eta$ and $\lambda - \phi$ planes. The grids have a staggered structure in all three directions. In the horizontal (the $\lambda - \phi$ plane) an Arakawa C-grid (Arakawa & Lamb 1977) is used whilst in the vertical (the $\lambda - \eta$ and $\phi - \eta$ planes) the Charney-Phillips grid staggering (Charney & Phillips 1953) is used. Thus, in each of the three co-ordinate planes, $(\lambda - \phi, \lambda - \eta, \phi - \eta)$, there are two distinct grid structures, each grid type alternating with the next. We distinguish the particular grid type by assigning to (i, j, k) either integral or half-integral values. Thus i has either an integral value, I, or a half-integral value, $I \pm 1/2$.

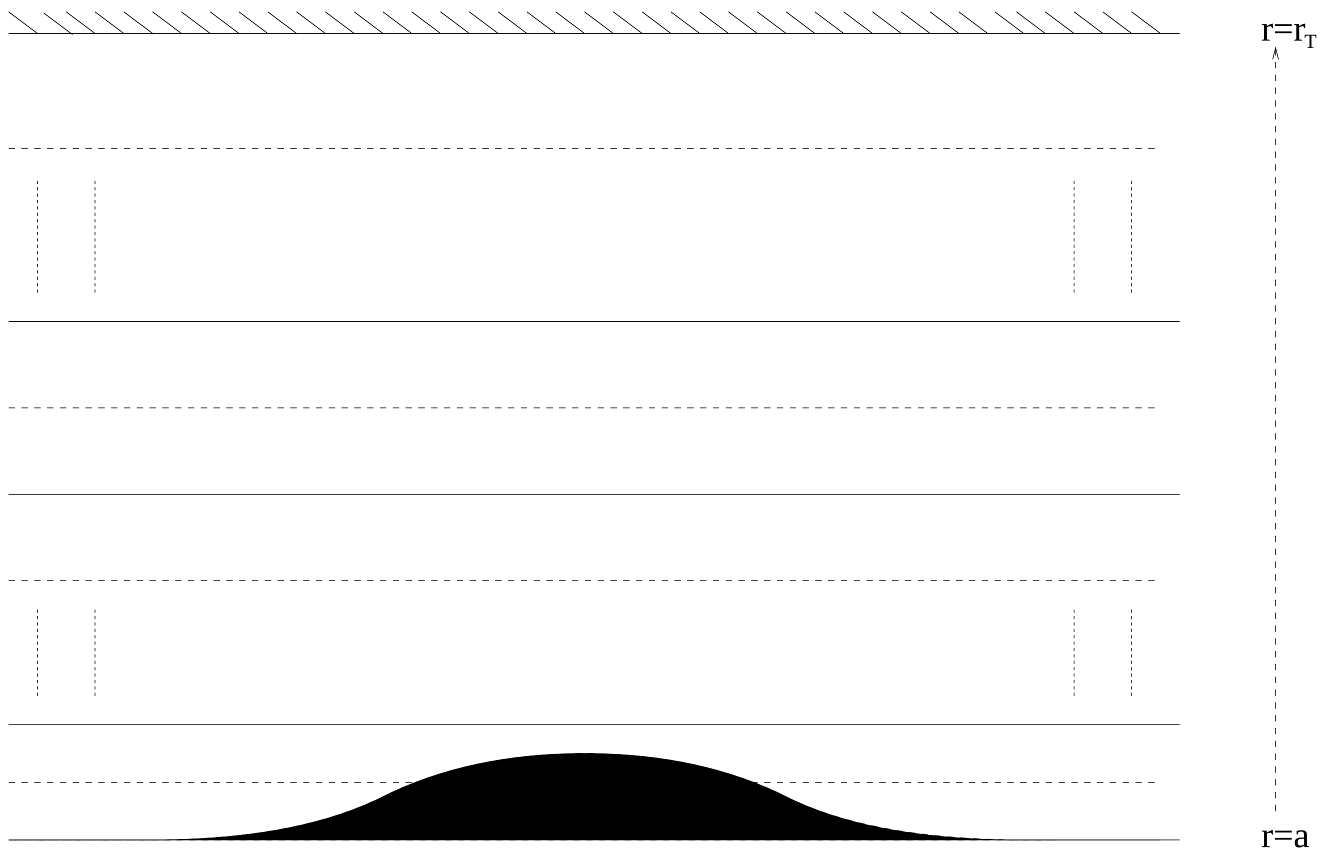

Figure 4.2: Schematic of surfaces of constant r.

Similarly, j takes values of either J or $J \pm 1/2$ and k takes values K or $K \pm 1/2$, for J and K integral.

In both horizontal directions, λ and ϕ, the grid spacing is uniform and equal respectively to $\Delta\lambda$ and $\Delta\phi$. Thus, $\lambda(i+1) = \lambda(i) + \Delta\lambda$ and $\phi(j+1) = \phi(j) + \Delta\phi$ for all i and j. Further, the integral and half-integral vertical planes are separated from each other by exactly one half grid length. Thus, $\lambda(i + 1/2) = \lambda(i) + \Delta\lambda/2$ and $\phi(j + 1/2) = \phi(j) + \Delta\phi/2$ for all i and j. In the vertical, however, a variable grid spacing is used and is determined from the prescribed values of $\eta(k)$ so that $\Delta\eta(k) \equiv \eta(k + 1/2) - \eta(k - 1/2)$. In general the half-integral horizontal planes (here horizontal means η held constant) are not equidistant from the two neighbouring integral horizontal planes and neither are the integral horizontal planes equidistant from their neighbouring half-integral horizontal planes. Thus, in general $\eta(k + 1/2) \neq \eta(k) + \Delta\eta(k + 1/2)/2$.

Aside :

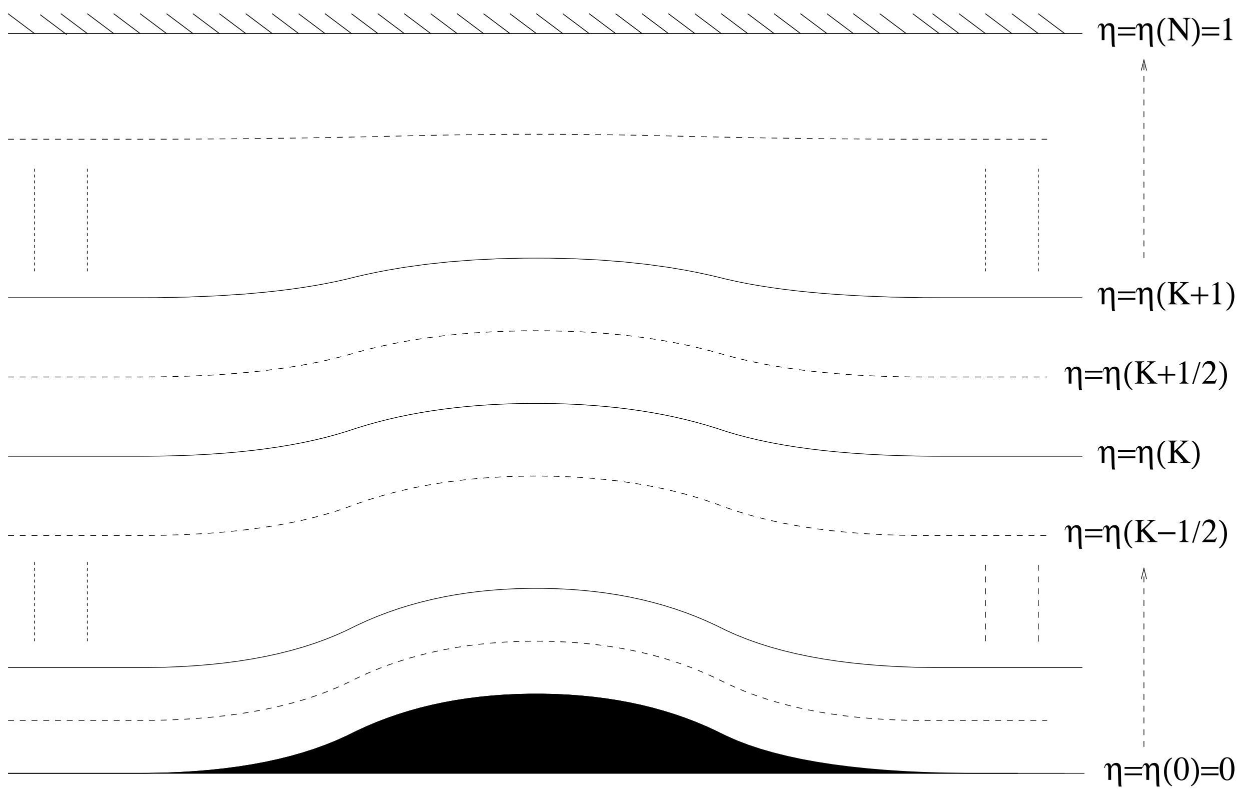

Figure 4.3: Schematic of surfaces of constant η.

ϕ is defined as latitude and is therefore zero at the equator. However, in the model's code, array indexing in the ϕ-direction starts at the South pole where $\phi = -\pi/2$.

Aside :

$\lambda_{1/2} \equiv 0$ is associated with v, w and scalar (Π, ρ, θ, m) points. For an unrotated mesh, $\lambda_{1/2} \equiv 0$ corresponds to the Greenwich meridian.

Aside :

Whilst the heights of the vertical grid levels are in principle arbitrary, to ensure that the finite-difference approximations to vertical spatial derivatives and vertical averages remain close to second-order accurate in the vertical spacing, the grid spacing between adjacent levels (integral to half-integral and half-integral to integral) should vary smoothly. Ideally, the height of each grid level should be obtained from a smooth, slowly varying analytic function of η (Kalnay de Rivas 1972).

Variable	Co-Location	i	j	k
Π		$I-1/2$	$J-1/2$	$K-1/2$
u		I	$J-1/2$	$K-1/2$
v		$I-1/2$	J	$K-1/2$
w		$I-1/2$	$J-1/2$	K
ρ	Π	$I-1/2$	$J-1/2$	$K-1/2$
θ	w	$I-1/2$	$J-1/2$	K
m	w	$I-1/2$	$J-1/2$	K
$\dot{\eta}$	w	$I-1/2$	$J-1/2$	K

Table 4.1: The storage of various model variables. (Here θ and m represent all variations of the thermodynamic and moisture variables respectively.)

All prognostic variables are co-located with one of the primary variables u, v, w or Π. Π is stored at the intersection of the three half-integral planes, i.e. it has index values of $(I \pm 1/2, J \pm 1/2, K \pm 1/2)$. u, v and w are each stored at points offset from Π-points by half a level in the direction of the wind component in question. Thus, u is stored at $(I, J \pm 1/2, K \pm 1/2)$ points, v at $(I \pm 1/2, J, K \pm 1/2)$ points and w at $(I \pm 1/2, J \pm 1/2, K)$ points. A schematic of the three-dimensional structure of the "grid molecule" is given in Fig. 4.4 and more details of this arrangement are given in Figs. 4.5, 4.6 and 4.7 for each of the half-integral planes. Note that in Figs. 4.6 and 4.7 a simple representation of the uneven grid spacing in the vertical, as discussed above, has been given.

Table 4.1 shows the arrangement of the primary and other variables. In FORTRAN only integer array referencing is permitted and so, for the chosen values of (i, j, k), the equivalent FORTRAN array indices for all the variables listed are identical and equal to (I, J, K). In general, a variable stored at the general point (i, j, k) has FORTRAN array indices of (I, J, K) where (I, J, K) are the nearest integers to (i, j, k) that are greater than or equal to (i, j, k). For example, $\Pi(i = I - 1/2, j = J - 1/2, k = K - 1/2)$ maps to the FORTRAN array element `exner`(I, J, K) so that specifically $\Pi(1/2, 1/2, 1/2)$ becomes `exner`$(1, 1, 1)$. Similarly, $u(1, 1/2, 1/2)$ maps to `u`$(1, 1, 1)$.

The structure of the integral planes can be deduced from the above figures and are not

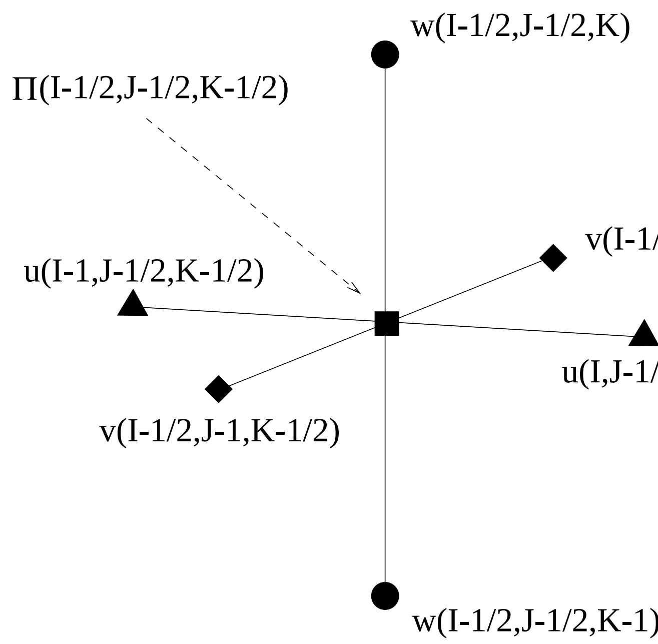

Figure 4.4: Schematic of the three-dimensional structure of the grid arrangement.

shown here. For i, j or k integral the plane only holds the u-, v-, and w-points respectively. (Note that none of the variables discussed here are stored at the intersection of the integral planes.)

4.3 Boundaries

4.3.1 Top and bottom boundaries

The formal top and bottom boundary conditions of an inviscid model, or sub-model, are those of a free-slip solid surface. Thus the normal vertical velocity ($\dot{\eta} \equiv D\eta/Dt$) is set to zero at the top and bottom of the model. It is therefore natural to place the upper and lower boundaries on w-points where $\dot{\eta}$ is stored. The resulting grid arrangement is shown in Fig. 4.8 for a vertical grid with $N+1$ w-points and N Π-points. It is important to note that the boundary condition is applied to $\dot{\eta}$ and not to w. $\dot{\eta}$ is the material rate of change of η whilst w is the material rate of change of r. Thus, $\dot{\eta}$ and w are equivalent only where surfaces of constant r and η coincide. Since the top of the domain is chosen to be a surface of constant r and, by construction, η is also constant there, surfaces of constant η and r coincide there and so the top boundary condition applies equally everywhere to both $\dot{\eta}$ and w. At the bottom of the domain whilst η, by definition takes a constant value, r does not

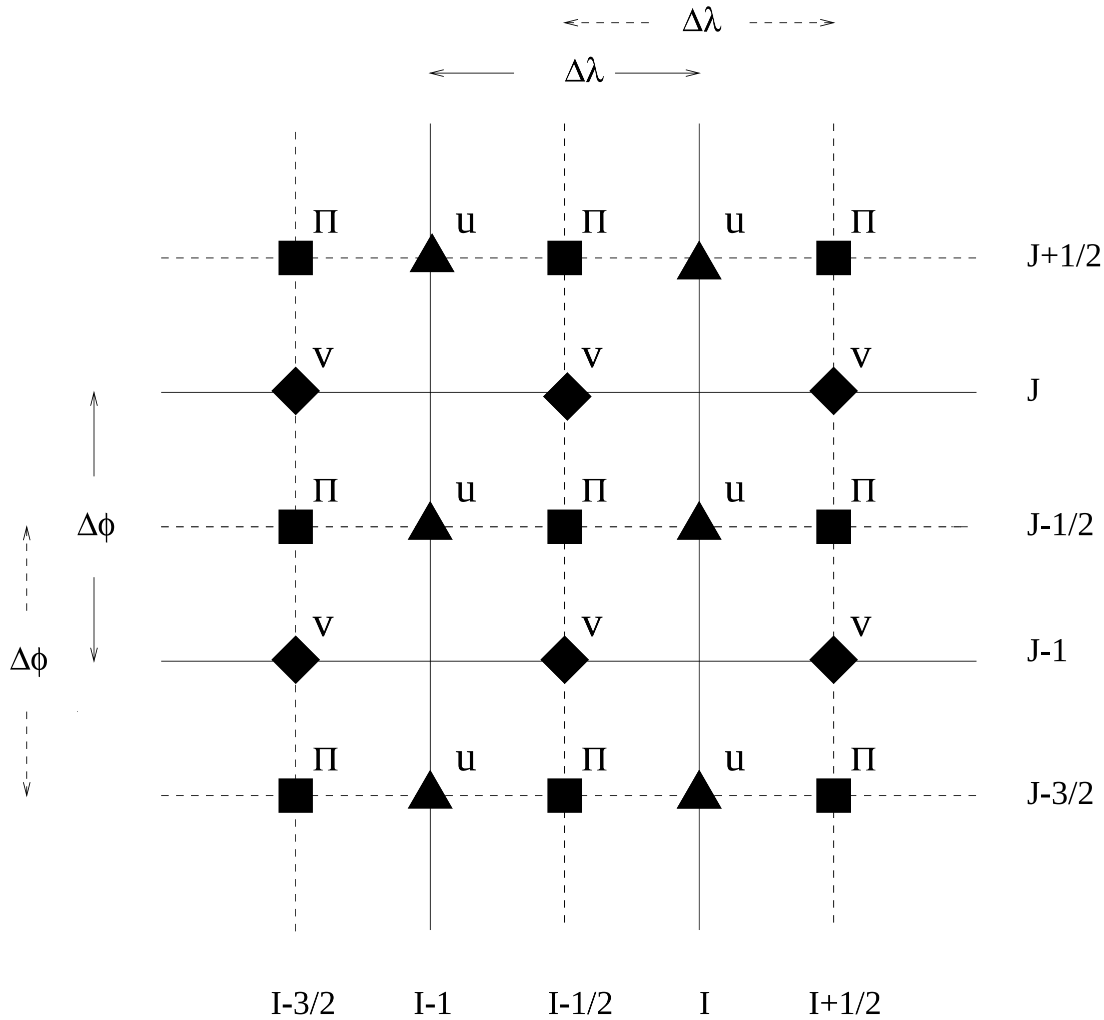

Figure 4.5: Arrangement of the primary variables, u, v and Π on the intermediate, horizontal ($k = K \pm 1/2$) planes of the Arakawa-C/Charney-Phillips grid.

and so, in general, w is non-zero at the surface. r only locally takes a constant value at the surface where the local surface is flat, i.e. over the ocean or over land in the absence of orography, and it is only in these special cases that w has a surface value of zero. This is shown schematically in Fig. 4.9.

4.3.2 Lateral boundaries

Global model For the global model, the lateral boundary conditions in the East-West, or λ-direction are those of periodicity. In the North-South, or ϕ-direction, there are two co-ordinate poles at $\phi = \pm\pi/2$. There is a choice as to whether the co-ordinate poles occur on integral or half-integral $\lambda - \eta$ planes. In the model the poles currently coincide with the

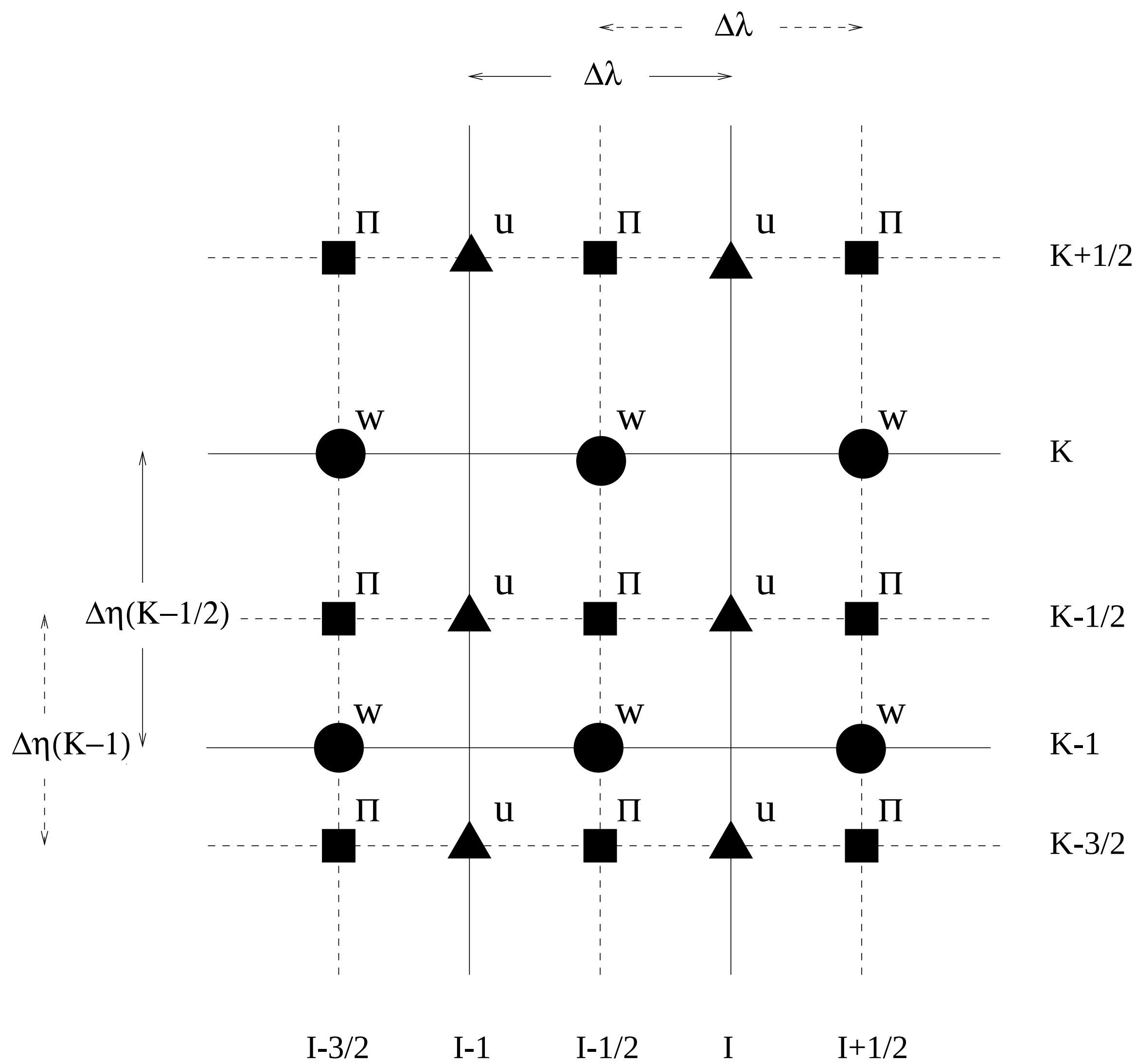

Figure 4.6: Arrangement of the primary variables, u, w and Π on the intermediate, vertical ($j = J \pm 1/2$) planes of the Arakawa-C/Charney-Phillips grid.

extreme half-integer planes, i.e. $j = 1/2$ and $M - 1/2$, where there are assumed to be M Π-points and $M - 1$ v-points, in the ϕ-direction. Thus, the Π- and u-points have pole points but the v-points do not. Figure 4.10 shows this arrangement. At the poles all values of Π are set equal. This is true also for the scalar variables ρ, θ, and m, as well as w, which are all stored at the poles. The values of u at the poles are diagnosed from the surrounding v components of the wind by a vector wind calculation (McDonald & Bates 1989). To show how this arrangement is accommodated in the array storage used in the model, Figure 4.11 is in the same form as 4.5 but shows the positions of the poles and the East-West boundaries. The South and North poles lie on the bold lines corresponding to $j = 1/2$ and

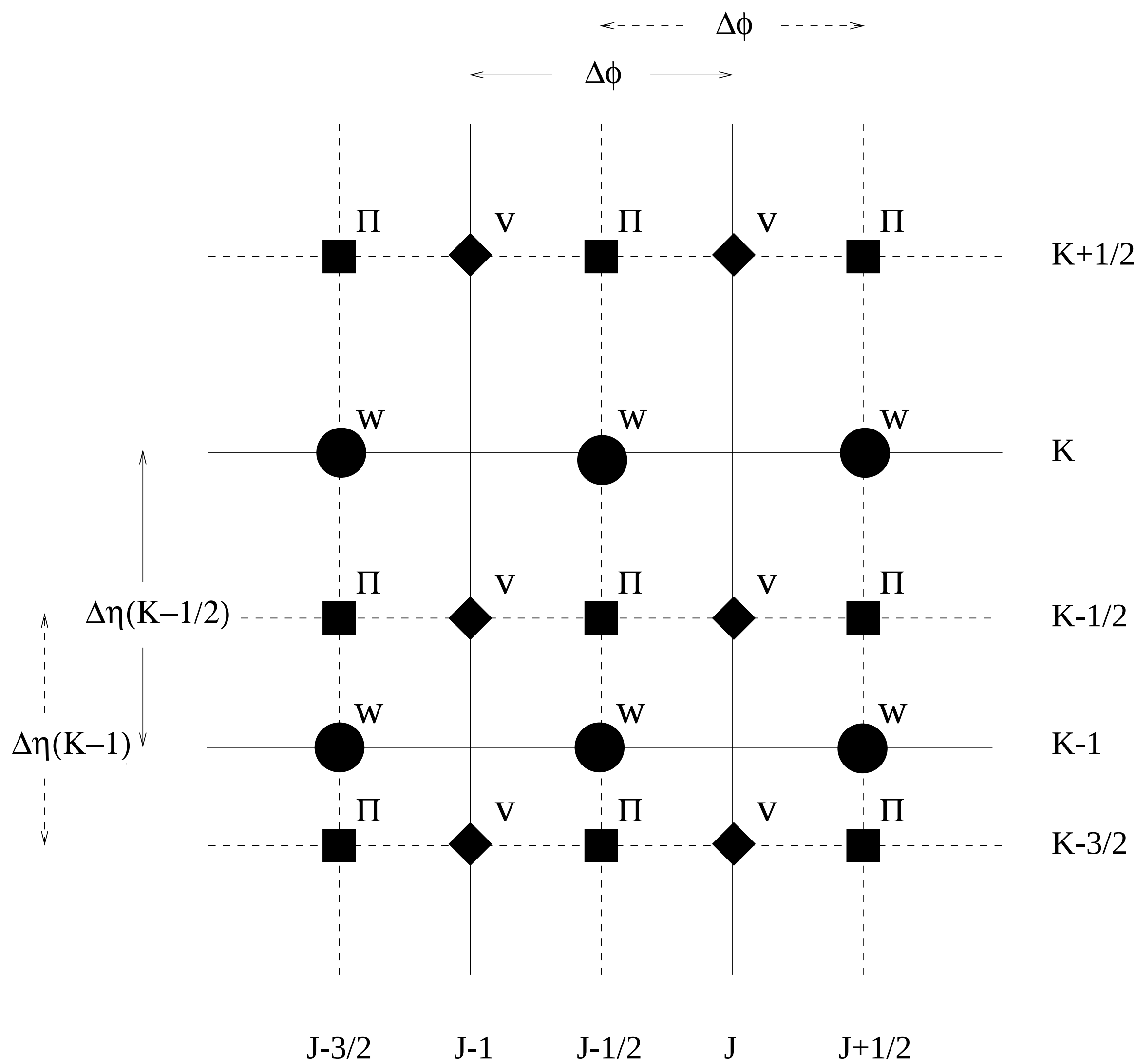

Figure 4.7: Arrangement of the primary variables, v, w and Π on the intermediate, vertical $(i = I \pm 1/2)$ planes of the Arakawa-C/Charney-Phillips grid.

$j = M - 1/2$, respectively. In the lateral, East-West, direction periodicity is obtained by requiring that $\lambda(-1/2) = \lambda(L - 1/2) - 2\pi$, $\lambda(0) = \lambda(L) - 2\pi$, $\lambda(L + 1/2) = \lambda(1/2) + 2\pi$ and $\lambda(L + 1) = \lambda(1) + 2\pi$ and that all functions, f, of λ satisfy $f(\lambda \pm 2\pi) = f(\lambda)$.

Limited area model For the limited area model the boundary values of the two horizontal components of wind, u and v, are specified. Their values are usually supplied from the global model. Figure 4.12 shows the positioning of the boundaries in the horizontal plane for a grid with L Π-points and $L - 1$ u-points, in the λ-direction, and M Π-points and $M - 1$ v-points, in the ϕ-direction (note though that all arrays are dimensioned to be $L \times M$). Where

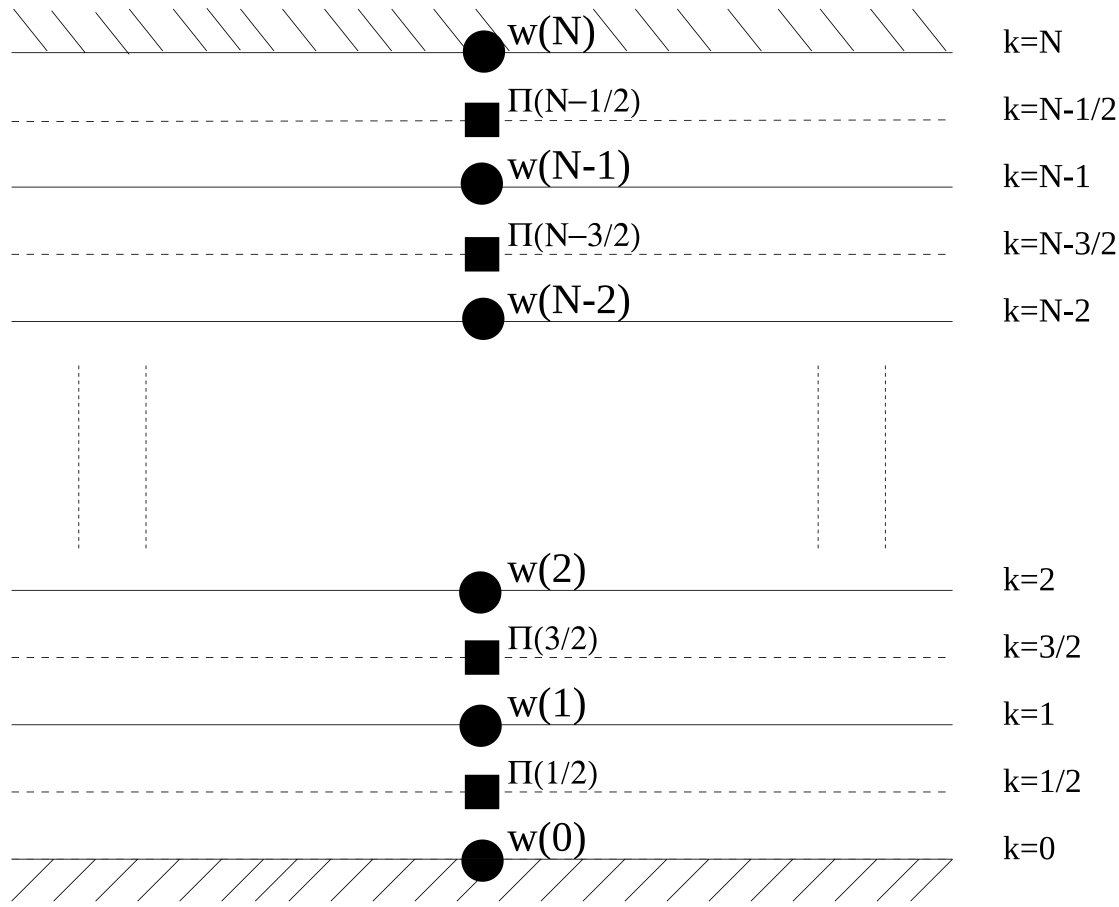

Figure 4.8: Arrangement of the vertical grid structure relative to the top and bottom boundaries.

information regarding boundary values of Π is required it is assumed that the boundary-normal Π'-gradient (equal to the gradient of $\Pi^{n+1} - \Pi^{n}$, where n indicates the time level) is zero on the boundary.

Aside :

The details and validity of the boundary conditions applied on Π need reconsideration.

Aside :

As can be seen from Fig. 4.12, currently the boundaries at the East and West sides of the limited area domain lie along the v-momentum points whilst those at the North and South sides of the domain lie along the u-momentum points. Since all the lateral boundaries coincide with surfaces of constant λ (for the East-West boundaries) and of constant ϕ (for the North-South boundaries) consideration of

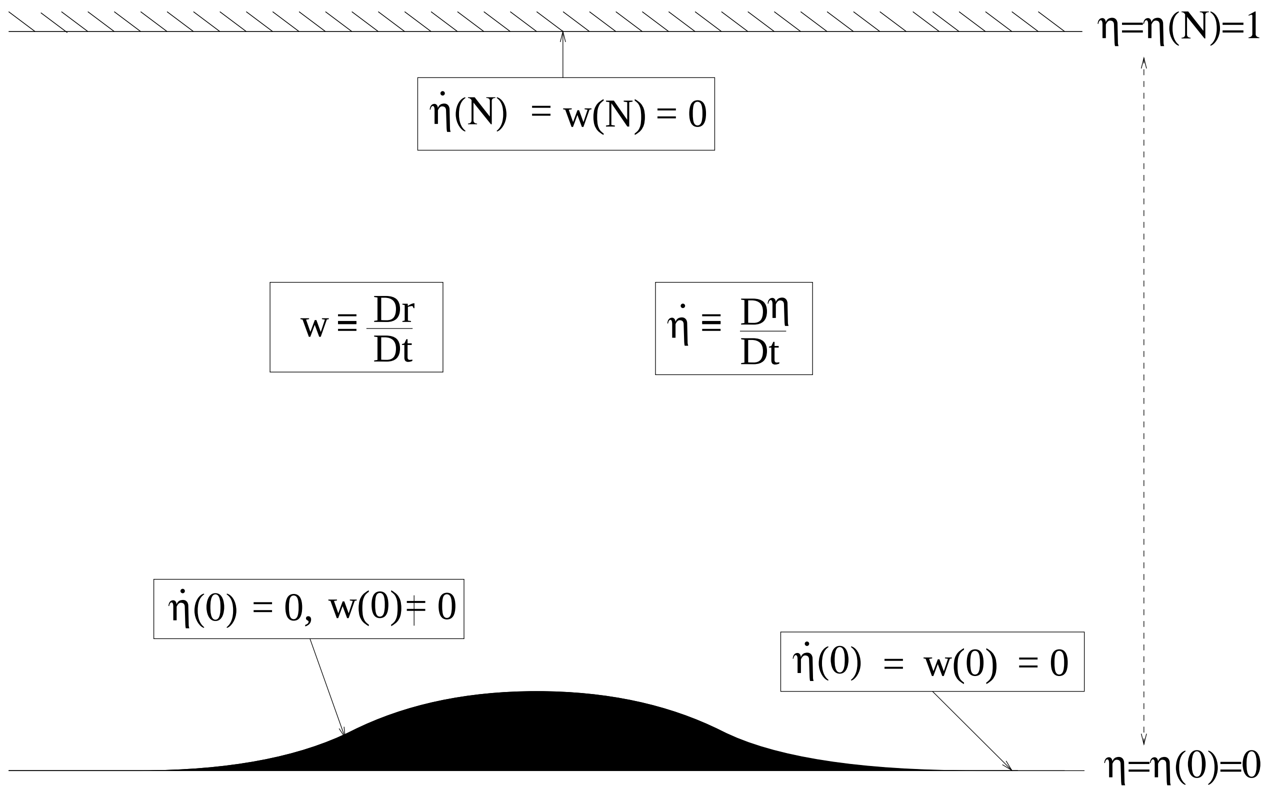

Figure 4.9: Top and bottom boundary conditions.

conservation of such quantities as mass and momentum within the limited area domain, applied to the continuous equations, suggests the natural boundary conditions (for the momentum equations) are specification of the normal velocity components at each of the domain sides. This then suggests that for the discrete model, the natural position for the boundaries is for them to lie on grid points associated with the velocity components normal to the boundaries. This would also both be consistent with the approach used for the vertical grid structure and also make it straightforward to simulate contained flows. With this arrangement the East and West sides of the limited area domain would lie along the u-momentum points and the North and South sides of the domain lie along the v-momentum points. This is how the model was originally coded (James 1997, unpublished) and this approach should be reconsidered. Figure 4.13 shows this alternative arrangement. Note that with the notation used here, whilst this grid has the same total number of grid points and the same number of interior Π*-points as there are*

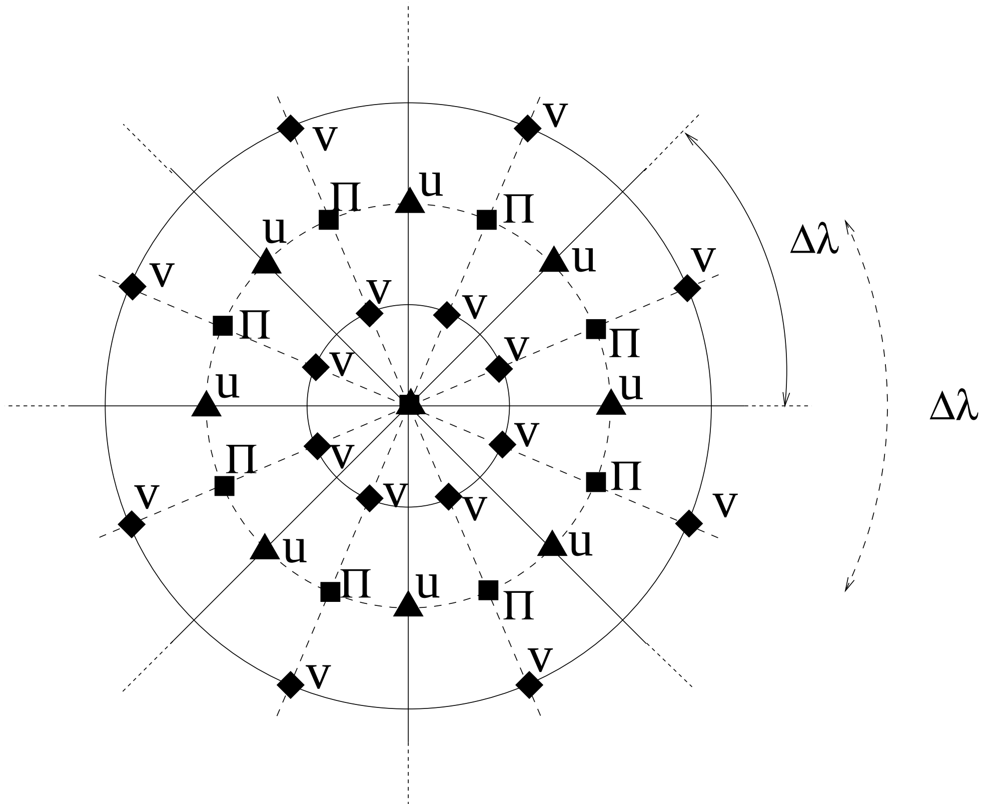

Figure 4.10: Arrangement of grid points and variables relative to either of the two co-ordinate poles. Note that the pole itself is both a u- and Π-point.

in Fig. 4.12, the number of interior u-points in the λ-direction, and the number of interior v-points in the ϕ-direction have both been reduced by 2.

Aside :

In addition to specifying values at the boundary itself, within an interior boundary zone the model's prognostic variables are relaxed, over a specified number of mesh lengths (currently up to 8 mesh lengths are used), towards values specified by the global model. Thus, for the generic variable F, say, within the interior boundary zone, its predicted value, F^L, is blended with its given global model value, F^G, to give the actual new value, F^{new}, as:

$$F^{new} = \omega(\lambda, \phi)F^G + (1 - \omega(\lambda, \phi))F^L, \tag{4.3}$$

where $\omega(\lambda, \phi)$ varies continuously and monotonically across the boundary zone from a value of unity at the outer boundary to zero at the inner one, varying only

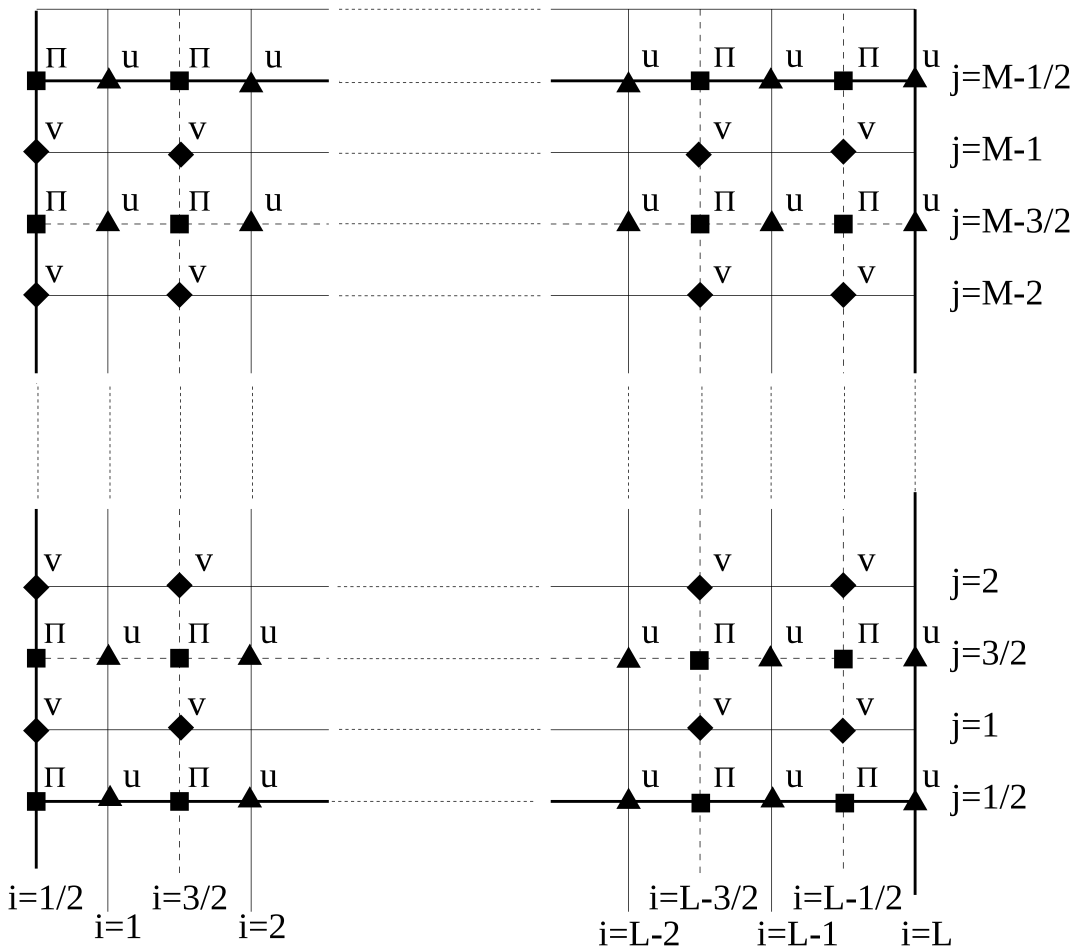

Figure 4.11: As for Fig. 4.5, but here showing the position of the lateral boundaries for the global model.

with λ across the East-West boundary zones and only with ϕ across the North-South boundary zones, the largest value of these two functions being used in the four corner zones where the North-South and East-West boundary zones overlap.

Staniforth (1997) highlights a potential danger of the use of this form of blending. If both the global model fields and the limited-area model fields are in horizontal geostrophic balance, with no vertical motion and in the absence of orography, then, if we consider the flow in the East-West direction, u^G, θ_v^G, Π^G and u^L, θ_v^L, Π^L satisfy the following, continuous equations (see Section 2):

$$f_3 u^G + \frac{c_p}{r}\theta_v^G \frac{\partial \Pi^G}{\partial \phi} = 0, \tag{4.4}$$

$$f_3 u^L + \frac{c_p}{r}\theta_v^L \frac{\partial \Pi^L}{\partial \phi} = 0. \tag{4.5}$$

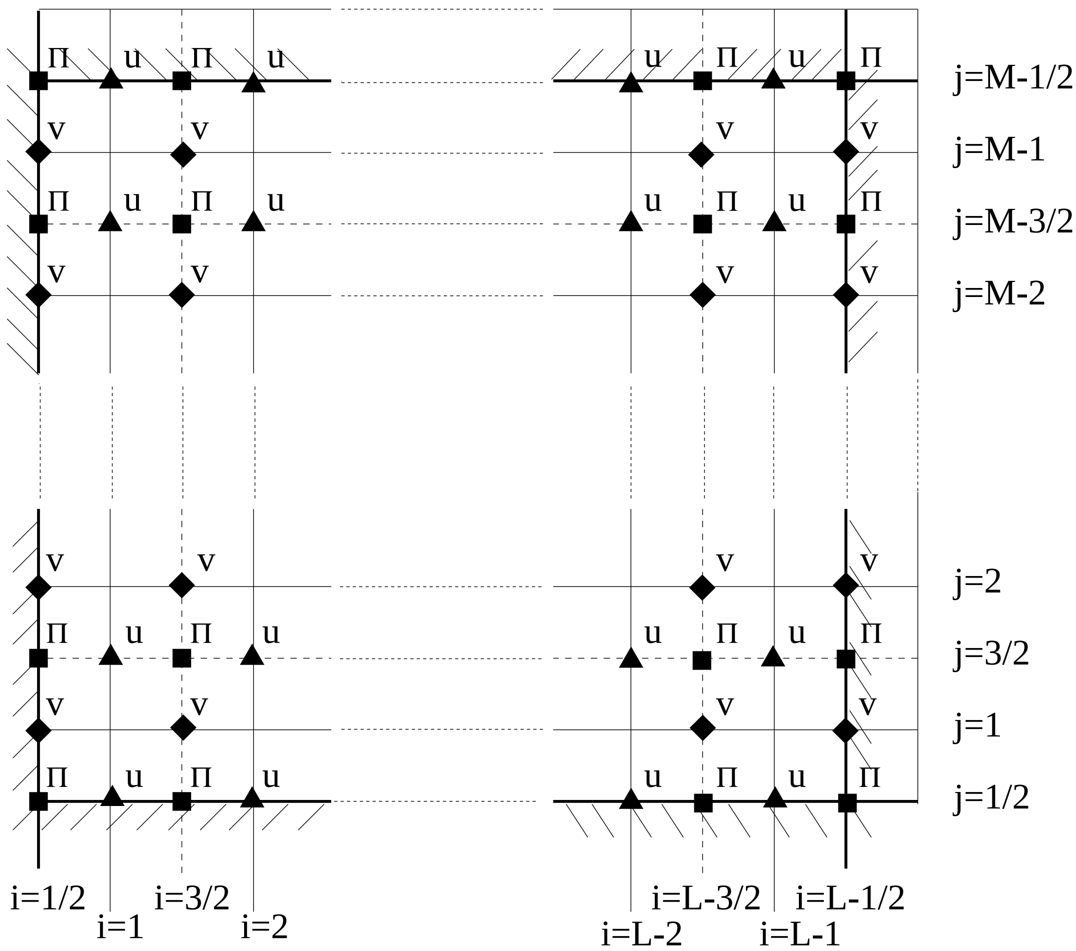

Figure 4.12: As for Fig. 4.5, but here showing the position of the lateral boundaries for the limited area model.

Here the metric terms have been neglected, as is usual in defining the geostrophic wind.

Using (4.3) *we can evaluate the blended values of* u, θ_v *and* Π *as* u^{new}, θ_v^{new} *and* Π^{new}. *Since the two original states are in geostrophic balance and the operator defined in* (4.3) *is linear, we might naively hope that the blended state is also in geostrophic balance so that:*

$$f_3 u^{new} + \frac{c_p}{r}\theta_v^{new}\frac{\partial \Pi^{new}}{\partial \phi} = 0. \tag{4.6}$$

However, inserting (4.4) *and* (4.5) *into* (4.3) *it can be seen that in fact:*

$$f_3 u^{new} + \frac{c_p}{r}\theta_v^{new}\frac{\partial \Pi^{new}}{\partial \phi} = \frac{c_p}{r}\left[\omega(1-\omega)(\theta_v^G - \theta_v^L)\frac{\partial}{\partial \phi}\left(\Pi^L - \Pi^G\right) + \frac{\partial \omega}{\partial \phi}\theta_v^{new}(\Pi^G - \Pi^L)\right]. \tag{4.7}$$

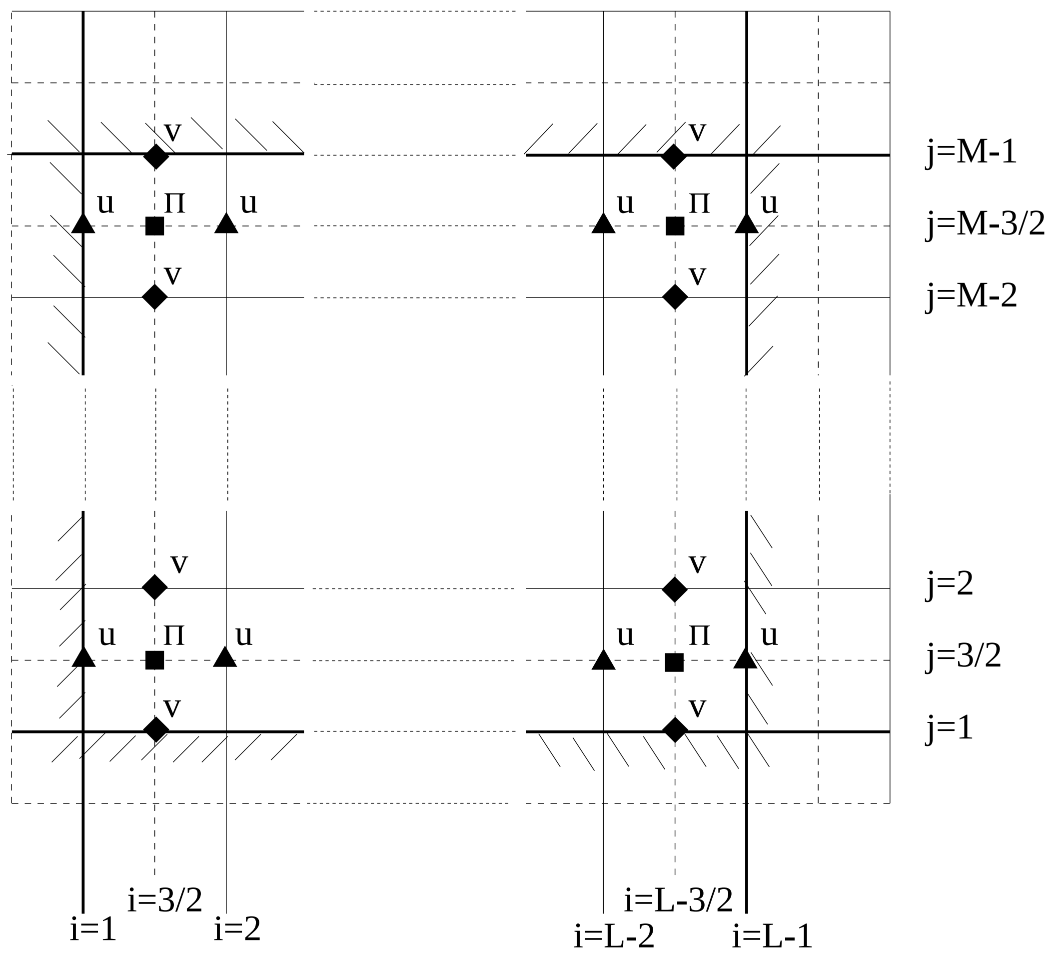

Figure 4.13: As for Fig. 4.12 but showing alternative positioning of the lateral boundaries.

The global and limited area fields will in general be different from each other, for example due to different grid resolutions. Therefore, in general, (4.7) *reduces to* (4.6) *only if both* $\omega(1-\omega) = 0$ *and also* $\partial\omega/\partial\phi = 0$. *Only in this case will the blended fields preserve the geostrophic balance of the original fields, otherwise the blending will introduce a spurious acceleration of, in this example, the North-South wind component,* v, *which may destabilise the dynamic balance of the flow. This departure from our naive anticipation* (4.6) *arises in the first place due to the non-linearity of the terms involving* θ_v *and* Π *in* (4.4) *and* (4.5) *(responsible for the term involving* $\omega(1-\omega)$ *in* (4.7)*) and in the second place due to the non-commutativity of differentiation with respect to either* λ *or* ϕ *and the operator defined by* (4.3) *(this aspect is responsible for the term involving* $\partial\omega/\partial\phi$ *in* (4.7)*).*

The departure of the blended flow from the balanced state can, in general, be *reduced by making ω vary slowly thereby reducing the impact of the term in* (4.7) *involving $\partial\omega/\partial\phi$. This slow variation can be achieved by making the width of the boundary zones as large as is feasible. However, this approach does not reduce the impact of the $\omega(1-\omega)$ term in* (4.7) *since whatever the particular functional form of ω, $\omega(1-\omega)$ attains its maximum value of* 1/4 *at some point within the boundary zone. Thus, the required geostrophic balance cannot in general be maintained within the boundary zone. Despite this though, it is clearly desirable that the blending procedure should not disrupt the balance at either the outer boundary or the inner one. Since, by construction $\omega = 1$ at the outer boundary and $\omega = 0$ at the inner, $\omega(1-\omega)$ is guaranteed to vanish at both of these boundaries and so the requirement for the maintenance of balance at both boundaries reduces to requiring that $\partial\omega/\partial\phi$ vanishes there. The simplest non-trivial polynomial that can be arranged to satisfy this requirement is a cubic. It would be interesting in the future to investigate what impact the use of such a blending function has on limited-area integrations of the model.*

4.4 Discretization

Discrete differential and averaging operators are defined on the grids described here using second-order, centred calculations. Thus, if the result of such an operation is required on a particular grid point the sums or differences of variables are calculated using values of the variable held on the grid points displaced half an integer in each appropriate direction from the grid point of interest. Further details of this procedure and associated notation are given in Appendix C.

Aside :

It is important to note that at present the model is coded in terms of a mix of the two vertical variables η and $r(\lambda,\phi,\eta)$. Since r is itself a function of λ and ϕ, the operation of averaging in the vertical over r does not commute with horizontal averaging in either the λ- or ϕ-directions. As, in the model, r is only stored on Π- and w-points, where mixed horizontal and vertical (in r) averages are required, the vertical averaging is performed first if the variable lies on a Π-or w-point followed by the horizontal average. But, for variables stored elsewhere, the horizontal *averaging is performed first in order to obtain an estimate of the variable on either a* Π*-or* w*-point where the vertical averaging can be straightforwardly performed. For example, if we wish to evaluate the vertical (in* r*) and horizontal (in the* λ*-direction for example) average of* Π*, we first average* Π *in the vertical direction to obtain an estimate of* Π *on a* w*-point and then we perform the horizontal average in the* λ*-direction, i.e. as* $\overline{\overline{\Pi}}^{r\lambda}$*. In contrast, if we wish to evaluate the vertical (in* r*) and horizontal average of* u*, we first perform the horizontal average in the* λ*-direction to obtain an estimate of* u *on a* Π*-point and then perform the average in the vertical, i.e. as* $\overline{\overline{u}}^{\lambda r}$*. In the documentation the order of the averaging operators has been given in the same order as it appears in the model code. Note, that this complication does not arise with vertical averaging over* η *as this operation does commute with averages in both the horizontal directions.*

5 Off-centred, semi-implicit, semi-Lagrangian time discretisation

For its time discretisation, the New Dynamics does not use the familiar Eulerian decomposition in which material derivatives are separated into local rates of change and advection terms. Instead it uses a *semi-Lagrangian* treatment. Material derivatives are retained intact, and next-timestep values at the gridpoints are found by integrating along interpolated trajectories.

An outline of the semi-Lagrangian technique is given in subsection 5.1. Later subsections deal with key features of the New Dynamics application of it: curvature aspects of the momentum equation in spherical polar coordinates (5.2), interpolation (5.3), and the trajectory calculation (5.4, 5.5). In our context, the advantages of the semi-Lagrangian technique are its stability even when long timesteps are taken, and the absence of Eulerian advection terms. The conceptual advantages of its trajectory emphasis are also worth noting. For detailed accounts of the technique's strengths and weaknesses, see Staniforth & Côté (1991) and Numerical Methods course notes available on the Internal Web.

The previous paragraphs give a simplified view in at least three respects. Although semi-Lagrangian treatments are used for the momentum, thermodynamic and moisture equations in the New Dynamics, an Eulerian treatment of the continuity equation is used in current versions; see Section 8. Also, the semi-Lagrangian treatment applied to the thermodynamic equation is of a mixed type ("non-interpolating in the vertical") which will be described in Section 9. Finally, as we shall note in Sections 5.2 and 5.4 below, semi-Lagrangian schemes may be subject to numerical instabilities if certain extrapolation procedures are used.

5.1 Outline of the semi-Lagrangian method

Consider the first order prognostic equation

$$\frac{DF}{Dt} = \Psi \, , \tag{5.1}$$

in which D/Dt is the material derivative, F is a scalar variable, and Ψ is a source term - which may involve F. (We consider later how a vector prognostic variable may be treated.)

Eq. (5.1) may be integrated *between times* $t^n = n\Delta t$ *and* $t^{n+1} = t^n + \Delta t$ *following the* *parcel of air that arrives at gridpoint* $\mathbf{x}_a$ *at time* t^{n+1}. The gridpoint $\mathbf{x}_a$ is called the *arrival point*. The change in F for the parcel that arrives at $\mathbf{x}_a$ at time t^{n+1} is simply the integral of Ψ along its trajectory over the relevant time interval:

$$F^{n+1} - F_d^n = \int_{t^n}^{t^n+\Delta t} \Psi dt = \overline{\Psi}\Delta t\,. \tag{5.2}$$

Here F^{n+1} is the value of F at time t^{n+1} at the arrival gridpoint $\mathbf{x}_a$, i.e.

$$F^{n+1} \equiv F\left(\mathbf{x}_a,\, t^{n+1}\right)\,, \tag{5.3}$$

and F_d^n is the value of F for the same parcel of air but at time t^n, i.e.

$$F_d^n \equiv F\left(\mathbf{x}_d,\, t^n\right), \tag{5.4}$$

where $\mathbf{x}_d$ is the location of the parcel at time t^n. The location $\mathbf{x}_d$ is called the *departure point* of the parcel. As shown in Fig. 5.1,thearrival point $\mathbf{x}_a$ is always a gridpoint, but the departure point $\mathbf{x}_d$ is generally **not** a gridpoint; we consider later how $\mathbf{x}_d$, and F_d^n, may be estimated from the available gridpoint fields. In (5.2), $\overline{\Psi}$ is the (time) average of Ψ along the trajectory from the departure point $\mathbf{x}_d$ (at $t = t^n$) to the arrival point $\mathbf{x}_a$ (at $t = t^{n+1}$). Like $\mathbf{x}_d$ and F_d^n, $\overline{\Psi}$ has to be estimated from the available gridpoint values.

Eq. (5.2), which contains no Eulerian advection terms, is an exact integral of (5.1);it involves *no* truncation error. In practice, errors are inevitably introduced: via the estimation of the departure point $\mathbf{x}_d$, via the estimation of the departure-point value F_d^n, and via the estimation of the trajectory time-average $\overline{\Psi}$. These estimations require interpolation and integration (but not differentiation). Eq. (5.2) does not explicitly involve the value (F^n) of F at the arrival point at the previous time-level n, but F^n will feature in the interpolation used to estimate F_d^n (see 5.3-5.5) if the Courant number $U\Delta t/\Delta x$ is sufficiently small. (Here U is the flow speed and Δx is the grid spacing.)

With local exceptions (to be signposted where they occur) the notationusedin (5.2) - (5.4) will be adhered to in this documentation:

- superscripts indicate the time-level (e.g. F^{n+1});
- quantities evaluated at the departure point ($\mathbf{x}_d$) carry a subscript d (e.g. F_d^n);
- the (generic) arrival point is indicated as $\mathbf{x}_a$;
- superscripted quantities evaluated at the arrival point are *not* subscripted (e.g. F^{n+1});

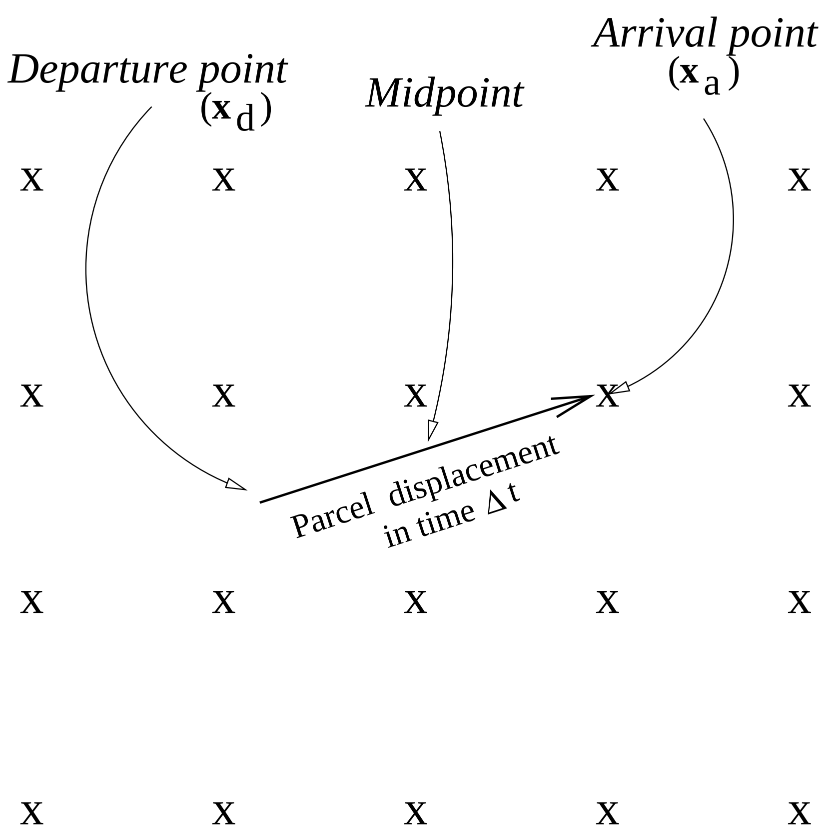

Figure 5.1: Illustrating in 2D an *arrival point* and the corresponding *departure point.* The arrival point is always at a gridpoint (**X**), but the departure point is generally not. The available gridpoint data must be used both to locate the departure point and to interpolate the advected fields to it.

• quantities having neither subscripts nor superscripts are to be regarded as continuously varying (e.g. t).

The use of a subscript to identify the arrival point $\mathbf{x}_a$ is largely limited to this section, and avoids confusion with the use of $\mathbf{x}$ to indicate a continuously-varying space coordinate.

Eq. (5.2) representsa *two-time-level* scheme, Δt being the time-step. [See the third *Aside* at the end of this subsection for discussion of *three-time-level* schemes.] The trajectory time-average $\overline{\Psi}$ may be approximated by a weighted average of the values of Ψ at the departure and arrival points:

$$\overline{\Psi} \equiv \alpha \Psi^{n+1} + (1-\alpha)\,\Psi_d^n\,. \tag{5.5}$$

The key parameter in (5.5) is α, the *trajectory weighting factor.* α is the next-time-level (t^{n+1}) weight, and $(1-\alpha)$ is the current time-level (t^n) weight. If Ψ involves F, $\alpha \geq 1/2$ is a necessary condition for stability (but, in the context of coupled equation sets, it is not necessarily sufficient - as we shall note in later subsections).

For a conventional *centred two-time-level* scheme, $\alpha = 1/2$ and (5.2) becomes

$$F^{n+1} - F_d^n = \frac{\Delta t}{2}\left(\Psi^{n+1} + \Psi_d^n\right)\,. \tag{5.6}$$

When divided by Δt, (5.6) gives an approximation to (5.1) having an $O\left(\Delta t^2\right)$ truncation error.

For an *off-centred two-time-level* scheme, $1/2 < \alpha \leq 1$, the truncation error becomes $O\left(\Delta t\right)$ and (5.2) becomes

$$F^{n+1} - F_d^n = \Delta t\left[\alpha\Psi^{n+1} + (1-\alpha)\,\Psi_d^n\right]\,. \tag{5.7}$$

This off-centred two-time-level scheme is generally more accurate and less damping the closer α is to $1/2$, and less accurate and more damping the closer α is to unity. Some off-centring is desirable to address spurious semi-Lagrangian orographic resonance (Rivest, Staniforth & Robert (1994)). Ways of restoring $O\left(\Delta t^2\right)$ accuracy when $\alpha \neq 1/2$ may be devised (Côté, Gravel & Staniforth (1995), Simmons & Temperton (1997)).

By grouping terms at the new time t^{n+1} on the left side and known quantities on the right, (5.7) may be rewritten as

$$F^{n+1} - \alpha\Delta t\Psi^{n+1} = F_d^n + (1-\alpha)\,\Delta t\Psi_d^n \equiv \left[F + (1-\alpha)\,\Delta t\Psi\right]_d^n\,. \tag{5.8}$$

Here $[\;\;]_d^n$ denotes evaluation at time t^n at the departure point $\mathbf{x}_d$.

Eq. (5.8) is the basis for calculating F^{n+1}, the new time-level value at the arrival point. The term $-\alpha\Delta t\Psi^{n+1}$ in (5.8) involves the forcing evaluated at the arrival point at the new time-level, and - as we have noted - that time-level of evaluation is necessary for stability ($\alpha \geq 1/2$) if Ψ involves F. The presence of the term $-\alpha\Delta t\Psi^{n+1}$ complicates the calculation of F^{n+1}, especially if all or part of Ψ is nonlinear in F (or indeed if all or part of Ψ is nonlinear in any of the prognostic variables of the model). The part of Ψ, if any, that is linear in F (or in any prognostic variable) can in principle be dealt with by algebraic elimination. The parts of Ψ^{n+1} that are nonlinear in F^{n+1} have to be accommodated using some iterative procedure, which in practice consists of a fixed (small) number of "predictor-corrector" steps; in the New Dynamics such a procedure is also used for some of the linear parts of Ψ. See 6 - 10.

To the extent that Ψ depends on F, (5.8) may be regarded as a *semi-implicit* form; Ψ has been represented (by (5.5)) as a weighted average of known and unknown values. We shall refer to (5.8) as an *off-centred, semi-implicit, semi-Lagrangian* form. [This use of the term *semi-implicit* is somewhat unconventional, but it is useful for current purposes.]

Evaluation of the departure-point quantities F_d^n and Ψ_d^n (see (5.8)) proceeds in two stages, both of which involve approximation (if not uncertainty):

(i) location of the departure point $\mathbf{x}_d$; and

(ii) interpolation to obtain $F_d^n \equiv F(\mathbf{x}_d,\, t^n)$ and $\Psi_d^n \equiv \Psi^n(\mathbf{x}_d,\, t^n)$ from available gridpoint values of F and Ψ at time-level n.

The departure-point calculation exploits the definition of the continuously-varying velocity field $\mathbf{u}$ as the rate of change of the positions $\mathbf{x}$ of parcels of air (both relative to the rotating Earth):

$$\frac{D\mathbf{x}(t)}{Dt} = \mathbf{u}(\mathbf{x}(t),\, t)\ . \tag{5.9}$$

This is applied in the integrated form

$$\mathbf{x}_a - \mathbf{x}_d = \int_{t^n}^{t^n+\Delta t} \mathbf{u}dt = \overline{\mathbf{u}}\Delta t\,, \tag{5.10}$$

where the integrand $\mathbf{u}$ is evaluated along the trajectory between departure point $\mathbf{x}_d$ and arrival point $\mathbf{x}_a$. Eq (5.10) is an implicit equation for $\mathbf{x}_d$ (because the spatial starting point for its velocity integral is $\mathbf{x}_d$ itself). It is solved iteratively, after appropriate discretization of the velocity integral; details of the scheme used are given in sections 5.4 and 5.5. A range of options exists for the interpolation of F_d^n and Ψ_d^n from available gridpoint values of F and Ψ; an account is given in 5.3.

If the quantity F in the general prognostic equation (5.1) is the component of a vector, and the corresponding source term is known, then the procedure outlined above may be applied without formal change. Each component of the velocity vector $\mathbf{u}$ ($\equiv (u,\, v,\, w)$) may be treated in this way, via (2.71), (2.72), (2.76); however, computational instabilities due to the metric terms become an issue (Desharnais & Robert (1990)). There are attractions, therefore, to treating the momentum equation in its vector form when a semi-Lagrangian time-discretisation is being used. The momentum equation (1.6) may be written as

$$\frac{D\mathbf{u}}{Dt} = \mathbf{\Psi}\,, \tag{5.11}$$

in which the vector field$\mathbf{\Psi}$ represents the Coriolis, centrifugal, pressure gradient and frictional forces. Eq. (5.11) may be integrated alongtrajectories in precisely the same way as the scalar equation (5.1); instead of (5.2), the result is

$$\mathbf{u}^{n+1} - \mathbf{u}_d^n = \overline{\mathbf{\Psi}}\Delta t\,. \tag{5.12}$$

The use of (5.12), with its beguiling simplicity, is considered in 5.2.

Aside :

Eq. (5.12) *depends on the momentum equation being of the form* (5.11)*. This is obviously the case for the virtually unapproximated equations used by the New Dynamics, but not for the hydrostatic primitive equations (HPEs). The HPEs have no prognostic equation for w, so a corresponding vector momentum equation of the form* (5.11) *does not exist; and if a "horizontal" form involving $D\mathbf{v}/Dt$ is accepted, allowance must be made for the fact that $D\mathbf{v}/Dt$ has a vertical component if $\mathbf{v}$ is the velocity in spherical surfaces. The latter aspect considerably complicates application of the semi-Lagrangian technique to HPE models on the sphere (Ritchie (1988), Côté (1988), Bates, Semazzi, Higgins & Barros (1990)).*

Aside :

There is a close formal similarity between the integrated vector momentum equation (5.12) *and the departure point equation* (5.10)*. Although they are applied in different ways ((*5.10*) is solved for the parcel location $\mathbf{x}_d$ at the current time t^n, but* (5.12) *is used to forecast $\mathbf{u}^{n+1}$) this formal similarity might be expected* *to lead to recognisably similar solution strategies. We shall note in later sections that the New Dynamics does not display such similarities.*

Aside :

In a three-time-level *(leapfrog) scheme,* (5.1) *is integrated along a trajectory between times* t^{n-1} $(\equiv t^n - \Delta t)$ *and* t^{n+1} $(\equiv t^n + \Delta t)$ *to give, in place of* (5.2),

$$F^{n+1} - F_d^{n-1} = 2\overline{\Psi}\Delta t\,. \tag{5.13}$$

Here $\overline{\Psi}$ *is the (time) average of* Ψ *along the trajectory from the departure point* $\mathbf{x}_d$ *(at* $t = t^{n-1}$*) to the arrival point* $\mathbf{x}_a$ *(at* $t = t^{n+1}$*). Eq.* (5.13) *is an exact integral of* (5.1). *The simplest approximation to* $\overline{\Psi}$ *is the mid-point rule* $\overline{\Psi} \cong \Psi^n_{mid} \equiv \Psi^n\left((\mathbf{x}_a + \mathbf{x}_d)/2\right)$*; conveniently, this requires no evaluation at time level* $n+1$*, but its explicit character leads to instability if* Ψ *involves* F*. Other approximations to* $\overline{\Psi}$ *are: the end-points rule* $\overline{\Psi} \cong \left(\Psi_d^{n-1} + \Psi^{n+1}\right)/2$ *(Robert (1981), Robert (1982)) and the trapezoid rule* $\overline{\Psi} \cong \left(\Psi_d^{n-1} + 2\Psi^n_{mid} + \Psi^{n+1}\right)/4$*, both of which have the same formal accuracy as the mid-point rule; and Simpson's rule* $\overline{\Psi} \cong \left(\Psi_d^{n-1} + 4\Psi^n_{mid} + \Psi^{n+1}\right)/6$*, which is more accurate. These alternatives to the mid-point rule all have better stability properties, but require evaluation of* Ψ *at time level* $n+1$ *and so involve the same complications as those noted above for the two-time-level scheme. The New Dynamics uses two-time-level schemes throughout: they require less storage, and for a given timestep (i.e.* Δt *in* (5.2), $2\Delta t$ *in* (5.13)*) they reach a given forecast time in 50% fewer steps because successive intervals do not overlap (see Côté & Staniforth (1988)).*

5.2 Semi-Lagrangian treatment of the momentum equation in spherical geometry

As noted above, the vector momentum equation (1.6) can be written in the form

$$\frac{D\mathbf{u}}{Dt} = \mathbf{\Psi}\,, \tag{5.14}$$

so that

$$\mathbf{u}^{n+1} - \mathbf{u}_d^n = \overline{\mathbf{\Psi}}\Delta t\,. \tag{5.15}$$

From (1.11) and (1.12) of Section 1,

$$\mathbf{\Psi} \equiv -2\mathbf{\Omega} \times \mathbf{u} - g\mathbf{k} - \frac{1}{\rho}\mathbf{grad}p + \mathbf{S^u} \, . \tag{5.16}$$

To apply (5.14) we need to isolate its zonal, meridional and radial components at the arrival point $\mathbf{x}_a$. Doing this is not straightforward because *the zonal, meridional and radial directions at the arrival point* $\mathbf{x}_a$ *are generally not the same as their counterparts at the departure point* $\mathbf{x}_d$. An outbreak of spherical coordinate geometry is therefore inevitable, but luckily we have already developed some of the required formulae in another context - see Fig. 2.5 of Section 2).

<u>Aside :</u>

> *Readers who are happy with the matrix representation of rotations in 3 dimensions may wish at this point to jump to* (5.67)*, noting that the* 3×3 *orthogonal matrix* $\mathbf{M}$ *that transforms a vector in the departure-point system to a vector in the arrival-point system has elements* M_{ij} *given by* (5.29) *and* (5.33) - (5.38).

The unit vectors $\mathbf{i}_a$, $\mathbf{j}_a$, $\mathbf{k}_a$ in the zonal, meridional and radial directions at the arrival point $(\lambda_a, \, \phi_a, \, r_a)$ may be expressed in terms of the unit vectors $\mathbf{I}$, $\mathbf{J}$, $\mathbf{K}$ in a geocentric Cartesian system (compare Fig. 2.5 of Section 2) as

$$\mathbf{i}_a \; = \; -\mathbf{I}\sin\lambda_a + \mathbf{J}\cos\lambda_a \, , \tag{5.17}$$

$$\mathbf{j}_a \; = \; -\mathbf{I}\sin\phi_a\cos\lambda_a - \mathbf{J}\sin\phi_a\sin\lambda_a + \mathbf{K}\cos\phi_a \, , \tag{5.18}$$

$$\mathbf{k}_a \; = \; \mathbf{I}\cos\phi_a\cos\lambda_a + \mathbf{J}\cos\phi_a\sin\lambda_a + \mathbf{K}\sin\phi_a \, . \tag{5.19}$$

Similar expressions relate the unit vectors $\mathbf{i}_d$, $\mathbf{j}_d$, $\mathbf{k}_d$ in the zonal, meridional and radial directions at the departure point $(\lambda_d, \, \phi_d, \, r_d)$ to the geocentric Cartesian unit vectors:

$$\mathbf{i}_d \; = \; -\mathbf{I}\sin\lambda_d + \mathbf{J}\cos\lambda_d \, , \tag{5.20}$$

$$\mathbf{j}_d \; = \; -\mathbf{I}\sin\phi_d\cos\lambda_d - \mathbf{J}\sin\phi_d\sin\lambda_d + \mathbf{K}\cos\phi_d \, , \tag{5.21}$$

$$\mathbf{k}_d \; = \; \mathbf{I}\cos\phi_d\cos\lambda_d + \mathbf{J}\cos\phi_d\sin\lambda_d + \mathbf{K}\sin\phi_d \, . \tag{5.22}$$

The velocities $\mathbf{u}_d^n$ and $\mathbf{u}^{n+1}$ at the departure and arrival points may be written in terms of their *local* unit vectors as

$$\mathbf{u}_d^n \; = \; u_d^n\mathbf{i}_d \; + v_d^n\mathbf{j}_d \; + w_d^n\mathbf{k}_d \, , \tag{5.23}$$

and

$$\mathbf{u}^{n+1} = \; u^{n+1}\mathbf{i}_a \; + v^{n+1}\mathbf{j}_a \; + w^{n+1}\mathbf{k}_a \, . \tag{5.24}$$

Expressions for the arrival-point velocity components u^{n+1}, v^{n+1}, w^{n+1} may be derived from (5.15) through scalar multiplication by the arrival-point unit vectors $\mathbf{i}_a$, $\mathbf{j}_a$, $\mathbf{k}_a$:

$$u^{n+1} = \mathbf{i}_a \cdot \mathbf{u}^{n+1} = \mathbf{i}_a \cdot \mathbf{u}^n_d \; + \; \mathbf{i}_a \cdot \overline{\mathbf{\Psi}} \Delta t \, , \tag{5.25}$$

$$v^{n+1} = \mathbf{j}_a \cdot \mathbf{u}^{n+1} = \mathbf{j}_a \cdot \mathbf{u}^n_d \; + \; \mathbf{j}_a \cdot \overline{\mathbf{\Psi}} \Delta t \, , \tag{5.26}$$

$$w^{n+1} = \mathbf{k}_a \cdot \mathbf{u}^{n+1} = \mathbf{k}_a \cdot \mathbf{u}^n_d \; + \; \mathbf{k}_a \cdot \overline{\mathbf{\Psi}} \Delta t \, . \tag{5.27}$$

Application of (5.17) - (5.23) to (5.25) - (5.27) enables u^{n+1}, v^{n+1}, w^{n+1} to be related to the components u^n_d, v^n_d, w^n_d at the departure point. For example, use of (5.17) and (5.20) - (5.22) in (5.23) gives

$$\mathbf{i}_a \cdot \mathbf{u}^n_d = \mathbf{i}_a \cdot (u^n_d \mathbf{i}_d + v^n_d \mathbf{j}_d + w^n_d \mathbf{k}_d) = u^n_d \cos(\lambda_a - \lambda_d) + v^n_d \sin\phi_d \sin(\lambda_a - \lambda_d) - w^n_d \cos\phi_d \sin(\lambda_a - \lambda_d) \, . \tag{5.28}$$

Thus, in terms of

$$M_{uu} = \cos(\lambda_a - \lambda_d) \, , \quad M_{uv} = \sin\phi_d \sin(\lambda_a - \lambda_d) \, , \quad M_{uw} = -\cos\phi_d \sin(\lambda_a - \lambda_d) \, , \tag{5.29}$$

(5.25) can be written as

$$u^{n+1} - \; M_{uu} u^n_d \; = \; M_{uv} v^n_d \; + \; M_{uw} w^n_d \; + \; \mathbf{i}_a \cdot \overline{\mathbf{\Psi}} \Delta t \, . \tag{5.30}$$

Similarly, use of (5.18) - (5.22) in (5.23) shows that (5.26) and (5.27) may be written as

$$v^{n+1} - \; M_{vv} v^n_d \; = \; M_{vu} u^n_d \; + \; M_{vw} w^n_d \; + \; \mathbf{j}_a \cdot \overline{\mathbf{\Psi}} \Delta t \, , \tag{5.31}$$

$$w^{n+1} - \; M_{ww} w^n_d \; = \; M_{wu} u^n_d \; + \; M_{wv} v^n_d \; + \; \mathbf{k}_a \cdot \overline{\mathbf{\Psi}} \Delta t \, , \tag{5.32}$$

where

$$M_{vu} = -\sin\phi_a \sin(\lambda_a - \lambda_d) \; , \tag{5.33}$$

$$M_{vv} = \cos\phi_a \cos\phi_d + \sin\phi_a \sin\phi_d \cos(\lambda_a - \lambda_d) \; , \tag{5.34}$$

$$M_{vw} = \cos\phi_a \sin\phi_d - \sin\phi_a \cos\phi_d \cos(\lambda_a - \lambda_d) \; , \tag{5.35}$$

$$M_{wu} = \cos\phi_a \sin(\lambda_a - \lambda_d) \; , \tag{5.36}$$

$$M_{wv} = \sin\phi_a \cos\phi_d - \cos\phi_a \sin\phi_d \cos(\lambda_a - \lambda_d) \; , \tag{5.37}$$

$$M_{ww} = \sin\phi_a \sin\phi_d + \cos\phi_a \cos\phi_d \cos(\lambda_a - \lambda_d) \ . \tag{5.38}$$

(Clearly the terms $\mathbf{i}_a \cdot \overline{\mathbf{\Psi}}$, $\mathbf{j}_a \cdot \overline{\mathbf{\Psi}}$, $\mathbf{k}_a \cdot \overline{\mathbf{\Psi}}$ in (5.30) - (5.32) can be treated in a similar way, and we shall discuss this later.)

Allowing for some minor differences in notation, expressions (5.29) and (5.33) - (5.38) for M_{uu}, M_{uv}, M_{uw}, M_{vu}, M_{vv}, M_{vw}, M_{wu}, M_{wv}, M_{ww} are the same as those given by Mawson (1998) (see his (3.17) - (3.19)) . The 3×3 matrix $\mathbf{M} \equiv \{M_{ij}\}$ is a finite rotation matrix. It is straightforward (and tedious) to show that $\mathbf{M}$ is orthogonal: the inverse of $\mathbf{M}$ is its transpose, i.e. $\mathbf{M}\mathbf{M}^{\mathbf{T}} = \mathbf{I}$. Some alternative forms of (5.29) and (5.33) - (5.38) are given in later *Aside*s.

The 6 off-diagonal elements of $\mathbf{M}$ (which appearon the right sides of (5.30) - (5.32)) *correspond to the 6 metric terms that appear in the spherical polar components* (2.71), (2.72) *and* (2.76) *of the momentum equation* [see below]*:* M_{uv} *and* M_{uw} *correspond to* $(uv\tan\phi)/r$ *and* $-uw/r$ *in* (2.71)*;* M_{vu} *and* M_{vw} *to* $-(u^2\tan\phi)/r$ *and* $-vw/r$ *in* (2.72)*;* M_{wu} *and* M_{wv} *to* u^2/r *and* v^2/r *in* (2.76)*.* For the reader's convenience, (2.71), (2.72) and (2.76) are reproduced here:

$$\frac{Du}{Dt} = \frac{uv\tan\phi}{r} - \frac{uw}{r} + f_3 v - f_2 w - \frac{c_{pd}\theta_v}{r\cos\phi}\left(\frac{\partial\Pi}{\partial\lambda} - \frac{\partial\Pi}{\partial r}\frac{\partial r}{\partial\lambda}\right) + S^u \ , \tag{5.39}$$

$$\frac{Dv}{Dt} = -\frac{u^2\tan\phi}{r} - \frac{vw}{r} + f_1 w - f_3 u - \frac{c_{pd}\theta_v}{r}\left(\frac{\partial\Pi}{\partial\phi} - \frac{\partial\Pi}{\partial r}\frac{\partial r}{\partial\phi}\right) + S^v \ , \tag{5.40}$$

$$\frac{Dw}{Dt} = \frac{u^2}{r} + \frac{v^2}{r} + f_2 u - f_1 v - g\left(1 + q_{cl} + q_{cf}\right) - c_{pd}\theta_v\frac{\partial\Pi}{\partial r} + S^w \ . \tag{5.41}$$

The correspondences noted above may be established by considering the limit $\Delta t \to 0$; then $\lambda_d \to \lambda_a$ and $\phi_d \to \phi_a$. For example, regarding M_{uv}, M_{uw} in the limit $\lambda_d \to \lambda_a$, $\phi_d \to \phi_a$, we find (from (5.29))

$$M_{uv}v_d^n = v_d^n \sin\phi_d \sin(\lambda_a - \lambda_d) \to (\lambda_a - \lambda_d)\, v_d^n \sin\phi_a \to \left(\frac{u^n \Delta t}{r_a\cos\phi_a}\right) v^n \sin\phi_a = \frac{u^n v^n \tan\phi_a}{r_a}\Delta t, \tag{5.42}$$

$$M_{uw}w_d^n = -w_d^n \cos\phi_d \sin(\lambda_a - \lambda_d) \to -(\lambda_a - \lambda_d)\, w_d^n \cos\phi_a \to -\frac{u^n w^n}{r_a}\Delta t \ . \tag{5.43}$$

The extreme right sides of (5.42) and (5.43) are the metric terms in (5.39), multiplied by Δt and evaluated at the arrival point $(\lambda_a,\ \phi_a,\ r_a)$. [The time-level of evaluation of the right sides of (5.42) and (5.43) is shown as n, but could just as well have been shown as $n+1$ since we are considering the limit $\Delta t \to 0$.] Note also that

$$u^{n+1} - M_{uu}u_d^n = u^{n+1} - u_d^n \cos(\lambda_a - \lambda_d) \to u^{n+1} - u_d^n \cong \frac{Du}{Dt}\Delta t \ . \tag{5.44}$$

Aside :

The other correspondences may be demonstrated in essentially the same way. From (5.33) - (5.35)*:*

$$M_{vu}u_d^n = -u_d^n \sin\phi_a \sin(\lambda_a - \lambda_d) \to -(\lambda_a - \lambda_d)\, u_d^n \sin\phi_a \to -\frac{(u^n)^2 \tan\phi_a}{r_a}\Delta t\,, \tag{5.45}$$

$$M_{vw}w_d^n = (\cos\phi_a \sin\phi_d - \sin\phi_a \cos\phi_d \cos(\lambda_a - \lambda_d))\, w_d^n \to -(\phi_a - \phi_d)\, w_d^n \to -\frac{v^n w^n}{r_a}\Delta t, \tag{5.46}$$

$$v^{n+1} - M_{vv}v_d^n = v^{n+1} - (\cos\phi_a \cos\phi_d + \sin\phi_a \sin\phi_d \cos(\lambda_a - \lambda_d))\, v_d^n \to v^{n+1} - v_d^n \cong \frac{Dv}{Dt}\Delta t. \tag{5.47}$$

The extreme right sides of (5.45) - (5.47) *are the metric and material derivative terms in* (5.40)*, multiplied by* Δt *and evaluated at the arrival point* $(\lambda_a,\ \phi_a,\ r_a)$*.*

From (5.36) - (5.38)*:*

$$M_{wu}u_d^n = u_n^d \cos\phi_a \sin(\lambda_a - \lambda_d) \to (\lambda_a - \lambda_d)\, u_n^d \cos\phi_a \to \frac{(u^n)^2}{r_a}\Delta t\,, \tag{5.48}$$

$$M_{wv}v_d^n = (\sin\phi_a \cos\phi_d - \cos\phi_a \sin\phi_d \cos(\lambda_a - \lambda_d))\, v_n^d \to (\phi_a - \phi_d)\, v_d^n \to \frac{(v^n)^2}{r_a}\Delta t, \tag{5.49}$$

$$w^{n+1} - M_{ww}w_d^n = w^{n+1} - (\sin\phi_a \sin\phi_d + \cos\phi_a \cos\phi_d \cos(\lambda_a - \lambda_d))\, w_d^n \to w^{n+1} - w_d^n \cong \frac{Dw}{Dt}\Delta t. \tag{5.50}$$

The extreme right sides of (5.48) - (5.50) *are the metric and material derivative terms in* (5.41)*, multiplied by* Δt *and evaluated at the arrival point* $(\lambda_a,\ \phi_a,\ r_a)$*.*

The correspondence between the 6 off-diagonal elements of $\mathbf{M}$ and the 6 metric terms in the spherical polar components of the momentum equation is entirely reasonable in physical terms. Although we started out with the vector form (5.14) of the momentum equation, our analysis became committed to a spherical polar coordinate system when we isolated the zonal, meridional and radial components of (5.15). We may have succeeded in disguising the metric terms, but we have not succeeded in removing them (neither should we expect that to be possible within the framework imposed by a curved, non-Cartesian coordinate system). Our derivation of (5.30) - (5.32) from the Lagrangian time-integrated momentum equation (5.15),and subsequent consideration of the limit $\Delta t \to 0$, could be regarded simply as a way of obtaining the zonal, meridional and radial components of the material derivative $D\mathbf{u}/Dt$

in the original momentum equation (5.11). [Issues of the relative accuracy of Eulerian and semi-Lagrangian schemes are clearly of interest here, but will not be pursued.]

Aside :

The metric terms in any of their guises could be avoided by working in terms of velocity and acceleration components in a (rotating) geocentric Cartesian coordinate system. This possibility is worth exploring. In section 5.5 we note that use of such a coordinate system is an attractive strategy in the trajectory calculation (which, as we have already noted, is a formally similar problem).

The superficial implication of the correspondence of the off-diagonal elements of $\mathbf{M}$ to the metric terms in (5.39), (5.40) and (5.41) is that nothing has been gained (or lost!) by working with the vector momentum equation (5.14) rather than with (5.39), (5.40) and (5.41) individually. The demonstration of this equivalence, as given in (5.42) - (5.50), also raises the suspicion that the terms $M_{ij}u_{dj}^n$ may represent the metric terms - at least partially - in a forward timestep.

Aside :

The stability of the current treatment of the metric terms should be examined. Since the off-diagonal terms of $\mathbf{M}$ *in the vector treatment are equivalent to the metric terms in* (5.39), (5.40) *and* (5.41)*, how does the vector treatment avoid the instability found by Desharnais & Robert (1990) ? The answer may lie in the nature of* $\mathbf{M}$*. The vector treatment represents the metric terms in the action of* $\mathbf{M}$ *on the discretization which would apply in their absence (see* (5.67)*, below); the orthogonality of* $\mathbf{M}$ *may ensure a neutral effect on stability (which the explicit evaluation of metric terms in the component equations would not achieve unless specifically arranged to mimic the action of* $\mathbf{M}$*).*

Aside :

As noted by Temperton (1997) (following M. Rochas), the vector Coriolis term of the HPEs may be expressed as the material derivative of a simple vector. A similar re-expression of the unapproximated momentum equation used in the New Dynamics can be carried out. Instead of (5.14) *and* (5.16) *in the form*

$$\frac{D\mathbf{u}}{Dt} = -2\mathbf{\Omega} \times \mathbf{u} - g\mathbf{k} - \frac{1}{\rho}\mathbf{grad}p + \mathbf{S^u}\,, \tag{5.51}$$

one may use the equivalent form

$$\frac{D}{Dt}\widehat{\mathbf{u}} \equiv \frac{D}{Dt}\left(\mathbf{u} + 2\boldsymbol{\Omega} \times \mathbf{r}\right) = -g\mathbf{k} - \frac{1}{\rho}\mathbf{grad}p + \mathbf{S}^{\mathbf{u}} \equiv \widehat{\boldsymbol{\Psi}}, \tag{5.52}$$

and advect the vector quantity $\widehat{\mathbf{u}} = \mathbf{u} + 2\boldsymbol{\Omega} \times \mathbf{r}$ $(= \mathbf{u} + 2\Omega\mathbf{i}\cos\phi)$. *This is a seductive possibility for two reasons. First, it offers a unified treatment of the Coriolis and metric terms. Second, although the analytical time integration leading from the material conservation law (such as* (5.14)*) to the semi-Lagrangian increment equation (such as* (5.15)*) treats both the advected quantity and the source term exactly, the source term is approximated later on - for example, by* (5.5)*. When the choice exists, it seems therefore good strategy to treat terms as part of the advected quantity rather than as part of the source. However, as noted by Temperton, Hortal & Simmons (2001) for the HPEs, use of a two-time-level scheme in conjunction with* (5.52) *amounts to forward timestepping the Coriolis terms - with implied potential for instability - if temporal extrapolation is used in the parcel displacement calculation (see Section 5.4); Temperton et al. (2001) use a predictor-corrector scheme instead. Use of* (5.52) *rather than* (5.51) *should not be contemplated in the New Dynamics until the instability issues have been clarified.*

Options exist in the New Dynamics code to omit all or some of the off-diagonal elements of $\mathbf{M}$ in (5.30) - (5.32). In the *"2d option"*, which is the default setting, $M_{uw} = M_{vw} = M_{wu} = M_{wv} = 0$; also, $M_{ww} = 1$. The *"1d geometry option"* sets all the off-diagonal elements of $\mathbf{M}$ to zero, and all the diagonal elements to unity. By noting the correspondence between the off-diagonal elements of $\mathbf{M}$ and the metric terms in (5.39), (5.40) and (5.41), it is easily seen that the *2d option* is equivalent to retaining the $\tan\phi$ metric terms in (5.39) and (5.40), but neglecting the other metric terms in (5.39), (5.40) and (5.41).

Aside :

Neglect of the metric terms not involving $\tan\phi$ *is an energetically consistent step, and it is reminiscent of the HPEs. However, the shallow atmosphere approximation is* not *made, and the* $\cos\phi$ *Coriolis terms are retained: it can be shown that this package is* not *consistent with respect to angular momentum and potential vorticity conservation. The terms omitted in the* "2d option" *are quantitatively very small, but their absence means that the model will not tend to a physically and mathematically well-behaved limit as time and spatial resolution are* *increased. Neither does the* "2d option" *preserve the orthogonality of the matrix* $\mathbf{M}$*: the property* $\mathbf{M}\mathbf{M}^{\mathbf{T}} = \mathbf{I}$ *does not survive (and* $\mathbf{M}$ *is no longer a true rotation matrix) if we set* $M_{uw} = M_{vw} = M_{wu} = M_{wv} = 0$ *and* $M_{ww} = 1$*. Amongst other undesirable effects, this means that the magnitude of vectors is not preserved by the transformation. An improved* "2d option" *is proposed in the* Aside *which terminates this subsection. All in all, it would appear safest to bear the extra computational cost of properly including all the elements of the rotation matrix* $\mathbf{M}$.

It remains to deal with the scalar product source terms $\mathbf{i}_a \cdot \overline{\mathbf{\Psi}}$, $\mathbf{j}_a \cdot \overline{\mathbf{\Psi}}$, $\mathbf{k}_a \cdot \overline{\mathbf{\Psi}}$ in (5.30) - (5.32). Extending the definition of the trajectory time-average (5.5) to vector fields, we have

$$\overline{\mathbf{\Psi}} \equiv \alpha \mathbf{\Psi}^{n+1} + (1-\alpha)\, \mathbf{\Psi}_d^n \, . \tag{5.53}$$

Our procedure now follows that already applied to the $\mathbf{u}^{n+1}$ and $\mathbf{u}_d^n$ terms in (5.15). Express $\mathbf{\Psi}^{n+1}$ in terms of unit vectors at the arrival point and $\mathbf{\Psi}_d^n$ in terms of unit vectors at the departure point:

$$\overline{\mathbf{\Psi}} \equiv \alpha \left(\Psi_\lambda^{n+1} \mathbf{i}_a + \Psi_\phi^{n+1} \mathbf{j}_a + \Psi_r^{n+1} \mathbf{k}_a \right) + (1-\alpha) \left(\Psi_{d\lambda}^n \mathbf{i}_d + \Psi_{d\phi}^n \mathbf{j}_d + \Psi_{dr}^n \mathbf{k}_d \right) \, . \tag{5.54}$$

Hence

$$\mathbf{i}_a \cdot \overline{\mathbf{\Psi}} \equiv \alpha \Psi_\lambda^{n+1} + (1-\alpha) \left(\Psi_{d\lambda}^n \mathbf{i}_a \cdot \mathbf{i}_d + \Psi_{d\phi}^n \mathbf{i}_a \cdot \mathbf{j}_d + \Psi_{dr}^n \mathbf{i}_a \cdot \mathbf{k}_d \right) \, , \tag{5.55}$$

$$\mathbf{j}_a \cdot \overline{\mathbf{\Psi}} \equiv \alpha \Psi_\phi^{n+1} + (1-\alpha) \left(\Psi_{d\lambda}^n \mathbf{j}_a \cdot \mathbf{i}_d + \Psi_{d\phi}^n \mathbf{j}_a \cdot \mathbf{j}_d + \Psi_{dr}^n \mathbf{j}_a \cdot \mathbf{k}_d \right) \, , \tag{5.56}$$

$$\mathbf{k}_a \cdot \overline{\mathbf{\Psi}} \equiv \alpha \Psi_r^{n+1} + (1-\alpha) \left(\Psi_{d\lambda}^n \mathbf{k}_a \cdot \mathbf{i}_d + \Psi_{d\phi}^n \mathbf{k}_a \cdot \mathbf{j}_d + \Psi_{dr}^n \mathbf{k}_a \cdot \mathbf{k}_d \right) \, . \tag{5.57}$$

The scalar products on the righthand sidesof (5.55) - (5.57) are simply the elements of the finite rotation matrix $\mathbf{M}$ (see, for example, (5.29) and (5.33)). Thus

$$\mathbf{i}_a \cdot \overline{\mathbf{\Psi}} \equiv \alpha \Psi_\lambda^{n+1} + (1-\alpha) \left(\Psi_{d\lambda}^n M_{uu} + \Psi_{d\phi}^n M_{uv} + \Psi_{dr}^n M_{uw} \right) \, , \tag{5.58}$$

$$\mathbf{j}_a \cdot \overline{\mathbf{\Psi}} \equiv \alpha \Psi_\phi^{n+1} + (1-\alpha) \left(\Psi_{d\lambda}^n M_{vu} + \Psi_{d\phi}^n M_{vv} + \Psi_{dr}^n M_{vw} \right) \, , \tag{5.59}$$

$$\mathbf{k}_a \cdot \overline{\mathbf{\Psi}} \equiv \alpha \Psi_r^{n+1} + (1-\alpha) \left(\Psi_{d\lambda}^n M_{wu} + \Psi_{d\phi}^n M_{wv} + \Psi_{dr}^n M_{ww} \right) \, . \tag{5.60}$$

Use of (5.58) - (5.60), some re-arrangement, and definition of $\beta = (1-\alpha)$, enables (5.30) - (5.32) to be written as

$$u^{n+1} - \alpha \Psi_\lambda^{n+1} \Delta t = M_{uu} \left\{ u_d^n + \beta \Psi_{d\lambda}^n \Delta t \right\} + M_{uv} \left\{ v_d^n + \beta \Psi_{d\phi}^n \Delta t \right\} + M_{uw} \left\{ w_d^n + \beta \Psi_{dr}^n \Delta t \right\} \, , \tag{5.61}$$

$$v^{n+1} - \alpha\Psi_{\phi}^{n+1}\Delta t = M_{vu}\left\{u_d^n + \beta\Psi_{d\lambda}^n\Delta t\right\} + M_{vv}\left\{v_d^n + \beta\Psi_{d\phi}^n\Delta t\right\} + M_{vw}\left\{w_d^n + \beta\Psi_{dr}^n\Delta t\right\} , \tag{5.62}$$

$$w^{n+1} - \alpha\Psi_{r}^{n+1}\Delta t = M_{wu}\left\{u_d^n + \beta\Psi_{d\lambda}^n\Delta t\right\} + M_{wv}\left\{v_d^n + \beta\Psi_{d\phi}^n\Delta t\right\} + M_{ww}\left\{w_d^n + \beta\Psi_{dr}^n\Delta t\right\} . \tag{5.63}$$

The terms involving the diagonal elements of the rotation matrix **M** are the dominant contributors to the right sides of (5.61) - (5.63); they would remain (except for uniform flows) even as curvature effects became vanishingly small. The other terms on the right sides of (5.61) - (5.63) involve the off-diagonal elements of **M**; they are minor contributors, and would become vanishingly small as curvature effects became vanishingly small. The diagonal elements M_{uu}, M_{vv}, M_{ww} are not generally equal to unity, but tend to that value as curvature vanishes.

Aside :

As might be expected on geometric grounds, M_{uu}, M_{vv}, $M_{ww} \leq 1$. This is readily demonstrated by writing the definitions (5.29), (5.34), (5.38) *in terms of $\lambda_- \equiv (\lambda_a - \lambda_d)/2$, $\phi_- \equiv (\phi_a - \phi_d)/2$ and $\phi_+ \equiv (\phi_a + \phi_d)/2$, and using elementary identities:*

$$M_{uu} = 1 - 2\sin^2\lambda_- , \tag{5.64}$$

$$M_{vv} = 1 - 2\sin^2\lambda_- \sin^2\phi_+ - 2\sin^2\phi_- \cos^2\lambda_- , \tag{5.65}$$

$$M_{ww} = 1 - 2\sin^2\lambda_- \cos^2\phi_+ - 2\sin^2\phi_- \cos^2\lambda_- . \tag{5.66}$$

*(Writing the off-diagonal elements of **M** in terms of λ_-, ϕ_- and ϕ_+ is not particularly helpful.)*

Eqs. (5.61) - (5.63) may be writtenconcisely in vector-matrix form as

$$\mathbf{u}^{n+1} - \alpha\boldsymbol{\Psi}^{n+1}\Delta t = \mathbf{M}\left\{\mathbf{u}_d^n + (1-\alpha)\boldsymbol{\Psi}_d^n\Delta t\right\} , \tag{5.67}$$

in which **M** is the rotation matrix $\{M_{ij}\}$. It is to be understood that the vectors on the left side are expressed as their components in the arrival-point coordinate system, and the vectors on the right side are expressed as their components in the departure-point coordinate system. The role of the matrix **M** in transforming vectors between the departure- and arrival-point systems is particularly clear in (5.67).

Eq. (5.67) provides a friendly context for the introduction of a sort of splitting technique used in the model: *different parts of the forcing may be represented with different values of the trajectory weighting factor* α. In symbolic terms, the source $\mathbf{\Psi}$ may be represented as a sum of parts $\mathbf{\Psi}_k$, with each of which a weighting factor α_k is associated:

$$\mathbf{\Psi} = \sum_k \mathbf{\Psi}_k \, .$$

The corresponding form of (5.67) is

$$\mathbf{u}^{n+1} - \sum_k \alpha_k \mathbf{\Psi}_k^{n+1} \Delta t \; = \mathbf{M} \left\{ \mathbf{u}_d^n + \sum_k \left(1 - \alpha_k\right) \mathbf{\Psi}_{kd}^n \Delta t \right\} \, . \tag{5.68}$$

The essential idea here is straightforward - to represent different terms in the momentum equation (such as the components of the Coriolis force or of the pressure gradient force) with different trajectory weighting factors α_k. The technique need not be limited to different treatments of different forces; it can be applied so as to treat different components of the same force differently (however arbitrary such a procedure might appear on physical grounds).

Aside :

The interpretation of $\mathbf{M}$ *as a transformation matrix suggests ways of factorising it into less formidable matrices. The orientation of the* $(\mathbf{i}, \mathbf{j}, \mathbf{k})$ *unit vector triad (UVT) at the arrival point may be achieved by a sequence of elementary rotations of the departure-point UVT. For example (see Fig. 5.2): (i) move the UVT from the departure point* (λ_d, ϕ_d) *to the equator via the meridian* λ_d*; this amounts to a rotation about the zonal direction through an angle* ϕ_d*, which is associated with the matrix*

$$\mathbf{A} = \begin{pmatrix} 1 & 0 & 0 \\ 0 & \cos\phi_d & \sin\phi_d \\ 0 & -\sin\phi_d & \cos\phi_d \end{pmatrix} , \tag{5.69}$$

(ii) move the UVT around the equator from longitude λ_d *to longitude* λ_a*; this amounts to a rotation about the local meridional direction through an angle* $(\lambda_a - \lambda_d)$*, the associated matrix being*

$$\mathbf{B} = \begin{pmatrix} \cos(\lambda_a - \lambda_d) & 0 & -\sin(\lambda_a - \lambda_d) \\ 0 & 1 & 0 \\ \sin(\lambda_a - \lambda_d) & 0 & \cos(\lambda_a - \lambda_d) \end{pmatrix} , \tag{5.70}$$

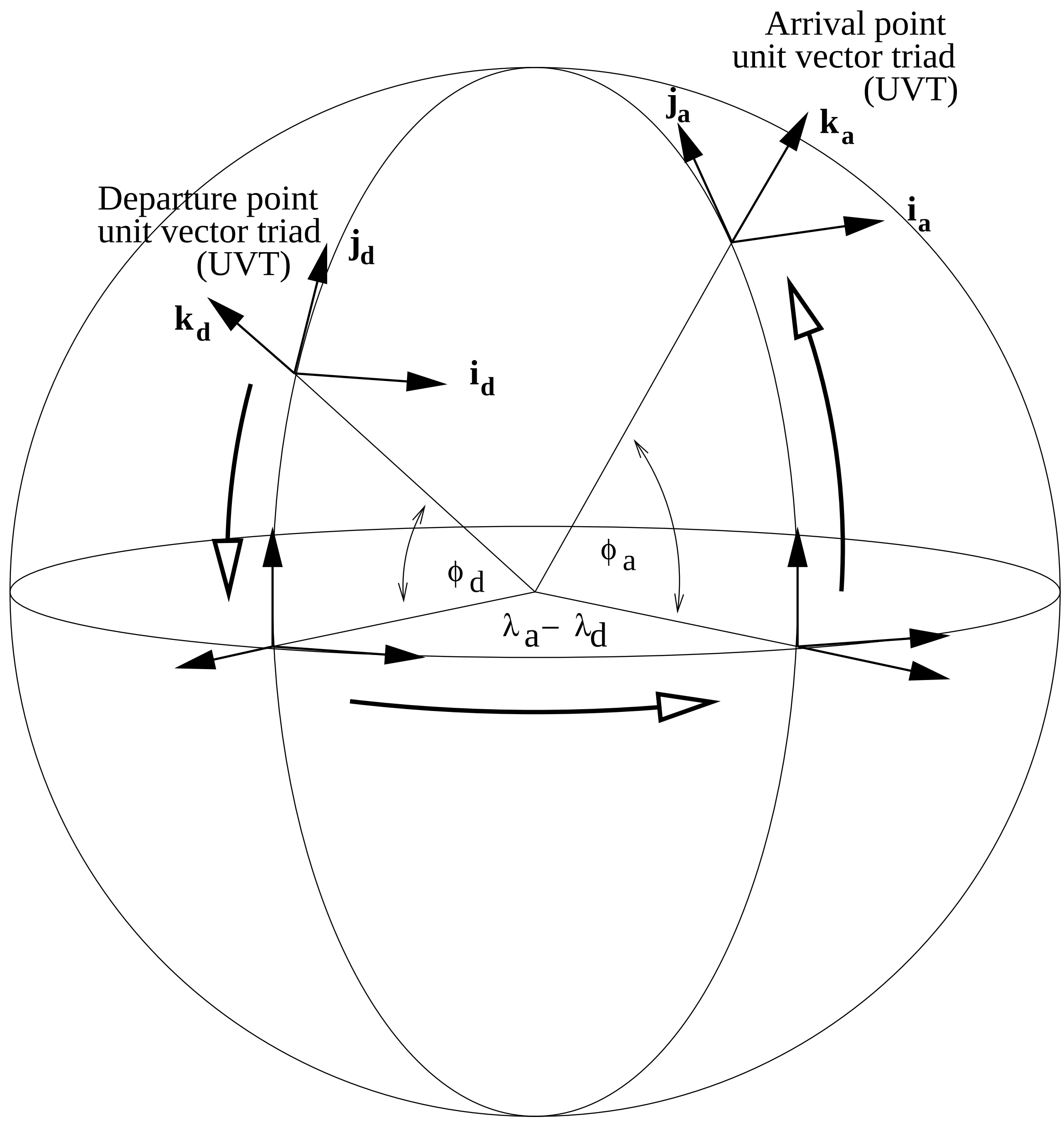

Figure 5.2: The **M** matrix, which represents the rotation of the unit vector triad (UVT) from the departure point to the arrival point, may be factorised into matrices representing rotations having the same cumulative effect. In this example, the UVT is rotated successively through ϕ_d about its initial zonal axis, through $(\lambda_a - \lambda_d)$ about its intermediate meridional axis, and finally through $-\phi_a$ about its intermediate zonal axis (which is therefore also its final zonal axis). See text for further discussion.

(iii) move the UVT to the arrival point (λ_a, ϕ_a)*; this amounts to a rotation about the local zonal direction through an angle* $-\phi_a$*, with associated matrix*

$$\mathbf{C} = \begin{pmatrix} 1 & 0 & 0 \\ 0 & \cos\phi_a & \sin\phi_a \\ 0 & -\sin\phi_a & \cos\phi_a \end{pmatrix} . \tag{5.71}$$

The net effect of the three rotations is represented by the matrix $\mathbf{CBA}$*, and it is readily verified by direct multiplication that* $\mathbf{CBA} = \mathbf{M}$*. An equally simple factorization can be constructed by moving the UVT from the departure point to the arrival point via the North pole and noting the 3 associated matrices (the second of which is identical to* $\mathbf{B}$ *as given by* (5.70)*).*

Aside :

A more important factorization may be achieved by noting the matrices $\mathbf{F}$, $\mathbf{G}$, $\mathbf{H}$ *associated with the following sequence of UVT rotations involving the great circle between the departure and arrival points (see Fig. 5.3):*

$\mathbf{F}$: *rotate the departure-point UVT about the local vertical so that the new* $\mathbf{i}$ *direction points along the great circle towards the arrival point;*

$\mathbf{G}$: *rotate the new UVT in the plane of the great circle until it reaches the arrival point;*

$\mathbf{H}$: *rotate the resulting UVT about the local vertical so that the final* $\mathbf{i}$ *direction points along the (geographical) latitude circle at the arrival point.*

Rotations $\mathbf{F}$ *and* $\mathbf{H}$ *are conveniently represented in terms of the angles* γ_d *and* γ_a *between the great circle and the (geographical) latitude circles at the departure and arrival points. Then* $\mathbf{F}$ *is a rotation about the local vertical through an angle* γ_d*, and* $\mathbf{H}$ *is a rotation about the local vertical through an angle* $-\gamma_a$*:*

$$\mathbf{F} = \begin{pmatrix} \cos\gamma_d & \sin\gamma_d & 0 \\ -\sin\gamma_d & \cos\gamma_d & 0 \\ 0 & 0 & 1 \end{pmatrix} , \qquad \mathbf{H} = \begin{pmatrix} \cos\gamma_a & -\sin\gamma_a & 0 \\ \sin\gamma_a & \cos\gamma_a & 0 \\ 0 & 0 & 1 \end{pmatrix} . \tag{5.72}$$

If the minor arc of the great circle between departure and arrival point subtends

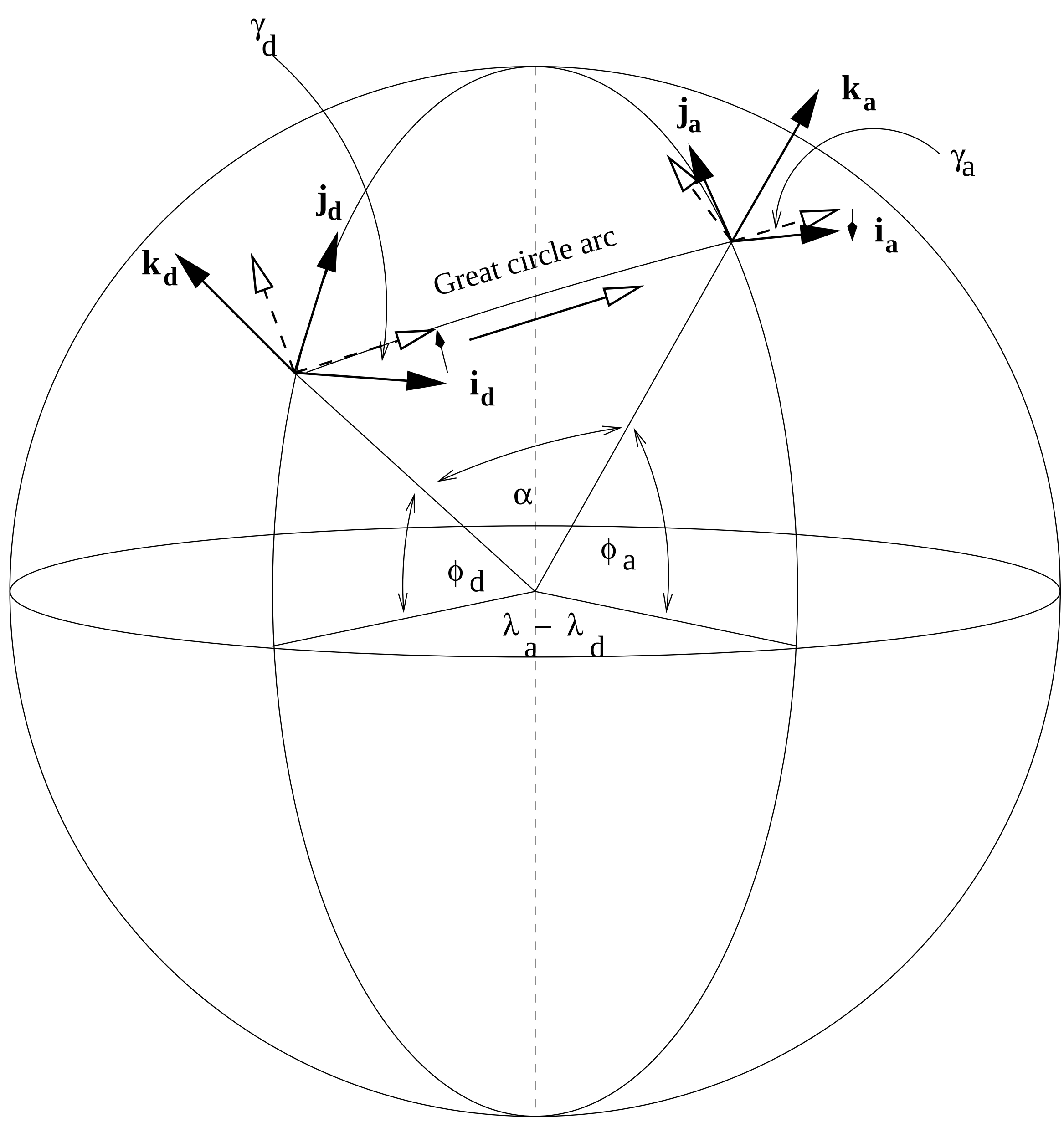

Figure 5.3: Another way of accomplishing in 3 easy stages the UVT rotation between departure point and arrival point: rotation about the local vertical through angle γ_d ; rotation in the plane of the great circle arc through angle α ; and finally rotation about the new local vertical through angle $-\gamma_a$. See text for analytical details.

an angle α at the centre of the Earth, then rotation $\boldsymbol{G}$ *has*

$$\mathbf{G} = \begin{pmatrix} \cos\alpha & 0 & -\sin\alpha \\ 0 & 1 & 0 \\ \sin\alpha & 0 & \cos\alpha \end{pmatrix}. \tag{5.73}$$

Hence the matrix of the total rotation is $\mathbf{N} = \mathbf{HGF}$. *Direct use of* (5.72) *and* (5.73) *shows that* $\mathbf{N}$ *is the matrix*

$$\begin{pmatrix} \cos\alpha\cos\gamma_a\cos\gamma_d+\sin\gamma_a\sin\gamma_d & \cos\alpha\cos\gamma_a\sin\gamma_d-\sin\gamma_a\cos\gamma_d & -\sin\alpha\cos\gamma_a \\ \cos\alpha\sin\gamma_a\cos\gamma_d-\cos\gamma_a\sin\gamma_d & \cos\alpha\sin\gamma_a\sin\gamma_d+\cos\gamma_a\cos\gamma_d & -\sin\alpha\sin\gamma_a \\ \sin\alpha\cos\gamma_d & \sin\alpha\sin\gamma_d & \cos\alpha \end{pmatrix}. \tag{5.74}$$

From (5.29) *and* (5.33) - (5.38), *and with* $\delta \equiv \lambda_a - \lambda_d$, *the* $\mathbf{M}$ *matrix is*

$$\begin{pmatrix} \cos\delta & \sin\phi_d\sin\delta & -\cos\phi_d\sin\delta \\ -\sin\phi_a\sin\delta & \cos\phi_a\cos\phi_d+\sin\phi_a\sin\phi_d\cos\delta & \cos\phi_a\sin\phi_d-\sin\phi_a\cos\phi_d\cos\delta \\ \cos\phi_a\sin\delta & \sin\phi_a\cos\phi_d-\cos\phi_a\sin\phi_d\cos\delta & \sin\phi_a\sin\phi_d+\cos\phi_a\cos\phi_d\cos\delta \end{pmatrix}. \tag{5.75}$$

The equality of $\mathbf{M}$ *and* $\mathbf{N}$ *is by no means obvious from* (5.74) *and* (5.75), *but it may be demonstrated by development and repeated application of spherical triangle formulae, as outlined in Appendix D. The main interest of the* $\mathbf{M} = \mathbf{N} = \mathbf{HGF}$ *factorization centres on what happens if the great circle rotation* $\mathbf{G}$ *is replaced by the identity operation, i.e. if the curvature of the great circle is neglected. Then we have simply*

$$\mathbf{N} \rightarrow \mathbf{HF} = \begin{pmatrix} \cos(\gamma_d-\gamma_a) & \sin(\gamma_d-\gamma_a) & 0 \\ -\sin(\gamma_d-\gamma_a) & \cos(\gamma_d-\gamma_a) & 0 \\ 0 & 0 & 1 \end{pmatrix}. \tag{5.76}$$

It can be shown (see Appendix D) that

$$\sin(\gamma_d-\gamma_a) = \frac{(\sin\phi_a+\sin\phi_d)\sin\delta}{(1+\cos\alpha)} \equiv q, \tag{5.77}$$

and

$$\cos(\gamma_d-\gamma_a) = \frac{\cos\phi_a\cos\phi_d+(1+\sin\phi_a\sin\phi_d)\cos\delta}{(1+\cos\alpha)} \equiv p\ . \tag{5.78}$$

The 2×2 *upper left submatrix of* $\mathbf{HF}$*, as given by* (5.76) *with* (5.78) *and* (5.77)*, is identical to the transformation matrix* $\Re$ *used in the semi-Lagrangian scheme of the (HPE) ECMWF model; see the Appendix of Temperton et al. (2001). In terms of* p *and* q *as defined by* (5.78) *and* (5.77)*, we consider that the* "2d option" *in the New Dynamics should have*

$$\mathbf{M}_{2d} = \mathbf{HF} = \begin{pmatrix} p & q & 0 \\ -q & p & 0 \\ 0 & 0 & 1 \end{pmatrix}, \tag{5.79}$$

and not (as at present)

$$\begin{pmatrix} \cos\delta & \sin\phi_d \sin\delta & 0 \\ -\sin\phi_a \sin\delta & \cos\phi_a \cos\phi_d + \sin\phi_a \sin\phi_d \cos\delta & 0 \\ 0 & 0 & 1 \end{pmatrix} \equiv \begin{pmatrix} p_1 & q_1 & 0 \\ -q_2 & p_2 & 0 \\ 0 & 0 & 1 \end{pmatrix}. \tag{5.80}$$

It is easily seen that $\mathbf{M}_{2d}$*, as given by* (5.79) *together with* (5.78) *and* (5.77)*, is orthogonal. Since*

$$p = \frac{(p_1 + p_2)}{(1 + \cos\alpha)}, \quad q = \frac{(q_1 + q_2)}{(1 + \cos\alpha)}, \tag{5.81}$$

and

$$\cos\alpha = M_{ww} = p_1 p_2 + q_1 q_2, \tag{5.82}$$

the necessary modifications are unlikely to be expensive in computational terms.

5.3 Interpolation

Section 5.1's brief account of the semi-Lagrangian method portrayed as separate and sequential steps (i) the departure-point calculation and (ii) the interpolation of fields to the departure point. This was correct only in broad-brush terms, since it glossed over the fact that the departure-point calculation itself involves interpolation. We discuss interpolation before the departure-point calculation in the present more detailed treatment. We consider interpolation in a Cartesian framework first, and then outline the approach used in the New Dynamics. Our discussion aims to provide a simple background and to illuminate the options available in the code.

5.3.1 *Cartesian Interpolation*

Suppose that we know the value of the function F at a number of gridpoints, and that we wish to estimate F at some point $\mathbf{x}$ which is not a gridpoint; in many cases, $\mathbf{x}$ will be the departure point $\mathbf{x}_d$. [Precisely the same problem arises regarding the source function Ψ; we use the symbol F generically.]

Linear interpolation

The 1-dimensional problem is straightforward. Suppose that F is known at gridpoints x_i and x_{i+1}, i.e. $F(x_i) = F_i$ and $F(x_{i+1}) = F_{i+1}$. Without loss of generality, choose $x_i = 0$ and define $\Delta x \equiv (x_{i+1} - x_i)$; then the linear interpolant for F at some intermediate point x is simply

$$F(x) = F_i + \frac{x}{\Delta x}\left[F_{i+1} - F_i\right] \ . \tag{5.83}$$

From (5.83) it is clear that $F(x)$ lies between F_i and F_{i+1} so long as x lies between 0 and Δx; the interpolant $F(x)$ is *monotonic* and lies within the range of the two gridpoint values of F. A useful equivalent of (5.83) is

$$F(x) = \left(1 - \frac{x}{\Delta x}\right) F_i + \frac{x}{\Delta x} F_{i+1} \ . \tag{5.84}$$

This expresses $F(x)$ as the sum of: (i) a term equal to F_i at $x = x_i = 0$ and to zero at $x = x_{i+1} = \Delta x$; and (ii) a term equal to F_{i+1} at $x = x_{i+1} = \Delta x$ and to zero at $x = x_i = 0$. See Fig. 5.4.

<u>Aside :</u>

How accurate is (5.84)*? Suppose that* $F(x)$ *can be expanded as a Taylor series about* $x = x_i = 0$*, i.e. that*

$$F(x) = F_i + xF_i' + \frac{x^2}{2}F_i'' + \frac{x^3}{6}F_i''' + ... , \tag{5.85}$$

where the primes and subscripts indicate differentiation and evaluation at $x = x_i = 0$*. At*$x = x_{i+1} = \Delta x$*,* (5.85) *gives*

$$F_{i+1} = F(\Delta x) = F_i + \Delta x F_i' + \frac{\Delta x^2}{2}F_i'' + \frac{\Delta x^3}{6}F_i''' + ... \tag{5.86}$$

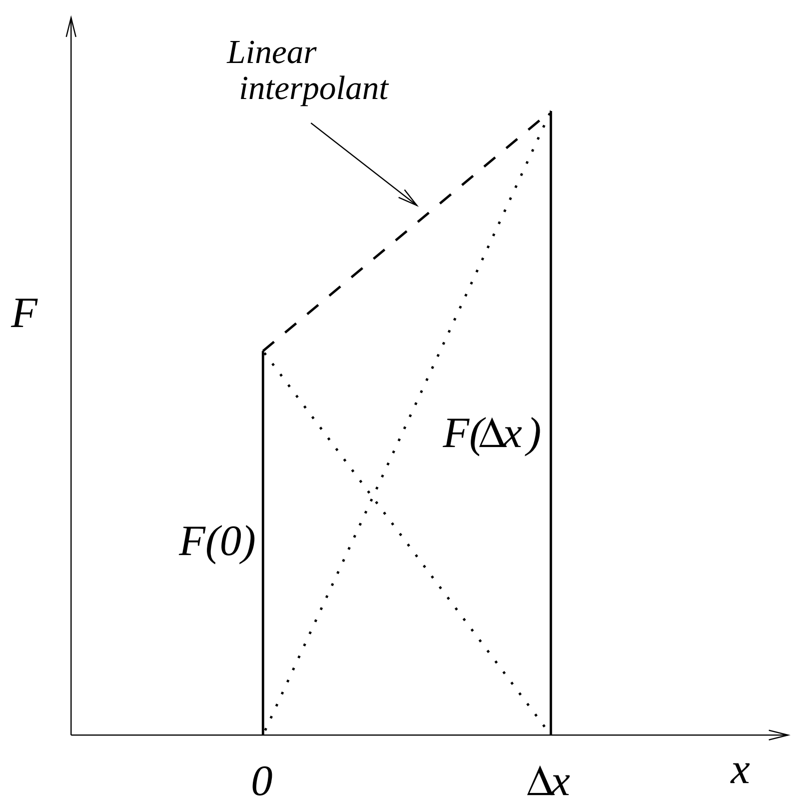

Figure 5.4: Illustrating linear interpolation (broken line) between known values of F at gridpoints at $x = x_i = 0$ and $x = x_{i+1} = \Delta x$. The dotted lines indicate linear functions which each reproduce the known value at one gridpoint and vanish at the other; their sum is equal to the linear interpolant.

By eliminating $F_i^{'}$ *between* (5.85) *and* (5.86)*, and truncating terms of third order and above, one obtains* (5.84) *augmented by a quadratic leading error term:*

$$F(x) = F_i + \frac{x}{\Delta x}\left(F_{i+1} - F_i\right) - \frac{x\left(\Delta x - x\right)}{2} F_i^{''}. \tag{5.87}$$

The term $-\left[x(\Delta x - x)/2\right] F_i^{''}$ *vanishes at the gridpoints* $x_i = 0$, $x_{i+1} = \Delta x$ *(as does the entire error) and attains the local extremum* $-\left[\Delta x^2/8\right] F_i^{''}$ *at* $x = \Delta x/2$. *[As an* extra*polation formula,* (5.87) *can lead to much larger errors.]*

The leading error term in (5.87) *may be usefully compared with those found in simple discrete approximations to integrals and derivatives. Eq.* (5.87) *leads directly to an end-points approximation (with leading error term) to the integral of* $F(x)$ *over the interval* $x = [x_i,\ x_{i+1}] = [0, \Delta x]$*:*

$$\int_0^{\Delta x} F dx = \Delta x \left(\frac{1}{2}\left(F_i + F_{i+1}\right) - \frac{\Delta x^2}{12} F_i^{''}\right). \tag{5.88}$$

From (5.86) *and the Taylor expansion* (5.85) *evaluated at*$x = x_{i-1} = -\Delta x$*,a familiar approximation to the first derivative of* F *at* $x = x_i = 0$ *may be obtained (with leading error term):*

$$F_i^{'} = \frac{\left(F_{i+1} - F_{i-1}\right)}{2\Delta x} - \frac{\Delta x^2}{6} F_i^{'''}, \tag{5.89}$$

(where $F_{i-1} = F(x_{i-1})$*). Thederivation of the simple (and crude) formulae* (5.87) - (5.89) *emphasises Taylor's theorem as their common origin, and shows that much the same analysis is needed whether the context is interpolation, integration or differentiation. The coefficients of the quadratic error terms in* (5.87) - (5.89) *are all of the same order of magnitude. More accurate formulae may be obtained in all cases by involving more gridpoint values so as to raise the order of the leading error terms.*

Linear interpolation in two Cartesian dimensions (*bilinear interpolation*) is somewhat more challenging. With reference to Fig. 5.5,suppose we know the function F at gridpoints $(x_i,\ y_j)$, $(x_{i+1},\ y_j)$, $(x_i,\ y_{j+1})$ and $(x_{i+1},\ y_{j+1})$, i.e. $F\left(x_i,\ y_j\right) = F_{i,\,j}$, $F\left(x_{i+1},\ y_j\right) = F_{i+1,\,j}$, $F\left(x_i,\ y_{j+1}\right) = F_{i,\,j+1}$ and $F\left(x_{i+1},\ y_{j+1}\right) = F_{i+1,\,j+1}$. Without loss of generality, choose $x_i = y_j = 0$ and define $\Delta x \equiv (x_{i+1} - x_i)$, $\Delta y \equiv (y_{j+1} - y_j)$. We can construct an interpolant for F at some intermediate point $(x,\ y)$ by three successive one-dimensional linear interpolations:

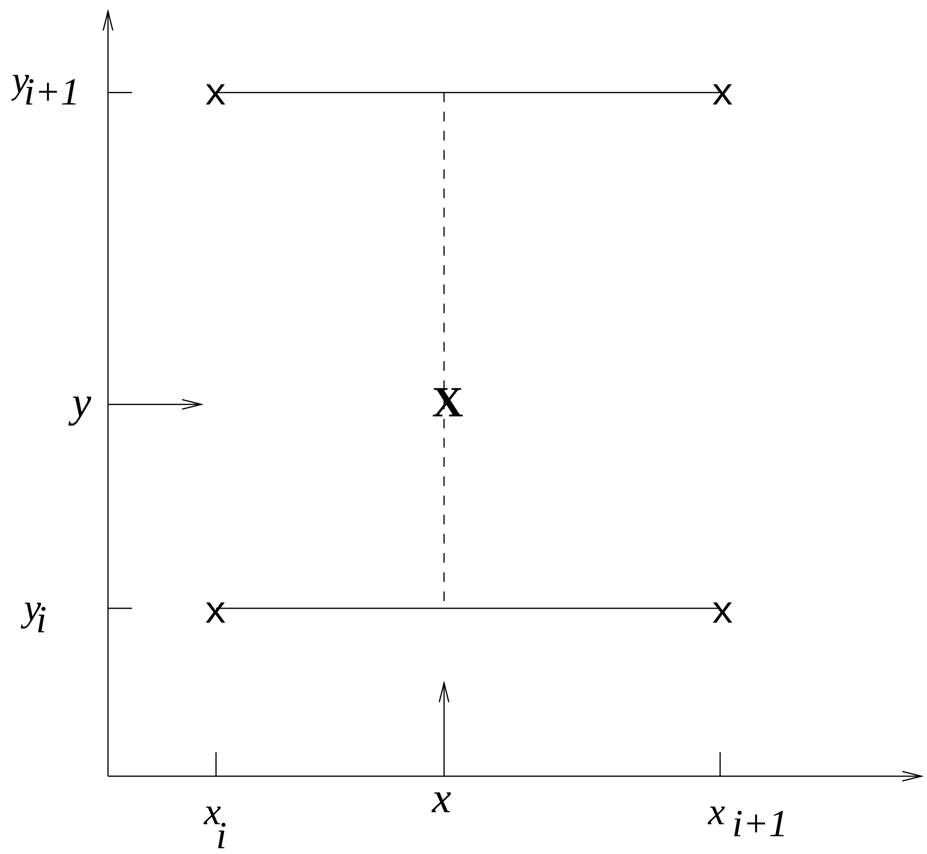

Figure 5.5: Illustrating linear interpolation in 2D. To construct an expression for interpolation to the target point $(x,\, y)$: (i) interpolate to $(x,\, y_i)$; (ii) interpolate to $(x,\, y_{i+1})$; and (iii) interpolate to $(x,\, y)$ using the results of (i) and (ii).

(a) between $F_{i,\,j}$ and $F_{i+1,\,j}$ to obtain F at point $(x,\, y_j)$:

$$F(x,\, y_j) = F_{i,\,j} + \frac{x}{\Delta x}\left[F_{i+1,\,j} - F_{i,\,j}\right]; \tag{5.90}$$

(b) between $F_{i,\,j+1}$ and $F_{i+1,\,j+1}$ to obtain F at point $(x,\, y_{j+1})$:

$$F(x,\, y_{j+1}) = F_{i,\,j+1} + \frac{x}{\Delta x}\left[F_{i+1,\,j+1} - F_{i,\,j+1}\right]; \tag{5.91}$$

(c) between $F\,(x,\, y_j)$ and $F\,(x,\, y_{j+1})$ to obtain F at point $(x,\, y)$:

$$F(x,\, y) = F\,(x,\, y_j) + \frac{y}{\Delta y}\left[F\,(x,\, y_{j+1}) - F\,(x,\, y_j)\right]. \tag{5.92}$$

The result (5.92) can be written in terms of $F_{i,\,j}$, $F_{i+1,\,j}$, $F_{i,\,j+1}$, $F_{i+1,\,j+1}$ as

$$F\,(x,\, y) =$$

$$\left(1-\frac{x}{\Delta x}\right)\left(1-\frac{y}{\Delta y}\right)F_{i,j}+\frac{x}{\Delta x}\left(1-\frac{y}{\Delta y}\right)F_{i+1,j}+\frac{y}{\Delta y}\left(1-\frac{x}{\Delta x}\right)F_{i,j+1}+\frac{x}{\Delta x}\frac{y}{\Delta y}F_{i+1,j+1}\,. \tag{5.93}$$

The four terms on the right side of (5.93) each reduce to a gridpoint value of F at one of the four gridpoints, and vanish at the other three (cf. (5.84)).

Eq. (5.93) has two important properties.

First, it gives a direction-independent interpolant. It is readily shown that the same result (5.93) is obtained by varying the order of operations (a), (b) and (c): by interpolating first in y to obtain F at point $(x_i,\ y)$, second in y to obtain F at point $(x_{i+1},\ y)$ and finally in x to obtain F at point $(x,\ y)$.

Second, (5.93) contains terms in the product xy as well as constants and terms linear in x and y. Hence (5.93) does not represent a plane. (This is to be expected anyway, since a plane would be uniquely specified by only 3 of the 4 gridpoint values $F_{i,\,j}$, $F_{i+1,\,j}$, $F_{i,\,j+1}$, $F_{i+1,\,j+1}$.) In geometric terms, the interpolant (5.93) represents a *ruled surface* having zero Newtonian (mean) curvature $\nabla^2 F$, rather than a plane; in analytic terms, it is a harmonic function - each of its components (constant + terms in x, y and xy) satisfies Laplace's equation $\nabla^2 F = 0$. [The interpolant has negative semi-definite Gaussian curvature: $\Delta x^2 \Delta y^2 \left(F_{xx}F_{yy} - F_{xy}^2\right) \;=\; -\left(F_{i,j} + F_{i+1,j+1} - F_{i,j+1} - F_{i+1,j}\right)^2$. This just reflects the fact that the surface is anticlastic: it lies between its principal centres of curvature, like the surface of a saddle - or a Pringle! Because $\nabla^2 F = 0$, the principal curvatures are numerically equal but of opposite sign (as is characteristic of a hyperbolic paraboloid).]

The harmonic character of (5.93) has the important consequence that the extremal values of the interpolant F within the domain of interpolation must lie on the boundary of the domain [$\nabla^2 F = 0 \;\Rightarrow\;$ no interior extrema, by Gauss's theorem]; and since F varies linearly on the boundaries of the interpolation domain, the extremal values of F must occur at gridpoints. Hence *2D linear interpolation does not generate values outside the range defined by the surrounding gridpoints.* In other words, 2D linear interpolation, like 1D linear interpolation, is automatically monotone in character. The same result applies to 3D linear interpolation (*trilinear interpolation)*, and for the same reasons: the 3D generalisation of (5.93) contains only terms that are harmonic functions.

Higher order interpolation

Over time, linear interpolation gives unacceptably large damping when used to interpolate fields to the departure point in semi-Lagrangian schemes (Bates & McDonald (1982)). [Linear interpolation is found to be sufficent in the departure-point calculation itself, however; see below.] Interpolation using higher degree polynomials is more accurate, and gives much less damping. Both *cubic and quintic Lagrange interpolation* are available in the New Dynamics and are particularly transparent in one dimension.

Suppose that F is known at gridpoints x_{i-1}, x_i, x_{i+1} and x_{i+2}, i.e. $F(x_{i-1}) = F_{i-1}$, $F(x_i) = F_i$, $F(x_{i+1}) = F_{i+1}$ and $F(x_{i+2}) = F_{i+2}$. To form a cubic polynomial $F(x)$ that reproduces these known values, observe that cubics reproducing *one* of the known values, but *vanishing* at the other gridpoints, are readily constructed. For example (see Fig. 5.6), a cubic $C_{i-1}(x)$ that vanishes at x_i, x_{i+1} and x_{i+2} must be expressible as

$$C_{i-1}(x) \;=\; A\,(x - x_i)\,(x - x_{i+1})\,(x - x_{i+2})\,. \tag{5.94}$$

The constant A may be chosen so that $C_{i-1}(x)$ gives the value F_{i-1} at $x = x_{i-1}$:

$$C_{i-1}(x) = \frac{(x - x_i)\,(x - x_{i+1})\,(x - x_{i+2})}{(x_{i-1} - x_i)\,(x_{i-1} - x_{i+1})\,(x_{i-1} - x_{i+2})} F_{i-1}. \tag{5.95}$$

Cubics $C_i\,(x)$, $C_{i+1}\,(x)$, $C_{i+2}\,(x)$ that give (respectively) F_i at $x = x_i$, F_{i+1} at $x = x_{i+1}$ and F_{i+2} at $x = x_{i+2}$, but vanish at the other gridpoints, may be constructed in the same way:

$$C_i(x) = \frac{(x - x_{i-1})\,(x - x_{i+1})\,(x - x_{i+2})}{(x_i - x_{i-1})\,(x_i - x_{i+1})\,(x_i - x_{i+2})} F_i, \tag{5.96}$$

$$C_{i+1}(x) = \frac{(x - x_{i-1})\,(x - x_i)\,(x - x_{i+2})}{(x_{i+1} - x_{i-1})\,(x_{i+1} - x_i)\,(x_{i+1} - x_{i+2})} F_{i+1}, \tag{5.97}$$

$$C_{i+2}(x) = \frac{(x - x_{i-1})\,(x - x_i)\,(x - x_{i+1})}{(x_{i+2} - x_{i-1})\,(x_{i+2} - x_i)\,(x_{i+2} - x_{i+1})} F_{i+2}. \tag{5.98}$$

The cubic that reduces to F_{i-1} at $x = x_{i-1}$, to F_i at $x = x_i$, to F_{i+1} at $x = x_{i+1}$ and to F_{i+2} at $x = x_{i+2}$ is just the sum of (5.95), (5.96), (5.97), (5.98):

$$F(x) = C_{i-1}(x) + C_i(x) + C_{i+1}(x) + C_{i+1}(x). \tag{5.99}$$

Equality of the intervals $(x_i - x_{i-1})$, $(x_{i+1} - x_i)$ and $(x_{i+2} - x_{i+1})$ has not been assumed and is not required.

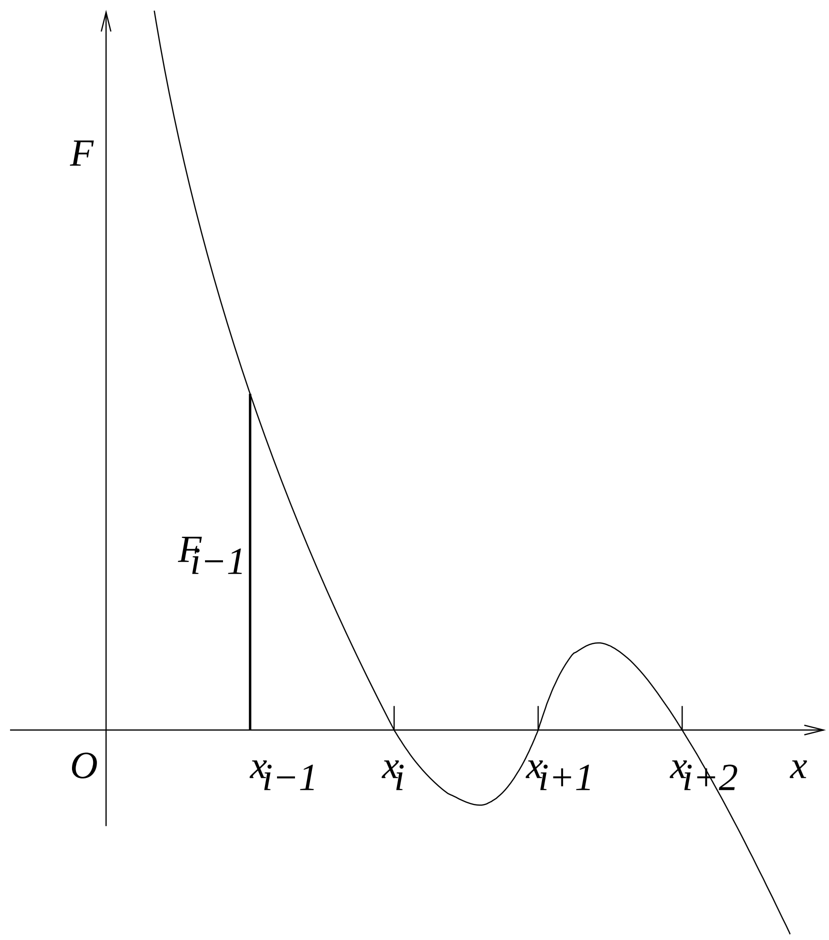

Figure 5.6: Sketch of a cubic polynomial which vanishes at gridpoints $x = x_i$, x_{i+1}, x_{i+2} and is equal to $F_{i-1} = F(x_{i-1})$ at $x = x_{i-1}$. The cubic necessarily tends to $\pm\infty$ for large $|x|$.

Quintic Lagrange interpolation proceeds in essentially the same way, the function F being known at the 6 gridpoints x_{i-2}, x_{i-1}, x_i, x_{i+1}, x_{i+2} and x_{i+3} [i.e. $F(x_{i-2}) = F_{i-2}$, $F(x_{i-1}) = F_{i-1}$, $F(x_i) = F_i$, $F(x_{i+1}) = F_{i+1}$, $F(x_{i+2}) = F_{i+2}$ and $F(x_{i+3}) = F_{i+3}$], and the quintic interpolant being the sum of 6 fifth order polynomials that each reduce to F at one of the gridpoints but vanish at the others.

Aside :

Another way of deriving interpolation formulae such as (5.99) *is simply to fit a polynomial to the gridpoint values. In the case of cubic interpolation, pose the polynomial*

$$P_3(x) = A + Bx + Cx^2 + Dx^3 \,, \tag{5.100}$$

and find A, B, C and D from the 4 linear inhomogeneous algebraic equations

$$P_3(x_{i-1}) = A + Bx_{i-1} + Cx_{i-1}^2 + Dx_{i-1}^3 = F_{i-1}, \tag{5.101}$$

$$P_3(x_i) = A \;+\; Bx_i \;+\; Cx_i^2 \;+\; Dx_i^3 = F_i \;\;, \tag{5.102}$$

$$P_3(x_{i+1}) = A + Bx_{i+1} + Cx_{i+1}^2 + Dx_{i+1}^3 = F_{i+1}, \tag{5.103}$$

$$P_3(x_{i+2}) = A + Bx_{i+2} + Cx_{i+2}^2 + Dx_{i+2}^3 = F_{i+2}. \tag{5.104}$$

This procedure may be rationalised by noting that the polynomial (5.100) *has the same form as a truncated Taylor series expansion of F about $x = 0$ (the location of which relative to the gridpoints we are of course free to choose):*

$$F(x) = F(0) + xF^{'}(0) + \frac{x^2}{2}F^{''}(0) + \frac{x^3}{6}F^{'''}(0) + O(x^4). \tag{5.105}$$

The constants A, B, C and D in (5.100) *may be identified with* $F(0)$, $F^{'}(0)$, $F^{''}(0)/2$ *and* $F^{'''}(0)/6$ *in* (5.105), *since there can be only one cubic that passes through four given gridpoint values of F. The Taylor series expansion* (5.105) *shows that cubic interpolation is accurate to fourth order, in the sense that the first term omitted,* $(x^4/24)\,F^{''''}(0)$, *is of this order. The leading order error in the cubic* (5.100), *once A, B, C and D have been determined, must vanish at the gridpoints x_{i-1}, x_i, x_{i+1} and x_{i+2}; since it must also be a quartic polynomial in x, it must have the form*

$$E_4(x) = a\,(x - x_{i-1})\,(x - x_i)\,(x - x_{i+1})\,(x - x_{i+2}) \;, \tag{5.106}$$

where a is a constant. If the grid interval Δx is uniform, and the origin of x is placed at $(x_i + x_{i+1})/2$, (5.106) *becomes*

$$E_4(x) = a\left(x^2 - \frac{\Delta x^2}{4}\right)\left(x^2 - \frac{9\Delta x^2}{4}\right), \tag{5.107}$$

(the gridpoints being now located at $x = \pm\Delta x/2$, $x = \pm 3\Delta x/2$). $E_4(x)$ has an extremum of $9a\Delta x^4/16$ at $x = 0$ and extrema of $-a\Delta x^4$at $x = \pm\sqrt{5}/2$. This suggests that the cubic interpolant (5.100) *is* numerically *more accurate between the inner pair of gridpoints ($|x| < \Delta x/2$) than between the outer pairs ($\Delta x/2 < |x| < 3\Delta x/2$). Integrating E_4 over the relevant ranges bears this out:*

$$\frac{1}{\Delta x}\int_{-\Delta x/2}^{\Delta x/2} E_4(x)dx = \frac{11a\Delta x^4}{30}, \tag{5.108}$$

$$\frac{1}{\Delta x}\int_{\Delta x/2}^{3\Delta x/2} E_4(x)dx = -\frac{19a\Delta x^4}{30}. \tag{5.109}$$

The constant a takes the value $-F''''(0)/24$. Note that the interpolant is of the same order *of accuracy (i.e. $O(\Delta x^4)$) throughout the range $x_{i-1} < x < x_{i+2}$. This result holds (with $\Delta x = \max\{\Delta x_i\}$) also for a variable mesh. However, the use of cubic interpolants except between the inner pair of gridpoints has been found to destabilise semi-Lagrangian schemes; see Bates & McDonald (1982) and McDonald (1984) for analytical stability treatments giving this result.*

Aside :

Interpolation using even-order polynomials (such as quadratics) is a perfectly respectable procedure but it is not used in the New Dynamics. See McDonald (1984) and Leslie & Dietachmayer (1997) for examples of the use of quadratic interpolation in semi-Lagrangian schemes.

The treatment is readily extended to 2 and 3 spatial dimensions. In 2 dimensions, for example, (see Fig. 5.7) cubic interpolation formulae for the point $(x,\, y)$ may be derived by successive interpolations to the 4 points $(x,\, y_{i-1})$, $(x,\, y_i)$, $(x,\, y_{i+1})$, $(x,\, y_{i+2})$ along 4 "rows" of points, and a final interpolation using the "column" of values thus obtained. The outcome is direction-independent: the same result is obtained if interpolation to the 4 points $(x_{i-1},\, y)$, $(x_i,\, y)$, $(x_{i+1},\, y)$, $(x_{i+2},\, y)$ along 4 "columns" of points is done first, and the

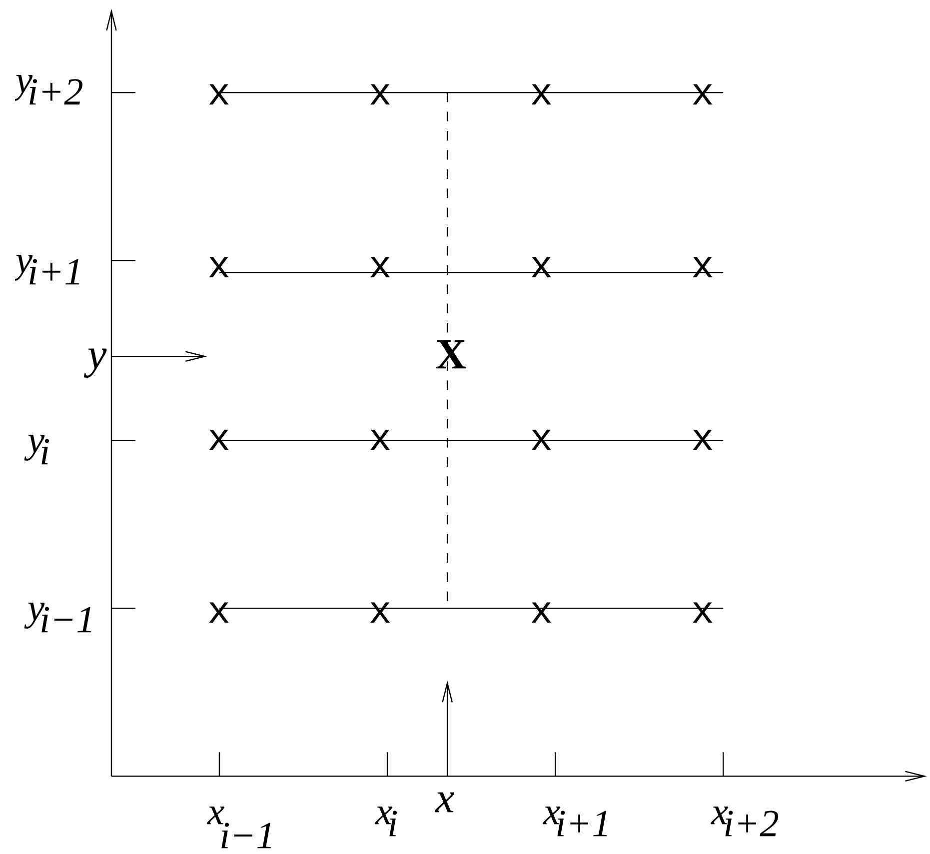

Figure 5.7: Illustrating cubic Lagrange interpolation in 2D. To derive an interpolation formula for the target point $(x,\, y)$, a two-stage process may be used. In the first stage, the 4 horizontal rows of points are used to interpolate to x at $y = y_{i-1},\, y_i,\, y_{i+1},\, y_{i+2}$. In the second stage, the column of 4 values thus obtained are used to interpolate to the target point (as indicated by the broken line).

final interpolation uses the resulting "row" of values. The amount of computation involved becomes considerable: cubic interpolation requires 16 gridpoint values of F in 2D and 64 in 3D, while the corresponding figures for quintic interpolation are 36 and 216.

An interpolation method that requires less computation, and is available in the New Dynamics, is the *quasi-cubic* scheme of Ritchie, Temperton, Simmons, Hortal, Davies, Dent & Hamrud (1995). This blends linear and cubic interpolation. In 2D, it requires only 12 values of F, the 4 unused values being those at the vertices of the 4×4 rectangle defined by the 16 gridpoints deployed in regular 2D cubic interpolation. (These 4 vertices are farther from the centre of the 4×4 rectangle than the other 12 gridpoints are; but points away from the centre may be closer to the omitted vertices than to some of the retained gridpoints.) In

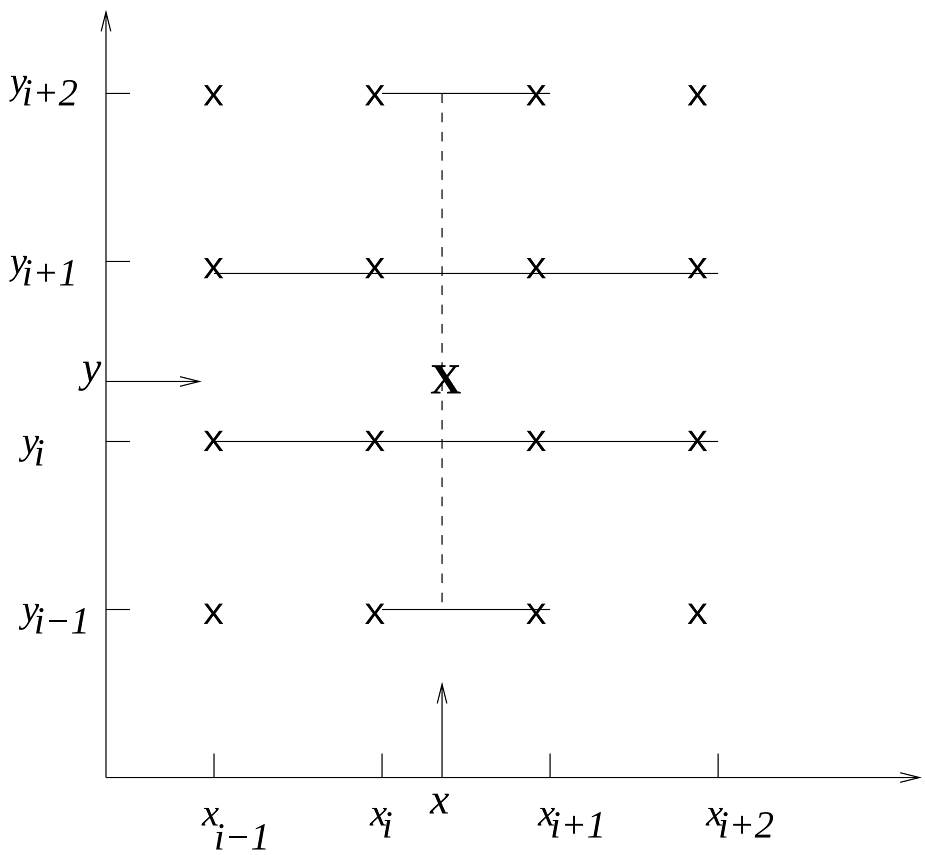

Figure 5.8: Illustrating 2D quasi-cubic interpolation to the target point $(x,\ y)$. The procedure for deriving the interpolation formula is the same as for 2D Lagrange cubic interpolation, except that the interpolant to x at the rows y_{i-1} and y_{i+2} is obtained simply by linear interpolation between the values at x_i and x_{i+1} .

3D, the quasi-cubic scheme requires only 32 values of F - half the number required in regular 3D cubic interpolation; the omitted values are those on the edges (and at the vertices) of the $4 \times 4 \times 4$ rectanguloid defined by the 64 gridpoints of regular cubic interpolation. We give an outline of the 2D algorithm.

Suppose that F is to be interpolated to the point $(x,\, y)$, and that $F_i = F(x_i)$ is known at the 4 gridpoints surrounding $(x,\, y)$ and at the 8 nearby gridpoints which together define a cross-shaped domain on the plane; see Fig. 5.8. To derive the formula, perform cubic Lagrange interpolations to the points $(x,\, y_i)\,,\, (x,\, y_{i+1})$ along the two 4-point "rows" of the cross. Next, perform *linear* interpolation to the points $(x,\, y_{i-1})\,,\, (x,\, y_{i+2})$ along the two 2-point rows of the cross. Finally, use the resulting values of F at points $(x,\, y_{i-1})\,,\, (x,\, y_i)$, $(x,\, y_{i+1})\,,\, (x,\, y_{i+2})$ to carry out a cubic Lagrange interpolation to the point $(x,\, y)$.

This quasi-cubic scheme is attractive because it feels more isotropic than regular cubic interpolation, as well as being less computationally demanding. However, as well as being less accurate, it suffers the disadvantage of being direction-dependent: the same result for $F(x,\, y)$ is *not* obtained if one first interpolates to $(x_i,\, y)\,,\, (x_{i+1},\, y)$ using the two 4-point *columns* of the cross, interpolates to $(x_{i-1},\, y)\,,\, (x_{i+2},\, y)$ using the two 2-point columns of the cross, and finally interpolates to $(x,\, y)$ by the cubic Lagrange method. [The scheme would obviously be direction-independent if re-defined as the mean of the two versions already described, but it would then involve even more cubic interpolations than the regular 2D scheme (whilst still being less accurate).]

Aside :

A promising way of efficiently improving the accuracy of interpolation would be to use the cascade scheme of Purser & Leslie (1991) and Nair, Côté & Staniforth (1999).

5.3.2 *Interpolation in the New Dynamics*

The previous subsection gave a basic introduction to some interpolation schemes; we now discuss their implementation in a model framed in spherical geometry and with rigid lower and upper boundaries.

Interpolation in the New Dynamics makes no concession to the sphericity of the coordinate system: all interpolation is carried out as if the relevant gridpoints were located on a

Cartesian grid. To the extent that even quintic interpolation involves points only two rows or levels away from the target volume, this seems a reasonable approximation. Within a few gridpoints of most grid volumes, a local Cartesian approximation to the spherical polar geometry is very good, given the high resolutions used in the New Dynamics.

Aside :

This locality argument does not extend to the time-stepping of the velocity components, for which sphericity effects over the displacement of a parcel during one timestep need to be - and are - included (see section 5.2).

Aside :

The grid volumes which abut either the North Pole or the South Pole are triangular in horizontal section, and the Cartesian (rectangular) approximation seems severe. Analysis of this specific issue is needed, and - more generally - of interpolation procedures in the vicinity of the poles.

Linear interpolation is used in the departure-point calculation (see next subsection) but - except close to the lower and upper boundaries - linear interpolation is *not* used to evaluate fields at the departure point once it has been calculated. Linear interpolants obtained on the Cartesian assumption are no longer strictly harmonic functions in spherical polar geometry, so - for the departure-point calculation - the consequences for monotonicity need to be considered. An intuitive topological argument shows that no interior extrema are generated by assuming Cartesian geometry and then applying the interpolant in spherical polars. In the Cartesian space, Gauss's theorem ensures that the extrema occur at gridpoints (see previous subsection). Application of the resulting interpolant in spherical geometry involves a simple deformation of the Cartesian field which can introduce no new interior extrema; hence they must remain at the gridpoints. Evidently, $\nabla^2 F = 0$ is a sufficient but not a necessary condition for the occurrence of extrema only at the boundaries of a domain.

Aside :

It is not difficult to construct interpolation schemes based on the requirement that $\nabla^2 F = 0$ when the interpolant F is evaluated between points on a λ, ϕ, r grid. For radial (r) interpolation we can require that

$$\nabla_r^2 F \equiv \frac{1}{r^2}\frac{\partial}{\partial r}\left(r^2 \frac{\partial F}{\partial r}\right) = 0, \tag{5.110}$$

which is satisfied by taking

$$F = \frac{A}{r} + B. \tag{5.111}$$

The constants A and B can be determined from $F(r_k) = F_k$ and $F(r_{k+1}) = F_{k+1}$. This defines the radial spherical polar equivalent of linear interpolation in one Cartesian dimension. The radial spherical polar equivalent of cubic interpolation in one Cartesian dimension may be defined by requiring $\nabla_r^4 F = 0$, which has the simple solution

$$F = \frac{A}{r} + B + Cr + Dr^2. \tag{5.112}$$

This result is readily extended to the case $\nabla_r^{2n} F = 0$. It is clear that the same interpolants would be obtained by applying Cartesian *interpolations (linear, cubic or higher odd order) to the quantity rF. Vertical interpolation schemes defined in these terms may be worth exploring further.*

We have already noted that linear interpolation is necessarily monotone. This property is not assured if cubic or quintic (or higher order) interpolation is used. The facility to impose monotonicity, and thus to suppress (supposedly) spurious overshoots, is included in the New Dynamics code. The scheme used is that of Bermejo & Staniforth (1992): if any departure point value is found to be outside the range defined by the 8 surrounding gridpoints, then it is replaced by the closer extremal value.

Aside :

Linear interpolation is not somehow "better" than higher order interpolation because it generates an interpolant which is automatically monotonic. Indeed, it is used routinely only in the departure-point calculation (as we have noted) and very close to the lower and upper boundaries (as we shall note soon), since it is generally found to be insufficiently accurate for the estimation of field values at the departure point. Linear interpolation on a rectangular grid concentrates all the curvature at the boundaries of the grid cells (in much the same way as the curvature in a polyhedron is concentrated at the edges and vertices). Higher order interpolation schemes allow curvature within grid cells as well as at their boundaries; they thus achieve a more even distribution of curvature, which is desirable in almost all respects - including better treatment of real maxima and *minima in the fields. [Spline interpolation, which is not used in the New Dynamics, is a technique which specifically aims to achieve an equitable distribution of curvature.] A consequence, however, is that monotonicity is no longer assured.*

The facility to enforce (first moment) conservation also exists in the code; the scheme of Priestley (1993) is used. In essence, a degree of smoothing greater than that of the monotonicity scheme of Bermejo & Staniforth (1992) is applied if this achieves conservation.

As is usual in semi-Lagrangian codes, cubic and quintic interpolants are actually used only in the central grid box of the region of fit. This almost certainly ensures that the best interpolant is used within each grid box, and avoids the instabilities that may be associated with other choices; see McDonald (1984) and the *Aside* following (5.99).

Interpolation near the boundaries of the domain proceeds as follows. If cubic interpolation is being applied in the interior, linear interpolation is applied in all grid boxes adjacent to the boundary; this procedure involves a reduction in formal accuracy near the boundaries, since linear interpolation is less accurate than cubic. If quintic interpolation is being applied in the interior, linear interpolation is applied in all grid boxes adjacent to the boundaries, and cubic interpolation in all grid boxes separated from a boundary by one grid volume. This procedure also involves a reduction in formal accuracy.

Aside :

In an earlier Aside it was noted that (1-D) cubic interpolation is most accurate between the central grid points, but is of the same order *of accuracy throughout the range defined by the four gridpoints. Using linear interpolation in gridboxes adjacent to boundaries is therefore less accurate than using the cubic interpolant centred on the next interior gridbox. Similar remarks apply to the use of linear and cubic interpolation close to the boundaries when quintic interpolation is being applied in the interior. The reason for the use of reduced-order interpolation near the boundaries is a desire to avoid the numerical instabilities that can arise if, for example, a cubic interpolant is used outside its inner interval (see earlier comments) but re-examination of the issue may be desirable. In general, linear interpolation is found to be insufficiently accurate for the estimation of field values at departure points, and it is globally used only in the departure-point calculation.*

Since the New Dynamics uses a terrain-following vertical coordinate η (see sections 2 and

4), it might be expected that all interpolation would be carried out in the $(\lambda,\ \phi,\ \eta)$ system (in which all fields are stored). The latest version uses interpolation in $(\lambda,\ \phi,\ \eta)$ except in the departure point calculation, where interpolation in $(\lambda,\ \phi,\ r)$ is used. Earlier versions used interpolation in $(\lambda,\ \phi,\ r)$ in both the departure-point calculation and the estimation of field values at the departure point, and this was shown in idealised experiments to degrade accuracy.

5.4 Trajectory estimation: the departure point calculation

Before the departure-point values $F_d^n \equiv F(\mathbf{x}_d,\ t^n)$ and $\Psi_d^n \equiv \Psi^n(\mathbf{x}_d,\ t^n)$ (see (5.8)) can be calculated using an interpolation scheme, the departure point $\mathbf{x}_d$ itself must be found.

The principle of departure point calculation is simple: the displacement of a parcel of air is its velocity integrated over the relevant time interval. From (5.9) [see (5.10)] the particular displacement $\mathbf{x}_a - \mathbf{x}_d$ is given by

$$\mathbf{x}_a - \mathbf{x}_d = \int_{t^n}^{t^n+\Delta t} \mathbf{u}dt, \tag{5.113}$$

in which it is understood (as for (5.2))that the integral is to be taken along the trajectory between $\mathbf{x}_d$ at time t^n and $\mathbf{x}_a$ at time t^{n+1}. The time integration along the trajectory requires knowledge of the velocity field at the parcel location throughout the time period $[t^n,\ t^n + \Delta t]$. The practical difficulty is that the velocity field is known only at the gridpoints at discrete time levels. In other words, (5.113) requires a continuous Lagrangian description, but only discrete Eulerian information is available.

Ironically, things are made worse by the ability of semi-Lagrangian schemes to maintain numerical stability even when Δt exceeds the CFL criterion for the stability of conventional schemes (see Staniforth & Côté (1991)): the large values of Δt that are likely to be used make the temporal resolution of all fields particularly coarse. However, the practical difficulties in evaluating the integral in (5.113) are no greater in principle than those in evaluating the integral involving the source function Ψ in (5.1). We seek a time-centred approximation to (5.113) that will make good use of the available information.

Aside :

We have already noted the formal similarity between the departure point equation (5.113) *andthe integrated vector velocity equation* (5.15) *which is used to calculate* *the next-time-level velocity components. This aspect will be referred to again later.*

Lagrangian time-centred approximation

According to the Mean Value Theorem (MVT), (5.113) must be expressible as

$$\mathbf{x}_a - \mathbf{x}_d = \int_{t^n}^{t^n+\Delta t} \mathbf{u}\,(t)\, dt = \mathbf{u}\,(t^n + \theta\Delta t)\,\Delta t, \qquad (5.114)$$

where $\mathbf{u} = \mathbf{u}(t)$ refers to the trajectory, and $0 \leq \theta \leq 1$. In general, θ will be different for each trajectory, i.e. for each gridpoint and time-level, but its existence on the interval $[0,\ 1]$ is assured. Centring in time corresponds to making the *approximation* $\theta = 1/2$ in (5.114) in all cases. The accuracy of this step may be established by expanding the parcel velocity $\mathbf{u}(t)$ as a Taylor series about time-level $n + 1/2$, i.e. $t^n + \Delta t/2$, and integrating the result over the interval $[t^n,\ t^n + \Delta t]$:

$$\int_{t^n}^{t^n+\Delta t} \mathbf{u}(t)dt = \Delta t \left[\mathbf{u}\,(t^n + \Delta t/2) + \frac{1}{24}\Delta t^2 \mathbf{u}''\,(t^n + \Delta t/2) + O\left(\Delta t^4\right)\right]. \qquad (5.115)$$

The error in time-centring is thus $O\,(\Delta t^2)$ - as might have been expected.

Aside :

More interesting, perhaps, is that the error in time-centring vanishes if $\mathbf{u}''(t)$ *vanishes. Integrating* $\mathbf{u}''(t) = 0$ *twice gives*

$$\mathbf{u}(t) = \mathbf{u}(t^n) + (t - t^n)\mathbf{a}, \qquad (5.116)$$

in which the acceleration $\mathbf{a}$ *is independent of time. A further time integration gives the parcel location as*

$$\mathbf{x}(t) = \mathbf{x}(t^n) + [t - t^n]\,\mathbf{u}(t^n) + \left[(t - t^n)^2/2\right]\mathbf{a}\,. \qquad (5.117)$$

[This is a vector version of the rote formula $x = ut + (1/2)\,ft^2$*, well known to generations of schoolpersons.] It is readily shown that* (5.117) *represents an arc of a parabola lying in the plane (not necessarily horizontal) containing* $\mathbf{a}$ *and* $\mathbf{u}(t^n)$ *and having its axis parallel to* $\mathbf{a}$*; if* $\mathbf{a}$ *is parallel to* $\mathbf{u}(t^n)$*, then the parabolic trajectory becomes a straight line in the same direction. The possibilities of parabolic trajectories may be worth exploring farther, but in this documentation we shall generally assume that time-centring is synonymous with straight-line trajectories (or great-circle arcs, their shallow-atmosphere counterparts).*

Aside :

The smallness of the coefficient of the Δt^2 error term in (5.115) *is also worth noting; see later comments on the coefficient of the Δt^2 error term in the extrapolation formula* (5.128). *[The coefficient of the Δt^2 error term in* (5.88) *is of opposite sign and twice as large; it resulted from an uncentred approximation.]*

Thus, by neglecting the Δt^2 error term in (5.115),we arrive at the expression

$$\mathbf{x}_a - \mathbf{x}_d = \mathbf{u}\left(t^n + \Delta t/2\right)\Delta t. \tag{5.118}$$

The quantity $\mathbf{u}\left(t^n + \Delta t/2\right)$, the parcel velocity at time-level $n + 1/2$, remains to be determined. The strategy is to replace $\mathbf{u}\left(t^n + \Delta t/2\right)$ by the Eulerian velocity field $\mathbf{u} = \mathbf{u}(\mathbf{x},\ t)$ evaluated at an appropriate point at time-level $n + 1/2$. This leads to an implicit equation for $\mathbf{x}_a - \mathbf{x}_d$ which is solved iteratively. Spatial interpolation and temporal extrapolation are required.

Aside :

An easy but crude way of estimating $\mathbf{u}\left(t^n + \Delta t/2\right)$ would be to use the arrival point value at the previous time-level, i.e. $\mathbf{u}^n = \mathbf{u}\left(\mathbf{x}_a,\ t^n\right)$. However, $\mathbf{u}^n = \mathbf{u}\left(\mathbf{x}_a,\ t^n\right)$ is an uncentred, first-order accurate approximation to $\mathbf{u}\left(t^n + \Delta t/2\right)$ both in time and space, and its use as an estimate of $\mathbf{u}\left(t^n + \Delta t/2\right)$ is found to give poor results unless Δt is chosen to be uneconomically small; see, for example, Staniforth & Pudykiewicz (1985) and Temperton & Staniforth (1987). Another easy option for estimating $\mathbf{u}\left(t^n + \Delta t/2\right)$ would be to use $\mathbf{u}^{n+1/2} = \mathbf{u}\left(\mathbf{x}_a,\ t^{n+1/2}\right)$, which can be calculated by extrapolation to $O\left(\Delta t^2\right)$ (see below). The reasons for condemning this are that it is uncentred in space, and involves error of order $\left(\nabla\mathbf{u}\right)\cdot\left(\mathbf{x}_a - \mathbf{x}_d\right)$; here $\nabla\mathbf{u}$ is the velocity gradient tensor.

Aside :

The emerging solution and approximation strategy for (5.113) *may be compared with that adopted for the formally similar time-integrated vector momentum equation* (5.15). *In that case (see* (5.53)*) a weighted mean of the righthand (source) term at time levels n and $n + 1$ was used, with "trajectory weighting factor" α. Eq.* (5.113) *is to be solved iteratively for $\mathbf{x}_d$, so it is clearly undesirable that*

$\mathbf{u}^{n+1}$ *should appear in the chosen discretised approximation to the time integral term;* $\mathbf{u}^{n+1}$ *will not be known until* (5.15) *has been applied, which in turn requires knowledge of the departure point! Hence, in pragmatic terms, the choice of a time-centred approximation to the time integral term in* (5.113)*; see* (5.118). *Note, however, that (i) an iterative procedure involving both* $\mathbf{x}_d$ *and* $\mathbf{u}^{n+1}$ *can be envisaged, and (ii) the appearance of terms at time-level* $n+1$ *on the rightside of* (5.15) *is itself computationally inconvenient (as noted in subsection 5.1). [The iterative procedure is used in the Canadian GEM model - see ECMWF report.]*

Midpoint approximation

If the particle velocity remained constant in magnitude and direction over the interval $[t^n,\ t^n+\Delta t]$, then its location at $t^n+\Delta t/2$ would be $\mathbf{x}_a - (\mathbf{x}_a - \mathbf{x}_d)/2 = (\mathbf{x}_a + \mathbf{x}_d)/2$. The particle velocity is generally *not* constant in this sense, of course, but it is an attractive approximation to estimate $\mathbf{u}(t^n+\Delta t/2)$ as if it were so. Then (5.118) becomes, to $O(\Delta t^2)$,

$$\mathbf{x}_a - \mathbf{x}_d = \mathbf{u}\left((\mathbf{x}_a + \mathbf{x}_d)/2,\ t^n + \Delta t/2\right)\Delta t. \tag{5.119}$$

This approximation may be thought of as replacing the location of the parcel at $t^n+\Delta t/2$ by the midpoint of a chord drawn from the departure point $\mathbf{x}_d$ to the arrival point $\mathbf{x}_a$. See Fig. 5.1.

Aside :

The formal accuracy of (5.119) *is readily established if the second derivative of the parcel velocity vanishes, i.e.* $\mathbf{u}''(t)=0$. *In this case the truncation error in the time-centring vanishes (see an earlier Aside), and parcel location as a function of time is given by* (5.117). *The error incurred in estimating* $\mathbf{x}(t^n+\Delta t/2)$*, the actual position of the parcel at time-level* $n+1/2$*, by the average of its positions* $\mathbf{x}(t^n)$ *and* $\mathbf{x}(t^n+\Delta t)$ *at time-levels* n *and* $n+1$*, may then be found:*

$$\mathbf{x}(t^n+\Delta t/2) - \left[\mathbf{x}(t^n) + \mathbf{x}(t^n+\Delta t)\right]/2 = -\left(\Delta t^2/8\right)\mathbf{a}\,. \tag{5.120}$$

Thus

$$\mathbf{x}(t^n+\Delta t/2) = \left[\mathbf{x}_a + \mathbf{x}_d\right]/2 - \left(\Delta t^2/8\right)\mathbf{a}\,, \tag{5.121}$$

in which the sign of the Δt^2 term correctly indicates that the displacement of an accelerating parcel ($\mathbf{a} > 0$) at time $t^n + \Delta t/2$ is overestimated by the average of its locations at t^n and $t^{n+1} = t^n + \Delta t$. Since

$$\mathbf{u}(t^n + \Delta t/2) = \mathbf{u}(\mathbf{x}(t^n + \Delta t/2),\ t^n + \Delta/2), \tag{5.122}$$

a Taylor expansion shows that

$$\mathbf{u}(t^n + \Delta t/2) = \mathbf{u}([\mathbf{x}_a + \mathbf{x}_d]/2,\ t^n + \Delta t/2) - \left(\Delta t^2/8\right)(\nabla\mathbf{u})\cdot\mathbf{a} + O\left(\Delta t^4\right). \tag{5.123}$$

The error incurred in replacing $\mathbf{u}(t^n + \Delta t/2)$ by the midpoint value is therefore

$$-\left(\Delta t^2/8\right)(\nabla\mathbf{u})\cdot\mathbf{a} + O\left(\Delta t^4\right). \tag{5.124}$$

[$\nabla\mathbf{u}$ is evaluated at the midpoint $(\mathbf{x}_a + \mathbf{x}_d)/2$.] The error in the midpoint approximation in the case $\mathbf{u}''(t) = 0$ is thus of order Δt^2 . Even when the $O(\Delta t^2)$ error introduced by time-centring vanishes, an $O(\Delta t^2)$ error is introduced by the midpoint approximation. Notice that, unless $\nabla\mathbf{u}$ and/or $\mathbf{a}$ vanish, the vector $(\nabla\mathbf{u})\cdot\mathbf{a}$ vanishes only in exceptional cases; for, even if the tensor $\nabla\mathbf{u}$ possesses a null space (itself a special circumstance) it is very unlikely that $\mathbf{a}$ will lie entirely within it.

Equation (5.119) may be written more concisely (and less argumentatively) as

$$\mathbf{x}_a - \mathbf{x}_d = \mathbf{u}_*\Delta t, \tag{5.125}$$

on the understanding that the velocity $\mathbf{u}_*$ isto be determined by extrapolation from gridpoint values at time-levels $n-1$ and n and interpolation of the resulting time-level $n+1/2$ values to the midpoint $(\mathbf{x}_a + \mathbf{x}_d)/2$.

Eulerian extrapolation in time

The velocities at gridpoints may be extrapolated to time-level $n + 1/2$ as

$$\mathbf{u}^{n+\frac{1}{2}} \equiv \mathbf{u}^n + \frac{1}{2}\left(\mathbf{u}^n - \mathbf{u}^{n-1}\right) = \frac{3}{2}\mathbf{u}^n - \frac{1}{2}\mathbf{u}^{n-1}. \tag{5.126}$$

Thissimple and intuitive extrapolation (and its accuracy) may be formally established by Taylor series expansion of $\mathbf{u}$ in time:

$$\mathbf{u}(t + \lambda\Delta t) = \mathbf{u}(t) + \lambda\Delta t\mathbf{u}'(t) + \frac{1}{2}\lambda^2\Delta t^2\mathbf{u}''(t) + O\left(\Delta t^3\right). \tag{5.127}$$

[The primes indicate *local* time differentiation.] Setting successively $\lambda = \frac{1}{2}$ and $\lambda = -1$, and then eliminating $\mathbf{u}'(t)$, leads to

$$\mathbf{u}\left(t + \frac{1}{2}\Delta t\right) = \frac{3}{2}\mathbf{u}(t) - \frac{1}{2}\mathbf{u}(t - \Delta t) + \frac{5}{4}\Delta t^2 \mathbf{u}''(t) + O\left(\Delta t^3\right). \tag{5.128}$$

The coefficient of the Δt^2 error term in (5.128) is 30 times as large as the coefficient of the corresponding term in (5.115).

Aside :

Schemes more accurate than (5.126) *can be constructed by bringing in values of* $\mathbf{u}$ *from earlier time-levels. For example, by also mobilising the Taylor series* (5.127) *for* $\mathbf{u}(t - 2\Delta t)$ *(i.e. setting* $\lambda = -2$*) one may obtain an* $O(\Delta t^3)$*-accurate, 3-time-level extrapolation for* $\mathbf{u}^{n+\frac{1}{2}}$*:*

$$\mathbf{u}^{n+\frac{1}{2}} = \frac{1}{8}\left(15\mathbf{u}^n - 10\mathbf{u}^{n-1} + 2\mathbf{u}^{n-2}\right). \tag{5.129}$$

See Temperton & Staniforth (1987) and McGregor (1993). The use of (5.129) *in the New Dynamics would require the retention of velocities at 3 time-levels, and the* $O(\Delta t^3)$ *accuracy achieved would be wasted unless the* $O(\Delta t^2)$ *errors elsewhere in the departure-point calculation could be removed. Also, use of equation* (5.129) *has been found to cause gravity mode destabilization, and countermeasures designed to suppress it tend to damp other modes unrealistically (Côté & Staniforth (1988), Gravel, Staniforth & Côté (1993)).*

Iteration and interpolation to find the displacement

The displacement $(\mathbf{x}_a - \mathbf{x}_d)$is determined implicitly by (5.125), and interpolation is required to evaluate the right side from gridpoint values of $\mathbf{u}^{n+\frac{1}{2}}$. In the New Dynamics, (5.125) is solved iteratively, using (5.126) to determine $\mathbf{u}^{n+\frac{1}{2}}$ at gridpoints, and *linear* interpolation to evaluate $\mathbf{u}$ at $(\mathbf{x}_a + \mathbf{x}_d)/2$. The iterative procedure is simply

$$(\mathbf{x}_a - \mathbf{x}_d)^{(K)} = \mathbf{u}\left(\mathbf{x}_a - (\mathbf{x}_a - \mathbf{x}_d)^{(K-1)}/2,\ t^n + \Delta t/2\right)\Delta t \equiv \mathbf{u}_*^{(K-1)}\Delta t, \tag{5.130}$$

where $(\mathbf{x}_a - \mathbf{x}_d)^{(K)}$ is the Kth iterate. The iteration is started by setting $(\mathbf{x}_a - \mathbf{x}_d)^{(0)} = 0$, and is terminated when $(\mathbf{x}_a - \mathbf{x}_d)^{(2)}$ has been found: (5.130) is applied only twice. All 3 components of (5.130) are iterated together.

Aside :

The use of linear *interpolation to evaluate* $\mathbf{u}$ *at* $(\mathbf{x}_a + \mathbf{x}_d)/2$ *in the iterative solution of* (5.126) *requires comment. Several studies have shown that the use of higher order interpolation gives no benefit here. This is in contrast to the finding - equally well founded in practical experience - that the use of linear interpolation to evaluate fields at the departure point* $\mathbf{x}_d$ *noticeably degrades results and that cubic or quasi-cubic interpolation is necessary. The situation has been illuminated by an analysis of a semi-Lagrangian treatment of the 1-D nonlinear advection equation by McDonald (1987). He examines the effect on formal accuracy of using (i) different orders of interpolation and different numbers of iterations in the departure point calculation, and (ii) different orders of interpolation in the evaluation of fields. For details of results the reader is referred to the original paper; suffice it to say that McDonald's analysis supports the conclusion that linear interpolation during the departure-point calculation, and the use of a small number of iterations, are consistent in terms of accuracy with the use of quadratic or cubic interpolation of field values. A physical explanation of these results is not yet forthcoming. It may be helpful to observe that the (scale-dependent) damping tendency of linear interpolation is likely to be more important in the interpolation of field values than in the departure-point calculation, that errors in estimating the departure point result mainly in phase errors, and that errors in estimating the field values at the departure point result mainly in amplitude errors.*

Although the issue is circumvented in practice by allowing only two iterations, the convergence properties of procedure (5.130) are clearly important. Pudykiewicz & Staniforth (1984) state that a sufficient condition for convergence in 2D Cartesian flow is

$$\max\{|u_x|, |u_y|, |v_x|, |v_y|\}\,\Delta t < 1. \tag{5.131}$$

Thisamounts to a restriction on the timestep Δt which is most severe where velocity gradients are largest; in 1D its violation may be related in physical terms to the crossing of adjacent characteristics, with consequent loss of solution uniqueness.

Aside :

Violation of the sufficient condition (5.131) *might lead to non-convergence of the procedure* (5.130) *(if a limit on the number of iterations were not applied).*

This possibility is of interest because it shows another way in which the semi-Lagrangian procedure might break down, notwithstanding its usual stability at any timestep Δt. A more familiar mechanism for instability has been noted by Bates, Li, Brandt, McCormack & Ruge (1995). They found that application of a semi-Lagrangian scheme to the conservation form of the barotropic vorticity equation led to an instability via the extrapolation scheme used to calculate parcel displacements; it could be obviated by restricting the timestep, or by reformulating so as to avoid use of an extrapolation scheme. This finding is consistent with the results of Temperton et al. (2001) noted in a previous Aside in connection with (5.52)*.Another instability associated with extrapolation was noted in connection with the $O(\Delta t^3)$-accurate scheme* (5.129) *discussed in a more recent Aside.*

Two aspects of the New Dynamics make the departure point calculation more complicated than our account has so far suggested: the staggered grid and spherical geometry. We consider these aspects in turn; the second warrants a complete subsection.

Treatment of individual velocity components

Eq. (5.125) implies three component equations, and during solution they are iterated simultaneously. The velocity components are, however, stored at different locations in the gridcell. As currently formulated, the code solves (5.125) for each of three different staggered sets of departure points. The first step in each of the three calculations is the linear interpolation of the other two velocity components onto the location of the current velocity component.

Aside :

It would be cheaper, and formally just as accurate, to solve for only one set of departure points (corresponding, say, to arrival points collocated with w) and then obtain the others by interpolation. This possibility deserves further study.

Aside :

As our discussion throughout this subsection has implied, the vector velocity is regarded as (u, v, w) in the departure point calculation. For example, it is w which is extrapolated to time-level $n+1/2$ using the vertical component of (5.126)*, and the vertical displacement calculated is $\Delta r \equiv r_a^{n+1} - r_d^n$ rather than $\Delta\eta \equiv$*

$\eta_a^{n+1} - \eta_d^n$ (see section 5.5 for more details). An alternative procedure would be to work in terms of $d\eta/dt$ and displacements in η; this would simplify both interpolation and the application of the lower boundary condition ($d\eta/dt = 0$).

5.5 *Spherical polar aspects of the departure-point calculation*

The spherical polar departure-point calculation in the HPE, shallow-atmosphere case was treated by Ritchie (1987). We outline in an *Aside*, below, how Ritchie's approach could be extended to our non-HPE context. The extension is actually simpler than the original because no correction has to be applied "to keep particles on the sphere", and although a few extra terms arise, the number of trigonometric functions that have to be evaluated at each iteration is the same as in the HPE case. The computational burden of these trig functions in the HPE case (which we believe to have been exaggerated) prompted the development of the approximate scheme described by Ritchie & Beaudoin (1994) which uses Taylor series expansions and does not require repeated evaluation of trig functions. A variant of this scheme is currently used in the New Dynamics: it is adapted for the use of a 2-level rather than a 3-level time integration scheme, and (to some extent) for the relaxation of the shallow atmosphere approximation. We present the relevant formulae and describe their application. (Derivations are outlined in Appendices B and C.)

In addition to terms in Δt, which trace the trajectory in the (λ, ϕ) system as if it were Cartesian, the Ritchie-Beaudoin algorithm involves terms of higher order (up to Δt^3) which represent corrections for the curvature of the (λ, ϕ) system. Even the retained higher order terms are insufficient near the coordinate poles, and poleward of 80^o the New Dynamics transforms into and out of appropriate rotated spherical polar systems so as to achieve the required accuracy. The algorithm of McDonald & Bates (1989) is used. The associated theory is similar to that presented in Section 2 for the rotated coordinate system used in mesoscale versions of the model. The present treatment, as we shall describe, differs from the mesoscale application in that a different rotated system is invoked for each gridpoint: the latitude, longitude origin of the rotated system is placed successively at each gridpoint.

Given the formal similarity between the departure point equation and the integrated vector momentum equation (see earlier *Asides*) it might be expected that similar methods and approximations would be applied in the solution of spherical polar versions of each. In fact, quite different approaches are used. In this description we shall concentrate on the methods used in the New Dynamics departure point calculation, and shall relegate to *Asides* all comment on contrasts with the treatment of the integrated vector momentum equation.

5.5.1 The Ritchie-Beaudoin algorithm

Consider the iterated displacement equation (5.130) written in the abbreviated form

$$(\mathbf{x}_a - \mathbf{x}_d)^{(K)} = \mathbf{u}_*^{(K-1)}\Delta t, \tag{5.132}$$

in which it is understood that $\mathbf{u}_*$ is the velocity evaluated (using the interpolation and extrapolation methods already described) at time $t^n + \Delta/2$ and at location $(\mathbf{x}_a + \mathbf{x}_d)^{(K-1)}/2$. Since the arrival point $\mathbf{x}_a$ is known, (5.130) may be regarded as an iterative equation for the departure point $\mathbf{x}_d$:

$$\mathbf{x}_d^{(K)} = \mathbf{x}_a - \mathbf{u}_*^{(K-1)}\Delta t. \tag{5.133}$$

In the New Dynamics, (5.133) is solved by using spherical trigonometric approximations following and extending (albeit in an *ad hoc* fashion) the shallow atmosphere, HPE method of Ritchie & Beaudoin (1994). The iteration is always stopped at the end of the second cycle ($K = 2$), and the three components of (5.133) are treated simultaneously.

Aside :

An earlier method (Ritchie 1987) is more computationally demanding but involves less approximation and does not break down as the coordinate poles are approached. Introduce a Cartesian coordinate system $OXYZ$ with origin O at the centre of the Earth, work in terms of X, Y, Z and the corresponding velocity components $U = DX/Dt$, $V = DY/Dt$, $W = DZ/Dt$, and transform to and from the spherical polar system as necessary. For a point $(\lambda,\ \phi,\ r)$ and velocity $(u,\ v,\ w)$ in the spherical polar system, the corresponding Cartesian coordinates and velocity components are:

$$X = r\cos\phi\cos\lambda, \tag{5.134}$$

$$Y = r\cos\phi\sin\lambda, \tag{5.135}$$

$$Z = r\sin\phi, \tag{5.136}$$

$$U = -u \sin\lambda - v \sin\phi \cos\lambda + w \cos\phi \cos\lambda, \tag{5.137}$$

$$V = \ \ u \cos\lambda - v \sin\phi \sin\lambda + w \cos\phi \sin\lambda, \tag{5.138}$$

$$W = \qquad v \cos\phi + w \sin\phi. \tag{5.139}$$

Eqs. (5.137) - (5.139) *may be obtained either by direct projection of* u, v *and* w *onto* U, V *and* W, *or by material differentiation of* (5.134) - (5.136) *(upon noting that* $ur \cos\phi = D\lambda/Dt$, $vr = D\phi/Dt$ *and* $w = Dr/Dt$*). Ritchie's HPE forms have* r *replaced by the constant mean value* a *(shallow atmosphere approximation) in* (5.134) - (5.136). *As a consequence, the terms in* w *in* (5.137) - (5.139) *do not appear in the HPE forms; note, however, that the trigonometric factors* $\cos\phi$, $\sin\phi$, $\cos\lambda$, $\sin\lambda$ *associated with the* w *terms in* (5.137) - (5.139) *are each also associated with one or more of the* u, v *terms, and so have to be evaluated even in the HPE case.*

The Cartesian components of (5.133) *are*

$$X_d^{(K)} = X_a - U_*^{(K-1)} \Delta t, \tag{5.140}$$

$$Y_d^{(K)} = Y_a - V_*^{(K-1)} \Delta t, \tag{5.141}$$

$$Z_d^{(K)} = Z_a - W_*^{(K-1)} \Delta t. \tag{5.142}$$

On each iteration of (5.140) - (5.142) *the "new" values of* r, λ *and* ϕ *must be calculated using the formulae inverse to* (5.134) - (5.136)*:*

$$r^2 = X^2 + Y^2 + Z^2, \tag{5.143}$$

$$\tan\lambda = Y/X, \tag{5.144}$$

$$\sin\phi = Z/r. \tag{5.145}$$

On each iteration, in either the HPE case or its extension, a number of trigonometric functions have to be evaluated: certainly $\arctan Y/X$ *and* $\arcsin Z/r$*; but note that only gridpoint values of* $\cos\phi$, $\sin\phi$, $\cos\lambda$, $\sin\lambda$ *seem necessary. This computational burden (which is repeated for every departure-point calculation at every timestep) prompted the development of Ritchie & Beaudoin (1994)'s approximate spherical trigonometric method, which we discuss below.*

Aside :

The use of a geocentric coordinate system (following Ritchie (1987)'s treatment for the HPEs) parallels a possible treatment, noted in Section 2, of the time-integrated vector momentum equation (5.15)*.The method actually used in the New Dynamics code for that problem is the rotation matrix method in which the spherical components of the velocity are time-stepped using* (5.67)*. By, for example, using it to transform the flow at the midpoint into the arrival-point coordinate system, the rotation matrix method could be applied in the departure-point calculation. This is done in the ECMWF model - see the Appendix of Temperton et al. (2001) - but not in the New Dynamics. The Ritchie-Beaudoin procedure must amount to an approximation of the rotation matrix method, but the precise relationship between the two is not clear. We recall also that the application of the rotation matrix method via* (5.67) *involves putting some of the elements* M_{ij} *to zero in a default setting known as "the 2D option".*

The central projection of a straight line onto a sphere is a great circle. In a shallow-atmosphere framework, consider the great circle which passes through the horizontal projection (λ_d, ϕ_d) of the departure point and the horizontal projection (λ_a, ϕ_a) of the arrival point; see Fig. 5.9. Let (λ_0, ϕ_0) be the midpoint of the minor arc of the great circle between (λ_d, ϕ_d) and (λ_a, ϕ_a). Let u_0 and v_0 be the velocity components at (λ_0, ϕ_0) at time $t^{n+1/2}$ and V_0 be the horizontal speed, i.e.

$$V_0 = \left(u_0^2 + v_0^2\right)^{1/2} . \tag{5.146}$$

Also, let γ_0 be the angle between the latitude circle ϕ_0 and the great circle (see Fig. 5.9); then

$$\tan\gamma_0 = \frac{v_0}{u_0}, \quad \sin\gamma_0 = \frac{v_0}{V_0}, \quad \cos\gamma_0 = \frac{u_0}{V_0}. \tag{5.147}$$

Finally, let α_0 be *half* the angle subtended at the centre of the great circle by the radii to the departure point and the arrival point. To the usual accuracy of the departure-point calculation,

$$\alpha_0 \equiv \frac{V_0 \Delta t}{2a} . \tag{5.148}$$

The quantity angle α_0 will nearly always be very much less than unity; it plays a key role in the analysis.

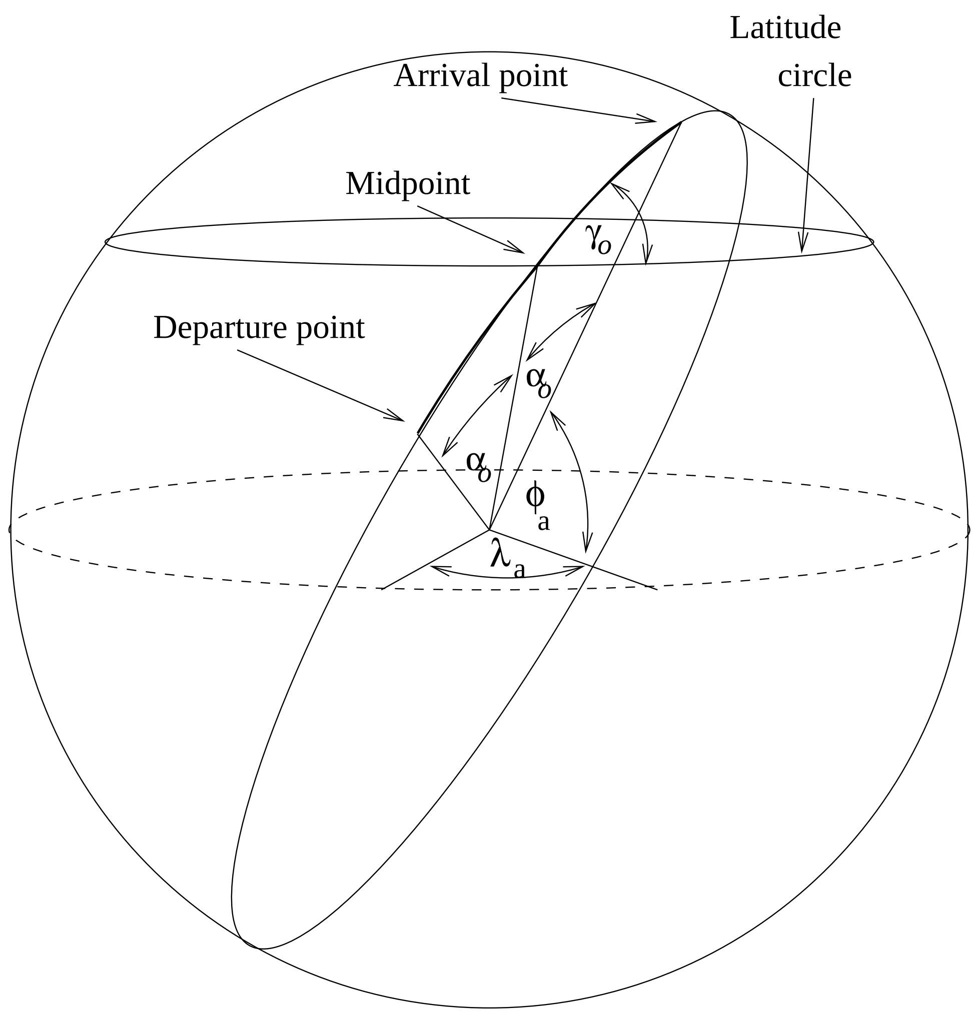

Figure 5.9: Showing an arrival point, the corresponding departure point, and the midpoint of the minor arc of the great circle between them. The minor arc subtends an angle $2\alpha_0$ at the centre of the Earth; γ_0 is the angle between the great circle and the latitude circle $\phi = \phi_0$; λ_a and ϕ_a are the longitude and latitude of the arrival point. In the interests of clarity, λ_d, ϕ_d λ_0 are ϕ_0 are not indicated, and the length of the minor arc is exaggerated.

Aside :

Each of equations (5.147) *gives an indeterminate result in the no-flow case (*$V_0 = 0$*). From* (5.148)*, however,* $\alpha_0 = 0$ *when* $V_0 = 0$*. This saves the day. All of the formulae* (5.149) - (5.164)*, below, are well-behaved both as* $V_0 \to 0$ *and when* $V_0 = 0$.

In terms of an amplitude $A_0 = A_0(\alpha_0, u_0, v_0)$ and a phase $\delta_0 = \delta_0(\alpha_0, u_0, v_0)$ defined by

$$A_0^2 = \cos^2\alpha_0 + \frac{v_0^2}{V_0^2}\sin^2\alpha_0 = 1 - \frac{u_0^2}{V_0^2}\sin^2\alpha_0, \tag{5.149}$$

and

$$\delta_0 = \arctan\left[\frac{v_0}{V_0}\tan\alpha_0\right], \tag{5.150}$$

(recall (5.146)) use of spherical triangle formulae (see Appendix E) leads to the following 6 relations involving α_0, u_0, v_0 and the coordinates (λ_d, ϕ_d), (λ_0, ϕ_0) and (λ_a, ϕ_a) of the departure point, the midpoint and the arrival point:

$$\sin\phi_a = A_0 \sin(\phi_0 + \delta_0)\ , \tag{5.151}$$

$$\cos\phi_a \cos(\lambda_a - \lambda_0) = A_0 \cos(\phi_0 + \delta_0)\ , \tag{5.152}$$

$$\cos\phi_a \sin(\lambda_a - \lambda_0) = \frac{u_0}{V_0}\sin\alpha_0\ , \tag{5.153}$$

$$\sin\phi_d = A_0 \sin(\phi_0 - \delta_0)\ , \tag{5.154}$$

$$\cos\phi_d \cos(\lambda_d - \lambda_0) = A_0 \cos(\phi_0 - \delta_0)\ . \tag{5.155}$$

$$\cos\phi_d \sin(\lambda_d - \lambda_0) = -\frac{u_0}{V_0}\sin\alpha_0\ . \tag{5.156}$$

Aside :

Only two of (5.151)*,* (5.152) *and* (5.153) *are independent, and only two of* (5.154)*,* (5.155) *and* (5.156) *are independent. For example,* (5.156) *may be derived by squaring and adding* (5.154) *and* (5.155)*, noting the definition of* A_0 *((5.149)), and determining a square root sign by inspection. From* (5.151) - (5.156) *we can obtain only four independent relations, but having all 6 to hand eases the derivation of the target formulae below. This redundancy is of course one of the characteristics of spherical trigonometry, and it has a number of consequences. Expressions which look entirely different may turn out to be equivalent, and derivations* *may be much simplified by inspired choices of route. The reader is invited to seek more direct derivations than those given in Appendix E (not to mention Appendices D and F).*

The use of (5.151) - (5.156) in the Ritchie-Beaudoin method is somewhat convoluted, both in approach and in approximation. The arrival point coordinates λ_a, ϕ_a being known, (5.153) and (5.151) are solved for the coordinates of the midpoint λ_0, ϕ_0 , with due regard to the fact that the velocity components u_0, v_0 and speed V_0 (and hence A_0 and δ_0) must be evaluated at the midpoint. Also involved in the iteration, and contributing to the determination of the midpoint, is the vertical component of the displacement equation, but for ease of presentation we shall discuss this aspect later (Section 5.5.3). The values of λ_0, ϕ_0, u_0, v_0 and V_0 (and A_0 and δ_0) obtained from this calculation are then used to solve for the departure point coordinates λ_d, ϕ_d.

In practice, approximate forms of (5.151) - (5.156) are used. As outlined in Appendix F (where some analytical obscurities are noted), from (5.148) - (5.156) the following expressions for λ_0 and ϕ_0 in terms of λ_a, ϕ_a, u_0 and v_0 can be derived:

$$\lambda_0 = \lambda_a - \frac{u_0 \Delta t}{2a\cos\phi_a}\left[1 + \frac{\Delta t^2}{24a^2}\left(u_0^2\tan^2\phi_a - v_0^2\right)\right] + O\left(\Delta t^5\right), \tag{5.157}$$

$$\phi_0 = \phi_a - \frac{v_0\Delta t}{2a} + \left(\frac{u_0\Delta t}{2a}\right)^2 \frac{\tan\phi_a}{2} - \frac{1}{3}\left(\frac{v_0\Delta t}{2a}\right)\left(\frac{u_0\Delta t}{2a}\right)^2 + O\left(\Delta t^4\right). \tag{5.158}$$

These may be solved iteratively for λ_0 and ϕ_0, giving also u_0 and v_0. The vertical coordinate of the midpoint is also involved in the iteration - see Section 5.5.3. From (5.148) - (5.158) can be derived (see Appendix F) expressions for λ_d and ϕ_d in terms of λ_a, ϕ_a and the values of u_0 and v_0 already determined:

$$\lambda_d = \lambda_a - \frac{u_0\Delta t}{a\cos\phi_a}\left[1 - \left(\frac{v_0\Delta t}{2a}\right)\tan\phi_a + \left(\frac{v_0\Delta t}{2a}\right)^2\left(2\tan^2\phi_a + \frac{5}{6}\right) + \left(\frac{u_0\Delta t}{2a}\right)^2\frac{\tan^2\phi_a}{6}\right] + O\left(\Delta t^4\right), \tag{5.159}$$

$$\phi_d = \phi_a - \frac{v_0\Delta t}{a} + \left(\sec^2\phi_a - \frac{2}{3}\right)\left(\frac{u_0\Delta t}{2a}\right)^2\frac{v_0\Delta t}{2a} + O\left(\Delta t^4\right). \tag{5.160}$$

These expressions are 2-time-level versions of those given in the Appendix of Ritchie & Beaudoin (1994). In the main text of that paper, and in the New Dynamics, the terms of order Δt^3 in the expressions (5.158) and (5.159) for $\phi_0$and $\lambda_d$are neglected. The procedure is therefore:

(i) to solve

$$\lambda_0 = \lambda_a - \frac{u_0 \Delta t}{2a \cos \phi_a} \left[1 + \frac{\Delta t^2}{24a^2} \left(u_0^2 \tan^2 \phi_a - v_0^2 \right) \right], \tag{5.161}$$

and

$$\phi_0 = \phi_a - \frac{v_0 \Delta t}{2a} + \left(\frac{u_0 \Delta t}{2a} \right)^2 \frac{\tan \phi_a}{2}, \tag{5.162}$$

(and the vertical component of the displacement equation) iteratively for λ_0 , ϕ_0 , u_0 and v_0;

(ii) to calculate λ_d and ϕ_d from

$$\lambda_d = \lambda_a - \frac{u_0 \Delta t}{a \cos \phi_a} \left[1 - \left(\frac{v_0 \Delta t}{2a} \right) \tan \phi_a \right], \tag{5.163}$$

and

$$\phi_d = \phi_a - \frac{v_0 \Delta t}{a} + \left(\sec^2 \phi_a - \frac{2}{3} \right) \left(\frac{u_0 \Delta t}{2a} \right)^2 \frac{v_0 \Delta t}{2a} . \tag{5.164}$$

Aside :

The terms of order Δt^2 *and higher in* (5.161) - (5.164) *allow for the curvature of the spherical polar coordinate system. The procedure used by Ritchie & Beaudoin (1994) in their main text, and that used by the New Dynamics, amounts to retaining in each of* (5.161) - (5.164) *only the term linear in* Δt *and the next higher term, irrespective of its order. Terms of order* Δt^3 *remain in* (5.161) *and* (5.164), *but no terms of order higher than* Δt^2 *in* (5.162) *and* (5.163). *Although the thinking behind this procedure can readily be appreciated, it leads to inconsistent results in the simple case* $v_0 = 0$, $u_0 \neq 0$. *In this case, the great circle must have a latitude extremum at* $\lambda = \lambda_0$, *and the formulae should deliver* $\phi_d = \phi_a$, $\phi_0 \neq \phi_a$ *and* $\lambda_a - \lambda_d = 2(\lambda_a - \lambda_0)$. *With* $v_0 = 0$, (5.161) - (5.164) *give*

$$\lambda_0 = \lambda_a - \frac{u_0 \Delta t}{2a \cos \phi_a} \left[1 + \frac{u_0^2 \Delta t^2}{24a^2} \tan^2 \phi_a \right] , \tag{5.165}$$

$$\phi_0 = \phi_a + \left(\frac{u_0 \Delta t}{2a} \right)^2 \frac{\tan \phi_a}{2} , \tag{5.166}$$

$$\lambda_d = \lambda_a - \frac{u_0 \Delta t}{a \cos \phi_a} , \tag{5.167}$$

$$\phi_d = \phi_a . \tag{5.168}$$

So, although the treatment of ϕ_0 *and* ϕ_d *is satisfactory, the treatment of* λ_0 *and* λ_d *is not: there is a* Δt^3 *term in* (5.165) *but not in* (5.167). *Consistent results in this case would be obtained by omitting the* Δt^3 *term in* (5.161), *i.e. by making* *no curvature correction in the equation for* λ_0*. Alternatively, the complete forms* (5.157) - (5.160) *could be used. With* $v_0 = 0$*they give* (5.165)*,* (5.166) *and* (5.168) *unchanged, but in place of* (5.167)*,*

$$\lambda_d = \lambda_a - \frac{u_0 \Delta t}{a \cos \phi_a} \left[1 + \frac{u_0^2 \Delta t^2}{24 a^2} \tan \phi_a \right], \tag{5.169}$$

which is consistent with (5.165)*. Both* (5.157) - (5.160) *and* (5.161) - (5.164) *give consistent behaviour in the simple case* $u_0 = 0$*,* $v_0 \neq 0$*; we find* $\lambda_d = \lambda_0 = \lambda_a$*,* $\phi_0 = \phi_a - v_0 \Delta t / 2a$ *and* $\phi_d = \phi_a - v_0 \Delta t / a$*.*

The New Dynamics in its Global version uses (5.161) - (5.164) to find the departure point corresponding to all latitudes equatorwards of 80° N and S. For arrival points at 80° N and S and poleward, a completely different procedure is used; it is described in a later subsection. The New Dynamics in its Mesoscale version uses simplified versions of (5.161) - (5.164) to find all arrival points - only the terms linear in Δt are retained. This procedure is justified by the small curvature of the chosen rotated latitude/longitude system in the Mesoscale model (see Section 2).

Application to the departure-point problem - deep atmosphere modifications

The Ritchie-Beaudoin expressions were derived in the shallow-atmosphere environment of the HPEs, but the New Dynamics is based on virtually unapproximated components of the momentum equation: the shallow atmosphere approximation is not made, and intrinsic metric terms are retained so that the $2\Omega \cos \phi$ Coriolis terms can be included whilst leaving conservation properties intact. Adjustments to the Ritchie-Beaudoin expressions to allow for the relaxation of the shallow atmosphere approximation are made in an *ad hoc* way. Wherever the Earth's mean radius, a, appears in (5.161) - (5.164), it is replaced by r_a, the value of r at the arrival point (be it a u, a v or a w gridpoint). The versions actually used are therefore

$$\lambda_0 = \lambda_a - \frac{u_0 \Delta t}{2 r_a \cos \phi_a} \left[1 + \frac{\Delta t^2}{24 r_a^2} \left(u_0^2 \tan^2 \phi_a - v_0^2 \right) \right], \tag{5.170}$$

$$\phi_0 = \phi_a - \frac{v_0 \Delta t}{2 r_a} + \left(\frac{u_0 \Delta t}{2 r_a} \right)^2 \frac{\tan \phi_a}{2}, \tag{5.171}$$

$$\lambda_d = \lambda_a - \frac{u_0 \Delta t}{r_a \cos \phi_a} \left[1 - \left(\frac{v_0 \Delta t}{2 r_a} \right) \tan \phi_a \right], \tag{5.172}$$

$$\phi_d = \phi_a - \frac{v_0 \Delta t}{r_a} + \left(\sec^2 \phi_a - \frac{2}{3}\right)\left(\frac{u_0 \Delta t}{2r_a}\right)^2 \frac{v_0 \Delta t}{2r_a} \, . \tag{5.173}$$

Aside :

These adaptations of the Ritchie-Beaudoin expressions are probably sufficiently accurate for all practical purposes, and it is not clear what else could be done within the spherical trigonometric framework of the method. Replacing r_a by the value of r $(= r_0)$ at the midpoint (and thus including it in the iteration) would be a more centred approximation, but it would probably make very little difference to results. If a more accurate treatment is required, the best course of action would either be to use the geocentric coordinate method of Ritchie (1987) extended as described in an earlier Aside, *or the local orthogonal great circle method of McDonald & Bates (1989) as described in the next subsection.*

5.5.2 Treatment near the poles

Inspection of (5.165) - (5.168) and (5.161) - (5.164) suggests that the procedure of Ritchie and Beaudoin breaks down close to the coordinate poles: terms in $\tan \phi_a$ and $\sec \phi_a$ appear. (This suggestion is reinforced by a glance at the derivations outlined in Appendix F.)

Poleward of 80°, the New Dynamics uses the rotated grid method of McDonald & Bates (1989) to locate departure points. The essence of the method is to use local orthogonal great circles *at each arrival point* to define a new coordinate system in which the departure point calculation is performed. One of the chosen local great circles is the meridian through the arrival point. As shown in Fig. 5.10, this choice means that the orthogonal great circle is co-tangential with the latitude circle through the arrival point, which in turn means that *at the arrival point* (and only at the arrival point) the zonal velocity component in the geographical latitude/longitude system is equal to the velocity component along the orthogonal great circle in the new system. Viewed as a coordinate transformation, the change from the geographical latitude/longitude system to the orthogonal great circle system involves a 2-stage coordinate rotation of the type discussed at length in Section 2 in connection with the rotated grid used in the Mesoscale version of the New Dynamics. See Fig. 5.11. The current application differs from the Mesoscale in two important respects:

(i) the origin of latitude and longitude in the rotated system is placed at each arrival point in turn, so *many different* rotated systems are used;

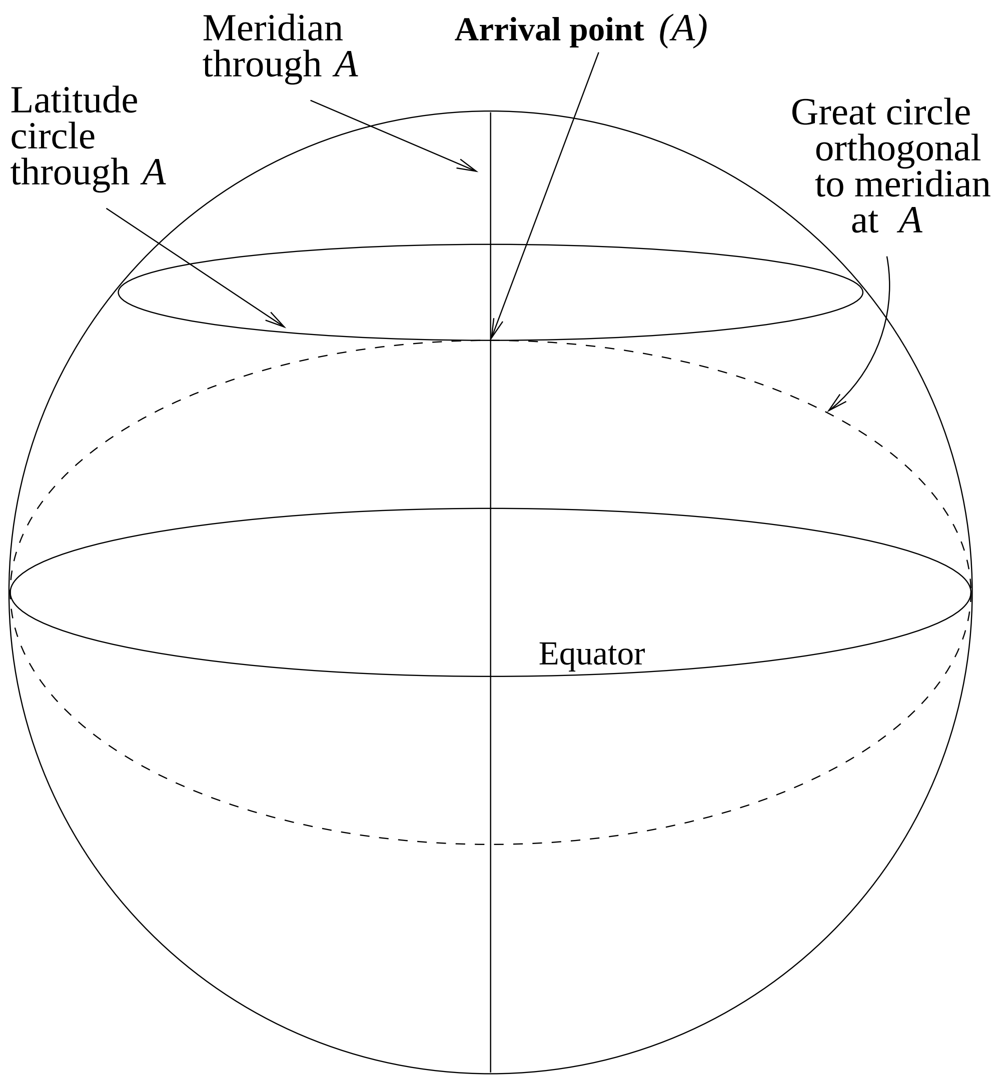

Figure 5.10: The latitude circle through the arrival point A is orthogonal to the meridian through A. The great circle orthogonal to the meridian at A therefore has, at A, the same tangent as the latitude circle. Thus, at A, the zonal velocity component is the same in both the geographical system and the rotated system in which the orthogonal great circle through A is the equator.

(ii) the transformation expressions may be simplified because the origin of latitude and longitude in the rotated system is at the arrival point (and, in terms of the *rotated* latitude and longitude, the departure point is close at hand).

Let primes denote quantities evaluated in the rotated latitude/longitude system having its origin $\lambda' = 0$, $\phi' = 0$ at the arrival point whose geographical latitude and longitude are $\lambda = \lambda_a$, $\phi = \phi_a$. The coordinates of the departure point *in the rotated system*, to the usual accuracy of calculation, may be found from the simple expressions

$$\lambda_d^{'} = -\frac{u_0^{'}\Delta t}{r_a \cos\phi_0^{'}}\ , \tag{5.174}$$

$$\phi_d^{'} = -\frac{v_0^{'}\Delta t}{r_a}\ . \tag{5.175}$$

[These are simple modifications of the shallow-atmosphere expressions originally used by McDonald & Bates (1989). The use of r_a, the arrival-point value of r, is reminiscent of the modifications of the Ritchie-Beaudoin scheme described above.]

Eqs. (5.174) and (5.175) are sufficiently accurate because we are working very close to the equator of the rotated system - the Ritchie-Beaudoin nonlinear terms are not required. The latitude $\phi_0^{'}$ and the velocity components $u_0^{'}$, $v_0^{'}$ are evaluated at the midpoint of the great circle arc between the departure point and the arrival point. To a very good approximation we have

$$\lambda_0^{'} = \lambda_d^{'}/2, \tag{5.176}$$

and

$$\phi_0^{'} = \phi_d^{'}/2. \tag{5.177}$$

If we were working solely in the rotated system, it would be very easy to use (5.174) and (5.175) to determine $\lambda_d^{'}$, $\phi_d^{'}$ iteratively. A final transformation back to the geographical system, using the following formulae (5.178) and (5.179), would then give us λ_d and ϕ_d:

$$\lambda_d = \lambda_a + \arctan\left[\frac{\cos\phi_d^{'}\sin\lambda_d^{'}}{\cos\phi_d^{'}\cos\lambda_d^{'}\cos\phi_a - \sin\phi_d^{'}\sin\phi_a}\right], \tag{5.178}$$

$$\phi_d = \arcsin\left[\cos\phi_d^{'}\cos\lambda_d^{'}\sin\phi_a + \sin\phi_d^{'}\cos\phi_a\right]. \tag{5.179}$$

[These formulae are readily obtained from (2.27) - (2.29) of Section 2, allowing for some minor differences in notation.] Unfortunately, the data we need for the interpolations to the midpoint $\lambda_0^{'}$, $\phi_0^{'}$ are on the geographical grid, so it is necessary to transform both coordinates

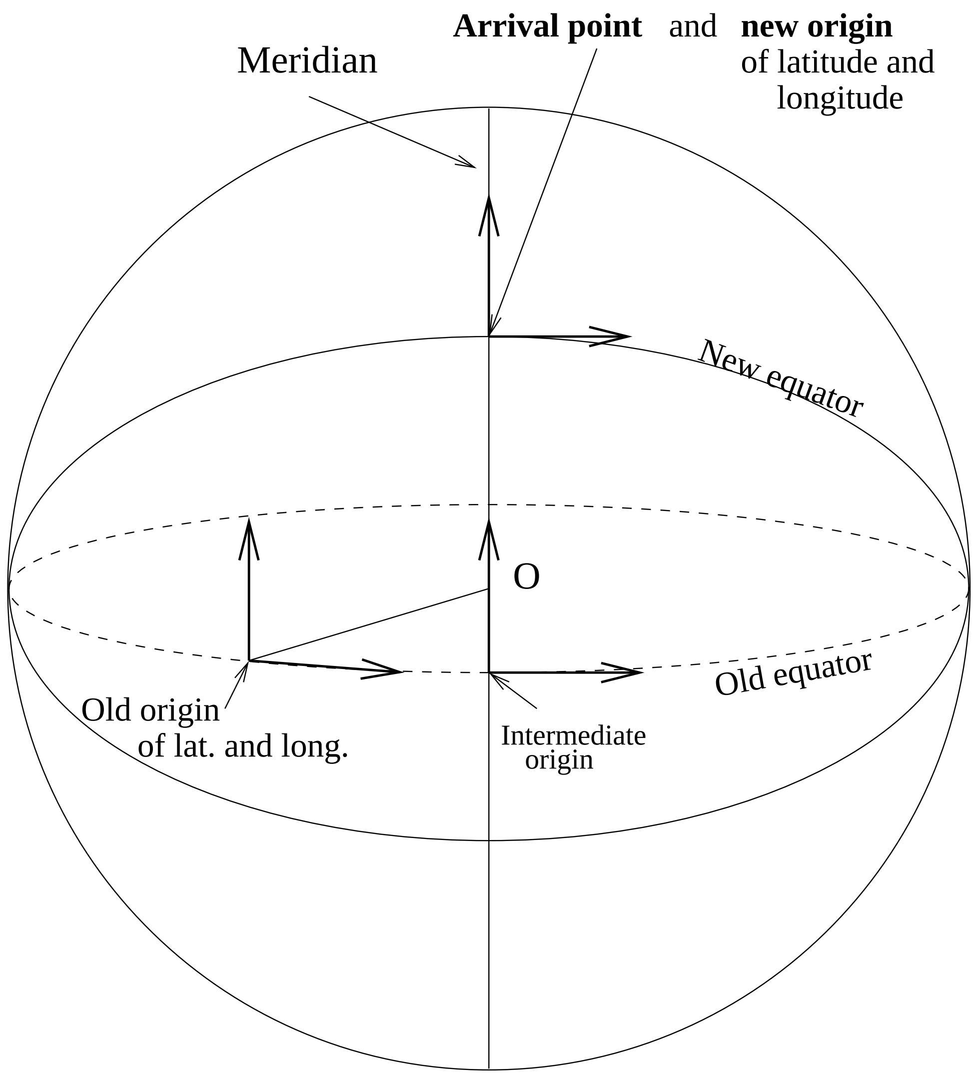

Figure 5.11: Illustrating the transformation to a rotated coordinate system in which the origin of latitude and longitude is moved to the arrival point. The transformation from the "old" to the "new" system can be made via an intermediate system which has its origin at the intersection of the "old" equator and the meridian through the arrival point.

and velocity components between the grids at each iteration. However, only two iterations are done (as ever), so the penalty is not great! The transformation formulae for the velocity components are

$$u_0^{'} = Gu_0 - Sv_0, \tag{5.180}$$

$$v_0^{'} = Su_0 + Gv_0. \tag{5.181}$$

The rotation matrix components G and S are given by

$$G \cos \phi^{'} = \cos \phi \cos \phi_a + \sin \phi \sin \phi_a \cos (\lambda - \lambda_a) , \tag{5.182}$$

$$S \cos \phi^{'} = \sin \phi_a \sin (\lambda - \lambda_a) . \tag{5.183}$$

[These formulae are the same as (2.38) - (2.39) of section 2, again allowing for some minor differences in notation and definition.] In the code, the transformation formulae (5.178) - (5.183) are applied as they stand, all trig formulae being evaluated using library routines.

<u>Aside :</u>

Since $\lambda_d^{'}$ and $\phi_d^{'}$ are both small quantities, there is scope for approximating the transformation formulae (5.178) - (5.183) *and thus for reducing the number of trig functions to be evaluated. Candidate formulae are*

$$\lambda_d = \lambda_a + \arctan \left[\frac{\lambda_d^{'}}{\cos \phi_a - \phi_d^{'} \sin \phi_a} \right] , \tag{5.184}$$

$$\phi_d = \arcsin \left[\sin \phi_a + \phi_d^{'} \cos \phi_a \right] , \tag{5.185}$$

$$G = \sqrt{1 - (\lambda - \lambda_a)^2 \sin^2 \phi_a} , \tag{5.186}$$

$$S = (\lambda - \lambda_a) \sin \phi_a . \tag{5.187}$$

The square root in (5.186) *ensuresretention of the property $G^2 + S^2 = 1$ under the approximations made.*

<u>Aside :</u>

Is it consistent in terms of accuracy to use the Ritchie-Beaudoin procedure equatorward of some latitude and the McDonald-Bates procedure poleward of it? A basis for comparing the accuracy of the two schemes should be devised, and adjustments made if necessary.

Aside :

The McDonald-Bates procedure is applicable at all latitudes, but the Ritchie-Beaudoin procedure is not. Since the Ritchie-Beaudoin procedure is analytically and conceptually the more complicated, consideration should be given to the possibility of using the McDonald-Bates procedure at all latitudes (perhaps using the simplified formulae (5.184) - (5.187)*). Another possibility - as noted earlier - is to use the geocentric Cartesian method of Ritchie (1987).*

5.5.3 Vertical displacements and boundary checks

In what is essentially an extension of the procedure used by Ritchie & Beaudoin (1994), the New Dynamics calculates vertical displacements on the assumption that sphericity is relevant only as it affects horizontal displacements.

Aside :

This would not be the case if the rotation matrix method of Section 1.2 were to be applied in the departure-point problem. However, we recall that a certain "2D option" is a default approximation in the code where the rotation matrix method is in use. This is probably similar in its effect to the assumption that vertical displacements may be found independently of horizontal displacements, although the issue has not been explored in detail.

The relevant expression is

$$r_d^n = r_a^{n+1} - w_* \Delta t \, , \tag{5.188}$$

where w_* is the vertical velocity evaluated at the midpoint $[\mathbf{r}_a + \mathbf{r}_d]/2$ at time-level $n + 1/2$, i.e.

$$w_* = w\left([\mathbf{r}_a + \mathbf{r}_d]/2, \; t^n + \Delta t/2\right) . \tag{5.189}$$

The radial coordinate r_0 of the midpoint obeys the equally simple form (used in the iteration)

$$r_0 = r_a^{n+1} - \frac{1}{2} w_* \Delta t \, . \tag{5.190}$$

The same treatment suffices (given the approximations already involved) whether or not a rotated local grid is in use for the horizontal part of the departure-point calculation.

Aside :

As previously noted, there would be some advantages to calculating vertical displacements in terms of η rather than r. This would appear to follow more closely the method of Ritchie & Beaudoin (1994), who calculated vertical displacements in terms of $\dot{\sigma}$ in a σ-coordinate HPE model. However, nonhydrostatic models which do not use height as vertical coordinate have an intrinsic ambivalence between $w = Dz/Dt$ and $\dot{\eta} = D\eta/Dt$, since the vertical component of the momentum equation is far simpler in terms of the former than the latter; so the issue is perhaps not clear-cut.

Boundary checks

Both during and after iteration to find departure points, checks are made to ensure that midpoints and departure points do not lie outside the fluid. Midpoints and departure points found to be out of bounds are re-located in the vertical to the first appropriate model level; horizontal location is not changed. When a vertical velocity arrival point is involved, midpoints or departure points lying outside the fluid are relocated to the nearer boundary. When a u or a v arrival point is involved, a slightly different adjustment is made: relocation is to the nearest u or v level within the domain. These boundary checks are made only for levels close to the boundaries (according to variable control parameters). If a layer near the top of the domain is found to give no midpoints or departure points above the upper boundary, it is assumed that no lower layer needs to be investigated for the same misbehaviour.

Aside :

The reason for relocating midpoints during iteration is not clear. It certainly reduces the need for extrapolation, but cannot aid convergence - which, of course, is not a visible issue given that only two iterations are done. It might be preferable to relocate only after iteration, or to relocate only departure points.

Aside :

The relocation of departure points found to be outside the domain can be seen to distort the solution in the vicinity of mountains. Assuming quasi-sinusoidal terrain height, the relocation will tend to raise departure points which lie in valleys, but a compensating reduction of departure-point heights over crests will tend not *to occur. A discriminator for this behaviour, given 2D sinusoidal terrain, is the local tangent: where the terrain lies* above *the local tangent, upward relocations will tend to be made, but where the terrain lies* below *the local tangent relocations will tend not to be made. The effect of this bias will be rectification of the terrain tending to falsely increase its mean height (by "filling in" the valleys). Quantification of this effect, and ways of compensating for it, should be sought. Indeed, a thorough investigation of the occurrence and extent of parcel relocations could be a good investment of time.*

5.5.4 The New Dynamics departure-point calculation: a summary

At each time-level, a departure-point calculation is carried out for each u gridpoint, each v gridpoint and each w gridpoint. The calculation in each case proceeds as follows.

1. The other wind components are linearly interpolated onto the grid of the component for which the departure point is sought.

2. For each arrival point equatorward of 80° (N or S), the (modified) Ritchie-Beaudoin expressions (5.170), (5.171) and (5.190) are applied twice to obtain an estimate of the midpoint (λ_0, ϕ_0, r_0). Linear interpolation is applied during this iteration, and the three expressions are iterated simultaneously. Having found (λ_0, ϕ_0, r_0), the departure point is evaluated using (5.172), (5.173) and (5.188). During the iteration of (5.170), (5.171) and (5.190), all midpoints lying above or below the model domain are relocated vertically to lie on the domain boundary (which is differently defined for horizontal and vertical wind components). Departure points (delivered by (5.172), (5.173) and (5.188)) lying outside the model domain are re-located in the same way.

3. For arrival points at or poleward of 80°, the calculation proceeds in all respects as before, *except* that the Bates-McDonald rotated grid method is used. In this method, the origin of latitude and longitude is moved to each arrival point in turn, and the simple formulae (5.174) - (5.177) are used to find the midpoint and the departure point. These formulae are sufficiently accurate because curvature effects are very small in the rotated system (since the arrival point lies on its equator). Since the model stores the wind components on the geographical grid, it is necessary to transform between the rotated and geographical grids during as well as after the iteration.

6 Discretisation of the horizontal components of the momentum equation

The forced horizontal components of the momentum equation are:

$$\frac{Du}{Dt} - f_3 v + f_2 w - \frac{uv\tan\phi}{r} + \frac{uw}{r} + \frac{c_{pd}\theta_v}{r\cos\phi}\left(\frac{\partial\Pi}{\partial\lambda} - \frac{\partial\Pi}{\partial r}\frac{\partial r}{\partial\lambda}\right) = S^u, \tag{6.1}$$

$$\frac{Dv}{Dt} + f_3 u - f_1 w + \frac{u^2\tan\phi}{r} + \frac{vw}{r} + \frac{c_{pd}\theta_v}{r}\left(\frac{\partial\Pi}{\partial\phi} - \frac{\partial\Pi}{\partial r}\frac{\partial r}{\partial\phi}\right) = S^v. \tag{6.2}$$

These equations are discretised using a predictor-corrector method having several correction steps. The discretisation is first developed in detail for the u-component of the momentum equation, and the corresponding result is then given for the v-component.

As described in Section 5.2, the vector momentum equation for $\mathbf{u} \equiv (u, v, w)$ is directly discretised in the form (see (5.68))

$$\mathbf{u}^{n+1} - \sum_k \alpha_k \Delta t \mathbf{\Psi}_k^{n+1} = \mathbf{M}\left\{\left[\mathbf{u} + \sum_k (1-\alpha_k)\,\Delta t \mathbf{\Psi}_k\right]_d^n\right\}. \tag{6.3}$$

Here $\mathbf{M}$ is the 3×3 rotation matrix, defined in Section 5.2, that transforms the components of a vector expressed in a coordinate system centred on a departure point into those expressed in the coordinate system associated with the corresponding arrival point. The role of this rotation matrix is to represent the curvature effects of spherical geometry and, specifically, to handle the associated metric terms. Because of the complexity of the current predictor/corrector discretisation of the momentum equation, it is convenient to develop this discretisation in component form as if the metric terms were absent, with the understanding that the missing metric terms are then included via (6.3) and application of the rotation matrix .

6.1 Discretisation of the u-component of the momentum equation at levels $k = 3/2,\ 5/2, \ldots,\ N - 3/2$

If (6.1) were to be discretised using a 2-time-level, off-centred, semi-implicit, semi-Lagrangian scheme, as outlined above, then at the u points of the Arakawa C grid this would give the approximation:

$$\frac{u^{n+1} - u_d^n}{\Delta t} = \alpha_3\left[f_3\overline{v}^{\lambda\phi} - \frac{c_{pd}}{\overline{r}^{\lambda}\cos\phi}\left(\overline{\theta_v}^{r\lambda}\delta_\lambda\Pi - \overline{\theta_v\delta_r\Pi}^{r\lambda}\delta_\lambda r\right)\right]^{n+1}$$

$$
\begin{aligned}
&+(1-\alpha_3)\left[f_3\overline{v}^{\lambda\phi}-\frac{c_{pd}}{\overline{r}^{\lambda}\cos\phi}\left(\overline{\theta_v}^{r\lambda}\delta_\lambda\Pi-\overline{\theta_v\delta_r\Pi}^{r\lambda}\delta_\lambda r\right)\right]_d^n \\
&-\alpha_4\left[f_2\overline{w}^{r\lambda}\right]^{n+1}-(1-\alpha_4)\left[f_2\overline{w}^{r\lambda}\right]_d^n \\
&+\alpha_p\left[S^u\right]^{n+1}+(1-\alpha_p)\left[S^u\right]_d^n, \qquad (6.4)
\end{aligned}
$$

where the departure-point terms are those evaluated in the arrival-point coordinate system using (6.3), and the usual horizontal and vertical, averaging and difference, operators are defined in Appendix C. However this is not what is presently done, principally because of the complexity associated with a time-implicit treatment of the $f_2 w$ Coriolis term, the non-linear pressure-gradient terms and the forcing, or "physics", term, S^u. This motivated the development of the predictor-corrector method developed below.

Aside :

Note that, as discussed further in Appendix C, the vertical ($\overline{(\ )}^r$) averaging operator does not commute with the horizontal ($\overline{(\ )}^\lambda$ and $\overline{(\ )}^\phi$) averaging operators and the order in which they are presented here reflects the order in which they occur in the model code.

Aside :

Eq. (6.4) *is only valid for levels* $k = 3/2,\ 5/2,\ \ldots,\ N-3/2$. *This is because some vertically averaged and differenced terms (e.g.* $\overline{\theta_v\delta_r\Pi}^{r\lambda}$*, which spans two vertical meshlengths) are undefined for* $k = 1/2$ *and* $k = N-3/2$*, and so additional constraints (see subsection 6.3) are imposed in the vicinity of the upper and lower boundaries.*

For the u-component of the momentum equation at the u points of the Arakawa C grid the predictor-corrector method is comprised of the following steps:

- **Predictor**

  Let $\tilde{u}^{(1)}$ be a first predictor for u^{n+1}. The basis for this predictor is first to neglect the forcing term, S^u, and then to replace all the remaining terms evaluated at meshpoints at time $(n+1)\,\Delta t$ in (6.4) by their values at the same meshpoints but at time $n\Delta t$. Thus

$$
\frac{\tilde{u}^{(1)}-u_d^n}{\Delta t} = \alpha_3\left[f_3\overline{v}^{\lambda\phi}-\frac{c_{pd}}{\overline{r}^{\lambda}\cos\phi}\left(\overline{\theta_v}^{r\lambda}\delta_\lambda\Pi-\overline{\theta_v\delta_r\Pi}^{r\lambda}\delta_\lambda r\right)\right]^n
$$

$$+\left(1-\alpha_3\right)\left[f_3\overline{v}^{\lambda\phi}-\frac{c_{pd}}{\overline{r}^{\lambda}\cos\phi}\left(\overline{\theta_v}^{r\lambda}\delta_\lambda\Pi-\overline{\theta_v\delta_r\Pi}^{r\lambda}\delta_\lambda r\right)\right]_d^n$$
$$-\alpha_4\left[f_2\overline{w}^{r\lambda}\right]^n-\left(1-\alpha_4\right)\left[f_2\overline{w}^{r\lambda}\right]_d^n. \tag{6.5}$$

This equation can be solved explicitly for $\tilde{u}^{(1)}$.

- **1st "Physics" Corrector**

The basis of how the forcing term, or "physics", S^u, is discretised is to write S^u as the sum of two terms $S^u = S_1^u + S_2^u$ and to let the value of the physics time-weight, α_p, associated with S_1^u be 0 (appropriate for slow processes) and that associated with S_2^u be 1 (appropriate for fast processes). Thus, the physics terms of S_1^u and S_2^u are evaluated at the departure and arrival points, respectively. In addition, the terms for S_1^u are evaluated as functions of the model state at the previous, n^{th}, time-step, denoted here as $\{u^n\}$. Therefore,

$$S_1^u = S_1^u\left(\{u^n\}\right) = G^u\left(\{u^n\}\right), \tag{6.6}$$

where G^u represents the effects of *sub-gridscale gravity-wave drag*. Let $\tilde{u}^{(P1)}$ be the first physics predictor for u^{n+1}. This can be written as the sum of the (1st) predictor $\tilde{u}^{(1)}$ plus a 1st physics corrector $\left(\tilde{u}^{(P1)}-\tilde{u}^{(1)}\right)$, i.e. as

$$\tilde{u}^{(P1)} = \tilde{u}^{(1)} + \left(\tilde{u}^{(P1)}-\tilde{u}^{(1)}\right). \tag{6.7}$$

This 1st physics corrector is defined as

$$\left(\tilde{u}^{(P1)}-\tilde{u}^{(1)}\right) = \Delta t\left[S_1^u\right]_d^n. \tag{6.8}$$

Aside :

The first physics corrector has the effect of simply adding to the right-hand side of (6.5) *the parallel, or process-split, physics term, where this term is evaluated at the departure point using time level n quantities. This can be seen by eliminating* $\tilde{u}^{(1)}$ *between the left-hand sides of* (6.5) *and* (6.8) *to get:*

$$\begin{aligned}\frac{\tilde{u}^{(P1)}-u_d^n}{\Delta t} = {} & \alpha_3\left[f_3\overline{v}^{\lambda\phi}-\frac{c_{pd}}{\overline{r}^{\lambda}\cos\phi}\left(\overline{\theta_v}^{r\lambda}\delta_\lambda\Pi-\overline{\theta_v\delta_r\Pi}^{r\lambda}\delta_\lambda r\right)\right]^n \\ & +\left(1-\alpha_3\right)\left[f_3\overline{v}^{\lambda\phi}-\frac{c_{pd}}{\overline{r}^{\lambda}\cos\phi}\left(\overline{\theta_v}^{r\lambda}\delta_\lambda\Pi-\overline{\theta_v\delta_r\Pi}^{r\lambda}\delta_\lambda r\right)\right]_d^n \\ & -\alpha_4\left[f_2\overline{w}^{r\lambda}\right]^n-\left(1-\alpha_4\right)\left[f_2\overline{w}^{r\lambda}\right]_d^n \\ & +\left[S_1^u\right]_d^n.\end{aligned} \tag{6.9}$$

Aside :

> S_1^u *is computed explicitly using data at time level* n*. It is not known whether or not, or under what conditions, this procedure is computationally stable. A stability analysis, if tractable, would be desirable.*

- **2nd "Physics" Corrector**

The target discretisation for the remaining part of the physics, S_2^u, is to evaluate it *implicitly* using model variables at time level $n+1$. To avoid using an iterative approach, rather than using time level $n+1$ information, this part of the physics uses the latest available predictors of all the model variables required. Let $\tilde{u}^{(P2)}$ be the second physics predictor for u^{n+1}. This can be written as the sum of the (1st physics) predictor $\tilde{u}^{(P1)}$ plus a 2nd physics corrector $\left(\tilde{u}^{(P2)} - \tilde{u}^{(P1)}\right)$, i.e. as

$$\tilde{u}^{(P2)} = \tilde{u}^{(P1)} + \left(\tilde{u}^{(P2)} - \tilde{u}^{(P1)}\right). \tag{6.10}$$

This 2nd physics corrector is defined as

$$\left(\tilde{u}^{(P2)} - \tilde{u}^{(P1)}\right) = \Delta t \left[S_2^u\right]^*. \tag{6.11}$$

The asterisk notation is used to indicate that S_2^u is based on an intermediate, unbalanced model state and not on time level $n+1$ values.

Aside :

> S_2^u *is made up of two physics components each of which updates the model variables used as the model state in the next component. The outcome of this part of the physics therefore depends on the order in which the components are evaluated. For this reason this part of the physics is known as "sequential", or "time-split" physics. For* u *and* v *there are two such physics components which are the effects due to* sub-gridscale convective momentum transport *and the effects due to* subgrid-scale boundary-layer turbulence. *Notionally,* $\tilde{u}^{(P2)} - \tilde{u}^{(P1)}$ *can itself be written as the sum of two correctors:*
>
> $$\tilde{u}^{(P2a)} - \tilde{u}^{(P1)} = \Delta t C^u \left(\left\{\tilde{u}^{(P1)}\right\}\right), \tag{6.12}$$
>
> $$\tilde{u}^{(P2b)} - \tilde{u}^{(P2a)} = \Delta t BL^u \left(\left\{\tilde{u}^{(P2a)}\right\}\right), \tag{6.13}$$

where $\tilde{u}^{(P2)} \equiv \tilde{u}^{(P2b)}$ *and* $\left\{\tilde{u}^{(P1)}\right\}$ *indicates the set of intermediate model variables, the various predictors, available at the same time as* $\tilde{u}^{(P1)}$*, and similarly for the other predictors for* u^{n+1}*. The other momentum variables available at the start of this process, i.e. at the same intermediate time as* $\tilde{u}^{(P1)}$*, are* $\tilde{v}^{(P1)}$ *and* $\tilde{w}^{(1)}$*, the available thermodynamic variable is* $\tilde{\theta}^{(P1)}$ *and the available moisture variables are* $\widetilde{m}_X^{(P1)}$ *(see sections 7, 9 and 10). The only available density is that at time level* n*, i.e.* ρ^n*, and similarly for the Exner field,* Π^n*, and the pressure field,* p^n*. Note that each of the physics components is evaluated simultaneously for each of the model variables* u*,* v*,* θ *and* m_X*, as appropriate.* BL^u *represents the implicit boundary-layer term and is defined by:*

$$BL^u\left(\left\{\tilde{u}^{(P2a)}\right\}\right) \equiv \frac{u^{**} - \tilde{u}^{(P2a)}}{\Delta t}, \tag{6.14}$$

where u^{**} *satisfies the implicit equation:*

$$\begin{aligned} \frac{u^{**} - u^n}{\Delta t} \quad = \quad & \frac{1}{r^2\rho^n}\delta_r\left(\alpha_{BL} r^2 \rho^n K_u \delta_r u^{**}\right) + \frac{1}{r^2\rho^n}\delta_r\left[\left(1-\alpha_{BL}\right) r^2\rho^n K_u\delta_r u^n\right] \\ & + \frac{\tilde{u}^{(P2a)} - u^n}{\Delta t}. \end{aligned} \tag{6.15}$$

$K_u = K_u\left(\{u^n\}\right)$ *is the eddy-viscosity. This is required on u-columns (at* θ*-levels) but it is initially calculated on* θ*-points, using horizontal winds which are averaged horizontally, and then it is averaged horizontally back onto the u-columns.* α_{BL} *is an off-centred, semi-implicit weighting factor which gives a fully implicit scheme when it is set equal to* 1*. However, the dependence of* K_u *on the timelevel* n *variables can lead to a non-linear instability which can be eliminated by making the scheme "overweighted" i.e. by choosing a value for* α_{BL} *which is greater than* 1 *(see the series of papers Kalnay & Kanamitsu (1988), Girard & Delage (1990) and Bénard, Marki, Neytchev & Prtenjak (2000), and also Teixeira (2000)).*

Setting $\tilde{u}^{(P2)} \equiv \tilde{u}^{(P2b)}$ *and summing the* 2 *correctors given by* (6.12)-(6.13)*,* (6.11) *is obtained with*

$$\left[S_2^u\right]^* \equiv C^u\left(\left\{\tilde{u}^{(P1)}\right\}\right) + BL^u\left(\left\{\tilde{u}^{(P2a)}\right\}\right), \tag{6.16}$$

though writing it this way masks the sequential nature of the scheme.

Aside :

> *The second physics corrector has the effect of simply adding the sequential, or time-split, physics term to the right-hand side of* (6.9)*. This can be seen by eliminating* $\tilde{u}^{(P1)}$ *between the left-hand sides of* (6.9) *and* (6.11) *to get:*
>
> $$\begin{aligned} \frac{\tilde{u}^{(P2)} - u^n_d}{\Delta t} &= \alpha_3 \left[f_3 \overline{v}^{\lambda\phi} - \frac{c_{pd}}{\overline{r}^\lambda \cos\phi} \left(\overline{\theta_v}^{r\lambda} \delta_\lambda \Pi - \overline{\theta_v \delta_r \Pi}^{r\lambda} \delta_\lambda r \right) \right]^n \\ &+ (1-\alpha_3) \left[f_3 \overline{v}^{\lambda\phi} - \frac{c_{pd}}{\overline{r}^\lambda \cos\phi} \left(\overline{\theta_v}^{r\lambda} \delta_\lambda \Pi - \overline{\theta_v \delta_r \Pi}^{r\lambda} \delta_\lambda r \right) \right]^n_d \\ &- \alpha_4 \left[f_2 \overline{w}^{r\lambda} \right]^n - (1-\alpha_4) \left[f_2 \overline{w}^{r\lambda} \right]^n_d \\ &+ \left[S^u_2 \right]^* + \left[S^u_1 \right]^n_d , \end{aligned} \tag{6.17}$$
>
> *but note that this masks the dependence of* $[S^u_2]^*$ *on the previous predictors for* u^{n+1}*.*

- **1st "Dynamics" Corrector**

Let $\tilde{u}^{(2)}$ be a 2nd dynamics predictor for u^{n+1}. This can be written as the sum of the (2nd physics) predictor $\tilde{u}^{(P2)}$ plus a 1st dynamics corrector $\left(\tilde{u}^{(2)} - \tilde{u}^{(P2)}\right)$, i.e. as

$$\tilde{u}^{(2)} = \tilde{u}^{(P2)} + \left(\tilde{u}^{(2)} - \tilde{u}^{(P2)}\right). \tag{6.18}$$

This 1st dynamics corrector is defined as

$$\left(\tilde{u}^{(2)} - \tilde{u}^{(P2)}\right) = -\alpha_3 \Delta t \left[\frac{c_{pd}}{\overline{r}^\lambda \cos\phi} \left(\overline{\left(\theta^*_v - \theta^n_v\right)}^{r\lambda} \delta_\lambda \Pi^n - \overline{\left(\theta^*_v - \theta^n_v\right) \delta_r \Pi^n}^{r\lambda} \delta_\lambda r \right) \right], \tag{6.19}$$

where

$$\theta^*_v = \theta^* \left(\frac{1 + \frac{1}{\varepsilon} m^*_v}{1 + m^*_v + m^*_{cl} + m^*_{cf}} \right), \tag{6.20}$$

$m^*_X = \widetilde{m}^{(P2)}_X$, $X = (v, cl, cf)$, and θ^* are the latest available predictors for m_X and θ at time $(n+1)\,\Delta t$ (see Sections 9 and 10 for details of how they are computed). Equations (6.18)-(6.19) can be explicitly solved for $\tilde{u}^{(2)}$.

Aside :

> *The asterisk notation, introduced in WP154 and appearing in* (6.20)*, is somewhat misleading. At first sight one might think that* θ^*_v *represents the virtual temperature intrinsically associated with a particular parcel of moist air with*

potential temperature θ^* and mixing ratios m_X^*, $X = (v, cl, cf)$, which are coherently transported (in the absence of sources and sinks) during a model timestep. In fact the asterisk in $\theta^*$and the one in m_X^* have somewhat different meanings. For θ^* the asterisk denotes the latest-availabl*e predictor $\widetilde{\theta}$ for θ (i.e.* before *solution of the Helmholtz equation and back substitution), but not the final one θ^{n+1}, obtained* after *solution of the Helmholtz equation by back substitution. For m_X^* the asterisk also denotes the latest available predictor for m_X. However, it is not transported in the same way as θ^* is (θ is advected using a so-called non-interpolating algorithm in the vertical, whereas advection of m_X is via 3-d interpolating semi-Lagrangian scheme with an a posteriori conservation correction). A danger here is that a parcel of moist air could spuriously supersaturate, and thereby generate spurious physical forcing via parameterised processes, due to the inconsistent transport of θ and m_X.*

Aside :

Although not obvious at first sight, adding the corrector (6.19) *is equivalent to replacing $\overline{\theta_v}^{r\lambda}$ where it appears in the 1st square-bracketed term on the right-hand side of* (6.17) *by $\overline{\theta_v^*}^{r\lambda}$, defined by* (6.20). *This can be seen by eliminating $\tilde{u}^{(P2)}$ from* (6.17)- (6.19) *to get*

$$\begin{aligned}\frac{\tilde{u}^{(2)} - u_d^n}{\Delta t} &= \alpha_3 \left[f_3 \overline{v^n}^{\lambda\phi} - \frac{c_{pd}}{\overline{r}^\lambda \cos\phi} \left(\overline{\theta_v^*}^{r\lambda} \delta_\lambda \Pi^n - \overline{\theta_v^* \delta_r \Pi^n}^{r\lambda} \delta_\lambda r \right) \right] \\ &+ (1 - \alpha_3) \left[f_3 \overline{v}^{\lambda\phi} - \frac{c_{pd}}{\overline{r}^\lambda \cos\phi} \left(\overline{\theta_v}^{r\lambda} \delta_\lambda \Pi - \overline{\theta_v \delta_r \Pi}^{r\lambda} \delta_\lambda r \right) \right]_d^n \\ &- \alpha_4 \left[f_2 \overline{w}^{r\lambda} \right]^n - (1 - \alpha_4) \left[f_2 \overline{w}^{r\lambda} \right]_d^n \\ &+ \left[S_2^u \right]^* + \left[S_1^u \right]_d^n . \end{aligned} \tag{6.21}$$

- **2nd "Dynamics" Corrector**

Let $\tilde{u}^{(3)}$ be a 3rd dynamics predictor for u^{n+1}. This can be written as the sum of the (2nd dynamics) predictor $\tilde{u}^{(2)}$ plus a 2nd dynamics corrector $\left(\tilde{u}^{(3)} - \tilde{u}^{(2)}\right)$, i.e. as

$$\tilde{u}^{(3)} = \tilde{u}^{(2)} + \left(\tilde{u}^{(3)} - \tilde{u}^{(2)} \right) . \tag{6.22}$$

This 2nd dynamics corrector is defined as

$$\left(\tilde{u}^{(3)}-\tilde{u}^{(2)}\right)=\alpha_3\Delta t\left[f_3\overline{v'}^{\lambda\phi}-\frac{c_{pd}}{\overline{r}^{\lambda}\cos\phi}\left(\overline{\theta_v^*}^{r\lambda}\delta_\lambda\Pi'-\overline{\theta_v^*\delta_r\Pi'}^{r\lambda}\delta_\lambda r\right)\right], \tag{6.23}$$

where

$$v'\equiv v^{n+1}-v^n,\quad \Pi'\equiv\Pi^{n+1}-\Pi^n. \tag{6.24}$$

Aside :

> *Adding the corrector* (6.22) *is equivalent to replacing* v *and* Π *where they appear in the 1st square-bracketed term on the right-hand side of* (6.21) *by their values at meshpoints at time* $(n+1)\,\Delta t$*. This can be seen by eliminating* $\tilde{u}^{(2)}$ *from* (6.21)- (6.24) *to get*
>
> $$\begin{aligned}\frac{\tilde{u}^{(3)}-u_d^n}{\Delta t} &= \alpha_3\left[f_3\overline{v^{n+1}}^{\lambda\phi}-\frac{c_{pd}}{\overline{r}^{\lambda}\cos\phi}\left(\overline{\theta_v^*}^{r\lambda}\delta_\lambda\Pi^{n+1}-\overline{\theta_v^*\delta_r\Pi^{n+1}}^{r\lambda}\delta_\lambda r\right)\right]\\ &\quad+(1-\alpha_3)\left[f_3\overline{v}^{\lambda\phi}-\frac{c_{pd}}{\overline{r}^{\lambda}\cos\phi}\left(\overline{\theta_v}^{r\lambda}\delta_\lambda\Pi-\overline{\theta_v\delta_r\Pi}^{r\lambda}\delta_\lambda r\right)\right]_d^n\\ &\quad-\alpha_4\left[f_2\overline{w}^{r\lambda}\right]^n-(1-\alpha_4)\left[f_2\overline{w}^{r\lambda}\right]_d^n\\ &\quad+\left[S_2^u\right]^*+\left[S_1^u\right]_d^n.\end{aligned} \tag{6.25}$$

Contrary to the 1st dynamics corrector, which is *explicit*, the 2nd dynamics corrector gives rise to an *implicit coupling* of the momentum equation with the other governing equations and eventually leads to a Helmholtz problem to be solved for the Exner pressure tendency Π'. Equation (6.25) is quite close to the target 2-time-level, off-centred, semi-implicit, semi-Lagrangian discretisation defined by (6.4). There are however three differences: (a) θ_v in the pressure gradient terms uses an intermediate value θ_v^* instead of its time $(n+1)\,\Delta t$ value θ_v^{n+1}; (b) the time-implicit Coriolis term f_2w^{n+1} is instead evaluated explicitly as f_2w^n; and (c) the physics terms are time discretised somewhat differently, as described above.

Aside :

> *A stability analysis of the inertial terms shows that the approximation of (b) above is computationally unstable (see Appendix G).*

- **3rd "Dynamics" Corrector**

If we stop at the 3rd dynamics predictor/2nd dynamics corrector stage (i.e. set $u^{n+1} \equiv \tilde{u}^{(3)}$), then elimination of v^{n+1} from (6.25) leads to a large stencil in the resulting Helmholtz equation for the Exner pressure tendency Π'. To avoid such a large stencil, a 4th dynamics predictor and 3rd dynamics corrector is applied. It will be shown that this allows $(v^{n+1} - v^n)$ to be eliminated from the equation for $(u^{n+1} - u^n)$ (and vice versa), leaving an equation for $(u^{n+1} - u^n)$ analogous to the one that would be obtained by finite-differencing the result of an analytic elimination (and similarly for the equation for $(v^{n+1} - v^n)$).

Let $\tilde{u}^{(4)}$ be the 4th dynamics and final predictor for u^{n+1}, i.e. $u^{n+1} \equiv \tilde{u}^{(4)}$. This can be written as the sum of the (3rd dynamics) predictor $\tilde{u}^{(3)}$ plus a 3rd dynamics corrector $u^{n+1} - \tilde{u}^{(3)}$, i.e. as

$$u^{n+1} = \tilde{u}^{(3)} + \left(u^{n+1} - \tilde{u}^{(3)}\right). \tag{6.26}$$

This 4th dynamics corrector is defined as

$$\left(u^{n+1} - \tilde{u}^{(3)}\right) = \frac{\alpha_3^2 f_3^2 \Delta t^2}{1 + \alpha_3^2 f_3^2 \Delta t^2} \left(I - \bar{I}^{\lambda\lambda\phi\phi}\right) \left(u^n - \tilde{u}^{(3)} + \alpha_3 f_3 \Delta t \overline{v}^{\lambda\phi}\right), \tag{6.27}$$

where I is the unit operator and

$$\overline{I}^{\lambda\phi} F \equiv \overline{F}^{\lambda\phi}. \tag{6.28}$$

Aside :

> *As the 4th dynamics predictor is the final one, the final discretisation of the u-component of the momentum equation can be written using* (6.24)-(6.25) *and* (6.27) *as:*
>
> $$\begin{aligned} \frac{u^{n+1} - u^n_d}{\Delta t} = & \left\{ \alpha_3 \left[f_3 \overline{v^{n+1}}^{\lambda\phi} - \frac{c_{pd}}{\overline{r}^\lambda \cos\phi} \left(\overline{\theta_v^*}^{r\lambda} \delta_\lambda \Pi^{n+1} - \overline{\theta_v^* \delta_r \Pi^{n+1}}^{r\lambda} \delta_\lambda r \right) \right] \right. \\ & + (1-\alpha_3) \left[f_3 \overline{v}^{\lambda\phi} - \frac{c_{pd}}{\overline{r}^\lambda \cos\phi} \left(\overline{\theta_v}^{r\lambda} \delta_\lambda \Pi - \overline{\theta_v \delta_r \Pi}^{r\lambda} \delta_\lambda r \right) \right]^n_d \\ & \left. - \left[\alpha_4 \left(f_2 \overline{w}^{r\lambda} \right)^n + (1-\alpha_4) \left(f_2 \overline{w}^{r\lambda} \right)^n_d \right] \right\} \\ & + \left[S_2^u \right]^* + \left[S_1^u \right]^n_d \\ & - \alpha_3^2 f_3^2 \Delta t^2 \left(1 + \alpha_3^2 f_3^2 \Delta t^2 \overline{I}^{\lambda\lambda\phi\phi} \right)^{-1} \left(I - \overline{I}^{\lambda\lambda\phi\phi} \right) \end{aligned}$$

$$\times \left[\frac{u^{n+1} - u^n}{\Delta t} - \alpha_3 f_3 \Delta t \overline{I}^{\lambda\phi} \left(\frac{v^{n+1} - v^n}{\Delta t} \right) \right]. \tag{6.29}$$

Eq. (6.29) *is exactly the same as* (6.25)*, except for the addition of some small residual terms introduced by the last corrector in order to simplify the elimination procedure for the Helmholtz solver.*

6.2 Formally-equivalent statement of the discretisation of the u-component of the momentum equation at levels $k = 3/2$, $5/2$,..., $N - 3/2$

By defining R_u, R_u^{P1}, R_u^{P2}, R_u^{+} and R_u^{++} as

$$R_u \equiv \tilde{u}^{(1)} - u^n, \quad R_u^{P1} \equiv \tilde{u}^{(P1)} - u^n, \quad R_u^{P2} \equiv \tilde{u}^{(P2)} - u^n,$$
$$R_u^{+} \equiv \tilde{u}^{(2)} - u^n, \quad R_u^{++} \equiv \tilde{u}^{(3)} - u^n - \alpha_3 f_3 \Delta t \overline{v'}^{\lambda\phi} \tag{6.30}$$

where $\tilde{u}^{(1)}$, $\tilde{u}^{(P1)}$, $\tilde{u}^{(P2)}$, $\tilde{u}^{(2)}$ and $\tilde{u}^{(3)}$ are given by (6.5), (6.8), (6.11), (6.19) and (6.23), the above predictor-corrector discretisation of the u-component of the momentum equation can be written as the equivalent following steps:

- Compute R_u at the u points of the Arakawa C grid:

$$R_u = -\left\{ u - \alpha_3 \Delta t \left[f_3 \overline{v}^{\lambda\phi} - \frac{c_{pd}}{\overline{r}^{\lambda} \cos\phi} \left(\overline{\theta_v}^{r\lambda} \delta_\lambda \Pi - \overline{\theta_v \delta_r \Pi}^{r\lambda} \delta_\lambda r \right) \right] + \alpha_4 \Delta t f_2 \overline{w}^{r\lambda} \right\}^n$$
$$+ \left\{ u + (1 - \alpha_3) \Delta t \left[f_3 \overline{v}^{\lambda\phi} - \frac{c_{pd}}{\overline{r}^{\lambda} \cos\phi} \left(\overline{\theta_v}^{r\lambda} \delta_\lambda \Pi - \overline{\theta_v \delta_r \Pi}^{r\lambda} \delta_\lambda r \right) \right] - (1 - \alpha_4) \Delta t f_2 \overline{w}^{r\lambda} \right\}_d^n. \tag{6.31}$$

- Compute R_u^{P1} at the u points of the Arakawa C grid:

$$R_u^{P1} = R_u + \Delta t \left[S_1^u \right]_d^n, \tag{6.32}$$

  where $\left[S_1^u \right]_d^n$, given by (6.6), is the parallel, or process-split, component of the physics increment.

- Compute R_u^{P2} at the u points of the Arakawa C grid:

$$R_u^{P2} = R_u^{P1} + \Delta t \left[S_2^u \right]^*, \tag{6.33}$$

  where $\left[S_2^u \right]^*$, given by (6.16), is the sequential, or time-split, component of the physics increment.

- Compute R_u^+ at the u points of the Arakawa C grid:

$$R_u^+ = R_u^{P2} - \alpha_3 \Delta t \left[\frac{c_{pd}}{\overline{r}^\lambda \cos\phi} \left(\overline{\left(\theta_v^* - \theta_v\right)}^{r\lambda} \delta_\lambda \Pi - \overline{\left(\theta_v^* - \theta_v\right) \delta_r \Pi}^{r\lambda} \delta_\lambda r \right) \right]^n , \tag{6.34}$$

where

$$\theta_v^* = \theta^* \left(\frac{1 + \frac{1}{\varepsilon} m_v^*}{1 + m_v^* + m_{cl}^* + m_{cf}^*} \right) , \tag{6.35}$$

is the latest available predictor for θ_v when R_u^+ is computed (see Section 9 for details), and $m_X^* = \widetilde{m}_X^{(P2)}$ is the latest available predictor for m_X (see Section 10 for details).

- Compute R_u^{++} at the u points of the Arakawa C grid:

$$R_u^{++} = R_u^+ - \alpha_3 \Delta t \left[\frac{c_{pd}}{\overline{r}^\lambda \cos\phi} \left(\overline{\theta_v^*}^{r\lambda} \delta_\lambda \Pi' - \overline{\theta_v^* \delta_r \Pi'}^{r\lambda} \delta_\lambda r \right) \right] , \tag{6.36}$$

where $\Pi' \equiv \Pi^{n+1} - \Pi^n$ is obtained from the solution of a Helmholtz problem (to be derived) .

- Approximate the time tendency u' as:

$$u' \equiv u^{n+1} - u^n = \alpha_3 \Delta t f_3 \overline{v'}^{\lambda\phi} + \left(\frac{I + \alpha_3^2 f_3^2 \Delta t^2 \bar{I}^{\lambda\lambda\phi\phi}}{1 + \alpha_3^2 f_3^2 \Delta t^2} \right) R_u^{++}, \tag{6.37}$$

where $v' \equiv v^{n+1} - v^n$.

6.3 Discretisation of the u-component of the momentum equation at levels $k = 1/2$ and $k = N - 1/2$

The discretisations of the u-component of the momentum equation for levels $k = 1/2$ and $k = N - 1/2$ are examined separately here. The discretisation proceeds exactly the same as that at intervening levels except that certain terms are modified, as described below, to account for the presence of the upper and lower boundaries.

- **k = 1/2**

  To compute $\left.(R_u)\right|_{\eta_{1/2}}$ (cf. (6.31)), the term

$$\left. \left(\overline{\theta_v^n}^{r\lambda} \delta_\lambda \Pi^n - \overline{\theta_v^n \delta_r \Pi^n}^{r\lambda} \delta_\lambda r \right) \right|_{\eta_{1/2}} , \tag{6.38}$$

  has to be evaluated, and both of its subterms involve an averaging over the layer $[\eta_0 \equiv 0, \eta_1]$. Since θ_v (or equivalently θ and q) is not prognostically carried at $\eta_0 \equiv 0$, to close the problem it is instead assumed that θ_v is isentropic (i.e. constant) in the layer $[\eta_0 \equiv 0, \eta_1]$. Thus $\left.(\theta_v)\right|_{\eta_0\equiv 0}$ is diagnostically related to $\left.(\theta_v)\right|_{\eta_1}$ by

$$\left.(\theta_v)\right|_{\eta_0\equiv 0} = \left.(\theta_v)\right|_{\eta_1}, \tag{6.39}$$

and

$$\left.\left(\overline{\theta_v^n}^{r\lambda}\delta_\lambda \Pi^n\right)\right|_{\eta_{1/2}} = \left.\left(\overline{\theta_v^n}^{\lambda}\right)\right|_{\eta_1} \left.(\delta_\lambda \Pi^n)\right|_{\eta_{1/2}}. \tag{6.40}$$

<u>**Aside :**</u>

> *In the limit that the meshlengths tend to zero, the use of* (6.39) *corresponds to applying the constraint that* $\left.(\partial\theta_v/\partial\eta)\right|_{\eta_0\equiv 0} = 0$*, which in general is not true. To address this,* θ *and* q *could be prognostically carried at* $\eta_0 \equiv 0$*. Since* $\dot{\eta} = 0$ *at* $\eta_0 \equiv 0$*, the thermodynamic and moisture equations would then reduce to 2-d advection along the bottom surface* $\eta_0 \equiv 0$ *and could be discretised in the usual semi-Lagrangian manner. The term* $\left.\left(\overline{\theta_v^n}^{r\lambda}\delta_\lambda \Pi^n\right)\right|_{\eta_{1/2}}$ *could then be computed as for any other layer without arbitrarily imposing* (6.39)*.*

For the second subterm, $\left.\left(\overline{\theta_v^n \delta_r \Pi^n}^{r\lambda}\delta_\lambda r\right)\right|_{\eta_{1/2}}$, there is an additional problem since the contribution due to the vertical derivative of Π normally spans two vertical meshlengths and data is unavailable below the surface. To address this, the contribution to $\left.\left(\overline{\theta_v^n \delta_r \Pi^n}^{r\lambda}\right)\right|_{\eta_{1/2}}$ at the bottom boundary ($\eta_0 \equiv 0$) is evaluated as

$$\left.\theta_v^n \delta_r \Pi^n\right|_{\eta_0\equiv 0} = -\frac{g}{c_{pd}}. \tag{6.41}$$

with the contribution at η_1 being computed in the usual way.

<u>**Aside :**</u>

> *Eq.* (6.41) *is equivalent to applying the "traditional" hydrostatic assumption at the bottom surface* $\eta_0 \equiv 0$*, and it corresponds to neglecting all terms (vertical acceleration, Coriolis, and metric) other than the two hydrostatically- balanced terms of* (6.41)*. Applying the "traditional" hydrostatic assumption at the surface can be considered to be a modification of the governing equations, rather than a discretisation of them, since in the limit that the meshlengths*

and timestep go to zero, the solution will converge to hydrostatic balance at the bottom surface rather than to the exact non-hydrostatic solution.

To compute $(R_u)|_{\eta_{1/2}}$, the term $\left(f_2\overline{w}^{r\lambda}\right)\big|_{\eta_{1/2}}$ also has to be evaluated and this is done by assuming

$$w|_{\eta_0\equiv 0} = 0. \tag{6.42}$$

Aside :

Condition (6.42) *is valid anywhere the bottom surface is flat (e.g. for oceans and lakes), since* $w = \dot{\eta} = 0$ *there, and also for viscous flow, for which the no-slip condition holds. However, it is not valid for inviscid flow (nor for an inviscid substep) over orography.*

To compute $(R_u^+)|_{\eta_{1/2}}$ and $(R_u^{++})|_{\eta_{1/2}}$ (cf. (6.34)-(6.36)), the terms $\left[\overline{\left(\theta_v^* - \theta_v\right)}^{r\lambda}\delta_\lambda\Pi\right]\Big|_{\eta_{1/2}}$ and $\left[\overline{\theta_v^*}^{r\lambda}\delta_\lambda\Pi'\right]\Big|_{\eta_{1/2}}$ are evaluated with analogous assumptions and in the same manner as that described above to evaluate $\left(\overline{\theta_v^n}^{r\lambda}\delta_\lambda\Pi^n\right)\Big|_{\eta_{1/2}}$ and $\left(\overline{\theta_v^n\delta_r\Pi^n}^{r\lambda}\delta_\lambda r\right)\Big|_{\eta_{1/2}}$, and $\left[\overline{\left(\theta_v^* - \theta_v\right)\delta_r\Pi}^{r\lambda}\delta_\lambda r\right]\Big|_{\eta_{1/2}}$ is evaluated by applying (6.41) with θ_v^n replaced by θ_v^*. The remaining term in $(R_u^{++})|_{\eta_{1/2}}$ is computed as

$$\left(\overline{\theta_v^*\delta_r\Pi'}^{r\lambda}\delta_\lambda r\right)\Big|_{\eta_{1/2}} = \overline{\left(\theta_v^*\right)\big|_{\eta_1}\frac{\left(r|_{\eta_{1/2}} - r|_{\eta_0}\right)}{\left(r|_{\eta_1} - r|_{\eta_0}\right)}\frac{\left(\Pi'|_{\eta_{3/2}} - \Pi'|_{\eta_{1/2}}\right)}{\left(r|_{\eta_{3/2}} - r|_{\eta_{1/2}}\right)}}^{\lambda}\left(\delta_\lambda r\right)|_{\eta_{1/2}}\,, \tag{6.43}$$

where the isentropic assumption has been made (as above) for θ_v in the layer $[\eta_0 \equiv 0, \eta_1]$.

- **k = N-1/2**

To compute $(R_u)|_{\eta_{N-1/2}}$ (cf. (6.31)), the term

$$\left(\overline{\theta_v^n}^{r\lambda}\delta_\lambda\Pi^n - \overline{\theta_v^n\delta_r\Pi^n}^{r\lambda}\delta_\lambda r\right)\Big|_{\eta_{N-1/2}}, \tag{6.44}$$

has to be evaluated, and both of its subterms involve an averaging over the layer $[\eta_{N-1}, \eta_N \equiv 1]$. The first subterm, $\left(\overline{\theta_v^n}^{r\lambda}\delta_\lambda\Pi^n\right)\Big|_{\eta_{N-1/2}}$, is straightforward. Since θ_v is carried at the rigid lid ($\eta_N \equiv 1$) and prognostically determined there, it is computed in exactly the same manner as for any other layer.

For the second subterm, $\left.\left(\overline{\theta_v^n \delta_r \Pi^n}^{r\lambda} \delta_\lambda r\right)\right|_{\eta_{N-1/2}}$, there is, in principle, a difficulty since the contribution due to the vertical derivative of Π normally spans two vertical mesh-lengths and data is unavailable above the rigid lid. To circumvent this, the coordinate η is defined in such a way as to make

$$\left. r\right|_{\eta_{N-1/2}} = \text{constant}, \tag{6.45}$$

and so

$$\left.\left(\overline{\theta_v^n \delta_r \Pi^n}^{r\lambda} \delta_\lambda r\right)\right|_{\eta_{N-1/2}} \equiv 0, \tag{6.46}$$

since $\left.(\delta_\lambda r)\right|_{\eta_{N-1/2}} \equiv 0$.

Aside :

Although the assumption (6.45) *is not overly restrictive, strictly speaking it is not valid over orography (but it is elsewhere) for the simple (linear) coordinate definition*

$$\eta = \frac{r - r_S(\lambda, \phi)}{r_T - r_S(\lambda, \phi)}, \tag{6.47}$$

where $r_T = \text{constant}$ *defines the rigid lid, and* $r_S(\lambda, \phi)$ *defines the orography. At some point it would be of interest to revisit this.*

One way of avoiding this restriction might be to compute $\theta_v^n \frac{\partial \Pi^n}{\partial r} \frac{\partial r}{\partial \lambda}$ *as* $\overline{\overline{\theta_v^n \delta_r \Pi^n}^{\lambda} \delta_\lambda r}^{r}$ *and then* $\left.\left(\overline{\theta_v^n \delta_r \Pi^n}^{\lambda} \delta_\lambda r\right)\right|_{\eta_N} \equiv 0$ *closes the problem since* $\left.(\delta_\lambda r)\right|_{\eta_N} \equiv 0$*. If this were done, similar expressions elsewhere should presumably be evaluated in an analogous manner.*

To compute $\left.(R_u)\right|_{\eta_{N-1/2}}$, the term $\left.\left(f_2 \overline{w}^{r\lambda}\right)\right|_{\eta_{N-1/2}}$ also has to be evaluated. This is computed using

$$\left. w\right|_{\eta_N \equiv 1} = 0. \tag{6.48}$$

Aside :

Since the lid is rigid, and thus $w(\eta_N \equiv 1) = \dot{\eta}(\eta_N \equiv 1) = 0$*, condition* (6.48) *is valid everywhere on the lid.*

To compute $\left.(R_u^+)\right|_{\eta_{N-1/2}}$ and $\left.(R_u^{++})\right|_{\eta_{N-1/2}}$ (cf. (6.34)-(6.36)), the terms $\left.\left[\overline{\left(\theta_v^* - \theta_v^n\right)}^{r\lambda} \delta_\lambda \Pi^n\right]\right|_{\eta_{N-1/2}}$, $\left.\left[\overline{\theta_v^*}^{r\lambda} \delta_\lambda \Pi'\right]\right|_{\eta_{N-1/2}}$, $\left.\left[\overline{\left(\theta_v^* - \theta_v^n\right) \delta_r \Pi^n}^{r\lambda} \delta_\lambda r\right]\right|_{\eta_{N-1/2}}$ and $\left.\left(\overline{\theta_v^* \delta_r \Pi'}^{r\lambda} \delta_\lambda r\right)\right|_{\eta_{N-1/2}}$ are evaluated in the same manner as that described above to evaluate $\left.\left(\overline{\theta_v^n}^{r\lambda} \delta_\lambda \Pi^n\right)\right|_{\eta_{N-1/2}}$ and $\left.\left(\overline{\theta_v^n \delta_r \Pi^n}^{r\lambda} \delta_\lambda r\right)\right|_{\eta_{N-1/2}}$.

6.4 Discretisation of the v-component of the momentum equation at levels $k = 1/2,\ 3/2,\ldots,\ N-1/2$

The v-component of the momentum equation is discretised in exactly the same manner as that described in the previous two subsections for the u-component. Thus the discretisation of the v-component of the momentum equation can be written as:

$$\begin{aligned}\frac{v^{n+1}-v_d^n}{\Delta t} = -\alpha_3\left[f_3\overline{u^{n+1}}^{\lambda\phi}+\frac{c_{pd}}{\overline{r}^{\phi}}\left(\overline{\theta_v^*}^{r\phi}\delta_\phi\Pi^{n+1}-\overline{\theta_v^*\delta_r\Pi^{n+1}}^{r\phi}\delta_\phi r\right)\right]\\ -(1-\alpha_3)\left[f_3\overline{u}^{\lambda\phi}+\frac{c_{pd}}{\overline{r}^{\phi}}\left(\overline{\theta_v}^{r\phi}\delta_\phi\Pi-\overline{\theta_v\delta_r\Pi}^{r\phi}\delta_\phi r\right)\right]_d^n\\ +\left[\alpha_4\left(f_1\overline{w}^{r\phi}\right)^n+(1-\alpha_4)\left(f_1\overline{w}^{r\phi}\right)_d^n\right]\\ +\left[S_2^v\right]^*+\left[S_1^v\right]_d^n\\ -\alpha_3^2f_3^2\Delta t^2\left(1+\alpha_3^2f_3^2\Delta t^2\overline{I}^{\lambda\lambda\phi\phi}\right)^{-1}\left(I-\overline{I}^{\lambda\lambda\phi\phi}\right)\\ \times\left[\frac{v^{n+1}-v^n}{\Delta t}+\alpha_3f_3\Delta t\overline{I}^{\lambda\phi}\left(\frac{u^{n+1}-u^n}{\Delta t}\right)\right].\end{aligned} \tag{6.49}$$

6.5 Formally-equivalent statement of the discretisation of the v-component of the momentum equation at levels $k = 1/2,\ 3/2,\ldots,\ N-1/2$

By defining R_v, R_v^{P1}, R_v^{P2}, R_v^{+} and R_v^{++} as

$$\begin{aligned}R_v\equiv\tilde{v}^{(1)}-v^n,\quad R_v^{P1}\equiv\tilde{v}^{(P1)}-v^n,\quad R_v^{P2}\equiv\tilde{v}^{(P2)}-v^n,\\ R_v^{+}\equiv\tilde{v}^{(2)}-v^n,\quad R_v^{++}\equiv\tilde{v}^{(3)}-v^n+\alpha_3f_3\Delta t\overline{u'}^{\lambda\phi}\end{aligned} \tag{6.50}$$

the above predictor-corrector discretisation of the v-component of the momentum equation can be written as the equivalent following steps:

- Compute R_v at the v points of the Arakawa C grid:

$$\begin{aligned}R_v = \left\{-v-\alpha_3\Delta t\left[f_3\overline{u}^{\lambda\phi}+\frac{c_{pd}}{\overline{r}^{\phi}}\left(\overline{\theta_v}^{r\phi}\delta_\phi\Pi-\overline{\theta_v\delta_r\Pi}^{r\phi}\delta_\phi r\right)\right]+\alpha_4\Delta tf_1\overline{w}^{r\phi}\right\}^n\\ +\left\{v-(1-\alpha_3)\Delta t\left[f_3\overline{u}^{\lambda\phi}+\frac{c_{pd}}{\overline{r}^{\phi}}\left(\overline{\theta_v}^{r\phi}\delta_\phi\Pi-\overline{\theta_v\delta_r\Pi}^{r\phi}\delta_\phi r\right)\right]+(1-\alpha_4)\Delta tf_1\overline{w}^{r\phi}\right\}_d^n.\end{aligned} \tag{6.51}$$

- Compute R_v^{P1} at the v points of the Arakawa C grid:

$$R_v^{P1} = R_v + \Delta t \left[S_1^v\right]_d^n , \tag{6.52}$$

where $\left[S_1^v\right]_d^n$ is the parallel, or process-split, component of the physics increment, computed in an exactly analogous way to $\left[S_1^u\right]_d^n$.

- Compute R_v^{P2} at the v points of the Arakawa C grid:

$$R_v^{P2} = R_v^{P1} + \Delta t \left[S_2^v\right]^* , \tag{6.53}$$

where $\left[S_2^v\right]^*$ is the sequential, or time-split, component of the physics increment, computed in an exactly analogous way to $\left[S_2^u\right]^*$.

- Compute R_v^{+} at the v points of the Arakawa C grid:

$$R_v^{+} = R_v^{P2} - \alpha_3 \Delta t \left[\frac{c_{pd}}{\overline{r}^{\phi}} \left(\overline{\left(\theta_v^* - \theta_v\right)}^{r\phi} \delta_\phi \Pi - \overline{\left(\theta_v^* - \theta_v\right) \delta_r \Pi}^{r\phi} \delta_\phi r \right) \right]^n , \tag{6.54}$$

where

$$\theta_v^* = \theta^* \left(\frac{1 + \frac{1}{\varepsilon} m_v^*}{1 + m_v^* + m_{cl}^* + m_{cf}^*} \right) \tag{6.55}$$

is the latest available predictor for θ_v when R_v^+ is computed (see Section 9 for details), and $m_X^* = \widetilde{m}_X^{(P2)}$ is the latest available predictor for m_X (see Section 10 for details).

- Compute R_v^{++} at the v points of the Arakawa C grid:

$$R_v^{++} = R_v^{+} - \alpha_3 \Delta t \left[\frac{c_{pd}}{\overline{r}^{\phi}} \left(\overline{\theta_v^*}^{r\phi} \delta_\phi \Pi' - \overline{\theta_v^* \delta_r \Pi'}^{r\phi} \delta_\phi r \right) \right] . \tag{6.56}$$

- Approximate the time tendency v' as:

$$v' \equiv v^{n+1} - v^n = -\alpha_3 \Delta t f_3 \overline{u'}^{\lambda\phi} + \left(\frac{I + \alpha_3^2 f_3^2 \Delta t^2 \bar{I}^{\lambda\lambda\phi\phi}}{1 + \alpha_3^2 f_3^2 \Delta t^2} \right) R_v^{++}, \tag{6.57}$$

where $\Pi' \equiv \Pi^{n+1} - \Pi^n$ is obtained from the solution of a Helmholtz problem (to be derived), and $u' \equiv u^{n+1} - u^n$.

6.6 Elimination of u' and v' between the discretised horizontal components of the momentum equation at levels $k = 1/2,\ 3/2, \ldots,\ N - 1/2$

v' can be eliminated between (6.37) and (6.57) by substituting (6.57) into (6.37) to obtain:

$$u' = -\alpha_3^2 f_3^2 \Delta t^2 \overline{I}^{\lambda\lambda\phi\phi} u' + \alpha_3 \Delta t f_3 \left(\frac{I + \alpha_3^2 f_3^2 \Delta t^2 \overline{I}^{\lambda\lambda\phi\phi}}{1 + \alpha_3^2 f_3^2 \Delta t^2} \right) \overline{I}^{\lambda\phi} R_v^{++}$$

$$+\left(\frac{I+\alpha_3^2 f_3^2 \Delta t^2 \overline{I}^{\lambda\lambda\phi\phi}}{1+\alpha_3^2 f_3^2 \Delta t^2}\right) R_u^{++}, \tag{6.58}$$

i.e.

$$\left(I+\alpha_3^2 f_3^2 \Delta t^2 \overline{I}^{\lambda\lambda\phi\phi}\right) u' = \left(\frac{I+\alpha_3^2 f_3^2 \Delta t^2 \overline{I}^{\lambda\lambda\phi\phi}}{1+\alpha_3^2 f_3^2 \Delta t^2}\right) \left(\alpha_3 \Delta t f_3 \overline{I}^{\lambda\phi} R_v^{++} + R_u^{++}\right). \tag{6.59}$$

Similarly, substituting (6.37) into (6.57) gives:

$$\left(I+\alpha_3^2 f_3^2 \Delta t^2 \overline{I}^{\lambda\lambda\phi\phi}\right) v' = \left(\frac{I+\alpha_3^2 f_3^2 \Delta t^2 \overline{I}^{\lambda\lambda\phi\phi}}{1+\alpha_3^2 f_3^2 \Delta t^2}\right) \left(-\alpha_3 \Delta t f_3 \overline{I}^{\lambda\phi} R_u^{++} + R_v^{++}\right). \tag{6.60}$$

The horizontal averaging operator $\left(I+\alpha_3^2 f_3^2 \Delta t^2 \overline{I}^{\lambda\lambda\phi\phi}\right)$ is invertible and so (6.59)-(6.60) reduce to:

$$u' = \frac{1}{1+\alpha_3^2 f_3^2 \Delta t^2} \left(\alpha_3 \Delta t f_3 \overline{I}^{\lambda\phi} R_v^{++} + R_u^{++}\right), \tag{6.61}$$

$$v' = \frac{1}{1+\alpha_3^2 f_3^2 \Delta t^2} \left(-\alpha_3 \Delta t f_3 \overline{I}^{\lambda\phi} R_u^{++} + R_v^{++}\right), \tag{6.62}$$

or

$$u' = A_u R_u^{++} + F_u \overline{R_v^{++}}^{\lambda\phi}, \tag{6.63}$$

$$v' = -F_v \overline{R_u^{++}}^{\lambda\phi} + A_v R_v^{++}, \tag{6.64}$$

where

$$A_u = \frac{1}{1+\alpha_3^2 f_3^2 \Delta t^2}, \tag{6.65}$$

$$A_v = \frac{1}{1+\alpha_3^2 f_3^2 \Delta t^2}, \tag{6.66}$$

$$F_u = \alpha_3 \Delta t f_3 A_u = \frac{\alpha_3 \Delta t f_3}{1+\alpha_3^2 f_3^2 \Delta t^2}, \tag{6.67}$$

and

$$F_v = \alpha_3 \Delta t f_3 A_v = \frac{\alpha_3 \Delta t f_3}{1+\alpha_3^2 f_3^2 \Delta t^2}. \tag{6.68}$$

Thus the role the 4th predictor and 3rd corrector play is to approximate the equations in such a way as to allow the finite-difference equations to decouple in the same way that the analytical ones do.

Caveat :

> *The above derivation assumes that the* $\overline{I}^{\lambda\phi}$ *operator is commutative with respect to variables appearing in* (6.37) *and* (6.57). α_3 *and* Δt *are spatially invariant and*

so this assumption is correct only if f_3 is also spatially invariant. In practice this is almost true, but not exactly so. The f_3 appearing in (6.37) is evaluated on a u-point, as f_3^u say, whilst that appearing in (6.57) is evaluated on a v-point, as f_3^v say. Thus, in general $f_3^u\overline{I}^{\lambda\phi}f_3^v\overline{I}^{\lambda\phi} \neq f_3^v\overline{I}^{\lambda\phi}f_3^u\overline{I}^{\lambda\phi}$, although the difference will be very small since the points are very close to one another.

6.7 Polar discretisation

Determination of u at the two poles

To close the discretisation of the horizontal components of the momentum equation, it is necessary to specify u at the two poles. Since the horizontal components of the momentum equation are singular at the two poles, this is done diagnostically, rather than prognostically. First a vector wind is computed at each pole using the surrounding values of v, and then u is obtained there diagnostically. In what follows, and for simplicity, only horizontal indices are retained since the procedure is diagnostic and all vertical levels are treated in exactly the same manner.

South pole

Let the vector wind at the S. Pole (see Fig. 6.1, as viewed from the Earth's centre) have speed v_{SP} in direction λ_{SP} relative to the reference longitude $\lambda = \lambda_{1/2} \equiv 0$. In terms of this vector wind, the v-component of the wind at the S. Pole (or more correctly at a latitude infinitesimally close to it) with longitude $\lambda = \lambda_{i-1/2}$ is

$$v_{i-1/2,1/2} \equiv v|_{\left(\lambda_{i-1/2},\phi_{1/2}\equiv-\pi/2\right)} = v_{SP}\cos\left(\lambda_{i-1/2} - \lambda_{SP}\right), i = 1, 2, ..., L. \tag{6.69}$$

It remains to obtain expressions for v_{SP} and λ_{SP} in terms of $v_{i-1/2,1} \equiv v|_{\left(\lambda_{i-1/2},\phi_1\right)}, i = 1, 2, ..., L$, where ϕ_1 is the closest latitude to the S. Pole on which v points are held. If the vector wind were uniform in a vicinity of the S. Pole, then $v_{i-1/2,1/2}$ would be equal to $v_{i-1/2,1}$ for $i = 1, 2, ..., L$, and then v_{SP} and λ_{SP} could be determined from (6.69) using two of these L equations (the other $L-2$ equations would be trivially consistent with these two). However the vector wind in general is **not** uniform in the vicinity of the S. Pole, so a least squares minimisation principle is applied to determine v_{SP} and λ_{SP}. To do this, let

$$v(\lambda,\phi) = v_{SP}\cos(\lambda - \lambda_{SP}) + \varepsilon(\lambda,\phi), \tag{6.70}$$

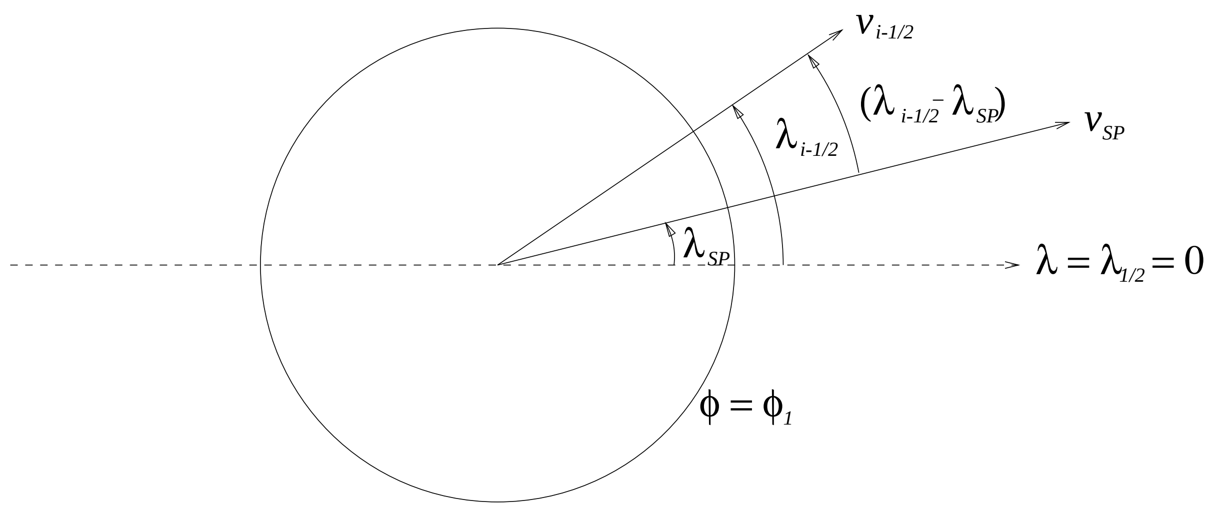

Figure 6.1: Vector wind at S. Pole as viewed from Earth's centre.

in the vicinity of the S. Pole, so $v(\lambda,\phi)$ is expressed as a perturbation about its polar value (i.e. the value at longitude λ, on a line of latitude ϕ infinitesimally close to the S. Pole).

The vector wind quantities v_{SP} and λ_{SP} are determined by minimising the area integral of the square perturbation $\varepsilon^2(\lambda,\phi)$ over the polar cap $\left\{0 \le \lambda \le 2\pi; -\pi/2 \equiv \phi_{1/2} \le \phi \le \phi_1\right\}$, i.e. by minimising

$$\begin{aligned}
I(\varepsilon) &= \int_0^{2\pi}\int_{\phi_{1/2}}^{\phi_1} \varepsilon^2(\lambda,\phi)\, r^2 \cos\phi d\phi d\lambda \\
&\approx r_{SP}^2 \int_0^{2\pi}\int_{\phi_{1/2}}^{\phi_1} \varepsilon^2(\lambda,\phi) \cos\phi d\phi d\lambda = r_{SP}^2 \sum_{i=1}^{L} \int_{\lambda_{i-1}}^{\lambda_i}\int_{\phi_{1/2}}^{\phi_1} \varepsilon^2(\lambda,\phi) \cos\phi d\phi d\lambda \\
&= r_{SP}^2 \sum_{i=1}^{L} \int_{\lambda_{i-1}}^{\lambda_i}\int_{\phi_{1/2}}^{\phi_1} \left[v(\lambda,\phi) - v_{SP}\cos(\lambda-\lambda_{SP})\right]^2 \cos\phi d\phi d\lambda, \qquad (6.71)
\end{aligned}$$

where r over the spherical cap has been approximated by its polar value $r_{SP} \equiv r|_{-\pi/2}$, and periodicity is assumed in decomposing the integral from 0 to 2π over λ into the sum of integrals from λ_{i-1} to λ_i.

Integrating over the individual control volumes $(\lambda_{i-1},\lambda_i)\otimes\left(\phi_{1/2},\phi_1\right)$ for $i = 1, 2, ..., L$, and assuming that $v(\lambda,\phi)$ is piecewise constant such that $v(\lambda,\phi) = v_{i-1/2,1}$, (6.71) is discretised as

$$I(v_{SP},\lambda_{SP}) = r_{SP}^2 \int_{\phi_{1/2}}^{\phi_1} \cos\phi d\phi \sum_{i=1}^{L} \Delta\lambda_{i-1/2}\left[v_{i-1/2,1} - v_{SP}\cos\left(\lambda_{i-1/2}-\lambda_{SP}\right)\right]^2, \qquad (6.72)$$

where $\Delta\lambda_{i-1/2} \equiv \lambda_i - \lambda_{i-1}$. $I(v_{SP},\lambda_{SP})$ is now minimised with respect to the two as-yet-undetermined parameters v_{SP} and λ_{SP}.

Setting $\partial I/\partial v_{SP} = 0$ yields

$$\sum_{i=1}^{L} \Delta\lambda_{i-1/2} \left[v_{i-1/2,1} - v_{SP}\cos\left(\lambda_{i-1/2} - \lambda_{SP}\right)\right] \cos\left(\lambda_{i-1/2} - \lambda_{SP}\right) = 0, \tag{6.73}$$

i.e.

$$v_{SP} \sum_{i=1}^{L} \Delta\lambda_{i-1/2} \cos^2\left(\lambda_{i-1/2} - \lambda_{SP}\right) = \sum_{i=1}^{L} \Delta\lambda_{i-1/2} v_{i-1/2,1} \cos\left(\lambda_{i-1/2} - \lambda_{SP}\right),$$

or

$$v_{SP}\left[1 + C\cos\left(2\lambda_{SP}\right) + D\sin\left(2\lambda_{SP}\right)\right] = A\cos\lambda_{SP} + B\sin\lambda_{SP}, \tag{6.74}$$

where

$$A = \frac{2}{2\pi}\sum_{i=1}^{L}\left(\Delta\lambda_{i-1/2} v_{i-1/2,1}\cos\lambda_{i-1/2}\right), B = \frac{2}{2\pi}\sum_{i=1}^{L}\left(\Delta\lambda_{i-1/2} v_{i-1/2,1}\sin\lambda_{i-1/2}\right), \tag{6.75}$$

$$C = \frac{1}{2\pi}\sum_{i=1}^{L}\left[\Delta\lambda_{i-1/2}\cos\left(2\lambda_{i-1/2}\right)\right], D = \frac{1}{2\pi}\sum_{i=1}^{L}\left[\Delta\lambda_{i-1/2}\sin\left(2\lambda_{i-1/2}\right)\right]. \tag{6.76}$$

Setting $\partial I/\partial \lambda_{SP} = 0$ yields

$$\sum_{i=1}^{L} \Delta\lambda_{i-1/2} \left[v_{i-1/2,1} - v_{SP}\cos\left(\lambda_{i-1/2} - \lambda_{SP}\right)\right] v_{SP}\sin\left(\lambda_{i-1/2} - \lambda_{SP}\right) = 0, \tag{6.77}$$

i.e.

$$v_{SP}\sum_{i=1}^{L} \Delta\lambda_{i-1/2}\cos\left(\lambda_{i-1/2} - \lambda_{SP}\right)\sin\left(\lambda_{i-1/2} - \lambda_{SP}\right) = \sum_{i=1}^{L} \Delta\lambda_{i-1/2} v_{i-1/2,1}\sin\left(\lambda_{i-1/2} - \lambda_{SP}\right),$$

or

$$B\cos\lambda_{SP} - A\sin\lambda_{SP} = v_{SP}\left[D\cos\left(2\lambda_{SP}\right) - C\sin\left(2\lambda_{SP}\right)\right]. \tag{6.78}$$

For a uniform mesh, where $\Delta\lambda = 2\pi/L$, the orthogonality properties of discrete Fourier transforms lead to $C = D = 0$. Eqs. (6.78) and (6.74) then respectively reduce to

$$\lambda_{SP} = \tan^{-1}\left(\frac{B}{A}\right), \tag{6.79}$$

$$v_{SP} = A\cos\lambda_{SP} + B\sin\lambda_{SP} = \sqrt{(A^2 + B^2)}. \tag{6.80}$$

Note that the inverse tangent in (6.79) is evaluated using the Fortran library routine ATAN2, in order for λ_{SP} to be determined such that v_{SP} is indeed the windspeed, i.e. a non-negative quantity - this avoids any directional ambiguity.

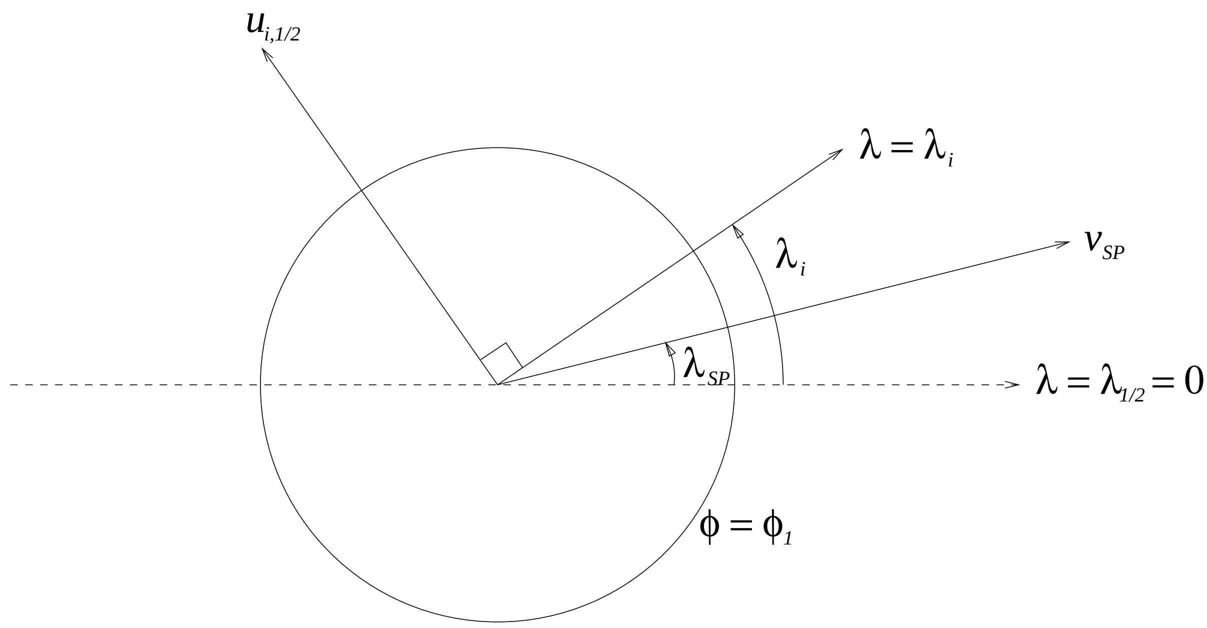

Figure 6.2: u-component of wind at S. Pole as viewed from Earth's centre.

Finally, having determined the vector wind quantities λ_{SP} and v_{SP} at the S. Pole, the u-component of the wind at longitude λ_i, on a line of latitude infinitesimally close to the S. Pole, is obtained (see Fig. 6.2) from

$$u_{i,1/2} \equiv u|_{\left(\lambda_i, \phi_{1/2} \equiv -\pi/2\right)} = -v_{SP} \sin\left(\lambda_i - \lambda_{SP}\right), i = 1, 2, ..., L. \tag{6.81}$$

Summarising, the procedure for determining the vector wind at the S. Pole using (6.79), (6.75) and (6.80) and, from this and (6.81), the u wind-component there, is:

- evaluate λ_{SP} from $\lambda_{SP} = \tan^{-1}(B/A)$, where $A = \frac{2}{L}\sum_{i=1}^{L}\left(v_{i-1/2,1}\cos\lambda_{i-1/2}\right)$, $B = \frac{2}{L}\sum_{i=1}^{L}\left(v_{i-1/2,1}\sin\lambda_{i-1/2}\right)$;
- obtain v_{SP} from $v_{SP} = A\cos\lambda_{SP} + B\sin\lambda_{SP} = \sqrt{(A^2 + B^2)}$;
- obtain $u_{i,1/2}$ from $u_{i,1/2} \equiv u|_{\left(\lambda_i, \phi_{1/2} \equiv -\pi/2\right)} = -v_{SP}\sin\left(\lambda_i - \lambda_{SP}\right), i = 1, 2, ..., L.$

Aside :

An alternative, equivalent, and slightly more efficient procedure, valid only for uniform resolution, is:

- *obtain* $u_{i,1/2}$ *from* $u_{i,1/2} = -A\sin\lambda_i + B\cos\lambda_i$, *where* $A = \frac{2}{L}\sum_{i=1}^{L}\left(v_{i-1/2,1}\cos\lambda_{i-1/2}\right)$, $B = \frac{2}{L}\sum_{i=1}^{L}\left(v_{i-1/2,1}\sin\lambda_{i-1/2}\right)$ *or, equivalently but less efficiently, from* $u_{i,1/2} = -\frac{2}{L}\sum_{k=1}^{L}\left[v_{k-1/2,1}\sin\left(\lambda_i - \lambda_{k-1/2}\right)\right]$.

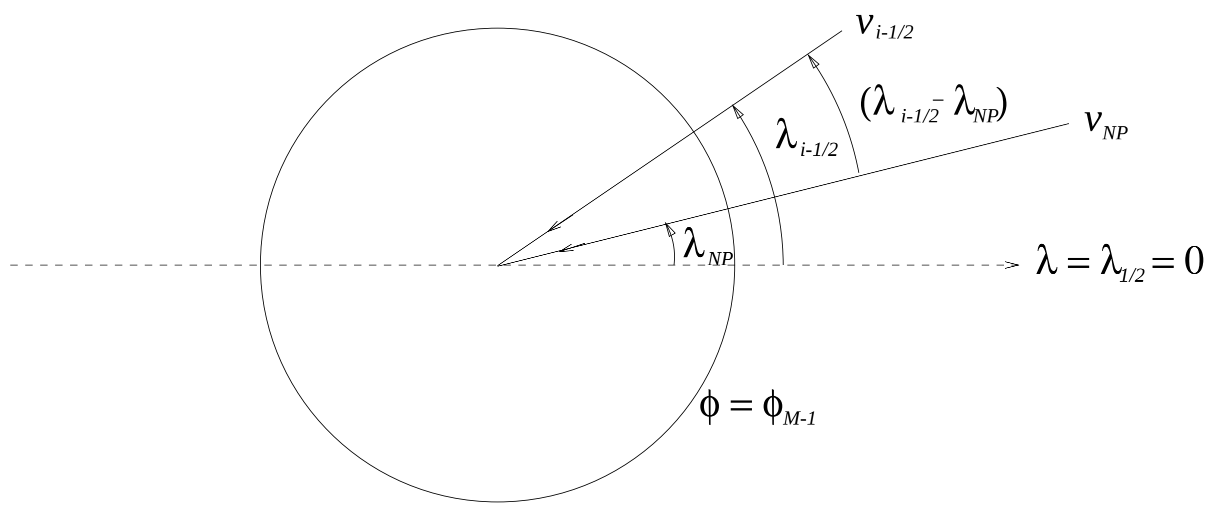

Figure 6.3: Vector wind at N. Pole as viewed from directly above the N. Pole.

Another advantage of this alternative procedure is that it simplifies the form of the expression for $u_{i,1/2}$ and thereby makes it clear that it depends linearly on $v(\phi_1)$, an important consideration for the formulation of adjoints.

North pole

Let the vector wind at the N. Pole (see Figs. 6.3-6.4, as viewed from directly above the N. Pole) have speed v_{NP} in direction λ_{NP} relative to the reference longitude $\lambda = \lambda_{1/2} \equiv 0$. Note that the v wind-component vector arrows in Figs. 6.1-6.4 all point in the direction of increasing coordinate ϕ. Thus in Figs. 6.3-6.4 they point *towards* the N. Pole, whereas in Figs. 6.1-6.2 they point *away from* the S. Pole. In terms of the vector wind at the N. Pole, the v-component of the wind at the N. Pole (or more correctly at a latitude infinitesimally close to it) with longitude $\lambda = \lambda_{i-1/2}$ is

$$v_{i-1/2,M-1/2} \equiv v|_{\left(\lambda_{i-1/2},\phi_{M-1/2}\equiv+\pi/2\right)} = v_{NP}\cos\left(\lambda_{i-1/2} - \lambda_{NP}\right), i = 1, 2, ..., L. \tag{6.82}$$

Proceeding in a similar manner to that used to derive results for the S. Pole leads to the following procedure to determine the vector wind at the N. Pole, and from this, the u wind-component there:

- evaluate λ_{NP} from

$$\lambda_{NP} = \tan^{-1}\left(\frac{B}{A}\right), \tag{6.83}$$

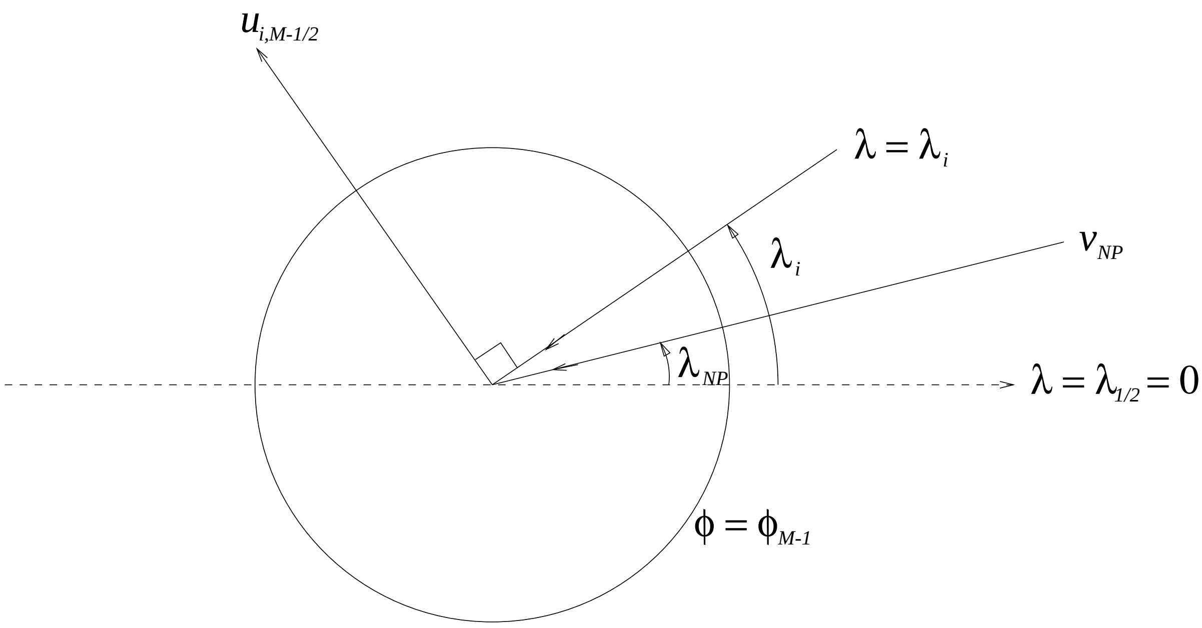

Figure 6.4: u-component of wind at N. Pole as viewed from directly above the N. Pole.

where

$$A = \frac{2}{L}\sum_{i=1}^{L}\left(v_{i-1/2,M-1}\cos\lambda_{i-1/2}\right), B = \frac{2}{L}\sum_{i=1}^{L}\left(v_{i-1/2,M-1}\sin\lambda_{i-1/2}\right), \tag{6.84}$$

- obtain v_{NP} from

$$v_{NP} = A\cos\lambda_{NP} + B\sin\lambda_{NP} = \sqrt{(A^2+B^2)}, \tag{6.85}$$

- obtain $u_{i,M-1/2}$ from

$$u_{i,M-1/2} \equiv u|_{\left(\lambda_i,\phi_{M-1/2}\equiv+\pi/2\right)} = +v_{NP}\sin\left(\lambda_i - \lambda_{NP}\right), i = 1, 2, ..., L. \tag{6.86}$$

Aside :

An alternative, equivalent and slightly more efficient procedure, valid only for uniform resolution, is:

- *obtain* $u_{i,M-1/2}$ *from* $u_{i,M-1/2} = +A\sin\lambda_i - B\cos\lambda_i$, *where* $A = \frac{2}{L}\sum_{i=1}^{L}\left(v_{i-1/2,M-1}\cos\lambda_{i-1/2}\right)$, $B = \frac{2}{L}\sum_{i=1}^{L}\left(v_{i-1/2,M-1}\sin\lambda_{i-1/2}\right)$ *or, equivalently but less efficiently, from* $u_{i,M-1/2} = +\frac{2}{L}\sum_{k=1}^{L}\left[v_{k-1/2,M-1}\sin\left(\lambda_i - \lambda_{k-1/2}\right)\right]$.

Another advantage of this alternative procedure is that it simplifies the form of the expression for $u_{i,M-1/2}$ and thereby makes it clear that it depends linearly on $v\left(\phi_{M-1}\right)$, an important consideration for the formulation of adjoints.

Near-polar determination of v

From (6.64), (6.36) and (6.56), at the near-polar latitudes ϕ_1 and ϕ_{M-1}, v' satisfies

$$
\begin{aligned}
(v')_{i-\frac{1}{2},j} &= (A_v)_{i-\frac{1}{2},j}\left(R_v^{++}\right)_{i-\frac{1}{2},j} - (F_v)_{i-\frac{1}{2},j}\left(\overline{R_u^{++}}^{\lambda\phi}\right)_{i-\frac{1}{2},j} \\
&= (A_v)_{i-\frac{1}{2},j}\left\{\left(R_v^{+}\right)_{i-\frac{1}{2},j} - \left[\frac{\alpha_3\Delta t c_{pd}}{\overline{r}^{\phi}}\left(\overline{\theta_v^*}^{r\phi}\delta_\phi\Pi' - \overline{\theta_v^*\delta_r\Pi'}^{r\phi}\delta_\phi r\right)\right]_{i-\frac{1}{2},j}\right\} \\
&\quad - (F_v)_{i-\frac{1}{2},j}\left\{\left(\overline{R_u^{+}}^{\lambda\phi}\right)_{i-\frac{1}{2},j} - \left[\overline{\frac{\alpha_3\Delta t c_{pd}}{\overline{r}^{\lambda}\cos\phi}\left(\overline{\theta_v^*}^{r\lambda}\delta_\lambda\Pi' - \overline{\theta_v^*\delta_r\Pi'}^{r\lambda}\delta_\lambda r\right)}^{\lambda\phi}\right]_{i-\frac{1}{2},j}\right\} \\
&\quad (i = 1, 2, ..., L;\ j = 1, M-1)
\end{aligned}
\tag{6.87}
$$

where, from (6.66) and (6.68),

$$
A_v = \frac{1}{1+\alpha_3^2 f^2\Delta t^2}, \tag{6.88}
$$

$$
F_v = \frac{\alpha_3\Delta t f}{1+\alpha_3^2 f^2\Delta t^2}, \tag{6.89}
$$

and $(\ )_{i,j}$ denotes evaluation at (λ_i, ϕ_j).

For the near-polar latitude ϕ_1, this means that the polar values $\left(R_u^+\right)_{i,\frac{1}{2}}$ and $\left[\frac{\alpha_3\Delta t c_{pd}}{\overline{r}^{\lambda}\cos\phi}\left(\overline{\theta_v^*}^{r\lambda}\delta_\lambda\Pi' - \overline{\theta_v^*\delta_r\Pi'}^{r\lambda}\delta_\lambda r\right)\right]_{i,\frac{1}{2}}$ are required when computing $\left(\overline{R_u^+}^{\lambda\phi}\right)_{i-\frac{1}{2},1}$. The polar value $\left(R_u^+\right)_{i,\frac{1}{2}}$ is computed from the near-polar values of $\left(R_v^+\right)_{i-\frac{1}{2},1}$ using the same procedure (outlined in the preceding subsection) used to determine the polar value $u_{i,\frac{1}{2}}$ from the near-polar values of $v_{i-\frac{1}{2},1}$. Single-valuedness of Π' and r at the pole implies that $\left(\delta_\lambda\Pi'\right)_{i,\frac{1}{2}} \equiv 0$ and $\left(\delta_\lambda r\right)_{i,\frac{1}{2}} \equiv 0$, and so $\left[\frac{\alpha_3\Delta t c_{pd}}{\overline{r}^{\lambda}\cos\phi}\left(\overline{\theta_v^*}^{r\lambda}\delta_\lambda\Pi' - \overline{\theta_v^*\delta_r\Pi'}^{r\lambda}\delta_\lambda r\right)\right]_{i,\frac{1}{2}}$ is set to zero.

Similarly for the near-polar latitude ϕ_{M-1}, the polar values $\left(R_u^+\right)_{i,M-\frac{1}{2}}$ and $\left[\frac{\alpha_3\Delta t c_{pd}}{\overline{r}^{\lambda}\cos\phi}\left(\overline{\theta_v^*}^{r\lambda}\delta_\lambda\Pi' - \overline{\theta_v^*\delta_r\Pi'}^{r\lambda}\delta_\lambda r\right)\right]_{i,M-\frac{1}{2}}$ are required when computing $\left(\overline{R_u^+}^{\lambda\phi}\right)_{i-\frac{1}{2},M-1}$. The polar value $\left(R_u^+\right)_{i,M-\frac{1}{2}}$ is computed from the near-polar values of $\left(R_v^+\right)_{i-\frac{1}{2},M-1}$ using the same procedure (outlined in the preceding subsection) used to determine the polar value $u_{i,M-\frac{1}{2}}$ from the near-polar values of $v_{i-\frac{1}{2},M-1}$. Single-valuedness of Π' and r at the pole implies that $(\delta_\lambda \Pi')_{i,M-\frac{1}{2}} \equiv 0$ and $(\delta_\lambda r)_{i,M-\frac{1}{2}} \equiv 0$, and so $\left[\frac{\alpha_3 \Delta t c_{pd}}{\overline{r}^\lambda \cos\phi}\left(\overline{\underset{v}{\theta^*}}^{r\lambda}\delta_\lambda\Pi' - \overline{\underset{v}{\theta^*}\delta_r\Pi'}^{r\lambda}\delta_\lambda r\right)\right]_{i,M-\frac{1}{2}}$ is set to zero.

7 Discretisation of the vertical component of the momentum equation

The unforced (see aside at the end of this section) vertical component of the momentum equation is:

$$\mathbf{I}_h \frac{Dw}{Dt} + \left(-f_2 u + f_1 v - \frac{u^2+v^2}{r}\right) + g + c_{pd}\theta_v \frac{\partial \Pi}{\partial r} = 0. \tag{7.1}$$

Here $\mathbf{I}_h$ is a hydrostatic switch. $\mathbf{I}_h = 0$ is the hydrostatic approximation of White & Bromley (1995) and $\mathbf{I}_h = 1$ is the unapproximated form of the equation.

This equation is discretised using a predictor-corrector method having several correction steps.

As described in Section 5.2, the vector momentum equation for $\mathbf{u} \equiv (u, v, w)$ is directly discretised in the form (see (5.68))

$$\mathbf{u}^{n+1} - \sum_k \alpha_k \Delta t \mathbf{\Psi}_k^{n+1} = \mathbf{M}\left\{\left[\mathbf{u} + \sum_k (1-\alpha_k)\,\Delta t \mathbf{\Psi}_k\right]_d^n\right\}. \tag{7.2}$$

Here $\mathbf{M}$ is the 3×3 rotation matrix, defined in Section 5.2, that transforms the components of a vector expressed in a coordinate system centred on a departure point into those expressed in the coordinate system associated with the corresponding arrival point. The role of this rotation matrix is to represent the curvature effects of spherical geometry and, specifically, to handle the associated metric terms. Because of the complexity of the current predictor/corrector discretisation of the momentum equation, it is convenient to develop this discretisation in component form as if the metric terms were absent, with the understanding that the missing metric terms are then included via (7.2) and application of the rotation matrix .

7.1 Discretisation of the w-component of the momentum equation at levels $k = 1,\ 2,\ \ldots,\ N-1$

If (7.1) were to be discretised using a 2-time-level off-centred semi-implicit semi-Lagrangian scheme, as outlined above, then at the w points of the Charney-Phillips/Arakawa C grid this would give the approximation:

$$\begin{aligned}\mathbf{I}_h \frac{w^{n+1} - w_d^n}{\Delta t} &= \alpha_4 \left[\left(f_2 \overline{u}^{\lambda r} - f_1 \overline{v}^{\phi r}\right) - g - c_{pd}\theta_v \delta_r \Pi\right]^{n+1} \\ &\quad + (1-\alpha_4)\left[\left(f_2 \overline{u}^{\lambda r} - f_1 \overline{v}^{\phi r}\right) - g - c_{pd}\theta_v \delta_r \Pi\right]_d^n,\end{aligned} \tag{7.3}$$

where the departure-point terms are those evaluated in the arrival-point coordinate system using (7.2), and the usual horizontal and vertical, averaging and difference, operators are defined in Appendix C. However this is not what is presently done, principally because of the complexity associated with a time-implicit treatment of the Coriolis terms and the non-linear pressure-gradient term. This motivated the development of the following predictor-corrector method.

For the w-component of the momentum equation at the w points of the Arakawa C grid it is comprised of the following steps:

- **Predictor**

  Let $\tilde{w}^{(1)}$ be a first predictor for w^{n+1}. The basis for this predictor is to replace all the terms evaluated at meshpoints at time $(n+1)\,\Delta t$ in (7.3) by their values at the same meshpoints but at time $n\Delta t$. Thus

$$\mathbf{I}_h \frac{\tilde{w}^{(1)} - w^n_{_d}}{\Delta t} = \alpha_4 \left[\left(f_2 \overline{u}^{\lambda r} - f_1 \overline{v}^{\phi r} \right) - g - c_{pd} \theta_v \delta_r \Pi \right]^n$$
$$+ (1 - \alpha_4) \left[\left(f_2 \overline{u}^{\lambda r} - f_1 \overline{v}^{\phi r} \right) - g - c_{pd} \theta_v \delta_r \Pi \right]^n_d . \tag{7.4}$$

  This equation can be solved explicitly for $\tilde{w}^{(1)}$.

- **1st Corrector**

  Let $\tilde{w}^{(2)}$ be a 2nd predictor for w^{n+1}. This can be written as the sum of the (1st) predictor $\tilde{w}^{(1)}$ plus a 1st corrector $\left(\tilde{w}^{(2)} - \tilde{w}^{(1)} \right)$, i.e. as

$$\tilde{w}^{(2)} = \tilde{w}^{(1)} + \left(\tilde{w}^{(2)} - \tilde{w}^{(1)} \right) . \tag{7.5}$$

  This 1st corrector is defined as

$$\left(\tilde{w}^{(2)} - \tilde{w}^{(1)} \right) = -\alpha_4 \Delta t \left[c_{pd} \left(\theta^*_{_v} - \theta^n_{_v} \right) \delta_r \Pi^n \right] , \tag{7.6}$$

  where

$$\theta^*_v = \theta^* \left(\frac{1 + m^*_v / \varepsilon}{1 + m^*_v + m^*_{cl} + m^*_{cf}} \right) , \tag{7.7}$$

  $m^*_X = m^{n+1}_X$, $X = (v, cl, cf)$, and $\theta^* \equiv \tilde{\theta}^{(P2)}$ is the latest available predictor for θ at time $(n+1)\,\Delta t$ (see the section on the discretisation of the thermodynamic equation for details of how it is computed). Equations (7.5)-(7.6) can be explicitly solved for $\tilde{w}^{(2)}$.

Aside :

Although not obvious at first sight, adding the corrector (7.6) *is equivalent to replacing θ_v where it appears in the 1st square-bracketed term on the right-hand side of* (7.4) *by θ_v^*, defined by* (7.7). *This can be seen by eliminating $\tilde{w}^{(1)}$ from* (7.4)- (7.6) *to get*

$$\mathbf{I}_h \frac{\tilde{w}^{(2)} - w_d^n}{\Delta t} = \alpha_4 \left[\left(f_2 \overline{u}^{\lambda r} - f_1 \overline{v}^{\phi r} \right) - g \right]^n - \alpha_4 c_{pd} \theta_v^* \delta_r \Pi^n$$
$$+ (1 - \alpha_4) \left[\left(f_2 \overline{u}^{\lambda r} - f_1 \overline{v}^{\phi r} \right) - g - c_{pd} \theta_v \delta_r \Pi \right]_d^n . \quad (7.8)$$

- **2nd Corrector**

Let $\tilde{w}^{(3)}$ be a 3rd predictor for w^{n+1}. This can be written as the sum of the (2nd) predictor $\tilde{w}^{(2)}$ plus a 2nd corrector $\left(\tilde{w}^{(3)} - \tilde{w}^{(2)}\right)$, i.e. as

$$\tilde{w}^{(3)} = \tilde{w}^{(2)} + \left(\tilde{w}^{(3)} - \tilde{w}^{(2)}\right). \quad (7.9)$$

This 2nd corrector is defined as

$$\left(\tilde{w}^{(3)} - \tilde{w}^{(2)}\right) = -\alpha_4 \Delta t c_{pd} \theta_v^* \delta_r \Pi', \quad (7.10)$$

where

$$\Pi' \equiv \Pi^{n+1} - \Pi^n. \quad (7.11)$$

Aside :

Adding the corrector (7.9) *is equivalent to replacing the first occurrence of* Π^n *on the right-hand side of* (7.8) *by its value at meshpoints at time* $(n+1)\,\Delta t$. *This can be seen by eliminating $\tilde{w}^{(2)}$ from* (7.8)- (7.11) *to get*

$$\mathbf{I}_h \frac{\tilde{w}^{(3)} - w_d^n}{\Delta t} = \alpha_4 \left[\left(f_2 \overline{u}^{\lambda r} - f_1 \overline{v}^{\phi r} \right) - g \right]^n - \alpha_4 c_{pd} \theta_v^* \delta_r \Pi^{n+1}$$
$$+ (1 - \alpha_4) \left[\left(f_2 \overline{u}^{\lambda r} - f_1 \overline{v}^{\phi r} \right) - g - c_{pd} \theta_v \delta_r \Pi \right]_d^n . \quad (7.12)$$

Contrary to the 1st corrector, which is *explicit*, the 2nd corrector gives rise to an *implicit coupling* of the momentum equation with the other governing equations and eventually leads to a Helmholtz problem to be solved for the Exner pressure tendency Π'.

- **3rd Corrector**

Thus far the development of the scheme has followed closely that used for the discretisation of the horizontal components of the momentum equation (before application of the 3rd corrector). The third and final corrector for the discretised horizontal components of the momentum equation favours a more time-implicit treatment of the Coriolis terms, whereas that for the discretised vertical component of the momentum equation favours a more time-implicit treatment of the pressure-gradient term. Let $\tilde{w}^{(4)} \equiv w^{n+1}$ be the 4th and final predictor. This can be written as the sum of the (3rd) predictor $\tilde{w}^{(3)}$ plus a 3rd corrector $w^{n+1} - \tilde{w}^{(3)}$, i.e. as

$$w^{n+1} = \tilde{w}^{(3)} + \left(w^{n+1} - \tilde{w}^{(3)}\right). \tag{7.13}$$

This 3rd corrector is defined as

$$\left(w^{n+1} - \tilde{w}^{(3)}\right) = -\alpha_4 \Delta t c_{pd} \left(\theta_v^{n+1} - \theta_v^*\right) \delta_r \Pi^n. \tag{7.14}$$

This corrector has the effect of adding the term $(\theta_v^{n+1} - \theta_v^*)\delta_r \Pi^n$ to the pressure gradient term $\theta_v^* \delta_r \Pi^{n+1}$ in (7.12) and thereby changes the form of the discretization of the pressure gradient term used in the vertical component of the momentum equation compared with that of the horizontal ones.

Aside :

The different forms of the pressure gradient terms used in the horizontal components of the momentum equation compared with that used in the vertical component can be seen schematically by writing the fully implicit, target form of both the horizontal and vertical pressure gradients as $A^{n+1}B^{n+1}$, where A is a generic representation of the potential temperature term and B represents the appropriate gradient of Π. If now A^{n+1} is written as

$A^{n+1} \equiv A^* + (A^{n+1} - A^*) \equiv A^* + A'$ *where* A^* *is some intermediate estimate of* A^{n+1}*, and* B^{n+1} *is written as* $B^{n+1} \equiv B^n + (B^{n+1} - B^n) \equiv B^n + B'$*, then:*

$$A^{n+1}B^{n+1} \equiv A^*B^n + A^*B' + A'B^n + A'B'. \tag{7.15}$$

In the horizontal components of the momentum equation only the first two terms on the right-hand side of (7.15) *are retained whereas the first three terms are retained in the vertical momentum equation. If the change in the* θ *and* Π*-gradient fields is small in one time-step compared with the absolute magnitude of the fields themselves, and if* A^* *is also an* $O(\Delta t)$ *approximation to* A^{n+1}*, then the vertical momentum equation approximation is the more accurate, dropping only second order* $(O(\Delta t^2))$ *terms. However, this increase comes at the expense of implicitly coupling the vertical component of the momentum equation with the* θ *equation. As will be shown below, it is relatively straightforward to decouple these two equations, whereas in the horizontal components of the momentum equation the analogous coupling would be harder to handle. Note though that this would not be the case if the standard interpolating semi-Lagrangian scheme were used for* θ*. It is also worth noting that, since* A *represents* θ*, the accuracy of the approximation made in the horizontal components of the momentum equation depends on* θ^* *being a good estimate for* θ^{n+1}*. The vertical momentum equation is less dependent on the accuracy of this estimate.*

Aside :

As the 4th predictor is the final one, the final discretisation of the w*-component of the momentum equation can be written using* (7.12) *and* (7.14) *as:*

$$\begin{aligned}\mathbf{I}_h \frac{w^{n+1} - w^n_d}{\Delta t} &= \alpha_4 \left[\left(f_2 \overline{u}^{\lambda r} - f_1 \overline{v}^{\phi r} \right) - g \right]^n \\ -\alpha_4 \left[c_{pd} \theta_v^{n+1} \delta_r \Pi^{n+1} - c_{pd} \left(\theta_v^{n+1} - \theta_v^* \right) \left(\delta_r \Pi^{n+1} - \delta_r \Pi^n \right) \right] \\ +(1-\alpha_4) \left[\left(f_2 \overline{u}^{\lambda r} - f_1 \overline{v}^{\phi r} \right) - g - c_{pd} \theta_v \delta_r \Pi \right]^n_d .\end{aligned} \tag{7.16}$$

Equation (7.16) *is quite close to the target 2-time-level off-centred semi-implicit semi-Lagrangian discretisation defined by* (7.3). *There are how-*

ever three differences: (a) the mass loading of water content in the gravitational acceleration term is evaluated at time $n\Delta t$ instead of $(n+1)\Delta t$; (b) the time-implicit Coriolis terms are evaluated explicitly; and (c) the time-implicit pressure gradient term $c_{pd}\theta_v^{n+1}\delta_r\Pi^{n+1}$ has an $O(\Delta t^2)$ term, $c_{pd}(\theta_v^{n+1}-\theta_v^*)\delta_r(\Pi^{n+1}-\Pi^n)$, subtracted from it, as discussed in the preceding aside.

As it stands (7.16) is coupled to the θ-equation by the term involving θ_v^{n+1}. The equation for θ^{n+1} ((9.36)) is:

$$\theta^{n+1} = \theta^* - \left[\Delta t\alpha_2\left(w^{n+1}-w^n\right)\delta_{2r}\theta_{ref}\right]. \tag{7.17}$$

Here δ_{2r} is a vertical difference operator over 2 gridlengths and is defined in Appendix C. Multiplying this equation by $(1+m_v^*/\varepsilon)/\left(1+m_v^*+m_{cl}^*+m_{cf}^*\right)$ and noting that $m_X^* = m_X^{n+1}$, $X=(v,cl,cf)$, leads to the following equation for θ_v^{n+1}:

$$\theta_v^{n+1} = \theta_v^* - \left[\Delta t\alpha_2\left(w^{n+1}-w^n\right)\left(\frac{1+m_v^*/\varepsilon}{1+m_v^*+m_{cl}^*+m_{cf}^*}\right)\delta_{2r}\theta_{ref}\right], \tag{7.18}$$

which can be substituted into (7.16) to give:

$$\begin{aligned}\mathbf{I}_h\frac{w^{n+1}-w_d^n}{\Delta t} &= \alpha_4\left[\left(f_2\overline{u}^{\lambda r}-f_1\overline{v}^{\phi r}\right)-g-c_{pd}\theta_v^*\delta_r\Pi\right]^n-\alpha_4\left[c_{pd}\theta_v^*\delta_r\Pi'\right]\\ &+(1-\alpha_4)\left[\left(f_2\overline{u}^{\lambda r}-f_1\overline{v}^{\phi r}\right)-g-c_{pd}\theta_v\delta_r\Pi\right]_d^n\\ &+c_{pd}\alpha_2\alpha_4\Delta t\left(\frac{1+m_v^*/\varepsilon}{1+m_v^*+m_{cl}^*+m_{cf}^*}\right)\delta_{2r}\theta_{ref}\delta_r\Pi^n\left(w^{n+1}-w^n\right)\end{aligned} \tag{7.19}$$

This can be rewritten as

$$\begin{aligned}\frac{G(w^{n+1}-w^n)+\mathbf{I}_h(w^n-w_d^n)}{\Delta t} &= \alpha_4\left[\left(f_2\overline{u}^{\lambda r}-f_1\overline{v}^{\phi r}\right)-g-c_{pd}\theta_v^*\delta_r\Pi\right]^n-\alpha_4\left[c_{pd}\theta_v^*\delta_r\Pi'\right]\\ &+(1-\alpha_4)\left[\left(f_2\overline{u}^{\lambda r}-f_1\overline{v}^{\phi r}\right)-g-c_{pd}\theta_v\delta_r\Pi\right]_d^n,\end{aligned} \tag{7.20}$$

where

$$G = \mathbf{I}_h - c_{pd}\alpha_2\alpha_4\Delta t^2\left(\frac{1+m_v^*/\varepsilon}{1+m_v^*+m_{cl}^*+m_{cf}^*}\right)\delta_{2r}\theta_{ref}\delta_r\Pi^n. \tag{7.21}$$

In (7.17), and hence in (7.21), normally θ_{ref} should be the most accurate available estimate for θ^{n+1}, which is $\theta^* = \widetilde{\theta}^{(P2)}$. However, to avoid the singular case of G vanishing, and to ensure the ellipticity of the equation for $\Pi'(\equiv \Pi^{n+1}-\Pi^n)$ and convergence of the iterative procedure for its solution, $\delta_{2r}\theta_{ref}$ is in fact chosen such that

$$\delta_{2r}\theta_{ref} = \max\left[\delta_{2r}\theta^*, \left(\frac{\mathbf{I}_h-G_{tol}}{c_{pd}\alpha_2\alpha_4\Delta t^2\delta_r\Pi^n}\right)\left(\frac{1+m_v^*+m_{cl}^*+m_{cf}^*}{1+m_v^*/\varepsilon}\right)\right], \tag{7.22}$$

so that $G \geq G_{tol} > 0$, where G_{tol} is user specified.

Aside :

$\delta_r \Pi^n$ is almost always strictly negative. Under this assumption, making $G > 0$ amounts to perturbing $\delta_{2r}\theta^*$ away from being statically unstable (i.e. $\delta_{2r}\theta^* < 0$) towards being neutrally stable (i.e. $\delta_{2r}\theta^* = 0$), or (when $\mathbf{I}_h = 0$) making the profile statically stable (i.e. $\delta_{2r}\theta^* > 0$) - a smaller perturbation is required for the nonhydrostatic case (when $\mathbf{I}_h = 1$) since a mildly unstable profile is then tolerable.

For the nonhydrostatic case (when $\mathbf{I}_h = 1$), ellipticity can always be assured by taking a sufficiently small timestep, albeit at the price of efficiency, with no adjustment to θ^* being needed. This simply corresponds to adequately resolving the Brunt-Vaisala frequency instead of artificially retarding fast modes by adjusting the potential temperature profile. This latter alternative is not a problem provided such modes carry negligible energy - this is generally so for vertically-propagating acoustic modes and for the fastest horizontally-propagating gravity modes. However if this is not so, then there is no alternative but to reduce the timestep appropriately.

If G_{tol} is chosen too close to zero (but still positive), then although the Helmholtz problem will be elliptic, it will not be well conditioned and this can be expected to have an adverse effect on computational stability.

In exactly the same way as $\delta_{2r}\theta$ is evaluated in Section 9, $\delta_{2r}\theta^*$ in (7.22) is evaluated as:

$$\delta_{2r}\theta^*|_{\eta_1} = \left(\frac{\theta^*|_{\eta_2} - \theta^*|_{\eta_1}}{r|_{\eta_2} - r|_{\eta_1}} \right), \tag{7.23}$$

$$\delta_{2r}\theta^*|_{\eta_k} = \left(\frac{\theta^*|_{\eta_{k+1}} - \theta^*|_{\eta_{k-1}}}{r|_{\eta_{k+1}} - r|_{\eta_{k-1}}} \right), k = 2, 3, ..., N-1. \tag{7.24}$$

Aside :

As also noted in Section 9, consideration should be given to using the value of θ^* at level $k = 0$ when calculating $\delta_{2r}\theta^*$ at level $k = 1$. This means prognostically carrying θ at level $k = 0$.

Aside :

Note that the particular form of (7.19) *arises due to the use of the non-interpolating semi-Lagrangian advection scheme used for θ. Were the standard interpolating scheme to be used instead, θ^{n+1} in* (7.16) *would simply be replaced by θ_d^n and w^{n+1} would not appear on the right-hand side of* (7.19)*. This would have the effect of removing all terms involving α_2 from the following equations. (Further, neglecting any issues regarding numerical stability of the resulting equations, such an approach would allow inclusion of all the $O(\Delta t)$ terms of the pressure gradient terms in the horizontal components of the momentum equation without coupling them implicitly to the vertical one.)*

7.2 Formally-equivalent statement of the discretisation of the w-component of the momentum equation at levels $k = 1, 2, ..., N-1$

By defining R_w and R_w^+ as

$$R_w \equiv \tilde{w}^{(1)} - w^n, \quad R_w^+ \equiv \tilde{w}^{(2)} - w^n, \tag{7.25}$$

where $\tilde{w}^{(1)}$ and $\tilde{w}^{(2)}$ are given by (7.4) and (7.6), the above predictor-corrector discretisation of the w-component of the momentum equation can be written as the equivalent following steps:

- Compute R_w at the w-points of the Arakawa C grid:

$$\begin{aligned} R_w &= \mathbf{I}_h w_d^n - \mathbf{I}_h w^n \\ &+\alpha_4 \Delta t \left[\left(f_2 \overline{u}^{\lambda r} - f_1 \overline{v}^{\phi r} \right) - g - c_{pd} \theta_v \delta_r \Pi \right]^n \\ &+(1-\alpha_4)\Delta t \left[\left(f_2 \overline{u}^{\lambda r} - f_1 \overline{v}^{\phi r} \right) - g - c_{pd} \theta_v \delta_r \Pi \right]_d^n . \end{aligned} \tag{7.26}$$

- Compute R_w^+ at the w-points of the Arakawa C grid:

$$R_w^+ = R_w - \alpha_4 \Delta t c_p \left(\theta_v^* - \theta_v^n \right) \delta_r \Pi^n, \tag{7.27}$$

where

$$\theta_v^* = \theta^* \left(\frac{1 + m_v^* / \varepsilon}{1 + m_v^* + m_{cl}^* + m_{cf}^*} \right), \tag{7.28}$$

$\theta^* \equiv \tilde{\theta}^{(P2)}$ is the latest available predictor for θ when R_w^+ is computed (see Section 9 for details), and $m_X^* = m_X^{n+1}$, $X = (v, cl, cf)$.

- Approximate the time tendency w' as:

$$\begin{aligned} \mathbf{I}_h w' &\equiv \mathbf{I}_h \left(w^{n+1} - w^n\right) \\ &= R_w^+ - \alpha_4 \Delta t c_{pd} \theta_v^* \delta_r \Pi' + c_{pd} \alpha_2 \alpha_4 \Delta t^2 \left(\frac{1 + m_v^* / \varepsilon}{1 + m_v^* + m_{cl}^* + m_{cf}^*} \right) \delta_{2r} \theta_{ref} \delta_r \Pi^n w', \end{aligned} \tag{7.29}$$

which can be written as:

$$w' = G^{-1} R_w^+ - K \delta_r \Pi', \tag{7.30}$$

where $\Pi' \equiv \Pi^{n+1} - \Pi^n$ is obtained from the solution of a Helmholtz problem (to be derived),

$$G = \mathbf{I}_h - c_{pd} \alpha_2 \alpha_4 \Delta t^2 \left(\frac{1 + m_v^* / \varepsilon}{1 + m_v^* + m_{cl}^* + m_{cf}^*} \right) \delta_{2r} \theta_{ref} \delta_r \Pi^n, \tag{7.31}$$

and

$$\begin{aligned} K &= \frac{\alpha_4 \Delta t c_p \theta_v^*}{\mathbf{I}_h - c_{pd} \alpha_2 \alpha_4 \Delta t^2 \left[(1 + m_v^* / \varepsilon) / \left(1 + m_v^* + m_{cl}^* + m_{cf}^*\right) \right] \delta_{2r} \theta_{ref} \delta_r \Pi^n} \\ &= \alpha_4 \Delta t c_{pd} \theta_v^* G^{-1} \end{aligned} \tag{7.32}$$

with $\delta_{2r} \theta_{ref}$ defined by (7.22).

Aside :

There are no explicit *forcing, or "physics", terms in the vertical component of the momentum equation. However, since the momentum equation is a vector equation, departure point values are evaluated as components of a vector calculation (see Section 5). This means that for the vertical component of the momentum equation, a departure point value is calculated as the vertical (in the sense of the unit vectors* at the arrival point*) component of a vector, whose components are initially known in terms of the unit vectors* at the departure point. *Then, since, in general, the unit vectors of the model's spherical co-ordinate system change direction over the sphere, the arrival point vertical component is not the same as the departure point vertical component.*

Specifically, the term

$$\left\{\mathbf{I}_h w^n + (1-\alpha_4)\Delta t\left[\left(f_2\overline{u}^{\lambda r} - f_1\overline{v}^{\phi r}\right) - g - c_{pd}\theta_v\delta_r\Pi\right]\right\}_d^n, \tag{7.33}$$

required in the evaluation of R_w, is calculated as part of a vector whose two (departure point) horizontal components are those terms whose departure point values are required to evaluate R_u^{P1} and R_v^{P1}, namely:

$$\left\{u + (1-\alpha_3)\,\Delta t\left[f_3\overline{v}^{\lambda\phi} - \frac{c_{pd}}{\overline{r}^{\lambda}\cos\phi}\left(\overline{\theta_v}^{r\lambda}\delta_\lambda\Pi - \overline{\theta_v\delta_r\Pi}^{r\lambda}\delta_\lambda r\right)\right] - (1-\alpha_4)\,\Delta t f_2\overline{w}^{r\lambda} + \Delta t\left[S_1^u\right]\right\}_d^n \tag{7.34}$$

and

$$\left\{v - (1-\alpha_3)\,\Delta t\left[f_3\overline{u}^{\lambda\phi} + \frac{c_{pd}}{\overline{r}^{\phi}}\left(\overline{\theta_v}^{r\phi}\delta_\phi\Pi - \overline{\theta_v\delta_r\Pi}^{r\phi}\delta_\phi r\right)\right] + (1-\alpha_4)\,\Delta t f_1\overline{w}^{r\phi} + \Delta t\left[S_1^v\right]\right\}_d^n, \tag{7.35}$$

(see equations (6.31)-(6.32) *and* (6.51)-(6.52)*, respectively) and whose vertical component is* (7.33)*. Due, then, to the rotation of the unit vectors between the departure and arrival points, the horizontal forcing terms appearing in* (7.34) *and* (7.35) *(i.e. $\Delta t\left[S_1^u\right]$ and $\Delta t\left[S_1^v\right]$) will manifest themselves in the vertical component of the arrival point vector. In this way* implicit *forcing, or "physics", terms arise in the vertical component of the momentum equation.*

7.3 Polar discretisation

The polar discretisation of the vertical component of the momentum equation is almost identical to that elsewhere. This is because horizontal derivatives only occur in the acceleration term Dw/Dt. These and the metric terms $\left(u^2+v^2\right)/r$ are handled using the semi-Lagrangian procedures given in Section 5.

Uniqueness of w at the two poles is assumed, i.e.

$$w_{SP} \equiv w_{\frac{1}{2},\frac{1}{2}} \equiv w_{\frac{3}{2},\frac{1}{2}} \equiv w_{\frac{5}{2},\frac{1}{2}} \equiv ... \equiv w_{L-\frac{1}{2},\frac{1}{2}}, \tag{7.36}$$

$$w_{NP} \equiv w_{\frac{1}{2},M-\frac{1}{2}} \equiv w_{\frac{3}{2},M-\frac{1}{2}} \equiv w_{\frac{5}{2},M-\frac{1}{2}} \equiv ... \equiv w_{L-\frac{1}{2},M-\frac{1}{2}}. \tag{7.37}$$

Currently the Coriolis terms $(f_2u - f_1v)$ are ignored where, from (2.77)-(2.78),

$$f_1 = 2\Omega\sin\lambda\cos\phi_P, \tag{7.38}$$

$$f_2 = 2\Omega\left(\cos\phi\sin\phi_P + \sin\phi\cos\lambda\cos\phi_P\right). \tag{7.39}$$

and ϕ_P is the geographical latitude of the North Pole of the model's rotated latitude/longitude system. For an unrotated coordinate system, for which $\phi_P = \pi/2$, this is valid since then $(f_2 u - f_1 v)$ simplifies to $2\Omega u\cos\phi$, and this is identically zero at the two poles $\phi = \pm\pi/2$. For a rotated coordinate system no such simplification occurs and $(f_2 u - f_1 v)$ then has a nonzero contribution at the two computational poles. Therefore **the model as presently formulated cannot work properly in global mode for the rotated coordinate system option**, but only in limited-area mode for which the two poles are excluded from the model domain.

Aside :

This deficiency in the formulation needs to be addressed. One possible way of doing this is as follows.

Eq. (7.1) *can be formally rewritten as*

$$F = f_2 u - f_1 v, \tag{7.40}$$

where F represents all terms other than $f_2 u$ and $-f_1 v$.

Integrating (7.40) *over the south polar cap* $\left\{0 \le \lambda \le 2\pi; -\pi/2 \equiv \phi_{1/2} \le \phi \le \phi_1\right\}$ *gives*

$$\int_{-\frac{\pi}{2}}^{\phi_1}\int_0^{2\pi} Fr^2\cos\phi d\lambda d\phi = \int_{-\frac{\pi}{2}}^{\phi_1}\int_0^{2\pi}\left(f_2 u - f_1 v\right) r^2\cos\phi d\lambda d\phi, \tag{7.41}$$

where $\phi_1 - \phi_{1/2} = \Delta\phi/2$. By approximating r and F over the spherical cap by their polar values $r_{SP} \equiv r|_{-\pi/2}$ and $F_{SP} \equiv F|_{-\pi/2}$, this simplifies to

$$F_{SP} = \frac{1}{A_{SP}}\int_{-\frac{\pi}{2}}^{\phi_1}\int_0^{2\pi}\left(f_2 u - f_1 v\right)\cos\phi d\lambda d\phi. \tag{7.42}$$

Here $A_{SP} = \int_{-\frac{\pi}{2}}^{\phi_1}\int_0^{2\pi}\cos\phi d\lambda d\phi$ is the area of a spherical cap of a sphere of unit radius. It could be taken to have its exact value $2\pi\left(1+\sin\phi_1\right)$, or it could be approximated, as in Section 8, by the area of a plane circle of radius $\Delta\phi/2$, i.e. by $\pi\left(\Delta\phi/2\right)^2$. It is simpler to use the latter since other terms are anyway approximated to this order of accuracy, so

$$A_{SP} = \pi\left(\frac{\Delta\phi}{2}\right)^2. \tag{7.43}$$

Approximating u (cf. (6.81)*) over the south polar cap by its polar representation (this is equivalent to assuming that the wind blows uniformly over the spherical cap)*

$$u\left(\lambda,\phi\right) = -v_{SP}\sin\left(\lambda-\lambda_{SP}\right), \tag{7.44}$$

the first right-hand-side integral of (7.42) *can be discretised as*

$$\begin{aligned}
I_1 &\equiv \frac{1}{A_{SP}}\int_{-\frac{\pi}{2}}^{\phi_1}\int_0^{2\pi} f_2 u\cos\phi d\lambda d\phi \\
&\approx -\frac{2\Omega v_{SP}}{A_{SP}}\int_{-\frac{\pi}{2}}^{\phi_1}\int_0^{2\pi}\left(\cos\phi\sin\phi_P+\sin\phi\cos\lambda\cos\phi_P\right)\sin\left(\lambda-\lambda_{SP}\right)\cos\phi d\lambda d\phi \\
&= -\frac{2\Omega v_{SP}\cos\phi_P}{A_{SP}}\left[\int_{-\frac{\pi}{2}}^{\phi_1}\frac{\sin 2\phi}{2}d\phi\right]\left[\int_0^{2\pi}\cos\lambda\left(\sin\lambda\cos\lambda_{SP}-\cos\lambda\sin\lambda_{SP}\right)d\lambda\right] \\
&= -\frac{2\Omega v_{SP}\cos\phi_P}{A_{SP}}\left[\frac{\cos\left(-\pi\right)-\cos\left(2\phi_1\right)}{4}\right]\left[-\pi\sin\lambda_{SP}\right] \\
&= -\frac{2\Omega v_{SP}\cos\phi_P\sin\lambda_{SP}}{A_{SP}}\left(\frac{1-\cos\Delta\phi}{4}\right)\pi \\
&\approx -\frac{2\Omega v_{SP}\cos\phi_P\sin\lambda_{SP}}{A_{SP}}\pi\frac{\Delta\phi^2}{8} \\
&\approx -\Omega v_{SP}\cos\phi_P\sin\lambda_{SP},
\end{aligned} \tag{7.45}$$

where (7.43) *has been used to obtain the last line.*

Similarly, approximating v (cf. (6.69)*) over the south polar cap by its polar representation*

$$v\left(\lambda,\phi\right) = v_{SP}\cos\left(\lambda-\lambda_{SP}\right), \tag{7.46}$$

the second right-hand-side integral can be discretised as

$$\begin{aligned}
I_2 &\equiv \frac{1}{A_{SP}}\int_{-\frac{\pi}{2}}^{\phi_1}\int_0^{2\pi} f_1 v\cos\phi d\lambda d\phi \\
&\approx \frac{2\Omega v_{SP}}{A_{SP}}\int_{-\frac{\pi}{2}}^{\phi_1}\int_0^{2\pi}\sin\lambda\cos\phi_P\cos\left(\lambda-\lambda_{SP}\right)\cos\phi d\lambda d\phi \\
&= \frac{2\Omega v_{SP}\cos\phi_P}{A_{SP}}\left[\int_{-\frac{\pi}{2}}^{\phi_1}\cos\phi d\phi\right]\left[\int_0^{2\pi}\sin\lambda\left(\cos\lambda\cos\lambda_{SP}+\sin\lambda\sin\lambda_{SP}\right)d\lambda\right] \\
&= \frac{2\Omega v_{SP}\cos\phi_P}{A_{SP}}\left[\sin\phi_1-\sin\left(-\frac{\pi}{2}\right)\right]\left[\pi\sin\lambda_{SP}\right] \\
&= \frac{2\Omega v_{SP}\cos\phi_P\sin\lambda_{SP}}{A_{SP}}\left(1-\cos\frac{\Delta\phi}{2}\right)\pi \\
&\approx \frac{2\Omega v_{SP}\cos\phi_P\sin\lambda_{SP}}{A_{SP}}\pi\frac{\Delta\phi^2}{8} \\
&\approx \Omega v_{SP}\cos\phi_P\sin\lambda_{SP}.
\end{aligned} \tag{7.47}$$

Thus, using (6.75), (6.79)-(6.80), (7.45) *and* (7.47), (7.42) *may be rewritten as*

$$\begin{aligned}(f_2u - f_1v)_{SP} &= F_{SP} = \frac{1}{A_{SP}} \int_{-\frac{\pi}{2}}^{\phi_1} \int_0^{2\pi} (f_2u - f_1v) \cos\phi d\lambda d\phi = I_1 - I_2 \\ &= -2\Omega \cos\phi_P v_{SP} \sin\lambda_{SP} \\ &= -2\Omega \cos\phi_P B, \end{aligned} \tag{7.48}$$

where

$$B = \frac{2}{L} \sum_{i=1}^{L} \left(v_{i-1/2,1} \sin\lambda_{i-1/2} \right). \tag{7.49}$$

Similarly, at the North Pole

$$\begin{aligned}(f_2u - f_1v)_{NP} &= F_{NP} = \frac{1}{A_{NP}} \int_{\phi_{M-1}}^{\frac{\pi}{2}} \int_0^{2\pi} (f_2u - f_1v) \cos\phi d\lambda d\phi \\ &= -2\Omega \cos\phi_P B, \end{aligned} \tag{7.50}$$

where

$$A_{NP} = \pi \left(\frac{\Delta\phi}{2} \right)^2, \tag{7.51}$$

$$B = \frac{2}{L} \sum_{i=1}^{L} \left(v_{i-1/2,M-1} \sin\lambda_{i-1/2} \right). \tag{7.52}$$

8 Discretisation of the continuity equation

8.1 Continuous form

The continuity equation in continuous form, i.e. (2.80) rewritten in Eulerian flux form, is:

$$\frac{\partial}{\partial t}\left(r^2\rho_y\frac{\partial r}{\partial \eta}\right)+\left[\frac{1}{\cos\phi}\frac{\partial}{\partial\lambda}\left(r^2\rho_y\frac{\partial r}{\partial\eta}\frac{u}{r}\right)+\frac{1}{\cos\phi}\frac{\partial}{\partial\phi}\left(r^2\rho_y\frac{\partial r}{\partial\eta}\frac{v\cos\phi}{r}\right)+\frac{\partial}{\partial\eta}\left(r^2\rho_y\frac{\partial r}{\partial\eta}\dot{\eta}\right)\right]=0, \tag{8.1}$$

where

$$\frac{\partial r}{\partial\eta}\dot{\eta}=w-\frac{u}{r\cos\phi}\frac{\partial r}{\partial\lambda}-\frac{v}{r}\frac{\partial r}{\partial\phi}, \tag{8.2}$$

and

$$\dot{\eta}\big|_{\eta=0}=\dot{\eta}\big|_{\eta=1}=0. \tag{8.3}$$

Using (8.2), (8.1) may be rewritten as

$$\begin{aligned}\frac{\partial}{\partial t}\left(r^2\rho_y\frac{\partial r}{\partial \eta}\right) \quad + \quad &\left\{\frac{1}{\cos\phi}\frac{\partial}{\partial\lambda}\left(r^2\rho_y\frac{\partial r}{\partial\eta}\frac{u}{r}\right)+\frac{1}{\cos\phi}\frac{\partial}{\partial\phi}\left(r^2\rho_y\frac{\partial r}{\partial\eta}\frac{v\cos\phi}{r}\right)\right.\\ &\left.-\frac{\partial}{\partial\eta}\left(r^2\rho_y\frac{u}{r\cos\phi}\frac{\partial r}{\partial\lambda}+r^2\rho_y\frac{v}{r}\frac{\partial r}{\partial\phi}\right)+\frac{\partial}{\partial\eta}\left(r^2\rho_y w\right)\right\}=0.\end{aligned} \tag{8.4}$$

8.2 Discrete form at levels $k = 1/2,\ 3/2,\ldots,\ N-1/2$

Eq. (8.1) is discretised using a predictor-corrector method. If it were to be discretised using a 2-time-level off-centred semi-implicit *Eulerian* scheme, then at the ρ points of the Arakawa C grid this would give the approximation:

$$\begin{aligned}\frac{\left(r^2\rho_y\right)^{n+1}-\left(r^2\rho_y\right)^{n}}{\Delta t} \quad = \quad -\frac{1}{\delta_\eta r}&\left[\overline{\frac{1}{\cos\phi}\delta_\lambda\left(\frac{\overline{r^2\rho_y\delta_\eta r}^{\lambda}}{\overline{r}^{\lambda}}u\right)}^{\alpha_1}+\overline{\frac{1}{\cos\phi}\delta_\phi\left(\frac{\overline{r^2\rho_y\delta_\eta r}^{\phi}}{\overline{r}^{\phi}}v\cos\phi\right)}^{\alpha_1}\right.\\ &\left.+\,\overline{\delta_\eta\left(\overline{r^2\rho_y}^{r}\dot{\eta}\delta_\eta r\right)}^{average}\right],\end{aligned} \tag{8.5}$$

where

$$\overline{F}^{\alpha_1}=\alpha_1F^{n+1}+\left(1-\alpha_1\right)F^n, \tag{8.6}$$

denotes a time-weighted average of F at a meshpoint (rather than along a trajectory) at times $n\Delta t$ and $(n+1)\,\Delta t$, $\overline{G}^{average}$ denotes some kind of time-weighting (to be specified) of G at a meshpoint, and it is assumed that $\partial r/\partial\eta$ is independent of time.

However this is not what is presently done, principally because of the complexity associated with a time-implicit treatment of the term for the product of density with other quantities. This motivated the development of the following predictor-corrector method.

For the continuity equation at the ρ points of the Arakawa C grid it is comprised of the following steps:

- **Predictor**

  Let $\tilde{\rho}_y^{(1)}$ be a predictor for ρ_y^{n+1}. The basis for this predictor is to replace all the terms evaluated as time averages of quantities at meshpoints at time levels $n\Delta t$ and $(n+1)\Delta t$ in (8.5) by their values at the same meshpoints but at time $n\Delta t$. Thus

$$\frac{\left(r^2\tilde{\rho}_y^{(1)}\right)-\left(r^2\rho_y^n\right)}{\Delta t} = -\frac{1}{\delta_\eta r}\left[\frac{1}{\cos\phi}\delta_\lambda\left(\frac{\overline{r^2\rho_y^n\delta_\eta r}^\lambda}{\overline{r}^\lambda}u^n\right)+\frac{1}{\cos\phi}\delta_\phi\left(\frac{\overline{r^2\rho_y^n\delta_\eta r}^\phi}{\overline{r}^\phi}v^n\cos\phi\right)\right.$$
$$\left.+\,\delta_\eta\left(\overline{r^2\rho_y^n}^r\dot{\eta}^n\delta_\eta r\right)\right], \tag{8.7}$$

  where

$$\dot{\eta}^n = \frac{1}{\delta_\eta r}\left(w^n - \frac{\overline{\overline{u}^\eta}^\lambda}{\overline{r}^\lambda\cos\phi}\delta_\lambda r - \frac{\overline{\overline{v}^\eta}^\phi}{\overline{r}^\phi}\delta_\phi r\right)^n, \tag{8.8}$$

  at levels $k=1,2,...,N-1$, and

$$\dot{\eta}^n|_{\eta_0\equiv 0} = \dot{\eta}^n|_{\eta_N\equiv 1} = 0. \tag{8.9}$$

  Eq. (8.7) can be solved explicitly for $\tilde{\rho}_y^{(1)}$.

  <u>**Aside :**</u>

  $\delta_\eta\left(\overline{r^2\rho_y^n\delta_\eta r}^r\dot{\eta}^n\right)$ *is arguably a more natural discretisation of* $\frac{\partial}{\partial\eta}\left(r^2\rho_y\frac{\partial r}{\partial\eta}\dot{\eta}\right)$ *than* $\delta_\eta\left(\overline{r^2\rho_y^n}^r\dot{\eta}^n\delta_\eta r\right)$.

- **Corrector**

  ρ_y^{n+1} can be written as the sum of the predictor $\tilde{\rho}_y^{(1)}$ plus a corrector $\left(\rho_y^{n+1}-\tilde{\rho}_y^{(1)}\right)$, i.e. as

$$\rho_y^{n+1} = \tilde{\rho}_y^{(1)} + \left(\rho_y^{n+1}-\tilde{\rho}_y^{(1)}\right). \tag{8.10}$$

This corrector is defined by

$$\left(r^2\rho_y^{n+1}\right) - \left(r^2\tilde{\rho}_y^{(1)}\right) = -\frac{\Delta t}{\delta_\eta r}\left\{\frac{1}{\cos\phi}\delta_\lambda\left(\frac{\overline{r^2\rho_y^n\delta_\eta r}^\lambda}{\overline{r}^\lambda}\alpha_1 u'\right) + \frac{1}{\cos\phi}\delta_\phi\left(\frac{\overline{r^2\rho_y^n\delta_\eta r}^\phi}{\overline{r}^\phi}\alpha_1 v'\cos\phi\right) + \delta_\eta\left[\overline{r^2\rho_y^n}^r\left(\overline{\dot{\eta}}^{average} - \dot{\eta}^n\right)\delta_\eta r\right]\right\}, \tag{8.11}$$

where

$$\overline{\dot{\eta}}^{average} = \frac{1}{\delta_\eta r}\left[\overline{w}^{\alpha_2} - \overline{\left(\overline{\frac{\overline{u}^\eta}{\overline{r}^\lambda\cos\phi}\delta_\lambda r}^\lambda + \overline{\frac{\overline{v}^\eta}{\overline{r}^\phi}\delta_\phi r}^\phi\right)}^{\alpha_1}\right], \tag{8.12}$$

at levels $k = 1, 2, ..., N-1$,

$$\left.\overline{\dot{\eta}}^{average}\right|_{\eta_0\equiv 0} = \left.\overline{\dot{\eta}}^{average}\right|_{\eta_N\equiv 1} = 0, \tag{8.13}$$

and

$$u' \equiv u^{n+1} - u^n, \quad v' \equiv v^{n+1} - v^n. \tag{8.14}$$

<u>Aside :</u>

By eliminating $\tilde{\rho}_y^{(1)}$ *from* (8.7) *and* (8.11), *it can be seen that adding the corrector* (8.11) *is equivalent to approximating* (8.5) *by*

$$\frac{r^2\rho_y'}{\Delta t} = -\frac{1}{\delta_\eta r}\left[\frac{1}{\cos\phi}\delta_\lambda\left(\frac{\overline{r^2\rho_y^n\delta_\eta r}^\lambda}{\overline{r}^\lambda}\overline{u}^{\alpha_1}\right) + \frac{1}{\cos\phi}\delta_\phi\left(\frac{\overline{r^2\rho_y^n\delta_\eta r}^\phi}{\overline{r}^\phi}\overline{v}^{\alpha_1}\cos\phi\right) + \delta_\eta\left(\overline{r^2\rho_y^n}^r\,\overline{\dot{\eta}}^{average}\delta_\eta r\right)\right], \tag{8.15}$$

where

$$\rho_y' \equiv \rho_y^{n+1} - \rho_y^n. \tag{8.16}$$

<u>Aside :</u>

Eliminating $\overline{\dot{\eta}}^{average}$ *from* (8.15) *using* (8.12), *gives the following equivalent discretisation of* (8.4) *at interior levels* $k = 3/2,\ 5/2, ...,\ N - 3/2$:

$$\frac{r^2\rho_y'}{\Delta t} = -\frac{1}{\delta_\eta r}\left\{\frac{1}{\cos\phi}\delta_\lambda\left(\frac{\overline{r^2\rho_y^n\delta_\eta r}^\lambda}{\overline{r}^\lambda}\overline{u}^{\alpha_1}\right) + \frac{1}{\cos\phi}\delta_\phi\left(\frac{\overline{r^2\rho_y^n\delta_\eta r}^\phi}{\overline{r}^\phi}\overline{v}^{\alpha_1}\cos\phi\right) - \delta_\eta\left[\overline{r^2\rho_y^n}^r\,\overline{\left(\overline{\frac{\overline{u}^\eta}{\overline{r}^\lambda\cos\phi}\delta_\lambda r}^\lambda + \overline{\frac{\overline{v}^\eta}{\overline{r}^\phi}\delta_\phi r}^\phi\right)}^{\alpha_1}\right] + \delta_\eta\left(\overline{r^2\rho_y^n}^r\,\overline{w}^{\alpha_2}\right)\right\}. \tag{8.17}$$

Aside :

The introduction of different time weightings for the horizontal and vertical pseudo-divergence when discretising (8.1) *should be re-examined. In particular, if the discrete total pseudo-divergence of the flow is identically zero everywhere at each timestep, then the time-averaged discrete total pseudo-divergence would in general only have this property when* $\alpha_1 = \alpha_2$.

The corrector is *implicit.* It couples the continuity equation to the other governing equations and eventually leads to a Helmholtz problem to be solved for the Exner pressure tendency, Π' . Eq. (8.15) is quite close to the target 2-time-level off-centred semi-implicit Eulerian discretisation defined by (8.5). The difference is that the density that multiplies the pseudo-divergence at meshpoints at time $(n+1)\,\Delta t$, is evaluated at meshpoints at time $n\Delta t$ instead of at time $(n+1)\,\Delta t$. This reduces the formal accuracy of the scheme to $O\,(\Delta t)$ even when the scheme is otherwise centred (i.e. even when $\alpha_1 = \alpha_2 = 1\,/2$).

Aside :

It would be possible to use either the discretisation (8.5) *instead of* (8.15)*, or-rewrite* (8.1) *in logarithmic form and then discretise it along the trajectory, at the expense of having to iteratively solve a more implicitly coupled set of equations. This has the advantage of providing a more centred, and therefore formally more accurate, discretisation.*

Aside :

It should be noted that unless $\alpha_1 = \alpha_2$*, the surface boundary condition* $\left.\overline{\dot{\eta}}^{average}\right|_{\eta_0 \equiv 0} = 0$, (8.13) *is not in general (i.e. in the presence of orography with non-zero wind) consistent with the boundary conditions applied elsewhere in the model, that* $\left.\overline{\dot{\eta}}^{n}\right|_{\eta_0 \equiv 0} = \left.\overline{\dot{\eta}}^{n+1}\right|_{\eta_0 \equiv 0} = 0$.

8.3 Polar discretisation

To complete the discretisation of the continuity equation, the definition of $\dot\eta$ and the continuity equation are both integrated over the two polar caps $\left\{0 \le \lambda \le 2\pi; -\pi/2 \equiv \phi_{1/2} \le \phi \le \phi_1\right\}$ and $\left\{0 \le \lambda \le 2\pi; \phi_{M-1} \le \phi \le \phi_{M-1/2} \equiv \pi/2\right\}$.

Evaluation of $\dot\eta$ over the south polar cap

Integrating the vertically-discretised definition (8.2) of $\dot\eta$ over the south polar cap $\left\{0 \le \lambda \le 2\pi; -\pi/2 \equiv \phi_{1/2} \le \phi \le \phi_1\right\}$ gives

$$\begin{aligned}\int_0^{2\pi}\int_{-\frac{\pi}{2}}^{\phi_1}\left[r^2\dot\eta\delta_\eta r\right]\cos\phi d\phi d\lambda &= \int_0^{2\pi}\int_{-\frac{\pi}{2}}^{\phi_1}\left[wr^2\right]\cos\phi d\phi d\lambda \\ &\quad -\int_0^{2\pi}\int_{-\frac{\pi}{2}}^{\phi_1}\left(\frac{\overline{u}^\eta}{r\cos\phi}\frac{\partial r}{\partial\lambda}+\frac{\overline{v}^\eta}{r}\frac{\partial r}{\partial\phi}\right)r^2\cos\phi d\phi d\lambda, \end{aligned} \tag{8.18}$$

where $\phi_1 - \phi_{1/2} = \Delta\phi/2$. Approximating the square-bracketed terms of the first two integrals by their values at the pole, this may be rewritten as

$$\dot\eta_{SP} = \frac{1}{(\delta_\eta r)_{SP}}\left[w_{SP} - \frac{1}{2\pi\left(1-\cos\frac{\Delta\phi}{2}\right)r_{SP}^2}\int_0^{2\pi}\int_{-\frac{\pi}{2}}^{\phi_1}\left(\frac{\overline{u}^\eta}{r\cos\phi}\frac{\partial r}{\partial\lambda}+\frac{\overline{v}^\eta}{r}\frac{\partial r}{\partial\phi}\right)r^2\cos\phi d\phi d\lambda\right], \tag{8.19}$$

where subscript "SP" denotes evaluation at the S. Pole. Using the identity

$$\frac{u}{r\cos\phi}\frac{\partial r}{\partial\lambda}+\frac{v}{r}\frac{\partial r}{\partial\phi} \equiv \frac{1}{\cos\phi}\left[\frac{\partial}{\partial\lambda}\left(r\frac{u}{r}\right)+\frac{\partial}{\partial\phi}\left(r\frac{v}{r}\cos\phi\right)\right] - \frac{r}{\cos\phi}\left[\frac{\partial}{\partial\lambda}\left(\frac{u}{r}\right)+\frac{\partial}{\partial\phi}\left(\frac{v}{r}\cos\phi\right)\right], \tag{8.20}$$

the integral in (8.19) may be rewritten as

$$\begin{aligned}\int_0^{2\pi}\int_{-\frac{\pi}{2}}^{\phi_1}\left(\frac{\overline{u}^\eta}{r\cos\phi}\frac{\partial r}{\partial\lambda}+\frac{\overline{v}^\eta}{r}\frac{\partial r}{\partial\phi}\right)r^2\cos\phi d\phi d\lambda &= \int_0^{2\pi}\int_{-\frac{\pi}{2}}^{\phi_1} r^2\left[\frac{\partial}{\partial\lambda}\left(r\frac{\overline{u}^\eta}{r}\right)+\frac{\partial}{\partial\phi}\left(r\frac{\overline{v}^\eta}{r}\cos\phi\right)\right]d\phi d\lambda \\ &\quad -\int_0^{2\pi}\int_{-\frac{\pi}{2}}^{\phi_1} r^3\left[\frac{\partial}{\partial\lambda}\left(\frac{\overline{u}^\eta}{r}\right)+\frac{\partial}{\partial\phi}\left(\frac{\overline{v}^\eta}{r}\cos\phi\right)\right]d\phi d\lambda \\ &\approx r_{SP}^2\int_0^{2\pi}\int_{-\frac{\pi}{2}}^{\phi_1}\left[\frac{\partial}{\partial\lambda}\left(r\frac{\overline{u}^\eta}{r}\right)+\frac{\partial}{\partial\phi}\left(r\frac{\overline{v}^\eta}{r}\cos\phi\right)\right]d\phi d\lambda \\ &\quad -r_{SP}^3\int_0^{2\pi}\int_{-\frac{\pi}{2}}^{\phi_1}\left[\frac{\partial}{\partial\lambda}\left(\frac{\overline{u}^\eta}{r}\right)+\frac{\partial}{\partial\phi}\left(\frac{\overline{v}^\eta}{r}\cos\phi\right)\right]d\phi d\lambda \\ &= r_{SP}^2\int_0^{2\pi}\int_{-\frac{\pi}{2}}^{\phi_1}\left\{\frac{\partial}{\partial\phi}\left[(r-r_{SP})\frac{\overline{v}^\eta}{r}\cos\phi\right]\right\}d\phi d\lambda \\ &= \cos\phi_1 r_{SP}^2\int_0^{2\pi}\left[(r-r_{SP})\frac{\overline{v}^\eta}{r}\right]\Bigg|_{\phi=\phi_1} d\lambda\end{aligned}$$

$$\approx \frac{\Delta\phi}{2}\cos\phi_1 r_{SP}^2 \Delta\lambda \sum_{i=1}^{L}\left[2\left(\frac{r-r_{SP}}{\Delta\phi}\right)\frac{\overline{v}^{\eta}}{r}\right]_{i-\frac{1}{2},1}, \quad (8.21)$$

where $L = 2\pi/\Delta\lambda$ is the number of gridpoints around a latitude circle. Since r is only carried at scalar points, $r_{i-1/2,1}$ is evaluated in the last line of (8.21) as $\left(\overline{r}^{\phi}\right)_{i-1/2,1} \equiv \left(r_{i-1/2,3/2} + r_{i-1/2,1/2}\right)/2$, and so $2\left[\left(\overline{r}^{\phi} - r_{SP}\right)/\Delta\phi\right]_{i-1/2,1} = \left(r_{i-1/2,3/2} - r_{i-1/2,1/2}\right)/\Delta\phi = \left(\delta_\phi r\right)_{i-1/2,1}$. Thus

$$\int_0^{2\pi}\int_{-\frac{\pi}{2}}^{\phi_1}\left(\frac{\overline{u}^{\eta}}{r\cos\phi}\frac{\partial r}{\partial\lambda} + \frac{\overline{v}^{\eta}}{r}\frac{\partial r}{\partial\phi}\right) r^2\cos\phi\, d\phi\, d\lambda \approx \pi\Delta\phi\cos\phi_1 r_{SP}^2 \frac{1}{L}\sum_{i=1}^{L}\left(\frac{\overline{v}^{\eta}}{\overline{r}^{\phi}}\delta_\phi r\right)_{i-\frac{1}{2},1}. \quad (8.22)$$

Substituting (8.22) into (8.18) then gives

$$\dot{\eta}_{SP} = \frac{1}{\left(\delta_\eta r\right)_{SP}}\left[w_{SP} - \frac{\Delta\phi\sin\frac{\Delta\phi}{2}}{2\left(1-\cos\frac{\Delta\phi}{2}\right)}\frac{1}{L}\sum_{i=1}^{L}\left(\frac{\overline{v}^{\eta}}{\overline{r}^{\phi}}\delta_\phi r\right)_{i-\frac{1}{2},1}\right]. \quad (8.23)$$

Expanding the trigonometric functions in powers of $\Delta\phi$ and neglecting $O\left(\Delta\phi\right)^2$ terms, (8.23) simplifies to

$$\dot{\eta}_{SP} = \frac{1}{\left(\delta_\eta r\right)_{SP}}\left[w_{SP} - \frac{2}{L}\sum_{i=1}^{L}\left(\frac{\overline{v}^{\eta}}{\overline{r}^{\phi}}\delta_\phi r\right)_{i-\frac{1}{2},1}\right]. \quad (8.24)$$

Evaluation of $\dot{\eta}$ over the north polar cap

Similarly, integrating the vertically-discretised definition (8.2) of $\dot{\eta}$ over the north polar cap $\left\{0 \le \lambda \le 2\pi; \phi_{M-1} \le \phi \le \phi_{M-1/2} \equiv \pi/2\right\}$ gives

$$\dot{\eta}_{NP} = \frac{1}{\left(\delta_\eta r\right)_{NP}}\left[w_{NP} - \frac{2}{L}\sum_{i=1}^{L}\left(\frac{\overline{v}^{\eta}}{\overline{r}^{\phi}}\delta_\phi r\right)_{i-\frac{1}{2},M-1}\right]. \quad (8.25)$$

Aside :

The sign for the sum in (8.25) *is the same as that in* (8.24)*. This is because although the direction of v relative to the appropriate pole changes sign, this is compensated by a corresponding sign change in $\delta_\phi r$.*

Integration of the continuity equation over the south polar cap

Integrating (8.15) with horizontal discretisation removed, or equivalently (8.1) after time discretisation and vertical discretisation, over the south polar cap $\left\{0 \leq \lambda \leq 2\pi; -\pi/2 \equiv \phi_{1/2} \leq \phi \leq \phi_1\right\}$ gives:

$$\begin{aligned}\int_{-\frac{\pi}{2}}^{\phi_1}\left[\int_0^{2\pi}\frac{F'}{\Delta t}d\lambda\right]\cos\phi d\phi &= -\int_{-\frac{\pi}{2}}^{\phi_1}\left\{\int_0^{2\pi}\left[\frac{\partial}{\partial\lambda}\left(\frac{F^n\overline{u}^{\alpha_1}}{r}\right)+\frac{\partial}{\partial\phi}\left(\frac{F^n\overline{v}^{\alpha_1}\cos\phi}{r}\right)\right]d\lambda\right\}d\phi \\ &\quad -\int_{-\frac{\pi}{2}}^{\phi_1}\left\{\int_0^{2\pi}\delta_\eta\left(\overline{r^2\rho_y^n}^r\,\overline{\dot\eta}^{average}\delta_\eta r\right)d\lambda\right\}\cos\phi d\phi, \qquad (8.26)\end{aligned}$$

where

$$F^n \equiv r^2\rho_y^n\delta_\eta r, F' \equiv F^{n+1}-F^n \equiv r^2\delta_\eta r\left(\rho_y^{n+1}-\rho_y^{n+1}\right), \qquad (8.27)$$

$$\overline{\dot\eta}^{average} = \frac{1}{\delta_\eta r}\left[\overline{w}^{\alpha_2}-\overline{\left(\frac{\overline{u}^\eta}{r\cos\phi}\delta_\lambda r+\frac{\overline{v}^\eta}{r}\delta_\phi r\right)}^{\alpha_1}\right], \qquad (8.28)$$

and $\phi_1 - \phi_{1/2} = \Delta\phi/2$. Note that the usual contribution of r^2 to the area weighting is not appropriate here since it was already effectively introduced in the manipulation of the continuity equation, given in Section 2.2, to derive (8.1).

Approximating F' in the left-hand-side integral by its value at the pole gives

$$I_1 \equiv \int_{-\frac{\pi}{2}}^{\phi_1}\left[\int_0^{2\pi}\frac{F'}{\Delta t}d\lambda\right]\cos\phi d\phi \approx \frac{F'_{SP}}{\Delta t}\int_0^{2\pi}\int_{-\frac{\pi}{2}}^{\phi_1}\cos\phi d\phi d\lambda, \qquad (8.29)$$

where subscript "SP" denotes evaluation at the S. Pole. Now $\int_0^{2\pi}\int_{-\frac{\pi}{2}}^{\phi_1}\cos\phi d\phi d\lambda$ is the area of a spherical cap of a sphere of unit radius. Analytically this is equal to $2\pi\left(1+\sin\phi_1\right)$. In the New Dynamics however, the area of this spherical cap is approximated by the area of a *plane* circle of radius $\Delta\phi/2$, i.e. by $\pi\left(\Delta\phi\right)^2/4$. This is an $O\left(\Delta\phi^2\right)$-accurate approximation to the exact *spherical* area, and it leads to the discretisation

$$I_1 \equiv \int_{-\frac{\pi}{2}}^{\phi_1}\left[\int_0^{2\pi}\frac{F'}{\Delta t}d\lambda\right]\cos\phi d\phi \approx 2\pi b\frac{F'_{SP}}{\Delta t}, \qquad (8.30)$$

where $b = \left(\Delta\phi\right)^2/8$.

The first right-hand-side integral is discretised as

$$I_2 \equiv \int_{-\frac{\pi}{2}}^{\phi_1}\left\{\int_0^{2\pi}\left[\frac{\partial}{\partial\lambda}\left(\frac{F^n\overline{u}^{\alpha_1}}{r}\right)+\frac{\partial}{\partial\phi}\left(\frac{F^n\overline{v}^{\alpha_1}\cos\phi}{r}\right)\right]d\lambda\right\}d\phi$$

$$
\begin{aligned}
&= \int_0^{2\pi}\left[\int_{-\frac{\pi}{2}}^{\phi_1}\frac{\partial}{\partial\phi}\left(\frac{F^n\overline{v}^{\alpha_1}\cos\phi}{r}\right)d\phi\right]d\lambda \\
&= \int_0^{2\pi}\left[\left(\frac{F^n\overline{v}^{\alpha_1}\cos\phi}{r}\right)\bigg|_{(\lambda,\phi_1)} - \left(\frac{F^n\overline{v}^{\alpha_1}\cos\phi}{r}\right)\bigg|_{\left(\lambda,-\frac{\pi}{2}\right)}\right]d\lambda \\
&= \cos(\phi_1)\int_0^{2\pi}\left(\frac{F^n\overline{v}^{\alpha_1}}{r}\right)\bigg|_{(\lambda,\phi_1)}d\lambda \\
&\approx \cos(\phi_1)\frac{2\pi}{L}\sum_{i=1}^{L}\left(\frac{F^n\overline{v}^{\alpha_1}}{r}\right)_{i-\frac{1}{2},1},
\end{aligned}
\tag{8.31}
$$

where $L = 2\pi/\Delta\lambda$ is the number of gridpoints around a latitude circle, and $F_{SP} = (F)_{\frac{1}{2},\frac{1}{2}} = (F)_{\frac{3}{2},\frac{1}{2}} = (F)_{\frac{5}{2},\frac{1}{2}} ... = (F)_{L-\frac{1}{2},\frac{1}{2}}$. Since r and F are only carried at scalar points, $r_{i-1/2,1}$ and $F_{i-1/2,1}$ are evaluated in the last line of (8.31) as $\overline{r}^{\phi}_{i-\frac{1}{2},1}$ and $\overline{F}^{\phi}_{i-\frac{1}{2},1}$, where

$$
\overline{F}^{\phi}_{i-\frac{1}{2},1} = \frac{1}{2}\left(F_{i-\frac{1}{2},\frac{1}{2}} + F_{i-\frac{1}{2},\frac{3}{2}}\right),
\tag{8.32}
$$

Thus

$$
\begin{aligned}
I_2 &\equiv \int_{-\frac{\pi}{2}}^{\phi_1}\left\{\int_0^{2\pi}\left[\frac{\partial}{\partial\lambda}\left(\frac{F^n\overline{u}^{\alpha_1}}{r}\right) + \frac{\partial}{\partial\phi}\left(\frac{F^n\overline{v}^{\alpha_1}\cos\phi}{r}\right)\right]d\lambda\right\}d\phi \\
&= 2\pi\cos(\phi_1)\frac{1}{L}\sum_{i=1}^{L}\left(\frac{\overline{F^n}^{\phi}\overline{v}^{\alpha_1}}{\overline{r}^{\phi}}\right)_{i-\frac{1}{2},1}.
\end{aligned}
\tag{8.33}
$$

Similarly

$$
I_3 \equiv \int_{-\frac{\pi}{2}}^{\phi_1}\left\{\int_0^{2\pi}\delta_\eta\left(\overline{r^2\rho_y^n}^{r}\,\overline{\dot{\eta}}^{average}\delta_\eta r\right)d\lambda\right\}\cos\phi d\phi \approx 2\pi b\delta_\eta\left[\left(\overline{r^2\rho_y^n}^{r}\right)_{SP}\overline{\dot{\eta}_{SP}}^{average}(\delta_\eta r)_{SP}\right],
\tag{8.34}
$$

where

$$
\overline{\dot{\eta}_{SP}}^{average} = \frac{1}{(\delta_\eta r)_{SP}}\left[\overline{w_{SP}}^{\alpha_2} - \frac{2}{L}\sum_{i=1}^{L}\left(\overline{\frac{\overline{v}^{\eta}}{\overline{r}^{\phi}}\delta_\phi r}^{\alpha_1}\right)_{i-\frac{1}{2},1}\right],
\tag{8.35}
$$

is obtained from (8.12) using the procedure of the immediately-preceding subsection, and $b = (\Delta\phi)^2/8$ again corresponds to approximating the area of a spherical cap by a plane circle.

Putting the above results together, the discretisation of the continuity equation over the south polar cap is:

$$
\frac{F'_{SP}}{\Delta t} = -\frac{\cos(\phi_1)}{b}\frac{1}{L}\sum_{i=1}^{L}\left(\frac{\overline{F^n}^{\phi}\overline{v}^{\alpha_1}}{\overline{r}^{\phi}}\right)_{i-\frac{1}{2},1} - \delta_\eta\left[\left(\overline{r^2\rho_y^n}^{r}\right)_{SP}\overline{\dot{\eta}_{SP}}^{average}(\delta_\eta r)_{SP}\right],
\tag{8.36}
$$

where $F'_{SP} = (F')_{\frac{1}{2},\frac{1}{2}} = (F')_{\frac{3}{2},\frac{1}{2}} = (F')_{\frac{5}{2},\frac{1}{2}} = ... = (F')_{L-\frac{1}{2},\frac{1}{2}}$.

Integration of the continuity equation over the north polar cap

Similarly, integrating (8.15) with horizontal discretisation removed, or equivalently (8.1) after time discretisation and vertical discretisation, over the north polar cap $\left\{0 \leq \lambda \leq 2\pi; \phi_{M-1} \leq \phi \leq \phi_{M-1/2} \equiv \pi/2\right\}$ gives:

$$\begin{aligned}\int_{\phi_{M-1}}^{\frac{\pi}{2}} \left[\int_0^{2\pi} \frac{F'}{\Delta t} d\lambda\right] \cos\phi d\phi &= -\int_{\phi_{M-1}}^{\frac{\pi}{2}} \left\{\int_0^{2\pi} \left[\frac{\partial}{\partial\lambda}\left(\frac{F^n \overline{u}^{\alpha_1}}{r}\right) + \frac{\partial}{\partial\phi}\left(\frac{F^n \overline{v}^{\alpha_1}\cos\phi}{r}\right)\right] d\lambda\right\} d\phi \\ &\quad -\int_{\phi_{M-1}}^{\frac{\pi}{2}} \left\{\int_0^{2\pi} \delta_\eta \left(\overline{r^2\rho_y^n}^r \overline{\dot{\eta}}^{average} \delta_\eta r\right) d\lambda\right\} \cos\phi d\phi, \end{aligned} \tag{8.37}$$

where

$$F^n \equiv r^2 \rho_y^n \delta_\eta r, F' \equiv F^{n+1} - F^n \equiv r^2 \delta_\eta r \left(\rho_y^{n+1} - \rho_y^n\right), \tag{8.38}$$

$$\overline{\dot{\eta}}^{average} = \frac{1}{\delta_\eta r}\left[\overline{w}^{\alpha_2} - \overline{\left(\frac{\overline{u}^\eta}{r\cos\phi}\delta_\lambda r + \frac{\overline{v}^\eta}{r}\delta_\phi r\right)}^{\alpha_1}\right], \tag{8.39}$$

and $\pi/2 - \phi_{M-1} = \Delta\phi/2$.

Following the same procedure as for the south polar cap, the only real difference being the different limits of integration for ϕ, leads to the following discretisation of the continuity equation over the north polar cap:

$$\frac{F'_{NP}}{\Delta t} = \frac{\cos\left(\phi_{M-1}\right)}{b}\frac{1}{L}\sum_{i=1}^{L}\left(\frac{\overline{F^n}^\phi \overline{v}^{\alpha_1}}{\overline{r}^\phi}\right)_{i-\frac{1}{2},M-1} - \delta_\eta\left[\left(\overline{r^2\rho_y^n}^r\right)_{NP} \overline{\dot{\eta}_{NP}}^{average}\left(\delta_\eta r\right)_{NP}\right], \tag{8.40}$$

where

$$\overline{\dot{\eta}_{NP}}^{average} = \frac{1}{\left(\delta_\eta r\right)_{NP}}\left[\overline{w_{NP}}^{\alpha_2} - \frac{2}{L}\sum_{i=1}^{L}\left(\overline{\frac{\overline{v}^\eta}{\overline{r}^\phi}\delta_\phi r}^{\alpha_1}\right)_{i-\frac{1}{2},M-1}\right], \tag{8.41}$$

$F'_{NP} = (F')_{\frac{1}{2},M-\frac{1}{2}} = (F')_{\frac{3}{2},M-\frac{1}{2}} = (F')_{\frac{5}{2},M-\frac{1}{2}} ... = (F')_{L-\frac{1}{2},M-\frac{1}{2}}$, subscript "$NP$" denotes evaluation at the N. Pole, and $b = (\Delta\phi)^2/8$.

Aside :

The sign of the the first right-hand-side term in (8.40) *is the opposite of the corresponding term in* (8.36) - *this is due to the different limits of integration for* ϕ.

8.4 Dry mass conservation

Non polar-cap contributions

Multiplying (8.15) through by $\cos\phi\delta_\eta r$, the discretised continuity equation, away from the polar caps, at each vertical level (1/2, 3/2,..., $N-1/2$) may be rewritten as

$$\frac{F'\cos\phi}{\Delta t} = -\delta_\lambda\left(\frac{\overline{F^n}^\lambda}{\overline{r}^\lambda}\overline{u}^{\alpha_1}\right) - \delta_\phi\left(\frac{\overline{F^n}^\phi}{\overline{r}^\phi}\overline{v}^{\alpha_1}\cos\phi\right) - \delta_\eta\left(\overline{r^2\rho_y^n}^r\overline{\dot{\eta}}^{average}\cos\phi\delta_\eta r\right), \quad (8.42)$$

where

$$F^n \equiv r^2\rho_y^n\delta_\eta r, F' \equiv F^{n+1} - F^n \equiv r^2\delta_\eta r\left(\rho_y^{n+1} - \rho_y^n\right), \quad (8.43)$$

$$\overline{\dot{\eta}}^{average} = \frac{1}{\delta_\eta r}\left[\overline{w}^{\alpha_2} - \overline{\left(\overline{\frac{\overline{u}^\eta}{\overline{r}^\lambda\cos\phi}\delta_\lambda r}^\lambda + \overline{\frac{\overline{v}^\eta}{\overline{r}^\phi}\delta_\phi r}^\phi\right)}^{\alpha_1}\right]. \quad (8.44)$$

Multiplying (8.42) by the layer thicknesses $\Delta\eta_{k-\frac{1}{2}} \equiv \eta_k - \eta_{k-1}$, summing over the N layers $[\eta_{k-1}, \eta_k], k = 1, ..., N$, and applying the no-normal flow boundary conditions (8.13) on $\overline{\dot{\eta}}^{average}$, then yields

$$\sum_{k=1}^{N}\left(\frac{F'\cos\phi\Delta\eta}{\Delta t}\right)_{i-\frac{1}{2},j-\frac{1}{2},k-\frac{1}{2}} = -\sum_{k=1}^{N}\Delta\eta_{k-\frac{1}{2}}\left[\delta_\lambda\left(\frac{\overline{F^n}^\lambda}{\overline{r}^\lambda}\overline{u}^{\alpha_1}\right) + \delta_\phi\left(\frac{\overline{F^n}^\phi}{\overline{r}^\phi}\overline{v}^{\alpha_1}\cos\phi\right)\right]_{i-\frac{1}{2},j-\frac{1}{2},k-\frac{1}{2}}, \quad (8.45)$$

for $i = 1, 2, ..., L$ and $j = 2, 3, ..., M-1$, where

$$\left(\overline{F}^\lambda\right)_{i,j-\frac{1}{2},k-\frac{1}{2}} = \frac{1}{2}\left(F_{i+\frac{1}{2},j-\frac{1}{2},k-\frac{1}{2}} + F_{i-\frac{1}{2},j-\frac{1}{2},k-\frac{1}{2}}\right), \quad (8.46)$$

$$\left(\overline{F}^\phi\right)_{i-\frac{1}{2},j,k-\frac{1}{2}} = \frac{1}{2}\left(F_{i-\frac{1}{2},j+\frac{1}{2},k-\frac{1}{2}} + F_{i-\frac{1}{2},j-\frac{1}{2},k-\frac{1}{2}}\right). \quad (8.47)$$

Multiplying by $\Delta\lambda\Delta\phi$ and summing over all control volumes $[\lambda_{i-1}, \lambda_i] \otimes [\phi_{j-1}, \phi_j]$, with the exception of the two polar caps, gives:

$$\begin{aligned}
&\sum_{i=1}^{L}\sum_{j=2}^{M-1}\sum_{k=1}^{N}\left(\frac{F'\cos\phi\Delta\lambda\Delta\phi\Delta\eta}{\Delta t}\right)_{i-\frac{1}{2},j-\frac{1}{2},k-\frac{1}{2}} \\
= & -\sum_{k=1}^{N}\Delta\eta_{k-\frac{1}{2}}\sum_{i=1}^{L}\Delta\lambda\sum_{j=2}^{M-1}\Delta\phi\left[\delta_\lambda\left(\frac{\overline{F^n}^\lambda}{\overline{r}^\lambda}\overline{u}^{\alpha_1}\right) + \delta_\phi\left(\frac{\overline{F^n}^\phi}{\overline{r}^\phi}\overline{v}^{\alpha_1}\cos\phi\right)\right]_{i-\frac{1}{2},j-\frac{1}{2},k-\frac{1}{2}} \\
= & -\sum_{k=1}^{N}\Delta\eta_{k-\frac{1}{2}}\sum_{i=1}^{L}\Delta\lambda\sum_{j=2}^{M-1}\left[\Delta\phi\delta_\phi\left(\frac{\overline{F^n}^\phi}{\overline{r}^\phi}\overline{v}^{\alpha_1}\cos\phi\right)\right]_{i-\frac{1}{2},j-\frac{1}{2},k-\frac{1}{2}} \\
= & -\sum_{k=1}^{N}\Delta\eta_{k-\frac{1}{2}}\sum_{i=1}^{L}\Delta\lambda\left[\left(\frac{\overline{F^n}^\phi}{\overline{r}^\phi}\overline{v}^{\alpha_1}\cos\phi\right)_{i-\frac{1}{2},M-1,k-\frac{1}{2}} - \left(\frac{\overline{F^n}^\phi}{\overline{r}^\phi}\overline{v}^{\alpha_1}\cos\phi\right)_{i-\frac{1}{2},1,k-\frac{1}{2}}\right]
\end{aligned} \quad (8.48)$$

South polar-cap contribution

Multiplying (8.36) by $\pi\left(\Delta\phi/2\right)^2\Delta\eta_{k-\frac{1}{2}}$, summing over the N layers $\left[\eta_{k-1},\eta_k\right], k=1,...,N$, and applying the no-normal flow boundary conditions (8.13) on $\overline{\dot{\eta}}^{average}$, yields

$$\sum_{k=1}^{N}\left[\frac{F'_{SP}}{\Delta t}\pi\left(\frac{\Delta\phi}{2}\right)^2\Delta\eta\right]_{k-\frac{1}{2}} = -\sum_{k=1}^{N}\Delta\eta_{k-\frac{1}{2}}\sum_{i=1}^{L}\Delta\lambda\left(\frac{\overline{F^n}^{\phi}}{\overline{r}^{\phi}}\overline{v}^{\alpha_1}\cos\phi\right)_{i-\frac{1}{2},1,k-\frac{1}{2}}, \tag{8.49}$$

where $\Delta\lambda=2\pi/L$ and $\Delta\eta_{k-\frac{1}{2}}\equiv\eta_k-\eta_{k-1}$ are the layer thicknesses.

North polar-cap contribution

Multiplying (8.40) by $\pi\left(\Delta\phi/2\right)^2\Delta\eta_{k-\frac{1}{2}}$, summing over the N layers $\left[\eta_{k-1},\eta_k\right], k=1,...,N$, and applying the no-normal flow boundary conditions (8.13) on $\overline{\dot{\eta}}^{average}$, yields

$$\sum_{k=1}^{N}\left[\frac{F'_{NP}}{\Delta t}\pi\left(\frac{\Delta\phi}{2}\right)^2\Delta\eta\right]_{k-\frac{1}{2}} = \sum_{k=1}^{N}\Delta\eta_{k-\frac{1}{2}}\sum_{i=1}^{L}\Delta\lambda\left(\frac{\overline{F^n}^{\phi}}{\overline{r}^{\phi}}\overline{v}^{\alpha_1}\cos\phi\right)_{i-\frac{1}{2},M-1,k-\frac{1}{2}}. \tag{8.50}$$

Summation of all contributions

Summing (8.48)-(8.50), i.e. summing all the dry mass contributions, finally gives

$$\sum_{k=1}^{N}\left(\frac{F'_{SP}+F'_{NP}}{\Delta t}\right)\pi\left(\frac{\Delta\phi}{2}\right)^2\Delta\eta_{k-\frac{1}{2}}+\sum_{i=1}^{L}\sum_{j=2}^{M-1}\sum_{k=1}^{N}\left(\frac{F'\cos\phi\Delta\lambda\Delta\phi\Delta\eta}{\Delta t}\right)_{i-\frac{1}{2},j-\frac{1}{2},k-\frac{1}{2}}=0. \tag{8.51}$$

This equation is the discrete analogue of the continuous conservation law

$$\frac{\partial}{\partial t}\int_0^1\int_{-\frac{\pi}{2}}^{\frac{\pi}{2}}\int_0^{2\pi}F\cos\phi d\lambda d\phi d\eta\equiv\frac{\partial}{\partial t}\int_{r_S}^{r_T}\int_{-\frac{\pi}{2}}^{\frac{\pi}{2}}\int_0^{2\pi}\rho_y r^2\cos\phi d\lambda d\phi dr=0, \tag{8.52}$$

where $r=r_S\left(\lambda,\phi\right)$ is the Earth's surface and $r=r_T$=constant is the model top.

Aside :

The Eulerian discretisation of the continuity equation implicitly defines a measure (cf (8.51) *with* (8.52)*) for the discrete evaluation of* $\int_{r_S}^{r_T}\int_{-\frac{\pi}{2}}^{\frac{\pi}{2}}\int_0^{2\pi}\rho_y r^2\cos\phi d\lambda d\phi dr$. *For consistency, this suggests that the same measure be used to evaluate the related analytically-conserved quantities (see Section 10)* $\int_{r_S}^{r_T}\int_{-\frac{\pi}{2}}^{\frac{\pi}{2}}\int_0^{2\pi}\rho_y m_X r^2\cos\phi d\lambda d\phi dr$, *where* $m_X=m_v$, m_{cl} *or* m_{cf}.

Aside :

One might hope that if ρ_y were unity and r_S constant, then the discrete sum over the domain, defined by (8.51)*, would lead to the exact result $4\pi\left(r_T^3 - r_S^3\right)/3$, the volume of a spherical shell confined by the spheres $r = r_S$ and $r = r_T$. This however is not the case since*

$$2\sum_{k=1}^{N}\left[r^2\pi\left(\frac{\Delta\phi}{2}\right)^2\Delta r\right]_{k-\frac{1}{2}} + \sum_{i=1}^{L}\sum_{j=2}^{M-1}\sum_{k=1}^{N}\left(r^2\cos\phi\Delta\lambda\Delta\phi\Delta r\right)_{i-\frac{1}{2},j-\frac{1}{2},k-\frac{1}{2}} \neq 4\pi\frac{\left(r_T^3 - r_S^3\right)}{3}. \tag{8.53}$$

It is not so for two reasons:

$$(1) \quad : \quad \left(\frac{\Delta\phi}{2}\right)^2 + \sum_{j=2}^{M-1}\left(\cos\phi\Delta\phi\right)_{j-\frac{1}{2}} \neq 2, \tag{8.54}$$

$$(2) \quad : \quad \sum_{k=1}^{N}\left(r^2\Delta r\right)_{k-\frac{1}{2}} \neq \frac{\left(r_T^3 - r_S^3\right)}{3}. \tag{8.55}$$

The first is associated with the horizontal discretisation. If the continuity equation were rewritten in terms of the variable $\mu = \sin\phi$, i.e. as

$$\frac{\partial F}{\partial t} + \frac{1}{\sqrt{1-\mu^2}}\frac{\partial}{\partial\lambda}\left(Fu\right) + \frac{\partial}{\partial\mu}\left(Fv\sqrt{1-\mu^2}\right) + \frac{\partial}{\partial\eta}\left(F\dot{\eta}\right) = 0, \tag{8.56}$$

where $F \equiv r^2\rho_y\delta_\eta r$, and the area element rewritten as $r^2\Delta\lambda\Delta\mu_{j-\frac{1}{2}}$, instead of as $r^2\cos\phi_{j-\frac{1}{2}}\Delta\lambda\Delta\phi$, then not only would all the horizontal flux terms still sum to zero, but the implicit discrete measure for $\int_0^{2\pi}\int_{-\frac{\pi}{2}}^{\frac{\pi}{2}} F d\mu d\lambda$ would also give the exact result 4π (the area of a unit circle) for F equal to unity.

The second is associated with the vertical discretisation. If F were discretised as $F \equiv \rho_y\delta_\eta\left(r^3/3\right)$ instead of as $F \equiv r^2\rho_y\delta_\eta r$, and the volume element further rewritten as $\Delta\lambda\Delta\mu_{j-\frac{1}{2}}\Delta\left(r^3/3\right)_{k-\frac{1}{2}}$ instead of as $\Delta\lambda\Delta\mu_{j-\frac{1}{2}}\left(r^2\Delta r\right)_{k-\frac{1}{2}}$, then not only would the vertical flux terms of the discrete continuity equation still sum to zero, but the implicit discrete measure for $\int_{r_S}^{r_T} Fr^2 dr$ would also give the exact result $\left(r_T^3 - r_S^3\right)/3$ for F equal to unity. Changing the discrete definition of the volume element for the continuity equation might however have consistency ramifications elsewhere in the model formulation.

9 Discretisation of the thermodynamic equation

9.1 Rewriting the continuous form

The forced thermodynamic equation, written in invariant form, is:

$$\frac{D\theta}{Dt} = S^\theta. \tag{9.1}$$

In the r and η coordinate systems, this respectively becomes:

$$\left(\frac{\partial\theta}{\partial t}\right)_r + \frac{u}{r\cos\phi}\left(\frac{\partial\theta}{\partial\lambda}\right)_r + \frac{v}{r}\left(\frac{\partial\theta}{\partial\phi}\right)_r + w\frac{\partial\theta}{\partial r} = S^\theta, \tag{9.2}$$

$$\left(\frac{\partial\theta}{\partial t}\right)_\eta + \frac{u}{r\cos\phi}\left(\frac{\partial\theta}{\partial\lambda}\right)_\eta + \frac{v}{r}\left(\frac{\partial\theta}{\partial\phi}\right)_\eta + \dot\eta\frac{\partial\theta}{\partial\eta} = S^\theta, \tag{9.3}$$

where $(\,)_r$ and $(\,)_\eta$ denote differentiation whilst r and η are respectively held fixed.

The following transformation relations hold between the r and η coordinate systems:

$$\left(\frac{\partial}{\partial t}\right)_\eta = \left(\frac{\partial}{\partial t}\right)_r, \tag{9.4}$$

$$\left(\frac{\partial}{\partial s}\right)_\eta = \left(\frac{\partial}{\partial s}\right)_r + \left(\frac{\partial\eta}{\partial r}\right)\left(\frac{\partial r}{\partial s}\right)_\eta\frac{\partial}{\partial\eta}, \tag{9.5}$$

$$\frac{\partial}{\partial\eta} = \frac{\partial r}{\partial\eta}\frac{\partial}{\partial r}, \tag{9.6}$$

where $s = \lambda$ or ϕ.

Aside :

Note that whilst constant-r and constant-η surfaces coincide in the absence of orography, these surfaces are very different in its presence and mutually intersect. Note also that it is assumed that the lid is rigid, otherwise there would be an additional contribution

$$\left(\frac{\partial r}{\partial t}\right)_\eta\left(\frac{\partial\eta}{\partial r}\right)\frac{\partial}{\partial\eta}, \tag{9.7}$$

to the right-hand side of (9.4).

Let the departure point be located at (λ_d, ϕ_d, r_d) of the r-coordinate system, with the corresponding location in the η-coordinate system being denoted by $(\lambda_d, \phi_d, \eta_d)$. Also let the vertical projection of this departure point onto the nearest model level be located at $(\lambda_d, \phi_d, r_{dl})$ of the r-coordinate system, corresponding to $(\lambda_d, \phi_d, \eta_{dl})$ of the η-coordinate system. Thus the coordinates of the departure point and its vertical projection onto the nearest model level are identical in the horizontal, and only differ in the vertical.

The vertical component of the velocity required to move a parcel of air in one timestep from the vertical projection of the departure point $(\lambda_d, \phi_d, r_{dl})$ to the arrival point (λ_a, ϕ_a, r_a) is

$$w^* = \frac{(r_a - r_{dl})}{\Delta t}. \tag{9.8}$$

Note however that if $r_d < r\,(\lambda_d, \phi_d, \eta = \eta_1)$, i.e. the departure point is located below $\eta = \eta_1$, then w^* is set to its value at the arrival point, i.e. $w^* = w_a$. The rationale for this is not obvious. Eq. (9.2) can be rewritten as

$$\left(\frac{\partial \theta}{\partial t}\right)_r + \frac{u}{r\cos\phi}\left(\frac{\partial \theta}{\partial \lambda}\right)_r + \frac{v}{r}\left(\frac{\partial \theta}{\partial \phi}\right)_r + w^*\frac{\partial \theta}{\partial r} = -\left(w - w^*\right)\frac{\partial \theta}{\partial r} + S^\theta. \tag{9.9}$$

This can also be rewritten as

$$\frac{D^*\theta}{Dt} = -\left(w - w^*\right)\frac{\partial \theta}{\partial r} + S^\theta = -\left(w - w^*\right)\frac{\partial \eta}{\partial r}\frac{\partial \theta}{\partial \eta} + S^\theta, \tag{9.10}$$

where

$$\begin{aligned}\frac{D^*\theta}{Dt} &\equiv \left(\frac{\partial \theta}{\partial t}\right)_r + \frac{u}{r\cos\phi}\left(\frac{\partial \theta}{\partial \lambda}\right)_r + \frac{v}{r}\left(\frac{\partial \theta}{\partial \phi}\right)_r + w^*\frac{\partial \theta}{\partial r} \\ &\equiv \left(\frac{\partial \theta}{\partial t}\right)_\eta + \frac{u}{r\cos\phi}\left(\frac{\partial \theta}{\partial \lambda}\right)_\eta + \frac{v}{r}\left(\frac{\partial \theta}{\partial \phi}\right)_\eta + \dot{\eta}^*\frac{\partial \theta}{\partial \eta}.\end{aligned} \tag{9.11}$$

In (9.11)

$$\dot{\eta}^* = \frac{(\eta_a - \eta_{dl})}{\Delta t}, \tag{9.12}$$

corresponds to w^* in r-coordinates, and it is the vertical component of the velocity in η-coordinates required to move a parcel of air in one timestep from the vertical projection $(\lambda_d, \phi_d, \eta_{dl})$ of the departure point $(\lambda_d, \phi_d, \eta_d)$, to the arrival point $(\lambda_a, \phi_a, \eta_a)$.

Aside :

An obvious question is, why rewrite the thermodynamic equation in terms of a residual vertical velocity, rather than simply discretising it directly in its 3-d form (9.1)*? The answer is that this would lead to an unstable scheme.*

9.2 Target discretisation

If (9.10) were to be discretised using a 2-time-level off-centred semi-implicit semi-Lagrangian scheme, as outlined in Section 5, then at θ gridpoints this would give the approximation:

$$\begin{aligned} \frac{\theta^{n+1}-\theta^n_{dl}}{\Delta t} &= -\alpha_2\left[\left(w-w^*\right)\delta_{2r}\theta\right]^{n+1}-\left(1-\alpha_2\right)\left[\left(w-w^*\right)\delta_{2r}\theta\right]^n_{dl} \\ &\quad +\alpha_p\left[S^\theta\right]^{n+1}+\left(1-\alpha_p\right)\left[S^\theta\right]^n_d, \end{aligned} \tag{9.13}$$

where

$$\delta_{2r}F_k \equiv \frac{F\left(r_{k+1}\right)-F\left(r_{k-1}\right)}{r_{k+1}-r_{k-1}}. \tag{9.14}$$

However this is not what is presently done, principally because of the complexity associated with an off-centred semi-implicit treatment of both the residual vertical advection, specifically the first term on the r.h.s. of (9.13), and the forcing, or "physics", term, S^θ. This motivated the development of the following predictor-corrector discretisation.

<u>Aside :</u>

Another obvious question is, why discretise the thermodynamic equation in r coordinates rather than in η coordinates? The answer is not obvious, particularly given the statement in WP154 that "... the vertical advection equation at the arrival point is explicit and is not stable if the thickness of the model layer at the arrival point is less than one half that at the departure point", which apparently led to the strategy of limiting the net vertical velocity $(w-w^*)$ at the arrival point so that it does not exceed the vertical CFL condition. This issue is worth revisiting.

9.3 Predictor-corrector discretisation at levels $k = 1, 2, ..., N-1$

For the θ points of the Arakawa C grid the discretisation of the thermodynamic equation (9.10) is comprised of the following steps:

- **Limiter**

  The residual vertical windspeed $(w-w^*)$ used for vertical advection is first limited such that

$$\left|\frac{\left(w-w^*\right)\big|_{\eta_1}\Delta t}{\left(r\big|_{\eta_2}-r\big|_{\eta_1}\right)}\right| \leq 1, \tag{9.15}$$

$$\left| \frac{(w - w^*)|_{\eta_k} \Delta t}{r|_{\eta_{k+1}} - r|_{\eta_{k-1}}} \right| \leq \frac{1}{2}, \quad k = 2, 3, ..., N - 1. \tag{9.16}$$

Aside :

> *The reason for the application of this limiter is not evident but, according to WP 154, it enhances the stability of the algorithm. It appears that this limiter is most likely to be activated near the ground over steep slopes.*

- **Predictor**

Let $\tilde{\theta}^{(1)}$ be a predictor for θ^{n+1}. The basis for this predictor is first to neglect the forcing term, S^θ, and then to replace all the terms evaluated at meshpoints at time $(n + 1)\,\Delta t$ in (9.13) by their values at the same meshpoints but at time $n\Delta t$. Thus:

$$\frac{\tilde{\theta}^{(1)} - \theta^n_{dl}}{\Delta t} = -\alpha_2 \left[(w - w^*)\, \delta_{2r}\theta\right]^n - (1 - \alpha_2) \left[(w - w^*)\, \delta_{2r}\theta\right]^n_{dl}, \tag{9.17}$$

where $(w - w^*)$ is the value of $(w - w^*)$ after being limited as described above. In (9.17), $(w - w^*)\, \delta_{2r}\theta$ is computed as:

$$\left[(w - w^*)\, \delta_{2r}\theta\right]|_{\eta_1} = (w - w^*)|_{\eta_1} \left(\frac{\theta|_{\eta_2} - \theta|_{\eta_1}}{r|_{\eta_2} - r|_{\eta_1}} \right), \tag{9.18}$$

$$\left[(w - w^*)\, \delta_{2r}\theta\right]|_{\eta_k} = (w - w^*)|_{\eta_k} \left(\frac{\theta|_{\eta_{k+1}} - \theta|_{\eta_{k-1}}}{r|_{\eta_{k+1}} - r|_{\eta_{k-1}}} \right), \quad k = 2, 3, ..., N - 1. \tag{9.19}$$

These predictor equations can be solved explicitly for $\tilde{\theta}^{(1)}$.

Aside :

> *Consideration should be given to using the value of θ at level $k = 0$ when computing $(w - w^*)\, \delta_{2r}\theta$ at level $k = 1$. This means prognostically carrying θ at level $k = 0$.*

- **1st "Dynamics" Corrector**

Let $\tilde{\theta}^{(2)}$ be a 2nd dynamics predictor for θ^{n+1}. This can be written as the sum of the (1st) predictor $\tilde{\theta}^{(1)}$ plus a 1st dynamics corrector $\left(\tilde{\theta}^{(2)} - \tilde{\theta}^{(1)}\right)$, i.e. as

$$\tilde{\theta}^{(2)} = \tilde{\theta}^{(1)} + \left(\tilde{\theta}^{(2)} - \tilde{\theta}^{(1)}\right). \tag{9.20}$$

This 1st (explicit) dynamics corrector is defined as

$$\left(\tilde{\theta}^{(2)} - \tilde{\theta}^{(1)}\right) = -\alpha_2 \Delta t \left(w^n - w^*\right) \delta_{2r} \left(\tilde{\theta}^{(1)} - \theta^n\right), \tag{9.21}$$

where $\left(w^n - w^*\right) \delta_{2r} \left(\tilde{\theta}^{(1)} - \theta^n\right)$ is computed in the same way as for $\left(w - w^*\right) \delta_{2r}\theta$ as described above.

__**Aside :**__

Adding the dynamics corrector (9.21) *is equivalent to replacing* θ^n *where it appears in the 1st square-bracketed term on the right-hand side of* (9.17) *by the predictor* $\tilde{\theta}^{(1)}$. *This can be seen by eliminating* $\tilde{\theta}^{(1)}$ *from the l.h. sides of* (9.17) *and* (9.21) *to get*

$$\frac{\tilde{\theta}^{(2)} - \theta^n_{dl}}{\Delta t} = -\alpha_2 \left[\left(w^n - w^*\right) \delta_{2r}\tilde{\theta}^{(1)}\right] - \left(1 - \alpha_2\right) \left[\left(w - w^*\right) \delta_{2r}\theta\right]^n_{dl}. \tag{9.22}$$

- **1st "Physics" Corrector**

The basis of how the forcing term, or "physics", S^θ, is discretised is to write S^θ as the sum of two terms $S^\theta = S^\theta_1 + S^\theta_2$ and to let the value of the physics time-weight, α_p, associated with S^θ_1 be 0 (appropriate for slow processes) and that associated with S^θ_2 be 1 (appropriate for fast processes). Thus, the physics terms of S^θ_1 and S^θ_2 are evaluated at the departure and arrival points, respectively. In addition, the terms for S^θ_1 are evaluated as functions of the model state at the previous, n^{th}, time-step, denoted here as $\{\theta^n\}$. Therefore, $S^\theta_1 = S^\theta_1\left(\{\theta^n\}\right) = \mu^\theta_{phys}\left(\{\theta^n\}\right) + R^\theta_{rad}\left(\{\theta^n\}\right)$ where μ^θ_{phys} represents the effects of *microphysical processes* and R^θ_{rad} represents the effects of *radiation*. Since the order of calculation of μ^θ_{phys} and R^θ_{rad} is interchangeable, this form of physics is known as "parallel", or "process-split", physics. Let $\tilde{\theta}^{(P1)}$ be the first physics predictor for θ^{n+1}. This can be written as the sum of the (2nd dynamics) predictor $\tilde{\theta}^{(2)}$ plus a 1st physics corrector $\left(\tilde{\theta}^{(P1)} - \tilde{\theta}^{(2)}\right)$, i.e. as

$$\tilde{\theta}^{(P1)} = \tilde{\theta}^{(2)} + \left(\tilde{\theta}^{(P1)} - \tilde{\theta}^{(2)}\right). \tag{9.23}$$

This 1st physics corrector is defined as

$$\left(\tilde{\theta}^{(P1)} - \tilde{\theta}^{(2)}\right) = \Delta t \left[S^\theta_1\right]^n_d. \tag{9.24}$$

__**Aside :**__

An obvious question is: why is the parallel, or process-split, physics added to the second predictor? It would seem more consistent with the rationale of the predictor/corrector approach if it were added to the first predictor, i.e. do the first physics corrector before *the first dynamics corrector. Then the* $(w^n - w^*)\,\delta_{2r}\tilde{\theta}^{(1)}$ *term appearing in* (9.22) *would be a function of a more complete, and therefore hopefully more accurate, predictor for* θ^{n+1}.

Aside :

The first physics corrector has the effect of simply adding to the right-hand side of (9.22) *the parallel, or process-split, physics term, where this term is evaluated at the departure point using time level* n *quantities. This can be seen by eliminating* $\tilde{\theta}^{(2)}$ *between the left-hand sides of* (9.22) *and* (9.24) *to get:*

$$\frac{\tilde{\theta}^{(P1)} - \theta^n_{dl}}{\Delta t} = -\alpha_2 \left[(w^n - w^*)\,\delta_{2r}\tilde{\theta}^{(1)}\right] - (1-\alpha_2)\left[(w - w^*)\,\delta_{2r}\theta\right]^n_{dl} + \left[S_1^\theta\right]^n_d . \tag{9.25}$$

Aside :

S_1^θ *is computed explicitly using data at time level* n*. It is not known whether or not, or under what conditions, this procedure is computationally stable. A stability analysis, if tractable, would be desirable.*

- **2nd "Physics" Corrector**

The target discretisation for the remaining part of the physics, S_2^θ, is to evaluate it *implicitly* using model variables at time level $n+1$. To avoid using an iterative approach, rather than using time level $n+1$ information, this part of the physics uses the latest available predictors of all the model variables required. Let $\tilde{\theta}^{(P2)}$ be the second physics predictor for θ^{n+1}. This can be written as the sum of the (1st physics) predictor $\tilde{\theta}^{(P1)}$ plus a 2nd physics corrector $\left(\tilde{\theta}^{(P2)} - \tilde{\theta}^{(P1)}\right)$, i.e. as

$$\tilde{\theta}^{(P2)} = \tilde{\theta}^{(P1)} + \left(\tilde{\theta}^{(P2)} - \tilde{\theta}^{(P1)}\right). \tag{9.26}$$

This 2nd physics corrector is defined as

$$\left(\tilde{\theta}^{(P2)} - \tilde{\theta}^{(P1)}\right) = \Delta t \left[S_2^\theta\right]^* . \tag{9.27}$$

The asterisk notation is used to indicate that S_2^θ is based on an intermediate, unbalanced model state and not on time level $n+1$ values.

Aside :

S_2^θ is made up of two physics components each of which updates the model variables used as the model state in the next component. The outcome of this part of the physics therefore depends on the order in which the components are evaluated. For this reason this part of the physics is known as "sequential", or "time-split" physics. For θ there are two such physics components which are the effects due to sub-gridscale convection *and the effects due to* subgrid-scale boundary-layer turbulence. *Notionally, $\tilde{\theta}^{(P2)}-\tilde{\theta}^{(P1)}$ can itself be written as the sum of a sequence of correctors:*

$$\tilde{\theta}^{(P2a)} - \tilde{\theta}^{(P1)} = \Delta t C^\theta\left(\left\{\tilde{\theta}^{(P1)}\right\}\right), \tag{9.28}$$

$$\tilde{\theta}^{(P2b)} - \tilde{\theta}^{(P2a)} = \Delta t BL^\theta\left(\left\{\tilde{\theta}^{(P2a)}\right\}\right), \tag{9.29}$$

where $\tilde{\theta}^{(P2)} \equiv \tilde{\theta}^{(P2b)}$ and $\left\{\tilde{\theta}^{(P1)}\right\}$ indicates the set of intermediate model variables, the various predictors, available at the same time as $\tilde{\theta}^{(P1)}$, and similarly for the other predictors for θ^{n+1}. The momentum variables available at the start of this process, i.e. at the same intermediate time as $\tilde{\theta}^{(P1)}$, are $\tilde{u}^{(P1)}$, $\tilde{v}^{(P1)}$ and $\tilde{w}^{(1)}$, and the available moisture variables are $\widetilde{m}_X^{(P1)}$ (see sections 6, 7 and 10 respectively). The only available density is that at time level n, i.e. ρ^n, and similarly for the pressure field, p^n. Note that each of the physics components is evaluated simultaneously for each of the model variables u, v, θ and m_X, as appropriate. BL^θ represents the implicit boundary-layer terms and is defined by:

$$BL^\theta\left(\left\{\tilde{\theta}^{(P2a)}\right\}\right) \equiv \frac{\theta^{**} - \tilde{\theta}^{(P2a)}}{\Delta t}. \tag{9.30}$$

The definition of θ^{**} requires the introduction of the moist static energy variable χ. [Since the variable χ is used only within the boundary layer, it would seem advisable to review the basis for this choice of thermodynamic variable and consider whether the simpler approach of using a potential temperature *based variable is acceptable.] The moist static energy is defined as:*

$$\chi = T + \frac{g\left(r - r_S\right)}{c_{pd}} - \frac{L_c q_{cl}}{c_{pd}} - \frac{\left(L_c + L_f\right) q_{cf}}{c_{pd}}, \tag{9.31}$$

where $T = \theta\Pi$ *is the temperature,* L_c *and* L_f *are the latent heats of condensation and fusion respectively, and* q_{cl} *and* q_{cf} *are the specific humidities of cloud liquid water and cloud frozen water respectively. [Note that to interface the dynamics with the physical parameterisations, the mixing ratios of water substance are converted to/ from specific humidities using* (1.56) - (1.57)*]. Therefore* $\chi = \chi\left(\theta, \Pi, q_{cl}, q_{cf}\right)$ *which in the current notation can be written as* $\chi = \chi\left(\{\theta\}\right)$*. Then, defining* $\chi^n \equiv \chi\left(\{\theta^n\}\right)$ *and* $\tilde{\chi}^{(P2a)} \equiv \chi\left(\left\{\tilde{\theta}^{(P2a)}\right\}\right)$*,* θ^{**} *is diagnosed from* χ^{**} *where* χ^{**} *satisfies the implicit equation:*

$$\begin{aligned} \frac{\chi^{**} - \chi^n}{\Delta t} &= \frac{1}{r^2 \rho^n}\delta_r\left(\alpha_{BL} r^2 \rho^n K_\chi \delta_r \chi^{**}\right) + \frac{1}{r^2\rho^n}\delta_r\left[\left(1 - \alpha_{BL}\right) r^2 \rho^n K_\chi \delta_r \chi^n\right] \\ &\quad + \frac{\tilde{\chi}^{(P2a)} - \chi^n}{\Delta t} + S^\chi_{CG}. \end{aligned} \tag{9.32}$$

$K_\chi = K_\chi\left(\{\theta^n\}\right)$ *is the eddy-diffusivity and* $S^\chi_{CG} = S^\chi_{CG}\left(\{\theta^n\}\right)$ *represents the source due to the counter-gradient, turbulent flux of moist static energy.* α_{BL} *is an off-centred, semi-implicit weighting factor which gives a fully implicit scheme when it is set equal to* 1*. However, the dependence of* K_χ *on the timelevel* n *variables can lead to a non-linear instability which can be eliminated by making the scheme "overweighted" i.e. by choosing a value for* α_{BL} *which is greater than* 1 *(see the series of papers Kalnay & Kanamitsu (1988), Girard & Delage (1990) and Bénard et al. (2000), and also Teixeira (2000)). The diagnosis of* $\theta^{**} \equiv \tilde{\theta}^{(P2)}$ *from* χ^{**} *is done by application of the cloud scheme to* χ^{**} *and* $\tilde{q}_v^{(P2)} + \tilde{q}_{cl}^{(P2)}$ *and* $\tilde{q}_{cf}^{(P2)}$*. The definition and evaluation of these moisture variables is discussed in Section 10. The only estimator available for* Π *is* Π^n *and it is this value which is used in the definitions of* χ*.*

Setting $\tilde{\theta}^{(P2)} \equiv \tilde{\theta}^{(P2b)}$ *and summing the 2 correctors given by* (9.28)-(9.29)*,* (9.27) *is obtained with*

$$\left[S_2^\theta\right]^* \equiv C^\theta\left(\left\{\tilde{\theta}^{(P1)}\right\}\right) + BL^\theta\left(\left\{\tilde{\theta}^{(P2a)}\right\}\right), \tag{9.33}$$

though writing it this way masks the sequential nature of the scheme.

Aside :

Again the obvious question is: why is the sequential, or time-split, physics added here and not, e.g. after the first predictor for θ^{n+1}, which, as argued above, could incorporate the parallel, or process-split, physics? The answer seems an open one which may be answered by experiment and/or by consideration of the relative speeds, or time scales, of the various processes, both physics and dynamics. Intuitively, the magnitude of the increments associated with the different processes seems likely also to be important: if the dynamics is the dominant process in a time step, i.e. if it leads to the largest change in θ in one time step, then placing the sequential, or time-split, physics after this process, so that this part of the physics is a function of the best predictor for θ^{n+1}, seems sensible. However, for those cases in which the sequential, or time-split, physics is the dominant process in a time step it would seem better to evaluate these terms earlier in the procedure in order to improve the later dynamics predictors, specifically $\tilde{\theta}^{(2)}$.

Aside :

The second physics corrector has the effect of simply adding the sequential, or time-split, physics term to the right-hand side of (9.25). *This can be seen by eliminating $\tilde{\theta}^{(P1)}$ between the left-hand sides of* (9.25) *and* (9.27) *to get:*

$$\frac{\tilde{\theta}^{(P2)} - \theta^n_{dl}}{\Delta t} = -\alpha_2 \left[(w^n - w^*)\, \delta_{2r} \tilde{\theta}^{(1)} \right] - (1-\alpha_2) \left[(w - w^*)\, \delta_{2r} \theta \right]^n_{dl} + \left[S^\theta_1 \right]^n_d + \left[S^\theta_2 \right]^* . \tag{9.34}$$

- **2nd "Dynamics" Corrector**

Let $\tilde{\theta}^{(3)} \equiv \theta^{n+1}$ be the 3rd dynamics and final predictor for θ^{n+1}. This can be written as the sum of the (2nd physics) predictor $\tilde{\theta}^{(P2)}$ plus a 2nd dynamics corrector $\left(\theta^{n+1} - \tilde{\theta}^{(P2)}\right)$, i.e. as

$$\theta^{n+1} = \tilde{\theta}^{(P2)} + \left(\theta^{n+1} - \tilde{\theta}^{(P2)} \right) . \tag{9.35}$$

This final, dynamics corrector is defined as

$$\left(\theta^{n+1} - \tilde{\theta}^{(P2)} \right) = -\alpha_2 \Delta t \left[\left(w^{n+1} - w^n \right) \delta_{2r} \theta_{ref} \right] , \tag{9.36}$$

where (see (7.22) and accompanying text)

$$\delta_{2r}\theta_{ref} = \max\left[\delta_{2r}\theta^*, \left(\frac{\mathbf{I}_h - G_{tol}}{c_{pd}\alpha_2\alpha_4\Delta t^2\delta_r\Pi^n}\right)\left(\frac{1+m_v^*+m_{cl}^*+m_{cf}^*}{1+m_v^*/\varepsilon}\right)\right], \tag{9.37}$$

with $\theta^* \equiv \tilde{\theta}^{(P2)}$ and $\mathbf{I}_h$ is a hydrostatic switch (see Section 7). The final corrector is implicit. It couples the thermodynamic equation to the other governing equations and eventually leads to a Helmholtz problem to be solved for the Exner pressure tendency Π'.

Aside :

As indicated by the notation, $\delta_{2r}\theta_{ref}$ *has a role akin to the reference profile usually present in semi-implicit schemes.* $\delta_{2r}\theta^* = \delta_{2r}\tilde{\theta}^{(P2)}$ *and* $\tilde{\theta}^{(P2)}$ *contains all the physics increments to* θ*. If* $\delta_{2r}\theta^*$ *is greater than the term involving* G_{tol} *in* (9.37)*, then* $\delta_{2r}\theta_{ref} = \delta_{2r}\theta^*$*. In this case the effective reference profile of the semi-implicit scheme contains contributions from the physics increments. This has the potentially dangerous result that the profile may be discontinuous. Exactly what effect this might have is unclear but it may lead to numerical inaccuracies. Use of a predetermined and smoothly varying reference profile should be considered.*

Aside :

Where the corrector (9.36) *comes from is not obvious. Eliminating* $\tilde{\theta}^{(P2)}$ *from the l.h. sides of* (9.34) *and* (9.36) *gives*

$$\begin{aligned}\frac{\theta^{n+1}-\theta^n_{dl}}{\Delta t} = -\alpha_2\left[\left(w^{n+1}-w^*\right)\delta_{2r}\theta_{ref} + \left(w^n - w^*\right)\delta_{2r}\left(\tilde{\theta}^{(1)}-\theta_{ref}\right)\right]& \\ -\left(1-\alpha_2\right)\left[\left(w-w^*\right)\delta_{2r}\theta\right]^n_{dl}.& \\ +\left[S_2^\theta\right]^* + \left[S_1^\theta\right]^n_d.&\end{aligned} \tag{9.38}$$

Without the term $-\alpha_2\left(w^n-w^*\right)\delta_{2r}\left(\tilde{\theta}^{(1)}-\theta_{ref}\right)$*,* (9.38) *would be very close to the target 2-time-level off-centred semi-implicit semi-Lagrangian discretisation defined by* (9.13)*, the differences being that* $\delta_{2r}\theta^{n+1}$ *in the term* $\left(w^{n+1}-w^*\right)\delta_{2r}\theta^{n+1}$ *has been replaced by* $\delta_{2r}\theta_{ref}$ *and the physics terms are time discretised somewhat differently, as described above. The additional term* $-\alpha_2\left(w^n-w^*\right)\delta_{2r}\left(\tilde{\theta}^{(1)}-\theta_{ref}\right)$ *is, however, of 2nd order and formally no worse than the leading truncation error of* (9.38) *without it.*

A stability analysis of the predictor-corrector algorithm for vertical advection, described above, is given in Appendix H. It turns out that it is unstable for $\alpha_2 < 4 - 2\sqrt{3} \approx 0.54$. Currently the model is usually run with $\alpha_2 = 1$.

9.4 Discretisation at level $k = 0$

When θ^{n+1} is needed at level $k = 0$, it is obtained by simple extrapolation of the value at level $k = 1$:

$$\theta^{n+1}\Big|_{\eta_0} = \theta^{n+1}\Big|_{\eta_1}. \tag{9.39}$$

9.5 Discretisation at level k = N

At level $k = N$, θ^{n+1} is obtained by horizontal advection using a 2-d interpolating semi-Lagrangian scheme together with the forcing, or "physics" term, due to radiation alone. For consistency with the discretisation at levels $k = 1, 2, ..., N-1$, it is convenient to still write this comparatively simple scheme in predictor-corrector form. Since $w \equiv 0$ at the rigid lid, the residual windspeed at level $k = N$ is identically zero, i.e.

$$(w - w^*)|_{\eta_{N \equiv 1}} \equiv 0. \tag{9.40}$$

From (9.40) and the absence of any sequential, or time-split, physics at the top level, so that $\left(S_2^\theta\right)\Big|_{\eta_N} = 0$, the expressions (9.17), (9.21), (9.24), (9.27) and (9.36) for the predictors respectively simplify at level $k = N$ to

$$\left(\tilde{\theta}^{(1)}\right)\Big|_{\eta_N} = (\theta_d^n)|_{\eta_N}, \tag{9.41}$$

$$\left(\tilde{\theta}^{(2)}\right)\Big|_{\eta_N} = \left(\tilde{\theta}^{(1)}\right)\Big|_{\eta_N}, \tag{9.42}$$

$$\left(\tilde{\theta}^{(P1)}\right)\Big|_{\eta_N} = \left(\tilde{\theta}^{(2)}\right)\Big|_{\eta_N} + \Delta t \left(\left[S_1^\theta\right]_d^n\right)\Big|_{\eta_N}, \tag{9.43}$$

$$\left(\tilde{\theta}^{(P2)}\right)\Big|_{\eta_N} = \left(\tilde{\theta}^{(P1)}\right)\Big|_{\eta_N}, \tag{9.44}$$

$$\left(\theta^{n+1}\right)\Big|_{\eta_N} = \left(\tilde{\theta}^{(P2)}\right)\Big|_{\eta_N}. \tag{9.45}$$

Here, $S_1^\theta = R_{rad}^\theta\left(\{\theta^n\}\right)$.

Aside :

Eliminating $\tilde{\theta}^{(1)}$, $\tilde{\theta}^{(2)}$, $\tilde{\theta}^{(P1)}$, *and* $\tilde{\theta}^{(P2)}$ *from* (9.41)-(9.45) *this predictor-corrector procedure may be equivalently written as the discretisation*

$$\frac{(\theta^{n+1})|_{\eta_N} - (\theta^n_d)|_{\eta_N}}{\Delta t} = \left(\left[S^\theta_1 \right]^n_d \right)\Big|_{\eta_N} . \tag{9.46}$$

9.6 A better alternative discretisation?

It is argued in WP154 [just after A.35], that it would be better to use $\tilde{\theta}^{(2)}$ instead of $\tilde{\theta}^{(1)}$ in the last term on the r.h.s. of A.35 [this is equivalent to the 1st term on the r.h.s. of (9.22) above], but that this is not done since it would lead to a tri-diagonal matrix system to solve. An alternative is proposed here that is a further step towards accomplishing the same objective but without the need to to solve a tridiagonal matrix system. It is not as implicit as solving a tri-diagonal system, but more implicit than the current scheme and relatively inexpensive. For reasons discussed in an aside below, this alternative scheme is developed here for the unforced problem, $S^\theta \equiv 0$, so that the physics correctors are null correctors and do not appear.

- **Revised 2nd "Dynamics" Corrector**

  Let $\tilde{\theta}^{(3)}$ be a 3rd dynamics predictor for θ^{n+1}. This can be written as the sum of the (2nd dynamics) predictor $\tilde{\theta}^{(2)}$ plus a 2nd dynamics corrector $\left(\tilde{\theta}^{(3)} - \tilde{\theta}^{(2)}\right)$, i.e. as

$$\tilde{\theta}^{(3)} = \tilde{\theta}^{(2)} + \left(\tilde{\theta}^{(3)} - \tilde{\theta}^{(2)}\right) . \tag{9.47}$$

  This (explicit) 2nd dynamics corrector is defined as

$$\left(\tilde{\theta}^{(3)} - \tilde{\theta}^{(2)}\right) = -\alpha_2 \Delta t \left(w^n - w^*\right) \delta_{2r} \left(\tilde{\theta}^{(2)} - \tilde{\theta}^{(1)}\right) . \tag{9.48}$$

Aside :

Adding the dynamics corrector (9.48) *is equivalent to replacing* $\tilde{\theta}^{(1)}$ *where it appears in the 1st square-bracketed term on the right-hand side of* (9.22) *by the 2nd predictor* $\tilde{\theta}^{(2)}$. *This can be seen by eliminating* $\tilde{\theta}^{(2)}$ *from the l.h. sides of* (9.22) *and* (9.48) *to get*

$$\frac{\tilde{\theta}^{(3)} - \theta^n_{dl}}{\Delta t} = -\alpha_2 \left[\left(w^n - w^*\right) \delta_{2r} \tilde{\theta}^{(2)} \right] - \left(1 - \alpha_2\right) \left[\left(w - w^*\right) \delta_{2r} \theta \right]^n_{dl} . \tag{9.49}$$

It can also be shown that the revised 3rd dynamics corrector is a further iterate of an iterative procedure to solve the tri-diagonal matrix system that would arise if $\tilde{\theta}^{(2)}$ instead of $\tilde{\theta}^{(1)}$ were to be used in the 1st term on the r.h.s. of (9.22) *as mentioned above and in WP 154. So the alternative procedure proposed herein corresponds to incomplete iteration of the better (but more costly) procedure mentioned in WP 154.*

- **3rd "Dynamics" Corrector**

Let $\tilde{\theta}^{(4)} \equiv \theta^{n+1}$ be an additional (4th dynamics and final) predictor for θ^{n+1}. This can be written as the sum of the revised (3rd dynamics) predictor $\tilde{\theta}^{(3)}$ plus a 3rd dynamics corrector $\left(\theta^{n+1} - \tilde{\theta}^{(3)}\right)$, i.e. as

$$\theta^{n+1} = \tilde{\theta}^{(3)} + \left(\theta^{n+1} - \tilde{\theta}^{(3)}\right). \tag{9.50}$$

This final, dynamics corrector is defined as

$$\left(\theta^{n+1} - \tilde{\theta}^{(3)}\right) = -\alpha_2 \Delta t \left[\left(w^{n+1} - w^*\right) - \left(w^n - w^*\right)\right] \delta_{2r}\theta_{ref} = -\alpha_2 \Delta t \left[\left(w^{n+1} - w^n\right) \delta_{2r}\theta_{ref}\right], \tag{9.51}$$

where (see (7.22) and accompanying text)

$$\delta_{2r}\theta_{ref} = \max\left[\delta_{2r}\theta^*, \left(\frac{\mathbf{I}_h - G_{tol}}{c_{pd}\alpha_2\alpha_4\Delta t^2 \delta_r \Pi^n}\right)\left(\frac{1 + m_v^* + m_{cl}^* + m_{cf}^*}{1 + m_v^*/\varepsilon}\right)\right]. \tag{9.52}$$

The final corrector is implicit. It couples the thermodynamic equation to the other governing equations and eventually leads to a Helmholtz problem to be solved for the Exner pressure tendency Π'.

<u>Aside :</u>

Adding the corrector (9.51) *is equivalent to replacing* $\left(w^n - w^*\right)\delta_{2r}\tilde{\theta}^{(2)}$ *where it appears in the 1st square-bracketed term on the right-hand side of* (9.49) *by* $\left(w^{n+1} - w^*\right)\delta_{2r}\theta_{ref}$ *and adding a 2nd-order correction term* $\left(w^n - w^*\right)\delta_{2r}\left(\tilde{\theta}^{(2)} - \theta_{ref}\right)$. *This can be seen by eliminating* $\tilde{\theta}^{(3)}$ *from the l.h. sides of* (9.49) *and* (9.51) *to get*

$$\frac{\theta^{n+1} - \theta^n_{dl}}{\Delta t} = -\alpha_2\left[\left(w^{n+1} - w^*\right)\delta_{2r}\theta_{ref} + \left(w^n - w^*\right)\delta_{2r}\left(\tilde{\theta}^{(2)} - \theta_{ref}\right)\right] - \left(1 - \alpha_2\right)\left[\left(w - w^*\right)\delta_{2r}\theta\right]^n_{dl}. \tag{9.53}$$

The computation of the 2nd and 3rd dynamics correctors can be collapsed into the following single corrector

$$\left(\theta^{n+1}-\theta^{*}\right)=-\alpha_2\Delta t\left[\left(w^{n+1}-w^{n}\right)\delta_{2r}\theta_{ref}\right]-\alpha_2\Delta t\left(w^{n}-w^{*}\right)\delta_{2r}\left(\theta^{*}-\tilde{\theta}^{(1)}\right), \tag{9.54}$$

where $\theta^{*}\equiv\tilde{\theta}^{(P2)}$.

Comparing this with the one used in the model reveals that it is identical except for the additional (last) term of (9.54). *Eq.* (9.53) *is quite close to the target 2-time-level off-centred semi-implicit semi-Lagrangian discretisation defined by* (9.13). *The difference is that the vertical derivative in the evaluation of the residual vertical advection term* $\left[\left(w-w^{*}\right)\delta_{2r}\theta\right]^{n+1}$ *at time* $(n+1)\,\Delta t$ *[cf.* (9.13)*], is evaluated using* $\tilde{\theta}^{(2)}$ *instead of* θ^{n+1}. *This reduces the formal accuracy of the scheme to* $O\left(\Delta t\right)$ *even when the scheme is otherwise centred (i.e. when* $\alpha_2=1\,/2$ *).*

A stability analysis of the alternative predictor-corrector algorithm for vertical advection, described above, is given in the second part of Appendix H. It turns out that it addresses the instability of the present scheme identified at the end of Section 9.3.

Aside :

This alternative discretisation has been developed in the absence of the forcing, or "physics" term, S^{θ}. *To introduce the physics, in the form discussed previously, i.e.* $S^{\theta}=S_1^{\theta}+S_2^{\theta}$, *the issue of where to place the physics correctors in relation to the dynamics correctors has to be addressed. If one is content with the position of the first physics corrector in the current scheme (though see the aside after* (9.24)*) it would seem natural to continue with that approach for this alternative scheme and place it immediately following the first dynamics corrector. However, even if one accepts as correct the position of the second physics corrector in the current scheme (though see the aside after* (9.33)*), the significance of its position is unclear: that is, does it appear where it does because this follows immediately the first physics corrector or, alternatively, because it precedes the final, implicit dynamics corrector- i.e. in the alternative discretisation, should the second physics corrector still be placed immediately after the first physics corrector* *or should it now occur after the second, explicit dynamics corrector and before the third, implicit one? To answer this the rationale of the positioning of the physics in the current scheme needs to be understood. Alternatively, a linear stability analysis of the equations, if tractable, might shed some light on the issue.*

Aside :

Note that to implement the proposed alternative discretisation, appropriate changes have to be made in the derivation of the Helmholtz problem (see Section 14) because of the changed form of (13.14).

9.7 Polar discretisation

The polar discretisation of the thermodynamic equation is almost identical to that elsewhere. This is because horizontal derivatives only occur for horizontal advection of θ and these are handled using the semi-Lagrangian procedures given in Section 5.

Uniqueness of θ at the two poles is assumed, i.e.

$$\theta_{SP} \equiv \theta_{\frac{1}{2},\frac{1}{2}} \equiv \theta_{\frac{3}{2},\frac{1}{2}} \equiv \theta_{\frac{5}{2},\frac{1}{2}} \equiv ... \equiv \theta_{L-\frac{1}{2},\frac{1}{2}}, \tag{9.55}$$

$$\theta_{NP} \equiv \theta_{\frac{1}{2},M-\frac{1}{2}} \equiv \theta_{\frac{3}{2},M-\frac{1}{2}} \equiv \theta_{\frac{5}{2},M-\frac{1}{2}} \equiv ... \equiv \theta_{L-\frac{1}{2},M-\frac{1}{2}}. \tag{9.56}$$

9.8 Further comments

It is probably better to discretise the thermodynamic equation in η coordinates rather than in r coordinates.

Evaluating the vertical advection in an Eulerian manner introduces differences over two meshlengths, which can lead to vertical decoupling. The vertical interpolation of a 3-d scheme should not suffer from this problem. Also semi-Lagrangian advection using cubic interpolation is more accurate than 1st or 2nd-order finite differences.

Rewriting the thermodynamic equation in terms of the perturbation from a reference profile should be considered. This would for example give

$$\frac{D}{Dt}\left(\theta - \theta_{ref}\right) + \frac{u}{r\cos\phi}\left(\frac{\partial\theta_{ref}}{\partial\lambda}\right)_{\eta} + \frac{v}{r}\left(\frac{\partial\theta_{ref}}{\partial\phi}\right)_{\eta} + \dot{\eta}\frac{\partial\theta_{ref}}{\partial\eta} = 0. \tag{9.57}$$

It has several potential advantages. First, it would significantly reduce the singular nature of θ at high altitude where the Exner pressure is very small by solving for a perturbation of a singular quantity rather than for the quantity itself. Second, it naturally gives rise to the last term in the above equation which is a crucial component for the stability of a semi-implicit scheme and needs to be treated semi-implicitly. Third, it in principle (there are however some further subtleties associated with this) permits a 3-d fully-interpolating scheme for the perturbation quantity (instead of the current 2-d/ 1-d scheme), more consistent with what is done for the other prognostic equations. Fourth, if $\theta_{ref} = \theta_{ref}\left(\lambda, \phi, \eta\right)$, then it may also reduce the intensity of spurious orographic resonance.

10 Discretisation of the moisture equations

The forced moisture equations are:

$$\frac{Dm_v}{Dt} = S^{m_v}, \tag{10.1}$$

$$\frac{Dm_{cl}}{Dt} = S^{m_{cl}}, \tag{10.2}$$

$$\frac{Dm_{cf}}{Dt} = S^{m_{cf}}. \tag{10.3}$$

These equations are discretised using a predictor-corrector method having several correction steps. Note that where appropriate the shorthand m_X is used generically to represent any of the three moisture variables, m_v, m_{cl} and m_{cf}.

10.1 Target discretisation of the m_X-equations

If (10.1) - (10.3) were to be discretised using a 2-time level, off-centred, semi-implicit, semi-Lagrangian scheme, as outlined in Section 5 then at the m points of the Arakawa C grid this would give the approximation:

$$\frac{m_v^{n+1} - (m_v)_d^n}{\Delta t} = \alpha_p \left[S^{m_v}\right]^{n+1} + (1 - \alpha_p) \left[S^{m_v}\right]_d^n, \tag{10.4}$$

$$\frac{m_{cl}^{n+1} - (m_{cl})_d^n}{\Delta t} = \alpha_p \left[S^{m_{cl}}\right]^{n+1} + (1 - \alpha_p) \left[S^{m_{cl}}\right]_d^n, \tag{10.5}$$

$$\frac{m_{cf}^{n+1} - (m_{cf})_d^n}{\Delta t} = \alpha_p \left[S^{m_{cf}}\right]^{n+1} + (1 - \alpha_p) \left[S^{m_{cf}}\right]_d^n. \tag{10.6}$$

This is not, however, what is presently done because of the complexity associated with the semi-implicit treatment of the forcing terms, or "physics", S^{m_X}. This motivated the development of the predictor-corrector method developed below.

10.2 Predictor-corrector discretisation for m_X at levels $k = 1, 2, ..., N-1$

For the m points of the Arakawa C grid the discretisation of the moisture equations (10.1) - (10.3) is comprised of the following steps:

- **Predictor**

  Let $\widetilde{m}_X^{(1)}$ be a predictor for m_X^{n+1}. The basis for this predictor is to neglect the forcing terms, or "physics", in (10.4) - (10.6). Thus:

$$\frac{\widetilde{m}_v^{(1)} - (m_v)_d^n}{\Delta t} = 0, \tag{10.7}$$

$$\frac{\widetilde{m}_{cl}^{(1)} - (m_{cl})_d^n}{\Delta t} = 0, \tag{10.8}$$

$$\frac{\widetilde{m}_{cf}^{(1)} - (m_{cf})_d^n}{\Delta t} = 0, \tag{10.9}$$

  where, as usual, subscript "d" denotes evaluation at the upstream point.

- **1st "Physics" Corrector**

Caveat :

> *Whilst the "physics" is written everywhere in this document in terms of mixing-ratio quantities m_X, currently the "physics" is coded in terms of specific quantities q_X with a mixing-ratio/ specific-humidity conversion interface between the "physics" and the "dynamics". Eventually the "physics" should be changed to work directly with mixing-ratio quantities as documented here.*

The basis of how the forcing term, or "physics", S^{m_X}, is discretised is to write S^{m_X} as the sum of two terms $S^{m_X} = S_1^{m_X} + S_2^{m_X}$ and to let the value of the physics time-weight, α_p, associated with $S_1^{m_X}$ be 0 (appropriate for slow processes) and that associated with $S_2^{m_X}$ be 1 (appropriate for fast processes). Thus, the physics terms of $S_1^{m_X}$ and $S_2^{m_X}$ are evaluated at the departure and arrival points, respectively. In addition, the terms for $S_1^{m_X}$ are evaluated as functions of the model state at the previous, n^{th}, time-step denoted here as $\{m_X^n\}$. Therefore:

$$S_1^{m_v} = S_1^{m_v}\left(\{m_v^n\}\right) = \mu_{phys}^{m_v}\left(\{m_v^n\}\right), \tag{10.10}$$

$$S_1^{m_{cl}} = S_1^{m_{cl}}\left(\{m_{cl}^n\}\right) = \mu_{phys}^{m_{cf}}\left(\{m_v^n\}\right) \tag{10.11}$$

and

$$S_1^{m_{cf}} = S_1^{m_{cf}}\left(\{m_{cf}^n\}\right) = \mu_{phys}^{m_{cf}}\left(\{m_{cf}^n\}\right), \tag{10.12}$$

where $\mu^{m_X}_{phys}$ represents the effects of *microphysical processes*. Let $\widetilde{m}_X^{(P1)}$ be the first physics predictor for m_X^{n+1}. This can be written as the sum of the (1st) predictor $\widetilde{m}_X^{(1)}$ plus a 1st physics corrector $\left(\widetilde{m}_X^{(P1)} - \widetilde{m}_X^{(1)}\right)$, i.e. as

$$\widetilde{m}_X^{(P1)} = \widetilde{m}_X^{(1)} + \left(\widetilde{m}_X^{(P1)} - \widetilde{m}_X^{(1)}\right). \tag{10.13}$$

These 1st physics correctors are defined as

$$\left(\widetilde{m}_v^{(P1)} - \widetilde{m}_v^{(1)}\right) = \Delta t \left[S_1^{m_v}\right]_d^n, \tag{10.14}$$

$$\left(\widetilde{m}_{cl}^{(P1)} - \widetilde{m}_{cl}^{(1)}\right) = \Delta t \left[S_1^{m_{cl}}\right]_d^n, \tag{10.15}$$

$$\left(\widetilde{m}_{cf}^{(P1)} - \widetilde{m}_{cf}^{(1)}\right) = \Delta t \left[S_1^{m_{cf}}\right]_d^n. \tag{10.16}$$

Interfacing procedure

Currently the physics routines work internally in terms of specific humidities, q_X, $X = (v, cl, cf)$, and the interfacing procedure is to:

- convert mixing ratios m_X to specific humidities q_X using (see (1.56))

$$q_X = m_X \bigg/ \left(1 + \sum_{X=(v,cl,cf)} m_X\right), \tag{10.17}$$

- compute the specific-humidity physics forcings $S_1^{q_X}$, $X = (v, cl, cf)$, using the physics routines;

- convert the specific-humidity forcings $S_1^{q_X}$, $X = (v, cl, cf)$ to equivalent mixing-ratio forcings $S_1^{m_X}$, $X = (v, cl, cf)$ using

$$\begin{aligned} S_1^{m_X} &= \left(1 + \sum_{X=(v,cl,cf)} m_X^n\right)\left[S_1^{q_X} + m_X^n \sum_{X=(v,cl,cf)} S_1^{q_X}\right] \\ &= \frac{1}{\left(1 - \sum_{X=(v,cl,cf)} q_X^n\right)}\left[S_1^{q_X} + \frac{q_X^n}{\left(1 - \sum_{X=(v,cl,cf)} q_X^n\right)} \sum_{X=(v,cl,cf)} S_1^{q_X}\right] \end{aligned} \tag{10.18}$$

  Eq. (10.18) can be obtained from (1.48)-(1.57) and (1.63)-(1.64).

<u>**Aside :**</u>

The first physics corrector has the effect of simply adding to the right-hand sides of (10.7) - (10.9) *the parallel, or process-split, physics terms, where these terms are evaluated at the departure point using time level* n *quantities. This can be seen by eliminating* $\widetilde{m}_X^{(1)}$ *between the left-hand sides of* (10.7) - (10.9) *and* (10.14) - (10.16) *to get:*

$$\frac{\widetilde{m}_v^{(P1)} - (m_v)_d^n}{\Delta t} = \left[S_1^{m_v}\right]_d^n, \tag{10.19}$$

$$\frac{\widetilde{m}_{cl}^{(P1)} - (m_{cl})_d^n}{\Delta t} = \left[S_1^{m_{cl}}\right]_d^n, \tag{10.20}$$

$$\frac{\widetilde{m}_{cf}^{(P1)} - (m_{cf})_d^n}{\Delta t} = \left[S_1^{m_{cf}}\right]_d^n. \tag{10.21}$$

In practice these equations are rewritten in the form $\widetilde{m}_X^{(P1)} = \left[m_X + \Delta t S_1^{m_X}\right]_d^n$. *This means that there is only one interpolation, instead of two, for each* m_X*, and the result, to machine precision, is the same.*

- **2nd "Physics" Corrector**

The target discretisation for the remaining part of the physics, $S_2^{m_X}$, is to evaluate it *implicitly* using model variables at time level $n+1$. To avoid using an iterative approach, rather than using time level $n+1$ information, this part of the physics uses the latest available predictors of all the model variables required. Let $\widetilde{m}_X^{(P2)}$ be the second physics predictor for m_X^{n+1}. This can be written as the sum of the (1st physics) predictor $\widetilde{m}_X^{(P1)}$ plus a 2nd physics corrector $\left(\widetilde{m}_X^{(P2)} - \widetilde{m}_X^{(P1)}\right)$, i.e. as

$$\widetilde{m}_X^{(P2)} = \widetilde{m}_X^{(P1)} + \left(\widetilde{m}_X^{(P2)} - \widetilde{m}_X^{(P1)}\right). \tag{10.22}$$

These 2nd physics correctors are defined as

$$\left(\widetilde{m}_v^{(P2)} - \widetilde{m}_v^{(P1)}\right) = \Delta t \left[S_2^{m_v}\right]^*, \tag{10.23}$$

$$\left(\widetilde{m}_{cl}^{(P2)} - \widetilde{m}_{cl}^{(P1)}\right) = \Delta t \left[S_2^{m_{cl}}\right]^*, \tag{10.24}$$

$$\left(\widetilde{m}_{cf}^{(P2)} - \widetilde{m}_{cf}^{(P1)}\right) = \Delta t \left[S_2^{m_{cf}}\right]^*. \tag{10.25}$$

The asterisk notation is used to indicate that $S_2^{m_X}$ is based on an intermediate, unbalanced model state and not on time level $n+1$ values. Note that currently the physics routines work internally in terms of specific humidities, $q_X,\ X = (v, cl, cf)$. The same interfacing procedure as that described immediately following (10.16) is used above to obtain $S_2^{m_X}$ in (10.23) - (10.23), and also in what follows below, but with S_1 replaced by S_2.

Aside :

– The $S_2^{m_v}$ term:

$S_2^{m_v}$ *is made up of two physics components each of which updates the model variables used as the model state in the next component. The outcome of this part of the physics therefore depends on the order in which the components are evaluated. For this reason this part of the physics is known as "sequential", or "time-split" physics. For* m_v *there are two such physics components which are the effects due to* sub-gridscale convection *and the effects due to* subgrid-scale boundary-layer turbulence. *Notionally,* $\widetilde{m}_v^{(P2)} - \widetilde{m}_v^{(P1)}$ *can itself be written as the sum of a sequence of predictors and correctors:*

$$\widetilde{m}_v^{(P2a)} - \widetilde{m}_v^{(P1)} = \Delta t C^{m_v}\left(\left\{\widetilde{m}_v^{(P1)}\right\}\right), \tag{10.26}$$

$$\widetilde{m}_v^{(P2b)} - \widetilde{m}_v^{(P2a)} = \Delta t BL^{m_v}\left(\left\{\widetilde{m}_v^{(P2a)}\right\}\right), \tag{10.27}$$

where $\widetilde{m}_v^{(P2)} \equiv \widetilde{m}_v^{(P2b)}$ *and* $\left\{\widetilde{m}_v^{(P2a)}\right\}$ *indicates the set of intermediate model variables, the various predictors, available at the same time as* $\widetilde{m}_v^{(P2a)}$*, and similarly for the other predictors for* m_v^{n+1}*. Note that each physics increment is evaluated simultaneously for each model variable. The equivalent momentum variables available at the start of this process, i.e. at the same intermediate time as* $\widetilde{m}_v^{(P1)}$*, are* $\tilde{u}^{(P1)}$*,* $\tilde{v}^{(P1)}$ *and* $\tilde{w}^{(1)}$*, and the available temperature variable is* $\tilde{\theta}^{(P1)}$ *(see sections 6, 7 and 9 respectively). The only available density is that at time level* n*, i.e.* ρ^n*, and similarly for the Exner field,* Π^n*, and the pressure field,* p^n*. The cloud liquid water and cloud frozen water variables available at the same time as both* $\widetilde{m}_v^{(P1)}$ *and* $\widetilde{m}_v^{(P2a)}$ *are* $\widetilde{m}_{cl}^{(P1)}$ *and* $\widetilde{m}_{cf}^{(P1)}$*, respectively. Setting* $\widetilde{m}_v^{(P2)} \equiv \widetilde{m}_v^{(P2b)}$ *and summing the 2 correctors given by* (10.26)-(10.27), (10.23) *is obtained with*

$$\left[S_2^{m_v}\right]^* \equiv C^{m_v}\left(\left\{\widetilde{m}_v^{(P1)}\right\}\right) + BL^{m_v}\left(\left\{\widetilde{m}_v^{(P2a)}\right\}\right), \tag{10.28}$$

though writing it this way masks the sequential nature of the scheme. BL^{m_v} represents the implicit boundary-layer terms and is discussed below.

– The $S_2^{m_{cl}}$ and $S_2^{m_{cf}}$ terms:

$S_2^{m_{cl}}$ and $S_2^{m_{cf}}$ consist only of the subgrid-scale boundary-layer turbulence component. $\widetilde{m}_{cl}^{(P2)}$ and $\widetilde{m}_{cf}^{(P2)}$ can be written as:

$$\widetilde{m}_{cl}^{(P2)} - \widetilde{m}_{cl}^{(P1)} = \Delta t BL^{m_{cl}} \left(\left\{ \widetilde{m}_v^{(P2a)} \right\} \right) \tag{10.29}$$

and

$$\widetilde{m}_{cf}^{(P2)} - \widetilde{m}_{cf}^{(P1)} = \Delta t BL^{m_{cf}} \left(\left\{ \widetilde{m}_v^{(P2a)} \right\} \right), \tag{10.30}$$

where $\left\{ \widetilde{m}_v^{(P2a)} \right\}$ indicates the set of intermediate model variables, the various predictors, available at the same time as $\widetilde{m}_v^{(P2a)}$, as discussed above. (10.29) *and* (10.30) *are equivalent to* (10.24) *and* (10.25) *with*

$$\left[S_2^{m_{cl}} \right]^* \equiv BL^{m_{cl}} \left(\left\{ \widetilde{m}_v^{(P2a)} \right\} \right) \tag{10.31}$$

and

$$\left[S_2^{m_{cf}} \right]^* \equiv BL^{m_{cf}} \left(\left\{ \widetilde{m}_v^{(P2a)} \right\} \right). \tag{10.32}$$

$BL^{m_{cl}}$ and $BL^{m_{cf}}$ represent the implicit boundary-layer terms and are discussed below.

– The boundary-layer terms, BL^{m_X}:

The principal role of the boundary-layer scheme for moisture is to diffuse the conserved, total water variable, m_{tot}, given by $m_{tot} \equiv m_v + m_{cl} + m_{cf}$. From the definition of m_{tot} the following relations follow: $m_{tot}^n \equiv m_v^n + m_{cl}^n + m_{cf}^n$ and $\widetilde{m}_{tot}^{(P2a)} \equiv \widetilde{m}_v^{(P2a)} + \widetilde{m}_{cl}^{(P1)} + \widetilde{m}_{cf}^{(P1)}$. Then, the boundary-layer increment to the total water, $BL^{m_{tot}}$, is defined by:

$$BL^{m_{tot}} \left(\left\{ \widetilde{m}_v^{(P2a)} \right\} \right) \equiv \frac{m_{tot}^{**} - \widetilde{m}_{tot}^{(P2a)}}{\Delta t}, \tag{10.33}$$

where m_{tot}^{**} satisfies the implicit equation:

$$\begin{aligned} \frac{m_{tot}^{**} - m_{tot}^n}{\Delta t} \quad = \quad & \frac{1}{r^2 \rho_y^n} \delta_r \left(\alpha_{BL} r^2 \rho_y^n K_{m_{tot}} \delta_r m_{tot}^{**} \right) \\ & + \frac{1}{r^2 \rho_y^n} \delta_r \left[\left(1 - \alpha_{BL} \right) r^2 \rho_y^n K_{m_{tot}} \delta_r m_{tot}^n \right] \\ & + \frac{\widetilde{m}_{tot}^{(P2a)} - m_{tot}^n}{\Delta t}. \end{aligned} \tag{10.34}$$

$K_{m_{tot}} = K_{m_{tot}}\left(\{m_v^n\}\right)$ is the eddy-diffusivity for moisture. α_{BL} is an off-centred, semi-implicit weighting factor which gives a fully implicit scheme when it is set equal to 1. However, the dependence of $K_{m_{tot}}$ on the timelevel n variables can lead to a non-linear instability which can be eliminated by making the scheme "overweighted" i.e. by choosing a value for α_{BL} which is greater than 1 (see the series of papers Kalnay & Kanamitsu (1988), Girard & Delage (1990) and Bénard et al. (2000), and also Teixeira (2000)).

The sum of the as yet unknown quantities, $\widetilde{m}_v^{(P2)}$, $\widetilde{m}_{cl}^{(P2)}$ and $\widetilde{m}_{cf}^{(P2)}$, is set equal to m_{tot}^{**} so that $m_{tot}^{**} = \widetilde{m}_v^{(P2)} + \widetilde{m}_{cl}^{(P2)} + \widetilde{m}_{cf}^{(P2)}$. This relationship, together with the definition of $\widetilde{m}_v^{(P2)}$, equations (10.29), (10.30), (10.33) and the definition of $\widetilde{m}_{tot}^{(P2a)}$ gives:

$$BL^{m_{tot}}\left(\left\{\widetilde{m}_v^{(P2a)}\right\}\right) = BL^{m_v}\left(\left\{\widetilde{m}_v^{(P2a)}\right\}\right) + BL^{m_{cl}}\left(\left\{\widetilde{m}_v^{(P2a)}\right\}\right) + BL^{m_{cf}}\left(\left\{\widetilde{m}_v^{(P2a)}\right\}\right). \tag{10.35}$$

The final step of the boundary-layer scheme is effectively to diagnose the division of the total boundary-layer contribution, $BL^{m_{tot}}$, between BL^{m_v}, $BL^{m_{cf}}$ and $BL^{m_{cf}}$ in order to calculate the predictors $\widetilde{m}_v^{(P2)}$, $\widetilde{m}_{cl}^{(P2)}$ and $\widetilde{m}_{cf}^{(P2)}$. There are two steps in this procedure. The first is based on the assumption that there is no conversion between frozen and non-frozen water due to turbulent boundary-layer mixing. Then $BL^{m_{cf}}$ can be evaluated in exactly the same way as $BL^{m_{tot}}$, i.e. as:

$$BL^{m_{cf}}\left(\left\{\widetilde{m}_v^{(P2a)}\right\}\right) \equiv \frac{m_{cf}^{**} - \widetilde{m}_{cf}^{(P1)}}{\Delta t}, \tag{10.36}$$

where m_{cf}^{**} satisfies the implicit equation:

$$\begin{aligned} \frac{m_{cf}^{**} - m_{cf}^n}{\Delta t} &= \frac{1}{r^2\rho_y^n}\delta_r\left(\alpha_{BL} r^2 \rho_y^n K_{m_{tot}} \delta_r m_{cf}^{**}\right) + \frac{1}{r^2\rho_y^n}\delta_r\left[\left(1-\alpha_{BL}\right) r^2 \rho_y^n K_{m_{tot}} \delta_r m_{cf}^n\right] \\ &\quad + \frac{\widetilde{m}_{cf}^{(P1)} - m_{cf}^n}{\Delta t}, \end{aligned} \tag{10.37}$$

with $K_{m_{tot}}$ as used in (10.34). $\widetilde{m}_{cf}^{(P2)}$ is then obtained directly as $\widetilde{m}_{cf}^{(P2)} \equiv m_{cf}^{**}$. Then

$$BL^{m_v}\left(\left\{\widetilde{m}_v^{(P2a)}\right\}\right) + BL^{m_{cl}}\left(\left\{\widetilde{m}_v^{(P2a)}\right\}\right) = BL^{m_{tot}}\left(\left\{\widetilde{m}_v^{(P2a)}\right\}\right) - BL^{m_{cf}}\left(\left\{\widetilde{m}_v^{(P2a)}\right\}\right), \tag{10.38}$$

where the two terms on the right-hand side are known. This equation can alternatively be written as:

$$\widetilde{m}_v^{(P2)} + \widetilde{m}_{cl}^{(P2)} = m_{tot}^{**} - m_{cf}^{**}. \tag{10.39}$$

The second step is to make the final split between $\widetilde{m}_v^{(P2)}$ *and* $\widetilde{m}_{cl}^{(P2)}$ *and this is achieved by applying the cloud scheme to the field* $\widetilde{m}_v^{(P2)} + \widetilde{m}_{cl}^{(P2)}$ *resulting from* (10.39), *together with* $\widetilde{m}_{cf}^{(P2)}$ *and the moist static energy* χ^{**} *(see Section 9).*

Aside :

The second physics corrector has the effect of simply adding the sequential, or time-split, physics terms to the right-hand sides of (10.19) - (10.21). *This can be seen by eliminating* $\widetilde{m}_X^{(P1)}$ *between the left-hand sides of* (10.19) - (10.21) *and* (10.23) - (10.25) *to get:*

$$\frac{\widetilde{m}_v^{(P2)} - (m_v)_d^n}{\Delta t} = [S_1^{m_v}]_d^n + [S_2^{m_v}]^*, \tag{10.40}$$

$$\frac{\widetilde{m}_{cl}^{(P2)} - (m_{cl})_d^n}{\Delta t} = [S_1^{m_{cl}}]_d^n + [S_2^{m_{cl}}]^* \tag{10.41}$$

and

$$\frac{\widetilde{m}_{cf}^{(P2)} - (m_{cf})_d^n}{\Delta t} = \left[S_1^{m_{cf}}\right]_d^n + \left[S_2^{m_{cf}}\right]^*. \tag{10.42}$$

- **1st "Conservation" Corrector**

Let $\widetilde{m}_X^{(2)}$ be the second dynamics predictor for m_X^{n+1}. This can be written as the sum of the (2nd physics) predictor $\widetilde{m}_X^{(P2)}$ plus a 1st conservation corrector $\left(\widetilde{m}_X^{(2)} - \widetilde{m}_X^{(P2)}\right)$, i.e. as

$$\widetilde{m}_X^{(2)} = \widetilde{m}_X^{(P2)} + \left(\widetilde{m}_X^{(2)} - \widetilde{m}_X^{(P2)}\right). \tag{10.43}$$

These 1st conservation correctors are given by

$$\left(\widetilde{m}_v^{(2)} - \widetilde{m}_v^{(P2)}\right) = \Delta t \left(D_{cons}^{m_v}\right)^n, \tag{10.44}$$

$$\left(\widetilde{m}_{cl}^{(2)} - \widetilde{m}_{cl}^{(P2)}\right) = \Delta t \left(D_{cons}^{m_{cl}}\right)^n, \tag{10.45}$$

$$\left(\widetilde{m}_{cf}^{(2)} - \widetilde{m}_{cf}^{(P2)}\right) = \Delta t \left(D_{cons}^{m_{cf}}\right)^n, \tag{10.46}$$

where the new departure point correction term, $(D^{m_X}_{cons})^n$, $X = (v, cl, cf)$, is obtained so that the following global, integral relationships hold:

$$\int_{\mathcal{V}} \rho_y^{n+1} \left\{ [m_X + \Delta t S_1^{m_X}]_d^n + \Delta t \left(D^{m_X}_{cons}\right)^n \right\} d\mathcal{V} = \int_{\mathcal{V}} \rho_y^n \left(m_X + \Delta t S_1^{m_X}\right)^n d\mathcal{V}, \qquad (10.47)$$

where $\mathcal{V}$ represents the model volume of the atmosphere and $d\mathcal{V}$ is the volume element $r^2 \cos\phi d\lambda d\phi dr$. This is achieved by applying the Priestley algorithm (Priestley 1993) to two estimates for $[m_X + \Delta t S_1^{m_X}]_d^n$, one of which is required to be monotonic (guaranteed by using linear interpolation) and the other is obtained using a higher-order (e.g. cubic) interpolation scheme. The returned field, $[m_X + \Delta t S_1^{m_X}]_d^n + \Delta t \left(D^{m_X}_{cons}\right)^n$, is monotonic. If conservation is required but the Priestley algorithm does not converge, then the higher-order interpolation-scheme estimate for $[m_X + \Delta t S_1^{m_X}]_d^n$ is simply multiplied by the appropriate constant to achieve formal conservation. Note it is assumed here that a montonicity constraint has already been applied to the higher-order interpolation estimate. If conservation is not enforced then the correctors $\left(\widetilde{m}_X^{(2)} - \widetilde{m}_X^{(P2)}\right)$ are null correctors and $D^{m_X}_{cons} \equiv 0$.

<u>Aside :</u>

> *A disadvantage of this corrector is that it is necessary to store the values of* $m_v^n + \Delta t \left(S_1^{m_X}\right)^n$ *and also* $[m_v + \Delta t S_1^{m_X}]_d^n \equiv \widetilde{m}_X^{(P1)}$ *or, alternatively, recalculate the latter.*

<u>Aside :</u>

> *The first conservation corrector has the effect of simply adding to the right-hand sides of* (10.40) - (10.42) *the departure point correction terms,* $(D^{m_X}_{cons})^n$*. This can be seen by eliminating* $\widetilde{m}_X^{(P2)}$ *between the left-hand sides of* (10.40) - (10.42) *and* (10.44) - (10.46) *to get:*

$$\frac{\widetilde{m}_v^{(2)} - (m_v)_d^n}{\Delta t} = [S_1^{m_v}]_d^n + [S_2^{m_v}]^* + \left(D^{m_v}_{cons}\right)^n, \qquad (10.48)$$

$$\frac{\widetilde{m}_{cl}^{(2)} - (m_{cl})_d^n}{\Delta t} = [S_1^{m_{cl}}]_d^n + [S_2^{m_{cl}}]^* + \left(D^{m_{cl}}_{cons}\right)^n, \qquad (10.49)$$

$$\frac{\widetilde{m}_{cf}^{(2)} - (m_{cf})_d^n}{\Delta t} = \left[S_1^{m_{cf}}\right]_d^n + \left[S_2^{m_{cf}}\right]^* + \left(D^{m_{cf}}_{cons}\right)^n. \qquad (10.50)$$

- **2nd "Conservation" Corrector**

Caveat :

Note that the 2nd "conservation" corrector has not, as yet, been coded.

Let $\widetilde{m}_X^{(3)} \equiv m_X^{n+1}$ be the third dynamics, and final, predictor for m_X^{n+1}. This can be written as the sum of the (1st dynamics) predictor $\widetilde{m}_X^{(2)}$ plus a 2nd conservation corrector $\left(m_X^{n+1} - \widetilde{m}_X^{(2)}\right)$, i.e. as

$$m_X^{n+1} = \widetilde{m}_X^{(2)} + \left(m_X^{n+1} - \widetilde{m}_X^{(2)}\right). \tag{10.51}$$

These 2nd conservation correctors are given by

$$\left(m_v^{n+1} - \widetilde{m}_v^{(2)}\right) = -\Delta t \left(\frac{\rho_y^{n+1} - \rho_y^n}{\rho_y^{n+1}}\right) [S_2^{m_v}]^*, \tag{10.52}$$

$$\left(m_{cl}^{n+1} - \widetilde{m}_{cl}^{(2)}\right) = -\Delta t \left(\frac{\rho_y^{n+1} - \rho_y^n}{\rho_y^{n+1}}\right) [S_2^{m_{cl}}]^*, \tag{10.53}$$

$$\left(m_{cf}^{n+1} - \widetilde{m}_{cf}^{(2)}\right) = -\Delta t \left(\frac{\rho_y^{n+1} - \rho_y^n}{\rho_y^{n+1}}\right) \left[S_2^{m_{cf}}\right]^*. \tag{10.54}$$

If conservation is not enforced then the correctors $\left(m_X^{n+1} - \widetilde{m}_X^{(2)}\right)$ and $\left(\widetilde{m}_X^{(2)} - \widetilde{m}_X^{(P2)}\right)$ are null correctors and $m_X^{n+1} \equiv \widetilde{m}_X^{(P2)}$.

Aside :

The 1st and 2nd conservation correctors may be collapsed into the following single corrector

$$\left(m_v^{n+1} - \widetilde{m}_v^{(P2)}\right) = \Delta t \left(D_{cons}^{m_v}\right)^n - \Delta t \left(\frac{\rho_y^{n+1} - \rho_y^n}{\rho_y^{n+1}}\right) [S_2^{m_v}]^*, \tag{10.55}$$

$$\left(m_{cl}^{n+1} - \widetilde{m}_{cl}^{(P2)}\right) = \Delta t \left(D_{cons}^{m_{cl}}\right)^n - \Delta t \left(\frac{\rho_y^{n+1} - \rho_y^n}{\rho_y^{n+1}}\right) [S_2^{m_{cl}}]^*, \tag{10.56}$$

$$\left(m_{cf}^{n+1} - \widetilde{m}_{cf}^{(P2)}\right) = \Delta t \left(D_{cons}^{m_{cf}}\right)^n - \Delta t \left(\frac{\rho_y^{n+1} - \rho_y^n}{\rho_y^{n+1}}\right) \left[S_2^{m_{cf}}\right]^*. \tag{10.57}$$

Aside :

Note that in this collapsed form, the second conservation correctors, $\left(m_X^{n+1} - \widetilde{m}_X^{(2)}\right)$, *in themselves do not require any further memory storage as* $[S_2^{m_X}]^*$ *can be evaluated from* $\widetilde{m}_X^{(P2)}$ *and* $\widetilde{m}_X^{(P1)}$ *(which needs to be stored or calculated for the evaluation of the* $(D_{cons}^{m_X})^n$ *terms) by application of* (10.23)-(10.25).

Aside :

The second conservation corrector has the effect of multiplying the $[S_2^{m_X}]^*$ *terms on the right-hand sides of* (10.48)-(10.50) *by* ρ_y^n/ρ_y^{n+1}*. This can be seen by eliminating* $\widetilde{m}_X^{(2)}$ *between the left-hand sides of* (10.48)-(10.50) *and* (10.52)-(10.54) *to get:*

$$\frac{m_v^{n+1} - (m_v)_d^n}{\Delta t} = [S_1^{m_v}]_d^n + \left(\frac{\rho_y^n}{\rho_y^{n+1}}\right)[S_2^{m_v}]^* + (D_{cons}^{m_v})^n , \tag{10.58}$$

$$\frac{m_{cl}^{n+1} - (m_{cl})_d^n}{\Delta t} = [S_1^{m_{cl}}]_d^n + \left(\frac{\rho_y^n}{\rho_y^{n+1}}\right)[S_2^{m_{cl}}]^* + (D_{cons}^{m_{cl}})^n , \tag{10.59}$$

$$\frac{m_{cf}^{n+1} - (m_{cf})_d^n}{\Delta t} = \left[S_1^{m_{cf}}\right]_d^n + \left(\frac{\rho_y^n}{\rho_y^{n+1}}\right)\left[S_2^{m_{cf}}\right]^* + \left(D_{cons}^{m_{cf}}\right)^n . \tag{10.60}$$

Except for the details of how the physics terms are handled and the addition of the departure calculation corrections to ensure global conservation, equations (10.58)-(10.60) are very close to the target discretisations, (10.4)-(10.6), where $S^{m_X} \equiv S_1^{m_X} + S_2^{m_X}$.

10.3 Discretisation at level $k = 0$

When m_X^{n+1} , $X = (v, cl, cf)$, are needed at level $k = 0$, they are obtained by simple extrapolation of their values at level $k = 1$:

$$m_X^{n+1}\Big|_{\eta_0} = m_X^{n+1}\Big|_{\eta_1} , \; X = (v, cl, cf) . \tag{10.61}$$

10.4 Discretisation at level k = N

At level $k = N$, m_X^{n+1}, $X = (v, cl, cf)$, is obtained by horizontal advection using a 2-d interpolating semi-Lagrangian scheme together with the forcing, or "physics" term, due to microphysics alone. For consistency with the discretisation at levels $k = 1, 2, ..., N-1$, it is convenient to still write this comparatively simple scheme in predictor-corrector form.

Fromthe absence of any sequential, or time-split, physics at the top level, i.e.

$$(S_2^{m_X})|_{\eta_N} = 0, \; X = (v, cl, cf) , \tag{10.62}$$

the expressions (10.7)-(10.9), (10.14)-(10.16), (10.23)-(10.25), (10.44)-(10.46) and (10.52)-(10.54) for the predictors respectively simplify at level $k = N$ to

$$\left\{\widetilde{m}_X^{(1)}\right\}\Big|_{\eta_N} = \{(m_X)_d^n\}|_{\eta_N} , \tag{10.63}$$

$$\left\{\widetilde{m}_X^{(P1)} - \widetilde{m}_X^{(1)}\right\}\Big|_{\eta_N} = \Delta t \left\{[S_1^{m_X}]_d^n\right\}\big|_{\eta_N}, \tag{10.64}$$

$$\left\{\widetilde{m}_X^{(P2)} - \widetilde{m}_X^{(P1)}\right\}\Big|_{\eta_N} = 0, \tag{10.65}$$

$$\left\{\widetilde{m}_X^{(2)} - \widetilde{m}_X^{(P2)}\right\}\Big|_{\eta_N} = \Delta t \left\{(D_{cons}^{m_X})^n\right\}\big|_{\eta_N}, \tag{10.66}$$

$$\left\{m_X^{n+1} - \widetilde{m}_X^{(2)}\right\}\Big|_{\eta_N} = 0. \tag{10.67}$$

Here, $S_1^{m_X} = \mu_{phys}^{m_X}(\{m_X^n\})$, $X = (v, cl, cf)$, and $D_{cons}^{m_X}$ is defined by (10.47) when conservation is imposed, but is otherwise zero.

Aside :

Eliminating $\widetilde{m}_X^{(1)}$, $\widetilde{m}_X^{(P1)}$, $\widetilde{m}_X^{(P2)}$, *and* $\widetilde{m}_X^{(2)}$ *from* (10.63)-(10.67) *this predictor-corrector procedure may be equivalently written as the discretisation*

$$\frac{\left\{m_X^{n+1}\right\}\big|_{\eta_N} - \left\{(m_X)_d^n\right\}\big|_{\eta_N}}{\Delta t} = \left\{[S_1^{m_X}]_d^n + (D_{cons}^{m_X})^n\right\}\Big|_{\eta_N}. \tag{10.68}$$

10.5 Conservation

The global conservation of water substance is an important requirement for long term climate simulations in which systematic trends in water content can have substantial feedbacks on the climate. Analytic conservation is given by (A.37). Since the model uses (10.1) in the form it is written, i.e. in its Lagrangian, and not in its Eulerian, form, exact conservation is not automatically obtained but is instead imposed. The form currently chosen to discretise (A.37) is

$$\int_{\mathcal{V}} \frac{\left(\rho_y^{n+1} m_X^{n+1}\right) - \left(\rho_y^n m_X^n\right)}{\Delta t} d\mathcal{V} = \int_{\mathcal{V}} \rho_y^n \left[(S_1^{m_X})^n + (S_2^{m_X})^*\right] d\mathcal{V}. \tag{10.69}$$

Substituting the expression for m_X^{n+1} given by (10.58) - (10.60) into (10.69), shows that global conservation of moisture requires:

$$\int_{\mathcal{V}} \rho_y^{n+1} \left\{[m_X + \Delta t S_1^{m_X}]_d^n + \Delta t\,(D_{cons}^{m_X})^n + \Delta t \left(\frac{\rho_y^n}{\rho_y^{n+1}}\right)[S_2^{m_X}]^*\right\} d\mathcal{V}$$
$$= \int_{\mathcal{V}} \rho_y^n \left\{(m_X + \Delta t S_1^{m_X})^n + \Delta t\,[S_2^{m_X}]^*\right\} d\mathcal{V}. \tag{10.70}$$

Application of the definition of $D_{cons}^{m_X}$, given by (10.47),to rewrite

$$\int_{\mathcal{V}} \rho_y^{n+1} \left\{[m_X + \Delta t S_1^{m_X}]_d^n + \Delta t\,(D_{cons}^{m_X})^n\right\} d\mathcal{V} \tag{10.71}$$

as

$$\int_{\mathcal{V}} \rho_y^n \left(m_X + \Delta t S_1^{m_X}\right)^n d\mathcal{V}, \tag{10.72}$$

shows that (10.70) is indeed satisfied and therefore global conservation of moisture obtains.

10.6 Vertical discretisation

A final consideration in evaluating conservation properties arises because the density and the moisture variables are not co-located, they are staggered with respect to one another in the vertical. The question is: should the combined conservation corrector, $\left(m_X^{n+1} - \widetilde{m}_X^{(P2)}\right)$, be constructed to conserve:

$$\int_{\mathcal{V}} \overline{\left(\rho_y^{n+1}\right)}^r m_X^{n+1} d\mathcal{V} \tag{10.73}$$

or alternatively:

$$\int_{\mathcal{V}} \rho_y^{n+1} \overline{\left(m_X^{n+1}\right)}^r d\mathcal{V}. \tag{10.74}$$

The correct choice becomes clear by considering the case where m_X is set equal to a constant everywhere with no sources or sinks, i.e. $S_1^{m_X} \equiv S_2^{m_X} \equiv 0$. The value of m_X will then (hopefully!) remain constant everywhere for all time. Conservation in the form of equations (10.73) and (10.74) then reduces, respectively, to:

$$\int_{\mathcal{V}} \overline{\left(\rho_y^{n+1}\right)}^r d\mathcal{V} = \int_{\mathcal{V}} \overline{\left(\rho_y^{n}\right)}^r d\mathcal{V}, \tag{10.75}$$

and

$$\int_{\mathcal{V}} \rho_y^{n+1} d\mathcal{V} = \int_{\mathcal{V}} \rho_y^{n} d\mathcal{V}. \tag{10.76}$$

The Eulerian scheme for the continuity equation has been used in the New Dynamics specifically to ensure that the total dry mass of the atmosphere is exactly conserved (see Section 8.4), i.e.:

$$\int_{\mathcal{V}} \rho_y^{n+1} d\mathcal{V} \equiv \int_{\mathcal{V}} \rho_y^{n} d\mathcal{V}. \tag{10.77}$$

Thus, (10.76) is guaranteed to hold. However, this property relies on the exact cancellation of the terms contributing to the vertical component of the divergence of the momentum vector after the discretised equation has been multiplied by the appropriate volume element (see Section 8.4). In general, if the density is first averaged in the vertical this exact cancellation will no longer occur and (10.75) will not hold. A further complication with this approach arises because density is only held on interior levels and therefore an issue arises as to what to do near the boundaries?

Aside :

Neglecting the complication of the boundaries, it is worth noting that the scheme outlined above could in fact be used to ensure that a conservation law in the *form of* (10.73) *is indeed satisfied. However, since* (10.75) *does not hold then in the example given, where* m_X *initially takes a constant value everywhere, such conservation could only be satisfied by perturbing the values of* m_X *away from the constant value. The conservation process itself would introduce spurious sources and sinks of moisture to exactly compensate for the lack of mass conservation, i.e. the amount by which* (10.75) *is not satisfied, and this despite the fact that* (10.76) *is always satisfied!*

It is clear then that the appropriate form for conservation is given by (10.74).

One consequence of this is that the spatially discretised form of (10.47) is:

$$\int_{\mathcal{V}} \rho_y^{n+1} \overline{\left\{ \left[m_X + \Delta t S_1^{m_X} \right]_d^n + \Delta t \left(D_{cons}^{m_X} \right)^n \right\}}^r d\mathcal{V} = \int_{\mathcal{V}} \rho_y^n \overline{\left(m_X + \Delta t S_1^{m_X} \right)^n}^r d\mathcal{V}. \tag{10.78}$$

The resultant complication in evaluating $D_{cons}^{m_X}$ can be relatively easily handled by the Priestley algorithm. Another consequence, though, is that, rather than taking the simple form of (10.52), the second conservation corrector has to be defined such that

$$\overline{\left(m_X^{n+1} - \widetilde{m}_X^{(2)} \right)}^r = -\Delta t \left(\frac{\rho_y^{n+1} - \rho_y^n}{\rho_y^{n+1}} \right) \overline{\left[S_2^{m_X} \right]^*}^r. \tag{10.79}$$

Solution of this equation for $\left(m_X^{n+1} - \widetilde{m}_X^{(2)} \right)$ requires application of a boundary condition on m_X, either an upper boundary or a lower boundary condition, so that the remaining values may be evaluated recursively. At present the lower boundary condition that m_X is constant in the lowest layer could be used. Alternatively, the second conservation corrector could be written as $\left(m_X^{n+1} - \widetilde{m}_X^{(2)} \right) = \Delta t D2_{cons}^{m_X}$ and $D2_{cons}^{m_X}$ could be obtained in some variational manner so that the following equation is satisfied:

$$\int_{\mathcal{V}} \rho_y^{n+1} \overline{\left[\left(S_2^{m_X} \right)^* + D2_{cons}^{m_X} \right]}^r d\mathcal{V} = \int_{\mathcal{V}} \rho_y^n \overline{\left(S_2^{m_X} \right)^*}^r d\mathcal{V}. \tag{10.80}$$

However, an important complication with the conservation form of (10.74) is that the physics schemes, specifically the boundary-layer scheme, are not conservative even when written correctly in flux form. This can be seen by considering (10.34). The spatial discretisation of the scheme was not discussed previously but assuming that the eddy-diffusivity, $K_{m_{tot}}$ is co-located with density, on half-integer levels, then the only vertical averaging required is on the density in the denominator. With this added, (10.34) becomes:

$$\frac{m_{tot}^{**} - m_{tot}^n}{\Delta t} = \frac{1}{r^2 \overline{\rho_y^n}^r} \delta_r \left(\alpha_{BL} r^2 \rho_y^n K_{m_{tot}} \delta_r m_{tot}^{**} \right) + \frac{1}{r^2 \overline{\rho_y^n}^r} \delta_r \left[\left(1 - \alpha_{BL} \right) r^2 \rho_y^n K_{m_{tot}} \delta_r m_{tot}^n \right]$$

$$+\frac{\widetilde{m}_{tot}^{(P2b)} - m_{tot}^{n}}{\Delta t}. \tag{10.81}$$

Within the interior of the flow the boundary-layer scheme is a transport scheme and as such should not introduce any sources or sinks of moisture except at the upper or lower boundaries of the model. Therefore, in order for the scheme to have the correct conservative form, when the integral

$$\int_{\mathcal{V}} \rho_y^n \overline{\left(\frac{m_{tot}^{**} - m_{tot}^{n}}{\Delta t}\right)}^r d\mathcal{V} \tag{10.82}$$

is evaluated, i.e. a component of the boundary-layer contribution to the right-hand side of (10.69), it is required that the only sources or sinks due to the diffusive terms, the first two terms on the right-hand side of (10.81), arise from the boundary conditions. This will only be the case if the multiplying density in (10.82), ρ_y^n, cancels the density contributions that appear in the denominators of the diffusive terms in (10.81), $\overline{\rho_y^n}^r$. This is clearly not the case in general. If the alternative form of the conservation law were used, (10.73), then the boundary-layer scheme would in fact retain the correct conservative properties. But as discussed above, this approach has its own problems.

From this discussion it would appear that **the conservation of moisture cannot be exactly and consistently imposed in the New Dynamics.** On the one hand, if conservation were imposed in the form of (10.73), then the conservation procedure itself would lead to spurious sources and sinks of moisture simply to maintain an incorrect measure of mass conservation which the underlying numerical schemes do not 'see'. On the other hand, if conservation were imposed in the form of (10.74), then the boundary-layer scheme will introduce spurious sources and sinks of moisture in the interior of the flow.

The only way in which it is possible to conserve moisture correctly and consistently within the New Dynamics is to store moisture on the same levels as the density. The relatively simple, alternative approach to conservation suggested here would then hold without the need for spatial averaging of the appropriate variables and the physics schemes, too, would retain their correct conservative form.

10.7 Polar discretisation

The polar discretisation of the moisture equations is almost identical to that elsewhere. This is because horizontal derivatives only occur for horizontal advection of m_X and these are handled using the semi-Lagrangian procedures given in Section 5.

Uniqueness of m_X at the two poles is assumed, i.e.

$$(m_X)_{SP} \equiv (m_X)_{\frac{1}{2},\frac{1}{2}} \equiv (m_X)_{\frac{3}{2},\frac{1}{2}} \equiv (m_X)_{\frac{5}{2},\frac{1}{2}} \equiv ... \equiv (m_X)_{L-\frac{1}{2},\frac{1}{2}}\,, \tag{10.83}$$

$$(m_X)_{NP} \equiv (m_X)_{\frac{1}{2},M-\frac{1}{2}} \equiv (m_X)_{\frac{3}{2},M-\frac{1}{2}} \equiv (m_X)_{\frac{5}{2},M-\frac{1}{2}} \equiv ... \equiv (m_X)_{L-\frac{1}{2},M-\frac{1}{2}}. \tag{10.84}$$

11 Discretisation of the equation of state, total gaseous density, virtual potential temperature and absolute temperature.

11.1 Nonlinear continuous form of the equation of state

The nonlinear equation of state is

$$\Pi^{\frac{(\kappa_d-1)}{\kappa_d}}\theta_v\rho = \frac{p_0}{\kappa_d c_{pd}}, \tag{11.1}$$

where

$$\Pi = \left(\frac{p}{p_0}\right)^{\kappa_d}, \tag{11.2}$$

is Exner pressure.

The equation of state is a diagnostic relation between θ_v, ρ and Π. In (11.1), θ_v and ρ are quantities that are prognostically determined by the thermodynamic and continuity equations. Thus the role that the equation of state plays in the model is to diagnostically relate the Exner pressure Π to the prognostic quantities θ_v and ρ.

11.2 Linearised continuous form of the equation of state

The equation of state is nonlinear. To avoid a nonlinear coupling between the discretised equations at the new time level, the equation of state is linearised in terms of the time tendencies

$$\rho' \equiv \rho^{n+1} - \rho^n, \quad \theta_v' \equiv \theta_v^{n+1} - \theta_v^n, \quad p' \equiv p^{n+1} - p^n, \quad \Pi' \equiv \Pi^{n+1} - \Pi^n. \tag{11.3}$$

Aside :

This strategy should be revisited. Note that the equation of state can be written in logarithmic form and this provides a linear relation between logarithmic quantities. The thermodynamic and continuity equations can be written in logarithmic form, and the pressure gradient terms in the components of the momentum equation can be written in terms of the logarithm of pressure. The end result would be a set of weakly nonlinear equations in terms of logarithmic quantities, and these could be solved via an efficient iterative solver.

Eq. (11.1) is first rewritten as

$$\Pi\theta_v\rho = \frac{p_0}{\kappa_d c_{pd}}\Pi^{\frac{1}{\kappa_d}}, \tag{11.4}$$

which can be evaluated at time $(n+1)\,\Delta t$ and then simplified by the use of (11.2) to give

$$\kappa_d \Pi^{n+1}\theta_v^{n+1}\rho^{n+1} = \frac{p^{n+1}}{c_{pd}}. \tag{11.5}$$

Using (11.3) this can be rewritten in terms of quantities at time $n\Delta t$ and their time tendencies:

$$\kappa_d\left(\Pi^n + \Pi'\right)\left(\theta_v^n + \theta_v'\right)\left(\rho^n + \rho'\right) = \frac{p^n + p'}{c_{pd}}. \tag{11.6}$$

Expanding (11.6) *and neglecting products of primed quantities*(caution: just because they are primed quantities does not necessarily mean that they are small, particularly for large timesteps!) yields

$$\kappa_d\Pi^n\theta_v^n\rho' + \kappa_d\theta_v^n\rho^n\Pi' + \kappa_d\Pi^n\rho^n\theta_v' - \frac{p'}{c_{pd}} \approx \frac{p^n}{c_{pd}} - \kappa_d\Pi^n\theta_v^n\rho^n. \tag{11.7}$$

To eliminate p' in favour of Π' in (11.7), (11.3) is first introduced into the definition (11.2) of Exner pressure, which is evaluated evaluated at time $(n+1)\,\Delta t$, so that

$$\Pi^n + \Pi' = \left(\frac{p^n + p'}{p_0}\right)^{\kappa_d} = \left(\frac{p^n}{p_0}\right)^{\kappa_d}\left(1 + \frac{p'}{p^n}\right)^{\kappa_d} = \Pi^n\left(1 + \frac{p'}{p^n}\right)^{\kappa_d} \approx \Pi^n\left(1 + \frac{\kappa_d p'}{p^n}\right). \tag{11.8}$$

An additional approximation has been introduced into (11.8). The term $\left(1 + p'/p^n\right)^{\kappa_d}$ is approximated by the 1st two terms of its binomial expansion, viz. by $\left(1 + \kappa_d p'/p^n\right)$. From (11.8) it is seen that

$$p' \approx \frac{p^n\Pi'}{\kappa_d\Pi^n}. \tag{11.9}$$

Substitution of (11.9) into (11.7) then yields

$$\kappa_d\Pi^n\theta_v^n\rho' + \left(\kappa_d\theta_v^n\rho^n - \frac{p^n}{\kappa_d c_{pd}\Pi^n}\right)\Pi' + \kappa_d\Pi^n\rho^n\theta_v' \approx \frac{p^n}{c_{pd}} - \kappa_d\Pi^n\theta_v^n\rho^n. \tag{11.10}$$

If the equation of state were exactly satisfied at time $n\Delta t$, then the right hand side of (11.10) would be identically zero. In general this will not be the case in the model, partly due to the adoption of the above linearisation strategy. The discrepancy should however be no larger than the individual terms on the left hand side. The extent to which (11.10) is a good approximation to the equation of state (11.1) evaluated at $(n+1)\,\Delta t$, i.e. to

$$\left(\Pi^{n+1}\right)^{\frac{(\kappa_d - 1)}{\kappa_d}}\theta_v^{n+1}\rho^{n+1} = \frac{p_0}{\kappa_d c_{pd}}, \tag{11.11}$$

is determined by the ratio in (11.10) of the neglected nonlinear terms with respect to the retained primed ones.

11.3 Discretisation of the linearised equation of state at levels $k = 1/2,\ 3/2,\ldots,\ N-1/2$

Because of the Charney-Phillips vertical staggering of variables, (11.10) is discretely approximated in the model by

$$\kappa_d \Pi^n \overline{\theta_v^n}^r \rho' + \left(\kappa_d \overline{\theta_v^n}^r \rho^n - \frac{p^n}{\kappa_d c_{pd} \Pi^n} \right) \Pi' + \kappa_d \Pi^n \rho^n \overline{\theta_v'}^r = \frac{p^n}{c_{pd}} - \kappa_d \Pi^n \overline{\theta_v^n}^r \rho^n. \qquad (11.12)$$

The vertical averaging operator introduced in (11.12) is defined at levels $k = 1/2, 3/2, \ldots, N-1/2$ by:

$$\begin{aligned} \overline{F(r_k)}^r \equiv \overline{F_k}^r &= \frac{\left(r_k - r_{k-1/2}\right) F\left(r_{k+1/2}\right) + \left(r_{k+1/2} - r_k\right) F\left(r_{k-1/2}\right)}{r_{k+1/2} - r_{k-1/2}} \\ &\equiv \frac{\left(r_k - r_{k-1/2}\right) F_{k+1/2} + \left(r_{k+1/2} - r_k\right) F_{k-1/2}}{r_{k+1/2} - r_{k-1/2}}. \end{aligned} \qquad (11.13)$$

where k is the vertical grid index (Section 4 gives further details).

11.4 Discretisation of the definition of total gaseous density at levels $k = 1/2,\ 3/2,\ldots,\ N-1/2$

The definition (1.99) of total gaseous density ρ is

$$\rho = \rho_y \left(1 + m_v + m_{cl} + m_{cf}\right) = \rho_y \left(1 + \sum_{X=(v,cl,cf)} m_X\right), \qquad (11.14)$$

where ρ_y is dry density and m_X, $X = (v, cl, cf)$, are the mixing ratios of water vapour, cloud liquid water and cloud frozen water respectively.

Bearing in mind that m_X is held on levels that are staggered with respect to those on which ρ and ρ_y are held, this is written in discrete form at levels $k = 1/2,\ 3/2,\ldots,\ N-1/2$ as

$$\rho = \rho_y \overline{\left(1 + \sum_{X=(v,cl,cf)} m_X\right)}^r, \qquad (11.15)$$

where the vertical averaging operator $\overline{(\ )}^r$ is defined by (C.4) of Appendix A. Note that $\left.(m_X)\right|_{\eta_0} = \left.(m_X)\right|_{\eta_1}$ when computing $\overline{(1 + \sum m_X)}^r$ at level $k = 1/2$ in the assumed isentropic layer $[\eta_0, \eta_1]$ where $\theta_0 = \theta_1$.

To obtain a Helmholtz problem (see Section 6) for Π', a diagnostic relation is required between ρ' and ρ'_y, where

$$\Pi' \equiv \Pi^{n+1} - \Pi^n, \rho' \equiv \rho^{n+1} - \rho^n, \rho'_y \equiv \rho_y^{n+1} - \rho_y^n. \tag{11.16}$$

Evaluating (11.15) at time levels $n+1$ and n, and subtracting, gives

$$\begin{aligned}
\rho' &= \rho_y^{n+1}\overline{\left(1 + \sum_{X=(v,cl,cf)} m_X^{n+1}\right)}^r - \rho_y^n\overline{\left(1 + \sum_{X=(v,cl,cf)} m_X^n\right)}^r \\
&= \left(\rho_y^{n+1} - \rho_y^n\right)\overline{\left(1 + \sum_{X=(v,cl,cf)} m_X^{n+1}\right)}^r + \rho_y^n\left[\sum_{X=(v,cl,cf)} \overline{\left(m_X^{n+1} - m_X^n\right)}^r\right].
\end{aligned} \tag{11.17}$$

If m_X^{n+1}, $X = (v, cl, cf)$, were known, then (11.17) could be used to obtain the Helmholtz problem. However this is not the case since two moisture conservation steps (see Section 10.2) remain to be applied during back substitution (see Section 16). Consequently (11.17) is instead rewritten as

$$\rho' = \rho'_y\overline{\left(1 + \sum_{X=(v,cl,cf)} m_X^*\right)}^r + \rho_y^n\left[\sum_{X=(v,cl,cf)} \overline{\left(m_X^* - m_X^n\right)}^r\right]. \tag{11.18}$$

where

$$m_X^* = \widetilde{m}_X^{(P2)}, \tag{11.19}$$

is the latest-available value of m_X.

11.5 Discretisation of the definition of virtual potential temperature at levels $k = 1/2,\ 3/2, \ldots,\ N - 1/2$

From the definitions (2.75) and (2.83), the potential temperature θ, the virtual potential temperature θ_v, and the mixing ratios of water vapour m_v, cloud liquid water m_{cl}, and cloud frozen water m_{cf}, are related by

$$\theta_v = \theta\left(\frac{1 + \frac{1}{\varepsilon}m_v}{1 + m_v + m_{cl} + m_{cf}}\right) = \theta\left(\frac{1 + \frac{1}{\varepsilon}m_v}{1 + \sum_{X=(v,cl,cf)} m_X}\right). \tag{11.20}$$

To obtain a Helmholtz problem (see Section 14) for Π', a diagnostic relation is required between θ'_v and θ', where

$$\theta'_v \equiv \theta_v^{n+1} - \theta_v^n, \theta' \equiv \theta^{n+1} - \theta^n. \tag{11.21}$$

Evaluating (11.20) at time levels $n+1$ and n, and subtracting, gives

$$\theta'_v = \theta^{n+1}\left(\frac{1+\frac{1}{\varepsilon}m_v^{n+1}}{1+\sum_{X=(v,cl,cf)} m_X^{n+1}}\right) - \theta^n\left(\frac{1+\frac{1}{\varepsilon}m_v^{n}}{1+\sum_{X=(v,cl,cf)} m_X^{n}}\right). \tag{11.22}$$

This can be rewritten as

$$\theta'_v = \left(\theta^{n+1}-\theta^n\right)\left(\frac{1+\frac{1}{\varepsilon}m_v^{n+1}}{1+\sum_{X=(v,cl,cf)} m_X^{n+1}}\right) + \theta^n\left(\frac{1+\frac{1}{\varepsilon}m_v^{n+1}}{1+\sum_{X=(v,cl,cf)} m_X^{n+1}}\right) - \theta^n\left(\frac{1+\frac{1}{\varepsilon}m_v^{n}}{1+\sum_{X=(v,cl,cf)} m_X^{n}}\right). \tag{11.23}$$

If m_X^{n+1}, $X=(v,cl,cf)$, were known, then (11.22) could be used to obtain the Helmholtz problem. However this is not the case since two moisture conservation steps (see Section 10.2) remain to be applied during back substitution (see Section 16). Consequently (11.22) is instead rewritten as

$$\theta'_v = \theta'\left(\frac{1+\frac{1}{\varepsilon}m_v^{*}}{1+\sum_{X=(v,cl,cf)} m_X^{*}}\right) + \theta^n\left(\frac{1+\frac{1}{\varepsilon}m_v^{*}}{1+\sum_{X=(v,cl,cf)} m_X^{*}}\right) - \theta^n\left(\frac{1+\frac{1}{\varepsilon}m_v^{n}}{1+\sum_{X=(v,cl,cf)} m_X^{n}}\right), \tag{11.24}$$

where

$$m_X^* = \widetilde{m}_X^{(P2)}, \tag{11.25}$$

is the latest-available value of m_X.

Eq. (11.24) is the pointwise discretisation of the definition of virtual potential temperature that is used in the derivation of the Helmholtz problem, and it is consistent (see Sections 6, 7 and 16) with the pointwise definition used in the three components of the momentum equation and, equivalently, at the back-substitution step.

11.6 Discretisation of the definition of absolute temperature at levels $k = 1, 2, \ldots, N$

The absolute temperature T is not required explicitly in the dynamics. However, it is required for the evaluation of the forcing, or "physics", terms. Specifically it is required by the boundary-layer scheme (BL^X of Sections 6, 9 and 10) and by the radiation scheme (R^θ_{rad} of Section 9). [Note that here only the evaluation of T at the levels $k=1,2,...,N$ is described since, where required, the surface value of absolute temperature ($k=0$) is evaluated from the physics surface energy balance scheme.] The value of T at time level $n+1$ is diagnosed from Π^{n+1} and θ^{n+1} as:

$$T^{n+1} = \theta^{n+1}\Pi^{n+1}. \tag{11.26}$$

Spatially, T^{n+1} is co-located with θ^{n+1} and so it is staggered, in the vertical, with respect to Π^{n+1}. Therefore, evaluation of (11.26) requires an estimate of Π^{n+1} at the (integer) θ-levels, denoted here as Π_θ^{n+1}. This is evaluated as the usual linear average of Π in the vertical. However, since an estimate for Π_θ^{n+1} on the top model level, $k = N$, is needed, an estimate has to be made of Π^{n+1} above the top model level, at an imaginary level, $k = N + 1/2$. This is done as follows:

- $\Pi^{n+1}\big|_{N+1/2}$ is obtained by estimating the value of the change in the vertical gradient of Π over a time step at the top model level, $\delta_r \Pi'|_N$, where $\Pi' \equiv \Pi^{n+1} - \Pi^n$. Then, $\Pi^{n+1}\big|_{N+1/2}$ is estimated as

$$\Pi^{n+1}\big|_{N+1/2} = \Pi^n|_{N+1/2} + \Pi'|_{N+1/2} = \Pi^n|_{N+1/2} + \Pi'|_{N-1/2} + \left(r_{N+1/2} - r_{N-1/2}\right) \delta_r \Pi'|_N . \tag{11.27}$$

  Currently $\delta_r \Pi'|_N$ is simply approximated as being 0. Then (11.27) reduces to:

$$\Pi^{n+1}\big|_{N+1/2} = \Pi^n|_{N+1/2} + \Pi'|_{N-1/2} . \tag{11.28}$$

  Note that equation (11.28) is equivalent to the diagnostic assumption that $\delta_r \Pi^{n+1}\big|_N =$ constant where the constant is determined from the initial data (see below).

- An initial value, $\Pi^0|_{N+1/2}$ is required to start the above procedure, where a superscript of 0 is used to indicate an initial value. The initial Exner field is obtained by assuming it is in hydrostatic balance with the initial, observed virtual temperature field, T_v^0. Therefore, for $k = 1, 2, ..., N$, the hydrostatic equation is written in the form:

$$\delta_r \Pi^0\big|_k = -\frac{g \overline{\Pi^0}^r}{c_{pd}\, T_v^0\big|_k}, \tag{11.29}$$

  where, see Appendix C,

$$\overline{\Pi^0}^r \equiv \frac{\left(r_k - r_{k-1/2}\right) \Pi^0|_{k+1/2} + \left(r_{k+1/2} - r_k\right) \Pi^0|_{k-1/2}}{r_{k+1/2} - r_{k-1/2}}. \tag{11.30}$$

  Solving (11.29) for $\Pi^0|_{k+1/2}$ leads to:

$$\Pi^0\big|_{k+1/2} = \Pi^0\big|_{k-1/2} - \frac{g\ \Pi_\theta^0|_k}{c_{pd}\, T_v^0\big|_k} \left(r_{k+1/2} - r_{k-1/2}\right), \tag{11.31}$$

  where

$$\Pi_\theta^0\big|_k \equiv \frac{\Pi^0\big|_{k-1/2}}{1 + g\left(r_k - r_{k-1/2}\right) \big/ \left(c_{pd}\, T_v^0\big|_k\right)}, \tag{11.32}$$

for $k = 1, 2, ..., N$. Note that $\Pi_\theta^0|_k$ is an estimate for $\Pi^0|_k$ which would be obtained by a one-sided approximation to (11.29). Applying (11.31) at $k = N$, it can be seen that (11.28) is equivalent to assuming

$$\delta_r \Pi^{n+1}\big|_N = -\frac{g\ \Pi_\theta^0|_N}{c_{pd}\ T_v^0|_N}. \tag{11.33}$$

Aside :

To be consistent with the dynamics $\delta_r \Pi'|_N$ *should be estimated from the vertical momentum equation,* (7.30)*, applied at the top level of the model where* $w \equiv 0$*, and therefore also* $w' \equiv 0$*. This gives:*

$$\delta_r \Pi'|_N = \left[(\alpha_4 \Delta t c_{pd} \theta_v^*)^{-1} R_w^+ \right]\big|_N , \tag{11.34}$$

where (7.31) *and* (7.32) *have been used. Given that an estimate of* $\delta_r \Pi^n|_N$ *will be available from the procedure described here applied at the previous time step, all terms needed to evaluate the right-hand side of* (11.34)*, including* $R_w^+|_N$*, see* (7.26)-(7.27)*, are available except for terms involving the vertical average of the horizontal velocities,* $\overline{u}^r$ *and* $\overline{v}^r$*. However, it would seem reasonable to evaluate these terms by assuming there is no vertical wind shear across the top level of the model. At present though no attempt is made to evaluate* $R_w^+|_N$ *and, as noted above, it is simply approximated as being* 0 *so that* $\delta_r \Pi'|_N = 0$ *also. Also as noted above this is equivalent to assuming that*

$$\delta_r \Pi^{n+1}\big|_N = -\frac{g\ \Pi_\theta^0|_N}{c_{pd}\ T_v^0|_N}, \tag{11.35}$$

which can also be viewed as equivalent to making the hydrostatic approximation but neglecting the time rate-of-change of the potential temperature. For climate simulations, for which there is often considerable spin-up from the initial conditions and in which there may be large temperature changes between winter and summer, especially in the region of the poles, this procedure may lead to errors and even a climate drift. An obvious potential improvement would be to simply make the proper hydrostatic approximation at every time step, which, in terms of θ_v *instead of* Π/T_v*, would give*

$$\delta_r \Pi^{n+1}\big|_N = -\frac{g}{c_{pd}\ \theta_v^{n+1}|_N}, \tag{11.36}$$

and should be a better approximation to the correct solution, (11.34)*, than* (11.28) *whilst still retaining the simplicity of* (11.28)*.*

Having obtained values for Π^{n+1} at the levels $k = 1/2, 3/2 ... N - 1/2, N + 1/2$, they are then averaged linearly (see Appendix C) onto θ-levels to give:

$$\Pi_\theta^{n+1}\Big|_k = \overline{\left(\Pi^{n+1}\right)}^r\Big|_k \equiv \frac{\left(r_k - r_{k-1/2}\right) \Pi^{n+1}\big|_{k+1/2} + \left(r_{k+1/2} - r_k\right) \Pi^{n+1}\big|_{k-1/2}}{r_{k+1/2} - r_{k-1/2}}, \; k = 1, 2 ..., N, \tag{11.37}$$

from which T^{n+1}, at $k = 1, ... N$, is finally evaluated by application of (11.26) as:

$$T^{n+1} = \theta^{n+1} \Pi_\theta^{n+1}. \tag{11.38}$$

Aside :

In order to evaluate $\overline{\left(\Pi^{n+1}\right)}^r\Big|_N$ *a value has to be assigned to the height,* $r_{i,j,k}$*, of the imaginary level,* $k = N+1/2$*. This is currently set so that the top model level,* $r_{i,j,N}$*, lies exactly half way between* $r_{i,j,N+1/2}$ *and* $r_{i,j,N-1/2}$*. This has the simplifying implication that the weights, used in the linear averaging of* $\Pi^{n+1}\big|_{N+1/2}$ *and* $\Pi^{n+1}\big|_{N-1/2}$ *to form* $\overline{\Pi}^r\Big|_N$*, are equal to* 1/2*.*

To summarise the above procedure: at the interior levels, $k = 1, 2, ... N - 1$, the absolute temperature, T^{n+1}, is evaluated as:

$$T^{n+1} = \theta^{n+1} \overline{\Pi^{n+1}}^r, \tag{11.39}$$

whilst at the top level, $k = N$, it is evaluated as:

$$T^{n+1}\Big|_N = \theta^{n+1}\Big|_N \left[\frac{1}{2}\left(\Pi^n\big|_{N+1/2} + \Pi'\big|_{N-1/2} + \Pi^{n+1}\big|_{N-1/2}\right)\right]. \tag{11.40}$$

Aside :

Whilst (11.40) *corresponds to how the procedure has been coded in the model, the diagnostic nature of* (11.40) *can be seen by using* (11.33)*, which leads to:*

$$T^{n+1}\Big|_N = \theta^{n+1}\Big|_N \left(\Pi^{n+1}\Big|_{N-1/2} - \frac{g\, \Pi_\theta^0\big|_N}{2c_{pd}\, T_v^0\big|_N}\left(r_{N+1/2} - r_{N-1/2}\right)\right), \tag{11.41}$$

with $\Pi_\theta^0\big|_k$ *given by* (11.32)*.*

12 Horizontal diffusion and polar filtering

Generally, explicit diffusion is added to numerical weather and climate prediction models for one, or both, of two reasons.

The first reason is to represent unresolved, subgrid scale mixing processes. The primary process is usually (though not exclusively) turbulence within the boundary layer and, in the large scale models, this is represented by vertical diffusion (in the New Dynamics the boundary-layer diffusion is in the vertical r-direction, rather than in the slope normal direction). Arguments can be made though that there is some non-zero mixing in the horizontal due to unresolved processes and as the horizontal resolution decreases this will become more of an issue (small scale process models tend always to employ fully three-dimensional turbulence parametrisations). This latter view leads, in addition to the vertical boundary-layer diffusion, to the inclusion of horizontal diffusion. In this Section only diffusion which is in addition to the boundary-layer turbulence parametrisation is considered.

The second reason is to control accumulation of noise and energy at the grid scale. This may arise from a physical cascade of energy from larger to smaller scales but may also be due to numerical misrepresentation of non-linear interactions (aliasing). It can also arise from grid scale forcing from the physics or from surface boundary conditions (the so-called ancillary fields, such as orography, land-sea mask, hydrology etc.). The resultant diffusion is normally restricted to be in the horizontal, as there is usually sufficient physical (turbulence parametrisation) or implicit numerical diffusion to control such noise in the vertical direction.

Whichever view of diffusion is taken, it has to be decided whether it is to be applied along physically horizontal surfaces (surfaces of constant r) or along horizontal coordinate surfaces (surfaces of constant η). Which it should be is not at all clear. If it is genuinely an attempt to represent subgrid-scale effects, in addition to those currently represented by the boundary-layer scheme, then it would seem sensible that it should operate orthogonally to the boundary-layer scheme. For the New Dynamics then, this would imply diffusion along surfaces of constant r. As will be seen below, this would have certain advantages. On the other hand if it is purely numerical a more pragmatic approach may be justified and diffusion along η-surfaces may suffice. This is the approach currently taken in the New Dynamics.

Various possible approaches are discussed below and that currently used in the New Dynamics is detailed. Discussion starts with the diffusion operator for scalars before the complications associated with diffusion of vector quantities are considered.

12.1 The scalar diffusion operator in r-coordinates

Consider a general scalar, Q, then the full three-dimensional diffusion operator in r-coordinates, $D^r_{3D}(Q)$ (where the superscript r indicates that the operator is written in terms of the r-coordinate and the subscript $3D$ indicates that it is the full three-dimensional operator), is given by:

$$\begin{aligned} D^r_{3D}(Q) &\equiv \sum_{i=1}^{3} \frac{\partial}{\partial x_i}\left(K_i \frac{\partial Q}{\partial x_i}\right) \\ &= \frac{1}{r\cos\phi}\frac{\partial}{\partial\lambda}\left(\frac{K_\lambda}{r\cos\phi}\frac{\partial Q}{\partial\lambda}\right) + \frac{1}{r\cos\phi}\frac{\partial}{\partial\phi}\left(\frac{K_\phi\cos\phi}{r}\frac{\partial Q}{\partial\phi}\right) + \frac{1}{r^2}\frac{\partial}{\partial r}\left(r^2 K_r\frac{\partial Q}{\partial r}\right), \\ &= \frac{1}{r^2}\frac{\partial}{\partial\lambda}\left(\frac{K_\lambda}{\cos^2\phi}\frac{\partial Q}{\partial\lambda}\right) + \frac{1}{r^2\cos\phi}\frac{\partial}{\partial\phi}\left(K_\phi\cos\phi\frac{\partial Q}{\partial\phi}\right) + \frac{1}{r^2}\frac{\partial}{\partial r}\left(r^2 K_r\frac{\partial Q}{\partial r}\right), \end{aligned} \quad (12.1)$$

where K_λ, K_ϕ and K_r are the coefficients of diffusion in the λ, ϕ and r directions, respectively. Isotropic diffusion is obtained by setting $K_\lambda = K_\phi = K_r$.

Consider the global volume integral, calculated in r-coordinates, V^r, of the operator $D^r_{3D}(Q)$:

$$V^r\left[D^r_{3D}(Q)\right] \equiv \int_{\lambda=0}^{\lambda=2\pi}\int_{\phi=-\pi/2}^{\phi=+\pi/2}\int_{r=r_S(\lambda,\phi)}^{r=r_T} D^r_{3D}(Q) r^2\cos\phi\, dr d\lambda d\phi. \quad (12.2)$$

Note the identity, for arbitrary F and constant r_T, that

$$\int_{r=r_S(\lambda,\phi)}^{r=r_T} \frac{\partial F}{\partial\lambda}dr \equiv \left(F\frac{\partial r}{\partial\lambda}\right)_{r=r_s} + \frac{\partial}{\partial\lambda}\left(\int_{r=r_S(\lambda,\phi)}^{r=r_T} F dr\right), \quad (12.3)$$

and similarly with $\partial/\partial\lambda$ replaced by $\partial/\partial\phi$. Then, using periodicity in the λ-direction and the fact that $\cos\phi$ vanishes at both poles, (12.2) with D^r_{3D} in the form (12.1) becomes:

$$\begin{aligned} V^r\left[D^r_{3D}(Q)\right] &= \int_{\lambda=0}^{\lambda=2\pi}\int_{\phi=-\pi/2}^{\phi=+\pi/2}\left(r^2\cos\phi K_r\frac{\partial Q}{\partial r}\right)_{r=r_T} d\lambda d\phi \\ &\quad - \int_{\lambda=0}^{\lambda=2\pi}\int_{\phi=-\pi/2}^{\phi=+\pi/2}\left(r^2\cos\phi K_r\frac{\partial Q}{\partial r} - \frac{K_\lambda}{\cos\phi}\frac{\partial Q}{\partial\lambda}\frac{\partial r}{\partial\lambda} - K_\phi\cos\phi\frac{\partial Q}{\partial\phi}\frac{\partial r}{\partial\phi}\right)_{r=r_S} d\lambda d\phi. \end{aligned} \quad (12.4)$$

By comparison with the case when the three coefficients of diffusion, K_λ, K_ϕ, and K_r, are all equal, the case of isotropic diffusion, the right-hand side of (12.1) can be written informally as $\nabla.(K\nabla Q)$ so that $K\nabla Q$ can be identified as the diffusive flux of Q given by

$$\left(\frac{K_\lambda}{r\cos\phi}\frac{\partial Q}{\partial\lambda}, \frac{K_\phi}{r}\frac{\partial Q}{\partial\phi}, K_r\frac{\partial Q}{\partial r}\right), \quad (12.5)$$

and the outward normal surface element, $d\mathbf{S}$, is

$$d\mathbf{S} = -r^2\cos\phi\left(-\frac{1}{r\cos\phi}\frac{\partial r}{\partial\lambda}, -\frac{1}{r}\frac{\partial r}{\partial\phi}, 1\right)d\lambda d\phi, \tag{12.6}$$

at the lower surface, $r = r_S$, and

$$d\mathbf{S} = r^2\cos\phi\,(0,0,1)\,d\lambda d\phi, \tag{12.7}$$

at the upper surface, $r = r_T$. Therefore (12.4) simply reflects the divergence theorem:

$$\int\int\int \nabla.\,(K\nabla Q)\,dV = \int\int K\nabla Q.d\mathbf{S}. \tag{12.8}$$

Thus, if the diffusive flux normal to the bounding upper (the first bracketed term on the right-hand side of (12.4)) and lower surfaces (the second bracketed term on the right-hand side of (12.4)) vanishes, then the global, volume integral of $D^r_{3D}(Q)$ vanishes and the diffusion operator has no net effect on the volume average of the quantity Q.

If this diffusion is viewed as a numerical artifact then it is clear that it should have no net effect on the global integral of a physically conserved quantity. Imposition of zero surface fluxes suffices to ensure this constraint is met. However, if the diffusion is viewed as a physical process then this will not necessarily be the case unless *all* surface fluxes (including the horizontal component of slope normal fluxes) are accounted for in the boundary-layer parametrisation. This is not currently the case in the New Dynamics over non-zero slopes as the boundary-layer scheme acts only in the r-direction.

Aside :

For moisture variables, such as the mixing ratio, the globally conserved quantity is the product of the mixing ratio and the density of the dry air. Since the density varies with position it will not in general commute with the diffusion operator, $D^r_{3D}(Q)$. Therefore, if $D^r_{3D}(Q)$ is designed to conserve Q, so that the global volume integral of $\rho D^r_{3D}(Q)$ vanishes, the integral of $\rho D^r_{3D}(Q)$ will, in general, not do so. Therefore, for quantities for which there is a conservation principle, it is important that the conservative diffusion operator acts on the conserved quantity. In particular for the example of mixing ratio, conservative diffusion should act on the product of the dry density and the mixing ratio. At present in the New Dynamics this is not the case, diffusion acts on the moisture variable directly.

12.1.1 Diffusion along surfaces of constant r, in r-coordinates

Diffusion along surfaces of constant r, denoted by $D_r^r(Q)$, is obtained by dropping partial derivatives with respect to r in (12.1), or equivalently by setting $K_r = 0$, and is given by:

$$\begin{aligned} D_r^r(Q) &= \frac{1}{r\cos\phi}\frac{\partial}{\partial\lambda}\left(\frac{K_\lambda}{r\cos\phi}\frac{\partial Q}{\partial\lambda}\right) + \frac{1}{r\cos\phi}\frac{\partial}{\partial\phi}\left(\frac{K_\phi\cos\phi}{r}\frac{\partial Q}{\partial\phi}\right), \\ &= \frac{1}{r^2}\frac{\partial}{\partial\lambda}\left(\frac{K_\lambda}{\cos^2\phi}\frac{\partial Q}{\partial\lambda}\right) + \frac{1}{r^2\cos\phi}\frac{\partial}{\partial\phi}\left(K_\phi\cos\phi\frac{\partial Q}{\partial\phi}\right). \end{aligned} \tag{12.9}$$

From (12.4) with K_r set equal to zero, this operator preserves the global, volume average property of $D_{3D}^r(Q)$ (i.e. that $V^r\left[D_r^r(Q)\right] = 0$) if

$$\left(\frac{K_\lambda}{\cos\phi}\frac{\partial Q}{\partial\lambda}\frac{\partial r}{\partial\lambda} + K_\phi\cos\phi\frac{\partial Q}{\partial\phi}\frac{\partial r}{\partial\phi}\right)_{r=r_S} = 0. \tag{12.10}$$

12.2 Diffusion in η-coordinates

Transforming (12.1) into the model's η-coordinates gives:

$$\begin{aligned} D_{3D}^\eta(Q) \equiv\; & \frac{1}{r^2}\frac{\partial}{\partial\lambda}\left[\frac{K_\lambda}{\cos^2\phi}\left(\frac{\partial Q}{\partial\lambda} - \frac{\partial\eta}{\partial r}\frac{\partial r}{\partial\lambda}\frac{\partial Q}{\partial\eta}\right)\right] \\ & -\frac{1}{r^2}\frac{\partial\eta}{\partial r}\frac{\partial r}{\partial\lambda}\frac{\partial}{\partial\eta}\left[\frac{K_\lambda}{\cos^2\phi}\left(\frac{\partial Q}{\partial\lambda} - \frac{\partial\eta}{\partial r}\frac{\partial r}{\partial\lambda}\frac{\partial Q}{\partial\eta}\right)\right] \\ & +\frac{1}{r^2\cos\phi}\frac{\partial}{\partial\phi}\left[K_\phi\cos\phi\left(\frac{\partial Q}{\partial\phi} - \frac{\partial\eta}{\partial r}\frac{\partial r}{\partial\phi}\frac{\partial Q}{\partial\eta}\right)\right] \\ & -\frac{1}{r^2\cos\phi}\frac{\partial\eta}{\partial r}\frac{\partial r}{\partial\phi}\frac{\partial}{\partial\eta}\left[K_\phi\cos\phi\left(\frac{\partial Q}{\partial\phi} - \frac{\partial\eta}{\partial r}\frac{\partial r}{\partial\phi}\frac{\partial Q}{\partial\eta}\right)\right] \\ & +\frac{1}{r^2}\frac{\partial\eta}{\partial r}\frac{\partial}{\partial\eta}\left(r^2K_r\frac{\partial\eta}{\partial r}\frac{\partial Q}{\partial\eta}\right). \end{aligned} \tag{12.11}$$

Noting that for general F

$$\frac{\partial F}{\partial\lambda} - \frac{\partial\eta}{\partial r}\frac{\partial r}{\partial\lambda}\frac{\partial F}{\partial\eta} \equiv \frac{\partial\eta}{\partial r}\left[\frac{\partial}{\partial\lambda}\left(\frac{\partial r}{\partial\eta}F\right) - \frac{\partial}{\partial\eta}\left(\frac{\partial r}{\partial\lambda}F\right)\right], \tag{12.12}$$

(12.11) can be written in the alternative, equivalent form:

$$\begin{aligned} D_{3D}^\eta(Q) \equiv\; & \left(\frac{1}{r^2}\frac{\partial\eta}{\partial r}\right)\Bigg(\frac{\partial}{\partial\lambda}\left\{\frac{K_\lambda}{\cos^2\phi}\left[\frac{\partial}{\partial\lambda}\left(\frac{\partial r}{\partial\eta}Q\right) - \frac{\partial}{\partial\eta}\left(\frac{\partial r}{\partial\lambda}Q\right)\right]\right\} \\ & -\frac{\partial}{\partial\eta}\left\{\frac{\partial r}{\partial\lambda}\frac{\partial\eta}{\partial r}\frac{K_\lambda}{\cos^2\phi}\left[\frac{\partial}{\partial\lambda}\left(\frac{\partial r}{\partial\eta}Q\right) - \frac{\partial}{\partial\eta}\left(\frac{\partial r}{\partial\lambda}Q\right)\right]\right\} \\ & +\frac{1}{\cos\phi}\frac{\partial}{\partial\phi}\left\{K_\phi\cos\phi\left[\frac{\partial}{\partial\phi}\left(\frac{\partial r}{\partial\eta}Q\right) - \frac{\partial}{\partial\eta}\left(\frac{\partial r}{\partial\phi}Q\right)\right]\right\} \\ & -\frac{1}{\cos\phi}\frac{\partial}{\partial\eta}\left\{\frac{\partial r}{\partial\phi}\frac{\partial\eta}{\partial r}K_\phi\cos\phi\left[\frac{\partial}{\partial\phi}\left(\frac{\partial r}{\partial\eta}Q\right) - \frac{\partial}{\partial\eta}\left(\frac{\partial r}{\partial\phi}Q\right)\right]\right\} \\ & +\frac{\partial}{\partial\eta}\left(r^2K_r\frac{\partial\eta}{\partial r}\frac{\partial Q}{\partial\eta}\right)\Bigg). \end{aligned} \tag{12.13}$$

This form more naturally preserves, in the η-coordinate system, the flux form of the diffusion operator.

The global, volume integral, calculated in η-coordinates, V^{η}, of the operator $D_{3D}^{\eta}(Q)$, is defined as:

$$V^{\eta}\left[D_{3D}^{\eta}(Q)\right] \equiv \int_{\lambda=0}^{\lambda=2\pi} \int_{\phi=-\pi/2}^{\phi=+\pi/2} \int_{\eta=0}^{\eta=1} D_{3D}^{\eta}(Q) r^2 \frac{\partial r}{\partial \eta} \cos\phi d\eta d\lambda d\phi. \tag{12.14}$$

From (12.13) it is clear that

$$\begin{aligned} V^{\eta}\left[D_{3D}^{\eta}(Q)\right] &= \int_{\lambda=0}^{\lambda=2\pi} \int_{\phi=-\pi/2}^{\phi=+\pi/2} \left(r^2 \cos\phi K_r \frac{\partial \eta}{\partial r} \frac{\partial Q}{\partial \eta} \right)_{\eta=1} d\lambda d\phi \\ &\quad - \int_{\lambda=0}^{\lambda=2\pi} \int_{\phi=-\pi/2}^{\phi=+\pi/2} \left\{ r^2 \cos\phi K_r \frac{\partial \eta}{\partial r} \frac{\partial Q}{\partial \eta} \right. \\ &\quad - \frac{\partial r}{\partial \lambda} \frac{\partial \eta}{\partial r} \frac{K_\lambda}{\cos\phi} \left[\frac{\partial}{\partial \lambda} \left(\frac{\partial r}{\partial \eta} Q \right) - \frac{\partial}{\partial \eta} \left(\frac{\partial r}{\partial \lambda} Q \right) \right] \\ &\quad \left. - \frac{\partial r}{\partial \phi} \frac{\partial \eta}{\partial r} K_\phi \cos\phi \left[\frac{\partial}{\partial \phi} \left(\frac{\partial r}{\partial \eta} Q \right) - \frac{\partial}{\partial \eta} \left(\frac{\partial r}{\partial \phi} Q \right) \right] \right\}_{\eta=0} d\lambda d\phi, \end{aligned} \tag{12.15}$$

which is simply the transformed version of (12.4). Therefore, as is to be expected, the global integral of $D_{3D}^{\eta}(Q)$ vanishes if the surface normal diffusive fluxes at the top and bottom of the domain vanish, exactly as for $D_{3D}^{r}(Q)$.

12.2.1 Diffusion along surfaces of constant r, in η-coordinates

Diffusion along surfaces of constant r, denoted by $D_r^{\eta}(Q)$, can be obtained by simply setting $K_r = 0$ in (12.13) (this does not afford much simplification of the equation though and so it is not reproduced here). This operator preserves the zero volume integral property (i.e. $V^{\eta}\left[D_r^{\eta}(Q)\right] = 0$) if

$$\left\{ \frac{\partial r}{\partial \lambda} \frac{K_\lambda}{\cos\phi} \left[\frac{\partial}{\partial \lambda} \left(\frac{\partial r}{\partial \eta} Q \right) - \frac{\partial}{\partial \eta} \left(\frac{\partial r}{\partial \lambda} Q \right) \right] + \frac{\partial r}{\partial \phi} K_\phi \cos\phi \left[\frac{\partial}{\partial \phi} \left(\frac{\partial r}{\partial \eta} Q \right) - \frac{\partial}{\partial \eta} \left(\frac{\partial r}{\partial \phi} Q \right) \right] \right\}_{\eta=0} = 0. \tag{12.16}$$

Due to the fact that (12.13) is written in a flux form, the application of this boundary condition to (12.13) with $K_r = 0$, is straightforward, at least for variables stored on half levels, i.e. those which are stored half a grid length above the surface $\eta = 0$. In this case, the boundary condition, (12.16), is applied by simply setting this quantity to zero where it is used in the discretised form of (12.13). Whilst (12.13) has a more complicated form than the two options currently available in the New Dynamics (see Sections 12.2.2 and 12.3), the property of being able to diffuse along r-surfaces quite naturally even in the presence of orography (see Section 12.4.4) is quite appealing and should be given further consideration.

12.2.2 Diffusion along surfaces of constant η, in η-coordinates

There is an issue as to how to derive the diffusion operator along an η-surface. By starting with (12.11) and dropping all derivatives with respect to η, a diffusion operator along surfaces or "levels" results. This operator does preserve the *surface integral* of the diffused quantity. However, the volume element has the form $r^2 \partial r/\partial\eta \cos\phi d\eta d\lambda d\phi$, and this operator has nothing to cancel the $\partial r/\partial\eta$ term (it has no information regarding the physical thicknesses of the model layers). This, together with the fact that it is not in flux form, means that it does not preserve the *global volume integral* of the diffused quantity. It is therefore not conservative. To derive an operator which does preserve the global volume integral, and is therefore conservative, the operator is first written in flux form, (12.13), and then all partial derivatives with respect to η are neglected, except for metric terms, $\partial r/\partial\eta$ and $\partial\eta/\partial r$. This approach gives a diffusion operator, denoted by $D^\eta_\eta(Q)$, along "layers" and it takes the form:

$$D^\eta_\eta(Q) = \left(\frac{1}{r^2}\frac{\partial\eta}{\partial r}\right)\left\{\frac{\partial}{\partial\lambda}\left[\frac{K_\lambda}{\cos^2\phi}\frac{\partial}{\partial\lambda}\left(\frac{\partial r}{\partial\eta}Q\right)\right] + \frac{1}{\cos\phi}\frac{\partial}{\partial\phi}\left[K_\phi\cos\phi\frac{\partial}{\partial\phi}\left(\frac{\partial r}{\partial\eta}Q\right)\right]\right\}. \quad (12.17)$$

It is the fact that this operator diffuses along "layers" rather than "levels" which leads to it preserving the global volume integral property. (Here, a level is the model surface, of vanishing thickness, defined by $\eta = \eta_k$, whereas a layer is defined as the volume lying between the staggered η surfaces which bound that level, and is therefore defined by $\eta_{k-1/2} < \eta < \eta_{k+1/2}$.) This operator is now optionally available in the New Dynamics and is colloquially known as the "conserving" option.

In contrast to D^η_r, the operator D^η_η identically preserves the global volume integral property, i.e. $V^\eta\left[D^\eta_\eta(Q)\right] = 0$, without any further restraint on Q. In this regard it might be argued that this is an inappropriate form for a physically based diffusion operator if non-zero, horizontal surface fluxes are to be applied!

12.3 The New Dynamics horizontal diffusion operator

The horizontal diffusion operator, $D^{\eta}_{ND}(Q)$, originally used in the New Dynamics and still optionally available (colloquially known as the "non-conserving" option) is given by:

$$D^{\eta}_{ND}(Q) = \frac{1}{r^2}\left[\frac{\partial}{\partial\lambda}\left(\frac{K_\lambda}{\cos^2\phi}\frac{\partial Q}{\partial\lambda}\right) + \frac{\partial}{\partial\phi}\left(K_\phi\frac{\partial Q}{\partial\phi}\right)\right]. \tag{12.18}$$

This is the same as D^{η}_{η} except the metric terms, $\partial\eta/\partial r$ and $\partial r/\partial\eta$, have been dropped (equivalent to neglecting the variation of $\partial r/\partial\eta$ in the λ- and ϕ-directions) and the $\cos\phi$ terms associated with the ϕ part of the operator have been neglected. Either of these approximations is sufficient to ensure that this form of the operator does not, in general, preserve the global volume integral property. That is, there is no natural constraint on the fluxes of Q which ensures that $V^{\eta}\left[D^{\eta}_{ND}(Q)\right] = 0$.

If the $\cos\phi$ terms were reintroduced into (12.18), then the resulting operator could equivalently be obtained from the form of D^{η}_{3D} given by (12.11) and neglecting *all* partial derivatives with respect to η, including the metric terms $\partial\eta/\partial r$ and $\partial r/\partial\eta$. Again $V^{\eta}\left[D^{\eta}_{ND}(Q)\right] \neq 0$. By approximating this form of the operator (12.11), rather than the more natural flux form, (12.13), the global volume integral property is lost (except in the special case of the absence of any orography at all when $\partial r/\partial\eta$ is independent of λ and ϕ).

It is therefore recommended that in the New Dynamics the operator $D^{\eta}_{ND}(Q)$, given by (12.18), be definitively abandoned in favour of D^{η}_{η}, given by (12.17). This is targeted for UM6.1.

12.4 Setting K_λ and K_ϕ

12.4.1 Stability issues

A somewhat separate issue to the discussion on the choice of operator, is the choice of the value of K_λ compared with that of K_ϕ. Ideally K_λ would be chosen equal to K_ϕ, thereby giving a locally isotropic form of diffusion. However, the diffusion operator is currently discretised in an explicit fashion, i.e. the value of Q used in the operator is that available at the present time step. This leads to an upper limit on the time step, Δt, required to prevent this scheme, in isolation, being numerically unstable. K_λ is therefore chosen to mitigate the impact of this restriction. The details of the stability analysis and the consequences are given below.

The stability analysis for the preferred ("conserving") diffusion operator, D_η^η, is complicated by the presence of the $\cos\phi$ factor multiplying K_ϕ in (12.17). In order to make the problem tractable the analysis is carried out locally so that $\cos\phi$ can be assumed to be approximately constant over the region of interest, a "frozen" approximation. Once this approximation is made, and in the absence of orography so that $\partial r/\partial\eta$ is independent of λ and ϕ, the two forms of diffusion operator, D_η^η and D_{ND}^η, are equivalent and the following analysis and discussion hold for both operators. In both cases:

$$\frac{\partial Q}{\partial t} \simeq \frac{1}{r^2}\left[\frac{\partial}{\partial\lambda}\left(\frac{K_\lambda}{\cos^2\phi}\frac{\partial Q}{\partial\lambda}\right) + \frac{\partial}{\partial\phi}\left(K_\phi\frac{\partial Q}{\partial\phi}\right)\right], \tag{12.19}$$

this equation being exact for D_{ND}^η.

<u>Aside :</u>

An idea of the stability requirements for the fully isotropic spherical case, without the above approximation, can be found by keeping the spatial derivatives continuous and only discretising the temporal aspects of (12.17). *Then* (12.17), *with* $K_\lambda = K_\phi = \mathrm{K}$, *a constant, becomes:*

$$\frac{Q^{n+1} - Q^n}{\Delta t} = \frac{K}{r^2}\left[\frac{\partial}{\partial\lambda}\left(\frac{1}{\cos^2\phi}\frac{\partial Q^n}{\partial\lambda}\right) + \frac{1}{\cos\phi}\frac{\partial}{\partial\phi}\left(\cos\phi\frac{\partial Q^n}{\partial\phi}\right)\right]. \tag{12.20}$$

In this case, Q can be expanded in terms of spherical harmonics, $Y_\ell^k(\lambda,\phi) = e^{ik\lambda}P_\ell^k(\cos\phi)$, *where here ℓ and k are used to denote the degree and rank of* $P_\ell^k(\cos\phi)$, *respectively, and the P_ℓ^k are the associated Legendre functions. The definition of the spherical harmonics and their orthogonality mean that* (12.20) *reduces to*

$$\frac{Q^{k,\ell,n+1} - Q^{k,\ell,n}}{\Delta t} = \frac{K}{r^2}\left\{\frac{-k^2}{\cos^2\phi}Q^{k,\ell,n} + \left[\frac{k^2}{\cos^2\phi} - \ell(\ell+1)\right]Q^{k,\ell,n}\right\}, \tag{12.21}$$

for each of the coefficients, $Q^{k,\ell,n}$, of Q in the spherical harmonic expansion. Following an analysis analogous to that discussed in more detail below, this shows that stability, with preservation of the sign of each component, requires

$$\frac{K\ell(\ell+1)\Delta t}{r^2} \leq 1. \tag{12.22}$$

Whilst this can only be suggestive of the stability requirement of the finite-difference operator, it is interesting to note that (12.22) *is independent of the zonal wavenumber, k, in contrast to what is obtained for the analysis of the "frozen" approximation with the anisotropic assumption, $K_\lambda = \cos^2\phi K_\phi$, Case 3 below. (But it* *should be noted that ℓ is* not *equivalent to the meridional wavenumber, k_ϕ, used below.)*

Consider the explicit time discretisation of this equation:

$$\frac{Q^{n+1}-Q^n}{\Delta t}=\frac{1}{r^2}\left[\delta_\lambda\left(\frac{K_\lambda}{\cos^2\phi}\delta_\lambda Q^n\right)+\delta_\phi\left(K_\phi\delta_\phi Q^n\right)\right], \qquad (12.23)$$

It is straightforward to analyse the stability of (12.23) for three special cases.

Case 1: $K_\lambda = 0$

(12.23) then reduces to

$$\frac{Q^{n+1}-Q^n}{\Delta t}=\frac{1}{r^2}\delta_\phi\left(K_\phi\delta_\phi Q^n\right). \qquad (12.24)$$

Assuming $K_\phi=$ constant and

$$Q=Q\left(\phi,t\right)=Q_0e^{i\left(k_\phi\phi+\omega t\right)}, \qquad (12.25)$$

where k_ϕ is meridional wavenumber and ω is frequency, then the response function E is given by

$$E\equiv e^{i\omega\Delta t}=1-\frac{K_\phi\Delta t}{r^2}\frac{\sin^2\left(k_\phi\Delta\phi/2\right)}{\left(\Delta\phi/2\right)^2}. \qquad (12.26)$$

For stability, we need to respect $|E|\leq 1$, which leads to

$$\frac{K_\phi\Delta t}{r^2\left(\Delta\phi\right)^2}\leq\frac{1}{2}. \qquad (12.27)$$

Aside :

Note however that while (12.24) *will be stable if* (12.27) *is satisfied, E may alternate sign on alternate time steps, which is not such a good idea. To prevent this, it is better to choose a two-times smaller time step such that $0\leq E\leq 1$, which then leads to*

$$\frac{K_\phi\Delta t}{r^2\left(\Delta\phi\right)^2}\leq\frac{1}{4}. \qquad (12.28)$$

Case 2: $K_\phi = 0$

(12.23) then reduces to

$$\frac{Q^{n+1} - Q^n}{\Delta t} = \frac{1}{r^2}\delta_\lambda\left(\frac{K_\lambda}{\cos^2\phi}\delta_\lambda Q^n\right), \tag{12.29}$$

Assuming $K_\lambda =$ constant and

$$Q = Q(\lambda, t) = Q_0 e^{i(k_\lambda\lambda + \omega t)}, \tag{12.30}$$

where k_λ is zonal wavenumber, then

$$E \equiv e^{i\omega\Delta t} = 1 - \frac{K_\lambda\Delta t}{r^2\cos^2\phi}\frac{\sin^2(k_\lambda\Delta\lambda/2)}{(\Delta\lambda/2)^2}. \tag{12.31}$$

For stability, we need to respect $|E| \le 1$, which leads to

$$\frac{K_\lambda\Delta t}{r^2\cos^2\phi\,(\Delta\lambda)^2} \le \frac{1}{2}, \tag{12.32}$$

or, if we additionally wish to avoid E alternating sign on alternate time steps, the twice as restrictive criterion

$$\frac{K_\lambda\Delta t}{r^2\cos^2\phi\,(\Delta\lambda)^2} \le \frac{1}{4}. \tag{12.33}$$

Contrasting the form of (12.33) with that of (12.28) strongly suggests that when $K = K_\lambda = K_\phi =$ constant (i.e. when the diffusion is approximately isotropic) the maximum permissible value of K for a given time step has, from (12.33), a $\cos^2\phi$ latitudinal dependence. This means that the maximum value of K is determined by the latitude closest to the pole and is very restrictive.

If instead we choose the functional form

$$K_\lambda/\cos^2\phi = K_\phi = \text{constant}, \tag{12.34}$$

then the severe restriction on K due to (12.33) is relaxed to that associated with (12.28). This is the choice currently made in the New Dynamics.

Aside :

The (high) price paid for this is that the diffusion becomes highly anisotropic, particularly in polar regions where diffusion is probably most needed, and noise is much less controlled in the East-West direction than in the North-South direction.

For the New Dynamics choice (12.34), it is straightforward to do a more complete (two-dimensional) analysis.

Case 3: $K_\lambda / \cos^2\phi = K_\phi = \text{constant}$

(12.23) then reduces to

$$\frac{Q^{n+1} - Q^n}{\Delta t} = \frac{K_\phi}{r^2}\left(\delta_{\lambda\lambda} Q^n + \delta_{\phi\phi} Q^n\right), \tag{12.35}$$

and

$$E \equiv e^{i\omega\Delta t} = 1 - \frac{K_\phi \Delta t}{r^2}\left[\frac{\sin^2\left(k_\lambda \Delta\lambda/2\right)}{\left(\Delta\lambda/2\right)^2} + \frac{\sin^2\left(k_\phi \Delta\phi/2\right)}{\left(\Delta\phi/2\right)^2}\right]. \tag{12.36}$$

For stability we must therefore respect

$$\frac{K_\phi \Delta t}{r^2}\left(\frac{1}{\Delta\lambda^2} + \frac{1}{\Delta\phi^2}\right) \leq \frac{1}{2}, \tag{12.37}$$

or, if we additionally wish to avoid E alternating sign on alternate time steps, the twice as restrictive criterion

$$\frac{K_\phi \Delta t}{r^2}\left(\frac{1}{\Delta\lambda^2} + \frac{1}{\Delta\phi^2}\right) \leq \frac{1}{4}. \tag{12.38}$$

Aside :

Note that, for a uniform grid such that $\Delta\lambda = \Delta\phi$, including both directions in the stability analysis leads in two dimensions to a twice as restrictive stability condition than that in one dimension.

Aside :

The r^2 contribution to all of the above stability conditions means that the stability condition of horizontal diffusion at the bottom of the atmosphere is slightly more restrictive than that at the top.

Aside :

The value of K_ϕ used in the New Dynamics is a user specified parameter. No check is made within the code to ensure its value is numerically stable. Caveat emptor!

Aside :

One way of removing the potential instability would be to use an implicit numerical scheme for the diffusion operator. This would allow K_λ to be chosen equal to K_ϕ giving an isotropic diffusion operator, and K_ϕ could be chosen as large as *required without causing numerical instability. Eq.* (12.23) *would then be replaced by:*

$$\frac{Q^{n+1}-Q^n}{\Delta t}=\frac{1}{r^2}\left[\delta_\lambda\left(\frac{K_\lambda}{\cos^2\phi}\delta_\lambda Q^{n+1}\right)+\delta_\phi\left(K_\phi\delta_\phi Q^{n+1}\right)\right], \tag{12.39}$$

or, symbolically, as the matrix equation:

$$\left[\mathbf{I}-\Delta t\left(\mathbf{D}_{\lambda\lambda}+\mathbf{D}_{\phi\phi}\right)\right]\mathbf{Q}^{n+1}_{\lambda,\phi}=\mathbf{Q}^{n}_{\lambda,\phi}, \tag{12.40}$$

where $\mathbf{D}_{\lambda\lambda}$ *represents the diffusion operator obtained when* $K_\phi\equiv 0$ *in the right-hand side of* (12.39), *and* $\mathbf{D}_{\phi\phi}$ *is that obtained when* $K_\lambda\equiv 0$. *However, inverting the resultant three-dimensional matrix,* $\left[\mathbf{I}-\Delta t\left(\mathbf{D}_{\lambda\lambda}+\mathbf{D}_{\phi\phi}\right)\right]$, *would be too computationally expensive for operational implementation. An alternative and viable approach, at least for the case in which diffusion is being applied for purely numerical reasons, is to approximate the matrix* $\left[\mathbf{I}-\Delta t\left(\mathbf{D}_{\lambda\lambda}+\mathbf{D}_{\phi\phi}\right)\right]$ *as:*

$$\left[\mathbf{I}-\Delta t\left(\mathbf{D}_{\lambda\lambda}+\mathbf{D}_{\phi\phi}\right)\right]\approx\left[\mathbf{I}-\Delta t\mathbf{D}_{\lambda\lambda}\right]\left[\mathbf{I}-\Delta t\mathbf{D}_{\phi\phi}\right], \tag{12.41}$$

equivalent to approximating (12.23) *by*

$$\begin{aligned}\frac{Q^{n+1}-Q^n}{\Delta t} &= \frac{1}{r^2}\left[\delta_\lambda\left(\frac{K_\lambda}{\cos^2\phi}\delta_\lambda Q^{n+1}\right)+\delta_\phi\left(K_\phi\delta_\phi Q^{n+1}\right)\right]\\ &\quad -\frac{\Delta t}{r^2}\delta_\lambda\left\{\frac{K_\lambda}{\cos^2\phi}\delta_\lambda\left[\frac{1}{r^2}\delta_\phi\left(K_\phi\delta_\phi Q^{n+1}\right)\right]\right\}.\end{aligned} \tag{12.42}$$

If diffusion is being applied for purely numerical reasons then the presence of the extra term, the last term on the right-hand side of (12.42), *is probably of little consequence. The advantage of including this extra term is that the problem is now separable and each of the operators* $\left(\mathbf{I}-\Delta t\mathbf{D}_{\lambda\lambda}\right)$ *and* $\left(\mathbf{I}-\Delta t\mathbf{D}_{\phi\phi}\right)$ *are two-dimensional, tri-diagonal matrices which can be inverted efficiently (though even the cost of this may not be insignificant on a massively parallel computer). In addition, in the absence of orography, for constant values of* K_λ *and* K_ϕ, *and if the variation of* $\cos\phi$ *with* ϕ *is neglected (a "frozen" approximation), the scheme is numerically stable for all values of* Δt. *One slight drawback though is that there is an arbitrariness in choosing in which order to write* (12.41). *Due to the presence of both the* r^2 *and the* $\cos^2\phi$ *factors, the operators* $\mathbf{D}_{\lambda\lambda}$ *and* $\mathbf{D}_{\phi\phi}$ *do not commute so that the approximation*

$$\left[\mathbf{I}-\Delta t\left(\mathbf{D}_{\lambda\lambda}+\mathbf{D}_{\phi\phi}\right)\right]\approx\left[\mathbf{I}-\Delta t\mathbf{D}_{\lambda\lambda}\right]\left[\mathbf{I}-\Delta t\mathbf{D}_{\phi\phi}\right], \tag{12.43}$$

is not the same as the approximation

$$[\mathbf{I} - \Delta t\,(\mathbf{D}_{\lambda\lambda} + \mathbf{D}_{\phi\phi})] \approx [\mathbf{I} - \Delta t \mathbf{D}_{\phi\phi}]\,[\mathbf{I} - \Delta t \mathbf{D}_{\lambda\lambda}]\,. \tag{12.44}$$

For relatively large diffusion coefficients, such that the explicit scheme might be close to being unstable, i.e. when an implicit scheme has most benefit, the difference between these two choices need not necessarily be small. The particular choice of (12.43) *or* (12.44) *could be made by choosing the form with the smallest truncation error or choosing that form with the best conservation behaviour. Note that the above discussion is exact for* D^{η}_{ND}*. For* D^{η}_{η} *the operators* $\mathbf{D}_{\lambda\lambda}$ *and* $\mathbf{D}_{\phi\phi}$ *are chosen by setting* K_ϕ *and* K_λ*equal to zero in* (12.17)*. In this case, and in contrast to* D^{η}_{ND}*, the order of the operators does not impact the volume integral conservation property.*

12.4.2 Some properties of the diffusion operator

Having analysed the stability for the specific choices of diffusion coefficients, it is instructive to quantify the degree of damping in the simple case of an explicit, one-dimensional diffusion operator. For convenience the case $K_\phi \equiv 0$ is considered, i.e. Case 2 of Section 12.4.1 and the assumptions relevant to that case are also assumed here, viz. the "frozen" approximation and the absence of orography. Additionally, it is here assumed that $\Delta\lambda$ is constant. A non-dimensional diffusion coefficient K^* is defined such that $K_\lambda = K^* r^2 \cos^2\phi \Delta\lambda^2/\Delta t$. Then, on applying the definition of δ_λ given by (C.6) of Appendix C, (12.29) takes the form

$$Q^{n+1}_{i,j,k} = Q^n_{i,j,k} + K^* \left(Q^n_{i+1,j,k} - 2Q^n_{i,j,k} + Q^n_{i-1,j,k}\right). \tag{12.45}$$

The response function, E, for (12.45) is given by (12.31) which may be rewritten as $E = 1 - S$ where $S \equiv 4K^* \sin^2(k_\lambda \Delta\lambda/2)$. E is largest when $k_\lambda = 0$ for which it takes the value 1. E is smallest when $k_\lambda = L/2$ (assuming L even, where L is the number of grid points around a latitude circle) and then E takes the value $1 - 4K^*$. [When L is indeed even, then the wave associated with $k_\lambda = L/2$ is commonly referred to as the two-gridlength wave.] As discussed in relation to Case 2 above, the scheme is stable and E does not alternate sign on alternate time steps (i.e. $0 \le E \le 1$) provided $0 \le K^* \le 1/4$. Choosing the upper limiting value for K^* (i.e. $K^* = 1/4$) gives $S = 1$ and $E = 0$. Therefore, the two-gridlength wave ($k_\lambda = L/2$) is eliminated by one application of the operator defined by (12.45). Table 12.1

k_λ	$L/2$	$L/3$	$L/4$	$L/5$	$L/6$	$L/8$	$L/10$	$L/20$
S	1.00	0.75	0.50	0.35	0.25	0.15	0.10	0.02
E	0.00	0.25	0.50	0.65	0.75	0.85	0.90	0.98

Table 12.1: Magnitude of S and the response function E for Case 2 when $K^* = 1/4$ for various wavenumbers.

gives values of S and E for various wavenumbers when $K^* = 1/4$. Choosing K^* to be a fraction of the limiting value will change S ($\equiv 1 - E$) proportionally.

A practical method for choosing K^* is to choose its value such that the two-gridlength wave, $k_\lambda = L/2$, (when it exists) is damped by a factor e over n applications. This value is given by $K^* = \left(1 - e^{-\frac{1}{n}}\right)/4$. Alternatively, instead of basing K^* on the e-folding time, it could be based on the halving time by setting $K^* = \left(1 - 0.5^{\frac{1}{n}}\right)/4$.

In addition to analysing the response of the operator at particular wavelengths, it is instructive to consider its local effect by analysing what it does to an isolated perturbation to Q in an otherwise uniform field. For a particular grid point (i, j, k), let $Q_{i,j,k}$ have a value $Q_0 + \Delta Q$ and all other surrounding points have values Q_0. Then the effect of applying the operator (12.46) to this distribution is to remove $2K^*\Delta Q$ from $Q_{i,j,k}$ and to add $K^*\Delta Q$ to both $Q_{i+1,j,k}$ and $Q_{i-1,j,k}$ thereby reducing the local excess at $Q_{i,j,k}$. This is the well known property of the diffusion operator, that it conserves the total amount of a substance but smooths its distribution.

More generally, though, Q will vary away from the ith point and then, with constant K^*, the diffusion operator will damp such variations too. These may be realistic variations which it would be undesirable to damp. This leads to the concept of "targeted diffusion" for which K^* varies horizontally. The generalisation of (12.45) is then:

$$Q^{n+1}_{i,j,k} = Q^n_{i,j,k} + K^*_{i+1/2,j,k}\left(Q^n_{i+1,j,k} - Q^n_{i,j,k}\right) - K^*_{i-1/2,j,k}\left(Q^n_{i,j,k} - Q^n_{i-1,j,k}\right). \tag{12.46}$$

Now suppose that $Q_{i,j,k}$ is again equal to $Q_0 + \Delta Q$ and that the immediately surrounding points have values $Q_{i\pm1,j,k} = Q_0$ but that Q is arbitrary elsewhere. Then by setting the diffusion coefficients to zero everywhere except at the points $(i \pm 1/2, j, k)$, for which $K^*_{i\pm1/2,j,k} = K^*$, the effect of the diffusion operator is exactly the same as before. The excess of Q_i is reduced by $2K^*\Delta Q$ and the values of both Q_{i+1} and Q_{i-1} are increased by an amount

$K^*\Delta Q$. All other values of Q are left unchanged (and will remain so even after successive applications of the diffusion operator) and hence the term "targeted diffusion".

12.4.3 Targeted diffusion

When running the complete model, it is possible for isolated grid points to develop strong upward motion with associated, intense, large-scale precipitation. These are referred to as grid-point storms. Since they are characterised by larger vertical velocities than is normally encountered in the model and, as they develop, their column humidity becomes significantly larger than surrounding points, it is possible to use a locally targeted diffusion to suppress them.

The basis of the targeted diffusion scheme is to use the conserving operator $D_\eta^\eta(Q)$ given by (12.17) but to set $K_\lambda = K_\phi = 0$ everywhere except at the points immediately surrounding the point for which the targeted-diffusion criterion has been identified as being met. The criterion for where to apply the targeted diffusion is to look for the maximum vertical velocity w_{max} in a column and where $w_{max} > w_{threshold}$. When this occurs, a value for K^* is chosen for the four staggered points surrounding the identified point. Then, at those points, K_λ in (12.17) is set according to:

$$K_\lambda = K^* r^2 \cos^2\phi \Delta\lambda^2/\Delta t, \tag{12.47}$$

and, by applying the analogy between Case 1 and Case 2, K_ϕ is set according to:

$$K_\phi = K^* r^2 \Delta\phi^2/\Delta t. \tag{12.48}$$

(Note however the aside following (12.34) regarding the anisotropic nature of this choice of coefficients.)

The chosen value of K^* is restricted by the requirement for numerical stability. With the above choice for K_λ and K_ϕ and under appropriate simplifying assumptions, the results of Case 3 then apply and the scheme is stable and the response function does not alternate sign on alternate time steps provided $K^* \leq 1/8$.

As noted above, at points where the threshold is not exceeded then the diffusion coefficients are set to zero. Note, however, that a point next to an active point will share one of its diffusion coefficients with the active point so that the operator works as a redistributing or smoothing operator, as described in the previous subsection. For example, at an active

i,j point the following diffusion coefficients are set: $K^*_{i+\frac{1}{2},j}$ and $K^*_{i-\frac{1}{2},j}$ in the longitudinal direction and $K^*_{i,j-\frac{1}{2}}$ and $K^*_{i,j+\frac{1}{2}}$ in the latitudinal direction. The local diffusion is applied only to the water vapour field and to the whole column apart from where the restriction due to sloping surfaces applies (Section 12.4.4). Although this means that the targeted diffusion is applied in the stratosphere (where it is not needed) it only significantly changes values where there are significant horizontal gradients which usually do not occur in the stratosphere.

The choice for $w_{threshold}$ is somewhat arbitrary and is resolution dependent. It is desirable not to make it too small otherwise the targeted diffusion will operate at more points than necessary. In practice a value can be identified for which no more than a handful of points have $w_{max} > w_{threshold}$ for any particular configuration. In low-resolution climate configurations, $w_{threshold} = 0.1$ or 0.2 ms^{-1} appears sufficient whereas in the operational global model $w_{threshold} = 0.5$ ms^{-1} has been found to be more appropriate. The value for the effective diffusion coefficient is normally set to $K^* = 0.1$.

12.4.4 Choosing K_ϕ over orography

The horizontal diffusion operator, by design, acts along levels of constant η, which, in physical space, approximately follow the underlying orography, at least near the surface. For any field which is strongly stratified in the vertical, e.g. in particular potential temperature and moisture, the application of horizontal diffusion along η surfaces over non-zero orography will lead to spurious transport of that field up or down the slopes of the orography, with a consequent negative impact on the dynamical response of the flow. For example, moisture generally has a strongly negative, *non-linear* lapse rate. Diffusing moisture, with such a lapse rate, up an orographic slope will lead to a moistening of the air higher up the slopes, where the air is generally colder. This may, in extreme circumstances, lead to condensation of the moisture with associated release of latent heat. This can then potentially trigger spurious convection. It is therefore desirable to do something to prevent this occurring. One approach might be to use diffusion along r-surfaces, as discussed in Section 12.2.1. Currently in the New Dynamics, however, the solution employed is to switch off the diffusion over orography which is such that the change in height of the orography over one horizontal grid length (keeping η constant) is, in some sense, significant.

Consider the East-West direction. Let the diffused field be stored on the (i, j, k) grid

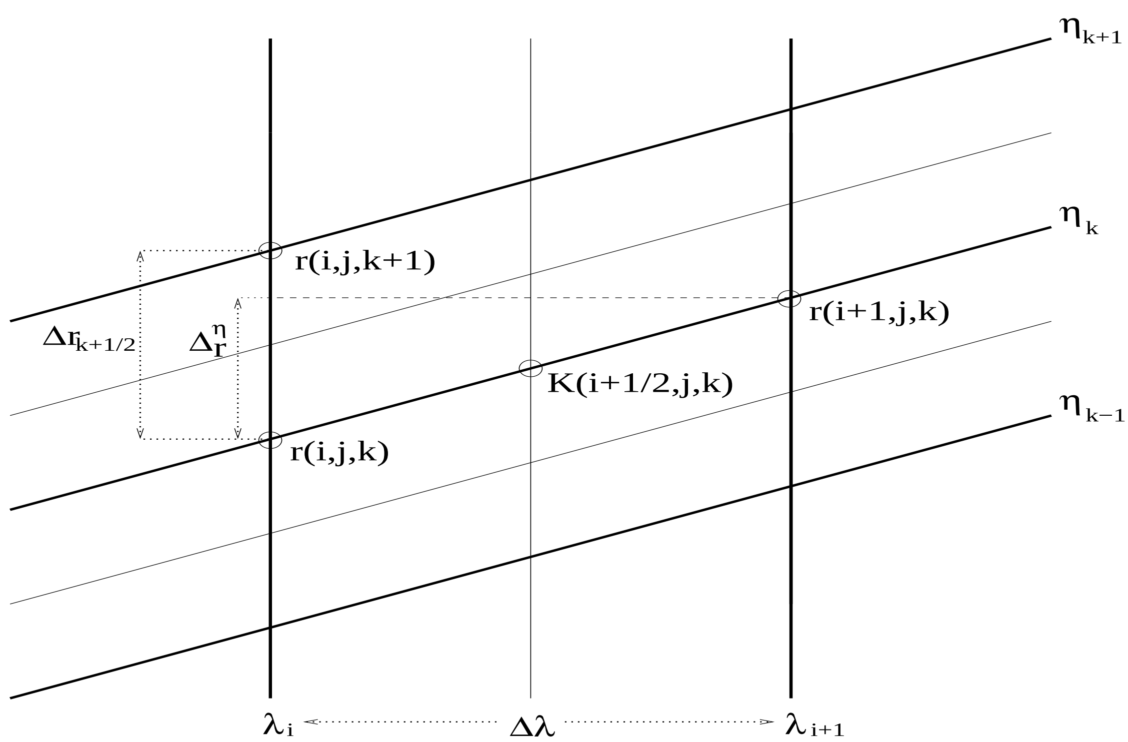

Figure 12.1: Schematic of the grid geometry over a sloping surface. Since $\Delta_r^\eta < \Delta r_{k+1/2}$ in this case, the diffusion coefficient K at the grid point $(i+1/2, j, k)$ will be non-zero.

point so that the diffusion coefficient, K_λ, is evaluated on the $(i+1/2, j, k)$ grid point (see Fig. 12.1). Then the variation of the grid in the East-West direction in the region of this point will determine whether diffusion is permitted there or should be switched off. The change in the height, along a surface of constant η, over one grid length centred on the grid point $(i+1/2, j, k)$ is

$$(\Delta_r^\eta)_{i+1/2,j,k} \equiv \left(\Delta r_{i+1/2,j,k}\right)\Big|_\eta = r_{i+1,j,k} - r_{i,j,k}. \tag{12.49}$$

When this quantity is positive, a pragmatic upper bound on this change in height, above which it is considered significant, is the difference in height between $r_{i,j,k}$ and $r_{i,j,k+1}$, i.e. in order to apply diffusion it is required that

$$(\Delta_r^\eta)_{i+1/2,j,k} < r_{i,j,k+1} - r_{i,j,k}. \tag{12.50}$$

When $(\Delta_r^\eta)_{i+1/2,j,k}$ is negative, the lower bound is the difference in height between $r_{i,j,k}$ and $r_{i,j,k-1}$, i.e.

$$(\Delta_r^\eta)_{i+1/2,j,k} > r_{i,j,k-1} - r_{i,j,k}. \tag{12.51}$$

This may be summarised as requiring

$$\left|(\delta_\lambda r)_{i+1/2,j,k}\right| < \frac{\Delta r_{i,j,k\pm1/2}}{\Delta\lambda}, \tag{12.52}$$

where Δr here denotes the usual spacing of grid levels keeping λ and ϕ constant. It is evaluated at $(i, j, k+1/2)$ when $(\delta_\lambda r)_{i+1/2,j,k}$ is positive, and at $(i, j, k-1/2)$ when $(\delta_\lambda r)_{i+1/2,j,k}$ is negative. An analogous expression is used in the North-South direction, i.e. it is required that

$$\left|(\delta_\phi r)_{i,j+1/2,k}\right| < \frac{\Delta r_{i,j,k\pm1/2}}{\Delta\phi}, \tag{12.53}$$

The above amounts to saying that horizontal diffusion is only applied where the slope of the coordinate surfaces is less than the vertical to horizontal aspect ratio of the grid. Another interpretation is that diffusion is only applied where the slope of the coordinate surface is such that, for a given grid point, its neighbouring grid points, along an η surface, do not have heights in physical space that are greater than (less than) the grid point immediately above (below) that point (see Fig. 12.1 for the case of positive sloping coordinate surfaces).

For points, $(i+1/2, j, k)$, where the condition, (12.52), is not met, K_λ is set equal to zero and for points, $(i, j+1/2, k)$, where the condition, (12.53), is not met, K_ϕ is set equal to zero. Setting the values of K_λ and K_ϕ to zero rather than making the whole diffusion operator zero at these points, ensures that the correct flux form of the operator is retained so that any global conservation properties of the operator are maintained.

Aside :

A more natural and symmetric condition, centred on $(i + 1/2, j, k)$*, would be to require*

$$\left|(\delta_\lambda r)_{i+1/2,j,k}\right| < \frac{\Delta r_{i+1/2,j,k}}{\Delta\lambda}, \tag{12.54}$$

for diffusion to be permitted, and similarly for the ϕ*-direction.*

Aside :

The choice of the above conditions, (12.52) *and* (12.53)*, to determine whether diffusion should be applied or not is based on pragmatic arguments evolved by experimentation. This leaves some questions unanswered. For example, it would seem quite legitimate to multiply the right-hand sides of* (12.52) *and* (12.53) *by some constant - there seems no objective reason why that constant should be* 1*. Also, the conditions do not relate to the actual structure of the field being diffused. For example, if there is little or no vertical stratification it would seem possible, and probably desirable, to still apply diffusion. Further, the condition is based not only on the slope of the coordinate surfaces, which is related to the underlying orography, but also on the grid aspect ratio. This seems likely to lead to a grid dependency in the model, in that for orography of the same slope and for the same stratification of the diffused field, simply adding more vertical resolution is going to reduce the number of grid points over the orography at which diffusion is applied. Indeed, in the limit of infinite vertical resolution, with the horizontal resolution fixed, no diffusion over any sloping surface would be permitted.*

12.5 Higher order operators

The second order operators considered thus far are not very scale selective and can therefore impact negatively on some of the well resolved scales. In the New Dynamics multiple applications of the diffusion operator are allowed each time step, effectively replacing the second-order diffusion operator by higher order operators, which are more scale selective. This is achieved by first writing the discretisation of the diffusion operator as:

$$Q^{n+1} - Q^n = \Delta t D^\eta(Q), \tag{12.55}$$

where D^η represents either of D^η_{ND} and D^η_η, and then generalising this form to:

$$Q^{n+1} - Q^n = (-1)^{d_o - 1} \left[\Delta t D^\eta\right]^{d_o} (Q). \tag{12.56}$$

d_o is a positive integer, denoting the order of the resultant diffusion operator, so that $d_0 = 1$ gives the appropriate flavour of ∇^2 diffusion, $d_0 = 2$ gives ∇^4 diffusion etc.

Repeating the above stability analysis but now with the operator given in (12.56), and with $K_\lambda / \cos^2\phi = K_\phi =$ constant, shows that (12.36) is replaced by

$$E \equiv e^{i\omega\Delta t} = 1 - \left\{\frac{K_\phi \Delta t}{r^2}\left[\frac{\sin^2(k_\lambda\Delta\lambda/2)}{(\Delta\lambda/2)^2} + \frac{\sin^2(k_\phi\Delta\phi/2)}{(\Delta\phi/2)^2}\right]\right\}^{d_o}. \tag{12.57}$$

For numerical stability and also to avoid E alternating sign on alternate time steps, the restriction on the time step is therefore unchanged from (12.33). This result is because the time step, Δt, is taken within the operator $(-1)^{d_o - 1}\left[\Delta t D^\eta\right]^{d_o}$ of (12.56).

The stability requirement means that for all wavenumbers, (k_λ, k_ϕ), with the possible exception of the pair $(\pi/\Delta\lambda, \pi/\Delta\phi)$, the term in curly braces in (12.57) is less than one and so the damping associated with the diffusion is reduced as d_o increases. However, it is important to note that it is only the operator with $d_o = 1$ which guarantees to preserve the monotonicity of the field being diffused; higher order operators can introduce spurious new extrema. This is not a good idea for moisture and tracer fields.

12.6 The discrete form of the preferred diffusion operator, D^η_η

In this section the preferred discrete form of D^η_η is given. In many respects the discretisation of the alternative form, D^η_{ND}, can be obtained analogously but where key differences do occur these are noted in Asides.

12.6.1 Non-polar discrete form

Q may be held on either ρ-levels, $k = 1/2, 3/2, ...N - 1/2$, or θ-levels $k = 0, 1, ...N$, (see Section 4 for details). Since r is stored on both sets of levels, the discretisation of (12.17) is symbolically the same for all interior levels, $k = 1/2, 1, 3/2, ...N-1, N-1/2$, and is given by:

$$D^{\eta}_{\eta}(Q) = \left(\frac{1}{r^2\delta_\eta r}\right)\left\{\delta_\lambda\left[\frac{K_\lambda}{\cos^2\phi}\delta_\lambda\left(Q\delta_\eta r\right)\right] + \frac{1}{\cos\phi}\delta_\phi\left[K_\phi\cos\phi\delta_\phi\left(Q\delta_\eta r\right)\right]\right\}, \tag{12.58}$$

where it has been assumed that K_λ and K_ϕ are staggered in the λ and ϕ directions respectively relative to Q. If required at the top level, $k = N$, use can be made of the fact that $r|_{\eta_{N-1/2}}$ and $r|_{\eta_N}$ are constants so that $\delta_\eta r$ is independent of both λ and ϕ. (This is also true in the absence of orography, a fact that was used in the stability analysis.) Then (12.17) can be straightforwardly discretised at $k = N$ as:

$$D^{\eta}_{\eta}(Q) = \left\{\left(\frac{1}{r^2}\right)\left[\delta_\lambda\left(\frac{K_\lambda}{\cos^2\phi}\delta_\lambda Q\right) + \frac{1}{\cos\phi}\delta_\phi\left(K_\phi\cos\phi\delta_\phi Q\right)\right]\right\}\Bigg|_{\eta_N}. \tag{12.59}$$

Aside :

If the constraint that $r|_{\eta_{N-1/2}}$ be constant were to be removed then to discretise (12.17) at $k = N$ some further knowledge of the behaviour of $\delta_\eta r$ at $k = N$ would have to be applied, which would depend on the particular transformation used. Alternatively, (12.58) could be applied but with $(\partial r/\partial\eta)_{\eta_N}$ evaluated as the one-sided difference, $\left(r_N - r_{N-1/2}\right)/\left(\eta_N - \eta_{N-1/2}\right)$, which is equivalent to adding a fictitious level at $\eta_{N+1/2}$ with $\eta_{N+1/2}$ chosen so that $\eta_{N+1/2} - 1 = 1 - \eta_{N-1/2}$.

At $k = 0$ the boundary condition on all scalars is that their vertical gradient is zero. Thus the values of all scalars at $k = 0$ are given directly by their values at $k = 1$ and so no discretisation of (12.17) is required.

12.6.2 Polar discrete form

To complete the discretisation of the diffusion operator D^{η}_{η} is integrated over the two polar caps $\left\{0 \le \lambda \le 2\pi;\ -\pi/2 \equiv \phi_{1/2} \le \phi \le \phi_1\right\}$ and $\left\{0 \le \lambda \le 2\pi;\ \phi_{M-1} \le \phi \le \phi_{M-1/2} \equiv \pi/2\right\}$.

Integration of the horizontal diffusion operator over the south polar cap

Integrating (12.17), multiplied by $\partial r/\partial\eta$, over the south polar cap, defined by $\{0 \le \lambda \le 2\pi;$ $-\pi/2 \equiv \phi_{1/2} \le \phi \le \phi_1\}$, gives:

$$\int_{-\frac{\pi}{2}}^{\phi_1}\left[\int_0^{2\pi}\left(\frac{\partial r}{\partial\eta}D^{\eta}_{\eta}\right)r^2 d\lambda\right]\cos\phi d\phi \quad = \quad \int_{-\frac{\pi}{2}}^{\phi_1}\left\{\int_0^{2\pi}\frac{\partial}{\partial\lambda}\left[\frac{K_\lambda}{\cos\phi}\frac{\partial}{\partial\lambda}\left(\frac{\partial r}{\partial\eta}Q\right)\right]d\lambda\right\}d\phi$$

$$+\int_{-\frac{\pi}{2}}^{\phi_1}\left\{\int_0^{2\pi}\frac{\partial}{\partial\phi}\left[K_\phi\cos\phi\frac{\partial}{\partial\phi}\left(\frac{\partial r}{\partial\eta}Q\right)\right]d\lambda\right\}d\phi, \tag{12.60}$$

where $\phi_1 - \phi_{1/2} = \Delta\phi/2$.

Approximating $\left(D_\eta^\eta \partial r/\partial\eta\right) r^2$ in the left-hand side integral by its value at the pole gives

$$I_1 \equiv \int_{-\frac{\pi}{2}}^{\phi_1}\left[\int_0^{2\pi}\left(\frac{\partial r}{\partial\eta}D_\eta^\eta\right)r^2 d\lambda\right]\cos\phi d\phi \approx \left[\left(\frac{\partial r}{\partial\eta}D_\eta^\eta\right)r^2\right]_{SP}\int_0^{2\pi}\int_{-\frac{\pi}{2}}^{\phi_1}\cos\phi d\phi d\lambda, \tag{12.61}$$

where subscript "SP" denotes evaluation at the South Pole. Now $\int_0^{2\pi}\int_{-\frac{\pi}{2}}^{\phi_1}\cos\phi d\phi d\lambda$ is the area of a spherical cap of a sphere of unit radius. Analytically this is equal to $2\pi\left(1+\sin\phi_1\right)$. In the New Dynamics however, the area of this spherical cap is approximated by the area of a *plane* circle of radius $\Delta\phi/2$, i.e. by $\pi\left(\Delta\phi\right)^2/4$. This is an $O\left(\Delta\phi^2\right)$-accurate approximation to the exact *spherical* area, and it leads to the discretisation

$$I_1 \equiv \int_{-\frac{\pi}{2}}^{\phi_1}\left[\int_0^{2\pi}\left(\frac{\partial r}{\partial\eta}D_\eta^\eta\right)r^2 d\lambda\right]\cos\phi d\phi \approx 2\pi b\left[\left(\frac{\partial r}{\partial\eta}D_\eta^\eta\right)r^2\right]_{SP}, \tag{12.62}$$

where $b = \left(\Delta\phi\right)^2/8$.

The right-hand side integrals of (12.60) are discretised as

$$\begin{aligned}
I_2 &\equiv \int_{-\frac{\pi}{2}}^{\phi_1}\left\{\int_0^{2\pi}\left\{\frac{\partial}{\partial\lambda}\left[\frac{K_\lambda}{\cos\phi}\frac{\partial}{\partial\lambda}\left(\frac{\partial r}{\partial\eta}Q\right)\right]+\frac{\partial}{\partial\phi}\left[K_\phi\cos\phi\frac{\partial}{\partial\phi}\left(\frac{\partial r}{\partial\eta}Q\right)\right]\right\}d\lambda\right\}d\phi \\
&= \int_0^{2\pi}\left\{\int_{-\frac{\pi}{2}}^{\phi_1}\frac{\partial}{\partial\phi}\left[K_\phi\cos\phi\frac{\partial}{\partial\phi}\left(\frac{\partial r}{\partial\eta}Q\right)\right]d\phi\right\}d\lambda \\
&= \int_0^{2\pi}\left\{\left[K_\phi\cos\phi\frac{\partial}{\partial\phi}\left(\frac{\partial r}{\partial\eta}Q\right)\right]\Bigg|_{(\lambda,\phi_1)} - \left[K_\phi\cos\phi\frac{\partial}{\partial\phi}\left(\frac{\partial r}{\partial\eta}Q\right)\right]\Bigg|_{\left(\lambda,-\frac{\pi}{2}\right)}\right\}d\lambda \\
&= \cos\left(\phi_1\right)\int_0^{2\pi}\left[K_\phi\frac{\partial}{\partial\phi}\left(\frac{\partial r}{\partial\eta}Q\right)\right]\Bigg|_{(\lambda,\phi_1)}d\lambda \\
&\approx \cos\left(\phi_1\right)\frac{2\pi}{L}\sum_{i=1}^{L}\left[K_\phi\frac{\partial}{\partial\phi}\left(\frac{\partial r}{\partial\eta}Q\right)\right]_{i-\frac{1}{2},1},
\end{aligned} \tag{12.63}$$

where $L = 2\pi/\Delta\lambda$ is the number of grid points around a latitude circle.

Putting the above results together, and discretising the various terms appropriately, the discrete form of the horizontal diffusion operator over the south polar cap is:

$$\left(D_{\eta}^{\eta}\right)_{SP} = \left(\frac{1}{r^2 \delta_\eta r}\right)_{SP} \frac{\cos\left(\phi_1\right)}{b} \frac{1}{L} \sum_{i=1}^{L} \left[K_\phi \delta_\phi \left(Q \delta_\eta r\right)\right]_{i-\frac{1}{2},1}, \tag{12.64}$$

where for general F, $F_{SP} = (F)_{\frac{1}{2},\frac{1}{2}} = (F)_{\frac{3}{2},\frac{1}{2}} = (F)_{\frac{5}{2},\frac{1}{2}} = ... = (F)_{L-\frac{1}{2},\frac{1}{2}}$.

Aside :

The equivalent form of (12.64) *but for the alternative diffusion operator* D_{ND}^{η}*, given by* (12.18)*, cannot strictly be obtained in a similar manner to above due to the omission of the* $\cos\phi$ *term discussed above. However, by replacing the* $\partial r/\partial\eta$ *term in* (12.60) *by* $1/\cos\phi$, (12.61) *becomes*

$$\begin{aligned} I_1 &\equiv \int_{-\frac{\pi}{2}}^{\phi_1} \left[\int_0^{2\pi} \left(D_{ND}^{\eta}\right) r^2 d\lambda\right] \left(\cos\phi / \cos\phi\right) d\phi \\ &\approx \left[\left(D_{ND}^{\eta}\right) r^2\right]_{SP} \int_0^{2\pi} \int_{-\frac{\pi}{2}}^{\phi_1} d\phi d\lambda \\ &= \left[\left(D_{ND}^{\eta}\right) r^2\right]_{SP} \pi \Delta\phi. \end{aligned} \tag{12.65}$$

(12.63) *can be developed similarly however, the equivalent of the last term on the right-hand side of the third line of* (12.63)*, namely*

$$-\int_0^{2\pi} \left\{ \left[K_\phi \cos\phi \frac{\partial}{\partial\phi}\left(\frac{\partial r}{\partial\eta} Q\right)\right]\Bigg|_{\left(\lambda,-\frac{\pi}{2}\right)} \right\} d\lambda, \tag{12.66}$$

which is identically zero, is replaced by

$$-\int_0^{2\pi} \left\{ \left[K_\phi \frac{\partial}{\partial\phi}\left(\frac{\partial r}{\partial\eta} Q\right)\right]\Bigg|_{\left(\lambda,-\frac{\pi}{2}\right)} \right\} d\lambda. \tag{12.67}$$

This term does not now vanish in general. However, assuming it can be neglected (12.63) *becomes*

$$I_2 \approx \frac{2\pi}{L} \sum_{i=1}^{L} \left[K_\phi \frac{\partial Q}{\partial\phi}\right]_{i-\frac{1}{2},1}. \tag{12.68}$$

giving the final discrete form as

$$\left(D_{ND}^{\eta}\right)_{SP} = \left(\frac{1}{r^2}\right)_{SP} \frac{1}{\Delta\phi} \frac{2}{L} \sum_{i=1}^{L} \left[K_\phi \delta_\phi Q\right]_{i-\frac{1}{2},1}, \tag{12.69}$$

which is what is currently used in the code for this option.

The neglect of the term in (12.67) *may, however, lead to non-smooth behaviour of the diffusion operator at the pole.*

Integration of the horizontal diffusion operator over the north polar cap

Similarly, integrating (12.17), multiplied by $\partial r/\partial\eta$, over the north polar cap, defined by $\left\{0 \le \lambda \le 2\pi;\ \ \phi_{M-1} \le \phi \le \phi_{M-1/2} \equiv \pi/2\right\}$, gives:

$$\begin{aligned}\int_{\phi_{M-1}}^{\frac{\pi}{2}}\left[\int_0^{2\pi}\left(\frac{\partial r}{\partial\eta}D_\eta^\eta\right)r^2 d\lambda\right]\cos\phi d\phi \ &= \ \int_{\phi_{M-1}}^{\frac{\pi}{2}}\left\{\int_0^{2\pi}\frac{\partial}{\partial\lambda}\left[\frac{K_\lambda}{\cos\phi}\frac{\partial}{\partial\lambda}\left(\frac{\partial r}{\partial\eta}Q\right)\right]d\lambda\right\}d\phi \\ &+\int_{\phi_{M-1}}^{\frac{\pi}{2}}\left\{\int_0^{2\pi}\frac{\partial}{\partial\phi}\left[K_\phi\cos\phi\frac{\partial}{\partial\phi}\left(\frac{\partial r}{\partial\eta}Q\right)\right]d\lambda\right\}d\phi,\end{aligned} \tag{12.70}$$

where $\pi/2 - \phi_{M-1} = \Delta\phi/2$.

Following the same procedure as for the south polar cap, the only real difference being the different limits of integration for ϕ, leads to the following discretisation of the horizontal diffusion operator over the north polar cap:

$$\left(D_\eta^\eta\right)_{NP} = -\left(\frac{1}{r^2\delta_\eta r}\right)_{NP}\frac{\cos\left(\phi_{M-1}\right)}{b}\frac{1}{L}\sum_{i=1}^{L}\left[K_\phi\delta_\phi\left(Q\delta_\eta r\right)\right]_{i-\frac{1}{2},M-1}, \tag{12.71}$$

where for general F, $F_{NP} = (F)_{\frac{1}{2},M-\frac{1}{2}} = (F)_{\frac{3}{2},M-\frac{1}{2}} = (F)_{\frac{5}{2},M-\frac{1}{2}} \cdots = (F)_{L-\frac{1}{2},M-\frac{1}{2}}$, subscript "$NP$" denotes evaluation at the North Pole, and $b = (\Delta\phi)^2/8$.

Aside :

The sign of the right-hand side term in (12.71) *is the opposite of the corresponding term in* (12.64) *- this is due to the different limits of integration for* ϕ*.*

Aside :

Similarly to the South Pole, the form of the alternative diffusion operator at the North Pole neglects the contribution due to

$$+\int_0^{2\pi}\left\{\left[K_\phi\frac{\partial}{\partial\phi}\left(\frac{\partial r}{\partial\eta}Q\right)\right]\bigg|_{\left(\lambda,\frac{\pi}{2}\right)}\right\}d\lambda, \tag{12.72}$$

and then

$$\left(D_{ND}^\eta\right)_{NP} = -\left(\frac{1}{r^2}\right)_{SP}\frac{1}{\Delta\phi}\frac{2}{L}\sum_{i=1}^{L}\left[K_\phi\delta_\phi Q\right]_{i-\frac{1}{2},M-1}. \tag{12.73}$$

12.7 Conservation properties of the discrete horizontal diffusion operator

Non polar-cap contributions

Multiplying (12.58) through by $r^2 \cos\phi \delta_\eta r$, the diffusion operator, away from the polar caps, at each vertical level (1/2, 3/2,..., $N-1/2$ or 1, 2,..., $N-1$) may be rewritten as

$$D_\eta^\eta r^2 \cos\phi \delta_\eta r = \delta_\lambda \left[\frac{K_\lambda}{\cos\phi} \delta_\lambda \left(Q \delta_\eta r \right) \right] + \delta_\phi \left[K_\phi \cos\phi \delta_\phi \left(Q \delta_\eta r \right) \right]. \tag{12.74}$$

Multiplying by $\Delta\eta_k \Delta\lambda \Delta\phi$, where $\Delta\eta_k \equiv \eta_{k+1/2} - \eta_{k-1/2}$, are the layer thicknesses, and summing over all control volumes $\left[\eta_{k-1/2}, \eta_{k+1/2}\right] \otimes [\lambda_{i-1}, \lambda_i] \otimes [\phi_{j-1}, \phi_j]$, with the exception of the two polar caps, gives:

$$\begin{aligned}
& \sum_{i=1}^{L} \sum_{j=2}^{M-1} \sum_k \left(D_\eta^\eta r^2 \cos\phi \delta_\eta r \Delta\eta \Delta\lambda \Delta\phi \right)_{i-\frac{1}{2}, j-\frac{1}{2}, k} \\
= & \sum_{i=1}^{L} \Delta\lambda \sum_{j=2}^{M-1} \Delta\phi \sum_k \Delta\eta_k \left\{ \delta_\lambda \left[\frac{K_\lambda}{\cos\phi} \delta_\lambda \left(Q \delta_\eta r \right) \right] + \delta_\phi \left[K_\phi \cos\phi \delta_\phi \left(Q \delta_\eta r \right) \right] \right\}_{i-\frac{1}{2}, j-\frac{1}{2}, k} \\
= & \sum_{i=1}^{L} \Delta\lambda \sum_k \Delta\eta_k \sum_{j=2}^{M-1} \left\{ \Delta\phi \delta_\phi \left[K_\phi \cos\phi \delta_\phi \left(Q \delta_\eta r \right) \right] \right\}_{i-\frac{1}{2}, j-\frac{1}{2}, k} \\
= & \sum_{i=1}^{L} \Delta\lambda \sum_k \Delta\eta_k \left\{ \left[K_\phi \cos\phi \delta_\phi \left(Q \delta_\eta r \right) \right]_{i-\frac{1}{2}, M-1, k} - \left[K_\phi \cos\phi \delta_\phi \left(Q \delta_\eta r \right) \right]_{i-\frac{1}{2}, 1, k} \right\}.
\end{aligned} \tag{12.75}$$

Note that the summation limits for the sum over k have been deliberately omitted. Since their details are not explicitly used in the algebraic manipulations of this section, the consequent results, as written, are valid for Q stored either on ρ-levels, for which $k = 1/2, 3/2 ... N - 1/2$ or on θ-levels, for which $k = 0, 1, ... N$. But in the latter case, to exactly span the domain in the vertical $\Delta\eta_0$ and $\Delta\eta_N$ are defined, respectively, as the half-layer thicknesses $\Delta\eta_0 \equiv \eta_{\frac{1}{2}} - \eta_0 = \eta_{\frac{1}{2}} - 0$ and $\Delta\eta_N \equiv \eta_N - \eta_{N-\frac{1}{2}} = 1 - \eta_{N-\frac{1}{2}}$.

South polar-cap contribution

Multiplying (12.64) by $\left[\left(r^2 \delta_\eta r \right)_{SP} \Delta\eta \right]_k \pi \left(\Delta\phi / 2 \right)^2$, and summing over k yields

$$\sum_k \Delta\eta_k \left[\left(r^2 \delta_\eta r D_\eta^\eta \right)_{SP} \right]_k \pi \left(\frac{\Delta\phi}{2} \right)^2 = \sum_{i=1}^{L} \Delta\lambda \sum_k \Delta\eta_k \left[K_\phi \cos\phi \delta_\phi \left(Q \delta_\eta r \right) \right]_{i-\frac{1}{2}, 1, k}, \tag{12.76}$$

where $\Delta\lambda = 2\pi / L$.

North polar-cap contribution

Multiplying (12.71) by $\left[\left(r^2\delta_\eta r\right)_{NP}\Delta\eta\right]_k \pi\left(\Delta\phi/2\right)^2$, and summing over k yields

$$\sum_k \Delta\eta_k\left[\left(r^2\delta_\eta r D_\eta^\eta\right)_{NP}\right]_k \pi\left(\frac{\Delta\phi}{2}\right)^2 = -\sum_{i=1}^{L}\Delta\lambda\sum_k \Delta\eta_k\left[K_\phi\cos\phi\delta_\phi\left(Q\delta_\eta r\right)\right]_{i-\frac{1}{2},M-1,k}. \tag{12.77}$$

Summation of all contributions

Summing (12.75)-(12.77), i.e. summing all the horizontal diffusion operator contributions, finally gives

$$\begin{aligned}\sum_k \Delta\eta_k\left[\left(r^2\delta_\eta r D_\eta^\eta\right)_{SP}+\left(r^2\delta_\eta r D_\eta^\eta\right)_{NP}\right]_k \pi\left(\frac{\Delta\phi}{2}\right)^2 + \\ \sum_{i=1}^{L}\sum_{j=2}^{M-1}\sum_k\left(D_\eta^\eta r^2\cos\phi\delta_\eta r\Delta\eta\Delta\lambda\Delta\phi\right)_{i-\frac{1}{2},j-\frac{1}{2},k} &= 0.\end{aligned} \tag{12.78}$$

This equation is the discrete analogue of the continuous conservation law ($V^\eta\left[D_\eta^\eta(Q)\right]=0$):

$$\int_{-\frac{\pi}{2}}^{\frac{\pi}{2}}\int_0^{2\pi}\int_0^1 D_\eta^\eta r^2\cos\phi\delta_\eta r d\eta d\lambda d\phi \equiv \int_{-\frac{\pi}{2}}^{\frac{\pi}{2}}\int_0^{2\pi}\int_{r_S}^{r_T} D_\eta^\eta r^2\cos\phi\delta_\eta r dr d\lambda d\phi = 0, \tag{12.79}$$

where $r=r_S\left(\lambda,\phi\right)$ is the Earth's surface and $r=r_T$=constant is the model top.

Such a result is not obtained using the alternative diffusion operator D_{ND}^η and so, as noted previously, this operator does not preserve the global volume integral property.

12.8 Implementation

Currently, scalar diffusion is applied to the potential temperature field, θ, and the moisture field, q_v. For the θ field the detailed procedure is as follows.

An increment is calculated based on the field at the current time step and, in the terminology of Section 9, this explicit increment is added after the 2nd physics predictor, $\tilde{\theta}^{(P2)}$, and before the implicit 3rd dynamics predictor, $\tilde{\theta}^{(3)}$, is evaluated. This procedure can be formalised as follows.

Replace the current "2nd Dynamics Corrector" in Section 9 with:

- **2nd "Dynamics" Corrector**

Let $\tilde{\theta}^{(3)}$ be the 3rd dynamics predictor for θ^{n+1}. This can be written as the sum of the (2nd physics) predictor $\tilde{\theta}^{(P2)}$ plus a 2nd dynamics corrector $\left(\tilde{\theta}^{(3)} - \tilde{\theta}^{(P2)}\right)$, i.e. as

$$\tilde{\theta}^{(3)} = \tilde{\theta}^{(P2)} + \left(\tilde{\theta}^{(3)} - \tilde{\theta}^{(P2)}\right). \tag{12.80}$$

This dynamics corrector is defined as

$$\left(\tilde{\theta}^{(3)} - \tilde{\theta}^{(P2)}\right) = (-1)^{d_o - 1} \left[\Delta t D^{\eta}\right]^{d_o} (\theta^n), \tag{12.81}$$

where, as before, D^{η} represents either of D^{η}_{ND} and D^{η}_{η}. This corrector is explicit and dependent only on the time level n value of the field.

Aside :

Eliminating $\tilde{\theta}^{(P2)}$ *from the left-hand sides of* (9.34) *and* (12.81) *gives*

$$\begin{aligned} \frac{\tilde{\theta}^{(3)} - \theta^n_{dl}}{\Delta t} &= -\alpha_2 \left[(w^n - w^*)\,\delta_{2r}\tilde{\theta}^{(1)}\right] - (1-\alpha_2)\left[(w - w^*)\,\delta_{2r}\theta\right]^n_{dl} \\ &+ \left[S^{\theta}_1\right]^n_d + \left[S^{\theta}_2\right]^* + (-\Delta t)^{d_o - 1}\left[D^{\eta}\right]^{d_o}(\theta^n). \end{aligned} \tag{12.82}$$

Then make the current "2nd Dynamics Corrector" the "3rd Dynamics Corrector" with the (2nd physics) predictor, $\tilde{\theta}^{(P2)}$, replaced by the (2nd dynamics) predictor, $\tilde{\theta}^{(3)}$.

Aside :

It would be interesting to know what effect applying the diffusion operator $(-1)^{d_o-1}\left[\Delta t D^{\eta}\right]^{d_o}$ *to* $\tilde{\theta}^{(P2)}$, *rather than to* θ^n *in* (12.81), *would have on the deleterious effect of possible grid scale noise associated with the physics forcing.*

For the moisture field, q_v, the procedure is exactly analogous, and is not repeated here. The explicit increment arising from the horizontal diffusion operator is added after the 2nd physics predictor, $\tilde{q}_v^{(P2)}$, and before the 2nd dynamics predictor, $\tilde{q}_v^{(2)}$, is evaluated.

12.9 The vector diffusion operator

So far only scalar diffusion operators have been considered. However, for controlling numerical noise in the momentum components, the form of the diffusion operator for these components must also be considered. First the current implementation is briefly described before a more general discussion is given.

12.9.1 Continuous form

Currently the model uses the same options for the diffusion operator which is, in the continuous case, exactly the same as that for scalar diffusion, i.e. either D^η_η or D^η_{ND}.

12.9.2 Discrete form

In the discretised form, the diffusion for the w field is exactly the same as for the scalar fields, including the polar boundary conditions and the setting of the diffusion coefficients over orography.

For the u and v fields there are very minor differences in the interior due to the storage of the fields r and $\cos\phi$.

The setting of the diffusion coefficients over orography is done in an analogous manner to the scalar case, allowing for a different positioning of the variables, except at the lowest internal u and v level, $k = 1/2$, and for negatively sloping coordinate surfaces. In this case the level $k-1$ is below the ground and is undefined. Therefore, the simple expedient of using the height of the ground itself, r_S, has been used. Thus, diffusion is applied only if

$$(\Delta^\eta_r)_{i+1/2,j,1/2} > (r_S)_{i,j} - r_{i,j,1/2}, \tag{12.83}$$

and similarly for the ϕ-direction. This is rather more restrictive than is obtained in the interior points and more so than would be obtained if, for example, there were a fictitious level below the surface.

Aside :

This aspect is quite worrying as it introduces an asymmetry into the model. This is because slopes are defined to be "positive" or "negative" only in respect of whether the height of the surface increases or decreases in the direction of increasing coordinate, i.e. independent of wind direction. Thus, if the model were rewritten with i increasing from East to West and j increasing from North to South, "negative" slopes that do not satisfy (12.83) *would now be "positive" slopes which may well then satisfy the associated, less stringent requirement for diffusion to be permitted. In principle at least(!) the meteorology of this situation would not have changed. A simple remedy might be to replace r_S in* (12.83) *by*

$(r_S)_{i,j} - \left[r_{i,j,1/2} - (r_S)_{i,j}\right]$ *which would more closely mimic what would happen if this were indeed an internal level.*

For the u field no diffusion is applied at either pole. Where required the values of u at the poles are those evaluated as the components of the polar vector wind calculation (see Section 6.7 for details).

At the South pole, the ϕ-direction gradient of v across the pole is evaluated as:

$$\left.\frac{\partial v}{\partial \phi}\right|_{i,1/2,k} = \frac{v_{i,1,k} - \left(-v_{i+L/2,1,k}\right)}{\Delta\phi} \quad \text{for} \quad i = 1/2, 3/2, ..., L/2 - 1/2, \tag{12.84}$$

and as

$$\left.\frac{\partial v}{\partial \phi}\right|_{i,1/2,k} = \frac{v_{i,1,k} - \left(-v_{i-L/2,1,k}\right)}{\Delta\phi} \quad \text{for} \quad i = L/2 + 1/2, ..., L - 1/2. \tag{12.85}$$

Similarly, at the North pole the ϕ-direction gradient of v across the pole is evaluated as:

$$\left.\frac{\partial v}{\partial \phi}\right|_{i,M-1/2,k} = \frac{\left(-v_{i+L/2,M-1,k}\right) - v_{i,M-1,k}}{\Delta\phi} \quad \text{for} \quad i = 1/2, 3/2, ..., L/2 - 1/2, \tag{12.86}$$

and as

$$\left.\frac{\partial v}{\partial \phi}\right|_{i,M-1/2,k} = \frac{\left(-v_{i-L/2,M-1,k}\right) - v_{i,M-1,k}}{\Delta\phi} \quad \text{for} \quad i = L/2 + 1/2, ..., L - 1/2. \tag{12.87}$$

The operators are also implemented in the same way as in the scalar case. That is it operates on the time level n fields and, for the u and v fields, is evaluated after the second physics predictors, $\tilde{u}^{(P2)}$ and $\tilde{v}^{(P2)}$, and before the second dynamics predictors, $\tilde{u}^{(2)}$ and $\tilde{v}^{(2)}$. For the w field it is evaluated after the first dynamics predictor, $\tilde{w}^{(1)}$, and before the second dynamics predictor, $\tilde{w}^{(2)}$.

12.9.3 Discussion

There are two aspects to be considered in designing the diffusion operator for the velocity field. The first is what general tensor form should the diffusion take? The general form can be written as

$$\frac{\partial u_i}{\partial t} = \frac{\partial \tau_{ij}}{\partial x_j}, \; i, j = 1, 2, 3, \tag{12.88}$$

where τ_{ij} can be considered as a stress tensor. Here, since diffusion is primarily considered to be a numerical artifact, the simple expedient of taking $\tau_{ij} = \partial u_i / \partial x_j$ is made. In developing a similar, numerically motivated operator, Becker (2001),however, effectively uses a symmetric stress tensor, i.e. $\tau_{ij} = \partial u_i/\partial x_j + \partial u_j/\partial x_i$. Further, Smagorinsky (1993) considers physically based diffusion and therefore uses what amounts, for a certain choice of his parameters α, β and γ, to the usual turbulent Reynolds stress, $\tau_{ij} = \partial u_i/\partial x_j + \partial u_j/\partial x_i - (2/3)\nabla.\mathbf{u}\delta_{ij}$, where δ_{ij} is the Kronecker δ. (For incompressible flows the diffusion operator (12.88) for each of these options is the same.) The resultant differences between all of these choices for the case of horizontal diffusion are discussed at the end of this section.

The second aspect of the problem is that, since u, v and w are the components of a vector, it is important that the vector form of the diffusion operator is considered to ensure that the operator preserves the correct conservation laws. Currently this is not the case - a form of the usual scalar operator is used, which, as has been discussed above, does not even conserve scalars. The full form of the vector diffusion operator, given below, is more complicated than its scalar equivalent and, at first (or even second!) sight, it is not at all clear how this operator should be simplified to give the desired horizontal diffusion whilst retaining appropriate conservation properties.

The full, three-dimensional vector diffusion operator in spherical polar coordinates is (Batchelor 1967):

$$\begin{aligned}\frac{\partial u}{\partial t} &= \frac{K_\lambda}{r^2}\frac{\partial}{\partial\lambda}\left(\frac{1}{\cos^2\phi}\frac{\partial u}{\partial\lambda}\right) + \frac{K_\phi}{r^2\cos\phi}\frac{\partial}{\partial\phi}\left(\cos\phi\frac{\partial u}{\partial\phi}\right) + \frac{K_r}{r^2}\frac{\partial}{\partial r}\left(r^2\frac{\partial u}{\partial r}\right)\\ &+ \left[-K_{u1}\frac{u}{r^2\cos^2\phi} + K_{u2}\frac{2}{r^2\cos\phi}\frac{\partial w}{\partial\lambda} - K_{u3}\frac{2\sin\phi}{r^2\cos^2\phi}\frac{\partial v}{\partial\lambda}\right],\end{aligned} \tag{12.89}$$

$$\begin{aligned}\frac{\partial v}{\partial t} &= \frac{K_\lambda}{r^2}\frac{\partial}{\partial\lambda}\left(\frac{1}{\cos^2\phi}\frac{\partial v}{\partial\lambda}\right) + \frac{K_\phi}{r^2\cos\phi}\frac{\partial}{\partial\phi}\left(\cos\phi\frac{\partial v}{\partial\phi}\right) + \frac{K_r}{r^2}\frac{\partial}{\partial r}\left(r^2\frac{\partial v}{\partial r}\right)\\ &+ \left[-K_{v1}\frac{v}{r^2\cos^2\phi} + K_{v2}\frac{2}{r^2}\frac{\partial w}{\partial\phi} + K_{v3}\frac{2\sin\phi}{r^2\cos^2\phi}\frac{\partial u}{\partial\lambda}\right],\end{aligned} \tag{12.90}$$

$$\begin{aligned}\frac{\partial w}{\partial t} &= \frac{K_\lambda}{r^2}\frac{\partial}{\partial\lambda}\left(\frac{1}{\cos^2\phi}\frac{\partial w}{\partial\lambda}\right) + \frac{K_\phi}{r^2\cos\phi}\frac{\partial}{\partial\phi}\left(\cos\phi\frac{\partial w}{\partial\phi}\right) + \frac{K_r}{r^2}\frac{\partial}{\partial r}\left(r^2\frac{\partial w}{\partial r}\right)\\ &+ \left[-K_{w1}\frac{2w}{r^2} - K_{w2}\frac{2}{r^2\cos\phi}\frac{\partial}{\partial\phi}(v\cos\phi) - K_{w3}\frac{2}{r^2\cos\phi}\frac{\partial u}{\partial\lambda}\right],\end{aligned} \tag{12.91}$$

where K_λ, K_ϕ and K_r are the usual coefficients of diffusion in the λ, ϕ and r directions, respectively. The K_{Xi} for $X = u, v, w$ and $i = 1, 2, 3$ are diffusion coefficients yet to be identified. Isotropic diffusion is obtained by setting all the K's to be equal. For simplicity, the K's have been assumed to be independent of position.

The first three terms on the right-hand side of (12.89)-(12.91) are the usual terms that constitute scalar diffusion in spherical (λ, ϕ, r) coordinates, i.e. D^r_{3D} as defined in (12.1). It is by analogy with this form that each of these terms has been associated uniquely with one of K_λ, K_ϕ and K_r, which seems a reasonable approximation. With all the K's set equal, the extra terms, those in square brackets, arise due to the spatial variation of the base vector triad, $(\mathbf{i}, \mathbf{j}, \mathbf{k})$, in spherical coordinates (see Section 1). With the exception of the first terms in each of the square brackets, these new terms are not necessarily negligible in comparison with those of the scalar diffusion operator. In addition, at least some of them are crucial in ensuring the diffusion operator conserves angular momentum.

There are two issues regarding the extra terms. The first is that in order to construct either a horizontal diffusion operator or, for the boundary-layer turbulence parametrisation, a vertical diffusion operator, it has to be known which of the new terms are associated with diffusion in the vertical or horizontal. In other words, each of the K_{Xi} needs to be associated in some way with one or more of K_λ, K_ϕ and K_r. (Becker (2001) indicates that the "conventional" horizontal form of (12.89)-(12.91) is achieved by setting all the K's equal, putting $w = 0$, neglecting all vertical derivatives and making the shallow-atmosphere approximation, $r = a$.) The second is that it is desirable for a finite-difference form of (12.89)-(12.91) to preserve any appropriate conservation properties. This is most easily achieved if, prior to discretisation, (12.89)-(12.91) are written in continuous form in the appropriate flux form. In assigning the K_{Xi}'s to K_λ, K_ϕ and K_r, the flux form will become evident.

One way of deciding the form of the K_{Xi}'s is to start with (12.88) and the appropriate form of τ_{ij}, retaining the distinction between K_λ, K_ϕ and K_r, and transform the equation into spherical coordinates. An alternative way, which hopefully gives some physical insight into the nature of the extra terms, is to find realisable, steady-state velocity fields, $\mathbf{u}$, for which it is known that $\nabla^2\mathbf{u} = 0$, so that diffusion should have no effect. Then when (12.89)-(12.91) are applied to the fields the time tendencies for u, v and w vanish. Four particular velocity fields are considered: solid body rotation about an arbitrary axis (in particular about a polar axis and an equatorial axis); flow due to a point source at the origin; flow due to a dipole at the origin (in particular, a dipole aligned with the polar axis); and uniform rectilinear flow.

Solid body rotation

Let the axis of rotation, $\mathbf{a}$, be defined by $(\lambda, \phi) = (\lambda_0, \phi_0)$, then in terms of the unit vectors at the point, (λ, ϕ, r), $\mathbf{a}$ is given by:

$$\left(-\cos\phi_0 \sin(\lambda - \lambda_0), -\cos\phi_0 \sin\phi \cos(\lambda - \lambda_0) + \sin\phi_0 \cos\phi, \cos\phi_0 \cos\phi \cos(\lambda - \lambda_0) + \sin\phi_0 \sin\phi\right), \tag{12.92}$$

and the velocity field for solid body rotation about this axis, with unit angular velocity, is:

$$(u, v, w) = r\left(-\cos\phi_0 \sin\phi \cos(\lambda - \lambda_0) + \sin\phi_0 \cos\phi, \cos\phi_0 \sin(\lambda - \lambda_0), 0\right). \tag{12.93}$$

The axial angular momentum , about $\mathbf{a}$, is given by

$$M = \rho\left(\mathbf{r} \times \mathbf{u}\right).\mathbf{a} = \rho r\left\{\cos\phi_0 \sin(\lambda - \lambda_0) v + \left[-\cos\phi_0 \sin\phi \cos(\lambda - \lambda_0) + \sin\phi_0 \cos\phi\right] u\right\}. \tag{12.94}$$

A particular, and meteorologically important, case is that of rotation about the polar axis, $\phi_0 = \pi/2$, with, for definiteness, $\lambda = \lambda_0$. (12.93) then reduces to:

$$(u, v, w) = r\left(\cos\phi, 0, 0\right). \tag{12.95}$$

Substituting this into (12.89)-(12.91) shows that both the v and w tendencies vanish. However, (12.89) becomes

$$\frac{\partial u}{\partial t} = \frac{1}{r\cos\phi}\left[-\left(\cos^2\phi - \sin^2\phi\right) K_\phi + 2\cos^2\phi K_r - K_{u1}\right]. \tag{12.96}$$

Setting $\partial u/\partial t = 0$ then determines that $K_{u1} = -\left(\cos^2\phi - \sin^2\phi\right) K_\phi + 2\cos^2\phi K_r$. Substituting this into (12.89) allows the equation to be written in the form:

$$\begin{aligned}\frac{\partial u}{\partial t} \quad = \quad & \frac{K_\lambda}{r^2}\frac{\partial}{\partial\lambda}\left(\frac{1}{\cos^2\phi}\frac{\partial u}{\partial\lambda}\right) + \frac{K_\phi}{r^2\cos^2\phi}\frac{\partial}{\partial\phi}\left[\cos^3\phi\frac{\partial}{\partial\phi}\left(\frac{u}{\cos\phi}\right)\right] + \frac{K_r}{r^3}\frac{\partial}{\partial r}\left[r^4\frac{\partial}{\partial r}\left(\frac{u}{r}\right)\right] \\ & + K_{u2}\frac{2}{r^2\cos\phi}\frac{\partial w}{\partial\lambda} - K_{u3}\frac{2\sin\phi}{r^2\cos^2\phi}\frac{\partial v}{\partial\lambda}.\end{aligned} \tag{12.97}$$

Since each of λ, ϕ and r commutes with the partial derivatives with respect to the other two variables, and assuming the density, ρ, to be a constant, (12.97) has the correct flux form for the natural conservation of the global volume integral of axial angular momentum (see Appendix A), given by

$$\frac{\partial}{\partial t}\int\int\int M r^2 \cos\phi d\lambda d\phi dr = \int\int\int\left(r\cos\phi\rho\frac{\partial u}{\partial t}\right) r^2\cos\phi d\lambda d\phi dr, \tag{12.98}$$

using (12.94) with $\phi_0 = \pi/2$ and $\lambda_0 = 0$.

<u>**Aside :**</u>

When ρ is not constant, conservation of global axial angular momentum would not be obtained as ρ would not commute with the diffusion operator so the requisite flux form is not achieved. A natural way of ensuring that conservation is indeed guaranteed by the diffusion operator in the presence of density variations, is to diffuse the true momentum components, $(\rho u, \rho v, \rho w)$, rather than just the velocity components as is currently done. This is analogous to diffusing $\rho\times$moisture variable instead of just the moisture variable. An alternative approach is to write $\nabla^2 \mathbf{u}$ as $(1/\rho)\nabla.(\rho\nabla\mathbf{u})$, analogous with molecular diffusion.

Further progress is made by considering now solid body rotation about an equatorial axis, $\phi_0 = 0$. (12.93) then reduces to

$$(u, v, w) = r\left(-\sin\phi\cos(\lambda - \lambda_0), \sin(\lambda - \lambda_0), 0\right). \tag{12.99}$$

Substituting this into (12.97) and (12.90)-(12.91) shows that

$$\frac{\partial u}{\partial t} = \frac{\cos(\lambda - \lambda_0)\sin\phi}{r\cos^2\phi}\left[K_\phi + K_\lambda - 2K_{u3}\right] \tag{12.100}$$

so that $K_{u3} = K_\phi/2 + K_\lambda/2$ so that (12.97) becomes

$$\begin{aligned}\frac{\partial u}{\partial t} &= \frac{K_\lambda}{r^2\cos^2\phi}\frac{\partial}{\partial\lambda}\left(\frac{\partial u}{\partial\lambda} - \sin\phi v\right) + \frac{K_\phi}{r^2\cos^2\phi}\left\{\frac{\partial}{\partial\phi}\left[\cos^3\phi\frac{\partial}{\partial\phi}\left(\frac{u}{\cos\phi}\right)\right] - \sin\phi\frac{\partial v}{\partial\lambda}\right\}\\ &\quad + \frac{K_r}{r^3}\frac{\partial}{\partial r}\left[r^4\frac{\partial}{\partial r}\left(\frac{u}{r}\right)\right] + K_{u2}\frac{2}{r^2\cos\phi}\frac{\partial w}{\partial\lambda}.\end{aligned} \tag{12.101}$$

Similarly, (12.99) in (12.90) shows that

$$\frac{\partial v}{\partial t} = \frac{\sin(\lambda - \lambda_0)}{r\cos^2\phi}\left(-K_\lambda + 2\cos^2\phi K_r - K_{v1} + 2\sin^2\phi K_{v3}\right). \tag{12.102}$$

Thus, $K_{v1} - 2\sin^2\phi K_{v3} = -K_\lambda + 2\cos^2\phi K_r$ or $K_{v1} = -K_\lambda + 2\cos^2\phi K_r + 2\sin^2\phi K_{v3}$. The v-equation, (12.90), can then be rewritten as:

$$\begin{aligned}\frac{\partial v}{\partial t} &= \frac{K_\lambda}{r^2\cos^2\phi}\left[\frac{\partial}{\partial\lambda}\left(\frac{\partial v}{\partial\lambda}\right) + v\right] + \frac{K_\phi}{r^2\cos\phi}\frac{\partial}{\partial\phi}\left(\cos\phi\frac{\partial v}{\partial\phi}\right) + \frac{K_r}{r^3}\frac{\partial}{\partial r}\left[r^4\frac{\partial}{\partial r}\left(\frac{v}{r}\right)\right]\\ &\quad + K_{v2}\frac{2}{r^2}\frac{\partial w}{\partial\phi} + K_{v3}\frac{2\sin\phi}{r^2\cos^2\phi}\left(\frac{\partial u}{\partial\lambda} - \sin\phi v\right).\end{aligned} \tag{12.103}$$

Also, (12.99) in (12.90) gives

$$\frac{\partial w}{\partial t} = \frac{2\sin(\lambda - \lambda_0)\sin\phi}{r\cos\phi}\left(K_{w2} - K_{w3}\right), \tag{12.104}$$

so that $K_{w3} = K_{w2}$.

Point source

For a point source at the origin, of strength 4π, the velocity field is purely radial and given by $(u,v,w)=(0,0,1/r^2)$. For this velocity field (12.101) and (12.103) give zero tendencies for u and v. Substituting this form into (12.91) gives

$$\frac{\partial w}{\partial t}=\frac{2}{r^4}\left(K_r-K_{w1}\right), \tag{12.105}$$

so that $K_{w1}=K_r$ and similarly to the u-equation, (12.91) can be written as:

$$\begin{aligned}\frac{\partial w}{\partial t} &= \frac{K_\lambda}{r^2}\frac{\partial}{\partial\lambda}\left(\frac{1}{\cos^2\phi}\frac{\partial w}{\partial\lambda}\right)+\frac{K_\phi}{r^2\cos\phi}\frac{\partial}{\partial\phi}\left(\cos\phi\frac{\partial w}{\partial\phi}\right)\\ &\quad+\frac{K_r}{r^3}\frac{\partial}{\partial r}\left[r^4\frac{\partial}{\partial r}\left(\frac{w}{r}\right)\right]-K_{w2}\frac{2}{r^2\cos\phi}\left[\frac{\partial}{\partial\phi}\left(v\cos\phi\right)+\frac{\partial u}{\partial\lambda}\right],\end{aligned} \tag{12.106}$$

where the above result that $K_{w3}=K_{w2}$ has been used.

Source dipole

For a source dipole of strength 4π, the velocity field is $(u,v,w)=(0,-\cos\phi/r^3,2\sin\phi/r^3)$. Substituting this into (12.101) leads to a zero tendency for u. (12.103) gives

$$\frac{\partial v}{\partial t}=\frac{1}{r^5\cos\phi}\left[-K_\lambda+\left(\cos^2\phi-\sin^2\phi\right)K_\phi-4\cos^2\phi K_r+4\cos^2\phi K_{v2}+2\sin^2\phi K_{v3}\right], \tag{12.107}$$

so that $4\cos^2\phi K_{v2}+2\sin^2\phi K_{v3}=K_\lambda-\left(\cos^2\phi-\sin^2\phi\right)K_\phi+4\cos^2\phi K_r$ or $2\sin^2\phi K_{v3}=K_\lambda-\left(\cos^2\phi-\sin^2\phi\right)K_\phi+4\cos^2\phi K_r-4\cos^2\phi K_{v2}$. Using this (12.103) becomes

$$\begin{aligned}\frac{\partial v}{\partial t} &= \frac{K_\lambda}{r^2\cos^2\phi}\frac{\partial}{\partial\lambda}\left(\frac{\partial v}{\partial\lambda}+\frac{u}{\sin\phi}\right)+\frac{K_\phi}{r^2\cos^2\phi}\left\{\frac{\partial}{\partial\phi}\left[\cos^3\phi\frac{\partial}{\partial\phi}\left(\frac{v}{\cos\phi}\right)\right]-\frac{\cos^2\phi-\sin^2\phi}{\sin\phi}\frac{\partial u}{\partial\lambda}\right\}\\ &\quad+\frac{K_r}{r^3}\left\{\frac{\partial}{\partial r}\left[r^4\frac{\partial}{\partial r}\left(\frac{v}{r}\right)\right]-4r\left(v-\frac{1}{\sin\phi}\frac{\partial u}{\partial\lambda}\right)\right\}+K_{v2}\frac{2}{r^2}\left[\frac{\partial w}{\partial\phi}+2\left(v-\frac{1}{\sin\phi}\frac{\partial u}{\partial\lambda}\right)\right].\end{aligned} \tag{12.108}$$

Substituting the velocity form into (12.107) shows that

$$\frac{\partial w}{\partial t}=\frac{4\sin\phi}{r^5}\left(-K_\phi+2K_r-K_{w2}\right), \tag{12.109}$$

so that $K_{w2}=-K_\phi+2K_r$. Using this, the final form of the w-equation is:

$$\begin{aligned}\frac{\partial w}{\partial t} &= \frac{K_\lambda}{r^2}\frac{\partial}{\partial\lambda}\left(\frac{1}{\cos^2\phi}\frac{\partial w}{\partial\lambda}\right)+\frac{K_\phi}{r^2\cos\phi}\left\{\frac{\partial}{\partial\phi}\left(\cos\phi\frac{\partial w}{\partial\phi}\right)+2\left[\frac{\partial}{\partial\phi}\left(v\cos\phi\right)+\frac{\partial u}{\partial\lambda}\right]\right\}\\ &\quad+\frac{K_r}{r^3}\left\{\frac{\partial}{\partial r}\left[r^4\frac{\partial}{\partial r}\left(\frac{w}{r}\right)\right]-\frac{4r}{\cos\phi}\left[\frac{\partial}{\partial\phi}\left(v\cos\phi\right)+\frac{\partial u}{\partial\lambda}\right]\right\}.\end{aligned} \tag{12.110}$$

Uniform flow

There now remain only two diffusion coefficients to be determined, K_{u2} and K_{v2}. In all the above tests the terms multiplying these coefficients in (12.101) and (12.108) identically vanish. In order to identify these terms a suitable flow with variation in the λ-direction is needed. A simple example of such a flow, with trivially vanishing $\nabla^2\mathbf{u}$, is the case of uniform flow in some direction. The axis, $\mathbf{a}$, defined and used above determines an arbitrary direction. Therefore, let the velocity have unit speed and be parallel in direction to $\mathbf{a}$. Then

$$(u,v,w) =$$

$$\left(-\cos\phi_0\sin(\lambda-\lambda_0), -\cos\phi_0\sin\phi\cos(\lambda-\lambda_0)+\sin\phi_0\cos\phi, \cos\phi_0\cos\phi\cos(\lambda-\lambda_0)+\sin\phi_0\sin\phi\right). \tag{12.111}$$

Substituting this into (12.101) gives

$$\frac{\partial u}{\partial t} = \frac{\cos\phi_0\sin(\lambda-\lambda_0)}{r^2}\left(K_\lambda - K_\phi + 2K_r - 2K_{u2}\right), \tag{12.112}$$

so that $K_{u2} = K_\lambda/2 - K_\phi/2 + K_r$. Substituting this expression for K_{u2} back into (12.101) gives the final form of the u-equation as:

$$\begin{aligned}
\frac{\partial u}{\partial t} &= \frac{K_\lambda}{r^2\cos^2\phi}\frac{\partial}{\partial\lambda}\left(\frac{\partial u}{\partial\lambda} - \sin\phi v + \cos\phi w\right) \\
&+\frac{K_\phi}{r^2\cos^2\phi}\left\{\frac{\partial}{\partial\phi}\left[\cos^3\phi\frac{\partial}{\partial\phi}\left(\frac{u}{\cos\phi}\right)\right] - \frac{\partial}{\partial\lambda}\left(\sin\phi v + \cos\phi w\right)\right\} \\
&+\frac{K_r}{r^3}\left\{\frac{\partial}{\partial r}\left[r^4\frac{\partial}{\partial r}\left(\frac{u}{r}\right)\right] + \frac{2r}{\cos\phi}\frac{\partial w}{\partial\lambda}\right\}.
\end{aligned} \tag{12.113}$$

Substituting (12.111) into (12.108) gives the interesting result that

$$\begin{aligned}
\frac{\partial v}{\partial t} &= \frac{1}{r^2\cos^2\phi}\left[-\frac{\cos(\lambda-\lambda_0)\cos\phi_0\cos^2\phi}{\sin\phi}\left(K_\lambda - K_\phi\right)\right. \\
&= \left.+2\cos^2\phi\cos\phi_0\left(3\cos(\lambda-\lambda_0)\sin\phi - 3\frac{\sin\phi_0\cos\phi}{\cos\phi_0} - 2\frac{\cos(\lambda-\lambda_0)}{\sin\phi}\right)\left(K_r - K_{v2}\right)\right],
\end{aligned} \tag{12.114}$$

which implies that $(K_r - K_{v2})$ is equal to $(K_\lambda - K_\phi)$ multiplied by a non-vanishing function of λ_0 and ϕ_0. However, λ_0 and ϕ_0 are arbitrary, in that $\partial v/\partial t$ vanishes whatever their value. This is only possible if $K_{v2} = K_r$ and also $K_\lambda = K_\phi$. Further, substituting (12.111) into (12.110) shows that $\partial w/\partial t$ vanishes in this case only if in addition $K_r = K_\lambda = K_\phi$. This is perhaps not surprising since the other test cases have all had a spherical geometry whereas this case does not and so it is only the true isotropic diffusion operator, $K_\lambda = K_\phi = K_r$ which preserves $\nabla^2\mathbf{u} = 0$. So finally, K_{v2} has been determined as being equal to K_r and so the final form of the v-equation is given by

$$\begin{aligned}\frac{\partial v}{\partial t} &= \frac{K_\lambda}{r^2\cos^2\phi}\frac{\partial}{\partial\lambda}\left(\frac{\partial v}{\partial\lambda}+\frac{u}{\sin\phi}\right)+\frac{K_\phi}{r^2\cos^2\phi}\left\{\frac{\partial}{\partial\phi}\left[\cos^3\phi\frac{\partial}{\partial\phi}\left(\frac{v}{\cos\phi}\right)\right]-\frac{\cos^2\phi-\sin^2\phi}{\sin\phi}\frac{\partial u}{\partial\lambda}\right\}\\ &+\frac{K_r}{r^3}\left\{\frac{\partial}{\partial r}\left[r^4\frac{\partial}{\partial r}\left(\frac{v}{r}\right)\right]+2r\frac{\partial w}{\partial\phi}\right\}. \end{aligned} \tag{12.115}$$

Summary and further comments

By considering a combination of simple translation, solid body rotation and the flow due to point sources and dipole sources, the appropriate forms of (12.89)-(12.91) are found to be:

$$\begin{aligned}\frac{\partial u}{\partial t} &= \frac{K_\lambda}{r^2\cos^2\phi}\frac{\partial}{\partial\lambda}\left(\frac{\partial u}{\partial\lambda}-\sin\phi v+\cos\phi w\right)\\ &+\frac{K_\phi}{r^2\cos^2\phi}\left\{\frac{\partial}{\partial\phi}\left[\cos^3\phi\frac{\partial}{\partial\phi}\left(\frac{u}{\cos\phi}\right)\right]-\frac{\partial}{\partial\lambda}\left(\sin\phi v+\cos\phi w\right)\right\}\\ &+\frac{K_r}{r^3}\left\{\frac{\partial}{\partial r}\left[r^4\frac{\partial}{\partial r}\left(\frac{u}{r}\right)\right]+\frac{2r}{\cos\phi}\frac{\partial w}{\partial\lambda}\right\}, \end{aligned} \tag{12.116}$$

$$\begin{aligned}\frac{\partial v}{\partial t} &= \frac{K_\lambda}{r^2\cos^2\phi}\frac{\partial}{\partial\lambda}\left(\frac{\partial v}{\partial\lambda}+\frac{u}{\sin\phi}\right)\\ &+\frac{K_\phi}{r^2\cos^2\phi}\left\{\frac{\partial}{\partial\phi}\left[\cos^3\phi\frac{\partial}{\partial\phi}\left(\frac{v}{\cos\phi}\right)\right]-\frac{\cos^2\phi-\sin^2\phi}{\sin\phi}\frac{\partial u}{\partial\lambda}\right\}\\ &+\frac{K_r}{r^3}\left\{\frac{\partial}{\partial r}\left[r^4\frac{\partial}{\partial r}\left(\frac{v}{r}\right)\right]+2r\frac{\partial w}{\partial\phi}\right\}, \end{aligned} \tag{12.117}$$

$$\begin{aligned}\frac{\partial w}{\partial t} &= \frac{K_\lambda}{r^2\cos^2\phi}\frac{\partial}{\partial\lambda}\left(\frac{\partial w}{\partial\lambda}\right)\\ &+\frac{K_\phi}{r^2\cos\phi}\left\{\frac{\partial}{\partial\phi}\left(\cos\phi\frac{\partial w}{\partial\phi}\right)+2\left[\frac{\partial}{\partial\phi}\left(v\cos\phi\right)+\frac{\partial u}{\partial\lambda}\right]\right\}\\ &+\frac{K_r}{r^3}\left\{\frac{\partial}{\partial r}\left[r^4\frac{\partial}{\partial r}\left(\frac{w}{r}\right)\right]-\frac{4r}{\cos\phi}\left[\frac{\partial}{\partial\phi}\left(v\cos\phi\right)+\frac{\partial u}{\partial\lambda}\right]\right\}. \end{aligned} \tag{12.118}$$

As noted above, the full equations of Smagorinsky (1993) for the vector diffusion operator use a considerably different, physically based, form for the stress tensor, τ_{ij}. As a result (12.116)-(12.118) differ slightly from Smagorinsky's (22). [Note though that his expression for S_{13}, his (20), is wrong. In place of

$$S_{13} = \frac{1}{2}\left(\frac{\partial u}{\partial z}+\frac{\partial w}{\partial x}\right), \tag{12.119}$$

the expression should read

$$S_{13} = \frac{1}{2}\left[r\frac{\partial\left(u/r\right)}{\partial z} + \frac{\partial w}{\partial x}\right], \tag{12.120}$$

see Batchelor (1967).]

Smagorinsky (1993) goes on to simplify the full equations in an energetically consistent manner to obtain a form appropriate to a quasi-hydrostatic, shallow-atmosphere approximation which results in diffusion only for the horizontal velocity components. This can be reduced further to obtain a form for horizontal diffusion by setting Smagorinsky's γ to zero. A comparable form of horizontal diffusion can be derived from (12.116)-(12.118) by setting K_r equal to zero. It is somewhat surprising, but reassuring, that, despite the significant differences in approach, when K_λ and K_ϕ are both set equal to Smagorinsky's β, (12.116) and (12.117) have exactly the same form as Smagorinsky's (35), with $\gamma = 0$. The only differences are that Smagorinsky retains the density, ρ, and also makes the shallow-atmosphere approximation, $r = a$, which has not been made here.

However, the horizontal diffusion of vertical velocity, (12.118), differs from Smagorinsky's form. Setting $K_r = 0$, which is analogous to setting Smagorinsky's $\gamma = 0$, does not eliminate the right-hand side of (12.118), in contrast to Smagorinsky's form for which the vertical diffusion vanishes. This is not a result of making the shallow-atmosphere approximation. This can be seen from Williams (1972) who derives the correct shallow-atmosphere approximation to the equation set (12.89)-(12.91), without also making the hydrostatic approximation. The resulting equations are identical to (12.116)-(12.118), when $K_\lambda = K_\phi = K_r = K$ and $r = a$, except for the appearance of the terms

$$\frac{2K}{r^2\cos\phi}\frac{\partial w}{\partial \lambda},$$

$$\frac{2K}{r^2}\frac{\partial w}{\partial \phi},$$

and

$$-\frac{2K}{r^2\cos\phi}\left[\frac{\partial}{\partial\phi}\left(v\cos\phi\right) + \frac{\partial u}{\partial\lambda}\right]$$

in (12.116), (12.117) and (12.118), respectively. Therefore, for an incompressible flow, as considered by Williams (1972), Williams' expression is obtained from (12.116)-(12.118) by setting all the K's equal, setting $r = a$ and subtracting the term $(2K/r)\nabla w$. Williams (1972) shows that his equation set still ensures a positive-definite energy dissipation rate. Thus, the lack of diffusion of the vertical velocity in the quasi-hydrostatic diffusion operator of

Smagorinsky (1993) would appear to be intrinsically linked to the hydrostatic approximation, which is consistent with the fact that the vertical velocity does not contribute to the kinetic energy of a hydrostatic model. For a non-hydrostatic model, such as the New Dynamics, it seems likely that the appropriate form of horizontal diffusion includes non-zero diffusion of the vertical velocity. It might be tentatively suggested that the appropriate form of this is given by (12.118) with $K_r = 0$. However, it is important that any proposed set preserves the positive-definiteness of the energy dissipation rate. Following a procedure similar to Williams (1972), it can be shown that this is the case for horizontal energy, $\rho\left(u^2+v^2\right)/2$, i.e. from consideration of (12.116) and (12.117) with $K_\lambda = K_\phi$ and $K_r = 0$. But, when these assumptions are made in (12.118) and the full energy is considered, such a result is only found if the term in (12.118) involving the product of K_ϕ and the horizontal divergence is either neglected or the horizontal divergence term is replaced by $-\partial w/\partial r$, as would be appropriate for an incompressible flow.

Clearly, the inclusion of diffusion of the vertical velocity in a simplified scheme complicates matters somewhat and in his approach, Williams (1972) found rather counter-intuitive results in this regard (qualitatively his results would be consistent with swapping the roles of the horizontal diffusion coefficients, K_λ and K_ϕ, with K_r in (12.118)). Further, the inclusion of this component, in whatever form, is not required to ensure any of the conservation or energetic constraints considered here.

Motivated by numerical considerations, Becker (2001) develops a “symmetric” form of the horizontal diffusion operator for a hydrostatic model. As he notes, this differs from that of Smagorinsky (1993) by the inclusion the horizontal gradient of the horizontal velocity divergence. The appearance of this extra term, compared with the form obtained here, is qualitatively clear from Becker's choice for τ_{ij}. The extra term, $\partial u_j/\partial x_i$, in τ_{ij} leads to an extra contribution to the diffusion operator equal to $\nabla\left(\nabla.\mathbf{u}\right)$. The gradient and divergence operators are then limited, by construction, to only be horizontal operators. For flow fields for which the horizontal divergence vanishes, the diffusion operators of Smagorinsky (1993) and Becker (2001) are equivalent. However, if the horizontal divergence does not vanish, in particular for the dipole source field discussed above, the two forms differ and Becker's “symmetric” form applies a spurious frictional drag to an otherwise steady flow.

All of the above forms for horizontal vector diffusion do preserve angular momentum. This is not the case for either of the optional forms currently available in the New Dynamics, that is either D^η_η or D^η_{ND} applied to each of u and v, nor for the "conventional" form discussed by Becker (2001). This latter operator is obtained from (12.89)-(12.90) by setting all the K's equal, setting $w = 0$, neglecting all vertical derivatives and making the shallow-atmosphere approximation, $r = a$. Further, the form proposed here is written in a flux form appropriate for the conservation of zonal angular momentum. Thus, it is straightforward to discretise the continuous form whilst retaining this important conservation property.

It is also worth noting the comment of Becker (2001) that it is important for the conservation of total energy, that when adding diffusion to the velocity components, the associated frictional heating, that is the dissipation of energy to heat, is allowed for in the thermodynamic equation.

Once the chosen form of the equations for horizontal diffusion are obtained, it is straightforward, though algebraically laborious, to repeat the analyses of the previous sections for the scalar operator, in order to obtain the appropriate vector equivalent of the various horizontal diffusion operators, either diffusion along r-surfaces in η-coordinates or diffusion along η-surfaces in η-coordinates.

12.10 Filtering in the region of the poles

Due to the anisotropic formulation of the diffusion (i.e. the current choice for K_λ, see Section 12.4.1), diffusion in the East-West, λ-direction, becomes weaker and weaker as the pole is approached. For this reason, near to the poles (where the horizontal grid length in the East-West direction can be of the order of 1 km) the model can suffer from the presence of small scale, $O(1)$-$O(10)$ km, signals which can then be transported away from the pole where they rapidly become grid scale and contaminate the resolved response in these regions. In addition, noise at the grid scale can significantly slow down the convergence of the Helmholtz solver (see Section 15 for details of the solver). Therefore, it is desirable to apply some form of spatial filtering near to each pole. Currently this filtering is applied to all three components of the velocity vector, u, v and w, and to the potential temperature field, θ.

Aside :

The introduction of a correctly isotropic diffusion operator, i.e. that proposed in Section 12.2.2 with $K_\lambda = K_\phi$, might be expected to eliminate the need for *additional polar filtering.*

Aside :

It is also possible that a contributory factor in the generation of noise in the region of the poles is that the globally applied horizontal diffusion, discussed earlier in this Section, is switched off over orography, such as might be the case at the edges of the Greenland and Antarctic plateaux.

Aside :

Applying the filter to one and only one of the thermodynamic variables, i.e. θ, means that, where that filter is applied, any balance between the thermodynamic variables is lost. In particular, the balance represented by the continuity equation, the definition of temperature, T, and the partitioning of water substances between vapour, cloud liquid water and cloud frozen water will be disturbed. However, for non-linear relationships, as all these are, applying a linear filter operator such as that described here, to all the related variables would not guarantee that those relationships still hold.

The polar filter is applied only in the East-West direction and is applied to the time-level n fields at the beginning of the time step (it is for this reason that the stability of the scheme is independent of any diffusion applied elsewhere in the model). As such it is not a time stepping procedure itself. However, for the general variable Q, the filter operation can formally be written as

$$\frac{\partial Q}{\partial t} = \frac{K_p}{r^2 \cos^2 \phi} \frac{\partial^2 Q}{\partial \lambda^2}, \tag{12.121}$$

and therefore has the same general form as (12.18) but with $K_\phi \equiv 0$ and K_λ replaced by the polar diffusivity K_p. Here, $\partial/\partial\lambda$ indicates the partial derivative keeping η constant, i.e. the transformed, (λ, ϕ, η) coordinates are assumed. (Note that the equivalence of (12.121) with (12.18) is only exact when K_λ is independent of λ, as is the case in the absence of orography.)

Eq. (12.121) is discretised in an explicit manner as

$$\frac{Q^f_{i,j,k} - Q^n_{i,j,k}}{\Delta t^*} = \frac{K_p}{r^2 \cos^2 \phi \Delta\lambda^2} \left(Q^n_{i+1,j,k} - 2Q^n_{i,j,k} + Q^n_{i-1,j,k} \right), \tag{12.122}$$

where Q^f indicates the filtered field and here Δt^* is a pseudo time step. The linear stability analysis of (12.122) is given in Case 2 of Section 12.4.1. Therefore, from (12.33), the scheme is stable and avoids oscillatory behaviour of the temporal response function E (see Section (12.4.1) for further details) provided

$$\frac{K_p \Delta t^*}{r^2 \cos^2\phi \Delta\lambda^2} \leq \frac{1}{4}. \qquad (12.123)$$

In the model, the parameter $K_p\Delta t^* / \left(r^2 \cos^2\phi\Delta\lambda^2\right)$ is replaced by the non-dimensional polar diffusivity K_p^*. Then (12.122) can be written as:

$$Q^f_{i,j,k} = \mathcal{P}\left(Q^n_{i,j,k}\right) \equiv Q^n_{i,j,k} + K_p^*\left(Q^n_{i+1,j,k} - 2Q^n_{i,j,k} + Q^n_{i-1,j,k}\right). \qquad (12.124)$$

When K_p^* is set equal to 1/4 (its typical value in the New Dynamics), (12.124) reduces to a simple 1-2-1 filter.

Aside :

From (12.123) *stability requires that* $K_p^* \leq 1/4$. *However, as for* K_ϕ*, the value of* K_p^* *used in the New Dynamics is a user specified parameter. No check is made within the code to ensure its value is numerically stable. Caveat emptor!*

Aside :

Since K_p^* *is specified as a single constant, independent of position and of the presence of orography, the factor of* r^2 *appearing in* (12.121) *is effectively lost. This means that the desired conservation properties of the polar filter,* $\mathcal{P}$*, (global volume integral conservation of* Q *itself for scalars and of* $r\cos\phi Q$*, i.e. angular momentum, for* $Q = u$*, see Appendix A for details) are lost when* $\partial r/\partial\lambda \neq 0$*, i.e. in the presence of orography.*

Polar filtering is applied in the region of the North pole (South pole) for latitudes greater than a base value of $+\phi_b$ (less than $-\phi_b$). In degrees, this distance is typically about 80°. Thus filtering is applied to variables located within the latitude ranges $-\pi/2 \leq \phi < -\phi_b$ and $+\phi_b < \phi \leq \pi/2$.

Aside :

Applying the polar filter to the full fields, Q^n*, acts to smooth the fields every time step. This can have an undesirable impact on the energy spectrum associated with the initial field, the impact of which increases as the model integration advances in time. It would be better to smooth the initial fields to the extent required and* *then, at each time step, to only apply the filter to the change in the field from the previous time step. That is it would be better to only apply the filter operator to* $Q^n - Q^{n-1}$ *and add this smoothed field onto* Q^{n-1} *to obtain the filtered field at time step* n*. This comment presumably also applies to any form of filtering or diffusion applied for numerical reasons, e.g. those forms discussed in the previous sections.*

Multiple sweeps

As the pole is approached the meridians converge and the physical distance over which polar filtering of the form (12.122) is effective becomes very small. Thus the small scale, $O(1)$-$O(10)$ km, signals which polar filtering is designed to remove may be left largely untouched by the filtering process. It is therefore considered desirable to apply the polar filter to an increasingly larger range of grid scales as the pole is approached. This is achieved by assigning a maximum number of filter applications, $d_p^{\max}$ (typically between 5 and 10), an increment in latitude, $\Delta\phi_p$ and a maximum (minimum) latitude of$+\phi_c$ $(-\phi_c)$ (typically about 88°). Then, as ϕ increases (decreases) by $\Delta\phi_p$ as the North (South) pole is approached, the number of times the polar filter is applied is increased by one, until the latitude is greater than (less than) the critical latitude, ϕ_c $(-\phi_c)$, beyond which the filter operation is applied $d_p^{\max}$ times. Thus, for a model latitude circle of latitude, ϕ_j, near the North pole such that $\phi_b < \phi_j$, the polar filter is applied d_p times where the integer d_p is given by:

$$d_p\left(\phi_j\right) = \left\{ \begin{array}{cl} \min\left[d_P^{\max}, 1 + \mathrm{INT}\left(\frac{\phi_j - \phi_b}{\Delta\phi_p}\right)\right] & \text{for} \quad \phi_b < \phi_j \le \phi_c \\ d_p^{\max} & \text{for} \quad \phi_c < \phi_j \end{array} \right. , \tag{12.125}$$

where INT denotes "integer part of". In the region of the South pole, where ϕ_j is negative, d_p is given by

$$d_p\left(\phi_j\right) = \left\{ \begin{array}{cl} \min\left[d_p^{\max}, 1 + \mathrm{INT}\left(-\frac{\phi_j + \phi_b}{\Delta\phi_p}\right)\right] & \text{for} \quad -\phi_c \le \phi_j < -\phi_b \\ d_p^{\max} & \text{for} \quad \phi_j < -\phi_c \end{array} \right. , \tag{12.126}$$

When $\Delta\phi_p$ is chosen such that

$$1 + \mathrm{INT}\left(\frac{\phi_c - \phi_b}{\Delta\phi_p}\right) \ge d_p^{\max}, \tag{12.127}$$

the number of applications of the filter will increase reasonably smoothly as the pole is approached. However, if this is not the case then there is potentially a large change in the level of diffusion applied to two neighbouring model rows.

When multiple sweeps are applied (12.124) becomes

$$Q^f_{i,j,k} = \mathcal{P}^{d_p}\left(Q^n_{i,j,k}\right). \tag{12.128}$$

The response function, for a zonal wavenumber k, of $\mathcal{P}^{d_p}$ is

$$E = \left[1 - 4K^*_P \sin^2\left(\frac{k\Delta\lambda}{2}\right)\right]^{d_p}, \tag{12.129}$$

from which, noting that $4K^*_p \leq 1$, it is evident that as d_p increases, waves of wavenumber $k > 0$ get progressively more damped.

Boundary conditions

Since $\mathcal{P}$ operates only in the zonal direction to which periodicity applies, boundary conditions are only required for variables stored at the two poles, $j = 1/2$ and $j = M - 1/2$. The vertical velocity component, w, and all scalars, in particular the potential temperature, θ, are single-valued at the poles. Therefore, $\mathcal{P}$ is a null operator on these variables and so it is not applied to them there. The filtered values of the zonal component of the wind, u, at the poles are evaluated by applying the polar vector wind calculation to the values of the filtered meridional wind component, v, at the model row surrounding each pole, i.e. to $v_{i,1,k}$ and $v_{i,M-1,k}$. For further details of this procedure see Section 6.

Filtering the increments

As well as u^n, v^n, w^n and θ^n being polar filtered at the beginning of each time step, the explicit increments for each of these variables (i.e. the sum of the first predictor and the explicit correctors) are also polar filtered immediately prior to their use in the solution of the Helmholtz problem for the implicit correctors. Thus, $\mathcal{P}$ is applied to each of R^+_u, R^+_v, R^+_w and $\left(\tilde{\theta}^{(P2)} - \theta^n\right)$ in exactly the same way as described above for u^n, v^n, w^n and θ^n.

13 The discrete equation set

The governing equations have been temporally and spatially discretised in the preceding sections. When the a posteriori moisture conservation option is not activated, they comprise a coupled set of linear equations for the unknown quantities at the new timestep $t_{n+1} \equiv (n+1)\,\Delta t$: when it is activated, the set becomes non-linear - see Section 16.7.2 for details of how the solution procedure is modified and how this may be algorithmically interpreted. There are $13N + 7$ levels of such unknown quantities, viz:

Unknowns at time t_{n+1}	Levels	# of levels
u_k	$k = 1/2, 3/2, ..., N - 1/2$	N
v_k	$k = 1/2, 3/2, ..., N - 1/2$	N
w_k	$k = 0, 1, ..., N$	$N + 1$
$\dot{\eta}_k$	$k = 0, 1, ..., N$	$N + 1$
$(\rho_y)_k$	$k = 1/2, 3/2, ..., N - 1/2$	N
ρ_k	$k = 1/2, 3/2, ..., N - 1/2$	N
θ_k	$k = 0, 1, ..., N$	$N + 1$
$(\theta_v)_k$	$k = 0, 1, ..., N$	$N + 1$
Π_k	$k = 1/2, 3/2, ..., N - 1/2$	N
p_k	$k = 1/2, 3/2, ..., N - 1/2$	N
$(m_v)_k$	$k = 0, 1, ..., N$	$N + 1$
$(m_{cl})_k$	$k = 0, 1, ..., N$	$N + 1$
$(m_{cf})_k$	$k = 0, 1, ..., N$	$N + 1$
	Total # of levels of unknowns =	$13N + 7$

Of the thirteen variables in the above table, eight (u, v, w, ρ_y, θ, m_v, m_{cl}, m_{cf}) are *prognostically* determined (i.e. there is an associated prognostic equation for the variable) whereas five ($\dot{\eta}$, ρ, θ_v, Π, p) are *diagnostically* related to the prognostic quantities.

To efficiently solve this coupled set of linear equations, it is *algebraically* decomposed into an equivalent discrete Helmholtz problem for $(\Pi')|_{\eta_k}$, where $\Pi' \equiv \Pi^{n+1} - \Pi^n$, and subscript k denotes evaluation at the N levels $\{\eta_{1/2}, \eta_{3/2}, ..., \eta_{N-1/2}\}$. Note that all operations to do so should be purely algebraic and that no further numerical approximations should be made beyond those of the preceding sections.

The purpose of this section is to gather together the required discretised equations to prepare the way for the derivation in the next section (Section 14) of the equivalent discrete Helmholtz problem. The remaining unknowns are then obtained via back-substitution - details for this are given in Section 16. Polar-specific equations are grouped together in Section 13.12.

13.1 Horizontal momentum at levels $k = 1/2, 3/2, ..., N - 1/2$

The discretised horizontal momentum equations (6.63) and (6.64) at levels k =1/2, 3/2, ..., $N - 1/2$ are:

$$\begin{aligned} u' &= A_u \left[R_u^+ - \alpha_3 \Delta t \frac{c_{pd}}{\overline{r}^{\lambda} \cos\phi} \left(\overline{\theta_v^*}^{r\lambda} \delta_\lambda \Pi' - \overline{\theta_v^* \delta_r \Pi'}^{r\lambda} \delta_\lambda r \right) \right] \\ &+ F_u \left[\overline{R_v^+}^{\lambda\phi} - \alpha_3 \Delta t \overline{\frac{c_{pd}}{\overline{r}^{\phi}} \left(\overline{\theta_v^*}^{r\phi} \delta_\phi \Pi' - \overline{\theta_v^* \delta_r \Pi'}^{r\phi} \delta_\phi r \right)}^{\lambda\phi} \right], \end{aligned} \tag{13.1}$$

$$\begin{aligned} v' &= A_v \left[R_v^+ - \alpha_3 \Delta t \frac{c_{pd}}{\overline{r}^{\phi}} \left(\overline{\theta_v^*}^{r\phi} \delta_\phi \Pi' - \overline{\theta_v^* \delta_r \Pi'}^{r\phi} \delta_\phi r \right) \right] \\ &- F_v \left[\overline{R_u^+}^{\lambda\phi} - \alpha_3 \Delta t \overline{\frac{c_{pd}}{\overline{r}^{\lambda} \cos\phi} \left(\overline{\theta_v^*}^{r\lambda} \delta_\lambda \Pi' - \overline{\theta_v^* \delta_r \Pi'}^{r\lambda} \delta_\lambda r \right)}^{\lambda\phi} \right], \end{aligned} \tag{13.2}$$

where

$$u' \equiv u^{n+1} - u^n, \quad v' \equiv v^{n+1} - v^n, \quad \Pi' \equiv \Pi^{n+1} - \Pi^n, \tag{13.3}$$

and the known quantities R_u^+, R_v^+, A_u, A_v, F_u, F_v and θ_v^* are respectively defined by (6.34), (6.54), (6.65)-(6.68) and (6.35). The special treatment of vertical averages and differences near the bottom and top boundaries to close the problem is described in Section 6.3.

13.2 Vertical momentum at levels $k = 0, 1, ..., N$

The discretised vertical momentum equation (7.30) at levels $k = 1, 2, ..., N - 1$ is

$$w' = G^{-1} R_w^+ - K \delta_r \Pi', \tag{13.4}$$

where

$$w' \equiv w^{n+1} - w^n, \tag{13.5}$$

and the known quantities R_w^+, G and K are respectively defined by (7.27), (7.31) and (7.32).

Although w_0 is not needed to derive the Helmholtz problem, it *is* used to compute the $f_1 w$ and $f_2 w$ terms in the horizontal momentum equations. From (6.42),w' at level $k=0$ is given by

$$w'|_{\eta_0 \equiv 0} = 0. \tag{13.6}$$

Since the lid is rigid, from (6.48) w' at level $k=N$ is given by

$$w'|_{\eta_N \equiv 1} = 0. \tag{13.7}$$

Aside :

Note that (13.6) *is only valid where the bottom is flat, and is invalid for inviscid flow in the presence of orography. This strategy needs revisiting.*

13.3 Continuity at levels $k = 1/2, 3/2, ..., N-1/2$

The discretised continuity equation (8.17) at levels k =3/2, 5/2, ..., $N-3/2$ is

$$\begin{aligned} r^2\rho'_y &= -\frac{\Delta t}{\delta_\eta r}\left\{\frac{1}{\cos\phi}\delta_\lambda\left(\frac{\overline{r^2\rho_y^n\delta_\eta r}^\lambda}{\overline{r}^\lambda}\overline{u}^{\alpha_1}\right)+\frac{1}{\cos\phi}\delta_\phi\left(\frac{\overline{r^2\rho_y^n\delta_\eta r}^\phi}{\overline{r}^\phi}\overline{v}^{\alpha_1}\cos\phi\right)\right.\\ &\left.-\delta_\eta\left[\overline{r^2\rho_y^n}^r\overline{\left(\overline{\frac{\overline{u}^\eta}{\overline{r}^\lambda\cos\phi}\delta_\lambda r}^\lambda+\overline{\frac{\overline{v}^\eta}{\overline{r}^\phi}\delta_\phi r}^\phi\right)}^{\alpha_1}\right]+\delta_\eta\left(\overline{r^2\rho_y^n}^r\overline{w}^{\alpha_2}\right)\right\}, \end{aligned} \tag{13.8}$$

where

$$\rho'_y \equiv \rho_y^{n+1}-\rho_y^n, \overline{F}^{\alpha_i} \equiv \alpha_i F^{n+1}+(1-\alpha_i)F^n \equiv F^n+\alpha_i F'. \tag{13.9}$$

Using (8.13), the discretised continuity equation (8.15) at levels $k=1/2$ and $k=N-1/2$ respectively reduces to

$$\begin{aligned} \left(r^2\rho'_y\right)\big|_{1/2} &= -\left(\frac{\Delta t}{\delta_\eta r}\right)\bigg|_{1/2}\left[\frac{1}{\cos\phi}\delta_\lambda\left(\frac{\overline{r^2\rho_y^n\delta_\eta r}^\lambda}{\overline{r}^\lambda}\overline{u}^{\alpha_1}\right)+\frac{1}{\cos\phi}\delta_\phi\left(\frac{\overline{r^2\rho_y^n\delta_\eta r}^\phi}{\overline{r}^\phi}\overline{v}^{\alpha_1}\cos\phi\right)\right]\bigg|_{1/2}\\ &-\left(\frac{\Delta t}{\delta_\eta r\Delta\eta}\right)\bigg|_{1/2}\left[\overline{r^2\rho_y^n}^r\overline{w}^{\alpha_2}-\overline{r^2\rho_y^n}^r\overline{\left(\overline{\frac{\overline{u}^\eta}{\overline{r}^\lambda\cos\phi}\delta_\lambda r}^\lambda+\overline{\frac{\overline{v}^\eta}{\overline{r}^\phi}\delta_\phi r}^\phi\right)}^{\alpha_1}\right]\bigg|_1, \end{aligned} \tag{13.10}$$

and

$$\begin{aligned} \left(r^2\rho'_y\right)\big|_{N-1/2} &= -\left(\frac{\Delta t}{\delta_\eta r}\right)\bigg|_{N-1/2}\left[\frac{1}{\cos\phi}\delta_\lambda\left(\frac{\overline{r^2\rho_y^n\delta_\eta r}^\lambda}{\overline{r}^\lambda}\overline{u}^{\alpha_1}\right)+\frac{1}{\cos\phi}\delta_\phi\left(\frac{\overline{r^2\rho_y^n\delta_\eta r}^\phi}{\overline{r}^\phi}\overline{v}^{\alpha_1}\cos\phi\right)\right]\bigg|_{N-1/2}\\ &+\left(\frac{\Delta t}{\delta_\eta r\Delta\eta}\right)\bigg|_{N-1/2}\left[\overline{r^2\rho_y^n}^r\overline{w}^{\alpha_2}-\overline{r^2\rho_y^n}^r\overline{\left(\overline{\frac{\overline{u}^\eta}{\overline{r}^\lambda\cos\phi}\delta_\lambda r}^\lambda+\overline{\frac{\overline{v}^\eta}{\overline{r}^\phi}\delta_\phi r}^\phi\right)}^{\alpha_1}\right]\bigg|_{N-1}. \end{aligned} \tag{13.11}$$

13.4 Definition of $\dot{\eta}$ at levels $k = 0, 1, ..., N$

The definition (8.8) of $\dot{\eta}$ leads to

$$\dot{\eta}' \equiv \dot{\eta}^{n+1} - \dot{\eta}^{n} = \frac{1}{\delta_\eta r}\left(w' - \overline{\frac{\overline{u'}^{\eta}}{\overline{r}^{\lambda}\cos\phi}\delta_\lambda r}^{\lambda} - \overline{\frac{\overline{v'}^{\eta}}{\overline{r}^{\phi}}\delta_\phi r}^{\phi} \right), \tag{13.12}$$

at levels $k = 1, 2, ..., N-1$, and to

$$\dot{\eta}'|_{\eta_0 \equiv 0} = \dot{\eta}'|_{\eta_N \equiv 1} = 0, \tag{13.13}$$

at levels $k = 0$ and $k = N$.

13.5 Thermodynamic at levels $k = 0, 1, ..., N$

The discretised thermodynamicequation (9.36) at levels $k = 1, 2, ..., N-1$ is

$$\theta' = (\theta^* - \theta^n) - \alpha_2 \Delta t \left(w' \delta_{2r} \theta_{ref} \right), \tag{13.14}$$

where

$$\theta' \equiv \theta^{n+1} - \theta^n, \tag{13.15}$$

$\theta^* \equiv \tilde{\theta}^{(P2)}$ (see (9.27)) is the latest available predictor for θ at time $(n+1)\Delta t$, and the known quantity $\delta_{2r}\theta_{ref}$ is defined by (9.37).

At the bottom ($k = 0$) level (see (9.39))

$$\theta'|_{\eta_0 \equiv 0} = \theta'|_{\eta_1}, \tag{13.16}$$

from the isentropic assumption, and at the top ($k = N$) level (see (9.45))

$$\theta'|_{\eta_N \equiv 1} = (\theta^* - \theta^n)|_{\eta_N \equiv 1}. \tag{13.17}$$

Note that (13.14) when evaluated at level 1 is handled a little differently from evaluation at intermediate levels because: (a) the limiter (9.15) has a different form from the general one (9.16),and (b) the computation (9.18) of the residual vertical advection has a different form from the general one (9.19).

13.6 Linearised gas law at levels $k = 1/2, 3/2, ..., N - 1/2$

Noting that $\kappa_d c_{pd} = R_d$, the discretisedlinearised gas law (11.12) at levels k =1/2, 3/2, ..., $N - 1/2$ is

$$\kappa_d \Pi^n \overline{\theta_v^n}^r \rho' + \left(\kappa_d \overline{\theta_v^n}^r \rho^n - \frac{p^n}{R_d \Pi^n} \right) \Pi' + \kappa_d \Pi^n \rho^n \overline{\theta_v'}^r = \frac{p^n}{c_{pd}} - \kappa_d \Pi^n \rho^n \overline{\theta_v^n}^r, \tag{13.18}$$

where

$$\theta_v' \equiv \theta_v^{n+1} - \theta_v^n, \rho' \equiv \rho^{n+1} - \rho^n, \tag{13.19}$$

and, from (11.15),

$$\rho^n = \overline{\rho_y^n \left(1 + \sum_{X=(v,cl,cf)} m_X^n \right)}^r. \tag{13.20}$$

13.7 Moisture at levels $k = 0, 1, ..., N$

The discretised moisture equations at levels $k = 1, 2, ..., N$ are

$$m_v^* \equiv \widetilde{m}_v^{(P2)}, \tag{13.21}$$

$$m_{cl}^* \equiv \widetilde{m}_{cl}^{(P2)}, \tag{13.22}$$

$$m_{cf}^* \equiv \widetilde{m}_{cf}^{(P2)}, \tag{13.23}$$

where $\widetilde{m}_X^{(P2)}$, $X = (v, cl, cf)$, are defined for $k = 1, 2, ..., N - 1$, by (10.23)-(10.25) or, equivalently, by (10.40)-(10.42), and, for $k = N$, by (10.63)-(10.65).

At level $k = 0$, $(m_X^*)|_{\eta_0 \equiv 0}$, $X = (v, cl, cf)$, are obtained by simple extrapolation of their values at $k = 1$ in an analogous manner to (10.61):

$$(m_v^*)|_{\eta_0 \equiv 0} = (m_v^*)|_{\eta_1}, \tag{13.24}$$

$$(m_{cl}^*)|_{\eta_0 \equiv 0} = (m_{cl}^*)|_{\eta_1}, \tag{13.25}$$

$$\left(m_{cf}^*\right)|_{\eta_0 \equiv 0} = \left(m_{cf}^*\right)|_{\eta_1}. \tag{13.26}$$

The procedure for determining the final moisture quantities at time $(n + 1) \Delta t$ depends upon whether moisture conservation corrections are imposed or not.

13.7.1 Without moisture conservation correction

When no moisture conservation correction is imposed, the moisture quantities at the new time at levels $k = 0, 1, ..., N$ are trivially obtained from

$$m_v^{n+1} = m_v^*, \tag{13.27}$$

$$m_{cl}^{n+1} = m_{cl}^*, \tag{13.28}$$

$$m_{cf}^{n+1} = m_{cf}^*, \tag{13.29}$$

where m_X^*, $X = (v, cl, cf)$, are defined by (13.21)-(13.23).

13.7.2 With moisture conservation correction

When the moisture conservation corrections are imposed, from (10.55)-(10.57) and (10.65)-(10.67), the moisture quantities at the new time at levels $k = 1, 2, ..., N$ are obtained from

$$m_v^{n+1} = m_v^* + \Delta t \left(D_{cons}^{m_v}\right)^n - \Delta t \left(\frac{\rho_y^{n+1} - \rho_y^n}{\rho_y^{n+1}}\right) \left[S_2^{m_v}\right]^*, \tag{13.30}$$

$$m_{cl}^{n+1} = m_{cl}^* + \Delta t \left(D_{cons}^{m_{cl}}\right)^n - \Delta t \left(\frac{\rho_y^{n+1} - \rho_y^n}{\rho_y^{n+1}}\right) \left[S_2^{m_{cl}}\right]^*, \tag{13.31}$$

$$m_{cf}^{n+1} = m_{cf}^* + \Delta t \left(D_{cons}^{m_{cf}}\right)^n - \Delta t \left(\frac{\rho_y^{n+1} - \rho_y^n}{\rho_y^{n+1}}\right) \left[S_2^{m_{cf}}\right]^*, \tag{13.32}$$

where m_X^*, $X = (v, cl, cf)$, are defined by (13.21)-(13.23), and $\left(D_{cons}^{m_X}\right)^n$ are given by imposition of (10.47). Also $\left[S_2^{m_X}\right]^*$ are given, for $k = 1, 2, ..., N - 1$, by (10.28) and (10.31)-(10.32) and, because of (10.62), are identically zero for $k = N$.

From (10.61), at level $k = 0$, $\left(m_X^{n+1}\right)\big|_{\eta_0 \equiv 0}$, $X = (v, cl, cf)$, are obtained by simple extrapolation of their values at $k = 1$:

$$\left(m_v^{n+1}\right)\big|_{\eta_0 \equiv 0} = \left(m_v^{n+1}\right)\big|_{\eta_1}, \tag{13.33}$$

$$\left(m_{cl}^{n+1}\right)\big|_{\eta_0 \equiv 0} = \left(m_{cl}^{n+1}\right)\big|_{\eta_1}, \tag{13.34}$$

$$\left(m_{cf}^{n+1}\right)\big|_{\eta_0 \equiv 0} = \left(m_{cf}^{n+1}\right)\big|_{\eta_1}. \tag{13.35}$$

Aside :

Note that when moisture conservation corrections are imposed in the above a posteriori manner, the formal algebraic consistency mentioned at the beginning of this section (just after the table) is lost (see Section 16.7.2 for further details).

13.8 Total gaseous density at levels $k = 1/2, 3/2, ..., N - 1/2$

The discrete definition of total gaseous density (11.18) at levels k =1/2, 3/2, ..., $N - 1/2$ is

$$\rho' = \rho'_y \overline{\left(1 + \sum_{X=(v,cl,cf)} m^*_X\right)}^r + \rho^n_y \left[\sum_{X=(v,cl,cf)} \overline{(m^*_X - m^n_X)}^r\right], \tag{13.36}$$

where m^*_X, $X = (v, cl, cf)$, are defined by (13.21)-(13.23).

13.9 Virtual potential temperature at levels $k = 0, 1, ..., N$

The discrete virtual potential temperature (11.24) at levels k =0, 1, ..., N is

$$\theta'_v = (\theta' + \theta^n)\left(\frac{1 + \frac{1}{\varepsilon} m^*_v}{1 + \sum_{X=(v,cl,cf)} m^*_X}\right) - \theta^n_v, \tag{13.37}$$

where m^*_X, $X = (v, cl, cf)$, are defined by (13.21)-(13.23).

13.10 Pressure at levels $k = 1/2, 3/2, ..., N - 1/2$

The definition of Exner pressure (11.2) at levels $k = 1/2, 3/2, ..., N - 1/2$ gives

$$p^{n+1} = p_0 \left(\Pi^{n+1}\right)^{\frac{1}{\kappa_d}}. \tag{13.38}$$

13.11 Number of equations vs. number of unknowns

From the table there are $13N + 7$ unknown quantities at the new timestep $t_{n+1} \equiv (n+1)\,\Delta t$. From (13.1)-(13.2), (13.4), (13.6)-(13.8), (13.12)-(13.14), (13.16)-(13.18) and (13.21)-(13.38), there are$13N + 7$ independent equations to determine these $13N + 7$ unknowns.

13.12 Polar equations

Polar-specific relations are grouped together here.

13.12.1 Uniqueness of scalars at the poles

All scalar quantities are unique at the two poles, i.e.

$$F_{SP} \equiv F_{\frac{1}{2},\frac{1}{2}} \equiv F_{\frac{3}{2},\frac{1}{2}} \equiv F_{\frac{5}{2},\frac{1}{2}} \equiv ... \equiv F_{L-\frac{1}{2},\frac{1}{2}}, \tag{13.39}$$

$$F_{NP} \equiv F_{\frac{1}{2},M-\frac{1}{2}} \equiv F_{\frac{3}{2},M-\frac{1}{2}} \equiv F_{\frac{5}{2},M-\frac{1}{2}} \equiv ... \equiv F_{L-\frac{1}{2},M-\frac{1}{2}}, \tag{13.40}$$

where F is any scalar quantity required at either of the two poles, $F_{i-\frac{1}{2},\frac{1}{2}} \equiv F|_{\left(\lambda_{i-1/2},\phi_{1/2}\equiv-\pi/2\right)}$ and $F_{i-\frac{1}{2},M-\frac{1}{2}} \equiv F|_{\left(\lambda_{i-1/2},\phi_{M-1/2}\equiv\pi/2\right)}$.

13.12.2 u wind component at the poles

The u wind component at the two poles is determined from (6.81) and (6.86):

$$u_{i,1/2} \equiv u|_{\left(\lambda_i,\phi_{1/2}\equiv-\pi/2\right)} = -v_{SP}\sin\left(\lambda_i - \lambda_{SP}\right), i = 1, 2, ..., L, \tag{13.41}$$

$$u_{i,M-1/2} \equiv u|_{\left(\lambda_i,\phi_{M-1/2}\equiv+\pi/2\right)} = +v_{NP}\sin\left(\lambda_i - \lambda_{NP}\right), i = 1, 2, ..., L. \tag{13.42}$$

where λ_{SP}, v_{SP}, λ_{NP} and v_{NP} are defined by (6.79), (6.80), (6.83) and (6.85).

13.12.3 v wind component at the poles

The v wind component at the two poles, if required, can be determined from (6.69) and (6.82):

$$v_{i-1/2,1/2} \equiv v|_{\left(\lambda_{i-1/2},\phi_{1/2}\equiv-\pi/2\right)} = v_{SP}\cos\left(\lambda_{i-1/2} - \lambda_{SP}\right), i = 1, 2, ..., L. \tag{13.43}$$

$$v_{i-1/2,M-1/2} \equiv v|_{\left(\lambda_{i-1/2},\phi_{M-1/2}\equiv+\pi/2\right)} = v_{NP}\cos\left(\lambda_{i-1/2} - \lambda_{NP}\right), i = 1, 2, ..., L. \tag{13.44}$$

where λ_{SP}, v_{SP}, λ_{NP} and v_{NP} are defined by (6.79), (6.80), (6.83) and (6.85).

13.12.4 w wind component at the poles

From (7.36)-(7.37) the w wind component is also unique at the two poles:

$$w_{SP} \equiv w_{\frac{1}{2},\frac{1}{2}} \equiv w_{\frac{3}{2},\frac{1}{2}} \equiv w_{\frac{5}{2},\frac{1}{2}} \equiv ... \equiv w_{L-\frac{1}{2},\frac{1}{2}}, \tag{13.45}$$

$$w_{NP} \equiv w_{\frac{1}{2},M-\frac{1}{2}} \equiv w_{\frac{3}{2},M-\frac{1}{2}} \equiv w_{\frac{5}{2},M-\frac{1}{2}} \equiv ... \equiv w_{L-\frac{1}{2},M-\frac{1}{2}}. \tag{13.46}$$

Aside :

When computing the right-hand-sides of the w momentum equation at the two poles, the terms $(f_2u - f_1v)_{SP}$ and $(f_2u - f_1v)_{NP}$ should be computed using (7.48) and (7.50) instead of setting them to zero as is presently done.

13.12.5 Continuity equation at the poles

The discretised continuity equations (8.36) and (8.40) over the southern and northern polar caps are

$$\frac{F'_{SP}}{\Delta t} = -\frac{\cos(\phi_1)}{b}\frac{1}{L}\sum_{i=1}^{L}\left(\frac{\overline{F^n}^{\phi}\overline{v}^{\alpha_1}}{\overline{r}^{\phi}}\right)_{i-\frac{1}{2},1} - \delta_\eta\left[\left(\overline{r^2\rho_y^n}^{r}\right)_{SP}\overline{\dot{\eta}_{SP}}^{average}(\delta_\eta r)_{SP}\right], \quad (13.47)$$

$$\frac{F'_{NP}}{\Delta t} = \frac{\cos(\phi_{M-1})}{b}\frac{1}{L}\sum_{i=1}^{L}\left(\frac{\overline{F^n}^{\phi}\overline{v}^{\alpha_1}}{\overline{r}^{\phi}}\right)_{i-\frac{1}{2},M-1} - \delta_\eta\left[\left(\overline{r^2\rho_y^n}^{r}\right)_{NP}\overline{\dot{\eta}_{NP}}^{average}(\delta_\eta r)_{NP}\right], \quad (13.48)$$

where

$$F^n \equiv r^2\rho_y^n\delta_\eta r, F' \equiv F^{n+1} - F^n \equiv r^2\delta_\eta r\left(\rho_y^{n+1} - \rho_y^n\right) \equiv r^2\delta_\eta r\rho'_y, \quad (13.49)$$

$$\overline{\dot{\eta}_{SP}}^{average} = \frac{1}{(\delta_\eta r)_{SP}}\left[\overline{w_{SP}}^{\alpha_2} - \frac{2}{L}\sum_{i=1}^{L}\left(\overline{\frac{\overline{v}^{\eta}}{\overline{r}^{\phi}}\delta_\phi r}^{\alpha_1}\right)_{i-\frac{1}{2},1}\right], \quad (13.50)$$

$$\overline{\dot{\eta}_{NP}}^{average} = \frac{1}{(\delta_\eta r)_{NP}}\left[\overline{w_{NP}}^{\alpha_2} - \frac{2}{L}\sum_{i=1}^{L}\left(\overline{\frac{\overline{v}^{\eta}}{\overline{r}^{\phi}}\delta_\phi r}^{\alpha_1}\right)_{i-\frac{1}{2},M-1}\right]. \quad (13.51)$$

13.12.6 Definition of $\dot{\eta}$ at poles

The definitions (8.24) and (8.25) are

$$\dot{\eta}_{SP} = \frac{1}{(\delta_\eta r)_{SP}}\left[w_{SP} - \frac{2}{L}\sum_{i=1}^{L}\left(\frac{\overline{v}^{\eta}}{\overline{r}^{\phi}}\delta_\phi r\right)_{i-\frac{1}{2},1}\right], \quad (13.52)$$

$$\dot{\eta}_{NP} = \frac{1}{(\delta_\eta r)_{NP}}\left[w_{NP} - \frac{2}{L}\sum_{i=1}^{L}\left(\frac{\overline{v}^{\eta}}{\overline{r}^{\phi}}\delta_\phi r\right)_{i-\frac{1}{2},M-1}\right]. \quad (13.53)$$

14 Derivation of the Helmholtz problem

14.1 Rewriting the discretised horizontal momentum equations at levels $k = 1/2, 3/2, ..., N-1/2$

The discretised horizontal momentum equations (13.1)-(13.2) may be rewritten as

$$\alpha_1 u' = \alpha_1 \left(A_u R_u^+ + F_u \overline{R_v^+}^{\lambda\phi} \right) - X = (u_* - u^n) - X, \tag{14.1}$$

$$\alpha_1 v' = \alpha_1 \left(A_v R_v^+ - F_v \overline{R_u^+}^{\lambda\phi} \right) - Y = (v_* - v^n) - Y, \tag{14.2}$$

where X and Y are defined by (I.1)-(I.6), and u_* and v_* by (I.32)-(I.33).

14.2 Obtaining an expression for $r^2\rho'$ at levels $k = 3/2, ..., N-3/2$

To obtain a Helmholtz problem from the discretised gas law an expression for $r^2\rho'$ is obtained from (13.8) and (13.36). The discretised continuity equation (13.8) is first rewritten as

$$\begin{aligned} r^2\rho_y' \quad = \quad & -\frac{\Delta t}{\delta_\eta r}\left[\frac{1}{\cos\phi}\delta_{\lambda 1}\left(C_{xx1}\overline{u}^{\alpha_1}\right) + \frac{1}{\cos\phi}\delta_{\phi 1}\left(C_{yy1}\overline{v}^{\alpha_1}\right)\right] \\ & -\frac{\Delta t}{\delta_\eta r}\delta_\eta\left[C_5\overline{w}^{\alpha_2} - C_5\overline{\left(\overline{C_{xz}\overline{u}^{\eta}}^{\lambda} + \overline{C_{yz}\overline{v}^{\eta}}^{\phi}\right)}^{\alpha_1}\right], \end{aligned} \tag{14.3}$$

where C_{xx1}, C_{yy1}, C_{xz}, C_{yz} and C_5 are defined by (I.7), (I.9), (I.13)-(I.14) and (I.26), and the operators $\delta_{\lambda 1}$ and $\delta_{\phi 1}$ are defined by (I.27)-(I.28). Inserting (14.3) into (13.36) then leads to:

$$\begin{aligned} r^2\rho' \quad = \quad & -\frac{\Delta t}{\delta_\eta r}\left(1 + \sum_{X=(v,cl,cf)} \overline{m_X^*}^r\right)\left[\frac{1}{\cos\phi}\delta_{\lambda 1}\left(C_{xx1}\overline{u}^{\alpha_1}\right) + \frac{1}{\cos\phi}\delta_{\phi 1}\left(C_{yy1}\overline{v}^{\alpha_1}\right)\right] \\ & -\frac{\Delta t}{\delta_\eta r}\left(1 + \sum_{X=(v,cl,cf)} \overline{m_X^*}^r\right)\delta_\eta\left[C_5\overline{w}^{\alpha_2} - C_5\overline{\left(\overline{C_{xz}\overline{u}^{\eta}}^{\lambda} + \overline{C_{yz}\overline{v}^{\eta}}^{\phi}\right)}^{\alpha_1}\right] \\ & + r^2\rho_y^n\left[\sum_{X=(v,cl,cf)} \overline{\left(m_X^* - m_X^n\right)}^r\right]. \end{aligned} \tag{14.4}$$

14.3 Obtaining an expression for $r^2\rho'$ at levels $k = 1/2$ and $k = N-1/2$

The procedure for obtaining the expression for $r^2\rho'$ at the near-boundary levels $k = 1/2$ and $k = N - 1/2$ closely follows that given in the previous sub-section for interior levels except that there are some differences in detail due to the influence of the boundary conditions. The expression for $r^2\rho'$ at levels $k = 1/2$ and $k = N - 1/2$ is now detailed.

14.3.1 $k = 1/2$

Eq. (13.10) is rewritten as

$$\begin{aligned}\left(r^2\rho'_y\right)\big|_{1/2} &= -\left\{\frac{\Delta t}{\delta_\eta r}\left[\frac{1}{\cos\phi}\delta_{\lambda 1}\left(C_{xx1}\overline{u}^{\alpha_1}\right)+\frac{1}{\cos\phi}\delta_{\phi 1}\left(C_{yy1}\overline{v}^{\alpha_1}\right)\right]\right\}\Bigg|_{1/2}\\ &\quad -\frac{\Delta t}{\left(\delta_\eta r\Delta\eta\right)_{1/2}}\left[C_5\overline{w}^{\alpha_2}-C_5\overline{\left(\overline{C_{xz}\overline{u}^{\eta}}^{\lambda}+\overline{C_{yz}\overline{v}^{\eta}}^{\phi}\right)}^{\alpha_1}\right]\Bigg|_1,\end{aligned}\tag{14.5}$$

where C_{xx1}, C_{yy1}, C_{xz}, C_{yz} and C_5 are defined by (I.7), (I.9), (I.13)-(I.14) and (I.26), and the operators $\delta_{\lambda 1}$ and $\delta_{\phi 1}$ are defined by (I.27)-(I.28). Inserting (14.5) into (13.36) then leads to:

$$\begin{aligned}\left(r^2\rho'\right)\big|_{1/2} &= -\left\{\frac{\Delta t}{\delta_\eta r}\left(1+\sum_{X=(v,cl,cf)}\overline{m_X^*}^{r}\right)\left[\frac{1}{\cos\phi}\delta_{\lambda 1}\left(C_{xx1}\overline{u}^{\alpha_1}\right)+\frac{1}{\cos\phi}\delta_{\phi 1}\left(C_{yy1}\overline{v}^{\alpha_1}\right)\right]\right\}\Bigg|_{1/2}\\ &\quad -\left[\frac{\Delta t}{\delta_\eta r\Delta\eta}\left(1+\sum_{X=(v,cl,cf)}\overline{m_X^*}^{r}\right)\right]\Bigg|_{1/2}\left[C_5\overline{w}^{\alpha_2}-C_5\overline{\left(\overline{C_{xz}\overline{u}^{\eta}}^{\lambda}+\overline{C_{yz}\overline{v}^{\eta}}^{\phi}\right)}^{\alpha_1}\right]\Bigg|_1\\ &\quad +\left[r^2\rho_y^n\sum_{X=(v,cl,cf)}\overline{\left(m_X^*-m_X^n\right)}^{r}\right]\Bigg|_{1/2}.\end{aligned}\tag{14.6}$$

14.3.2 $k = N - 1/2$

Eq. (13.11) is rewritten as

$$\begin{aligned}\left(r^2\rho'_y\right)\big|_{N-1/2} &= -\left\{\frac{\Delta t}{\delta_\eta r}\left[\frac{1}{\cos\phi}\delta_{\lambda 1}\left(C_{xx1}\overline{u}^{\alpha_1}\right)+\frac{1}{\cos\phi}\delta_{\phi 1}\left(C_{yy1}\overline{v}^{\alpha_1}\right)\right]\right\}\Bigg|_{N-1/2}\\ &\quad +\frac{\Delta t}{\left(\delta_\eta r\Delta\eta\right)_{N-1/2}}\left[C_5\overline{w}^{\alpha_2}-C_5\overline{\left(\overline{C_{xz}\overline{u}^{\eta}}^{\lambda}+\overline{C_{yz}\overline{v}^{\eta}}^{\phi}\right)}^{\alpha_1}\right]\Bigg|_{N-1},\end{aligned}\tag{14.7}$$

where C_{xx1}, C_{yy1}, C_{xz}, C_{yz} and C_5 are defined by (I.7), (I.9), (I.13)-(I.14) and (I.26), and the operators $\delta_{\lambda 1}$ and $\delta_{\phi 1}$ are defined by (I.27)-(I.28). Inserting (14.7) into (13.36) then leads to:

$$\begin{aligned}\left(r^2\rho'\right)\big|_{N-1/2} &= -\left\{\frac{\Delta t}{\delta_\eta r}\left(1+\sum_{X=(v,cl,cf)}\overline{m_X^*}^{r}\right)\left[\frac{1}{\cos\phi}\delta_{\lambda 1}\left(C_{xx1}\overline{u}^{\alpha_1}\right)+\frac{1}{\cos\phi}\delta_{\phi 1}\left(C_{yy1}\overline{v}^{\alpha_1}\right)\right]\right\}\Bigg|_{N-1/2}\\ &\quad +\left[\frac{\Delta t}{\delta_\eta r\Delta\eta}\left(1+\sum_{X=(v,cl,cf)}\overline{m_X^*}^{r}\right)\right]\Bigg|_{N-1/2}\left[C_5\overline{w}^{\alpha_2}-C_5\overline{\left(\overline{C_{xz}\overline{u}^{\eta}}^{\lambda}+\overline{C_{yz}\overline{v}^{\eta}}^{\phi}\right)}^{\alpha_1}\right]\Bigg|_{N-1}\end{aligned}$$

$$+\left[r^2\rho_y^n \sum_{X=(v,cl,cf)} \overline{(m_X^* - m_X^n)}^r\right]\Bigg|_{N-1/2} . \tag{14.8}$$

14.4 Obtaining an expression for $\overline{\theta_v'}^r$ at levels $k = 3/2, 5/2, ..., N-3/2$

An expression for $\overline{\theta_v'}^r$ is obtained from (13.14), (13.37) and (6.20). Thus:

$$\overline{\theta_v'}^r = -\Delta t \overline{\left(\frac{1+\frac{1}{\varepsilon}m_v^*}{1+\sum_{X=(v,cl,cf)} m_X^*}\right)(\alpha_2\delta_{2r}\theta_{ref}w')}^r + \overline{\theta_v^*}^r - \overline{\theta_v^n}^r . \tag{14.9}$$

Using (13.4) to eliminate w' from (14.9) gives

$$\begin{aligned}\overline{\theta_v'}^r &= \Delta t\overline{C_z\delta_\eta\Pi'}^r + \overline{\theta_v^*}^r - \overline{\theta_v^n}^r \\ &\quad -\Delta t\overline{\left(\frac{1+\frac{1}{\varepsilon}m_v^*}{1+\sum_{X=(v,cl,cf)} m_X^*}\right)(\alpha_2\delta_{2r}\theta_{ref}G^{-1}R_w^+)}^r ,\end{aligned} \tag{14.10}$$

where C_z is defined by (I.12).

14.5 Obtaining an expression for $\overline{\theta_v'}^r$ at levels $k = 1/2$ and $k = N-1/2$

14.5.1 $k = 1/2$

An expression for $\overline{\theta_v'}^r$ at level $k = 1/2$ is obtained from (13.14), (13.16), (13.24)-(13.26) and (13.37). Thus:

$$\left(\overline{\theta_v'}^r\right)\Big|_{1/2} = -\Delta t\left[\left(\frac{1+\frac{1}{\varepsilon}m_v^*}{1+\sum_{X=(v,cl,cf)} m_X^*}\right)(\alpha_2\delta_{2r}\theta_{ref}w')\right]\Bigg|_1 + \left(\overline{\theta_v^*}^r - \overline{\theta_v^n}^r\right)\Big|_{1/2} . \tag{14.11}$$

Using (13.4) to eliminate w' from (14.11) gives

$$\begin{aligned}\left(\overline{\theta_v'}^r\right)\Big|_{1/2} &= \Delta t\left(C_z\delta_\eta\Pi'\right)\big|_1 + \left(\overline{\theta_v^*}^r - \overline{\theta_v^n}^r\right)\Big|_{1/2} \\ &\quad -\Delta t\left[\left(\frac{1+\frac{1}{\varepsilon}m_v^*}{1+\sum_{X=(v,cl,cf)} m_X^*}\right)\left(\alpha_2\delta_{2r}\theta_{ref}G^{-1}R_w^+\right)\right]\Bigg|_1 ,\end{aligned} \tag{14.12}$$

where C_z is defined by (I.12).

14.5.2 $k = N-1/2$

An expression for $\overline{\theta_v'}^r$ at level $k = N-1/2$ is obtained from (13.14), (13.17) and (13.37). Thus:

$$\left(\overline{\theta_v'}^r\right)\Big|_{N-1/2} = -\Delta t\left(\frac{r_N - r_{N-1/2}}{r_N - r_{N-1}}\right)\left[\left(\frac{1+\frac{1}{\varepsilon}m_v^*}{1+\sum_{X=(v,cl,cf)} m_X^*}\right)(\alpha_2\delta_{2r}\theta_{ref}w')\right]\Bigg|_{N-1}$$

$$+ \left(\overline{\theta_v^*}^r - \overline{\theta_v^n}^r \right) \Big|_{N-1/2} . \qquad (14.13)$$

Using (13.4) to eliminate w' from (14.13) gives

$$\begin{aligned}
\left(\overline{\theta_v'}^r \right) \Big|_{N-1/2} &= \Delta t \left(\frac{r_N - r_{N-1/2}}{r_N - r_{N-1}} \right) \left(C_z \delta_\eta \Pi' \right) \big|_{N-1} \\
&\quad - \Delta t \left(\frac{r_N - r_{N-1/2}}{r_N - r_{N-1}} \right) \left[\left(\frac{1 + \frac{1}{\varepsilon} m_v^*}{1 + \sum_{X=(v,cl,cf)} m_X^*} \right) \left(\alpha_2 \delta_{2r} \theta_{ref} G^{-1} R_w^+ \right) \right] \Big|_{N-1} \\
&\quad + \left(\overline{\theta_v^*}^r - \overline{\theta_v^n}^r \right) \Big|_{N-1/2} , \qquad (14.14)
\end{aligned}$$

where C_z is defined by (I.12).

14.6 Using the discretised linearised gas law at levels $k = 3/2, 5/2, ..., N-3/2$

Introducing (14.4) and (14.10) into (13.18) gives

$$\begin{aligned}
& -\frac{\Delta t}{\delta_\eta r} \left(1 + \sum_{X=(v,cl,cf)} \overline{m_X^*}^r \right) \left[\frac{1}{\cos\phi} \delta_{\lambda 1} \left(C_{xx1} \overline{u}^{\alpha_1} \right) + \frac{1}{\cos\phi} \delta_{\phi 1} \left(C_{yy1} \overline{v}^{\alpha_1} \right) \right] \\
& -\frac{\Delta t}{\delta_\eta r} \left(1 + \sum_{X=(v,cl,cf)} \overline{m_X^*}^r \right) \delta_\eta \left[C_5 \overline{w}^{\alpha_2} - C_5 \overline{\left(\overline{C_{xz} \overline{u}^\eta}^\lambda + \overline{C_{yz} \overline{v}^\eta}^\phi \right)}^{\alpha_1} \right] \\
& + \frac{1}{\kappa_d \Pi^n \overline{\theta_v^n}^r} \left(\kappa_d r^2 \rho^n \overline{\theta_v^n}^r - \frac{r^2 p^n}{R_d \Pi^n} \right) \Pi' + \frac{r^2 \rho^n \Delta t^r}{\overline{\theta_v^n}^r} \overline{C_z \delta_\eta \Pi'}^r \\
& = -\frac{1}{\kappa_d \Pi^n \overline{\theta_v^n}^r} \left(\kappa_d r^2 \rho^n \Pi^n \overline{\theta_v^*}^r - \frac{r^2 p^n}{c_{pd}} \right) + r^2 \rho_y^n \sum_{X=(v,cl,cf)} \overline{\left(m_X^n - m_X^* \right)}^r \\
& \quad + \frac{r^2 \rho^n \Delta t}{\overline{\theta_v^n}^r} \overline{\left(\frac{1 + \frac{1}{\varepsilon} m_v^*}{1 + \sum_{X=(v,cl,cf)} m_X^*} \right) \left(\alpha_2 \delta_{2r} \theta_{ref} G^{-1} R_w^+ \right)}^r . \qquad (14.15)
\end{aligned}$$

Using (13.4), (13.9), (13.12) and (13.20), this may be rearranged as

$$\begin{aligned}
& - \left[\frac{1}{\cos\phi} \delta_{\lambda 1} \left(C_{xx1} \alpha_1 u' \right) + \frac{1}{\cos\phi} \delta_{\phi 1} \left(C_{yy1} \alpha_1 v' \right) \right] \\
& + \delta_\eta \left[C_{zz} \delta_\eta \Pi' + C_5 \left(\overline{C_{xz} \overline{\alpha_1 u'}^\eta}^\lambda + \overline{C_{yz} \overline{\alpha_1 v'}^\eta}^\phi \right) \right] + C_3 \overline{C_z \delta_\eta \Pi'}^r - C_4 \Pi' \\
& = -\frac{\delta_\eta r \left(\kappa_d r^2 \rho^n \Pi^n \overline{\theta_v^*}^r - \frac{r^2 p^n}{c_{pd}} \right)}{\Delta t \kappa_d \Pi^n \overline{\theta_v^n}^r \left(1 + \sum_{X=(v,cl,cf)} \overline{m_X^*}^r \right)} \\
& \quad - \frac{r^2 \rho^n \delta_\eta r}{\Delta t \left(1 + \sum_{X=(v,cl,cf)} \overline{m_X^n}^r \right)} \left(\frac{\sum_{X=(v,cl,cf)} \overline{\left(m_X^* - m_X^n \right)}^r}{1 + \sum_{X=(v,cl,cf)} \overline{m_X^*}^r} \right)
\end{aligned}$$

$$+\frac{1}{\cos\phi}\delta_{\lambda 1}\left(C_{xx1}u^n\right)+\frac{1}{\cos\phi}\delta_{\phi 1}\left(C_{yy1}v^n\right)+\delta_\eta\left[C_5\left(\dot{\eta}^n\delta_\eta r+\alpha_2 G^{-1}R_w^+\right)\right]$$
$$+C_3\overline{\left(\frac{1+\frac{1}{\varepsilon}m_v^*}{1+\sum_{X=(v,cl,cf)}m_X^*}\right)\left(\alpha_2\delta_{2r}\theta_{ref}G^{-1}R_w^+\right)}^r\ , \qquad (14.16)$$

where C_{zz}, C_3 and C_4 are defined by (I.11), (I.24) and (I.25).

Eliminating u' and v' using (14.1)-(14.2) yields:

$$\frac{1}{\cos\phi}\delta_{\lambda 1}\left(C_{xx1}X\right)+\frac{1}{\cos\phi}\delta_{\phi 1}\left(C_{yy1}Y\right)+C_3\overline{C_z\delta_\eta\Pi'}^r-C_4\Pi'$$
$$+\delta_\eta\left[C_{zz}\delta_\eta\Pi'-C_5\left(\overline{C_{xz}\overline{X}^\eta}^\lambda+\overline{C_{yz}\overline{Y}^\eta}^\phi\right)\right] \quad = \quad RHS, \qquad (14.17)$$

where RHS, u_* and v_* are defined by (I.30)-(I.33).

14.7 Using the discretised linearised gas law at levels $k=1/2$ and $k=N-1/2$

14.7.1 $k=1/2$

Introducing (14.6) and (14.12) into (13.18) gives

$$-\left[\frac{\Delta t}{\delta_\eta r}\left(1+\sum_{X=(v,cl,cf)}\overline{m_X^*}^r\right)\right]\Bigg|_{1/2}\left[\frac{1}{\cos\phi}\delta_{\lambda 1}\left(C_{xx1}\overline{u}^{\alpha_1}\right)+\frac{1}{\cos\phi}\delta_{\phi 1}\left(C_{yy1}\overline{v}^{\alpha_1}\right)\right]\Bigg|_{1/2}$$
$$-\left[\frac{\Delta t}{\delta_\eta r\Delta\eta}\left(1+\sum_{X=(v,cl,cf)}\overline{m_X^*}^r\right)\right]\Bigg|_{1/2}\left[C_5\overline{w}^{\alpha_2}-C_5\overline{\left(\overline{C_{xz}\overline{u}^\eta}^\lambda+\overline{C_{yz}\overline{v}^\eta}^\phi\right)}^{\alpha_1}\right]\Bigg|_1$$
$$+\left[\frac{1}{\kappa_d\Pi^n\overline{\theta_v^n}^r}\left(\kappa_d r^2\rho^n\overline{\theta_v^n}^r-\frac{r^2p^n}{R_d\Pi^n}\right)\Pi'\right]\Bigg|_{1/2}+\left(\frac{r^2\rho^n\Delta t}{\overline{\theta_v^n}^r}\right)\Bigg|_{1/2}\left(C_z\delta_\eta\Pi'\right)\big|_1$$
$$=\ -\left[\frac{1}{\kappa_d\Pi^n\overline{\theta_v^n}^r}\left(\kappa_d r^2\rho^n\Pi^n\overline{\theta_v^*}^r-\frac{r^2p^n}{c_{pd}}\right)\right]\Bigg|_{1/2}+\left[r^2\rho_y^n\sum_{X=(v,cl,cf)}\overline{\left(m_X^n-m_X^*\right)}^r\right]\Bigg|_{1/2}$$
$$+\left(\frac{r^2\rho^n\Delta t}{\overline{\theta_v^n}^r}\right)\Bigg|_{1/2}\left[\left(\frac{1+\frac{1}{\varepsilon}m_v^*}{1+\sum_{X=(v,cl,cf)}m_X^*}\right)\left(\alpha_2\delta_{2r}\theta_{ref}G^{-1}R_w^+\right)\right]\Bigg|_1 . \qquad (14.18)$$

Using (13.4), (13.9), (13.12) and (13.20), this may be rearranged as

$$-\left[\frac{1}{\cos\phi}\delta_{\lambda 1}\left(C_{xx1}\alpha_1 u'\right)+\frac{1}{\cos\phi}\delta_{\phi 1}\left(C_{yy1}\alpha_1 v'\right)\right]\Bigg|_{1/2}+\left(C_3\right)\big|_{1/2}\left(C_z\delta_\eta\Pi'\right)\big|_1-\left(C_4\Pi'\right)\big|_{1/2}$$
$$+\left(\frac{1}{\Delta\eta}\right)\Bigg|_{1/2}\left[C_{zz}\delta_\eta\Pi'+C_5\left(\overline{C_{xz}\overline{\alpha_1 u'}^\eta}^\lambda+\overline{C_{yz}\overline{\alpha_1 v'}^\eta}^\phi\right)\right]\Bigg|_1$$

$$
\begin{aligned}
= & - \left[\frac{\delta_\eta r \left(\kappa_d r^2 \rho^n \Pi^n \overline{\theta_v^*}^r - \frac{r^2 p^n}{c_{pd}} \right)}{\Delta t \kappa_d \Pi^n \overline{\theta_v^n}^r \left(1 + \sum_{X=(v,cl,cf)} \overline{m_X^*}^r \right)} \right] \Bigg|_{1/2} \\
& - \left[\frac{r^2 \rho^n \delta_\eta r}{\Delta t \left(1 + \sum_{X=(v,cl,cf)} \overline{m_X^n}^r \right)} \left(\frac{\sum_{X=(v,cl,cf)} \overline{(m_X^* - m_X^n)}^r}{1 + \sum_{X=(v,cl,cf)} \overline{m_X^*}^r} \right) \right] \Bigg|_{1/2} \\
& + \left[\frac{1}{\cos\phi} \delta_{\lambda 1} \left(C_{xx1} u^n \right) + \frac{1}{\cos\phi} \delta_{\phi 1} \left(C_{yy1} v^n \right) \right] \Bigg|_{1/2} + \left(\frac{1}{\Delta\eta} \right) \Bigg|_{1/2} \left[C_5 \left(\dot{\eta}^n \delta_\eta r + \alpha_2 G^{-1} R_w^+ \right) \right] \Big|_1 \\
& + \left(C_3 \right)\big|_{1/2} \left[\left(\frac{1 + \frac{1}{\varepsilon} m_v^*}{1 + \sum_{X=(v,cl,cf)} m_X^*} \right) \left(\alpha_2 \delta_{2r} \theta_{ref} G^{-1} R_w^+ \right) \right] \Bigg|_1 ,
\end{aligned}
\tag{14.19}
$$

where C_{zz}, C_3 and C_4 are defined by (I.11), (I.24) and (I.25).

Eliminating u' and v' using (14.1)-(14.2) yields:

$$
\begin{aligned}
& \left[\frac{1}{\cos\phi} \delta_{\lambda 1} \left(C_{xx1} X \right) + \frac{1}{\cos\phi} \delta_{\phi 1} \left(C_{yy1} Y \right) \right] \Bigg|_{1/2} + \left(C_3 \right)\big|_{1/2} \left(C_z \delta_\eta \Pi' \right)\big|_1 - \left(C_4 \Pi' \right)\big|_{1/2} \\
& \qquad + \left(\frac{1}{\Delta\eta} \right) \Bigg|_{1/2} \left[C_{zz} \delta_\eta \Pi' - C_5 \left(\overline{C_{xz} \overline{X}^\eta}^\lambda + \overline{C_{yz} \overline{Y}^\eta}^\phi \right) \right] \Bigg|_1 = \left(RHS \right)\big|_{1/2} ,
\end{aligned}
\tag{14.20}
$$

where $(RHS)|_{1/2}$, $(u_*)|_{1/2}$ and $(v_*)|_{1/2}$ are defined by (I.29) and (I.32)-(I.33).

14.7.2 $k = N - 1/2$

Introducing (14.8) and (14.14) into (13.18) gives

$$
\begin{aligned}
& - \left[\frac{\Delta t}{\delta_\eta r} \left(1 + \sum_{X=(v,cl,cf)} \overline{m_X^*}^r \right) \right] \Bigg|_{N-1/2} \left[\frac{1}{\cos\phi} \delta_{\lambda 1} \left(C_{xx1} \overline{u}^{\alpha_1} \right) + \frac{1}{\cos\phi} \delta_{\phi 1} \left(C_{yy1} \overline{v}^{\alpha_1} \right) \right] \Bigg|_{N-1/2} \\
& + \left[\frac{\Delta t}{\delta_\eta r \Delta\eta} \left(1 + \sum_{X=(v,cl,cf)} \overline{m_X^*}^r \right) \right] \Bigg|_{N-1/2} \left[C_5 \overline{w}^{\alpha_2} - C_5 \overline{\left(\overline{C_{xz} \overline{u}^\eta}^\lambda + \overline{C_{yz} \overline{v}^\eta}^\phi \right)}^{\alpha_1} \right] \Bigg|_{N-1} \\
& + \left[\frac{1}{\kappa_d \Pi^n \overline{\theta_v^n}^r} \left(\kappa_d r^2 \rho^n \overline{\theta_v^n}^r - \frac{r^2 p^n}{R_d \Pi^n} \right) \Pi' \right] \Bigg|_{N-1/2} \\
& + \left(\frac{r_N - r_{N-1/2}}{r_N - r_{N-1}} \right) \left(\frac{r^2 \rho^n \Delta t}{\overline{\theta_v^n}^r} \right) \Bigg|_{N-1/2} \left(C_z \delta_\eta \Pi' \right)\big|_{N-1} \\
= & - \left[\frac{1}{\kappa_d \Pi^n \overline{\theta_v^n}^r} \left(\kappa_d r^2 \rho^n \Pi^n \overline{\theta_v^*}^r - \frac{r^2 p^n}{c_{pd}} \right) \right] \Bigg|_{N-1/2} + \left[r^2 \rho_y^n \sum_{X=(v,cl,cf)} \overline{(m_X^n - m_X^*)}^r \right] \Bigg|_{N-1/2} \\
& + \left(\frac{r_N - r_{N-1/2}}{r_N - r_{N-1}} \right) \left(\frac{r^2 \rho^n \Delta t}{\overline{\theta_v^n}^r} \right) \Bigg|_{N-1/2} \left[\left(\frac{1 + \frac{1}{\varepsilon} m_v^*}{1 + \sum_{X=(v,cl,cf)} m_X^*} \right) \left(\alpha_2 \delta_{2r} \theta_{ref} G^{-1} R_w^+ \right) \right] \Bigg|_{N-1} .
\end{aligned}
\tag{14.21}
$$

Using (13.4), (13.9), (13.12) and (13.20), this may be rearranged as

$$
\begin{aligned}
&- \left[\frac{1}{\cos\phi} \delta_{\lambda 1} \left(C_{xx1} \alpha_1 u' \right) + \frac{1}{\cos\phi} \delta_{\phi 1} \left(C_{yy1} \alpha_1 v' \right) \right] \Bigg|_{N-1/2} \\
&+ \left(\frac{r_N - r_{N-1/2}}{r_N - r_{N-1}} \right) \left(C_3 \right)|_{N-1/2} \left(C_z \delta_\eta \Pi' \right)|_{N-1} - \left(C_4 \Pi' \right)|_{N-1/2} \\
&- \left(\frac{1}{\Delta\eta} \right) \Bigg|_{N-1/2} \left[C_{zz} \delta_\eta \Pi' + C_5 \left(\overline{C_{xz} \overline{\alpha_1 u'}^{\eta}}^{\lambda} + \overline{C_{yz} \overline{\alpha_1 v'}^{\eta}}^{\phi} \right) \right] \Bigg|_{N-1} \\
&= - \left[\frac{\delta_\eta r \left(\kappa_d r^2 \rho^n \Pi^n \overline{\theta_v^*}^r - \frac{r^2 p^n}{c_{pd}} \right)}{\Delta t \kappa_d \Pi^n \overline{\theta_v^n}^r \left(1 + \sum_{X=(v,cl,cf)} \overline{m_X^*}^r \right)} \right] \Bigg|_{N-1/2} \\
&\quad - \left[\frac{r^2 \rho^n \delta_\eta r}{\Delta t \left(1 + \sum_{X=(v,cl,cf)} \overline{m_X^n}^r \right)} \left(\frac{\sum_{X=(v,cl,cf)} \overline{\left(m_X^* - m_X^n \right)}^r}{1 + \sum_{X=(v,cl,cf)} \overline{m_X^*}^r} \right) \right] \Bigg|_{N-1/2} \\
&\quad - \left(\frac{1}{\Delta\eta} \right) \Bigg|_{N-1/2} \left[C_5 \left(\dot{\eta}^n \delta_\eta r + \alpha_2 G^{-1} R_w^+ \right) \right] \Big|_{N-1} \\
&\quad + \left(\frac{r_N - r_{N-1/2}}{r_N - r_{N-1}} \right) \left(C_3 \right)|_{N-1/2} \left[\left(\frac{1 + \frac{1}{\varepsilon} m_v^*}{1 + \sum_{X=(v,cl,cf)} m_X^*} \right) \left(\alpha_2 \delta_{2r} \theta_{ref} G^{-1} R_w^+ \right) \right] \Bigg|_{N-1} \\
&\quad + \left[\frac{1}{\cos\phi} \delta_{\lambda 1} \left(C_{xx1} u^n \right) + \frac{1}{\cos\phi} \delta_{\phi 1} \left(C_{yy1} v^n \right) \right] \Bigg|_{N-1/2}, \qquad (14.22)
\end{aligned}
$$

where C_{zz}, C_3 and C_4 are defined by (I.11), (I.24) and (I.25).

Eliminating u' and v' using (14.1)-(14.2) yields:

$$
\begin{aligned}
&\left[\frac{1}{\cos\phi} \delta_{\lambda 1} \left(C_{xx1} X \right) + \frac{1}{\cos\phi} \delta_{\phi 1} \left(C_{yy1} Y \right) \right] \Bigg|_{N-1/2} \\
&+ \left(\frac{r_N - r_{N-1/2}}{r_N - r_{N-1}} \right) \left(C_3 \right)|_{N-1/2} \left(C_z \delta_\eta \Pi' \right)|_{N-1} - \left(C_4 \Pi' \right)|_{N-1/2} \\
&- \left(\frac{1}{\Delta\eta} \right) \Bigg|_{N-1/2} \left[C_{zz} \delta_\eta \Pi' - C_5 \left(\overline{C_{xz} \overline{X}^{\eta}}^{\lambda} + \overline{C_{yz} \overline{Y}^{\eta}}^{\phi} \right) \right] \Bigg|_{N-1} = (RHS)|_{N-1/2}, \qquad (14.23)
\end{aligned}
$$

where $(RHS)|_{N-1/2}$, $(u_*)|_{N-1/2}$ and $(v_*)|_{N-1/2}$ are defined by (I.31) and (I.32)-(I.33).

14.8 Southern boundary condition at levels $k = 3/2, 5/2, ..., N - 3/2$

The southern boundary condition for the Helmholtz problem for Π' is obtained in an analogous manner to that for non-polar points but using the special discretisations for the south polar cap.

The discretised horizontal momentum equation (14.2) at points around the near-polar latitude circle ϕ_1 may be rewritten as

$$\begin{aligned}(\alpha_1 v')_{i-\frac{1}{2},1} &= \alpha_1 \left(A_v R_v^+ - F_v \overline{R_u^+}^{\lambda\phi} \right)_{i-\frac{1}{2},1} - Y_{i-\frac{1}{2},1} = (v_* - v^n)_{i-\frac{1}{2},1} - Y_{i-\frac{1}{2},1}, \\ &\quad (i = 1, 2, ..., L) \qquad (14.24)\end{aligned}$$

where subscript "$i - \frac{1}{2}, 1$" denotes evaluation at $\left(\lambda_{i-\frac{1}{2}}, \phi_1\right)$, Y is defined by (I.4)-(I.6), and v_* by (I.33).

The discretised continuity equation (13.47) over the southern polar cap is rewritten, using (13.50), as

$$\begin{aligned}\left(r^2 \rho_y'\right)_{SP} &= -\frac{\Delta t}{(\delta_\eta r)_{SP}} \frac{\Delta\phi}{b} \frac{1}{L} \sum_{i=1}^{L} \left(C_{yy1} \overline{v}^{\alpha_1}\right)_{i-\frac{1}{2},1} \\ &\quad - \frac{\Delta t}{(\delta_\eta r)_{SP}} \delta_\eta \left[\left(C_5 \overline{w}^{\alpha_2}\right)_{SP} - (C_5)_{SP} \frac{2}{L} \sum_{i=1}^{L} \left(\overline{C_{yz} \overline{v}^{\eta}}^{\alpha_1}\right)_{i-\frac{1}{2},1} \right], \qquad (14.25)\end{aligned}$$

where

$$b = \frac{(\Delta\phi)^2}{8},$$

C_{yy1}, C_{yz} and C_5 are defined by (I.9), (I.14) and (I.26), and subscript "SP" denotes evaluation at the South Pole. Inserting (14.25) into (13.36) then leads to:

$$\begin{aligned}\left(r^2 \rho'\right)_{SP} &= -\left[\frac{\Delta t}{\delta_\eta r} \left(1 + \sum_{X=(v,cl,cf)} \overline{m_X^*}^r \right) \right]_{SP} \frac{\Delta\phi}{b} \frac{1}{L} \sum_{i=1}^{L} \left(C_{yy1} \overline{v}^{\alpha_1}\right)_{i-\frac{1}{2},1} \\ &\quad - \left[\frac{\Delta t}{\delta_\eta r} \left(1 + \sum_{X=(v,cl,cf)} \overline{m_X^*}^r \right) \right]_{SP} \delta_\eta \left[\left(C_5 \overline{w}^{\alpha_2}\right)_{SP} - (C_5)_{SP} \frac{2}{L} \sum_{i=1}^{L} \left(\overline{C_{yz} \overline{v}^{\eta}}^{\alpha_1}\right)_{i-\frac{1}{2},1} \right] \\ &\quad + \left(r^2 \rho_y^n\right)_{SP} \left[\sum_{X=(v,cl,cf)} \overline{(m_X^* - m_X^n)}^r \right]_{SP}. \qquad (14.26)\end{aligned}$$

Evaluating (14.10) at the South Pole gives

$$\begin{aligned}\left(\overline{\theta_v'}^r\right)_{SP} &= \left(\Delta t \overline{C_z \delta_\eta \Pi'}^r + \overline{\theta_v^*}^r - \overline{\theta_v^n}^r \right)_{SP} \\ &\quad - \left[\overline{\Delta t \left(\frac{1 + \frac{1}{\varepsilon} m_v^*}{1 + \sum_{X=(v,cl,cf)} m_X^*} \right) \left(\alpha_2 \delta_{2r} \theta_{ref} G^{-1} R_w^+\right)}^r \right]_{SP}, \qquad (14.27)\end{aligned}$$

where C_z is defined by (I.12).

Introducing (14.26) and (14.27) into (13.18) evaluated at the South Pole gives

$$-\left[\frac{\Delta t}{\delta_\eta r} \left(1 + \sum_{X=(v,cl,cf)} \overline{m_X^*}^r \right) \right]_{SP} \frac{\Delta\phi}{b} \frac{1}{L} \sum_{i=1}^{L} \left(C_{yy1} \overline{v}^{\alpha_1}\right)_{i-\frac{1}{2},1}$$

$$
\begin{aligned}
&-\left[\frac{\Delta t}{\delta_\eta r}\left(1+\sum_{X=(v,cl,cf)}\overline{m_X^*}^r\right)\right]_{SP}\delta_\eta\left[(C_5\overline{w}^{\alpha_2})_{SP}-(C_5)_{SP}\frac{2}{L}\sum_{i=1}^{L}\left(\overline{C_{yz}\overline{v}^{\eta}}^{\alpha_1}\right)_{i-\frac{1}{2},1}\right]\\
&+\left[\frac{1}{\kappa_d\Pi^n\overline{\theta_v^n}^r}\left(\kappa_d r^2\rho^n\overline{\theta_v^n}^r-\frac{r^2p^n}{R_d\Pi^n}\right)\Pi'+\frac{r^2\rho^n\Delta t}{\overline{\theta_v^n}^r}\overline{C_z\delta_\eta\Pi'}^r\right]_{SP}\\
&=\left[-\frac{1}{\kappa_d\Pi^n\overline{\theta_v^n}^r}\left(\kappa_d r^2\rho^n\Pi^n\overline{\theta_v^*}^r-\frac{r^2p^n}{c_{pd}}\right)+r^2\rho_y^n\sum_{X=(v,cl,cf)}\overline{(m_X^n-m_X^*)}^r\right]_{SP}\\
&+\left[\frac{r^2\rho^n\Delta t}{\overline{\theta_v^n}^r}\overline{\left(\frac{1+\frac{1}{\varepsilon}m_v^*}{1+\sum_{X=(v,cl,cf)}m_X^*}\right)(\alpha_2\delta_{2r}\theta_{ref}G^{-1}R_w^+)}^r\right]_{SP}. \qquad (14.28)
\end{aligned}
$$

Using (13.4), (13.9), (13.12), (13.20) and (13.52), this may be rearranged as

$$
\begin{aligned}
&-\frac{\Delta\phi}{b}\frac{1}{L}\sum_{i=1}^{L}(C_{yy1}\alpha_1v')_{i-\frac{1}{2},1}+\left(C_3\overline{C_z\delta_\eta\Pi'}^r-C_4\Pi'\right)_{SP}\\
&+\delta_\eta\left[(C_{zz}\delta_\eta\Pi')_{SP}+(C_5)_{SP}\frac{2}{L}\sum_{i=1}^{L}\left(C_{yz}\overline{\alpha_1v'}^{\eta}\right)_{i-\frac{1}{2},1}\right]\\
&=-\left[\frac{\delta_\eta r}{\Delta t\kappa_d\Pi^n\overline{\theta_v^n}^r\left(1+\sum_{X=(v,cl,cf)}\overline{m_X^*}^r\right)}\left(\kappa_d r^2\rho^n\Pi^n\overline{\theta_v^*}^r-\frac{r^2p^n}{c_{pd}}\right)\right]_{SP}\\
&\quad-\left[\frac{r^2\rho^n\delta_\eta r}{\Delta t\left(1+\sum_{X=(v,cl,cf)}\overline{m_X^n}^r\right)}\left(\frac{\sum_{X=(v,cl,cf)}\overline{(m_X^*-m_X^n)}^r}{1+\sum_{X=(v,cl,cf)}\overline{m_X^*}^r}\right)\right]_{SP}\\
&\quad+\frac{\Delta\phi}{b}\frac{1}{L}\sum_{i=1}^{L}(C_{yy1}v^n)_{i-\frac{1}{2},1}+\left\{\delta_\eta\left[C_5\left(\dot\eta^n\delta_\eta r+\alpha_2G^{-1}R_w^+\right)\right]\right\}_{SP}\\
&\quad+\left[C_3\overline{\left(\frac{1+\frac{1}{\varepsilon}m_v^*}{1+\sum_{X=(v,cl,cf)}m_X^*}\right)(\alpha_2\delta_{2r}\theta_{ref}G^{-1}R_w^+)}^r\right]_{SP}, \qquad (14.29)
\end{aligned}
$$

where C_{zz}, C_3 and C_4 are defined by (I.11), (I.24) and (I.25).

Eliminating v' using (14.24) yields:

$$
\begin{aligned}
&\frac{\Delta\phi}{b}\frac{1}{L}\sum_{i=1}^{L}(C_{yy1}Y)_{i-\frac{1}{2},1}+\left(C_3\overline{C_z\delta_\eta\Pi'}^r-C_4\Pi'\right)_{SP}\\
&+\delta_\eta\left[(C_{zz}\delta_\eta\Pi')_{SP}-(C_5)_{SP}\frac{2}{L}\sum_{i=1}^{L}\left(C_{yz}\overline{Y}^{\eta}\right)_{i-\frac{1}{2},1}\right]=(RHS)_{SP}, \qquad (14.30)
\end{aligned}
$$

where

$$
(RHS)_{SP}=-\left[\frac{\delta_\eta r}{\Delta t\kappa_d\Pi^n\overline{\theta_v^n}^r\left(1+\sum_{X=(v,cl,cf)}\overline{m_X^*}^r\right)}\left(\kappa_d r^2\rho^n\Pi^n\overline{\theta_v^*}^r-\frac{r^2p^n}{c_{pd}}\right)\right]_{SP}
$$

$$
\begin{aligned}
&-\left[\frac{r^2\rho^n\delta_\eta r}{\Delta t\left(1+\sum_{X=(v,cl,cf)}\overline{m_X^n}^r\right)}\left(\frac{\sum_{X=(v,cl,cf)}\overline{(m_X^*-m_X^n)}^r}{1+\sum_{X=(v,cl,cf)}\overline{m_X^*}^r}\right)\right]_{SP}\\
&+\frac{\Delta\phi}{b}\frac{1}{L}\sum_{i=1}^{L}\left(C_{yy1}v_*\right)_{i-\frac{1}{2},1}+\left\{\delta_\eta\left[C_5\left(\dot{\eta}^n\delta_\eta r+\alpha_2G^{-1}R_w^+\right)\right]\right\}_{SP}\\
&-\delta_\eta\left[\left(C_5\right)_{SP}\left(\frac{2}{L}\sum_{i=1}^{L}\left[C_{yz}\overline{(v_*-v^n)}^\eta\right]_{i-\frac{1}{2},1}\right)\right]\\
&+\left[\overline{C_3\left(\frac{1+\frac{1}{\varepsilon}m_v^*}{1+\sum_{X=(v,cl,cf)}m_X^*}\right)\left(\alpha_2\delta_{2r}\theta_{ref}G^{-1}R_w^+\right)}^r\right]_{SP},
\end{aligned}
\tag{14.31}
$$

and v_* is defined by (I.33).

14.9 Northern boundary condition at levels $k = 3/2, 5/2, ..., N - 3/2$

The northern boundary condition for the Helmholtz problem for Π' is obtained in an analogous manner to that for non-polar points but using the special discretisations for the north polar cap.

The discretised horizontal momentum equation (14.2) at points around the near-polar latitude circle ϕ_{M-1} may be rewritten as

$$
\begin{aligned}
\left(\alpha_1 v'\right)_{i-\frac{1}{2},M-1} &= \alpha_1\left(A_vR_v^+-F_v\overline{R_u^+}^{\lambda\phi}\right)_{i-\frac{1}{2},M-1}-Y_{i-\frac{1}{2},M-1}=\left(v_*-v^n\right)_{i-\frac{1}{2},M-1}-Y_{i-\frac{1}{2},M-1},\\
&\quad (i=1,2,...,L)
\end{aligned}
\tag{14.32}
$$

where subscript "$i-\frac{1}{2}, M-1$" denotes evaluation at $\left(\lambda_{i-\frac{1}{2}},\phi_{M-1}\right)$, Y is defined by (I.4)-(I.6), and v_* by (I.33).

The discretised continuity equation (13.48) over the northern polar cap is rewritten, using (13.51), as

$$
\begin{aligned}
\left(r^2\rho_y'\right)_{NP} &= +\frac{\Delta t}{\left(\delta_\eta r\right)_{NP}}\frac{\Delta\phi}{b}\frac{1}{L}\sum_{i=1}^{L}\left(C_{yy1}\overline{v}^{\alpha_1}\right)_{i-\frac{1}{2},M-1}\\
&\quad-\frac{\Delta t}{\left(\delta_\eta r\right)_{NP}}\delta_\eta\left[\left(C_5\overline{w}^{\alpha_2}\right)_{NP}-\left(C_5\right)_{NP}\frac{2}{L}\sum_{i=1}^{L}\left(\overline{C_{yz}\overline{v}^\eta}^{\alpha_1}\right)_{i-\frac{1}{2},M-1}\right],
\end{aligned}
\tag{14.33}
$$

where

$$
b=\frac{(\Delta\phi)^2}{8},
$$

C_{yy1}, C_{yz} and C_5 are defined by (I.9), (I.14) and (I.26), and subscript "NP" denotes evaluation at the North Pole. Inserting (14.33) into (13.36) then leads to:

$$\begin{aligned}
\left(r^2\rho'\right)_{NP} &= +\left[\frac{\Delta t}{\delta_\eta r}\left(1+\sum_{X=(v,cl,cf)}\overline{m_X^*}^r\right)\right]_{NP}\frac{\Delta\phi}{b}\frac{1}{L}\sum_{i=1}^{L}\left(C_{yy1}\overline{v}^{\alpha_1}\right)_{i-\frac{1}{2},M-1}\\
&\quad-\left[\frac{\Delta t}{\delta_\eta r}\left(1+\sum_{X=(v,cl,cf)}\overline{m_X^*}^r\right)\right]_{NP}\delta_\eta\left[\left(C_5\overline{w}^{\alpha_2}\right)_{NP}-\left(C_5\right)_{NP}\frac{2}{L}\sum_{i=1}^{L}\left(\overline{C_{yz}\overline{v}^\eta}^{\alpha_1}\right)_{i-\frac{1}{2},M-1}\right]\\
&\quad+\left(r^2\rho_y^n\right)_{NP}\left[\sum_{X=(v,cl,cf)}\overline{\left(m_X^*-m_X^n\right)}^r\right]_{NP}. \qquad (14.34)
\end{aligned}$$

Evaluating (14.10) at the North Pole gives

$$\begin{aligned}
\left(\overline{\theta_v'}^r\right)_{NP} &= \left[\Delta t\overline{C_z\delta_\eta\Pi'}^r+\overline{\theta_v^*}^r-\overline{\theta_v^n}^r\right]_{NP}\\
&\quad-\left[\Delta t\overline{\left(\frac{1+\frac{1}{\varepsilon}m_v^*}{1+\sum_{X=(v,cl,cf)}m_X^*}\right)\left(\alpha_2\delta_{2r}\theta_{ref}G^{-1}R_w^+\right)}^r\right]_{NP}, \qquad (14.35)
\end{aligned}$$

where C_z is defined by (I.12).

Introducing (14.34) and (14.35) into (13.18) evaluated at the North Pole gives

$$\begin{aligned}
&+\left[\frac{\Delta t}{\delta_\eta r}\left(1+\sum_{X=(v,cl,cf)}\overline{m_X^*}^r\right)\right]_{NP}\frac{\Delta\phi}{b}\frac{1}{L}\sum_{i=1}^{L}\left(C_{yy1}\overline{v}^{\alpha_1}\right)_{i-\frac{1}{2},M-1}\\
&-\left[\frac{\Delta t}{\delta_\eta r}\left(1+\sum_{X=(v,cl,cf)}\overline{m_X^*}^r\right)\right]_{NP}\delta_\eta\left[\left(C_5\overline{w}^{\alpha_2}\right)_{NP}-\left(C_5\right)_{NP}\frac{2}{L}\sum_{i=1}^{L}\left(\overline{C_{yz}\overline{v}^\eta}^{\alpha_1}\right)_{i-\frac{1}{2},M-1}\right]\\
&+\left[\frac{1}{\kappa_d\Pi^n\overline{\theta_v^n}^r}\left(\kappa_d r^2\rho^n\overline{\theta_v^n}^r-\frac{r^2p^n}{R_d\Pi^n}\right)\Pi'+\frac{r^2\rho^n\Delta t}{\overline{\theta_v^n}^r}\overline{C_z\delta_\eta\Pi'}^r\right]_{NP}\\
&=\left[-\frac{1}{\kappa_d\Pi^n\overline{\theta_v^n}^r}\left(\kappa_d r^2\rho^n\Pi^n\overline{\theta_v^*}^r-\frac{r^2p^n}{c_{pd}}\right)+r^2\rho_y^n\sum_{X=(v,cl,cf)}\overline{\left(m_X^n-m_X^*\right)}^r\right]_{NP}\\
&\quad+\left[\frac{r^2\rho^n\Delta t}{\overline{\theta_v^n}^r}\overline{\left(\frac{1+\frac{1}{\varepsilon}m_v^*}{1+\sum_{X=(v,cl,cf)}m_X^*}\right)\left(\alpha_2\delta_{2r}\theta_{ref}G^{-1}R_w^+\right)}^r\right]_{NP}. \qquad (14.36)
\end{aligned}$$

Using (13.4), (13.9), (13.12), (13.20) and (13.53), this may be rearranged as

$$\begin{aligned}
&+\frac{\Delta\phi}{b}\frac{1}{L}\sum_{i=1}^{L}\left(C_{yy1}\alpha_1 v'\right)_{i-\frac{1}{2},M-1}+\left(C_3\overline{C_z\delta_\eta\Pi'}^r-C_4\Pi'\right)_{NP}\\
&+\delta_\eta\left[\left(C_{zz}\delta_\eta\Pi'\right)_{NP}+\left(C_5\right)_{NP}\frac{2}{L}\sum_{i=1}^{L}\left(C_{yz}\overline{\alpha_1 v'}^\eta\right)_{i-\frac{1}{2},M-1}\right]
\end{aligned}$$

$$\begin{aligned}
= & -\left[\frac{\delta_\eta r}{\Delta t\kappa_d \Pi^n \overline{\theta_v^n}^r \left(1+\sum_{X=(v,cl,cf)} \overline{m_X^*}^r\right)}\left(\kappa_d r^2\rho^n\Pi^n\overline{\theta_v^*}^r - \frac{r^2p^n}{c_{pd}}\right)\right]_{NP} \\
& -\left[\frac{r^2\rho^n\delta_\eta r}{\Delta t\left(1+\sum_{X=(v,cl,cf)}\overline{m_X^n}^r\right)}\left(\frac{\sum_{X=(v,cl,cf)}\overline{(m_X^*-m_X^n)}^r}{1+\sum_{X=(v,cl,cf)}\overline{m_X^*}^r}\right)\right]_{NP} \\
& -\frac{\Delta\phi}{b}\frac{1}{L}\sum_{i=1}^{L}\left(C_{yy1}v^n\right)_{i-\frac{1}{2},M-1} + \left\{\delta_\eta\left[C_5\left(\dot{\eta}^n\delta_\eta r + \alpha_2 G^{-1}R_w^+\right)\right]\right\}_{NP} \\
& +\left[C_3\overline{\left(\frac{1+\frac{1}{\varepsilon}m_v^*}{1+\sum_{X=(v,cl,cf)}m_X^*}\right)\left(\alpha_2\delta_{2r}\theta_{ref}G^{-1}R_w^+\right)}^r\right]_{NP}, \qquad (14.37)
\end{aligned}$$

where C_{zz}, C_3 and C_4 are defined by (I.11), (I.24) and (I.25).

Eliminating v' using (14.32) yields:

$$\begin{aligned}
& -\frac{\Delta\phi}{b}\frac{1}{L}\sum_{i=1}^{L}\left(C_{yy1}Y\right)_{i-\frac{1}{2},M-1} + \left(C_3\overline{C_z\delta_\eta\Pi'}^r - C_4\Pi'\right)_{NP} \\
& +\delta_\eta\left[\left(C_{zz}\delta_\eta\Pi'\right)_{NP} - \left(C_5\right)_{NP}\frac{2}{L}\sum_{i=1}^{L}\left(C_{yz}\overline{Y}^\eta\right)_{i-\frac{1}{2},M-1}\right] \; = \; (RHS)_{NP}, \qquad (14.38)
\end{aligned}$$

where

$$\begin{aligned}
(RHS)_{NP} = & -\left[\frac{\delta_\eta r}{\Delta t\kappa_d \Pi^n \overline{\theta_v^n}^r \left(1+\sum_{X=(v,cl,cf)} \overline{m_X^*}^r\right)}\left(\kappa_d r^2\rho^n\Pi^n\overline{\theta_v^*}^r - \frac{r^2p^n}{c_{pd}}\right)\right]_{NP} \\
& -\left[\frac{r^2\rho^n\delta_\eta r}{\Delta t\left(1+\sum_{X=(v,cl,cf)}\overline{m_X^n}^r\right)}\left(\frac{\sum_{X=(v,cl,cf)}\overline{(m_X^*-m_X^n)}^r}{1+\sum_{X=(v,cl,cf)}\overline{m_X^*}^r}\right)\right]_{NP} \\
& -\frac{\Delta\phi}{b}\frac{1}{L}\sum_{i=1}^{L}\left(C_{yy1}v_*\right)_{i-\frac{1}{2},M-1} + \left\{\delta_\eta\left[C_5\left(\dot{\eta}^n\delta_\eta r + \alpha_2 G^{-1}R_w^+\right)\right]\right\}_{NP} \\
& -\delta_\eta\left[\left(C_5\right)_{NP}\left(\frac{2}{L}\sum_{i=1}^{L}\left[C_{yz}\overline{(v_*-v^n)}^\eta\right]_{i-\frac{1}{2},M-1}\right)\right] \\
& +\left[C_3\overline{\left(\frac{1+\frac{1}{\varepsilon}m_v^*}{1+\sum_{X=(v,cl,cf)}m_X^*}\right)\left(\alpha_2\delta_{2r}\theta_{ref}G^{-1}R_w^+\right)}^r\right]_{NP}, \qquad (14.39)
\end{aligned}$$

and v_* is defined by (I.33).

14.10 Southern boundary condition at levels $k = 1/2$ and $k = N-1/2$

14.10.1 $k = 1/2$

The southern boundary condition for the Helmholtz problem for Π' at level $k = 1/2$ is obtained in an analogous manner to that for non-polar points but using the special discretisations for the south polar cap. Thus:

$$\left[\frac{\Delta\phi}{b}\frac{1}{L}\sum_{i=1}^{L}\left(C_{yy1}Y\right)_{i-\frac{1}{2},1}\right]\Bigg|_{\eta_{1/2}} + \left[(C_3)|_{\eta_{1/2}}\left(C_z\delta_\eta\Pi'\right)|_{\eta_1} - \left(C_4\Pi'\right)|_{\eta_{1/2}}\right]_{SP}$$
$$+\left(\frac{1}{\Delta\eta}\right)\Bigg|_{\eta_{1/2}}\left[\left(C_{zz}\delta_\eta\Pi'\right)_{SP} - (C_5)_{SP}\frac{2}{L}\sum_{i=1}^{L}\left(C_{yz}\overline{Y}^{\eta}\right)_{i-\frac{1}{2},1}\right]\Bigg|_{\eta_1} = \; = \; \left[(RHS)|_{\eta_{1/2}}\right]_{SP}, \tag{14.40}$$

where

$$\begin{aligned}
\left[(RHS)|_{\eta_{1/2}}\right]_{SP} = &-\left\{\left[\frac{\delta_\eta r}{\Delta t\kappa_d\Pi^n\overline{\theta_v^n}^r\left(1+\sum_{X=(v,cl,cf)}\overline{m_X^*}^r\right)}\left(\kappa_d r^2\rho^n\Pi^n\overline{\theta_v^*}^r - \frac{r^2p^n}{c_{pd}}\right)\right]\Bigg|_{\eta_{1/2}}\right\}_{SP}\\
&-\left\{\left[\frac{r^2\rho^n\delta_\eta r}{\Delta t\left(1+\sum_{X=(v,cl,cf)}\overline{m_X^n}^r\right)}\left(\frac{\sum_{X=(v,cl,cf)}\overline{\left(m_X^*-m_X^n\right)}^r}{1+\sum_{X=(v,cl,cf)}\overline{m_X^*}^r}\right)\right]\Bigg|_{\eta_{1/2}}\right\}_{SP}\\
&+\left[\frac{\Delta\phi}{b}\frac{1}{L}\sum_{i=1}^{L}\left(C_{yy1}v_*\right)_{i-\frac{1}{2},1}\right]\Bigg|_{\eta_{1/2}} + \left\{\left(\frac{1}{\Delta\eta}\right)\Bigg|_{\eta_{1/2}}\left[C_5\left(\dot\eta^n\delta_\eta r + \alpha_2G^{-1}R_w^+\right)\right]\big|_{\eta_1}\right\}_{SP}\\
&-\left(\frac{1}{\Delta\eta}\right)\Bigg|_{\eta_{1/2}}\left\{(C_5)_{SP}\frac{2}{L}\sum_{i=1}^{L}\left[C_{yz}\overline{(v_*-v^n)}^{\eta}\right]_{i-\frac{1}{2},1}\right\}\Bigg|_{\eta_1}\\
&+\left\{(C_3)|_{\eta_{1/2}}\left[\left(\frac{1+\frac{1}{\varepsilon}m_v^*}{1+\sum_{X=(v,cl,cf)}m_X^*}\right)\left(\alpha_2\delta_{2r}\theta_{ref}G^{-1}R_w^+\right)\right]\Bigg|_{\eta_1}\right\}_{SP},
\end{aligned} \tag{14.41}$$

and v_* is defined by (I.33).

14.10.2 $k = N - 1/2$

The southern boundary condition for the Helmholtz problem for Π' at level $k = N - 1/2$ is obtained in an analogous manner to that for non-polar points but using the special discretisations for the south polar cap. Thus:

$$\left[\frac{\Delta\phi}{b}\frac{1}{L}\sum_{i=1}^{L}\left(C_{yy1}Y\right)_{i-\frac{1}{2},1}\right]\Bigg|_{\eta_{N-1/2}} + \left[\left(\frac{r_N - r_{N-\frac{1}{2}}}{r_N - r_{N-1}}\right)(C_3)|_{\eta_{N-\frac{1}{2}}}\left(C_z\delta_\eta\Pi'\right)|_{\eta_{N-1}} - \left(C_4\Pi'\right)|_{\eta_{N-\frac{1}{2}}}\right]_{SP}$$

$$
-\left(\frac{1}{\Delta\eta}\right)\Bigg|_{\eta_{N-\frac{1}{2}}}\left[\left(C_{zz}\delta_\eta\Pi'\right)_{SP}-\left(C_5\right)_{SP}\frac{2}{L}\sum_{i=1}^{L}\left(C_{yz}\overline{Y}^{\eta}\right)_{i-\frac{1}{2},1}\right]\Bigg|_{\eta_{N-1}}=\left[(RHS)|_{\eta_{N-\frac{1}{2}}}\right]_{SP}, \tag{14.42}
$$

where

$$
\begin{aligned}
\left[(RHS)|_{\eta_{N-\frac{1}{2}}}\right]_{SP} = & -\left\{\left[\frac{\delta_\eta r}{\Delta t\kappa_d\Pi^n\overline{\theta_v^n}^r\left(1+\sum_{X=(v,cl,cf)}\overline{m_X^*}^r\right)}\left(\kappa_d r^2\rho^n\Pi^n\overline{\theta_v^*}^r-\frac{r^2p^n}{c_{pd}}\right)\right]\Bigg|_{\eta_{N-\frac{1}{2}}}\right\}_{SP} \\
& -\left\{\left[\frac{r^2\rho^n\delta_\eta r}{\Delta t\left(1+\sum_{X=(v,cl,cf)}\overline{m_X^n}^r\right)}\left(\frac{\sum_{X=(v,cl,cf)}\overline{(m_X^*-m_X^n)}^r}{1+\sum_{X=(v,cl,cf)}\overline{m_X^*}^r}\right)\right]\Bigg|_{\eta_{N-\frac{1}{2}}}\right\}_{SP} \\
& +\left[\frac{\Delta\phi}{b}\frac{1}{L}\sum_{i=1}^{L}\left(C_{yy1}v_*\right)_{i-\frac{1}{2},1}\right]\Bigg|_{\eta_{N-\frac{1}{2}}} \\
& -\left\{\left(\frac{1}{\Delta\eta}\right)\Bigg|_{\eta_{N-\frac{1}{2}}}\left[C_5\left(\dot\eta^n\delta_\eta r+\alpha_2G^{-1}R_w^+\right)\right]\big|_{\eta_{N-1}}\right\}_{SP} \\
& +\left(\frac{1}{\Delta\eta}\right)\Bigg|_{\eta_{N-\frac{1}{2}}}\left\{\left(C_5\right)_{SP}\frac{2}{L}\sum_{i=1}^{L}\left[C_{yz}\overline{(v_*-v^n)}^{\eta}\right]_{i-\frac{1}{2},1}\right\}\Bigg|_{\eta_{N-1}} \\
& +\Bigg\{\left(\frac{r_N-r_{N-\frac{1}{2}}}{r_N-r_{N-1}}\right)\left(C_3\right)|_{\eta_{N-\frac{1}{2}}} \\
& \quad\times\left[\left(\frac{1+\frac{1}{\varepsilon}m_v^*}{1+\sum_{X=(v,cl,cf)}m_X^*}\right)\left(\alpha_2\delta_{2r}\theta_{ref}G^{-1}R_w^+\right)\right]\Bigg|_{\eta_{N-1}}\Bigg\}_{SP},
\end{aligned} \tag{14.43}
$$

and v_* is defined by (I.33).

14.11 Northern boundary condition at levels $k = 1/2$ and $k = N-1/2$

14.11.1 $k = 1/2$

The northern boundary condition for the Helmholtz problem for Π' at level $k = 1/2$ is obtained in an analogous manner to that for non-polar points but using the special discretisations for the north polar cap. Thus

$$
\begin{aligned}
& -\left[\frac{\Delta\phi}{b}\frac{1}{L}\sum_{i=1}^{L}\left(C_{yy1}Y\right)_{i-\frac{1}{2},M-1}\right]\Bigg|_{\eta_{1/2}}+\left[\left(C_3\right)|_{\eta_{1/2}}\left(C_z\delta_\eta\Pi'\right)|_{\eta_1}-\left(C_4\Pi'\right)|_{\eta_{1/2}}\right]_{NP} \\
& \quad+\left(\frac{1}{\Delta\eta}\right)\Bigg|_{\eta_{1/2}}\left[\left(C_{zz}\delta_\eta\Pi'\right)_{NP}-\left(C_5\right)_{NP}\frac{2}{L}\sum_{i=1}^{L}\left(C_{yz}\overline{Y}^{\eta}\right)_{i-\frac{1}{2},M-1}\right]\Bigg|_{\eta_1}=\left[(RHS)|_{\eta_{1/2}}\right]_{NP},
\end{aligned}
$$

(14.44)

where

$$\left[(RHS)|_{\eta_{1/2}} \right]_{NP} = -\left\{ \left[\frac{\delta_\eta r}{\Delta t \kappa_d \Pi^n \overline{\theta_v^n}^r \left(1 + \sum_{X=(v,cl,cf)} \overline{m_X^*}^r \right)} \left(\kappa_d r^2 \rho^n \Pi^n \overline{\theta_v^*}^r - \frac{r^2 p^n}{c_{pd}} \right) \right] \Bigg|_{\eta_{1/2}} \right\}_{NP}$$
$$- \left\{ \left[\frac{r^2 \rho^n \delta_\eta r}{\Delta t \left(1 + \sum_{X=(v,cl,cf)} \overline{m_X^n}^r \right)} \left(\frac{\sum_{X=(v,cl,cf)} \overline{(m_X^* - m_X^n)}^r}{1 + \sum_{X=(v,cl,cf)} \overline{m_X^*}^r} \right) \right] \Bigg|_{\eta_{1/2}} \right\}_{NP}$$
$$- \left[\frac{\Delta \phi}{b} \frac{1}{L} \sum_{i=1}^{L} \left(C_{yy1} v_* \right)_{i-\frac{1}{2}, M-1} \right] \Bigg|_{\eta_{1/2}}$$
$$+ \left\{ \left(\frac{1}{\Delta \eta} \right) \Bigg|_{\eta_{1/2}} \left[C_5 \left(\dot{\eta}^n \delta_\eta r + \alpha_2 G^{-1} R_w^+ \right) \right] \big|_{\eta_1} \right\}_{NP}$$
$$- \left(\frac{1}{\Delta \eta} \right) \Bigg|_{\eta_{1/2}} \left\{ \left[(C_5)_{NP} \frac{2}{L} \sum_{i=1}^{L} \left[C_{yz} \overline{(v_* - v^n)}^\eta \right]_{i-\frac{1}{2}, M-1} \right] \right\} \Bigg|_{\eta_1}$$
$$+ \left\{ (C_3)|_{\eta_{1/2}} \left[\left(\frac{1 + \frac{1}{\varepsilon} m_v^*}{1 + \sum_{X=(v,cl,cf)} m_X^*} \right) \left(\alpha_2 \delta_{2r} \theta_{ref} G^{-1} R_w^+ \right) \right] \Bigg|_{\eta_1} \right\}_{NP}, \quad (14.45)$$

and v_* is defined by (I.33).

14.11.2 $k = N - 1/2$

The northern boundary condition for the Helmholtz problem for Π' at level $k = N - 1/2$ is obtained in an analogous manner to that for non-polar points but using the special discretisations for the north polar cap. Thus

$$- \left[\frac{\Delta \phi}{b} \frac{1}{L} \sum_{i=1}^{L} \left(C_{yy1} Y \right)_{i-\frac{1}{2}, M-1} \right] \Bigg|_{\eta_{N-\frac{1}{2}}} + \left[\left(\frac{r_N - r_{N-\frac{1}{2}}}{r_N - r_{N-1}} \right) (C_3)|_{\eta_{N-\frac{1}{2}}} \left(C_z \delta_\eta \Pi' \right)|_{\eta_{N-1}} - \left(C_4 \Pi' \right)|_{\eta_{N-\frac{1}{2}}} \right]_{NP}$$
$$- \left(\frac{1}{\Delta \eta} \right) \Bigg|_{\eta_{N-\frac{1}{2}}} \left[\left(C_{zz} \delta_\eta \Pi' \right)_{NP} - (C_5)_{NP} \frac{2}{L} \sum_{i=1}^{L} \left(C_{yz} \overline{Y}^\eta \right)_{i-\frac{1}{2}, M-1} \right] \Bigg|_{\eta_{N-1}} = \left[(RHS)|_{\eta_{N-\frac{1}{2}}} \right]_{NP},$$

(14.46)

where

$$\left[(RHS)|_{\eta_{N-\frac{1}{2}}} \right]_{NP} = -\left\{ \left[\frac{\delta_\eta r}{\Delta t \kappa_d \Pi^n \overline{\theta_v^n}^r \left(1 + \sum_{X=(v,cl,cf)} \overline{m_X^*}^r \right)} \left(\kappa_d r^2 \rho^n \Pi^n \overline{\theta_v^*}^r - \frac{r^2 p^n}{c_{pd}} \right) \right] \Bigg|_{\eta_{N-\frac{1}{2}}} \right\}_{NP}$$

$$
\begin{aligned}
&- \left\{ \left[\frac{r^2 \rho^n \delta_\eta r}{\Delta t \left(1 + \sum_{X=(v,cl,cf)} \overline{m_X^n}^r\right)} \left(\frac{\sum_{X=(v,cl,cf)} \overline{(m_X^* - m_X^n)}^r}{1 + \sum_{X=(v,cl,cf)} \overline{m_X^*}^r} \right) \right] \Bigg|_{\eta_{N-\frac{1}{2}}} \right\}_{NP} \\
&- \left[\frac{\Delta\phi}{b} \frac{1}{L} \sum_{i=1}^{L} \left(C_{yy1} v_*\right)_{i-\frac{1}{2},M-1} \right] \Bigg|_{\eta_{N-\frac{1}{2}}} \\
&- \left\{ \left(\frac{1}{\Delta\eta} \right) \Bigg|_{\eta_{N-\frac{1}{2}}} \left[C_5 \left(\dot{\eta}^n \delta_\eta r + \alpha_2 G^{-1} R_w^+ \right) \right] \big|_{\eta_{N-1}} \right\}_{NP} \\
&+ \left(\frac{1}{\Delta\eta} \right) \Bigg|_{\eta_{N-\frac{1}{2}}} \left\{ \left[\left(C_5\right)_{NP} \frac{2}{L} \sum_{i=1}^{L} \left[C_{yz} \overline{(v_* - v^n)}^\eta \right]_{i-\frac{1}{2},M-1} \right] \right\} \Bigg|_{\eta_{N-1}} \\
&+ \left\{ \left(\frac{r_N - r_{N-\frac{1}{2}}}{r_N - r_{N-1}} \right) \left(C_3\right)\big|_{\eta_{N-\frac{1}{2}}} \right. \\
&\quad \left. \times \left[\left(\frac{1 + \frac{1}{\varepsilon} m_v^*}{1 + \sum_{X=(v,cl,cf)} m_X^*} \right) \left(\alpha_2 \delta_{2r} \theta_{ref} G^{-1} R_w^+ \right) \right] \Bigg|_{\eta_{N-1}} \right\}_{NP},
\end{aligned}
\qquad (14.47)
$$

and v_* is defined by (I.33).

15 Solution of the discrete Helmholtz problem

This section describes the application of a preconditioned generalised conjugate residual method for the solution of the elliptic Helmholtz problem arising from the discretisation of the governing equations in the New Dynamics (Section 14). The necessary mathematical background and algorithmic details of iterative solvers are given in Appendix J.

15.1 The Helmholtz operator

The elliptic operator H resulting from the discretisation of the model's equations is of a Helmholtz type (see details in Section 14) and can be written as:

$$\begin{aligned} H(\cdot) &= \frac{\Delta\lambda}{\cos\phi}\delta_\lambda\left(C_{xx1}X\right) + \frac{\Delta\phi}{\cos\phi}\delta_\phi\left(C_{yy1}Y\right) \\ &+ \delta_\eta\left[C_{zz}\delta_\eta(\cdot) - C_5\left(\overline{C_{xz}\overline{X}^{\eta}}^{\lambda} + \overline{C_{yz}\overline{Y}^{\eta}}^{\phi}\right)\right] \\ &+ C_3\overline{C_z\delta_\eta(\cdot)}^{r} - C_4(\cdot), \end{aligned} \tag{15.1}$$

where

$$X = C_{xx2}\left(\Delta\lambda\delta_\lambda(\cdot) - C_{xp}\overline{C_2\delta_r(\cdot)}^{r\lambda}\right) + C_{xy1}\overline{C_{xy2}\left(\Delta\phi\delta_\phi(\cdot) - C_{yp}\overline{C_2\delta_r(\cdot)}^{r\phi}\right)}^{\lambda\phi}, \tag{15.2}$$

$$Y = C_{yy2}\left(\Delta\phi\delta_\phi(\cdot) - C_{yp}\overline{C_2\delta_r(\cdot)}^{r\phi}\right) - C_{yx1}\overline{C_{yx2}\left(\Delta\lambda\delta_\lambda(\cdot) - C_{xp}\overline{C_2\delta_r(\cdot)}^{r\lambda}\right)}^{\lambda\phi}, \tag{15.3}$$

$(\lambda, \phi, (r, \eta))$ is the coordinate system, and the C's are spatially-dependent coefficients. Due to the singularity of the term $(1/\cos\phi)$ at the poles, the GCR(k) solves a modified system $\cos\phi H(x) = b\cos\phi$, i.e. it uses a modified operator $A \equiv L(\cdot) = \cos\phi H(\cdot)$.

15.2 Ellipticity and definiteness of the Helmholtz operator

The *ellipticity* of the operator H is important for the *existence* of the solution of the second-order boundary-value problem, i.e. the non-singularity of the system, $Hx = b$, subject to typical Dirichlet, Neumann or mixed type boundary conditions, according to the maximum principle (see chapters 7, 8 and 9 of Garabedian (1964) for details). The class of any operator is usually determined by examining the coefficients related to the higher degree terms. For a second-order operator such as (15.1), the coefficients associated with $\delta_{\lambda\lambda}$, $\delta_{\lambda\phi}$, $\delta_{\lambda\eta}$, $\delta_{\phi\lambda}$, $\delta_{\phi\phi}$, $\delta_{\phi\eta}$, $\delta_{\eta\lambda}$, $\delta_{\eta\phi}$ and $\delta_{\eta\eta}$ determine the elliptic, hyperbolic or parabolic nature of the operator

(15.1) - see e.g. Garabedian (1964), page 73. If the operator (15.1) is written in the following form:

$$\begin{aligned}
H &= C_{\lambda\lambda}\delta_{\lambda\lambda} + C_{\lambda\phi}\delta_{\lambda\phi} + C_{\lambda\eta}\delta_{\lambda\eta} \\
&+ C_{\phi\lambda}\delta_{\phi\lambda} + C_{\phi\phi}\delta_{\phi\phi} + C_{\phi\eta}\delta_{\phi\eta} \\
&+ C_{\eta\lambda}\delta_{\eta\lambda} + C_{\eta\phi}\delta_{\eta\phi} + C_{\eta\eta}\delta_{\eta\eta} + \text{lower order terms,}
\end{aligned} \tag{15.4}$$

where the C's are the associated second-order coefficients, then the operator (15.4) is *elliptic* when the following matrix,

$$\hbar = \begin{bmatrix} C_{\lambda\lambda} & C_{\lambda\phi} & C_{\lambda\eta} \\ C_{\phi\lambda} & C_{\phi\phi} & C_{\phi\eta} \\ C_{\eta\lambda} & C_{\eta\phi} & C_{\eta\eta} \end{bmatrix}, \tag{15.5}$$

is either *positive* or *negative definite*. [If $C_{\lambda\lambda} > 0$, then the operator H is elliptic provided the matrix $\hbar$ is positive definite and, conversely, if $C_{\lambda\lambda} < 0$, then $\hbar$ should be negative definite. See e.g. Garabedian (1964), page 73.] Since the operator δ_{xy} is commutative, i.e. $\delta_{xy} = \delta_{yx}$, the matrix (15.5) can be equivalently replaced by the following symmetrised form:

$$\hbar_{symmetrised} = \begin{bmatrix} C_{\lambda\lambda} & \frac{1}{2}\left(C_{\lambda\phi} + C_{\phi\lambda}\right) & \frac{1}{2}\left(C_{\lambda\eta} + C_{\eta\lambda}\right) \\ \frac{1}{2}\left(C_{\phi\lambda} + C_{\lambda\phi}\right) & C_{\phi\phi} & \frac{1}{2}\left(C_{\phi\eta} + C_{\eta\phi}\right) \\ \frac{1}{2}\left(C_{\eta\lambda} + C_{\lambda\eta}\right) & \frac{1}{2}\left(C_{\eta\phi} + C_{\phi\eta}\right) & C_{\eta\eta} \end{bmatrix}. \tag{15.6}$$

Assume that the coefficients, C, are continuous and differentiable over the staggered grid (i.e. omit the averaging operations in (15.1), (15.2) and (15.3)). Using the definitions of the Helmholtz coefficients (see Appendix I for details), the operator (15.1) can then be locally put into the form (15.4) with the following, considered locally-constant, coefficients:

$$C_{\lambda\lambda} = \frac{(\Delta\lambda)^2}{\cos\phi} C_{xx1} C_{xx2}, \tag{15.7}$$

$$C_{\lambda\phi} = \frac{\Delta\lambda\Delta\phi}{\cos\phi} C_{xx1} C_{xy1} C_{xy2}, \tag{15.8}$$

$$C_{\lambda\eta} = -\frac{\Delta\lambda}{\cos\phi} C_{xx1}\left(C_{xx2}C_{xp} + C_{xy1}C_{xy2}C_{yp}\right) C_2 \delta_r \eta, \tag{15.9}$$

$$C_{\phi\lambda} = -\frac{\Delta\lambda\Delta\phi}{\cos\phi} C_{yy1} C_{yx1} C_{yx2}, \tag{15.10}$$

$$C_{\phi\phi} = \frac{(\Delta\phi)^2}{\cos\phi} C_{yy1} C_{yy2}, \tag{15.11}$$

$$C_{\phi\eta} = -\frac{\Delta\phi}{\cos\phi} C_{yy1}\left(C_{yy2}C_{yp} - C_{yx1}C_{yx2}C_{xp}\right) C_2 \delta_r \eta, \tag{15.12}$$

$$C_{\eta\lambda} = -\Delta\lambda C_5 \left(C_{xz}C_{xx2} - C_{yz}C_{yx1}C_{yx2}\right), \tag{15.13}$$

$$C_{\eta\phi} = -\Delta\phi C_5 \left(C_{yz}C_{yy2} + C_{xz}C_{xy1}C_{xy2}\right), \tag{15.14}$$

$$C_{\eta\eta} = C_{zz} + \left[C_{xz}\left(C_{xx2}C_{xp} + C_{xy1}C_{xy2}C_{yp}\right) + C_{yz}\left(C_{yy2}C_{yp} - C_{yx1}C_{yx2}C_{xp}\right)\right] C_2C_5\delta_r\eta. \tag{15.15}$$

These may be explicitly written as:

$$C_{\lambda\lambda} = \frac{\omega A_u}{\cos^2\phi}, \tag{15.16}$$

$$C_{\lambda\phi} = \frac{\omega F_u}{\cos\phi}, \tag{15.17}$$

$$C_{\lambda\eta} = -\frac{\omega}{\delta_\eta r\cos\phi}\left(\frac{A_u\delta_\lambda r}{\cos\phi} + F_u\delta_\phi r\right), \tag{15.18}$$

$$C_{\phi\lambda} = -\frac{\omega F_v}{\cos\phi}, \tag{15.19}$$

$$C_{\phi\phi} = \omega A_v, \tag{15.20}$$

$$C_{\phi\eta} = -\frac{\omega}{\delta_\eta r}\left(A_v\delta_\phi r - \frac{F_v\delta_\lambda r}{\cos\phi}\right), \tag{15.21}$$

$$C_{\eta\lambda} = -\frac{\omega}{\delta_\eta r\cos\phi}\left(\frac{A_u\delta_\lambda r}{\cos\phi} - F_v\delta_\phi r\right), \tag{15.22}$$

$$C_{\eta\phi} = -\frac{\omega}{\delta_\eta r}\left(A_v\delta_\phi r + \frac{F_u\delta_\lambda r}{\cos\phi}\right), \tag{15.23}$$

$$\begin{aligned} C_{\eta\eta} &= C_{zz} + C_{\lambda\lambda}\left(\frac{\delta_\lambda r}{\delta_\eta r}\right)^2 + C_{\phi\phi}\left(\frac{\delta_\phi r}{\delta_\eta r}\right)^2, \\ &= \frac{\alpha_2 K r^2\rho_y^n}{\delta_\eta r} + C_{\lambda\lambda}\left(\frac{\delta_\lambda r}{\delta_\eta r}\right)^2 + C_{\phi\phi}\left(\frac{\delta_\phi r}{\delta_\eta r}\right)^2, \end{aligned} \tag{15.24}$$

where

$$\omega = \alpha_1\alpha_3\Delta t c_{pd}\rho_y^n\theta_v^*\delta_\eta r, \tag{15.25}$$

$$0 < A_u = A_v = \frac{1}{1+\alpha_3^2\Delta t^2 f_3^2} = A \leq 1, \tag{15.26}$$

$$F_u = \alpha_3\Delta t f_3 A_u = \alpha_3\Delta t f_3 A,\ F_v = \alpha_3\Delta t f_3 A_v = \alpha_3\Delta t f_3 A, \tag{15.27}$$

$$K = \frac{\alpha_4\Delta t c_p\theta_v^*}{\mathbf{I}_h - c_{pd}\alpha_2\alpha_4\Delta t^2\left[\left(1+m_v^*/\varepsilon\right)/\left(1+m_v^*+m_{cl}^*+m_{cf}^*\right)\right]\delta_{2r}\theta_{ref}\delta_r\Pi^n}. \tag{15.28}$$

Insertion into form (15.6) then gives the simplified symmetric form

$$\hbar_{symmetrised} = \begin{bmatrix} C_{\lambda\lambda} & 0 & -C_{\lambda\lambda}\left(\delta_\lambda r/\delta_\eta r\right) \\ 0 & C_{\phi\phi} & -C_{\phi\phi}\left(\delta_\phi r/\delta_\eta r\right) \\ -C_{\lambda\lambda}\left(\delta_\lambda r/\delta_\eta r\right) & -C_{\phi\phi}\left(\delta_\phi r/\delta_\eta r\right) & C_{\eta\eta} \end{bmatrix}. \tag{15.29}$$

Recall that the Helmholtz operator H is *elliptic* if the matrix $\hbar$, given by (15.6), is either *positive* or *negative definite*. [If $C_{\lambda\lambda} > 0$, then $\hbar$ should be positive definite and, if $C_{\lambda\lambda} < 0$, then $\hbar$ should be negative definite.] A necessary and sufficient condition for a matrix to be positive definite (e.g. Strang (1980), p. 250) is that all the upper left submatrices have positive determinants. Thus, with the above assumption that the Helmholtz coefficients are continuous over the staggered grid (i.e. the averaging operators are omitted) then, using (15.29), the Helmholtz operator is *elliptic* when all three of the following determinants D_1, D_2 and D_3 are positive definite:

$$D_1 = C_{\lambda\lambda} = \frac{\omega A}{\cos^2\phi}, \tag{15.30}$$

$$D_2 = \begin{vmatrix} C_{\lambda\lambda} & 0 \\ 0 & C_{\phi\phi} \end{vmatrix} = C_{\lambda\lambda}C_{\phi\phi} = \left(\frac{\omega A}{\cos\phi}\right)^2, \tag{15.31}$$

$$\begin{aligned} D_3 &= \begin{vmatrix} C_{\lambda\lambda} & 0 & -C_{\lambda\lambda}\left(\delta_\lambda r/\delta_\eta r\right) \\ 0 & C_{\phi\phi} & -C_{\phi\phi}\left(\delta_\phi r/\delta_\eta r\right) \\ -C_{\lambda\lambda}\left(\delta_\lambda r/\delta_\eta r\right) & -C_{\phi\phi}\left(\delta_\phi r/\delta_\eta r\right) & C_{\eta\eta} \end{vmatrix} \\ &= C_{\lambda\lambda}C_{\phi\phi}\left\{C_{\eta\eta} - \left[C_{\lambda\lambda}\left(\frac{\delta_\lambda r}{\delta_\eta r}\right)^2 + C_{\phi\phi}\left(\frac{\delta_\phi r}{\delta_\eta r}\right)^2\right]\right\} \\ &= C_{\lambda\lambda}C_{\phi\phi}C_{zz} = C_{\lambda\lambda}C_{\phi\phi}\frac{\alpha_2 K r^2 \rho_y^n}{\delta_\eta r}, \end{aligned} \tag{15.32}$$

where (15.16), (15.20) and (15.24) have been used.

D_1 and D_2 are both positive definite since, from (15.25) and (15.26), $\omega \equiv \alpha_1\alpha_3\Delta t c_{pd}\rho_y^n\theta_v^*\delta_\eta r > 0$ and $A \equiv 1/\left(1+\alpha_3^2 f_3^2\Delta t^2\right) > 0$. [It is assumed here that $\rho_y^n > 0$, although this may not be numerically guaranteed when the model top is very high and ρ_y^n is correspondingly small.] The remaining condition, i.e. $D_3 > 0$, simply requires $C_{zz} > 0$. This means that *the ellipticity of the Helmholtz operator* (15.1) *is essentially controlled by the sign of the coefficient* C_{zz}*, i.e. by* $sign(C_{zz})$*. Moreover,* $sign(C_{zz}) = sign(K) = sign(G)$ *where* G *is ensured to be positive* $(G > 0)$ *by the imposed algorithmic condition* $G \geq G_{tol} > 0$ (see Sections 7 and 9). Imposing a lower limit on G is equivalent to imposing a restriction on the maximum magnitude of static instability allowed in the model for a given time step. *Note that the ellipticity of the Helmholtz operator at the poles only requires* $C_{zz} > 0$ *since terms associated with* λ *and* ϕ *which are second order in the interior, reduce to lower-order ones at the poles.*

Since under the above simplifying assumptions the operator H has been shown to be elliptic (provided $G \geq G_{tol} > 0$), it is either negative definite or positive definite. It is easy to verify that H is *not positive definite*. Since $C_{\lambda\lambda}$, $C_{\phi\phi}$, $C_{\eta\eta}$ and C_4 are positive, this and the properties of the difference operators occurring in (15.1) imply that the diagonal of H is negative, i.e. $diag(H) < 0$ ($diag(H)$ refers to the vector containing the diagonal elements of H). Thus $(Hy)^T y < 0$ for the choice $y = (1, 0, ..., 0)^T$. Hence, the Helmholtz operator (15.1) cannot be positive definite, and so H is therefore negative definite and $-H$ is positive definite. Note, though, that the definiteness of the operator H under the assumed continuity conditions does not guarantee the definiteness of the associated matrix after discretisation of the operator on a given grid, especially on a non-smooth one (Golub, Silvester & Wathen 1996), and therefore the above argument, albeit highly suggestive, is not rigorously true.

Under various hypotheses about the smoothness of the boundary and the behaviour of the coefficients, C, it is possible (Garabedian (1964), Chapter 7) to use the maximum principle to establish the *uniqueness* of a non-trivial solution of any special case of the general *elliptic boundary-value problem* $H(u) = C_{\lambda\lambda}\delta_{\lambda\lambda}u + ... + C_{\lambda}\delta_{\lambda}u + ... - C_4 u = 0$ with a *positive definite* $\hbar$ given by (15.5), subject to the usual Dirichlet, Neumann or mixed type boundary conditions, provided that $C_4 \geq 0$. For the present Helmholtz problem, C_4 is given by (see Appendix I):

$$C_4 = \frac{\delta_\eta r}{\kappa_d \Delta t \Pi^n \overline{\theta_v^n}^r \left(1 + \sum_{X=(v,cl,cf)} \overline{m_X^*}^r\right)} \left(\frac{r^2 p^n}{R_d \Pi^n} - \kappa_d r^2 \rho^n \overline{\theta_v^n}^r\right). \tag{15.33}$$

Therefore C_4 is certainly positive for $\rho^n > 0$ if the thermodynamic variables are balanced (i.e. they exactly satisfy the gas law) since, after discretisation of (11.5), (15.33) then reduces to

$$C_4 = \frac{r^2 \rho^n \delta_\eta r}{\kappa_d \Delta t \Pi^n \left(1 + \sum_{X=(v,cl,cf)} \overline{m_X^*}^r\right)} (1 - \kappa_d). \tag{15.34}$$

The expression (15.33) can however, in principle, become negative (though only for an extremely unbalanced situation).

The condition $C_4 \geq 0$ is also a good property for the definiteness of the operator H. This can be seen from the fact that if $H(u)$ is written in the form $H(u) = H_1(u) - C_4 u$, where H_1 is negative definite (i.e. $\langle u, H_1(u)\rangle < -\sigma \|u\|_2$, $\sigma > 0$), then:

$$\langle u, H(u)\rangle = \langle u, H_1(u)\rangle - C_4 \|u\|_2 < -(\sigma + C_4)\|u\|_2 < 0, \tag{15.35}$$

from which it can be seen that no further constraint for the negative definiteness of H (i.e. $\langle u, H(u)\rangle < 0$) is required.

15.3 Preconditioning

The preconditioning stage seeks to solve the following system:

$$Mq = R, \tag{15.36}$$

where M is the preconditioning matrix or operator. The system (15.36) is solved using an ADI scheme (described in Appendix J), i.e. by solving the following system, equivalent to (J.44) of Appendix J with $\xi = 1$, viz:

$$\begin{aligned}
\left[(\psi\delta\tau)_l^{-1} I + M_x\right] s_l^x &= b_l^x \ \left(b_l^x = R - Mq_l, \ \ s_l^x = q_{l+1/3} - q_l \ , \ q_0 = 0\right), \\
\left[(\psi\delta\tau)_l^{-1} I + M_y\right] s_l^y &= b_l^y \ \left(b_l^y = R - Mq_l - M_x s_l^x, \ \ s_l^y = q_{l+2/3} - q_l\right), \\
\left[(\psi\delta\tau)_l^{-1} I + M_z\right] s_l^z &= b_l^z \ \left(b_l^z = R - Mq_l - M_x s_l^x - M_y s_l^y, \ s_l^z = q_{l+1} - q_l\right),
\end{aligned} \tag{15.37}$$

where l is an iteration index.

<u>**Aside :**</u>

It would be better (see comments in Appendix J around (J.44)*) to set* $\xi = 1/2$ *instead of* $\xi = 1$.

The preconditioning matrix M should be as close as possible to $L = \cos\phi H$. For an elliptic operator, in principle the preconditioning matrix or operator M could range from a Laplacian ∇^2 to the complete $M = L$ operator. The algorithm used in the New Dynamics has the following two options

$$M = L, \tag{15.38}$$

or

$$\begin{aligned}
M &= \Delta\lambda\delta_\lambda\left[C_{xx1}C_{xx2}\Delta\lambda\delta_\lambda\left(\cdot\right)\right] + \Delta\phi\delta_\phi\left[C_{yy1}C_{yy2}\Delta\phi\delta_\phi\left(\cdot\right)\right] \\
&+ \cos\phi\left\{\delta_\eta\left[C_{zz}\delta_\eta\left(\cdot\right)\right] + C_3\overline{C_z\delta_\eta\left(\cdot\right)}^r - C_4\left(\cdot\right)\right\}.
\end{aligned} \tag{15.39}$$

It is emphasised that the choice of $M = L$ does not necessarily mean $M^{-1} = L^{-1}$ unless the ADI scheme (15.37) is iterated until convergence, which makes the use of GCR redundant. At each iteration of the GCR, the ADI scheme provides a cheap M^{-1}, which resembles L^{-1} using only a few ADI iterations. This reduces the magnitude of the condition number $\kappa\left(M^{-1}L\right)$, hence improving the convergence rate of the GCR. It is also worth mentioning that although M could be, in principle, any elliptic operator, including $M = L$, the rate of convergence of

M^{-1} to L^{-1} is mainly dominated by the implicit terms M_x, M_y and M_z in the ADI scheme (15.37). These terms form only a part of M when $M = L$, i.e. $(|M_x| + |M_y| + |M_z|) < |M|$.

Due to the fact that M^{-1} is only a cheap approximation to L^{-1}, the splitting of M neglects mixed derivatives when the full L operator is used. This results in three TriDiagonal (TD) matrices, M_x, M_y and M_z, and the system (15.37) is simply three TD systems, which can be solved using an efficient fast TD solver, and this is the main attraction of using the ADI in the first place. The M-directional operators are given by:

$$\begin{aligned} M_x \equiv L_\lambda(\cdot) &\cong \Delta\lambda\delta_\lambda\left[C_{xx1}C_{xx2}\Delta\lambda\delta_\lambda(\cdot)\right] - C_4(\cdot), && (15.40)\\ M_y \equiv L_\phi(\cdot) &\cong \Delta\phi\delta_\phi\left[C_{yy1}C_{yy2}\Delta\phi\delta_\phi(\cdot)\right] - C_4(\cdot), && (15.41)\\ M_z \equiv L_\eta(\cdot) &\cong \cos\phi\left\{\delta_\eta\left[C_{zz}\delta_\eta(\cdot)\right] + C_3\overline{C_z\delta_\eta(\cdot)}^r - C_4(\cdot)\right\}. && (15.42)\end{aligned}$$

When M is split into the three TD matrices (15.40)-(15.42), i.e. $M = M_x + M_y + M_z$, this option will be referred to as *3D-ADI preconditioner* (3DADIP). Furthermore, a simpler splitting, which will be referred to as the *Block Vertical ADI Preconditioner* (BVADIP), is provided which can be used on its own or in combination with the 3DADIP (for instance one iteration of the system (15.37) with BVADIP followed by one iteration with 3DADIP). The BVADIP is simply $M = \widehat{M_x} + \widehat{M_y} + \widehat{M_z}$, where $\widehat{M_x}$, $\widehat{M_y}$ and $\widehat{M_z}$ are given by:

$$\begin{aligned} \widehat{M_x} &= diag\left(M_x + C_4\right), && (15.43)\\ \widehat{M_y} &= diag\left(M_y + C_4\right), && (15.44)\\ \widehat{M_z} &= M_z, && (15.45)\end{aligned}$$

where $diag\,(A)$ refers to the vector containing the diagonal elements of A. In other words, instead of three TD systems, BVADIP option solves only one TD system given by:

$$(\widehat{M_x} + \widehat{M_y} + \widehat{M_z})q = \widetilde{M}q = R, \qquad (15.46)$$

where $\widetilde{M}$ is given by:

$$\widetilde{M} = \delta_\eta\left[C_{zz}\delta_\eta(\cdot)\right] + C_3\overline{C_z\delta_\eta(\cdot)}^r - \left[2\overline{C_{xx1}C_{xx2}}^\lambda + 2\overline{C_{yy1}C_{yy2}}^\phi + C_4\right](\cdot). \qquad (15.47)$$

Note also that in the GCR(k) used in the New Dynamics, a special case of the general system (15.37), namely the 2D $x - z$ preconditioner (XZADIP), is available. It consists of the system (15.37) with $s_l^y = 0$.

To permit an efficient solution of the TD systems (15.37), especially for multiple right-hand sides as is the case for the iterative process in (15.37), the three TD matrices M_x, M_y and M_z are factorised using an LU-decomposition ($M_{x,y,z} = L_{x,y,z}U_{x,y,z}$, where here L and U are respectively lower and upper triangular matrices). Dropping the subscripts (x, y, z) for neatness, any TD M is decomposed as

$$M_{n\times n} = \begin{bmatrix} \ddots & \ddots & 0 \\ a2_j & a0_j & a1_j \\ 0 & \ddots & \ddots \end{bmatrix} = \begin{bmatrix} \ddots & & 0 \\ f_j & 1 & \\ 0 & \ddots & \ddots \end{bmatrix} \begin{bmatrix} \ddots & \ddots & 0 \\ & d_j^{-1} & a1_j \\ 0 & & \ddots \end{bmatrix}, \tag{15.48}$$

where

$$d_j = \left(a0_j - a2_j d_{j-1} a1_{j-1}\right)^{-1}, \quad j = 1, n \quad (d_0 = 0)\,, \tag{15.49}$$

$$f_j = d_{j-1} a2_j, \quad j = 1, n. \tag{15.50}$$

Then, the solution for any TD system $Mx = b$ is carried out in the following two efficient forward and backward steps:

$$Ly = b \quad (\text{i.e. } y_0 = 0,\ y_j = b_j - f_j y_{j-1},\ j = 1, n)\,, \tag{15.51}$$

$$Ux = y \quad (\text{i.e. } y_{N+1} = 0,\ x_j = d_j\left(y_j - a1_j y_{j+1}\right),\ j = n, 1)\,. \tag{15.52}$$

15.4 Boundary conditions and treatment of the poles

The Helmholtz problem (15.1) is subject to the usual periodic boundary conditions in λ. The top and bottom boundary conditions

$$\dot{\eta}|_{\eta=0} = \dot{\eta}|_{\eta=1} = 0, \tag{15.53}$$

have been incorporated into the definition of H via the discretisation of the individual governing equations.

Due to the singularity of the poles, the Helmholtz operator $H_{SP,NP}$ at the poles has been derived by integrating the governing equations over the South polar cap, $\phi_{1/2} = -\pi/2 \leq \phi \leq \phi_1 = \phi_{1/2} + \Delta\phi,\ 0 \leq \lambda \leq 2\pi$, and the North polar cap, $\phi_{M-1} \leq \phi \leq \phi_{M-1/2} = \pi/2,\ 0 \leq \lambda \leq 2\pi$, where $j = 1/2$ and $j = M - 1/2$ denote the ϕ-index corresponding to the South and North poles, respectively. (Note that for consistency with previous sections the use of L and M as the upper limits for the indices i and j has been retained and these should not be confused with the elliptical and preconditioning matrices of the same name). This results in (see details in Sections 14.8 and 14.9):

$$\begin{aligned} H\left(\cdot\right)_{SP} &= \left(\frac{8}{\Delta\phi}\right)\frac{1}{L}\sum_{i=1}^{L}\left(C_{yy1}Y\right)_{i-1/2,1} + \left(C_3\overline{C_z\delta_\eta\left(\cdot\right)}^r - C_4\left(\cdot\right)\right)_{SP} \\ &\quad + \delta_\eta\left[\left(C_{zz}\delta_\eta\left(\cdot\right)\right)_{SP} - \left(C_5\right)_{SP}\frac{2}{L}\sum_{i=1}^{L}\left(C_{yz}\overline{Y}^\eta\right)_{i-1/2,1}\right], \end{aligned} \tag{15.54}$$

$$\begin{aligned} H\left(\cdot\right)_{NP} &= -\left(\frac{8}{\Delta\phi}\right)\frac{1}{L}\sum_{i=1}^{L}\left(C_{yy1}Y\right)_{i-1/2,M-1} + \left(C_3\overline{C_z\delta_\eta\left(\cdot\right)}^r - C_4\left(\cdot\right)\right)_{NP} \\ &\quad + \delta_\eta\left[\left(C_{zz}\delta_\eta\left(\cdot\right)\right)_{NP} - \left(C_5\right)_{NP}\frac{2}{L}\sum_{i=1}^{L}\left(C_{yz}\overline{Y}^\eta\right)_{i-1/2,M-1}\right], \end{aligned} \tag{15.55}$$

where $i = 1, 2, ..., L$ is the λ-index counter.

The GCR(k) solves the modified system with a modified operator $L = H\cos\phi$ where $\cos\phi$ at the poles is replaced in the New Dynamics by $\Delta\phi/8$ (see following aside). Hence, the modified operators $L\left(\cdot\right)_{NP,SP}$ at the poles are given by:

$$L\left(\cdot\right)_{SP} = \left(\Delta\phi/8\right)H\left(\cdot\right)_{SP}, \tag{15.56}$$

$$L\left(\cdot\right)_{NP} = \left(\Delta\phi/8\right)H\left(\cdot\right)_{NP}. \tag{15.57}$$

Aside :

It is not obvious, at first sight, why the polar equations are scaled with respect to $\Delta\phi/8$. However this choice is consistent with defining the individual area elements within the polar cap in the same discrete (rectangular) manner as elsewhere in the domain, viz. as $\Delta\lambda\Delta\phi\cos\phi$. Note though that the individual polar elements degenerate from rectangles to triangles. An alternative would therefore be to instead define thediscretearea to be $(\Delta\lambda\Delta\phi/2)\cos\phi$, and then the corresponding polar $\cos\phi$ would be $\Delta\phi/4$.

Special forms of $\widetilde{M}$ (i.e. BVADIP, see (15.47)) for the poles, $\widetilde{M}_{SP,NP}$, are given by:

$$\widetilde{M}_{SP} = \delta_\eta\left[C_{zz}\delta_\eta\left(\cdot\right)\right] + C_3\overline{C_z\delta_\eta\left(\cdot\right)}^r - C_4\left(\cdot\right) - \frac{8}{\Delta\phi L}\sum_{i=1}^{L}\left(C_{yy1}C_{yy2}\right)_{i-1/2,1}\left(\cdot\right) \tag{15.58}$$

$$\widetilde{M}_{NP} = \delta_\eta \left[C_{zz}\delta_\eta\left(\cdot\right)\right] + C_3\overline{C_z\delta_\eta\left(\cdot\right)}^r - C_4\left(\cdot\right) - \frac{8}{\Delta\phi L}\sum_{i=1}^{L}\left(C_{yy1}C_{yy2}\right)_{i-1/2,M-1}\left(\cdot\right) \tag{15.59}$$

Also special forms of M_x, M_y and M_z (see (15.40)-(15.42)) for the poles are given by:

$$\begin{aligned}
\left(M_x\right)_{SP} &= 0, && (15.60)\\
\left(M_x\right)_{NP} &= 0, && (15.61)\\
\left(M_y\right)_{SP} &= +\frac{8}{\Delta\phi}\frac{1}{L}\sum_{i=1}^{L}\left(C_{yy1}C_{yy2}\Delta\phi\delta_\phi\left(\cdot\right)\right)_{i-1/2,1} - C_4\left(\cdot\right)_{SP}, && (15.62)\\
\left(M_y\right)_{NP} &= -\frac{8}{\Delta\phi}\frac{1}{L}\sum_{i=1}^{L}\left(C_{yy1}C_{yy2}\Delta\phi\delta_\phi(\cdot)\right)_{i-1/2,M-1} - C_4\left(\cdot\right)_{NP}, && (15.63)\\
\left(M_z\right)_{SP} &= \delta_\eta\left[\left(C_{zz}\delta_\eta\left(\cdot\right)\right)_{SP}\right] + \left(C_3\overline{C_z\delta_\eta\left(\cdot\right)}^r - C_4\left(\cdot\right)\right)_{SP}, && (15.64)\\
\left(M_z\right)_{NP} &= \delta_\eta\left[\left(C_{zz}\delta_\eta\left(\cdot\right)\right)_{NP}\right] + \left(C_3\overline{C_z\delta_\eta\left(\cdot\right)}^r - C_4\left(\cdot\right)\right)_{NP}. && (15.65)
\end{aligned}$$

Note that the decomposition (15.60)-(15.65) means that at the poles, the preconditioner M is always a 2D $y-z$ preconditioner (YZADIP).

15.5 Details of GCR(k) used in the New Dynamics

In this section, details of the GCR(k) algorithm used in the New Dynamics are given. Note that there are a few minor sign differences between the following algorithm and those presented in Appendix J, which are highlighted wherever they occur. The reason is that the original code was written for a negative definite instead of a positive definite operator. Although this can be changed to a standard algorithm, it is not worth the effort. Highlighting these differences will suffice in removing any confusion.

Aside :

One general comment about the structure of the code is that it is not very flexible. The reason is that all the modules are problem-dependent. In other words, parameters such as solver options, domain geometry, averaging, and other high level parameters are carried out deep down throughout all modules. This makes testing and implementing changes more laborious than it should be. Simplicity and clarity can sometimes take second priority to optimisation efficiency and parallelisation for operational codes. However, for research and development purposes, *features such as clarity and ease of modification should at least be given a higher priority, even at the expense of computational efficiency.*

Typical options and parameter values for the GCR(k) algorithm used in the New Dynamics, which is detailed in "GCR(k) Algorithm" below, are:

- **Stopping Criteria:** This is usually based on $\|R\| \leq \epsilon \|R_0\|$ (line 14 of "GCR(k) Algorithm"), where ϵ is of the order of $\epsilon = 10^{-7}$. It is worth mentioning that using this stopping criteria, the final $\|R\|$ is dependent on $\|R_0\|$ and, therefore, producing a consistent $\|R\|$ at every time-step requires consistently using a $\|R_0\|$ of a given order. Consequently, the same precision $\|R\|$ can be achieved with a smaller ϵ given an initial guess with a smaller $\|R_0\|$. When the alternative criterion $|R_s| \equiv \|R_s\|_\infty = \max|(R_s)_i| \leq R_m$ is used, a typical value is $R_m = 10^{-5}$ (here the norm of the residual is independent of the initial guess). $|R_s|$ is the l_∞-norm of a non-dimensional scaled residual (see below) and R_m is a small non-dimensional constant. In principle the GCR(k) can be iterated until convergence to machine precision. However, this is not necessary from an application point of view, as the solution of the Helmholtz problem is only a sub-part of the overall physical solution. Hence, a precision of the Helmholtz problem that has little effect on the overall solution is usually not required. Therefore, the stopping criteria can be at a point beyond which any further reduction in the norms $\|R\|$ or $|R|$ will result in a negligible effect on the flow. The discretised continuity equation can be rewritten as $[r^2\rho/(\Delta t\delta_r\eta)](\rho'/\rho) = \Phi$ where Φ is a pseudo-divergence (see details in Section 8). Neglecting the horizontal components of Φ, it can be shown that a change of the residual $\delta R = L(\delta\Pi')$ will result in a change of $\delta\Phi$ of the same order, i.e. $\delta\Phi = O(\delta R)$ and consequently $\delta\Phi \simeq \delta R \simeq [r^2\rho/(\Delta t\delta_r\eta)]\,\delta(\rho'/\rho)$. Therefore, if a scaled residual $|R_s = R \times c|$, is defined, where $c = [\Delta t\delta_r\eta/(r^2\rho)]$, then the relative density change, $\delta(\rho'/\rho)$, will be of a similar order to that achieved for the scaled residual δR_s in the Helmholtz solution, i.e. an $|R_s| \leq 0.01$ will result in no more than a 1% change in the density or the pseudo-divergence. The scaled $|R_s|$ can be more useful in interpreting the effect of the Helmholtz precision on the physical flow than the unscaled l_2-norm $\|R\|$.

- **GCR(k) Options:**

- A typical k for the GCR(k) is $k = 1$.
- The maximum number of iterations allowed $i_{max} = 50$. i_{max} is a limit imposed beyond which the GCR(k) is deemed not converged and the results of the last iteration is taken as a reasonable solution of the Helmholtz problem for that particular time step.
- The initial guess to the solution is usually $x_0 = 0$ (line 3 of "GCR(k) Algorithm"). As mentioned previously, the choice $x_0 = 0$ makes the residual $\|R\|$ dependent on the norm of the right-hand side $\|b\|$ ($\|R_0\| = \|b\|$) of the Helmholtz problem $L(\Pi') = b$. Therefore as long as $\|b\|$ does not vary considerably from one step to another, the precision of the Helmholtz solution remains consistent.

• **ADI Options:**

- A typical option for the ADI-preconditioner is a combination of BVADIP (i.e. (15.43)-(15.45)) and XZADIP (i.e. (15.37) with $s_l^y = 0$). This is option 4 in the code. By "combination" of two preconditioners, it is meant that the first preconditioner is applied at line 4 of the "GCR(k) Algorithm" whilst the second is applied at line 15 of the same algorithm.
- The typical number of ADI-iterations is $l = 2$ in the system (15.37).
- The typical pseudo-time step is $\delta\tau = 0.013$.
- The damping coefficient ψ in (15.37) (and (J.45) of Appendix J) is introduced to make $\delta\tau$ dimensionless. Since q ($\equiv \Pi'$ in the New Dynamics) in (15.37) is dimensionless, a dimensional analysis suggests that $\psi = \varsigma_1/C_4$, where ς_1 is a dimensionless constant. Since C_4, in the elliptic operator, can be written as $C_4 = \varsigma_2\left(r^2\rho\delta_r\eta/\Delta t\right)$ (ς_2 is a dimensionless constant*)*, $\psi = \varsigma\left[\Delta t/\left(r^2\rho\delta_r\eta\right)\right]$ and for the obvious choice of $\varsigma = \varsigma_1/\varsigma_2 = 1$, $\psi = \left[\Delta t\delta_\eta r/\left(r^2\rho\right)\right]$.

Aside :

The use of the above "combination" of preconditioners, by which one preconditioner is used to initialise the search directions whilst another is used within the iterative loop, was chosen empirically. However, it is not clear that this approach *is in general robust and in some situations it seems possible that it may lead to slow or even non-convergence of the scheme. This approach should be reviewed.*

GCR(k) Algorithm

01- Given an initial solution x_0

02- Compute $R_0 = Ax_0 \equiv L\,(x_0)$ (L is the elliptic operator)

03- Compute$R_0 \;=\; Ax_0 - b\;\cos\phi \equiv R_0 - b\;\cos\phi$ (*see footnotes 1 and 2*)

If $x_0 = 0$ **then** $R_0 = -b\;\cos\phi$

04- Compute $p_0 \;=\; M^{-1}R_0$

05- Compute$\|R_0\|$ or $\left|\widehat{R}_0\right|$ (*see footnote* 3)

06- Compute $Ap_0 \;\equiv\; L\,(p_0)$

07- Start with $(x, R, \|R\|\,, \left|\widehat{R}\right|) = (x_0, R_0, \|R_0\|\,, \left|\widehat{R}_0\right|)$

08- **Do While** $(\|R\| > \epsilon\,\|R_0\|$ or $\left|\widehat{R}\right| > R_m)$

09- **Do** $i = 0, k-1$ (*see footnote* 4)

10- $\alpha = -\,\langle R, Ap_i\rangle\,/\,\langle Ap_i, Ap_i\rangle$ (*see footnote* 5)

11- $x \;\leftarrow\; x + \alpha p_i$

12- $R \;\leftarrow\; R + \alpha Ap_i$ (*see footnote* 6)

13- Compute $\|R\|$ or $\left|\widehat{R}\right|$

14- **If** $(\|R\| \le \epsilon\,\|R_0\|$ or $\left|\widehat{R}\right| \le R_m)$ **STOP**

15- Compute $p_{i+1} = \;M^{-1}R$

16- Compute $Ap_{i+1} \equiv\; L(p_{i+1})$

17- **Do** $j = 0, i$

18- $\beta_j = -\,\langle Ap_{i+1}, Ap_j\rangle\,/\,\langle Ap_j, Ap_j\rangle$ (*see footnote* 7)

19- **EndDo**

20- **Do** $j = 0, i$

21- $p_{i+1} \;\leftarrow\; p_{i+1} + \beta_j p_j$

22- $Ap_{i+1} \;\leftarrow\; Ap_{i+1} + \beta_j Ap_j$

23- **EndDo**

24- **EndDo**

25- Restart with $\left(x_0, R_0, p_0, Ap_0, \|R_0\|\,, \left|\widehat{R}_0\right|\right) = \left(x, R, p_k, Ap_k, \|R\|\,, \left|\widehat{R}\right|\right)$

26- **GOTO** line **07**

27- **EndWhile**

Footnotes for "GCR(k) Algorithm"

(1) Note that the sign of R here is the opposite of that used in Appendix J. This is due to the fact that the algorithm used here was written for a negative definite L instead of the more appropriate positive definite $-L$.

(2) The $\cos\phi$ factor is due to the fact that the system $Ax\cos\phi = b\cos\phi$ is being solved instead of the original $Ax = b$.

(3) The norm $\|R\| = \sqrt{\frac{1}{n}\sum_{i=1}^{n} R_i^2} = \left(\frac{1}{n}\right)^{1/2}\|R\|_2$, where n is the total number of unknowns (dimension of the vector R), is a scaled Euclidean norm to avoid large numbers for the intrinsic function $\sqrt{(...)}$. This scaling does not affect the stopping criteria in line 14 as both $\|R\|$ and $\|R_0\|$are scaled with same factor $(1/n)^{1/2}$.$\left|\widehat{R}\right| \equiv \left\|\widehat{R}\right\|_\infty = \max_{i=1,\dots,n}\left|\widehat{R}_i\right|$where$\widehat{R}$ is a scaled residual given by $\widehat{R} = c\,R$ (see details mentioned previously).

(4) The inner-loop index, i, runs from 0 to $k-1$, where GCR(k) has k inner-loops, and in particular *one inner-loop corresponds to* GCR(1).

(5) Again due to the definition of R(footnote 1), the sign of $\alpha$is of opposite sign to that used in Appendix J. Also note that this $\alpha$is denoted in the code as "*beta*"

(6) Again due to footnote 1, $R = R + \alpha Ap$instead of $R = R - \alpha Ap$ as in Appendix J.

(7) The coefficients $\beta_j$in line 18 are referred to as "*alpha* (j)" in the code.

16 Back substitution to complete timestep

Once the elliptic-boundary-value problem has been solved for the pressure tendencies $\Pi'(\equiv \Pi^{n+1} - \Pi^n)$ at levels $k = 1/2,\ 3/2,\ ...,\ N-1/2$, the remaining unknown variables should be obtained by a step-by-step process of back substitution into the original linear set of discretised equations summarised in Section 13. Polar-specific computations are grouped together in Section 16.11.

Aside :

As discussed in the aside in Section 16.7.2, this back substitution is entirely consistent with the original linear set in the absence of imposed a posteriori moisture conservation constraints. However, this is **not** *so when a posteriori moisture conservation constraints are imposed, although the differences are in general very small.*

16.1 Pressure at levels $k = 1/2, 3/2, ..., N-1/2$

From (13.3), the Exner pressure Π^{n+1} at the new time at levels $k = 1/2,\ 3/2,\ ...,\ N-1/2$ is given by

$$\Pi^{n+1} = \Pi^n + \Pi', \tag{16.1}$$

from whichp^{n+1} (required in (13.18)) is diagnostically obtained at the same levels as

$$p^{n+1} = p_0 \left(\Pi^{n+1}\right)^{\frac{1}{\kappa_d}}. \tag{16.2}$$

16.2 Horizontal momentum at levels $k = 1/2, 3/2, ..., N-1/2$

From (13.1)-(13.3) the horizontal momentum tendencies u' and v' at levels $k = 1/2,\ 3/2,\ ...,\ N-1/2$ are obtained from

$$\begin{aligned} u' \equiv u^{n+1} - u = \ & A_u \left[R_u^+ - \alpha_3 \Delta t \frac{c_{pd}}{\overline{r}^{\lambda} \cos\phi} \left(\overline{\theta_v^*}^{r\lambda} \delta_\lambda \Pi' - \overline{\theta_v^* \delta_r \Pi'}^{r\lambda} \delta_\lambda r \right) \right] \\ & + F_u \left[\overline{R_v^+}^{\lambda\phi} - \alpha_3 \Delta t \overline{\frac{c_{pd}}{\overline{r}^{\phi}} \left(\overline{\theta_v^*}^{r\phi} \delta_\phi \Pi' - \overline{\theta_v^* \delta_r \Pi'}^{r\phi} \delta_\phi r \right)}^{\lambda\phi} \right], \end{aligned} \tag{16.3}$$

$$\begin{aligned} v' \equiv v^{n+1} - v^n = \ & A_v \left[R_v^+ - \alpha_3 \Delta t \frac{c_{pd}}{\overline{r}^{\phi}} \left(\overline{\theta_v^*}^{r\phi} \delta_\phi \Pi' - \overline{\theta_v^* \delta_r \Pi'}^{r\phi} \delta_\phi r \right) \right] \\ & - F_v \left[\overline{R_u^+}^{\lambda\phi} - \alpha_3 \Delta t \overline{\frac{c_{pd}}{\overline{r}^{\lambda} \cos\phi} \left(\overline{\theta_v^*}^{r\lambda} \delta_\lambda \Pi' - \overline{\theta_v^* \delta_r \Pi'}^{r\lambda} \delta_\lambda r \right)}^{\lambda\phi} \right], \end{aligned} \tag{16.4}$$

where the known quantities R_u^+, R_v^+, A_u, A_v, F_u, F_v and θ_v^* are respectively defined by (6.34), (6.54), (6.65)-(6.68) and (6.35). The special treatment of vertical averages and differences near the bottom and top boundaries is described in Section 6.3.

Having determined u' and v' from these two equations, the horizontal momentum components u^{n+1} and v^{n+1} at the new time level are trivially obtained from

$$u^{n+1} = u^n + u', \tag{16.5}$$

$$v^{n+1} = v^n + u'. \tag{16.6}$$

16.3 Vertical momentum at levels $k = 0, 1, ..., N$

From (13.4)-(13.5) the vertical momentum tendency w' at levels $k = 1, 2, ..., N-1$ is obtained from

$$w' \equiv w^{n+1} - w^n = G^{-1}R_w^+ - K\delta_r \Pi', \tag{16.7}$$

where the known quantities R_w^+, G and K are respectively defined by (7.27), (7.31) and (7.32), and at levels $k = 1$ and $k = N$ it is trivially obtained from (13.6)-(13.7) as

$$w'|_{\eta_0 \equiv 0} = 0, \tag{16.8}$$

$$w'|_{\eta_N \equiv 1} = 0. \tag{16.9}$$

Aside :

> *Whilst* (16.8) *is consistent with the original discrete linear set of equations, it is only valid where the bottom is flat, and is invalid for inviscid flow in the presence of orography. As mentioned in an aside in Section 13, this needs revisiting.*

Having determined w' from the above equations, the vertical momentum component w^{n+1} at the new time is trivially obtained at levels $k = 0, 1, ..., N$ from

$$w^{n+1} = w^n + w'. \tag{16.10}$$

16.4 Vertical motion $\dot{\eta}$ at levels $k = 0, 1, ..., N$

From (13.12)-(13.13), the vertical motion tendency $\dot{\eta}'$ is obtained at levels $k = 1, 2, ..., N-1$ as

$$\dot{\eta}' \equiv \dot{\eta}^{n+1} - \dot{\eta}^n = \frac{1}{\delta_\eta r}\left(w' - \overline{\frac{\overline{u'}^\eta}{\overline{r}^\lambda \cos\phi}\delta_\lambda r}^\lambda - \overline{\frac{\overline{v'}^\eta}{\overline{r}^\phi}\delta_\phi r}^\phi \right), \tag{16.11}$$

where u' and v' are given by (16.3)-(16.4), and at levels $k=0$ and $k=N$ as

$$\dot{\eta}'|_{\eta_0\equiv 0} = \dot{\eta}'|_{\eta_N\equiv 1} = 0. \tag{16.12}$$

Having determined $\dot{\eta}'$ from these equations, the vertical motion $\dot{\eta}$ at the new time is then trivially obtained at levels $k=0$, 1, ..., N from

$$\dot{\eta}^{n+1} = \dot{\eta}^n + \dot{\eta}'. \tag{16.13}$$

16.5 Dry density at levels $k = 1/2, 3/2, ..., N-1/2$

From (13.8), the dry densitytendency ρ_y' at levels $k=3/2$, 5/2, ..., $N-3/2$ is obtained from

$$\begin{aligned} r^2\rho_y' &= -\frac{\Delta t}{\delta_\eta r}\left\{\frac{1}{\cos\phi}\delta_\lambda\left(\frac{\overline{r^2\rho_y^n\delta_\eta r}^\lambda}{\overline{r}^\lambda}\overline{u}^{\alpha_1}\right)+\frac{1}{\cos\phi}\delta_\phi\left(\frac{\overline{r^2\rho_y^n\delta_\eta r}^\phi}{\overline{r}^\phi}\overline{v}^{\alpha_1}\cos\phi\right)\right.\\ &\left.-\delta_\eta\left[\overline{r^2\rho_y^n}^r\overline{\left(\overline{\frac{\overline{u}^\eta}{\overline{r}^\lambda\cos\phi}\delta_\lambda r}^\lambda+\overline{\frac{\overline{v}^\eta}{\overline{r}^\phi}\delta_\phi r}^\phi\right)}^{\alpha_1}\right]+\delta_\eta\left(\overline{r^2\rho_y^n}^r\overline{w}^{\alpha_2}\right)\right\}, \end{aligned} \tag{16.14}$$

where

$$\overline{F}^{\alpha_i} \equiv \alpha_i F^{n+1} + (1-\alpha_i)F^n \equiv F^n + \alpha_i F', \tag{16.15}$$

and u', v' and w' are given by (16.3)-(16.4) and (16.7)-(16.9).

Similarly, from (13.10)-(13.11), the dry densitytendency ρ_y' at levels $k=1/2$ and $k=N-1/2$ are respectively obtained from

$$\begin{aligned} \left(r^2\rho_y'\right)\big|_{1/2} &= -\left(\frac{\Delta t}{\delta_\eta r}\right)\bigg|_{1/2}\left[\frac{1}{\cos\phi}\delta_\lambda\left(\frac{\overline{r^2\rho_y^n\delta_\eta r}^\lambda}{\overline{r}^\lambda}\overline{u}^{\alpha_1}\right)+\frac{1}{\cos\phi}\delta_\phi\left(\frac{\overline{r^2\rho_y^n\delta_\eta r}^\phi}{\overline{r}^\phi}\overline{v}^{\alpha_1}\cos\phi\right)\right]\bigg|_{1/2}\\ &-\left(\frac{\Delta t}{\delta_\eta r\Delta\eta}\right)\bigg|_{1/2}\left[\overline{r^2\rho_y^n}^r\overline{w}^{\alpha_2}-\overline{r^2\rho_y^n}^r\overline{\left(\overline{\frac{\overline{u}^\eta}{\overline{r}^\lambda\cos\phi}\delta_\lambda r}^\lambda+\overline{\frac{\overline{v}^\eta}{\overline{r}^\phi}\delta_\phi r}^\phi\right)}^{\alpha_1}\right]\bigg|_1, \end{aligned} \tag{16.16}$$

and

$$\begin{aligned} \left(r^2\rho_y'\right)\big|_{N-1/2} &= -\left(\frac{\Delta t}{\delta_\eta r}\right)\bigg|_{N-1/2}\left[\frac{1}{\cos\phi}\delta_\lambda\left(\frac{\overline{r^2\rho_y^n\delta_\eta r}^\lambda}{\overline{r}^\lambda}\overline{u}^{\alpha_1}\right)+\frac{1}{\cos\phi}\delta_\phi\left(\frac{\overline{r^2\rho_y^n\delta_\eta r}^\phi}{\overline{r}^\phi}\overline{v}^{\alpha_1}\cos\phi\right)\right]\bigg|_{N-1/2}\\ &+\left(\frac{\Delta t}{\delta_\eta r\Delta\eta}\right)\bigg|_{N-1/2}\left[\overline{r^2\rho_y^n}^r\overline{w}^{\alpha_2}-\overline{r^2\rho_y^n}^r\overline{\left(\overline{\frac{\overline{u}^\eta}{\overline{r}^\lambda\cos\phi}\delta_\lambda r}^\lambda+\overline{\frac{\overline{v}^\eta}{\overline{r}^\phi}\delta_\phi r}^\phi\right)}^{\alpha_1}\right]\bigg|_{N-1}. \end{aligned} \tag{16.17}$$

Having determined ρ_y', the dry densityat the new time is then trivially obtained at levels $k=1/2$, 3/2, ..., $N-1/2$ from

$$\rho_y^{n+1} = \rho_y^n + \rho_y'. \tag{16.18}$$

16.6 Potential temperature at levels $k = 0, 1, ..., N$

From (13.14)-(13.15), the potential temperature tendency θ' at levels $k = 1, 2, ..., N-1$ is obtained from

$$\theta' \equiv \theta^{n+1} - \theta^n = (\theta^* - \theta^n) - \alpha_2 \Delta t \left(w' \delta_{2r} \theta_{ref} \right), \tag{16.19}$$

where $\theta^* \equiv \tilde{\theta}^{(P2)}$ (see (9.27)) is the latest available predictor for θ at time $(n+1)\Delta t$, and the known quantity $\delta_{2r}\theta_{ref}$ is defined by (9.37).

At the bottom ($k = 0$) level (see (13.16))

$$\theta'|_{\eta_0 \equiv 0} = \theta'|_{\eta_1}, \tag{16.20}$$

and at the top ($k = N$) level (see (13.17))

$$\theta'|_{\eta_N \equiv 1} = (\theta^* - \theta^n)|_{\eta_N \equiv 1}. \tag{16.21}$$

Having determined θ', the potential temperature at the new time is then trivially obtained at levels $k = 0, 1, ..., N$ from

$$\theta^{n+1} = \theta^n + \theta'. \tag{16.22}$$

16.7 Moisture at levels $k = 0, 1, ..., N$

The procedure for determining the final moisture quantities at time $(n+1)\,\Delta t$ depends upon whether moisture conservation corrections are imposed or not.

16.7.1 Without moisture conservation correction

From (13.21)-(13.29), when no moisture conservation correction is imposed, the moisture quantities at the new time at levels $k = 0, 1, ..., N$ are trivially obtained from

$$m_v^{n+1} = m_v^* \equiv \widetilde{m}_v^{(P2)}, \tag{16.23}$$

$$m_{cl}^{n+1} = m_{cl}^* \equiv \widetilde{m}_{cl}^{(P2)}, \tag{16.24}$$

$$m_{cf}^{n+1} = m_{cf}^* \equiv \widetilde{m}_{cf}^{(P2)}, \tag{16.25}$$

where $\widetilde{m}_X^{(P2)}$, $X = (v, cl, cf)$, are defined for $k = 1, 2, ..., N-1$, by (10.23)-(10.25) or, equivalently, by (10.40)-(10.42), and, for $k = N$, by (10.63)-(10.65). At level $k = 0$, $(m_X^*)|_{\eta_0 \equiv 0}$, $X = (v, cl, cf)$, are defined by (13.24)-(13.26).

16.7.2 With moisture conservation correction

From (13.21)-(13.23) and (13.30)-(13.32), when the a posteriori moisture conservation constraints are imposed, the moisture quantities at the new time at levels $k = 1, 2, ..., N$ are obtained from

$$m_v^{n+1} = \widetilde{m}_v^{(P2)} + \Delta t \left(D_{cons}^{m_v}\right)^n - \Delta t \left(\frac{\rho_y^{n+1} - \rho_y^n}{\rho_y^{n+1}}\right) \left[S_2^{m_v}\right]^*, \tag{16.26}$$

$$m_{cl}^{n+1} = \widetilde{m}_{cl}^{(P2)} + \Delta t \left(D_{cons}^{m_{cl}}\right)^n - \Delta t \left(\frac{\rho_y^{n+1} - \rho_y^n}{\rho_y^{n+1}}\right) \left[S_2^{m_{cl}}\right]^*, \tag{16.27}$$

$$m_{cf}^{n+1} = \widetilde{m}_{cf}^{(P2)} + \Delta t \left(D_{cons}^{m_{cf}}\right)^n - \Delta t \left(\frac{\rho_y^{n+1} - \rho_y^n}{\rho_y^{n+1}}\right) \left[S_2^{m_{cf}}\right]^*, \tag{16.28}$$

where $\widetilde{m}_X^{(P2)}$, $X = (v, cl, cf)$, are defined for $k = 1, 2, ..., N-1$, by (10.23)-(10.25) or, equivalently, by (10.40)-(10.42) and, for $k = N$, by (10.63)-(10.65). Also $\left(D_{cons}^{m_X}\right)^n$ is given by imposition of (10.47); and $\left[S_2^{m_X}\right]^*$ are given, for $k = 1, 2, ..., N-1$, by (10.28) and (10.31)-(10.32), and, because of (10.62), are identically zero for $k = N$.

From (13.33)-(13.35),at level $k = 0$, $\left(m_X^{n+1}\right)\big|_{\eta_0 \equiv 0}$, $X = (v, cl, cf)$, are obtained by simple extrapolation of their values at $k = 1$:

$$\left(m_v^{n+1}\right)\big|_{\eta_0 \equiv 0} = \left(m_v^{n+1}\right)\big|_{\eta_1}, \tag{16.29}$$

$$\left(m_{cl}^{n+1}\right)\big|_{\eta_0 \equiv 0} = \left(m_{cl}^{n+1}\right)\big|_{\eta_1}, \tag{16.30}$$

$$\left(m_{cf}^{n+1}\right)\big|_{\eta_0 \equiv 0} = \left(m_{cf}^{n+1}\right)\big|_{\eta_1}. \tag{16.31}$$

Aside :

Note that when moisture conservation corrections are imposed in the above a posteriori manner, the formal algebraic consistency mentioned at the beginning of Section 13 (just after the table) is lost. This is because the total gaseous density ρ^{n+1} and the virtual potential temperature θ_v^{n+1} are obtained (using (16.36)-(16.37)*) with values of m_X (determined from* (16.26)-(16.31)*) which are different to those in* (13.36)-(13.37) *used during the Helmholtz elimination procedure. In contradistinction, when moisture conservation constraints are not imposed, the values of m_X obtained from* (16.23)-(16.25) *and those used in* (13.36)-(13.37) *are then mutually consistent, and algebraic consistency between the Helmholtz elimination procedure and the back substitution step consequently ensues.*

An alternative interpretation of the dynamics discretisation when moisture conservation constraints are applied is as follows. Eqs. (16.36)-(16.37) *could be equivalently replaced by*

$$\rho^{\#} = \rho_y^{n+1} \overline{\left(1 + \sum_{X=(v,cl,cf)} m_X^* \right)}^r , \tag{16.32}$$

$$\theta_v^{\#} = \theta^{n+1} \left(\frac{1 + \frac{1}{\varepsilon} m_v^*}{1 + m_v^* + m_{cl}^* + m_{cf}^*} \right) , \tag{16.33}$$

$$\rho^{n+1} = \rho^{\#} + \rho_y^{n+1} \overline{\left(1 + \sum_{X=(v,cl,cf)} \left(m_X^{n+1} - m_X^* \right) \right)}^r , \tag{16.34}$$

$$\theta_v^{n+1} = \theta_v^{\#} + \theta^{n+1} \left[\left(\frac{1 + \frac{1}{\varepsilon} m_v^{n+1}}{1 + m_v^{n+1} + m_{cl}^{n+1} + m_{cf}^{n+1}} \right) - \left(\frac{1 + \frac{1}{\varepsilon} m_v^*}{1 + m_v^* + m_{cl}^* + m_{cf}^*} \right) \right] . \tag{16.35}$$

The provisional atmospheric state comprised of $\{\Pi^{n+1}$, p^{n+1}, u^{n+1}, v^{n+1}, w^{n+1}, $\dot{\eta}^{n+1}$, ρ_y^{n+1}, θ^{n+1}, m_v^*, m_{cl}^*, m_{cf}^*, $\rho^{\#}$, $\theta_v^{\#}\}$ *would then be the algebraically-consistent solution of the linear equation set of Section 13 in the absence of moisture conservation corrections. The final atmospheric state* $\{\Pi^{n+1}$, p^{n+1}, u^{n+1}, v^{n+1}, w^{n+1}, $\dot{\eta}^{n+1}$, ρ_y^{n+1}, θ^{n+1}, m_v^{n+1}, m_{cl}^{n+1}, m_{cf}^{n+1}, ρ^{n+1}, $\theta_v^{n+1}\}$ *at time* $(n+1)\,\Delta t$ *would then be obtained from this provisional atmospheric state by applying the final correctors (to impose the moisture conservation constraints) defined by* (16.26)-(16.31) *and subsequently used in* (16.34)-(16.35).

16.8 Total gaseous density at levels $k = 1/2, 3/2, ..., N - 1/2$

The total gaseous density at the new time at levels k =1/2, 3/2, ..., $N - 1/2$ is obtained from

$$\rho^{n+1} = \rho_y^{n+1} \overline{\left(1 + \sum_{X=(v,cl,cf)} m_X^{n+1} \right)}^r , \tag{16.36}$$

where ρ_y^{n+1} and m_X^{n+1}, $X = (v, cl, cf)$, are respectively given by (16.18) and(depending on whether moisture conservation is imposed or not)by (16.26)-(16.28) or (16.23)-(16.25).

16.9 Virtual potential temperature at levels $k = 0, 1, ..., N$

The virtual potential temperature at the new time level at levels $k = 0, 1, ..., N$ is

$$\theta_v^{n+1} = \theta^{n+1} \left(\frac{1 + \frac{1}{\varepsilon} m_v^{n+1}}{1 + m_v^{n+1} + m_{cl}^{n+1} + m_{cf}^{n+1}} \right), \tag{16.37}$$

where θ^{n+1} and m_X^{n+1}, $X = (v, cl, cf)$, are respectively given by (16.22) and(depending on whether moisture conservation is imposed or not)by (16.26)-(16.28) or (16.23)-(16.25).

16.10 Absolute temperature at levels $k = 1, 2, ..., N$

The absolute temperature (needed only for the physics/dynamics coupling) at the new time level, at the interior levels, $k = 1, 2, ...N - 1$, is given by:

$$T^{n+1} = \theta^{n+1} \left[\overline{\left(\Pi^{n+1}\right)^{\frac{1}{\kappa_d}}}^{r} \right]^{\kappa_d}, \tag{16.38}$$

with Π^{n+1} given by (16.1). At the top level, $k = N$, T^{n+1} is evaluated as:

$$T^{n+1}\big|_N = \theta^{n+1}\big|_N \left\{ \frac{1}{2} \left[\left(\Pi^{n+1}\big|_{N+1/2} \right)^{\frac{1}{\kappa_d}} + \left(\Pi^{n+1}\big|_{N-1/2} \right)^{\frac{1}{\kappa_d}} \right] \right\}^{\kappa_d}, \tag{16.39}$$

where $\Pi^{n+1}\big|_{N+1/2}$ is obtained from (see (11.28)):

$$\Pi^{n+1}\big|_{N+1/2} = \Pi^{n}\big|_{N+1/2} + \Pi'\big|_{N-1/2}. \tag{16.40}$$

16.11 Polar computations

Polar-specific relations are grouped together here.

16.11.1 u wind component at the poles

The u wind component at the two poles is obtained from (13.41) and (13.42):

$$u_{i,1/2} \equiv u\big|_{\left(\lambda_i, \phi_{1/2} \equiv -\pi/2\right)} = -v_{SP} \sin\left(\lambda_i - \lambda_{SP}\right), i = 1, 2, ..., L, \tag{16.41}$$

$$u_{i,M-1/2} \equiv u\big|_{\left(\lambda_i, \phi_{M-1/2} \equiv +\pi/2\right)} = +v_{NP} \sin\left(\lambda_i - \lambda_{NP}\right), i = 1, 2, ..., L. \tag{16.42}$$

where λ_{SP}, v_{SP}, λ_{NP} and v_{NP} are defined by (6.79), (6.80), (6.83) and (6.85).

16.11.2 v wind component at the poles

The v wind component at the two poles, if required, can be obtained from (13.43) and (13.44):

$$v_{i-1/2,1/2} \equiv v|_{\left(\lambda_{i-1/2},\phi_{1/2}\equiv-\pi/2\right)} = v_{SP}\cos\left(\lambda_{i-1/2}-\lambda_{SP}\right), i=1,2,...,L. \tag{16.43}$$

$$v_{i-1/2,M-1/2} \equiv v|_{\left(\lambda_{i-1/2},\phi_{M-1/2}\equiv+\pi/2\right)} = v_{NP}\cos\left(\lambda_{i-1/2}-\lambda_{NP}\right), i=1,2,...,L. \tag{16.44}$$

where λ_{SP}, v_{SP}, λ_{NP} and v_{NP} are defined by (6.79), (6.80), (6.83) and (6.85).

16.11.3 w wind component at the poles

From (13.45)-(13.46), uniqueness of the w wind component at the two poles is imposed:

$$w_{\frac{1}{2},\frac{1}{2}} \equiv w_{\frac{3}{2},\frac{1}{2}} \equiv w_{\frac{5}{2},\frac{1}{2}} \equiv ... \equiv w_{L-\frac{1}{2},\frac{1}{2}} = w_{SP}, \tag{16.45}$$

$$w_{\frac{1}{2},M-\frac{1}{2}} \equiv w_{\frac{3}{2},M-\frac{1}{2}} \equiv w_{\frac{5}{2},M-\frac{1}{2}} \equiv ... \equiv w_{L-\frac{1}{2},M-\frac{1}{2}} = w_{NP}. \tag{16.46}$$

16.11.4 Definition of $\dot{\eta}$ at poles

From (13.52)-(13.53), $\dot{\eta}$ at the two poles is determined from

$$\dot{\eta}_{SP} = \frac{1}{\left(\delta_\eta r\right)_{SP}}\left[w_{SP} - \frac{2}{L}\sum_{i=1}^{L}\left(\frac{\overline{v}^{\eta}}{\overline{r}^{\phi}}\delta_\phi r\right)_{i-\frac{1}{2},1}\right], \tag{16.47}$$

$$\dot{\eta}_{NP} = \frac{1}{\left(\delta_\eta r\right)_{NP}}\left[w_{NP} - \frac{2}{L}\sum_{i=1}^{L}\left(\frac{\overline{v}^{\eta}}{\overline{r}^{\phi}}\delta_\phi r\right)_{i-\frac{1}{2},M-1}\right]. \tag{16.48}$$

16.11.5 Continuity equation at the poles

From (13.47)-(13.51), the density at the two poles is updated from

$$\frac{F'_{SP}}{\Delta t} = -\frac{\cos\left(\phi_1\right)}{b}\frac{1}{L}\sum_{i=1}^{L}\left(\frac{\overline{F^n}^{\phi}\overline{v}^{\alpha_1}}{\overline{r}^{\phi}}\right)_{i-\frac{1}{2},1} - \delta_\eta\left[\left(\overline{r^2\rho_y^n}^{r}\right)_{SP}\overline{\dot{\eta}_{SP}}^{average}\left(\delta_\eta r\right)_{SP}\right], \tag{16.49}$$

$$\frac{F'_{NP}}{\Delta t} = \frac{\cos\left(\phi_{M-1}\right)}{b}\frac{1}{L}\sum_{i=1}^{L}\left(\frac{\overline{F^n}^{\phi}\overline{v}^{\alpha_1}}{\overline{r}^{\phi}}\right)_{i-\frac{1}{2},M-1} - \delta_\eta\left[\left(\overline{r^2\rho_y^n}^{r}\right)_{NP}\overline{\dot{\eta}_{NP}}^{average}\left(\delta_\eta r\right)_{NP}\right], \tag{16.50}$$

where

$$F^n \equiv r^2\rho_y^n\delta_\eta r, F' \equiv F^{n+1} - F^n \equiv r^2\delta_\eta r\left(\rho_y^{n+1} - \rho_y^n\right) \equiv r^2\delta_\eta r\rho'_y, \tag{16.51}$$

$$\overline{\dot{\eta}_{SP}}^{average} = \frac{1}{(\delta_\eta r)_{SP}} \left[\overline{w_{SP}}^{\alpha_2} - \frac{2}{L} \sum_{i=1}^{L} \left(\overline{\frac{\overline{v}^\eta}{\overline{r}^\phi} \delta_\phi r}^{\alpha_1} \right)_{i-\frac{1}{2},1} \right], \tag{16.52}$$

$$\overline{\dot{\eta}_{NP}}^{average} = \frac{1}{(\delta_\eta r)_{NP}} \left[\overline{w_{NP}}^{\alpha_2} - \frac{2}{L} \sum_{i=1}^{L} \left(\overline{\frac{\overline{v}^\eta}{\overline{r}^\phi} \delta_\phi r}^{\alpha_1} \right)_{i-\frac{1}{2},M-1} \right]. \tag{16.53}$$

16.11.6 Uniqueness of scalars at the poles

From (13.39)-(13.40), scalar quantities are updated to have unique values at the two poles, i.e.

$$F_{\frac{1}{2},\frac{1}{2}} \equiv F_{\frac{3}{2},\frac{1}{2}} \equiv F_{\frac{5}{2},\frac{1}{2}} \equiv ... \equiv F_{L-\frac{1}{2},\frac{1}{2}} = F_{SP}, \tag{16.54}$$

$$F_{\frac{1}{2},M-\frac{1}{2}} \equiv F_{\frac{3}{2},M-\frac{1}{2}} \equiv F_{\frac{5}{2},M-\frac{1}{2}} \equiv ... \equiv F_{L-\frac{1}{2},M-\frac{1}{2}} = F_{NP}, \tag{16.55}$$

where F is any scalar quantity required at either of the two poles, $F_{i-\frac{1}{2},\frac{1}{2}} \equiv F|_{\left(\lambda_{i-1/2},\phi_{1/2}\equiv-\pi/2\right)}$ and $F_{i-\frac{1}{2},M-\frac{1}{2}} \equiv F|_{\left(\lambda_{i-1/2},\phi_{M-1/2}\equiv\pi/2\right)}$.

17 A stability analysis of the coupled equation set.

17.1 The governing equations: continuous and time-discretised forms.

The continuous set of governing equations (2.71) - (2.84), written in Cartesian $x-z$ coordinates, in the absence of rotation ($f_i \equiv 0, \forall i = 1, ..., 3$) and forcing ($S^u = S^v = S^w = S^\theta \equiv 0$), for a dry atmosphere ($\theta_v = \theta,\ \rho_y = \rho$), and neglecting variations in the $y-$direction ($\partial/\partial y \equiv 0$) is:

$$\frac{Du}{Dt} = -c_{pd}\theta\frac{\partial\Pi}{\partial x}, \tag{17.1}$$

$$\frac{Dv}{Dt} = 0, \tag{17.2}$$

$$\frac{Dw}{Dt} = -g - c_{pd}\theta\frac{\partial\Pi}{\partial z}, \tag{17.3}$$

$$\frac{D\theta}{Dt} = 0, \tag{17.4}$$

$$\frac{D\rho}{Dt} = -\rho\left(\frac{\partial u}{\partial x} + \frac{\partial w}{\partial z}\right), \tag{17.5}$$

$$\Pi^{\frac{\kappa_d - 1}{\kappa_d}}\rho\theta = \frac{p_0}{\kappa_d c_{pd}}, \tag{17.6}$$

where $D/Dt \equiv \partial/\partial t + u\partial/\partial x + w\partial/\partial z$, $\Pi \equiv (p/p_0)^{\kappa_d}$, and $\kappa_d \equiv R_d/c_{pd}$.

The time-discretised forms of (17.1) - (17.6) are obtained from the corresponding discrete equations reported in other sections of this document, but: rewritten under the simplifying assumptions stated above for the continuous equations, and in the absence of a spatial discretisation (i.e. with partial spatial derivatives in place of their finite difference counterparts and dropping spatial averages - this could be viewed as being equivalent to using a spectral spatial discretisation instead of a finite-difference one).

Using (6.31) - (6.34), (6.65), (6.67) and (13.3) in (13.1) and dividing by Δt implies

$$\frac{u^{n+1} - u_d^n}{\Delta t} = -\left(1-\alpha_3\right)c_{pd}\left[\theta\frac{\partial\Pi}{\partial x}\right]_d^n - \alpha_3 c_{pd}\theta^*\frac{\partial\Pi^{n+1}}{\partial x}, \tag{17.7}$$

where, under the simplifying assumptions considered in this analysis, θ^* is as defined in (17.11) - (17.13).

Using (6.51) - (6.54), (6.66), (6.68) and (13.3) in (13.2) and dividing by Δt implies

$$\frac{v^{n+1} - v_d^n}{\Delta t} = 0. \tag{17.8}$$

Using (13.5), (7.26) - (7.27) and (7.31) - (7.32) in (13.4) and dividing by Δt implies

$$\begin{aligned}\mathbf{I}_h\frac{w^{n+1}-w_d^n}{\Delta t} &= -g \\ &\quad -(1-\alpha_4)\,c_{pd}\left[\theta^n\frac{\partial\Pi^n}{\partial z}\right]_d-\alpha_4 c_{pd}\theta^*\frac{\partial\Pi^{n+1}}{\partial z} \\ &\quad +c_{pd}\alpha_2\alpha_4\Delta t\frac{\partial\theta^*}{\partial z}\frac{\partial\Pi^n}{\partial z}\left(w^{n+1}-w^n\right),\end{aligned}\tag{17.9}$$

where $\mathbf{I}_h$ is the hydrostatic switch introduced in Section 7 ($\mathbf{I}_h=0$ in the hydrostatic case, $\mathbf{I}_h=1$ otherwise).

Using (13.15), (9.37) and (13.5) in (13.14) and dividing by Δt implies

$$\frac{\theta^{n+1}-\theta^n}{\Delta t}=\frac{\theta^*-\theta^n}{\Delta t}-\alpha_2\left(w^{n+1}-w^n\right)\frac{\partial\theta^*}{\partial z},\tag{17.10}$$

where, under the simplifying assumptions considered in this analysis, θ^* is defined by:

$$\theta^*\equiv\tilde{\theta}^{(2)},\tag{17.11}$$

$\tilde{\theta}^{(2)}$ is obtained by adding (9.17) multiplied by Δt and (9.21), i.e. :

$$\tilde{\theta}^{(2)}=\theta_{dl}^n-\alpha_2\Delta t\left(w^n-w^*\right)\frac{\partial\tilde{\theta}^{(1)}}{\partial z}-(1-\alpha_2)\,\Delta t\left[\left(w-w^*\right)\frac{\partial\theta}{\partial z}\right]_{dl}^n,\tag{17.12}$$

and, from (9.17), $\tilde{\theta}^{(1)}$ is given by:

$$\tilde{\theta}^{(1)}=\theta_{dl}^n-\alpha_2\Delta t\left[\left(w-w^*\right)\frac{\partial\theta}{\partial z}\right]^n-(1-\alpha_2)\,\Delta t\left[\left(w-w^*\right)\frac{\partial\theta}{\partial z}\right]_{dl}^n.\tag{17.13}$$

In (17.12) and (17.13) $w^*=\left(z_a-z_{dl}\right)/\Delta t$, $z_{a/dl}$ being the vertical heights of the arrival and departure points respectively (cf. (9.8) and the accompanying text).

Using (13.9) in (13.8), rewritten appropriately for Cartesian geometry, implies

$$\begin{aligned}\frac{\rho^{n+1}-\rho^n}{\Delta t} &= -\alpha_1\frac{\partial}{\partial x}\left(\rho^n u^{n+1}\right)-(1-\alpha_1)\frac{\partial}{\partial x}\left(\rho^n u^n\right) \\ &\quad -\alpha_2\frac{\partial}{\partial z}\left(\rho^n w^{n+1}\right)-(1-\alpha_2)\frac{\partial}{\partial z}\left(\rho^n w^n\right),\end{aligned}\tag{17.14}$$

and using (13.19) in (13.18), gives:

$$\begin{aligned}&\kappa_d\theta^n\Pi^n\left(\rho^{n+1}-\rho^n\right)+\left(\kappa_d\rho^n\theta^n-\frac{p^n}{\kappa_d c_{pd}\Pi^n}\right)\left(\Pi^{n+1}-\Pi^n\right) \\ &\qquad +\kappa_d\Pi^n\rho^n\left(\theta^{n+1}-\theta^n\right)=\frac{p^n}{c_{pd}}-\kappa_d\Pi^n\rho^n\theta^n.\end{aligned}\tag{17.15}$$

Note that prior to UM5.3, the semi-implicit weights $\alpha_i,\ i = 1, ..., 4$ in (17.7), (17.9), (17.10) and (17.12) - (17.14) were almost always assigned the following values: $\alpha_1 = \alpha_3 = 0.6$ and $\alpha_2 = \alpha_4 = 1$. At UM 5.3, users became more adventurous.

For the equation of state the form (17.15) has been considered (in place of the time-discretised version of the nonlinear continuous equation (17.6)),since it is derived from the linearised gas law (13.18), which is the one actually used in the model (see Section 11).

17.2 Basic (steady) state solution to the governing equations.

To progress in the stability analysis, linear perturbations to the dependent variables are considered. Each dependent variable $F(x, z, t)$ is represented as the sum of a basic steady (i.e. independent of time) state part, $F_s(x, z)$, and a perturbation, $F'(x, z, t)$, under the assumptions that:

1. the basic state variables satisfy the governing equations
2. the perturbations are so small that terms involving their products can be neglected in the equations.

Let the basic steady state solution be:

$$u_s = u_s(x, z),\ v_s = v_s(x, z),\ w_s = w_s(x, z),\ \theta_s = \theta_s(x, z),\ \rho_s = \rho_s(x, z) \text{ and } \Pi_s = \Pi_s(x, z). \tag{17.16}$$

By substituting (17.16) into the governing equations (17.1) - (17.6), where, for the basic state variables D/Dt reduces to $D/Dt \equiv u_s\partial/\partial x$, a horizontally uniform basic steady state solution is found to be:

$$u_s = \text{constant},\ v_s = w_s \equiv 0,\ \theta_s = \theta_s(z),\ \rho_s = \rho_s(z),\ \Pi_s = \Pi_s(z), \tag{17.17}$$

(i.e. uniform wind in the $x-$direction, with potential temperature, density and Exner pressure function independent of x) such that:

$$c_{pd}\theta_s \frac{d\Pi_s}{dz} = -g, \tag{17.18}$$

$$\Pi_s^{\frac{\kappa_d - 1}{\kappa_d}} \rho_s \theta_s = \frac{p_0}{\kappa_d c_{pd}}. \tag{17.19}$$

Eqs. (17.18) and (17.19) (which mean that the basic state solution is in hydrostatic balance and satisfies the ideal gas law) are obtained from (17.3) and (17.6) respectively, the other governing equations being trivially satisfied by (17.17). Note that the basic steady state solution might be determined analytically for some particular thermal structure, such as for an isothermal (T_s = constant, where T_s is the basic steady state temperature) or an isentropic (θ_s = constant) basic state. The isothermal structure is assumed later and so its form is developed in Section 17.2.1.

17.2.1 The isothermal (T_s = constant) basic steady state solution.

For an isothermal basic steady state, by expressing the potential temperature θ_s in terms of the temperature T_s as (cf. (1.44))

$$\theta_s(z) = \frac{T_s}{\Pi_s(z)}, \tag{17.20}$$

and using (17.20) to eliminate θ_s in favour of the Exner pressure function Π_s in the hydrostatic relation (17.18), the latter can be vertically integrated to give:

$$\Pi_s(z) = \exp\left(-\frac{\kappa_d}{H} z\right), \tag{17.21}$$

where

$$H \equiv \frac{R_d T_s}{g}, \tag{17.22}$$

is the scale height of the isothermal atmosphere, and $p_s(0)$ has been set to p_0.

Substituting for Π_s from (17.21) into (17.20) yields the following expression for the potential temperature θ_s:

$$\theta_s(z) = T_s \exp\left(\frac{\kappa_d}{H} z\right), \tag{17.23}$$

and using (17.21) and (17.23) to eliminate Π_s and θ_s from the ideal gas law (17.19), the latter can be solved for the density ρ_s yielding:

$$\rho_s(z) = \frac{p_0}{\kappa_d c_{pd} T_s} \exp\left(-\frac{z}{H}\right). \tag{17.24}$$

Furthermore, the following quantities are defined, that will be used in the dispersion relation of the governing equations (Section 17.5):

$$\frac{1}{H_\theta} \equiv \frac{1}{\theta_s}\frac{d\theta_s}{dz}, \tag{17.25}$$

$$\frac{1}{H_\rho} \equiv -\frac{1}{\rho_s}\frac{d\rho_s}{dz}. \tag{17.26}$$

Also the expressions for the basic state buoyancy frequency, N_s, and sound speed, c_s, are:

$$N_s^2 \equiv \frac{g}{\theta_s}\frac{d\theta_s}{dz} = \frac{g}{H_\theta}, \tag{17.27}$$

$$c_s^2 \equiv \frac{\kappa_d}{1-\kappa_d} c_{pd} T_s. \tag{17.28}$$

For the isothermal basic steady state considered here the above quantities take the following values:

$$\frac{1}{H_\theta} = \frac{\kappa_d}{H}, \tag{17.29}$$

$$\frac{1}{H_\rho} = \frac{1}{H}, \tag{17.30}$$

$$N_s^2 = g\frac{\kappa_d}{H} = c_{pd} T_s \frac{\kappa_d^2}{H^2}, \tag{17.31}$$

and the square of the Froude number $F_k \equiv u_s k/N_s$ (where k is the horizontal wavenumber introduced in Section 17.5) can be written as:

$$F_k^2 = \frac{F_H^2 \left(kH\right)^2}{\kappa_d}, \tag{17.32}$$

where

$$F_H^2 \equiv \frac{u_s^2}{R_d T_s} \tag{17.33}$$

and kH are non-dimensional parameters that will be used in the dispersion relation of the governing equations (Section 17.5).

17.3 Linearisation of the time-discretised equations.

The time-discretised equations (17.7), (17.8) - (17.9), and (17.10) - (17.15) are linearised about the steady state defined by (17.17) - (17.19). This is accomplished by writing each dependent variable as the sum of its basic state value (denoted by the subscript s and defined by (17.17)) and a perturbation (denoted by primes), i.e. :

$$u(x,z,t) = u_s + u'(x,z,t), \tag{17.34}$$

$$v(x,z,t) = v'(x,z,t), \tag{17.35}$$

$$w(x,z,t) = w'(x,z,t), \tag{17.36}$$

$$\theta(x,z,t) = \theta_s(z) + \theta'(x,z,t), \tag{17.37}$$

$$\rho(x,z,t) = \rho_s(z) + \rho'(x,z,t), \tag{17.38}$$

$$\Pi(x,z,t) = \Pi_s(z) + \Pi'(x,z,t); \tag{17.39}$$

and substituting (17.34) - (17.39) into the time-discretised equations, neglecting the terms which are nonlinear in the perturbations, and using (17.18) - (17.19) to simplify the resulting expressions.

The following linearised time-discretised equations for the perturbed quantities, u, v, w, θ, ρ and Π (where primes have been dropped for convenience) are thus obtained, where $\mathbf{I}_a$, an anelastic switch ($\mathbf{I}_a = 0$ in the anelastic case and $\mathbf{I}_a = 1$ otherwise), has been added to the equations, which is of use in Section 17.7.

Note that the basic state variables are independent of x and the basic state advection is only in the x-direction. Therefore for a perturbation $Y(x,z,t)$, terms of the form $[X_s(z)Y(x,z,t)]_d$ reduce after linearisation to $X_s(z)[Y(x,z,t)]_d$ and $[Y(x,z,t)]_{dl} \equiv [Y(x,z,t)]_d$. Further, for the linearisation underpinning the stability analysis to be valid, the perturbations are assumed to be small, so that the vertical velocity w satisfies $w\Delta t/\Delta z < 1/2$. Under this assumption $w^* \equiv 0$, since $z_a \equiv z_{dl}$ (i.e. the heights of the arrival and of the nearest model level are the same). The equations are:

$$\frac{u^{n+1} - u_d^n}{\Delta t} = -\left(1-\alpha_3\right) c_{pd}\theta_s \left[\frac{\partial \Pi^n}{\partial x}\right]_d - \alpha_3 c_{pd}\theta_s \frac{\partial \Pi^{n+1}}{\partial x}, \tag{17.40}$$

$$\frac{v^{n+1} - v_d^n}{\Delta t} = 0, \tag{17.41}$$

$$\begin{aligned} \mathbf{I}_h \frac{w^{n+1} - w_d^n}{\Delta t} &= -c_{pd}\theta_s \left\{ \left(1-\alpha_4\right) \left[\frac{\partial \Pi^n}{\partial z}\right]_d + \alpha_4 \frac{\partial \Pi^{n+1}}{\partial z} \right\} \\ &\quad - \left(1-\mathbf{I}_a\right) c_{pd} \frac{d\theta_s}{dz} \left[\left(1-\alpha_4\right)\Pi_d^n + \alpha_4 \Pi^{n+1}\right] \\ &\quad - c_{pd} \frac{d\Pi_s}{dz} \left[\left(1-\alpha_4\right)\theta_d^n + \alpha_4 \theta^{n+1}\right], \end{aligned} \tag{17.42}$$

$$\frac{\theta^{n+1} - \theta_d^n}{\Delta t} = -\frac{d\theta_s}{dz} \left[\left(1-\alpha_2\right) w_d^n + \alpha_2 w^{n+1}\right], \tag{17.43}$$

$$\begin{aligned} \mathbf{I}_a \frac{\rho^{n+1} - \rho^n}{\Delta t} &= -\mathbf{I}_a u_s \frac{\partial \rho^n}{\partial x} - \frac{d\rho_s}{dz}\left[\left(1-\alpha_2\right) w^n + \alpha_2 w^{n+1}\right] \\ &\quad - \rho_s \left[\left(1-\alpha_1\right)\frac{\partial u^n}{\partial x} + \alpha_1 \frac{\partial u^{n+1}}{\partial x} + \left(1-\alpha_2\right)\frac{\partial w^n}{\partial z} + \alpha_2 \frac{\partial w^{n+1}}{\partial z}\right], \end{aligned} \tag{17.44}$$

$$\left(\frac{1-\kappa_d}{\kappa_d}\right)\frac{\Pi^{n+1}}{\Pi_s} = \frac{\rho^{n+1}}{\rho_s} + \frac{\theta^{n+1}}{\theta_s}. \tag{17.45}$$

In the derivation of the $w-$momentum equation, (17.42), (17.18) and (17.43) (solved for θ^{n+1}) have been used. In the derivation of the linearised gas law (17.45), (17.15) has been divided by $\kappa_d \Pi_s \rho_s \theta_s$ and the gas law (17.6) written for the basic state variables, i.e :

$$\frac{p_s}{c_{pd}} = \kappa_d \Pi_s \rho_s \theta_s, \tag{17.46}$$

and the linearised definition of the Exner pressure function, i.e. :

$$\Pi^n = \kappa_d \frac{p^n}{p_s} \left(\frac{p_s}{p_0} \right)^{\kappa_d}, \tag{17.47}$$

have been used in the resulting expression.

17.4 Rewriting the linearised time-discretised equations in operator form.

Following Gravel et al. (1993) the linearised time-discretised equations (17.40) - (17.45) can be written in a way which preserves their continuous form by introducing a number of operators. Let:

$$\begin{aligned}
\frac{D^L F}{Dt} &\equiv \frac{F^{n+1} - F^n_d}{\Delta t}, && (17.48)\\
\frac{D^E F}{Dt} &\equiv \frac{F^{n+1} - F^n}{\Delta t} + u_s \frac{\partial F^n}{\partial x}, && (17.49)\\
\overline{F}^{\alpha_i} &\equiv (1 - \alpha_i) F^n_d + \alpha_i F^{n+1}, && (17.50)\\
\overline{F}^{\tilde{\alpha}_i} &\equiv (1 - \alpha_i) F^n + \alpha_i F^{n+1}, && (17.51)\\
\overline{F}^{\hat{\alpha}_i} &\equiv (1 - \alpha_i) F^n_d + \alpha_i F^n. && (17.52)
\end{aligned}$$

Note that since all operators are linear and have constant coefficients (as u_s is independent of z) they, together with $\partial/\partial x$ and $\partial/\partial z$, all commute. (Note also that the analysis can be applied to the case of a semi-Lagrangian treatment of the density equation by therein redefining $D^E F/Dt$ to be $D^L F/Dt$ and $\overline{F}^{\tilde{\alpha}_i}$ to be $\overline{F}^{\alpha_i}$.)

By using the operators (17.48) - (17.52),the linearised time-discretised equations (17.40) - (17.45) can then be written as:

$$\begin{aligned}
\frac{D^L u}{Dt} &= -c_{pd} \theta_s \frac{\partial \overline{\Pi}^{\alpha_3}}{\partial x}, && (17.53)\\
\frac{D^L v}{Dt} &= 0, && (17.54)
\end{aligned}$$

$$\mathbf{I}_h \frac{D^L w}{Dt} = -c_{pd}\theta_s \frac{\partial \overline{\Pi}^{\alpha_4}}{\partial z} - c_{pd}\left(1-\mathbf{I}_a\right)\frac{d\theta_s}{dz}\overline{\Pi}^{\alpha_4} - c_{pd}\frac{d\Pi_s}{dz}\overline{\theta}^{\alpha_4}, \tag{17.55}$$

$$\frac{D^L \theta}{Dt} = -\frac{d\theta_s}{dz}\overline{w}^{\alpha_2}, \tag{17.56}$$

$$\mathbf{I}_a \frac{D^E \rho}{Dt} = -\frac{d\rho_s}{dz}\overline{w}^{\tilde{\alpha}_2} - \rho_s\left(\frac{\partial \overline{u}^{\tilde{\alpha}_1}}{\partial x} + \frac{\partial \overline{w}^{\tilde{\alpha}_2}}{\partial z}\right), \tag{17.57}$$

together with

$$\left(\frac{1-\kappa_d}{\kappa_d}\right)\frac{\Pi}{\Pi_s} = \frac{\rho}{\rho_s} + \frac{\theta}{\theta_s}. \tag{17.58}$$

17.5 Dispersion relation for the linearised time-discretised equations and vertical decomposition.

$D^L\left[(17.57)/\rho_s\right]/Dt$and $D^E\left[(17.56)/\theta_s\right]/Dt$in $\mathbf{I}_a\left[D^L\left(D^E\,(17.58)/Dt\right)/Dt\right]$ together with $\partial(17.53)/\partial x$ gives:

$$\left(-\frac{1}{H_\rho} + \frac{\partial}{\partial z}\right)\frac{D^L}{Dt}\overline{w}^{\tilde{\alpha}_2} + \mathbf{I}_a \frac{1}{H_\theta}\frac{D^E}{Dt}\overline{w}^{\alpha_2} = c_{pd}\theta_s\Pi_s\frac{\partial^2}{\partial x^2}\left(\frac{\overline{\Pi}^{\alpha_3,\tilde{\alpha}_1}}{\Pi_s}\right) - \mathbf{I}_a\left(\frac{1-\kappa_d}{\kappa_d}\right)\frac{D^E}{Dt}\frac{D^L}{Dt}\left(\frac{\Pi}{\Pi_s}\right), \tag{17.59}$$

and $1/\left(c_{pd}\theta_s\Pi_s\right)\left(D^L\,(17.55)/Dt\right)$with $(17.56)/\theta_s$and grouping together the terms depending on $D^L\left(\overline{\Pi}^{\alpha_4}/\Pi_s\right)/Dt$ on the left-hand side gives:

$$\left[(1-\mathbf{I}_a)\frac{1}{H_\theta} + \frac{1}{\Pi_s}\frac{d\Pi_s}{dz} + \frac{\partial}{\partial z}\right]\frac{D^L}{Dt}\left(\frac{\overline{\Pi}^{\alpha_4}}{\Pi_s}\right) = \frac{1}{H_\theta}\left(\frac{1}{\Pi_s}\frac{d\Pi_s}{dz}\right)\overline{w}^{\alpha_2,\alpha_4} - \mathbf{I}_h\frac{1}{c_{pd}\theta_s\Pi_s}\frac{D^L}{Dt}\left(\frac{D^L w}{Dt}\right). \tag{17.60}$$

A single equation for w (or Π) can be obtained by eliminating Π (or w) between (17.59) and (17.60) for a general reference profile. However, to simplify things an isothermal state (see Section 17.2.1)is chosen so that

$$\theta_s\Pi_s = T_s,\ H_\rho = H,\ H_\theta = \frac{H}{\kappa_d},\ \frac{1}{\Pi_s}\frac{d\Pi_s}{dz} = -\frac{1}{H_\theta} = -\frac{\kappa_d}{H},\ \text{where } H \equiv \frac{R_d T_s}{g} = \text{constant}. \tag{17.61}$$

Then eliminating Π/Π_s between (17.59) and (17.60) gives:

$$\begin{aligned}\left(-\frac{\kappa_d}{H}\mathbf{I}_a + \frac{\partial}{\partial z}\right)\frac{D^L}{Dt}&\left\{\left(-\frac{1}{H} + \frac{\partial}{\partial z}\right)\frac{D^L}{Dt}\left(\overline{w}^{\tilde{\alpha}_2,\alpha_4}\right) + \mathbf{I}_a\frac{\kappa_d}{H}\frac{D^E}{Dt}\left(\overline{w}^{\alpha_2,\alpha_4}\right)\right\} \\ &= c_{pd}T_s\frac{\partial^2}{\partial x^2}\left\{-\frac{\kappa_d^2}{H^2}\overline{w}^{\alpha_2,\alpha_4,\alpha_3,\tilde{\alpha}_1} - \mathbf{I}_h\frac{1}{c_{pd}T_s}\frac{D^L}{Dt}\left(\frac{D^L\overline{w}^{\alpha_3,\tilde{\alpha}_1}}{Dt}\right)\right\} \\ &- \mathbf{I}_a\left(\frac{1-\kappa_d}{\kappa_d}\right)\frac{D^E}{Dt}\frac{D^L}{Dt}\left\{-\frac{\kappa_d^2}{H^2}\overline{w}^{\alpha_2,\alpha_4} - \mathbf{I}_h\frac{1}{c_{pd}T_s}\frac{D^L}{Dt}\left(\frac{D^L w}{Dt}\right)\right\} \quad .\end{aligned} \tag{17.62}$$

Aside :

For an isothermal basic steady state, using (17.61) *in* (17.60) *leads to:*

$$\left(-\mathbf{I}_a\frac{\kappa_d}{H}+\frac{\partial}{\partial z}\right)\frac{D^L}{Dt}\left(\frac{\overline{\Pi}^{\alpha_4}}{\Pi_s}\right)=-\frac{\kappa_d^2}{H^2}\overline{w}^{\alpha_2,\alpha_4}-\mathbf{I}_h\frac{1}{c_{pd}T_s}\frac{D^L}{Dt}\left(\frac{D^L w}{Dt}\right). \quad (17.63)$$

Taking $(-\mathbf{I}_a\kappa_d/H+\partial/\partial z)\left(\overline{D^L}^{\alpha_4}\ (17.59)/Dt\right)$ *and eliminating the terms depending on* $(-\mathbf{I}_a\kappa_d/H+\partial/\partial z)\left[D^L\left(\overline{\Pi}^{\alpha_4}/\Pi_s\right)/Dt\right]$ *via* (17.63) *in the resulting expression, finally yields* (17.62).

The continuous form of (17.62) is recovered by setting $D^L/Dt \equiv D/Dt$, $D^E/Dt \equiv D/Dt$, and removing all the flavours of the α_i averaging operators. Thiscontinuous equation is fourth order in time with only even powers of the time derivative appearing. The four physical modes are two acoustic ones and two gravity wave ones (the slow "Rossby" mode has been lost by dropping the v-momentum equation which was decoupled by dropping the Coriolis terms). Either of the hydrostatic or anelastic approximations reduces the equation to only second order in time and thereby filters out the acoustic modes.

Analysis of the continuous form of (17.62) yields normal modes of the form discussed in Section 3.

This therefore suggests a vertical decomposition for the discrete equation (17.62) of the form:

$$w(x,z,t)=\sum_m w_m(x,t)\exp\left[i\left(m+\frac{1}{2H}\right)z\right], \quad (17.64)$$

with m real. This expansion only holds for the "internal" modes. The "external" mode is excluded from the analysis since $w=0$ for this mode. Its analysis is however considered in Appendix K.

Further, to derive the dispersion relation, w_m is expressed as:

$$w_m(x,t)=\hat{w}_m\exp\left[i\left(kx+\omega t\right)\right]. \quad (17.65)$$

Define:

$$C=ku_s\Delta t,\qquad E=\exp\left(i\omega\Delta t\right),\qquad P=\exp\left(-iC\right),\qquad \text{and}\qquad P_E=1-iC. \quad (17.66)$$

The discretisation operators (17.48) - (17.52) then take the following forms:

$$\frac{D^L F}{Dt} \equiv \frac{1}{\Delta t}\left(E-P\right)F, \quad (17.67)$$

$$\begin{aligned}
\frac{D^E F}{Dt} &\equiv \frac{1}{\Delta t}\left(E - P_E\right) F, &(17.68)\\
\overline{F}^{\alpha_i} &\equiv \left[\alpha_i E + (1-\alpha_i) P\right] F, &(17.69)\\
\overline{F}^{\tilde{\alpha}_i} &\equiv \left[\alpha_i E + (1-\alpha_i)\right] F, &(17.70)\\
\overline{F}^{\hat{\alpha}_i} &\equiv \left[\alpha_i + (1-\alpha_i) P\right] F, &(17.71)\\
\frac{\partial F}{\partial x} &\equiv ikF, &(17.72)\\
\frac{\partial F}{\partial z} &\equiv i\left[m - i/(2H)\right] F. &(17.73)
\end{aligned}$$

Eq. (17.62) then becomes a fourth order complex-coefficient polynomial in E. (The following analysis is comparable to that of Tanguay et al. (1990) except they use centred time averaging, so that all α's take the value 1/2, and so instead of using $\exp(i\omega\Delta t)$ they work in terms of $\tan(\omega\Delta t)$.) In general, this quartic has to be solved numerically - this is done in Sections 17.8 and 17.9. However, some analytical results can be obtained for the special cases examined in the following Sections 17.6 and 17.7.

17.6 Semi-Lagrangian discretisation of the continuity equation.

To start with, the stability properties of the scheme can be considered analytically if all advection (including that of density) is evaluated using the semi-Lagrangian method. Then:

$$\frac{D^E F}{Dt} \longrightarrow \frac{D^L F}{Dt}, \qquad (17.74)$$

and

$$\overline{F}^{\tilde{\alpha}_i} \longrightarrow \overline{F}^{\alpha_i}. \qquad (17.75)$$

If further, $\alpha_i = \alpha$ for all i, and $X = (E/P - 1)^{-1}$ then (17.62) can be written as:

$$\frac{C^2\kappa_d}{F_H^2 (kH)^2}(X+\alpha)^4 + \left[\frac{m^2 + 1/(4H^2)}{k^2} + \mathbf{I}_h\right](X+\alpha)^2 + \mathbf{I}_a\mathbf{I}_h(1-\kappa_d)\frac{F_H^2}{C^2} = 0, \qquad (17.76)$$

where $F_H^2 = u_s^2/(R_d T_s)$.

The solution for $(X+\alpha)^2$ is:

$$(X+\alpha)^2 = \frac{-Y \pm \sqrt{Y^2 - Z}}{2C^2\kappa_d/\left[F_H^2 (kH)^2\right]}, \qquad (17.77)$$

where

$$Y = \frac{m^2 + 1/(4H^2)}{k^2} + \mathbf{I}_h, \qquad (17.78)$$

and

$$Z = \frac{4\kappa_d (1 - \kappa_d)}{(kH)^2} \mathbf{I}_a \mathbf{I}_h, \tag{17.79}$$

with both Y and Z positive.

Then, since $(kH - 1/2)^2 + (mH)^2 > 0$ and $1 > 4\kappa_d (1 - \kappa_d) = 40/49$, it can be shown that:

$$\left[1 + \frac{m^2 + 1/(4H^2)}{k^2}\right]^2 > \frac{4\kappa_d (1 - \kappa_d)}{(kH)^2}, \tag{17.80}$$

so that $Y^2 - Z > 0$ and also $\sqrt{Y^2 - Z} < Y$ from which it follows that $(X + \alpha)^2 < 0$ (true also for $\mathbf{I}_a = 0$ and $\mathbf{I}_h = 0$). Hence

$$X + \alpha = \pm a i, \tag{17.81}$$

for some real number a. Substituting now for X in terms of E/P gives:

$$\left|\frac{E}{P}\right|^2 = 1 - \frac{(2\alpha - 1)}{(a^2 + \alpha^2)}, \tag{17.82}$$

so $2\alpha - 1 \geq 0$, or $\alpha \geq 1/2$, is required for the stability of the scheme. Note that this is a necessary condition for stability. It may not be sufficient since all possible terms of the governing equations are not included in this analysis (e.g. the Coriolis terms). Despite the limitations of this analysis, this result is however of interest, since it shows that the governing equations may be stably integrated using the semi-Lagrangian scheme, in contrast with the results obtained with the Eulerian approximation of the continuity equation (the standard New Dynamics implementation, i.e. mixed semi-Lagrangian and Eulerian advection), in which case, for any settings of the semi-implicit weights α_i, there are values of the non-dimensional parameters for which the scheme is unstable, as discussed in Sections 17.8 and 17.9.

17.7 Eulerian discretisation of the continuity equation.

The dispersion relation associated with the Eulerian discretisation of the continuity equation is (17.62). To make further progress analytically, further simplification is needed in this case. This is provided by either the anelastic ($\mathbf{I}_a = 0$) or the hydrostatic ($\mathbf{I}_h = 0$) approximations, which are examined in Sections 17.7.1 and 17.7.2.

17.7.1 The anelastic ($\mathbf{I}_a = 0$) case.

First consider the anelastic case, $\mathbf{I}_a = 0$, which is of interest since then, unless the semi-implicit weights are chosen so that $\alpha_1 = \alpha_2$ and $\alpha_3 = \alpha_4$, the dispersion relation admits two computational modes, alongside the two physical gravity modes. In fact inspection of (17.62) shows that the equation remains fourth order in E in contrast to the continuous form, i.e. two numerical modes have been introduced. Noting the multiplicative form of the averaging operators it is clear that if α_4 is equal to α_3 and α_2 is equal to α_1 then these two computational modes factorise out. For this anelastic case the terms involving α_1 and α_2 occur in the density equation and the potential computational mode arises due to use of different temporal averaging of the two components of the divergence field. Setting $\alpha_1 = \alpha_2$ sets the time averages equal to each other and leads to a spurious temporal averaging operator which can be ignored. The other computational mode arises from the potentially different time weighting employed to calculate both the pressure terms in the $u-$ and $w-$momentum equations. Setting $\alpha_3 = \alpha_4$ leads to the terms involving these parameters factorising out of the dispersion equation and leaves a computational solution:

$$E = -\frac{(1-\alpha_3)}{\alpha_3} P. \tag{17.83}$$

This mode is stable for $\alpha_3 \geq 1/2$ and is strongly damped for values of α_3 close to one but is undamped or neutrally stable when this parameter takes the value $1/2$. It is a temporal computational mode as it changes sign at alternate timesteps. The mode arises because in the anelastic case pressure is no longer a prognostic quantity, its role is to respond to the momentum accelerations in order to maintain the now time-independent continuity requirement. Therefore, it has no real time level associated with it and applying a time-averaging operator leads to the introduction of this computational mode. Further, if $\alpha_3 \neq \alpha_4$ the effect of this mode does not factorise out of the equations and will contaminate the physical gravity modes. Currently α_3 takes the value 0.6. Resetting it to unity would better control this mode, but at the expense of increasing the damping of physical modes.

The numerical form of the two physical gravity modes is determined by the quadratic:

$$(\alpha_1\alpha_3 + \beta)\left(\frac{E}{P}\right)^2 + \left[\alpha_1(1-\alpha_3) + \alpha_3(1-\alpha_1) - 2\beta\right]\left(\frac{E}{P}\right) + \left[(1-\alpha_1)(1-\alpha_3) + \beta\right] = 0, \tag{17.84}$$

where

$$\beta = \frac{m^2 + 1/\left(4H^2\right) + \mathbf{I}_h k^2}{k^2 N_s^2 \Delta t^2}, \tag{17.85}$$

and $\varpi = \pm\beta^{-1/2}/\Delta t$ is the dispersion relation for both the anelastic and hydrostatic forms of the continuous equations.

Eq. (17.84) has solutions:

$$\frac{E}{P} = \frac{-\alpha_1 - \alpha_3 + 2\left(\alpha_1\alpha_3 + \beta\right) \pm \sqrt{\left(\alpha_1 + \alpha_3\right)^2 - 4\left(\alpha_1\alpha_3 + \beta\right)}}{2\left(\alpha_1\alpha_3 + \beta\right)}. \tag{17.86}$$

If $\left(\alpha_1 + \alpha_3\right)^2 - 4\alpha_1\alpha_3 \geq 4\beta$ then stable solutions require $4\beta \geq \alpha_1 + \alpha_3 - 4\alpha_1\alpha_3$ and $4\beta \geq \alpha_1 + \alpha_3 - 4\alpha_1\alpha_3 - \left(1 - \alpha_1 - \alpha_3\right)$. These are both satisfied for all non-negative β if $\alpha_1 \geq 1/2$ and $\alpha_3 \geq 1/2$ as then $\alpha_1 + \alpha_3 - 4\alpha_1\alpha_3 - \left(1 - \alpha_1 - \alpha_3\right) = -\left(1 - 2\alpha_1\right)\left(1 - 2\alpha_3\right) \leq 0$.

If $\left(\alpha_1 + \alpha_3\right)^2 - 4\alpha_1\alpha_3 < 4\beta$ then stability requires:

$$\left(\beta + \alpha_1\alpha_3\right)\left(1 - \alpha_1 - \alpha_3\right) \leq 0, \tag{17.87}$$

i.e. $\alpha_1 + \alpha_3 \geq 1$.

Combining these it is seen that stable solutions are found for all non-negative values of β provided both α_1 and α_3 are greater than or equal to $1/2$.

17.7.2 The hydrostatic ($\mathbf{I}_h = 0$) case.

Now consider the hydrostatic case $\mathbf{I}_h = 0$. With $\mathbf{I}_h = 0$ (17.62) factorises to a third order polynomial times $\left[\alpha_4 E + \left(1 - \alpha_4\right) P\right]$. This term arises due to what is now an unnecessary temporal averaging of the $w-$momentum equation and is spurious. The remaining computational mode arises due to the different form of averaging used in the density and temperature equations (i.e. $\overline{F}^{\tilde{\alpha}_2}$ compared with $\overline{F}^{\alpha_2}$). This mode can be removed by setting $\alpha_2 = 1$, as is currently done in the New Dynamics, which leaves a spurious solution $E = 0$. However, this will unfortunately damp the horizontally propagating gravity modes via the right-hand side of (17.56). These two physical gravity modes are determined by the remaining quadratic given by:

$$\begin{aligned}\left(\beta + \alpha_1\alpha_3\right) E^2 + \left\{\beta\left[-2P + B\left(P_E - P\right)\right] + P\left(1 - \alpha_3\right)\alpha_1 + \alpha_3\left(1 - \alpha_1\right)\right\} E \\ +P\left\{\beta\left[P - B\left(P_E - P\right)\right] + \left(1 - \alpha_1\right)\left(1 - \alpha_3\right)\right\} = 0,\end{aligned} \tag{17.88}$$

where

$$B = \left(\frac{\kappa_d \mathbf{I}_a}{H}\right)\left(\frac{-\frac{1}{2H} + im}{\frac{1}{4H^2} + m^2}\right), \tag{17.89}$$

is complex, and β is as defined in (17.85) with $\mathbf{I}_h = 0$.

If we denote the two roots of this equation by E_1 and E_2 then it follows that:

$$|E_1|\,|E_2| = \left|\frac{\beta\left[1 - B\left(\frac{P_E}{P} - 1\right)\right] + P^{-1}\left(1-\alpha_1\right)\left(1-\alpha_3\right)}{\beta + \alpha_1\alpha_3}\right|, \tag{17.90}$$

where $|P| = 1$ has been used. Therefore, since β is non-negative, instability is guaranteed ($|E_1||E_2| > 1$) if:

$$\Re\left\{\beta B\left(1 - \frac{P_E}{P}\right) + P^{-1}\left(1-\alpha_1\right)\left(1-\alpha_3\right)\right\} > \alpha_1\alpha_3, \tag{17.91}$$

where $\Re$ denotes "real part of". This can be written as:

$$\begin{aligned} &-1 + \cos(C) + C\sin(C) + (2Hm)\left[\sin(C) - C\cos(C)\right] \\ &\qquad > \frac{2C^2}{F_H^2}\left[\alpha_1\alpha_3 - \left(1-\alpha_1\right)\left(1-\alpha_3\right)\cos(C)\right]. \end{aligned} \tag{17.92}$$

Then if α_1 and α_3 are restricted to lie between 1/2 and 1, for fixed value of α_1 (α_3), the right-hand side of (17.92) is an increasing function of α_3 (α_1). Therefore, reducing the values of α_1 and α_3 from some value will make the instability more likely to occur. Thus, if instability is found for $\alpha_1 = \alpha_3 = 1$, instability is also guaranteed for smaller values of α_1 and α_3. Therefore these values are chosen for further analysis. Some further progress can be made analytically by considering certain limits of the various parameters.

Typically $mH \gg 1$ and therefore for large values of C the left hand side is maximised for values of C close to $(2n+1)\pi$ for some integer n. For this value of C, after multiplying through by $2F_H^2$ and rearranging, (17.92) then reduces to:

$$4C^2 - 4\left(mH\right)CF_H^2 < -4F_H^2. \tag{17.93}$$

Completing the square on the left-hand side of (17.93) and rearranging yields:

$$\left[\left(mH\right)F_H^2 - 2C\right]^2 < F_H^2\left[\left(mH\right)^2 F_H^2 - 4\right], \tag{17.94}$$

so that instability is possible only if $2C$ is close in value to $\left(mH\right)F_H^2$ and $\left(mH\right)^2 F_H^2 > 4$.

For small values of C the trigonometric functions can be expanded and, to leading order in C, the inequality then approximates to:

$$\frac{16}{3}\left(mH\right)C > \frac{16}{F_H^2} - 4. \tag{17.95}$$

Noting that typically $F_H^2 \ll 1$ this further approximates to the requirement $(mH)\,F_H^2 > 3/C$.

With these values of α_1 and α_3 numerical investigation of (17.92) shows that instability is possible for:

$$(mH)\,F_H^2 \gtrsim 10, \tag{17.96}$$

for which values there is then a range of values of C for which instability is possible, this range increasing with $(mH)\,F_H^2$. Further, for $\alpha_1 = \alpha_3 = 1/2$, the range of values of C for which instability occurs increases and also the critical value of $(mH)\,F_H^2$ decreases. The requirement that mH exceed some value implies that it is the shortest vertical wavelengths which are the most unstable. Also, for small values of C, the presence of C on the left-hand side of (17.95) suggests that the shortest horizontal wavelengths are the most unstable. Finally, note that instability is always guaranteed for sufficiently large values of mH and therefore for sufficiently high vertical resolution.

17.8 Numerical solution of the dispersion relation.

In Sections 17.7.1 and 17.7.2 the analytical solutions to the dispersion relation associated with the mixed semi-Lagrangian and Eulerian time-discretisation of the governing equations, (17.62), have been discussed in the simplified hydrostatic and anelastic cases. In this section the dispersion relation is solved numerically and the results obtained in the hydrostatic (see Section 17.8.1) and nonhydrostatic (see Section 17.8.2)cases are compared. Note that the effect of interpolation in the semi-Lagrangian discretisation has not been included in this analysis. Since the response function of the interpolation operator is known to introduce numerical damping (Gravel et al. 1993), it may help to control instabilities, except for integer Courant numbers, for which interpolation is exact. This aspect is examined in Section 17.9.

The algebraic form of the dispersion relation associated with the mixed semi-Lagrangian and Eulerian time-discretisation of the governing equations (17.53) - (17.58) is obtained by substituting for the discretisation operators (17.67) - (17.73) into (17.62), i.e. (after multiplying by Δt^2):

$$\begin{aligned}\left[-\frac{\kappa_d}{H}\mathbf{I}_a + i\left(m - \frac{i}{2H}\right)\right]\left[\alpha_4 E + (1-\alpha_4)\,P\right]\Bigg\{\left[-\frac{1}{H} + i\left(m - \frac{i}{2H}\right)\right](E-P)^2\left[\alpha_2 E + (1-\alpha_2)\right] \\ +\mathbf{I}_a\frac{\kappa_d}{H}(E-P)\,(E-P_E)\left[\alpha_2 E + (1-\alpha_2)\,P\right]\Bigg\} \\ = \left\{c_{pd}T_s k^2\Delta t^2\left[\alpha_3 E + (1-\alpha_3)\,P\right]\left[\alpha_1 E + (1-\alpha_1)\right] + \mathbf{I}_a\frac{1-\kappa_d}{\kappa_d}(E-P)\,(E-P_E)\right\}\end{aligned}$$

$$\times \left\{ \frac{\kappa_d^2}{H^2} \left[\alpha_2 E + (1-\alpha_2) P\right] \left[\alpha_4 E + (1-\alpha_4) P\right] + \mathbf{I}_h \frac{1}{c_{pd} T_s} \frac{(E-P)^2}{\Delta t^2} \right\}. \tag{17.97}$$

By noting that

$$c_{pd} T_s k^2 \Delta t^2 = \frac{1}{\kappa_d} \frac{R_d T_s}{u_s^2} (k u_s \Delta t)^2 = \frac{1}{\kappa_d} \frac{C^2}{F_H^2}, \tag{17.98}$$

(17.97), after multiplying by H^2, can be rewritten in terms of the non-dimensional parameters

$$mH, \ kH, \ F_H^2 \equiv u_s^2 / (R_d T_s), \text{ and } C \equiv k u_s \Delta t, \tag{17.99}$$

as

$$\begin{aligned}
&\left[-\mathbf{I}_a \kappa_d + \frac{i}{2}(2mH - i)\right] \left[\alpha_4 E + (1-\alpha_4) P\right] \left\{ \frac{i}{2} (2mH + i)(E-P)^2 \left[\alpha_2 E + (1-\alpha_2)\right] \right.\\
&\qquad \left. + \mathbf{I}_a \kappa_d (E-P)(E-P_E) \left[\alpha_2 E + (1-\alpha_2) P\right] \right\}\\
&= \left\{ \frac{1}{\kappa_d} \frac{C^2}{F_H^2} \left[\alpha_3 E + (1-\alpha_3) P\right] \left[\alpha_1 E + (1-\alpha_1)\right] + \mathbf{I}_a \frac{1-\kappa_d}{\kappa_d} (E-P)(E-P_E) \right\}\\
&\quad \times \kappa_d \left\{ \kappa_d \left[\alpha_2 E + (1-\alpha_2) P\right] \left[\alpha_4 E + (1-\alpha_4) P\right] + \mathbf{I}_h (kH)^2 \frac{F_H^2}{C^2} (E-P)^2 \right\}.
\end{aligned} \tag{17.100}$$

Eq. (17.100) has been solved numerically using the *NAG* (Numerical Algorithm Group) library routine $C02AFF$ for an isothermal basic state with $T_s = 273.15K$ (which corresponds to a constant value of the scale height of the atmosphere $H \equiv R_d T_s / g \approx 7993m$), considering first the hydrostatic case (i.e. $\mathbf{I}_h = 0$ in (17.100), see Section 17.8.1), and generalising then the analysis to the nonhydrostatic case (i.e. $\mathbf{I}_h = 1$ in (17.100), see Section 17.8.2). Since the routine $C02AFF$ has been found to fail for some choices of the parameters, some of the results have been obtained by solving the dispersion relation using the routine $ZROOTS$ (Press, Teukolsky, Vetterling & Flannery 1992).

17.8.1 The hydrostatic ($\mathbf{I}_h = 0$) case.

Since kH only appears in the dispersion relation (17.100) multiplied by $\mathbf{I}_h$, the non-dimensional parameters governing the dispersion relation in the hydrostatic case are mH, F_H^2, and C. Solutions to (17.100) have been obtained for a range of values of each of these parameters. They have been varied independently in the ranges $mH \in [\pi, 15\pi]$, $F_H^2 \equiv u_s^2/R_d T \in [0, 0.3]$, and $C \equiv k u_s \Delta t \in [0, 1000]$, these ranges being chosen in such a way that the corresponding values of the horizontal wavenumber index and windspeed vary approximately in the physically relevant range $k \in [2\pi \cdot 10^{-6},\, 2\pi \cdot 10^{-3}]m^{-1}$ and $u_s \in [0,\, 150]ms^{-1}$, respectively. More specifically, the intervals in which mH and F_H^2 vary have been sampled using 30 and 50 equidistant points, and for F_H^2, the first sampling point is 10^{-17}, instead of zero (this is done to prevent u_s from being zero, which is needed to avoid dividing by zero in the code used to solve the dispersion relation). As to the parameter C, the tests have been performed by varying its value in the subintervals [0.01, 10], [10, 100], and [100, 1000] and sampling each of them using 100 points. Again the value of zero has not been used for C, since u_s is nonzero. A timestep of $\Delta t = 1000s$ is initially used: note that the timestep does not appear explicitly in the dispersion relation, it enters however in the definition of the parameter C.

When the semi-implicit weights are set to $\alpha_i = 1$ for all i (i.e. for the purely implicit scheme which is expected, a priori, to favour stability), a very weak instability starts to manifest itself for $(mH)\, F_H^2 \approx 2.2$ and for fairly small values of C ($C \in [1.7, 2.1]$ approximately). Increasing the value of $(mH)\, F_H^2$, the range of values of C for which instability occurs becomes wider, up to a maximum range of approximately $0.2 < C < 4$, which is attained for $(mH)\, F_H^2 > 8$. For $(mH)\, F_H^2 > 9$, as well as for the aforementioned range of values of C, a very weak instability (at most $\max|E| \approx 1.009$) also appears for $8.5 < C < 10.2$ approximately. Note however that with the values of the parameters considered in the tests, such a value of $(mH)\, F_H^2$ may only be achieved for $mH > 10\pi$, i.e. for vertical wavelengths shorter than would be typically associated with the height of the boundary layer (if one were present), given by $h_{BL} \approx H/10$. These numerical results are consistent with the approximation of the dispersion relation for small values of C, (17.95), and also with the condition derived from its further approximation, (17.96). They also show that instability is however possible even for values of $(mH)\, F_H^2$ smaller than those predicted by (17.96), as expected, since the latter has been derived by the approximation of a sufficient condition.

The numerical results have been examined by plotting the values of the maximum modulus of the roots of the dispersion relation as a function of the parameters $C \equiv ku_s\Delta t$, and $F_H^2 \equiv u_s^2/\left(R_dT_s\right)$, for fixed values of the parameter mH. Looking at the plots corresponding to each of the $mH-$sections shows that, for fixed values of the parameter mH, the instability grows more rapidly (albeit always very slowly) as F_H^2 increases. Furthermore, comparing the results obtained for different $mH-$sections and for fixed values of $(mH)\, F_H^2$, it is found that the instability is more rapid for smaller values of the parameter mH (i.e. for longer vertical wavelengths). Note however that the instability observed for the values of the semi-implicit weights of $\alpha_i = 1$ for all i is always very weak, with the maximum modulus of the roots of the dispersion relation reaching at most the value of $|E| \approx 1.013$. It is also worth noting that in this case ($\alpha_i = 1$ for all i), and when the parameter space is sampled as explained at the beginning of the Section, the scheme becomes stable when the effect of interpolation is taken into account (see Section 17.9).

As an example of the numerical results, in Figs. 17.1 and 17.2, the plots obtained for $mH \approx 16.79$ and $mH = 15\pi \approx 47.12$, respectively are displayed. The former is the $mH-$section for which the modulus of the roots of the dispersion relation attains its maximum value; the latter shows the second of the previously discussed ranges of values of the parameter C leading to instability, i.e. $8.5 < C < 10.2$. In the figures only the contours corresponding to values of the maximum of the modulus of the roots of the dispersion relation close to one, which are those of interest for the stability analysis, are shown. The continuous contours are associated with values of the maximum of the modulus of the roots of the dispersion relation larger than one (i.e. they denote regions of the parameter space for which instability occurs), the dashed ones correspond to values smaller than one. The x axis in the plot is associated with the parameter C, whose range of values in the plots is restricted to that for which instability has been observed. On the y axis the values of the product $(mH)\,F_H^2$ are displayed.

When the semi-implicit weights are set to their current values of $\alpha_1 = \alpha_3 = 0.6$, and $\alpha_2 = \alpha_4 = 1$, as expected, the instability is more rapid (the maximum modulus of the roots of the dispersion relation reaches at most the value of $|E| \approx 1.15$). Furthermore the critical value of $(mH)\,F_H^2$, for which instability starts to appear, becomes smaller, the ranges of values of the parameter C leading to instability are more numerous, and they are not necessarily limited to small values of C. These results are consistent with the discussion following (17.96). Also, with this setting of the semi-implicit weights, the damping effect of interpolation is not sufficient to stabilise the scheme (see Section 17.9 for the details).

Unlike the purely implicit scheme ($\alpha_i = 1$ for all i), the critical value of $(mH)\,F_H^2$ which gives rise to instability varies between the sections obtained for different values of the parameter mH in the range considered in the present study (i.e. $mH \in [\pi, 15\pi]$), ranging between $(mH)\,F_H^2 \approx 0.02$ for $mH = \pi$ and $(mH)\,F_H^2 \approx 0.22$ for $mH = 15\pi$. Similarly,

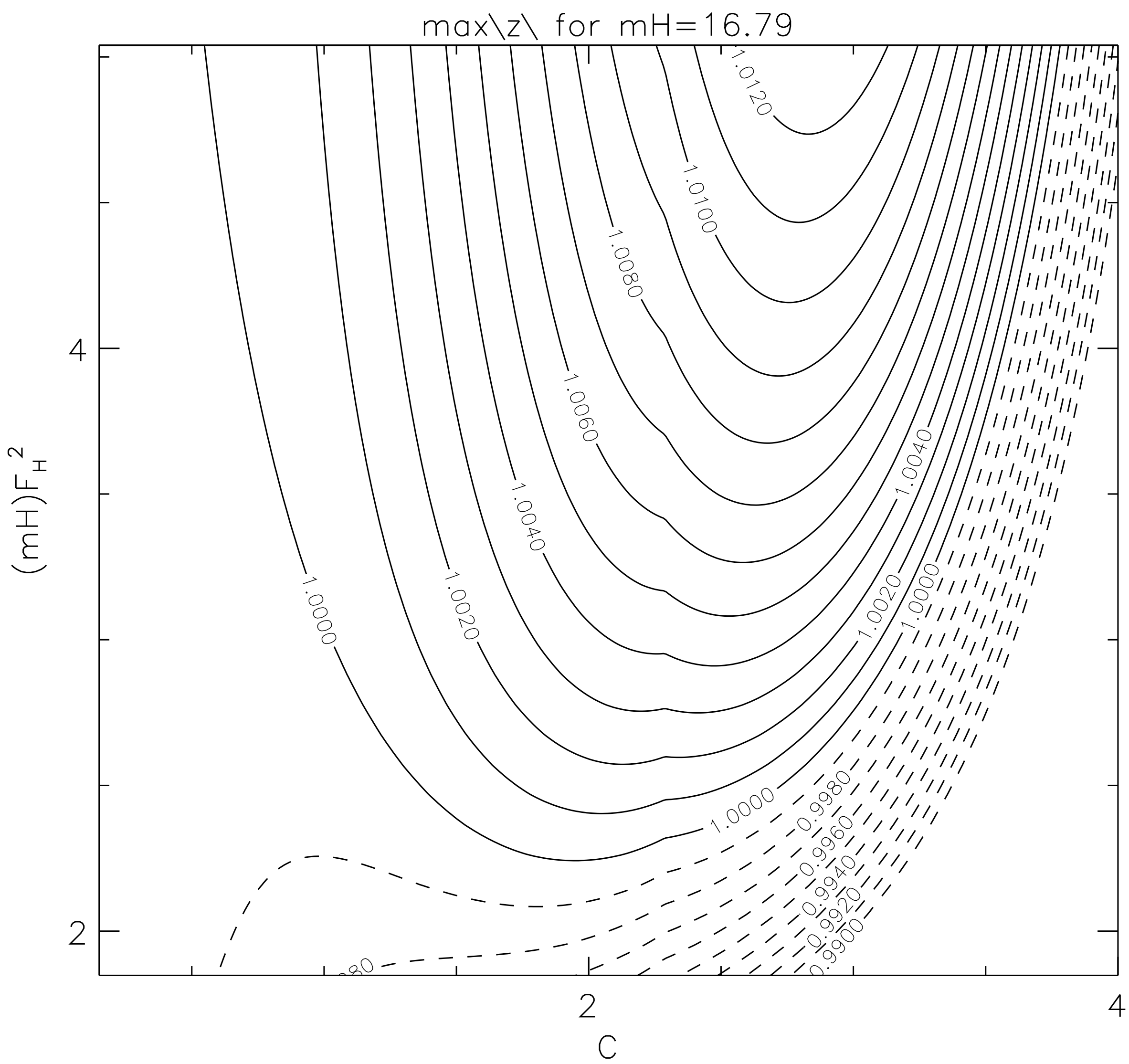

Figure 17.1: Maximum modulus of the roots of the dispersion relation plotted as a function of C and $(mH)F_H^2$ in the hydrostatic case with $\alpha_i = 1$ for all i, and for $mH \approx 16.79$. The scale on the C axis is restricted to four since instability has been not observed for larger values of C.

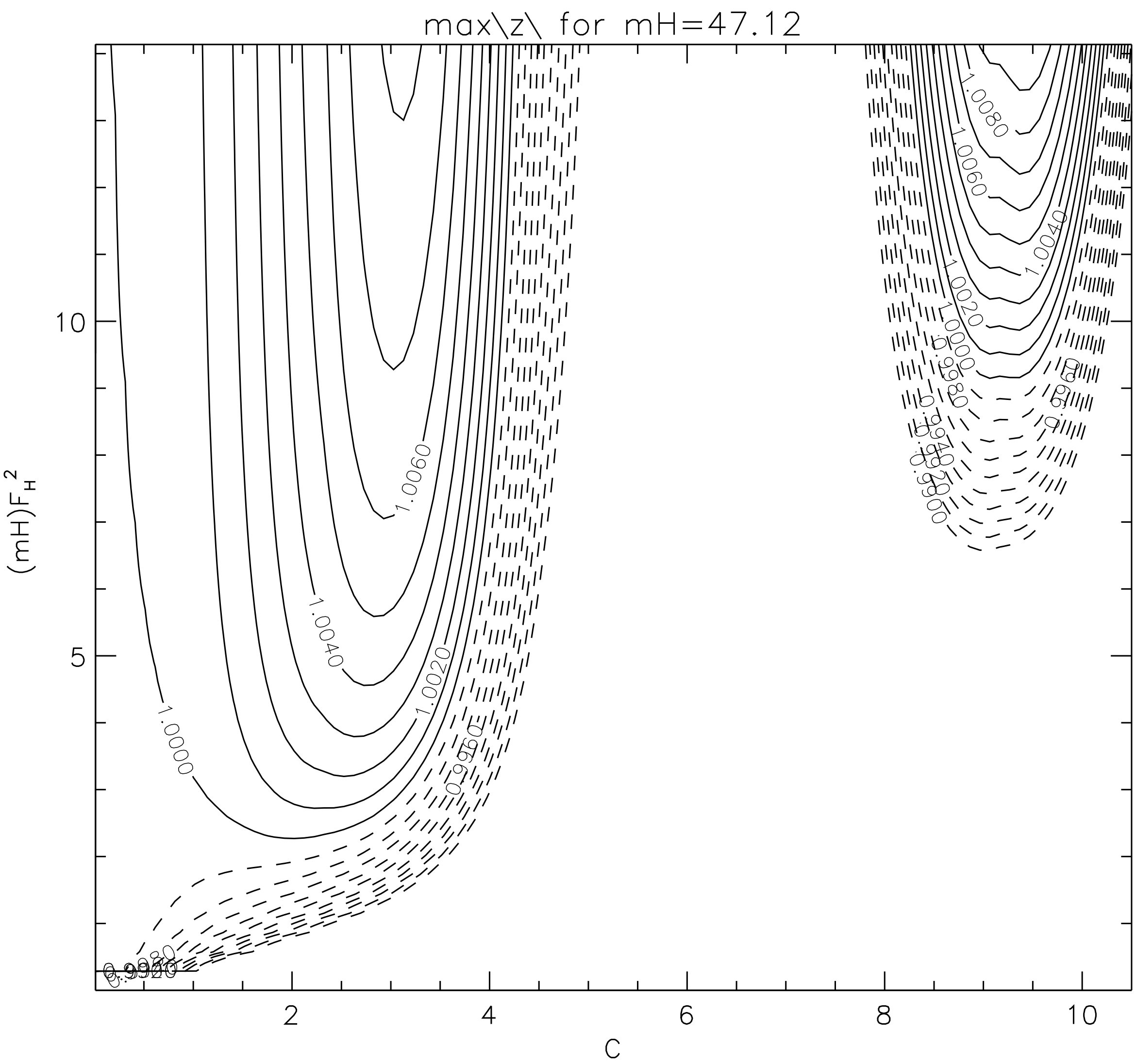

Figure 17.2: Maximum modulus of the roots of the dispersion relation plotted as a function of C and $(mH)F_H^2$ in the hydrostatic case with $\alpha_i = 1$ for all i, and for $mH \approx 47.12$. The values of C for which instability is observed do not exceed $C \approx 10.2$.

the associated ranges of values of the parameter C for which instability occurs, differ from one $mH-$section to another. Apart from the differences in the specific values of the parameters, however, the plots obtained for each of the sections show that, for small values of $(mH)\,F_H^2$ the instability starts to appear for small values of the parameter C (approximately $C < 3$). As $(mH)\,F_H^2$ increases, the instability also progressively spreads to other ranges of the parameter C (approximately $3.5 < C < 5.5$ and $7 < C < 9$), eventually reaching values of C increasingly larger than 10, for sufficiently large values of $(mH)\,F_H^2$, which again vary depending on the $mH-$section considered. The required value of $(mH)\,F_H^2$ becomes smaller and the corresponding values of the parameter C become larger for larger values of mH. These general features of the results are also consistent with those of the previously discussed plots obtained for the purely implicit scheme.

To illustrate the results summarised above, in Figs. 17.3 and 17.4 the maximum of the modulus of the roots of the dispersion relation is plotted as a function of C and $(mH)\,F_H^2$ for

Fig. 17.3 $mH \approx 9.2$ and (a): $C < 10$; (b): $10 < C < 20$

Fig. 17.4 $mH \approx 31.96$ and (a): $C < 10$; (b): $10 < C < 30$; (c): $30 < C < 60$; (d): $60 < C < 80$.

The former has been chosen as one of the sections for which the maximum modulus of the roots of the dispersion relation attains the largest value. The latter provides an example of the largest ranges of values of the parameter C leading to instability observed in our tests.

17.8.2 The nonhydrostatic ($\mathbf{I}_h = 1$) case.

In the nonhydrostatic case, the dispersion relation (17.100) depends upon the four non-dimensional parameters defined in (17.99), so that, in addition to those already discussed in the hydrostatic case, namely mH, $F_H^2 \equiv u_s^2/\left(R_dT_s\right)$, and $C \equiv ku_s\Delta t$, the further non-dimensional quantity kH, in principle, should be varied independently of the others. However, for given values of mH, F_H^2, and C, choosing H, or equivalently T_s, determines u_s as:

$$u_s \equiv \sqrt{F_H^2 R_d T_s}. \tag{17.101}$$

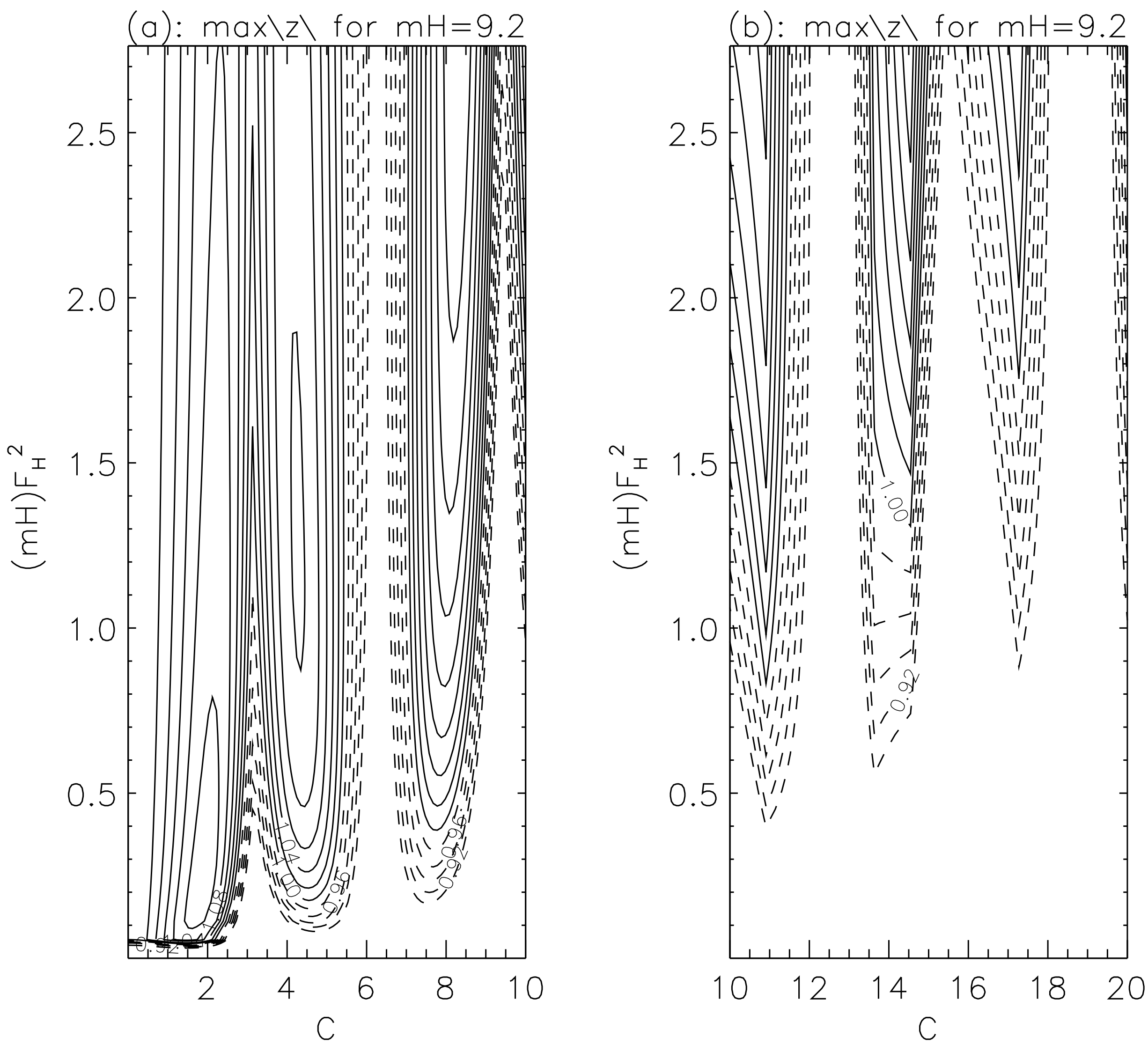

Figure 17.3: Maximum modulus of the roots of the dispersion relation as a function of C and $(mH)F_H^2$ in the hydrostatic case, with $\alpha_1 = \alpha_3 = 0.6$, $\alpha_2 = \alpha_4 = 1$, and for $mH = 9.2$. The contour interval is 0.02 and the maximum modulus of the roots reaches the values: 1.15751 in (a), and 1.11946 in (b).

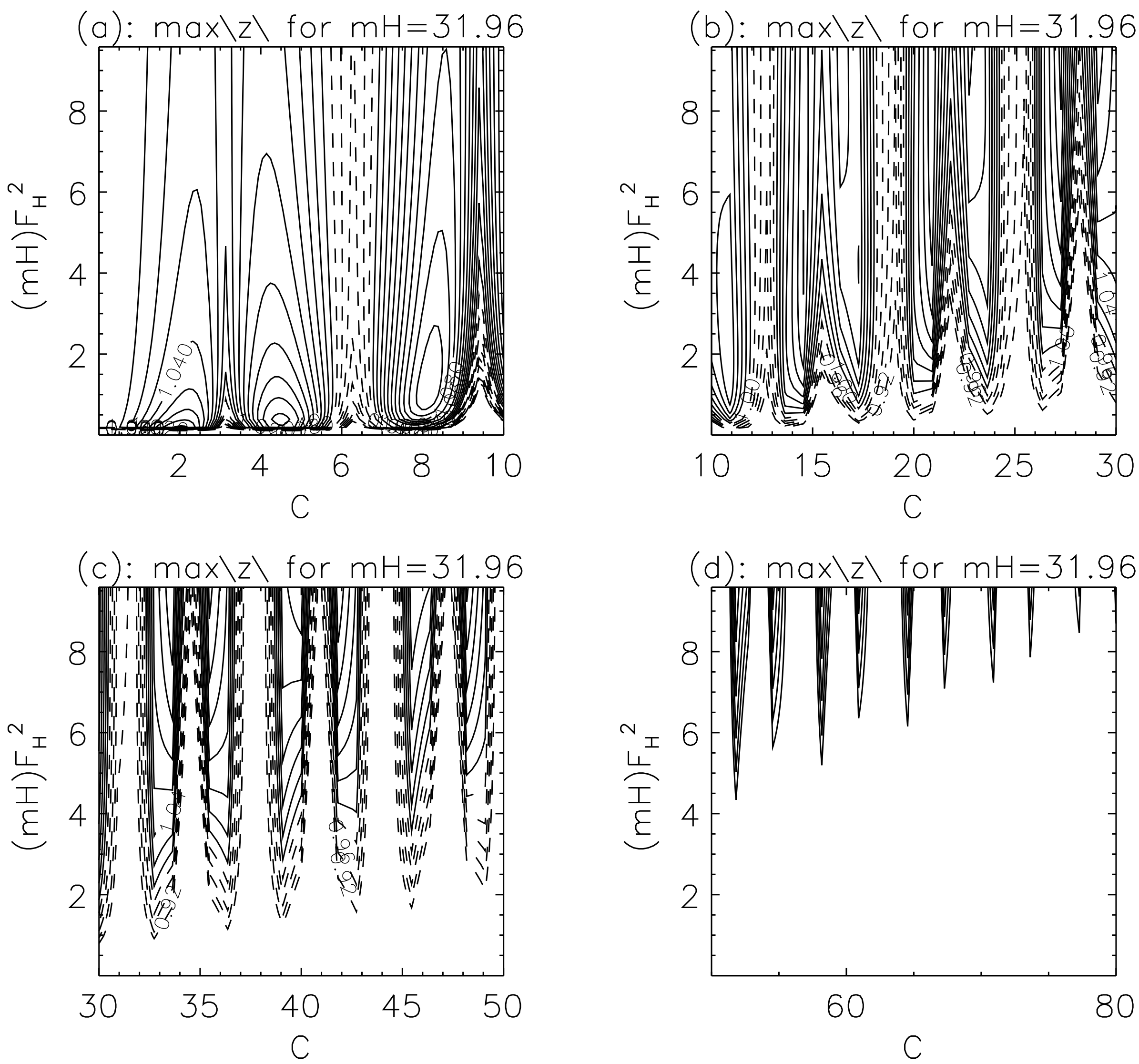

Figure 17.4: Maximum modulus of the roots of the dispersion relation as a function of C and $(mH)F_H^2$ in the hydrostatic case, with $\alpha_1 = \alpha_3 = 0.6$, $\alpha_2 = \alpha_4 = 1$, and for $mH = 31.96$. The contour interval is 0.01 in (a), 0.02 in (b)-(d) and the maximum modulus of the roots reaches the values 1.10738 in (a), (b) and 1.14765 in (c), (d).

Then choosing Δt determines k as $k = C/(u_s \Delta t)$, and hence, since H is a constant, kH is determined too. Therefore, for a given isothermal profile and an assumed value of Δt, the non-hydrostatic case can be compared with the hydrostatic one by choosing:

$$kH = \frac{C\sqrt{R_d T_s}}{F_H g \Delta t}. \tag{17.102}$$

It is also worth noting that, since the previous analysis reveals that the hydrostatic case is independent of the timestep, each of the nonhydrostatic runs performed with a different timestep may be interpreted as a generalisation of the same hydrostatic one, obtained by varying Δt (instead of kH) independently of mH, F_H^2, and C, and defining kH as in (17.102).

The numerical results obtained in the nonhydrostatic case for a timestep of $\Delta t = 1000s$ and a basic state temperature of $T_s = 273.15K$ are very similar to those of the hydrostatic case: the plots corresponding to each of the $mH-$sections - in all the ranges of values of the parameter C, and both when the weights are set to $\alpha_1 = \alpha_3 = 0.6$, $\alpha_2 = \alpha_4 = 1$ (the current settings) and in the purely implicit case ($\alpha_i = 1$ for all i) - are in fact indistinguishable from those obtained for the hydrostatic case and are not reproduced here. The differences become more pronounced as the timestep is reduced for the case when the weights are $\alpha_1 = \alpha_3 = 0.6$, $\alpha_2 = \alpha_4 = 1$.

These features may be explained by noting that the difference between the dispersion relation (17.97) written for the nonhydrostatic ($\mathbf{I}_h = 1$) and for the hydrostatic ($\mathbf{I}_h = 0$) cases is given by:

$$(E-P)^2 \left\{ k^2 \left[\alpha_3 E + (1-\alpha_3) P\right]\left[\alpha_1 E + (1-\alpha_1)\right] + \mathbf{I}_a \frac{1-\kappa_d}{R_d T_s} \frac{(E-P_E)(E-P)}{\Delta t^2} \right\}. \tag{17.103}$$

With the standard setting of the weights ($\alpha_1 = \alpha_3 = 0.6$, $\alpha_2 = \alpha_4 = 1$) the first term in (17.103) is a complete second order polynomial, whereas, in the purely implicit case ($\alpha_i = 1$ for all i) it reduces to $k^2 E^2$, so that the dispersion relation solved in the hydrostatic / nonhydrostatic cases differs for the second degree coefficient only: this presumably accounts for the more pronounced differences observed with the standard setting of the weights.

The second term in (17.103), which grows increasingly larger as the timestep is reduced (it becomes 10^4 times larger when the timestep is reduced from $\Delta t = 1000s$ to $\Delta t = 10s$), explains the results obtained when varying the timestep. It is worth noting that the first coefficient in (17.103) also grows larger as the horizontal wavenumber index, k increases, i.e. for smaller horizontal scales. This means that, when comparing the results obtained for the same $mH-$section (i.e. in the isothermal case for which the equivalent depth H is a constant, for constant m), the differences between the results obtained for the hydrostatic and for the nonhydrostatic runs are larger for smaller values of m/k . This is consistent, since smaller values of m/k, which is the ratio between the horizontal and the vertical scales, correspond to regimes for which the vertical scale becomes larger compared with the horizontal one, so that the hydrostatic approximation of the equations is less justified. Finally, for a given isothermal temperature T_s, for fixed values of the parameters C and u_s, reducing the timestep corresponds to considering larger horizontal wavenumbers, i.e. smaller horizontal scales.

As an example of the results obtained in the nonhydrostatic case for a timestep of $\Delta t = 10s$, in Figs. 17.5 and 17.6 the same case is reproduced as that illustrated in Figs. 17.3(a) and 17.4(a) for the hydrostatic one. In the nonhydrostatic case, and for values of the parameter C larger than 10, the dispersion relation could not be solved with the NAG library routine $C02AFF$, which failed, so in the results plotted in Figs. 17.5 and 17.6, the parameter C takes values up to 10. For $C > 10$ the nonhydrostatic tests with $\Delta t = 10s$ have been rerun solving the dispersion relation with the routine $ZROOTS$ (Press et al. 1992). In the case of Fig. 17.3(b), with $C \in [10, 20]$ it is found that the scheme is always stable, whereas, compared to Fig. 17.4, in cases (b) and (c) the instability is reduced (the maximum modulus of the roots is $\max|z| = 1.03279$ and $\max|z| = 1.005$ in (b) and (c) respectively); for $C > 50$, (d), the scheme is found to be stable. The results obtained in the nonhydrostatic case and with a timestep of $\Delta t = 10s$ and summarised above are not shown.

Note that, even when the results obtained in the nonhydrostatic case differ from those for the hydrostatic one, similar conclusions hold (differing however in the specific values of the parameters): in all the cases instability occurs for sufficiently large values of $(mH)\, F_H^2$ and for wider and more numerous ranges of the parameter C as $(mH)\, F_H^2$ increases. For each of the $mH-$sections and for values of C in each of the aforementioned ranges, the instability grows more rapidly as the parameter F_H^2 increases.

Finally, comparing the results obtained in the nonhydrostatic case varying Δt shows that, as expected, instability becomes weaker as the timestep Δt is reduced. As an example, in Tables 17.1-17.4 are summarized the maximum values of the modulus of the roots of the dis-

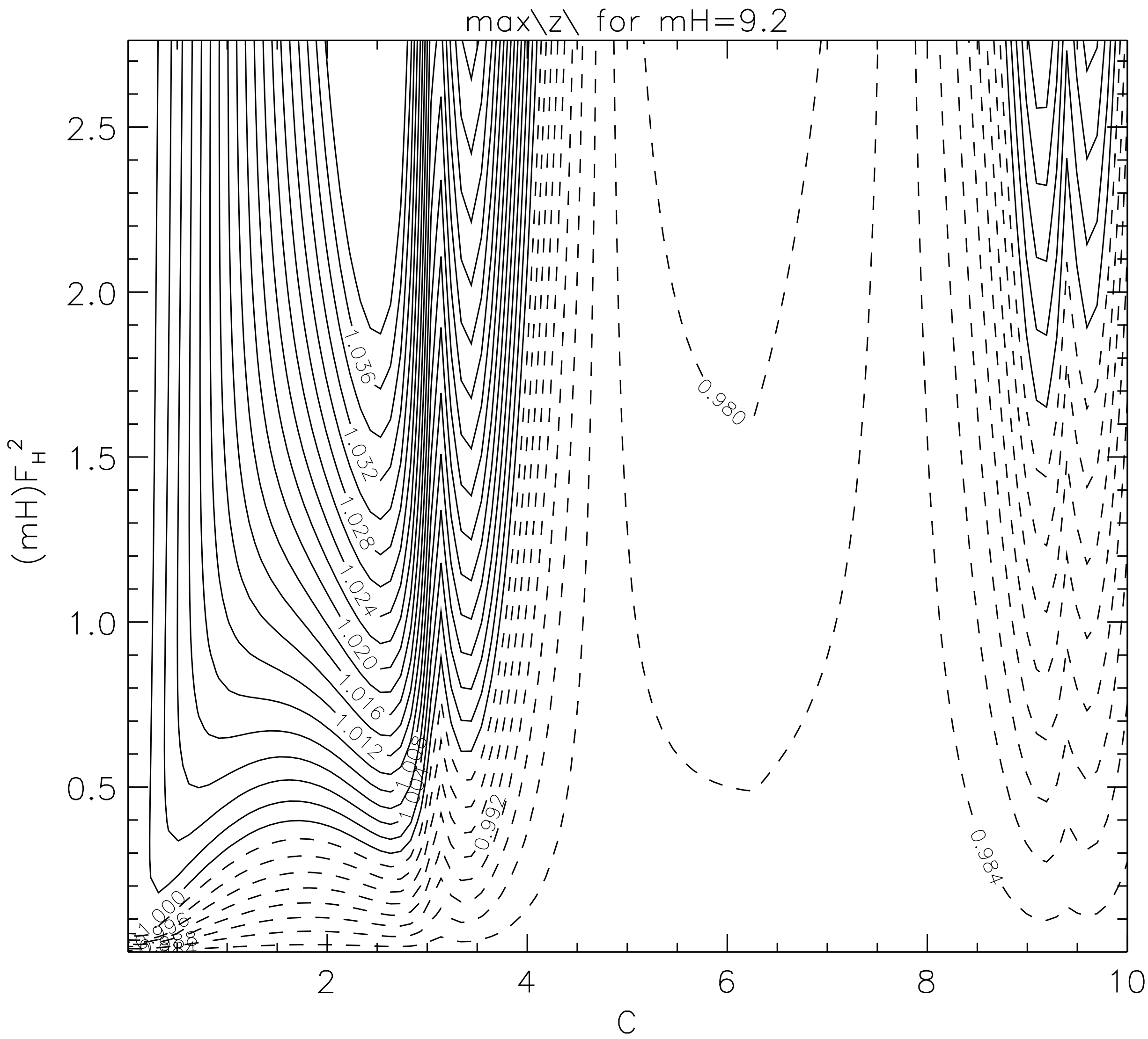

Figure 17.5: Maximum modulus of the roots of the dispersion relation as a function of C and $(mH)F_H^2$ in the nonhydrostatic case with $\Delta t = 10s$, $\alpha_1 = \alpha_3 = 0.6$, $\alpha_2 = \alpha_4 = 1$, and for $mH = 9.2$

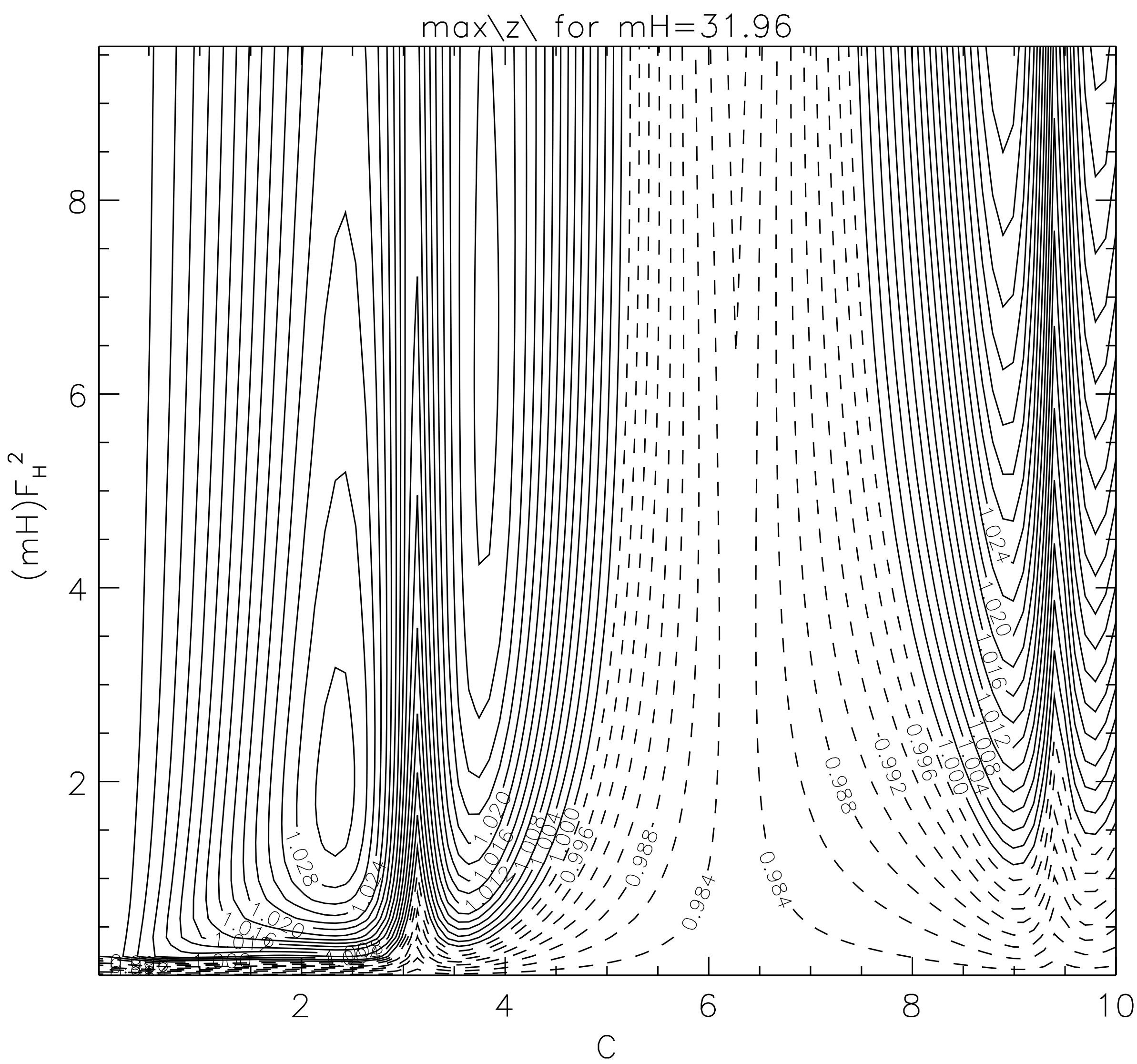

Figure 17.6: Maximum modulus of the roots of the dispersion relation as a function of C and $(mH)F_H^2$ in the nonhydrostatic case with $\Delta t = 10s$, $\alpha_1 = \alpha_3 = 0.6$, $\alpha_2 = \alpha_4 = 1$, and for $mH = 31.96$.

$mH \approx 9.2$	hydrostatic ($\mathbf{I}_h = 0$)	nonhydrostatic ($\mathbf{I}_h = 1$)
$\alpha_i = 1 \quad \forall i$	$\max\|z\| \approx 1.00568$	$\Delta t = 1000s$: $\max\|z\| \approx 1.00568$; $\Delta t = 10s$: $\max\|z\| \approx 1.00234$
$\alpha_1 = \alpha_3 = 0.6, \quad \alpha_2 = \alpha_4 = 1$	$\max\|z\| \approx 1.15751$	$\Delta t = 1000s$: $\max\|z\| \approx 1.15734$; $\Delta t = 10s$: $\max\|z\| \approx 1.04535$

Table 17.1: Comparison between the maximum modulus of the roots of the dispersion relation in the hydrostatic and nonhydrostatic cases for $mH \approx 9.2$.

$mH \approx 16.79$	hydrostatic ($\mathbf{I}_h = 0$)	nonhydrostatic ($\mathbf{I}_h = 1$)
$\alpha_i = 1 \quad \forall i$	$\max\|z\| \approx 1.0129$	$\Delta t = 1000s$: $\max\|z\| \approx 1.0129$; $\Delta t = 10s$: $\max\|z\| \approx 1.00736$
$\alpha_1 = \alpha_3 = 0.6$, $\alpha_2 = \alpha_4 = 1$	$\max\|z\| \approx 1.12755$	$\Delta t = 1000s$: $\max\|z\| \approx 1.12755$; $\Delta t = 10s$: $\max\|z\| \approx 1.03947$

Table 17.2: Comparison between the maximum modulus of the roots of the dispersion relation in the hydrostatic and nonhydrostatic cases for $mH \approx 16.79$.

persion relation corresponding to the sections illustrated in Figs. 17.1-17.6 in the hydrostatic / nonhydrostatic cases, for values of the parameters C and mH in the ranges $C \in [0, 10]$, $F_H^2 \in [0, 0.3]$ with both settings of the semi-implicit weights, and, in the nonhydrostatic case, for $T_s = 273.15K$, $\Delta t = 1000s$ and $\Delta t = 10s$.

17.9 Numerical solutions of the dispersion relation including interpolation

After discussing the analytical (Section 17.7)and numerical (Section 17.8)solutions to the dispersion relation (17.100), in this section the effect of the interpolation associated with the semi-Lagrangian discretisation of the governing equations (except the continuity equation, in the case of the mixed Eulerian semi-Lagrangian scheme) is considered. Specifically, since the value of the physical quantities involved in the time-discretised governing equations (17.40) - (17.45) is not known at the departure points of the trajectories (denoted by subscript d), it needs to be expressed in terms of the values of these quantities at the surrounding

$mH \approx 31.96$	hydrostatic ($\mathbf{I}_h = 0$)	nonhydrostatic ($\mathbf{I}_h = 1$)
$\alpha_i = 1 \quad \forall i$	$\max\|z\| \approx 1.01062$	$\Delta t = 1000s$: $\max\|z\| \approx 1.01062$; $\Delta t = 10s$: $\max\|z\| \approx 1.00850$
$\alpha_1 = \alpha_3 = 0.6$, $\alpha_2 = \alpha_4 = 1$	$\max\|z\| \approx 1.10738$	$\Delta t = 1000s$: $\max\|z\| \approx 1.10727$; $\Delta t = 10s$: $\max\|z\| \approx 1.04016$

Table 17.3: Comparison between the maximum modulus of the roots of the dispersion relation in the hydrostatic and nonhydrostatic cases for $mH \approx 31.96$.

$mH \approx 47.12$	hydrostatic ($\mathbf{I}_h = 0$)	nonhydrostatic ($\mathbf{I}_h = 1$)
$\alpha_i = 1 \quad \forall i$	$\max\|z\| \approx 1.00998$	$\Delta t = 1000s$: $\max\|z\| \approx 1.00998$; $\Delta t = 10s$: $\max\|z\| \approx 1.00733$
$\alpha_1 = \alpha_3 = 0.6$, $\alpha_2 = \alpha_4 = 1$	$\max\|z\| \approx 1.10140$	$\Delta t = 1000s$: $\max\|z\| \approx 1.10131$; $\Delta t = 10s$: $\max\|z\| \approx 1.03965$

Table 17.4: Comparison between the maximum modulus of the roots of the dispersion relation in the hydrostatic and nonhydrostatic cases for $mH \approx 47.12$.

gridpoints. This is done via cubic Lagrange interpolation based on the four gridpoints (two on the left- and two on the right-hand side) closest to the departure points. The value of each of the variables at the departure points at any time instant $n\Delta t$, denoted by $F_d^n \equiv F\left(x - u_s\Delta t,\, n\Delta t\right)$, is therefore replaced by the interpolated value:

$$\begin{aligned}\tilde{F}_d^n &= \left[c_1 \exp\left(-2ik\Delta x\right) + c_2 \exp\left(-ik\Delta x\right) + c_3 + c_4 \exp\left(ik\Delta x\right)\right] \\ &\times \exp\left(-ik\left[C_n\right]\Delta x\right) F\left(x,\, n\Delta t\right) \end{aligned} \tag{17.104}$$

where

$$C_n \equiv \frac{u_s\Delta t}{\Delta x} = \frac{k u_s \Delta t}{k\Delta x} = \frac{C}{k\Delta x} \tag{17.105}$$

denotes the Courant number, $[C_n]$ its integer part and the coefficients of the cubic Lagrange polynomial, c_j for $j = 1, ..., 4$ are given by:

$$\begin{aligned} c_1 = -\frac{1}{6}\left(1-\hat{C}_n\right)\left(1+\hat{C}_n\right)\hat{C}_n, \qquad & c_2 = \frac{1}{2}\left(2-\hat{C}_n\right)\left(1+\hat{C}_n\right)\hat{C}_n, \\ c_3 = \frac{1}{2}\left(2-\hat{C}_n\right)\left(1-\hat{C}_n\right)\left(1+\hat{C}_n\right), \qquad & c_4 = -\frac{1}{6}\left(2-\hat{C}_n\right)\left(1-\hat{C}_n\right)\hat{C}_n, \end{aligned} \tag{17.106}$$

where $\hat{C}_n \equiv C_n - [C_n]$ is the fractional part of the Courant number.

In (17.104), which assumes an expansion of F of the form (17.65), the terms in square brackets account for the distances between the gridpoints involved in the interpolation, the remaining exponential factor counts the number of complete gridlengths between the arrival and departure points. Noting that(from (17.105)):

$$\begin{aligned}\exp\left(-ik[C_n]\Delta x\right) &= \exp\left(-ikC_n\Delta x\right)\exp\left(ik\hat{C}_n\Delta x\right) \\ &= \exp\left(-iC\right)\exp\left(ik\hat{C}_n\Delta x\right), \end{aligned} \tag{17.107}$$

and recalling that $P = \exp(-iC)$, $\tilde{F}_d^n$ can be rewritten as

$$\begin{aligned}\tilde{F}_d^n &= \left[c_1 \exp\left(-2ik\Delta x\right) + c_2 \exp\left(-ik\Delta x\right) + c_3 + c_4 \exp\left(ik\Delta x\right)\right] \\ &\times \exp\left(ik\hat{C}_n\Delta x\right) PF\left(x,\, n\Delta t\right) \\ &= \tilde{\rho} PF\left(x,\, n\Delta t\right), \end{aligned} \tag{17.108}$$

where $\tilde{\rho}P = \rho = \tilde{F}_d^n / F\left(x,\, n\Delta t\right)$ is the response function for interpolation at departure points as defined in Gravel et al. (1993). It follows from (17.108) that incorporating interpolation into the analysis amounts to replacing P in the definitions of the discretised operators (17.67)

- (17.71) and in the following equations (and therefore in the dispersion relation (17.100) to be solved numerically),by $\tilde{\rho}P$. Note that for integer Courant numbers (i.e. $\hat{C}_n = 0$) interpolation is exact: $\tilde{\rho}P = P$ (see (17.106) and (17.108)) and the analysis of section 17.8 holds. This is consistent, since $\hat{C}_n = 0$ implies that the departure points coincide with gridpoints, in which case interpolation is not required (since the values of the dependent variables are available at gridpoints). Also in this documentation cubic interpolation has been considered (see (17.104)), but the same analysis can be repeated for different interpolating polynomials, by defining the appropriate response function.

The purpose of this analysis is to examine the impact of interpolation on the stability properties of the scheme by repeating the tests of Section 17.8 and comparing the results with and without interpolation. Specifically, this is to assess whether the numerical damping associated with interpolation may be sufficient to stabilise the scheme. To do so, however, note that when interpolation is considered, a spatial grid needs to be introduced: this implies that, alongside the non-dimensional quantities mH, F_H^2, C (and kH in the nonhydrostatic case), a further parameter (owing to the presence of a gridlength Δx) is required to define the stability problem under examination. Thiscorresponds to the fact that (17.104) - (17.108) depend on the new parameters $k\Delta x$ and $C_n = [C_n] + \hat{C}_n$, which are related (between them and with C) via:

$$k\Delta x = \frac{C}{C_n}. \tag{17.109}$$

Since there is a limitation on the smallest horizontal wavelengths that can be resolved on a spatial grid (i.e. $k\Delta x \leq \pi$), it follows from (17.109) that, unlike the continuous analysis and the tests of Sections 17.7 and 17.8, for each value of the Courant number C_n, the range of physically meaningful values for the parameter C is restricted to $C \in C_n \times [0, \pi]$. For consistency with the results without including interpolation, however, the tests have been performed using a uniform sample of 100 values of the parameter C spanning the interval [0.01, 10] (so that the dispersion relation is solved for the same values of the parameters in all cases), and then reducing the range as required when plotting the results.

In the hydrostatic case, with the purely implicit setting of the weights ($\alpha_i = 1$ for all i), sampling the parameter space as explained above and choosing as representative values of the Courant number $C_n = \{0.25, 0.5, 1, 1.25, 1.5\}$, it is found that interpolation stabilises the scheme - the results are not plotted here. (Note that for $C_n = 1$, as expected, the results without interpolation, see Figs. 17.1 and 17.2, are recovered.) However, changing the sampling points for the parameter C (100 points are considered but spanning the interval [0.1, 10] instead of [0.01, 10]) there are cases in which a very slow instability ($\max|E| \approx 1.001$) is still found, although it appears to be reduced at least by a factor of ten with respect to the results with no interpolation. The differences observed in the results when different sampling points are chosen, are an indication of the sensitivity of the roots of polynomial equations to (even small) changes in their coefficients. In fact the dispersion relation is in general a fourth order complex coefficient polynomial, whose coefficients depend, among others, on the parameter C, so that changing the points at which the range of feasible values of C is sampled, amounts to modifying (slightly) the coefficients of the dispersion relation to be solved.

With the standard setting of the weights ($\alpha_1 = \alpha_3 = 0.6$, $\alpha_2 = \alpha_4 = 1$), and for different values of the Courant number C_n, it is found that interpolation alone is not sufficient to stabilise the scheme, although instability becomes less rapid. To compare the results with and without interpolation on a specific example, the case illustrated in Figs. 17.3 and 17.4 is considered. In Fig. 17.7 the same test as that of Fig. 17.3 is reproduced, but for Courant numbers of: $C_n = 1$, (a), $C_n = 1.25$, (b), and $C_n = 1.5$ (c). Also the results have been plotted varying the horizontal non-dimensional wavenumber $k\Delta x$ on the $x-$axis instead of the parameter C, and $k\Delta x$ is restricted to be less than π.

To interpret the results shown, note that the response function for interpolation at departure points, $\tilde{\rho}P$, is a function of the horizontal non-dimensional wavenumber, $k\Delta x$, of the fractional part of the Courant number, $\hat{C}_n$ (see (17.108)), and through $P = \exp(-iC)$, of the parameter C :

$$\tilde{\rho}P = \tilde{\rho}\left(k\Delta x \equiv \frac{C}{C_n}, \hat{C}_n\right) P(C) . \tag{17.110}$$

Looking at (the same) fixed point in the different plots of Fig. 17.7 corresponds to comparing the results obtained for the same value of mH, F_H^2, and $k\Delta x$, but varying $\hat{C}_n$ (while keeping $[C_n]$ constant), and therefore varying also $C = C_n k\Delta x$.

Keeping $k\Delta x$ constant means that a specified wavelength is examined on a fixed grid - or the points at which the wave solution is sampled are the same. Varying $\hat{C}_n$ for the same $[C_n]$ and keeping the grid fixed amounts to moving the departure points on a particular gridlength, located $[C_n]$ gridlengths apart from the corresponding arrival points. So the

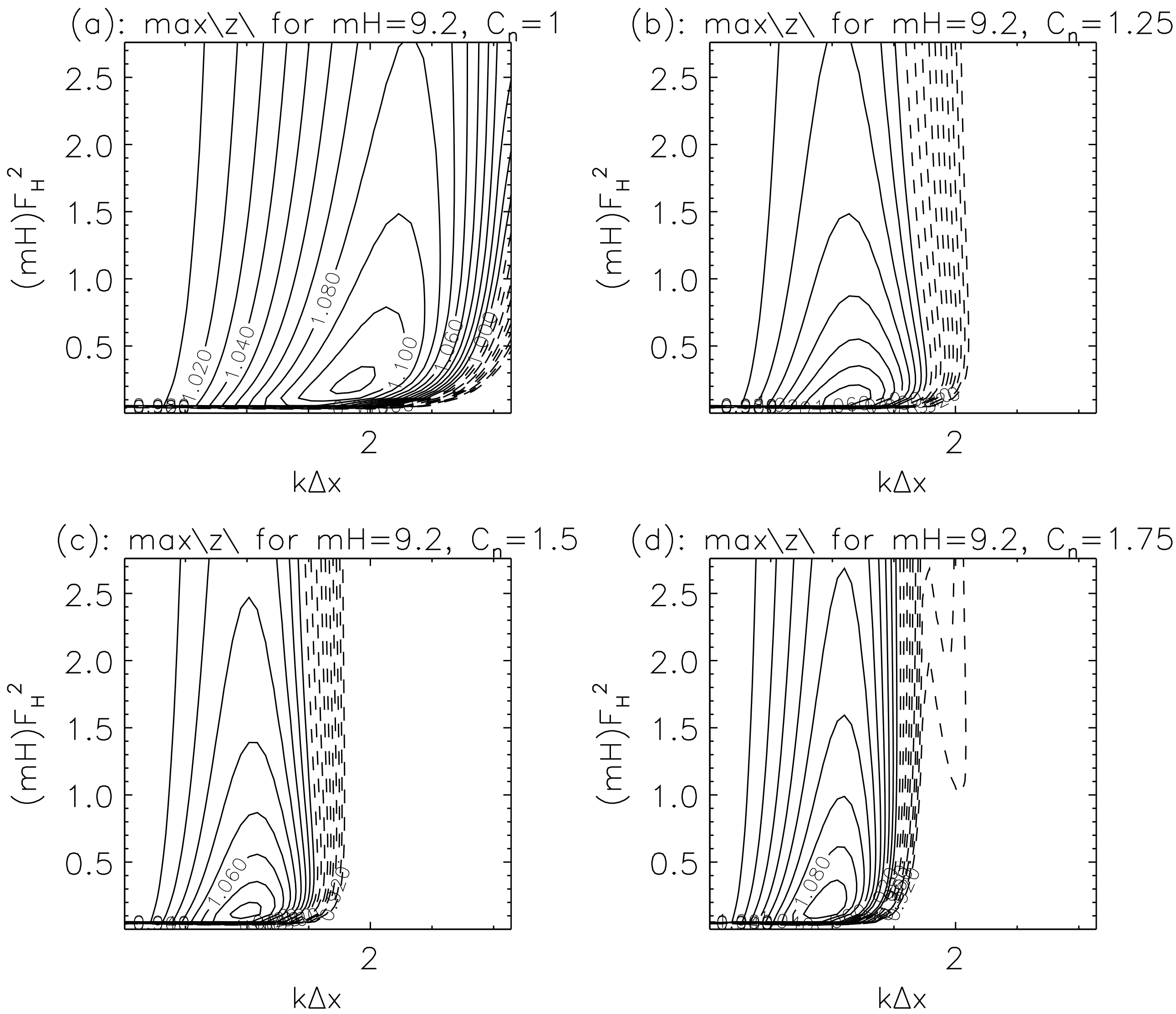

Figure 17.7: Maximum modulus of the roots of the dispersion relation as a function of $k\Delta x \equiv C/C_n$ and $(mH)F_H^2$ in the hydrostatic case, with $\alpha_1 = \alpha_3 = 0.6$, $\alpha_2 = \alpha_4 = 1$, and for $mH = 9.2$, for different values of C_n. It compares with Fig. 17.3(a), but with $k\Delta x$ (restricted to vary in the range $[0, \pi]$) on the $x-$axis and a contour interval of 0.01. Each of the plots corresponds to a different Courant number C_n. $C_n = 1$, plot (a), corresponds to the test with no interpolation.

different plots of Fig. 17.7 illustrate the effect of interpolation on the resolvable waves of a fixed spatial grid, when departure points are moved on a particular gridlength of the grid. In (a) the departure point coincides with the nearest gridpoint on the left of the arrival point; from (b) to (d) it is moved further to the left by a quarter of gridlength at a time. Since $[C_n] = 1$, the gridlength on which the departure point moves is located one gridlength apart form the departure point. This value is chosen because it corresponds to a meaningful range of values of the Courant number ($C_n \in [1, 1.75]$) in plots (a) - (d) and also because, for the integer value of the Courant number $C_n = 1$, plot (a), which corresponds to the base plot without interpolation, $C = k\Delta x$, so that the plots varying C or $k\Delta x$ coincide.

In the plots of Fig. 17.7 it is seen that including interpolation leaves the longest horizontal waves or lowest frequencies (small $k\Delta x$) unaffected, while damping shorter horizontal waves or higher frequencies. In particular in Fig. 17.7: at the longest horizontal wavelengths all the plots are almost identical (the first two contours on the left of each plots are approximately the same); at medium horizontal wavelengths the plots differ because of interpolation, and at the shortest ones the modes are damped; for $k\Delta x \approx \pi$ the maximum modulus of the roots reaches the values of $|z| = 0.7$, $|z| = 0.4$, and $|z| = 0.6$ in (b), (c), and (d) respectively - the corresponding contours are not drawn in the plots, where only those closest to one are shown. The maximum damping occurs for $C_n = 1.5$, i.e. when the departure point is at the midpoint of a gridlength, as expected theoretically (Gravel et al. 1993). Note however that, as mentioned above, for a fixed $k\Delta x$, C varies with C_n between the plots in Fig. 17.7. Since C is one of the parameters defining the original stability problem (in the absence of a spatial grid, Section 17.8), varying C changes the definition of the original problem to be solved, so that the comparison between the results is not exact. This needs to be born in mind, particularly given that, as already noted, the coefficients of the dispersion relation governing the stability properties of the scheme depend on the parameter C and that the roots of polynomial equations may be sensitive to variations in their coefficients. This problem does not arise in the special case $C_n = 1$, (a), for which $C = k\Delta x$, so that the same values of the parameter C correspond to the same wavelengths and the results without interpolation (Fig. 17.3) are in fact recovered - the differences between the plots are owing to the fact that in Fig. 17.7(a) the scale on the $x-$axis is restricted to $[0.01, \pi]$. Also, since for a fixed point in the plots u_s is the same, and Δt is assumed to be constant in the code, a different

$\Delta x = u_s \Delta t / C_n$ is used in the different plots (for the same $k\Delta x$).

In order to compare the results for the same values of the non-dimensional parameters defining the original problem, mH, F_H^2, and C, in Fig. 17.8 the same plots as in Fig. 17.7 are shown, but with C varying on the $x-$axis instead of $k\Delta x$. Note that, in principle, given the requirement $k\Delta x < \pi$, the appropriate range of values to be considered for C in the plots is $C \in [0.01,\, C_n\pi]$, yielding $C \in [0.01,\, 3.927]$, $C \in [0.01,\, 4.712]$, and $C \in [0.01,\, 5.498]$ for Fig. 17.8 (b), (c), and (d) respectively. The $C-$axis values are instead restricted to the same range, i.e. $C \in [0.01,\, \pi]$ (which is the appropriate one for plot (a) and is chosen as a reference interval), in order to have the same scale when comparing the plots. This means that horizontal wavelengths no shorter than $k\Delta x \approx 2.5$, $k\Delta x \approx 2.1$, and $k\Delta x \approx 1.8$ have been considered in plots (b), (c), and (d) respectively, although it has been verified that there is no instability for shorter waves, up to the smallest resolvable scale. This is consistent, since it is the longest horizontal wavelengths that are the most unstable, the shorter ones being damped by interpolation, as shown in Fig. 17.7. The features of the different plots look similar: this is again consistent with the fact that the damping effect of interpolation is weaker at large scales (i.e. long wavelengths). The plots differ in the magnitude of the maximum modulus of the roots, which is largest in the absence of interpolation, (a), so that interpolation does reduce the instability, without eliminating it.

Although for a fixed point in the different plots of Fig. 17.8 the value of the non-dimensional parameters mH, F_H^2, and C is the same (so that the original stability problem being solved - with no spatial grid and no interpolation - is the same), $k\Delta x = C/C_n$ and $\hat{C}_n$, both of which enter the definition of the response function (17.110), vary. This means examining the effect of interpolation on the modes of the original problem (mH, F_H^2, and C constant) but for: different spatial grids or relative sampling of the points (since $k\Delta x$ varies), and different position of the departure points on a prescribed gridlength of the grid (defined by the same $[C_n]$), since $\hat{C}_n$ varies.

In order to consider the effect of varying the spatial grid while keeping the same position of the departure point on a gridlength, the tests have been repeated for different values of the Courant number C_n, i.e. $C_n = \{0.5,\, 1.5,\, 2.5\}$, but with the same fractional part, $\hat{C}_n = 0.5$. Note that in doing so the integer part of the Courant number, $[C_n]$, varies between the different plots: this means that the number of gridlengths lying between the arrival and

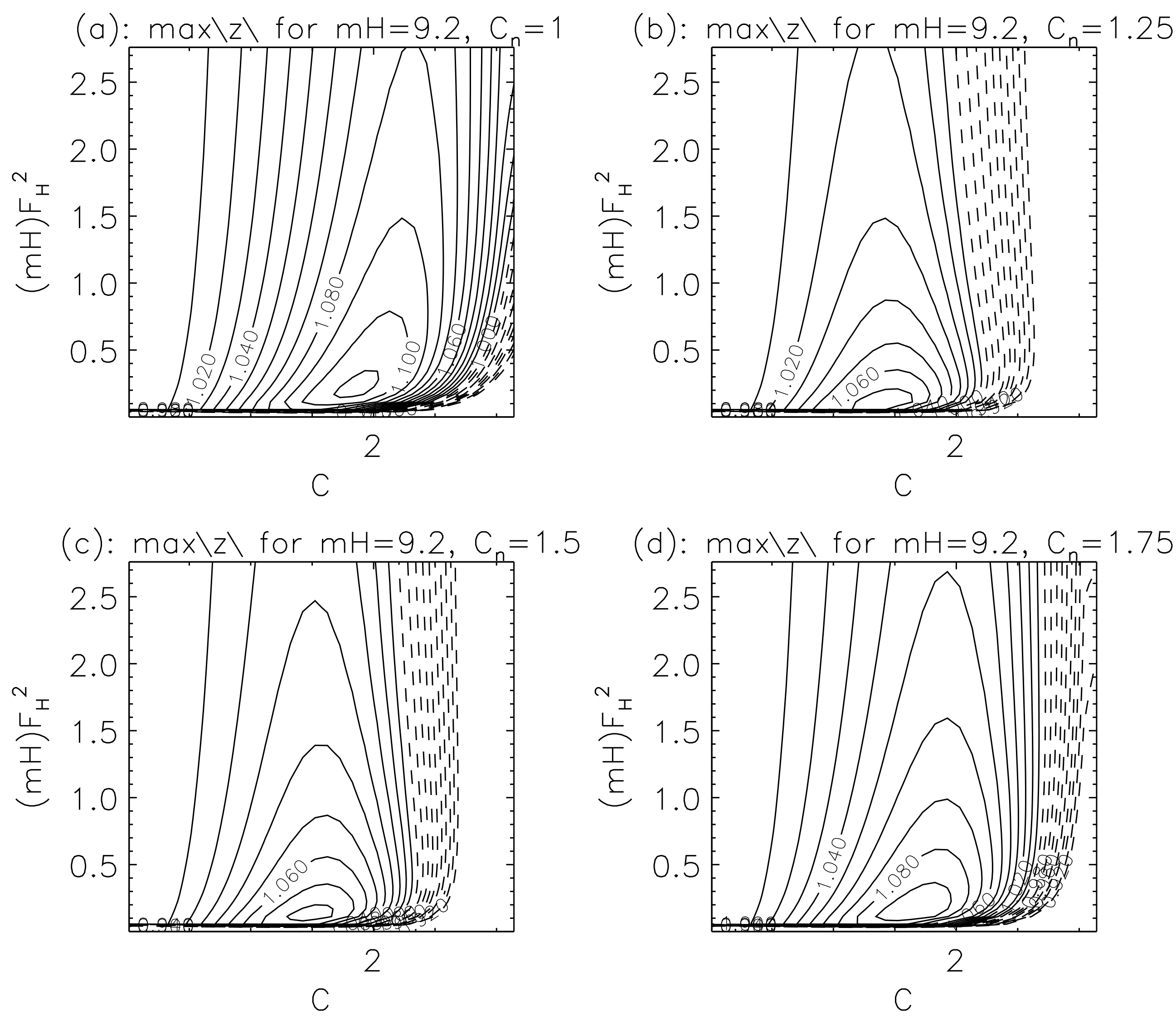

Figure 17.8: Same as in Fig. 17.7 but with C varying on the $x-$axis instead of $k\Delta x$. The parameter C has been restricted to vary in the range $C \in [0.01, \pi]$.

the departure points changes, so that the gridlength on which the departure points move is not the same, although the position of the departure points on it (i.e. at the midpoint of gridlengths, since $\hat{C}_n = 0.5$) is the same. This means that again, the comparison between the results is not exact, although the difference in this case arises from $[C_n]$, which does not explicitly enter the definition of the response function (17.110) or that of the coefficients of the dispersion relation (17.100). The results obtained are displayed in Fig. 17.9(b)-(d), where, for comparison with the case without interpolation, the plot corresponding to $C_n = 1$ is also shown in (a).

The plots of Fig. 17.9 confirm that instability is reduced but not eliminated by interpolation alone. When interpolation is considered, instability is more rapid for larger values of the Courant number C_n (but always less rapid than the case with no interpolation): this effect is more evident in the plots of Fig. 17.9, where the Courant number varies between $C_n = 0.5$, in (b) and $C_n = 2.5$ in (d), than in those of Figs. 17.7 and 17.8, where the variation of the Courant number is smaller ($C_n = 1$ in (a), and $C_n = 1.75$ in (c)). Also, comparing Fig. 17.9(b)-(d) shows that the effect of interpolation is stronger (and the differences between the plots more pronounced) for smaller values of the Courant number (see plot (b), where $C_n = 0.5$), which correspond, for the same value of the parameter C, to shorter horizontal wavelengths $k\Delta x = C/C_n$. This is consistent with the results of Figs. 17.7 and 17.8: for the same values of the non-dimensional quantities defining the stability problem, interpolation introduces more damping at the shortest horizontal wavelengths (i.e. for highest frequencies, or less resolved waves). Finally the same tests have been repeated in the nonhydrostatic case and, both with the purely implicit ($\alpha_i = 1$ for all i) and for the standard ($\alpha_1 = \alpha_3 = 0.6$, $\alpha_2 = \alpha_4 = 1$) settings of the semi-implicit weights, and similar results were found. Note that in the nonhydrostatic case, as explained at the beginning of Section 17.8.2,of the non-dimensional quantities governing the original stability problem, mH, F_H^2, and C have been varied independently, while kH has been defined as in (17.102), where the basic state temperature and timestep have been set to $T_s = 273.15K$ and $\Delta t = 1000s$.

From the results obtained it is concluded that interpolation alone is not sufficient to stabilise the scheme, although its damping effect helps to alleviate it.

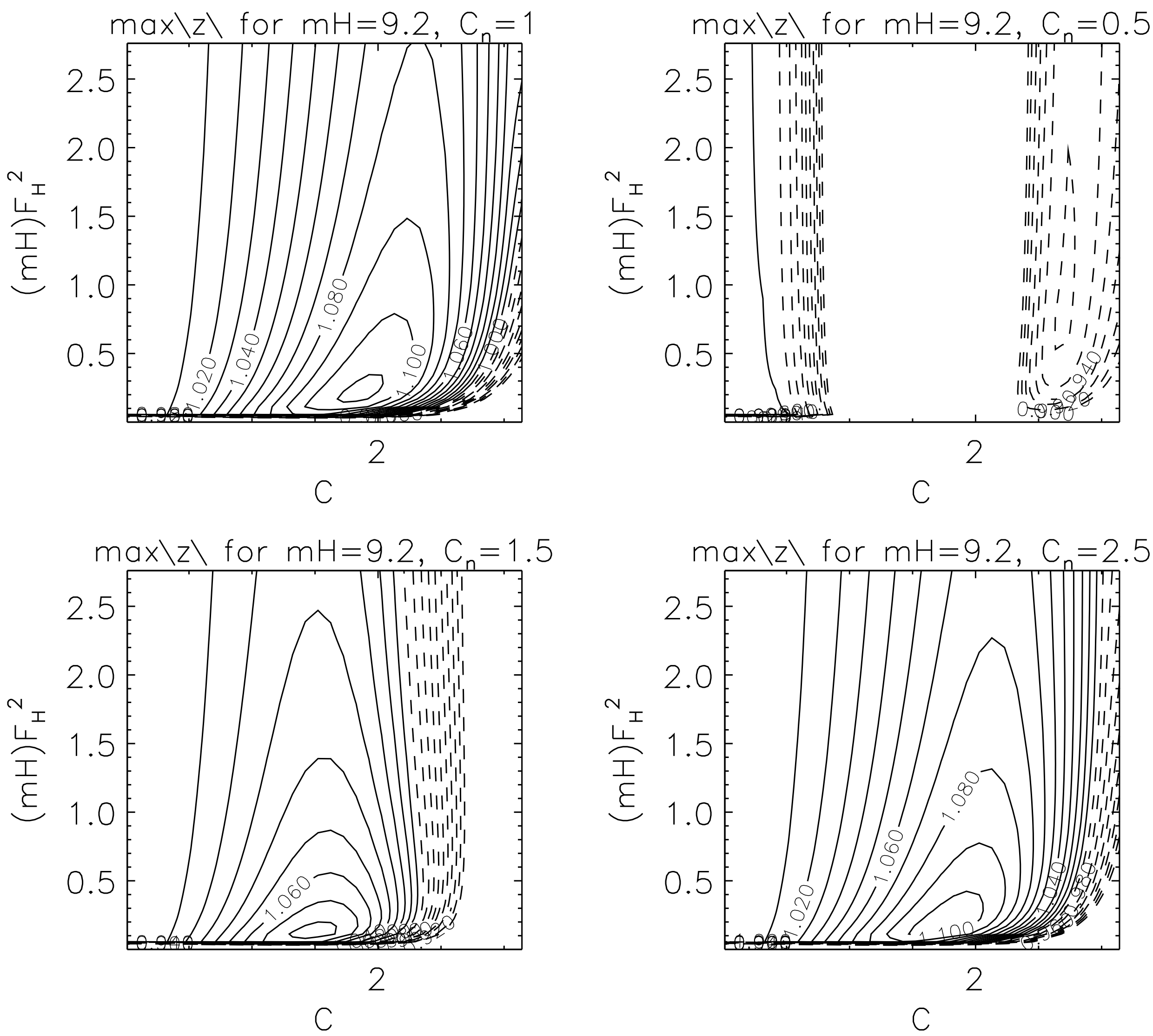

Figure 17.9: Maximum modulus of the roots of the dispersion relation as a function of C and $(mH)F_H^2$ in the hydrostatic case, with $\alpha_1 = \alpha_3 = 0.6$, $\alpha_2 = \alpha_4 = 1$, $mH = 9.2$, and for different values of the Courant number C_n: $C_n = 1$, i.e. no interpolation, in (a), and with the same fractional part of the Courant number, $\hat{C}_n = 0.5$, but varying the integer part, $[C_n]$, in (b)-(d). As in Fig. 17.8, $C_n \in [0.01, \pi]$ is chosen as a reference range of values for the Courant number in all the plots.

17.10 Summary

A linear stability analysis of the New Dynamics governing equations, written in Cartesian $x - z$ geometry, for a dry atmosphere, in the absence of rotation and forcing, and neglecting variations in the $y-$direction, has been considered. The linearised time-discretised equations have been examined in the simplified case of an isothermal basic steady state and manipulated to form a single equation for the vertical velocity w. By decomposing w vertically and Fourier expanding it in the horizontal, the dispersion relation obtained for both the semi-Lagrangian and the Eulerian discretisation of the continuity equation is obtained. With the semi-Lagrangian discretisation of the continuity equation, and for equal values of the semi-implicit weights ($\alpha_i = \alpha$ for all i) it is found that the scheme is stable, provided that $\alpha > 1/2$ (Section 17.6). With the Eulerian discretisation of the continuity equation, the dispersion relation is examined analytically in the anelastic ($\mathbf{I}_a = 0$) and hydrostatic ($\mathbf{I}_h = 0$) cases (Section 17.7), and solved numerically in the hydrostatic ($\mathbf{I}_h = 0$) and nonhydrostatic ($\mathbf{I}_h = 1$) cases, first neglecting the damping effect of interpolation (Section 17.8), then including it into the analysis (Section 17.9). The following conclusions are drawn from the approximate analysis of Section 17.7.

For the anelastic case the finite-difference form of the equations introduces two computational modes. These arise from potentially allowing differently weighted temporal averaging of terms in the density (α_1 and α_2) and the $u-$ and $w-$momentum equations (α_3 and α_4), as is current practice. Setting $\alpha_1 = \alpha_2$ removes the first of these modes as then for the anelastic case the resulting averaging becomes a redundant operator. Setting $\alpha_3 = \alpha_4 \geq 1/2$ leads to a stable computational mode that is damped as the value of $\alpha_{3,4}$ increases. This mode then factors out of the dispersion relation equation leading to a quadratic for the two physical gravity modes. These are stable provided all remaining values of α_i are greater than or equal to 1/2.

For the hydrostatic case terms involving α_4 factor out of the equation set. The dispersion relation is governed by the non-dimensional parameters mH, F_H^2, and C. The scheme introduces one computational mode which arises from the different time weighting of w in the density and temperature equations. This mode can be removed by setting $\alpha_2 = 1$, thereby damping it altogether. It is then found that the remaining physical gravity modes can exhibit an instability if $(mH)\, F_H^2$ exceeds some critical value and if C lies within some range of values, the size of which range increases as $(mH)\,F_H^2$ increases. This has been demonstrated analytically for $\alpha_1 = \alpha_3 = 1$.

The dispersion relation for the mixed semi-Lagrangian and Eulerian scheme, (17.100),is then solved numerically and the following results are found.

In the hydrostatic case, when the weights are set to $\alpha_i = 1$ for all i, a weak instability appears for $(mH)\,F_H^2 \approx 2.2$ and small values of C (approximately $C \in [1.7, 2.1]$). Increasing $(mH)\,F_H^2$ the range of values of C leading to instability becomes wider and for sufficiently large values of $(mH)\,F_H^2$, a very weak instability also manifests itself for larger values of C $(8.5 < C < 10.2)$. For fixed $(mH)\,F_H^2$, the instability is more rapid for smaller mH. When the weights are reduced to $\alpha_1 = \alpha_3 = 0.6$, $\alpha_2 = \alpha_4 = 1$, the critical value of $(mH)\,F_H^2$ leading to instability is smaller; the ranges of values for which instability appear are more numerous and not necessarily limited to small values of C.

In the nonhydrostatic case, the dispersion relation is governed by the independent non-dimensional parameters mH, F_H^2, C, and kH. However in the numerical tests kH has not been varied independently, but it has been chosen in such a way as to correspond to the value it attains in the hydrostatic case. The results obtained in the nonhydrostatic case for a timestep of $\Delta t = 1000s$ (i.e. large horizontal scale) and a basic state temperature of $T_s = 273.15K$ with both settings of the weights (i.e. $\alpha_1 = \alpha_3 = 0.6$, $\alpha_2 = \alpha_4 = 1$, and $\alpha_i = 1$ for all i) are very similar to those of the corresponding hydrostatic one.

The numerical results obtained both for the hydrostatic and nonhydrostatic case and summarised above are consistent with the approximate analysis of Section 17.7. From these results it seems sensible therefore to choose values of the α's such that $\alpha_1 = \alpha_2 \geq 1/2$ and $\alpha_3 = \alpha_4 \geq 1/2$. Further, to minimise the likelihood of instability and to damp the computational modes would require both these values to be as large as possible. However, this would presumably lead to excessive damping also of the physical modes. For the problems associated with the α_1 and α_2 parameters, the better solution seems to be to remove the source of the instability and computational mode which arises from the Eulerian scheme employed in the density equation.

Examining the differences between the hydrostatic and nonhydrostatic results shows that they become larger (although the general features of the results are the same, differing only in the specific values of the parameters) when the timestep is reduced and the weights are set to $\alpha_1 = \alpha_3 = 0.6$, $\alpha_2 = \alpha_4 = 1$ (compared to the implicit setting, $\alpha_i = 1$ for all i). When the differences are larger, the hydrostatic case is more prone to instability. It is verified that these larger differences correspond to smaller values of the ratio m/k, namely regimes for which the vertical scale becomes larger than the horizontal one, so that the hydrostatic approximation is less justified. It is therefore concluded that the analysis of the hydrostatic model provides some useful guidance for investigating the stability properties of the more complex nonhydrostatic one.

Finally the interpolation associated with the semi-Lagrangian discretisation of the governing equations (except the continuity equation, which is discretised in Eulerian fashion) has been incorporated into the stability analysis via its response function - cubic Lagrange interpolation has been examined in this document (see Section (17.9)). Both in the hydrostatic and nonhydrostatic cases, and for both the purely implicit ($\alpha_i = 1$ for all i) and the standard ($\alpha_1 = \alpha_3 = 0.6$, $\alpha_2 = \alpha_4 = 1$) settings of the weights, interpolation is found to damp the modes, particularly at the highest horizontal frequencies (i.e. shortest or less resolved waves), so that in all cases instability is reduced by interpolation. However, interpolation alone is not sufficient to stabilise the modes (this is also consistent with the fact that it is the longest waves that are the most unstable and interpolation is less damping at the longest horizontal wavelengths). It is therefore thought that other stabilising mechanisms are active in the model, such as the enforcement of a monotonicity constraint on the potential temperature, θ, the enforcement of conservation properties, and also vertical interpolation in the nonlinear model. These effects have not been included in this analysis. Further simplifications have also been made, such as the assumptions of a non-rotating and isothermal atmosphere: these too can have an impact on the stability properties of the model.

References

Arakawa, A. & Lamb, V. R. 1977 , Computational design of the basic dynamical processes of the UCLA general circulation model, *Methods in Comp. Phys.* **17**, 174–265.

Arnoldi, W. E. 1951 , The principle of minimized iterations in the solution of the matrix eigenvalue problem, *Quart. Appl. Math.* **9**, 17–29.

Axelsson, O. 1996 , Iterative solution methods, Cambridge University Press, Cambridge UK.

Barnes, R. T. H., Hide, R., White, A. A. & Wilson, C. A. 1983 , Atmospheric angular momentum fluctuations, length of day changes and polar motion, *Proc. R. Soc. Lond. A* **387**, 31–73.

Barrett, R., Berry, M., Chan, T. F., Demmel, J., Donato, J. M., Dongarra, J., Eijkhout, V., Pozo, R., Romine, C. & van der Vorst, H. A. 1994 , Templates for the solution of linear systems: Building blocks for iterative methods, SIAM, Philadelphia PA.

Batchelor, G. K. 1967 , An introduction to fluid dynamics, 1st edn, Cambridge University Press, Cambridge.

Bates, J. R. & McDonald, A. 1982 , Multiply-upstream, semi-Lagrangian advective schemes: analysis and application to a multi-level primitive equation model, *Mon. Wea. Rev.* **110**, 1831–1842.

Bates, J. R., Li, Y., Brandt, A., McCormack, S. F. & Ruge, J. 1995 , A global shallow-water numerical model based on the semi-Lagrangian advection of potential vorticity, *Q. J. R. Meteorol. Soc.* **121**, 1981–2005.

Bates, J. R., Semazzi, F. H. M., Higgins, R. W. & Barros, S. R. M. 1990 , Integration of the shallow water equations on the sphere using a semi-Lagrangian scheme with a multigrid solver, *Mon. Wea. Rev.* **118**, 1615–1627.

Becker, E. 2001 , Symmetric stress tensor formulation of horizontal momentum diffusion in global models of atmospheric circulation, *J. Atmos. Sci.* **58**, 269–282.

Beckmann, A. & Diebels, S. 1994 , Effects of the horizontal component of the Earth's rotation on wave propagation on an f-plane, *Geophys. Astrophys. Fluid Dynamics* **76**, 95–119.

Bénard, P., Marki, A., Neytchev, P. & Prtenjak, M. 2000 , Stabilization of nonlinear vertical diffusion schemes in the context of NWP models, *Mon. Wea. Rev.* **128**, 1937–1948.

Bermejo, R. & Staniforth, A. 1992 , The conversion of semi-Lagrangian advection schemes to quasi-monotone schemes, *Mon. Wea. Rev.* **120**, 2622–2632.

Brussino, G. & Sonnad, V. 1989 , A comparison of direct and preconditioned iterative techniques for sparse unsymmetric systems of linear equations, *Int. J. Numer. Meth. Eng.* **28**, 801–815.

Charney, J. G. & Phillips, N. A. 1953 , Numerical integration of the quasi-geostrophic equations for barotropic and simple baroclinic flows, *J. Meteor.* **10**, 71–99.

Colin de Verdière, A. & Schopp, R. 1994 , Flows in a rotating spherical shell: the equatorial case, *J. Fluid Mech.* **276**, 233–260.

Côté, J. 1988 , A Lagrange multiplier approach for the metric terms of semi-Lagrangian models on the sphere, *Q. J. R. Meteorol. Soc.* **114**, 1347–1352.

Côté, J. & Staniforth, A. 1988 , A two-time-level semi-Lagrangian semi-implicit scheme for spectral models, *Mon. Wea. Rev.* **116**, 2003–2021.

Côté, J., Gravel, S. & Staniforth, A. 1995 , A generalized family of schemes that eliminate the spurious resonant response of semi-Lagrangian schemes to orographic forcing, *Mon. Wea. Rev.* **123**, 3605–3613.

Cullen, M. J. P. 1993 , The unified forecast/ climate model, *Meteorol. Mag.* **122**, 81–94.

Cullen, M. J. P., Davies, T., Mawson, M. H., James, J. A., Coulter, S. C. & Malcolm, A. 1997 , An overview of numerical methods for the next generation UK NWP and climate model, *in* C. Lin, R. Laprise & H. Ritchie, eds, 'Numerical Methods in Atmospheric Modelling, The André Robert memorial volume', Canadian Meteorological and Oceanographical Society, Ottawa, Canada, pp. 425–444.

Daley, R. 1988 , The normal modes of the spherical non-hydrostatic equations with applications to the filtering of acoustic modes, *Tellus* **40A**, 96–106.

Desharnais, F. & Robert, A. 1990 , Errors near the poles generated by a semi-Lagrangian integration scheme in a global spectral model, *Atmos. Ocean* **78**, 162–176.

Douglas, J. & Rachford, H. H. 1956 , On the solution of heat conduction problems in two and three space variables, *Trans. Amer. Math. Soci.* **82**, 421–439.

Draghici, I. 1987 , Non-hydrostatic Coriolis effects in an isentropic coordinate frame, *Meteorol. Hydrol.* **19**, 13–27.

Eisentat, S. C., Elman, H. C. & Schultz, M. H. 1983 , Variational iterative methods for nonsymmetric systems of linear equations, *SIAM J. Numer. Anal.* **20**, 345–357.

Emanuel, K. A. 1994 , Atmospheric convection, 1st edn, Oxford University Press, Oxford.

Fletcher, R. 1975 , Conjugate gradient methods for indefinite systems, *in* G. Watson, ed., 'Proceedings of the Dundee Biennal Conference on Numerical Analysis', Springer-Verlag, New York, pp. 73–89.

Freund, R. & Nachtigal, N. 1991 , QMR: A quasi-minimal residual method for non-Hermetian linear systems, *Numer. Math.* **60**, 315–339.

Freund, R. W., Golub, G. H. & Nachtigal, N. M. 1992 , Iterative solution of linear systems, *Acta Numerica* **8**, 57–100.

Gal-Chen, T. & Somerville, R. C. J. 1975 , On the use of a coordinate transformation for the solution of the Navier-Stokes equations, *J. Comp. Phys.* **17**, 209–228.

Garabedian, P. R. 1964 , Partial differential equations, John Wiley, New York.

Garwood, R. W., Gallacher, C. G. & Muller, P. 1985 , Wind direction and equilibrium mixed layer depth: general theory, *J. Phys. Oceanogr.* **15**, 1325–1331.

Gill, A. 1982 , Atmosphere-ocean dynamics, 1st edn, Academic Press, London.

Girard, C. & Delage, Y. 1990 , Stable schemes for nonlinear vertical diffusion in atmospheric circulation models, *Mon. Wea. Rev.* **118**, 737–745.

Goldstein, H. 1959 , Classical mechanics, 6th edn, Addison-Wesley, London.

Golub, G., Silvester, D. & Wathen, A. 1996 , Diagonal dominance and positive definiteness of upwind approximations for advection-diffusion problems, *in* G. Watson, ed., 'Numerical Analysis: A.R. Mitchell 75th Birthday Volume', World Scientific, Singapore.

Gravel, S., Staniforth, A. & Côté, J. 1993 , A stability analysis of a family of baroclinic semi-Lagrangian forecast models, *Mon. Wea. Rev.* **121**, 815–824.

Heading, J. 1970 , Mathematical methods in science and engineering, 2nd edn, Edward Arnold, London.

Holton, J. R. 1992 , An introduction to dynamic meteorology, 3rd edn, Academic Press, New York.

Kadioglu, M. & Mudrick, S. 1992 , On the implementation of the GMRES(m) method to elliptic equations in meteorology, *J. Comput. Phys.* **102**, 348–359.

Kalnay de Rivas, E. 1972 , On the use of non-uniform grids in finite-difference equations, *J. Comput. Phys.* **10**, 202–210.

Kalnay, E. & Kanamitsu, M. 1988 , Time schemes for strongly nonlinear damping equations, *Mon. Wea. Rev.* **116**, 1945–1958.

Kao, C. Y. J. & Auer, L. H. 1990 , An iterative solver with convergence acceleration technique for pressure field in an uneven spacing grid, *Mon. Wea. Rev.* **118**, 1551–118.

Kasahara, A. & Qian, J.-H. 2000 , Normal modes of a global nonhydrostatic atmospheric model, *Mon. Wea. Rev.* **128**, 3357–3375.

Lamb, H. 1932 , Hydrodynamics, 6th edn, Cambridge university Press, Cambridge.

Leslie, L. M. & Dietachmayer, G. S. 1997 , Comparing schemes for integrating the euler equations, *Mon. Wea. Rev.* **125**, 1687–1691.

Longuet-Higgins, M. S. 1968 , The eigenfunctions of Laplace's tidal equations over a sphere, *Philos. Trans. Roy. Soc. London* **A262**, 511–607.

Lorenz, E. N. 1967 , The nature and theory of the general circulation of the atmosphere, 1st edn, W.M.O., Geneva.

Ma, S. & Saad, Y. 1992 , Block-ADI preconditioners for solving sparse nonsymmetric linear systems of equations, Technical Report UMSI-92-161, Computer Science Department, University of Minnesota, Minneapolis MN.

Marshall, J., Hill, C., Perelman, L. & Adcroft, A. 1997 , Hydrostatic, quasi-hydrostatic, and non-hydrostatic ocean modeling, *J. Geophys. Res.* **102**, 5733–5752.

Mason, P. J. & Thompson, D. J. 1987 , Large-eddy simulations of the neutral-static-stability planetary boundary layer, *Q. J. R. Meteorol. Soc.* **113**, 413–443.

Mawson, M. H. 1998 , The semi-Lagrangian advection scheme for the semi-implicit Unified Model integration scheme, FR Working Paper No 162.

McDonald, A. 1984 , Accuracy of multiply-upstream, semi-Lagrangian advective schemes, *Mon. Wea. Rev.* **112**, 1267–1275.

McDonald, A. 1987 , Accuracy of multiply upstream, semi-Lagrangian advective schemes ii, *Mon. Wea. Rev.* **115**, 1446–1450.

McDonald, A. & Bates, J. R. 1989 , Semi-Lagrangian integration of a gridpoint shallow water model on the sphere, *Mon. Wea. Rev.* **117**, 130–137.

McGregor, J. L. 1993 , Economical determination of departure points for semi-Lagrangian models, *Mon. Wea. Rev.* **121**, 221–230.

Müller, R. 1989 , A note on the relation between the 'traditional approximation' and the metric of the primitive equations, *Tellus* **41A**, 175–178.

Munk, W. & Macdonald, G. 1960 , The rotation of the Earth. a geophysical discussion., 1st edn, Cambridge University Press, Cambridge.

Nair, R., Côté, J. & Staniforth, A. 1999 , Cascade interpolation for semi-Lagrangian advection over the sphere, *Q. J. R. Meteorol. Soc.* **125**, 1445–1468.

Navara, A. 1987 , An application of Arnoldi's method to geophysical fluid dynamics problem, *J. Comput. Phys.* **69**, 143–162.

Newton, C. W. 1971 , Global angular momentum balance: Earth torques and atmospheric fluxes, *J. Atmos. Sci.* **28**, 1329–1341.

Peaceman, D. W. & Rachford, H. H. 1955 , The numerical solution of parabolic and elliptic differential equations, *J. Soc. Ind. Appl. Math.* **3**, 28–41.

Phillips, N. A. 1966 , The equations of motion for a shallow rotating atmosphere and the 'traditional' approximation, *J. Atmos. Sci.* **23**, 626–628.

Phillips, N. A. 1968 , Reply to 'Comments on Phillips' proposed simplification of the equations of motion for a shallow rotating atmosphere' by G. Veronis, *J. Atmos. Sci.* **25**, 1155–1157.

Phillips, N. A. 1973 , Principles of large-scale numerical weather prediction, in Dynamic Meteorology (ed. P. Morel) Reidel, Dordrecht, pp. 1–96.

Phillips, N. A. 1990 , Dispersion processes in large-scale weather prediction, World Meteorological Organization Report No. 700, Geneva.

Press, W., Teukolsky, S., Vetterling, W. & Flannery, B. 1992 , Numerical recipes in Fortran 77, Cambridge University Press, Cambridge UK.

Priestley, A. 1993 , A quasi-conservative version of the semi-Lagrangian advection scheme, *Mon. Wea. Rev.* **121**, 621–629.

Pudykiewicz, J. & Staniforth, A. 1984 , Some properties and comparative performance of the semi-Lagrangian method of Robert in the solution of the advection-diffusion equation, *Atmos.-Ocean* **22**, 283–308.

Purser, J. & Leslie, L. M. 1991 , An interpolation procedure for high-order three- dimensional semi-Lagrangian models, *Mon. Wea. Rev.* **119**, 2492–2498.

Richardson, L. F. 1922 , Weather prediction by numerical process, 1st edn, Cambridge University Press, Cambridge.

Ritchie, H. 1987 , Semi-Lagrangian advection on a Gaussian grid, *Mon. Wea. Rev.* **115**, 608–619.

Ritchie, H. 1988 , Application of the semi-Lagrangian method to a spectral model of the shallow-water equations, *Mon. Wea. Rev.* **116**, 1587–1598.

Ritchie, H. & Beaudoin, C. 1994 , Approximations and sensitivity experiments with a baroclinic semi-Lagrangian spectral model, *Mon. Wea. Rev.* **122**, 2391–2399.

Ritchie, H., Temperton, C., Simmons, A., Hortal, M., Davies, T., Dent, D. & Hamrud, M. 1995 , Implementation of the semi-Lagrangian method in a high resolution version of the ECMWF forecast model, *Mon. Wea. Rev.* **123**, 489–514.

Rivest, C., Staniforth, A. & Robert, A. 1994 , Spurious resonant response of semi-Lagrangian discretisations to orographic forcing: diagnosis and solution, *Mon. Wea. Rev.* **122**, 366–376.

Roache, P. J. 1976 , Computational fluid dynamics, Hermosa Publishers, Albuquerque NM.

Robert, A. 1981 , A stable numerical integration scheme for the primitive meteorological equations, *Atmos.-Ocean* **19**, 35–46.

Robert, A. 1982 , A semi-Lagrangian and semi-implicit numerical integration scheme for the primitive meteorological equations, *Japan Meteor. Soc.* **60**, 319–325.

Roulstone, I. S. & Brice, I. S. J. 1995 , On the Hamiltonian formulation of the quasi-hydrostatic equations, *Q. J. R. Meteorol. Soc.* **121**, 927–936.

Saad, Y. 1996 , Iterative methods for sparse linear systems, PWS Publishing Company, Boston MA.

Saad, Y. & Schultz, M. H. 1986 , GMRES: A generalized minimal residual algorithm for solving nonsymmetric linear systems, *SIAM J. Sci. Stat. Comput.* **7**, 856–869.

Saad, Y. & van der Vorst, H. 1999 , Iterative solution of linear systems in the 20th century, Technical Report UMSI-99-152, Computer Science Department, University of Minnesota, Minneapolis MN.

Simmons, A. J. & Temperton, C. 1997 , Stability of a two-time-level semi-implicit integration scheme for gravity wave motion, *Mon. Wea. Rev.* **125**, 600–615.

Skamarock, W. C., Smolarkiewicz, P. K. & Kemp, J. B. 1997 , Preconditioned conjugate residual solvers for Helmholtz equations in nonhydrostatic model, *Mon. Wea. Rev.* **125**, 587–599.

Smagorinsky, J. 1993 , Some historical remarks on the use of nonlinear viscosities, *in* B. Galperin & S. A. Orszag, eds, 'Large eddy simulation of complex engineering and geophysical flows', Cambridge University Press, Cambridge, UK, pp. 3–36.

Smolarkiewicz, P. K. & Margolin, L. G. 1994 , Variational elliptic solver for atmospheric applications, Technical Report LA-12712-MS, Los Alamos.

Sonneveld, P. 1989 , CGS a fast Lanczos-type solver for nonsymmetric linear systems, *SIAM J. Sci. Stat. Comput.* **10**, 36–52.

Staniforth, A. 1997 , Regional modelling: A theoretical discussion, *Meteorol. Atmos. Phys.* **63**, 15–29.

Staniforth, A. & Côté, J. 1991 , Semi-Lagrangian integration schemes for atmospheric models - a review, *Mon. Wea. Rev.* **119**, 2206–2223.

Staniforth, A. & Pudykiewicz, J. 1985 , Reply to comments on and addenda to 'Some properties and comparative performance of the semi-Lagrangian method of Robert in the solution of the advection-diffusion equation', *Atmos.-Ocean* **23**, 195–200.

Staniforth, A. N., Williams, R. T. & Neta, B. 1993 , Influence of linear depth variation on Poincaré, Kelvin, and Rossby waves, *J. Atmos. Sci.* **50**, 929–940.

Strang, G. 1980 , Linear algebra and its applications, 2nd edn, Academic Press, New York.

Tanguay, M., Robert, A. & Laprise, R. 1990 , A semi-implicit semi-Lagrangian fully compressible regional forecast model, *Mon. Wea. Rev.* **118**, 1970–1980.

Teixeira, J. 2000 , Boundary layer clouds in large scale atmospheric models: cloud schemes and numerical aspects, PhD thesis, European Centre for Medium-Range Weather Forecasts, Reading, UK, pp. 190.

Temperton, C. 1997 , Treatment of the Coriolis terms in semi-Lagrangian spectral models, *Pp. 293-302 in The André Robert memorial volume, Canadian Meteorological and Oceanographical Society, Ottawa.*

Temperton, C. & Staniforth, A. 1987 , An efficient two-time-level semi-Lagrangian semi-implicit integration scheme, *Q. J. R. Meteorol. Soc.* **113**, 1025–1039.

Temperton, C., Hortal, M. & Simmons, A. 2001 , A two-time-level semi-Lagrangian global spectral model, *Q. J. R. Meteorol. Soc.* **127**, 111–128.

Thuburn, J., Wood, N. & Staniforth, A. 2002*a* , Normal modes of deep atmospheres. I: spherical geometry, *Q. J. R. Meteorol. Soc.* **128**, 1771–1792.

Thuburn, J., Wood, N. & Staniforth, A. 2002*b* , Normal modes of deep atmospheres. II: $f-F-$plane geometry, *Q. J. R. Meteorol. Soc.* **128**, 1793–1806.

Tompkins, A. M. & Craig, G. C. 1998 , Radiative-convective equilibrium in a three-dimensional cloud ensemble model, *Q. J. R. Meteorol. Soc.* **124**, 2073–2097.

Tong, C. 1992 , A comparative study of preconditioned Lanczos methods for nonsymmetric linear systems, Technical Report SAND91-8240, Sandia Nat. Lab, Livermore CA.

van der Vorst, H. A. 1992 , A fast and smoothly converging variant of BiCG for the solution of nonsymmetric linear systems, *SIAM J. Sci. Stat. Comput.* **13**, 631–644.

White, A. A. & Bromley, R. A. 1995 , Dynamically consistent, quasi-hydrostatic equations for global models with a complete representation of the Coriolis force, *Q. J. R. Meteorol. Soc.* **121**, 399–418.

Williams, G. P. 1972 , Friction term formulation and convective instability in a shallow atmosphere, *J. Atmos. Sci.* **29**, 870–876.

Wong, Y. S., Zang, T. A. & Hussaini, M. Y. 1986 , Preconditioned conjugate residual methods for the solution of spectral equations, *Computers and Fluids* **14**, 85–95.

APPENDIX A

Conservation properties

A.1 Dry and moist forms of the continuity equation

The dry continuity equation (2.80) can be rewritten as

$$\frac{\partial}{\partial t}\left(r^2\rho_y\frac{\partial r}{\partial \eta}\right)+\frac{1}{\cos\phi}\frac{\partial}{\partial\lambda}\left(r^2\rho_y\frac{\partial r}{\partial \eta}\frac{u}{r}\right)+\frac{1}{\cos\phi}\frac{\partial}{\partial\phi}\left(r^2\rho_y\frac{\partial r}{\partial \eta}\frac{v\cos\phi}{r}\right)+\frac{\partial}{\partial \eta}\left(r^2\rho_y\frac{\partial r}{\partial \eta}\dot{\eta}\right)=0. \tag{A.1}$$

An expression of similar form, but with source/ sink terms, is now obtained for ρ instead of ρ_y. First, the moisture equations (2.85)-(2.87), the definition (2.81), and the identity

$$\frac{\partial}{\partial t}\left(r^2\rho\frac{\partial r}{\partial \eta}\right)=\left(1+m_v+m_{cl}+m_{cf}\right)\frac{\partial}{\partial t}\left(r^2\rho_y\frac{\partial r}{\partial \eta}\right)+r^2\rho_y\frac{\partial r}{\partial \eta}\frac{\partial}{\partial t}\left(m_v+m_{cl}+m_{cf}\right), \tag{A.2}$$

lead to

$$\begin{aligned}\frac{\partial}{\partial t}\left(r^2\rho\frac{\partial r}{\partial \eta}\right) &= \left(1+m_v+m_{cl}+m_{cf}\right)\frac{\partial}{\partial t}\left(r^2\rho_y\frac{\partial r}{\partial \eta}\right)+r^2\rho_y\frac{\partial r}{\partial \eta}\left(S^{m_v}+S^{m_{cl}}+S^{m_{cf}}\right)\\ &\quad -r^2\rho_y\frac{\partial r}{\partial \eta}\left(\frac{1}{\cos\phi}\frac{u}{r}\frac{\partial}{\partial\lambda}+\frac{1}{\cos\phi}\frac{v\cos\phi}{r}\frac{\partial}{\partial\phi}+\dot{\eta}\frac{\partial}{\partial\eta}\right)\left(m_v+m_{cl}+m_{cf}\right)\end{aligned} \tag{A.3}$$

Substitution of the rewritten continuity equation (A.1) into this, and use of (2.81), then yields

$$\begin{aligned}\frac{\partial}{\partial t}\left(r^2\rho\frac{\partial r}{\partial \eta}\right) &= -\left(1+m_v+m_{cl}+m_{cf}\right)\times\\ &\quad\left[\frac{1}{\cos\phi}\frac{\partial}{\partial\lambda}\left(r^2\rho_y\frac{\partial r}{\partial \eta}\frac{u}{r}\right)+\frac{1}{\cos\phi}\frac{\partial}{\partial\phi}\left(r^2\rho_y\frac{\partial r}{\partial \eta}\frac{v\cos\phi}{r}\right)+\frac{\partial}{\partial \eta}\left(r^2\rho_y\frac{\partial r}{\partial \eta}\dot{\eta}\right)\right]\\ &\quad -r^2\rho_y\frac{\partial r}{\partial \eta}\left(\frac{1}{\cos\phi}\frac{u}{r}\frac{\partial}{\partial\lambda}+\frac{1}{\cos\phi}\frac{v\cos\phi}{r}\frac{\partial}{\partial\phi}+\dot{\eta}\frac{\partial}{\partial\eta}\right)\left(1+m_v+m_{cl}+m_{cf}\right)\\ &\quad +r^2\rho_y\frac{\partial r}{\partial \eta}\left(S^{m_v}+S^{m_{cl}}+S^{m_{cf}}\right)\end{aligned}$$

i.e.

$$\begin{aligned}&\frac{\partial}{\partial t}\left(r^2\rho\frac{\partial r}{\partial \eta}\right)+\frac{1}{\cos\phi}\frac{\partial}{\partial\lambda}\left(r^2\rho\frac{\partial r}{\partial \eta}\frac{u}{r}\right)+\frac{1}{\cos\phi}\frac{\partial}{\partial\phi}\left(r^2\rho\frac{\partial r}{\partial \eta}\frac{v\cos\phi}{r}\right)+\frac{\partial}{\partial \eta}\left(r^2\rho\frac{\partial r}{\partial \eta}\dot{\eta}\right)\\ &\qquad = r^2\rho_y\frac{\partial r}{\partial \eta}\left(S^{m_v}+S^{m_{cl}}+S^{m_{cf}}\right).\end{aligned} \tag{A.4}$$

This has the same form as (A.1) for the dry density, but with the addition of source terms. In the absence of moisture and sources and sinks thereof (i.e. $m_v = m_{cl} = m_{cf} = S^{m_v} = S^{m_{cl}} = S^{m_{cf}} = 0$), (A.4) reduces to (A.1) as it should.

The following identity, where $F \equiv r^2 \rho \partial r/\partial \eta$, $F_y \equiv r^2 \rho_y \partial r/\partial \eta$ and G is any scalar, is useful for deriving various conservation properties and follows from (A.4):

$$\begin{aligned} F\cos\phi \frac{DG}{Dt} &= \frac{\partial}{\partial t}\left(GF\cos\phi\right) + \frac{\partial}{\partial \lambda}\left(\frac{u}{r}GF\right) + \frac{\partial}{\partial \phi}\left(\frac{v}{r}GF\cos\phi\right) + \frac{\partial}{\partial \eta}\left(\dot{\eta}GF\cos\phi\right) \\ & -G\left(S^{m_v} + S^{m_{cl}} + S^{m_{cf}}\right)F_y\cos\phi. \end{aligned} \tag{A.5}$$

A.2 Conservation of axial angular momentum

Since axial angular momentum is a vector quantity, conservation of axial angular momentum takes its simplest form for the unrotated coordinate system, where $\phi_0 = \pi/2$ in (2.78)-(2.79), and then the only component of the momentum equation required is the u one.

Eq. (A.5) may be rewritten as

$$\begin{aligned} \frac{\partial}{\partial t}\left(GF\cos\phi\right) &= G\left(S^{m_v} + S^{m_{cl}} + S^{m_{cf}}\right)F_y\cos\phi + \frac{DG}{Dt}F\cos\phi \\ & -\frac{\partial}{\partial \lambda}\left(\frac{u}{r}GF\right) - \frac{\partial}{\partial \phi}\left(\frac{v}{r}GF\cos\phi\right) - \frac{\partial}{\partial \eta}\left(\dot{\eta}GF\cos\phi\right). \end{aligned} \tag{A.6}$$

To apply (A.6) with $G = (u + \Omega r\cos\phi)\, r\cos\phi$, first note that then

$$\begin{aligned} \frac{DG}{Dt} &= \frac{D}{Dt}\left[(u+\Omega r\cos\phi)\, r\cos\phi\right] = \frac{Du}{Dt}r\cos\phi + (u + 2\Omega r\cos\phi)\frac{D}{Dt}\left(r\cos\phi\right) \\ &= \left[\frac{uv\tan\phi}{r} - \frac{uw}{r} + 2\Omega\sin\phi v - 2\Omega\cos\phi w - \frac{c_{pd}\theta_v}{r\cos\phi}\left(\frac{\partial \Pi}{\partial \lambda} - \frac{\partial \Pi}{\partial r}\frac{\partial r}{\partial \lambda}\right) + S^u\right] r\cos\phi \\ & + (u + 2\Omega r\cos\phi)\left(w\cos\phi - v\sin\phi\right) \\ &= \left[S^u - \frac{c_{pd}\theta_v}{r\cos\phi}\left(\frac{\partial \Pi}{\partial \lambda} - \frac{\partial \Pi}{\partial r}\frac{\partial r}{\partial \lambda}\right)\right] r\cos\phi \\ &= S^u r\cos\phi - \frac{R_d}{\rho}\left[\frac{\partial}{\partial \lambda}\left(\rho\theta_v\Pi\right) - \frac{\partial}{\partial r}\left(\rho\theta_v\Pi\right)\frac{\partial r}{\partial \lambda}\right], \end{aligned} \tag{A.7}$$

where Du/Dt has been eliminated using (2.71) with ϕ_0 set equal to $\pi/2$ in (2.78)-(2.79), the definitions $v \equiv rD\phi/Dt$ and $w \equiv Dr/Dt$ have been used, and the penultimate line has been simplified using the equation of state (2.84) and the definition (2.74) of Exner pressure. Thus applying (A.6) with G set to $(u + \Omega r\cos\phi)\, r\cos\phi$, and using (A.7), gives

$$\frac{\partial}{\partial t}\left\{\left[(u+\Omega r\cos\phi)\, r\cos\phi\right]F\cos\phi\right\} = \left[S^u F + (u + \Omega r\cos\phi)\left(S^{m_v} + S^{m_{cl}} + S^{m_{cf}}\right)F_y\right] r\cos^2\phi$$

$$
\begin{aligned}
&-R_d\left[\frac{\partial}{\partial\lambda}\left(\rho\theta_v\Pi\right)-\frac{\partial}{\partial r}\left(\rho\theta_v\Pi\right)\frac{\partial r}{\partial\lambda}\right]r^2\frac{\partial r}{\partial\eta}\cos\phi\\
&-\frac{\partial}{\partial\lambda}\left[\frac{u}{r}\left(u+\Omega r\cos\phi\right)r\cos\phi F\right]\\
&-\frac{\partial}{\partial\phi}\left[\frac{v}{r}\left(u+\Omega r\cos\phi\right)r\cos\phi F\cos\phi\right]\\
&-\frac{\partial}{\partial\eta}\left[\dot{\eta}\left(u+\Omega r\cos\phi\right)r\cos\phi F\cos\phi\right],
\end{aligned}
\tag{A.8}
$$

where $F\equiv r^2\rho\partial r/\partial\eta$ has been used to write the second term on the right-hand side.

Integrating over λ, ϕ and η, and noting that the $\partial/\partial\lambda$, $\partial/\partial\phi$ and $\partial/\partial\eta$ flux terms do not contribute due to periodicity and the upper and lower boundary conditions $\dot{\eta}=0$ at $\eta=0,1$ of no-normal flow, yields

$$
\begin{aligned}
\frac{\partial M}{\partial t} &\equiv \frac{\partial}{\partial t}\left\{\int_0^1\int_{-\pi/2}^{+\pi/2}\int_0^{2\pi}\left[\rho\left(u+\Omega r\cos\phi\right)r\cos\phi\right]r^2\cos\phi\frac{\partial r}{\partial\eta}d\lambda d\phi d\eta\right\}\\
&= \int_0^1\int_{-\pi/2}^{+\pi/2}\int_0^{2\pi}\left\{\left[\rho S^u+\rho_y\left(u+\Omega r\cos\phi\right)\left(S^{m_v}+S^{m_{cl}}+S^{m_{cf}}\right)\right]r\cos\phi\right\}r^2\cos\phi\frac{\partial r}{\partial\eta}d\lambda d\phi d\eta\\
&\quad -\int_0^1\int_{-\pi/2}^{+\pi/2}\int_0^{2\pi}\left\{R_d\left[\frac{\partial}{\partial\lambda}\left(\rho\theta_v\Pi\right)-\frac{\partial}{\partial r}\left(\rho\theta_v\Pi\right)\frac{\partial r}{\partial\lambda}\right]\right\}r^2\cos\phi\frac{\partial r}{\partial\eta}d\lambda d\phi d\eta,
\end{aligned}
\tag{A.9}
$$

where M is the magnitude of the atmospheric axial angular momentum vector $\mathbf{M}$, directed along the Earth's rotation axis.

The last integral simplifies to

$$
\begin{aligned}
I &\equiv \int_0^1\int_{-\pi/2}^{+\pi/2}\int_0^{2\pi}R_d\left[\frac{\partial}{\partial\lambda}\left(\rho\theta_v\Pi\right)-\frac{\partial}{\partial r}\left(\rho\theta_v\Pi\right)\frac{\partial r}{\partial\lambda}\right]r^2\cos\phi\frac{\partial r}{\partial\eta}d\lambda d\phi d\eta\\
&= \int_0^1\int_{-\pi/2}^{+\pi/2}\int_0^{2\pi}R_d\left[r^2\frac{\partial}{\partial\lambda}\left(\rho\theta_v\Pi\cos\phi\frac{\partial r}{\partial\eta}\right)-r^2\frac{\partial}{\partial\eta}\left(\rho\theta_v\Pi\cos\phi\frac{\partial r}{\partial\lambda}\right)\right]d\lambda d\phi d\eta\\
&= \int_0^1\int_{-\pi/2}^{+\pi/2}\int_0^{2\pi}R_d\left[\frac{\partial}{\partial\lambda}\left(\rho\theta_v\Pi r^2\cos\phi\frac{\partial r}{\partial\eta}\right)-\frac{\partial}{\partial\eta}\left(\rho\theta_v\Pi r^2\cos\phi\frac{\partial r}{\partial\lambda}\right)\right]d\lambda d\phi d\eta\\
&= \int_{-\pi/2}^{+\pi/2}\int_0^{2\pi}R_d\left[\rho\theta_v\Pi r^2\cos\phi\frac{\partial r}{\partial\lambda}\right]_S d\lambda d\phi,
\end{aligned}
\tag{A.10}
$$

where the integral of the $\partial/\partial\lambda$ flux was set to zero by periodicity in λ, the contribution at the upper boundary of the integral of the $\partial/\partial\eta$ flux is zero since $\partial r/\partial\lambda\equiv 0$ there, and subscript "S" denotes evaluation at the lower boundary ($\eta=0$).

Putting (A.10) into (A.9) finally yields

$$
\frac{\partial M}{\partial t} \equiv \frac{\partial}{\partial t}\left\{\int_0^1\int_{-\pi/2}^{+\pi/2}\int_0^{2\pi}\left[\rho\left(u+\Omega r\cos\phi\right)r\cos\phi\right]r^2\cos\phi\frac{\partial r}{\partial\eta}d\lambda d\phi d\eta\right\}
$$

$$= \int_0^1 \int_{-\pi/2}^{+\pi/2} \int_0^{2\pi} \left\{ \left[\rho S^u + \rho_y \left(u + \Omega r \cos\phi \right) \left(S^{m_v} + S^{m_{cl}} + S^{m_{cf}} \right) \right] r \cos\phi \right\} r^2 \cos\phi \frac{\partial r}{\partial \eta} d\lambda d\phi d\eta$$
$$- \int_{-\pi/2}^{+\pi/2} \int_0^{2\pi} \left(R_d \rho \theta_v \Pi \frac{\partial r}{\partial \lambda} \right)_S r_S^2 \cos\phi d\lambda d\phi, \tag{A.11}$$

The first term on the right-hand side represents the influence of sources and sinks of momentum and moisture, whereas the second is the mountain torque. In the absence of orography and of sources and sinks of momentum and moisture, atmospheric axial angular momentum is exactly conserved.

Aside :

Using the equation of state (2.84) *and the definition* (2.74) *of Exner pressure, the mountain torque term can be rewritten in a more familiar form as*

$$\int_{-\pi/2}^{+\pi/2} \int_0^{2\pi} \left(R_d \rho \theta_v \Pi \frac{\partial r}{\partial \lambda} \right)_S r_S^2 \cos\phi d\lambda d\phi = \int_{-\pi/2}^{+\pi/2} \int_0^{2\pi} \left(p_S \frac{\partial r_S}{\partial \lambda} \right) r_S^2 \cos\phi d\lambda d\phi. \tag{A.12}$$

Aside :

Eq. (A.11) *is only valid for the unrotated coordinated system, where the poles of the spherical polar coordinates are coincident with the geographical ones. At the expense of some algebra, it would be possible to derive the analogous expression for the rotated coordinate system, but this would require at least the use of the v-momentum equation, and possibly also the w-momentum one.*

Aside :

One contribution to S^u in (2.71)*, which also appears in* (A.11) *and thereby contributes to the axial angular momentum budget,is the parameterisation of sub-grid-scale boundary-layer turbulence. As noted in an aside in Section 6.1, the coupling to the model of the boundary-layer terms is incorrect because their functional form should be in terms of vertical fluxes and these, when integrated over the domain, should only result in fluxes at the lower boundary. In fact they do not, and the consequence is that momentum, heat and moisture are spuriously created and destroyed within the atmosphere and, in particular, axial angular momentum. Although this effect is, probably, instantaneously unimportant, it could arguably have a systematic effect and a non-negligible impact on the general atmospheric* *circulation. This needs to be further investigated, as should the coupling to the model of other parametrisations, particularly the parameterisation of convective momentum transport.*

Aside :

The above derivation suggests that it may be advantageous to rewrite the horizontal pressure gradient term in the u-momentum equations in flux form, i.e. as

$$\frac{c_{pd}\theta_v}{r\cos\phi}\left(\frac{\partial\Pi}{\partial\lambda}-\frac{\partial\Pi}{\partial r}\frac{\partial r}{\partial\lambda}\right)=\frac{R_d}{\rho r^3\cos^2\phi\frac{\partial r}{\partial\eta}}\left[\frac{\partial}{\partial\lambda}\left(\rho\theta_v\Pi r^2\cos\phi\frac{\partial r}{\partial\eta}\right)-\frac{\partial}{\partial\eta}\left(\rho\theta_v\Pi r^2\cos\phi\frac{\partial r}{\partial\lambda}\right)\right], \tag{A.13}$$

since this form leads more directly to the angular momentum principle (A.11). *To obtain* (A.11) *would then only require multiplication of the u- momentum equation by* $\rho r^3\cos^2\phi\partial r/\partial\eta$*, followed by integration over the domain. Discretisation of the right-hand side of* (A.13)*, rather than the left-hand side, would then lead naturally to a discrete angular momentum principle. This principle would be obtained by muliplying the discretisation of the u- momentum equation by a discrete form of* $\rho r^3\cos^2\phi\partial r/\partial\eta$*, and then summing all contributions over the domain, exploiting the fact that the discrete flux terms would automatically exactly cancel one another.*

A.3 Conservation of energy

A.3.1 Kinetic energy evolution equation

Multiplying the momentum equations (2.71)-(2.72) and (2.76) through by $Fu\cos\phi$, $Fv\cos\phi$ and $Fw\cos\phi$, where $F \equiv r^2\rho\partial r/\partial\eta$ and $\mathbf{I}_h$ is the non-hydrostatic switch, and summing gives

$$\begin{aligned} F\cos\phi\frac{D}{Dt}\left(\frac{u^2+v^2+\mathbf{I}_h w^2}{2}\right) &= -u\left[\frac{c_{pd}\theta_v}{r\cos\phi}\left(\frac{\partial\Pi}{\partial\lambda}-\frac{\partial\Pi}{\partial r}\frac{\partial r}{\partial\lambda}\right)-S^u\right]F\cos\phi \\ &\quad -v\left[\frac{c_{pd}\theta_v}{r}\left(\frac{\partial\Pi}{\partial\phi}-\frac{\partial\Pi}{\partial r}\frac{\partial r}{\partial\phi}\right)-S^v\right]F\cos\phi \\ &\quad -w\left[c_{pd}\theta_v\frac{\partial\Pi}{\partial r}+g-S^w\right]F\cos\phi. \end{aligned} \tag{A.14}$$

Using (A.5) or (A.6) with G set equal to $K \equiv \left(u^2+v^2+\mathbf{I}_h w^2\right)/2$, this can be rewritten as

$$\begin{aligned} \frac{\partial}{\partial t}\left(KF\cos\phi\right) &= -u\left[\frac{c_{pd}\theta_v}{r\cos\phi}\left(\frac{\partial\Pi}{\partial\lambda}-\frac{\partial\Pi}{\partial r}\frac{\partial r}{\partial\lambda}\right)\right]F\cos\phi - v\left[\frac{c_{pd}\theta_v}{r}\left(\frac{\partial\Pi}{\partial\phi}-\frac{\partial\Pi}{\partial r}\frac{\partial r}{\partial\phi}\right)\right]F\cos\phi \\ &\quad -w\left[c_{pd}\theta_v\frac{\partial\Pi}{\partial r}+g\right]F\cos\phi - \frac{\partial}{\partial\lambda}\left(\frac{u}{r}KF\right) - \frac{\partial}{\partial\phi}\left(\frac{v}{r}KF\cos\phi\right) - \frac{\partial}{\partial\eta}\left(\dot{\eta}KF\cos\phi\right) \\ &\quad +\left[\left(uS^u+vS^v+wS^w\right)F + K\left(S^{m_v}+S^{m_{cl}}+S^{m_{cf}}\right)F_y\right]\cos\phi. \end{aligned} \tag{A.15}$$

Using (2.61), this simplifies to

$$\begin{aligned} \frac{\partial}{\partial t}\left(KF\cos\phi\right) &= -c_{pd}\theta_v\left(\frac{u}{r\cos\phi}\frac{\partial\Pi}{\partial\lambda}+\frac{v}{r}\frac{\partial\Pi}{\partial\phi}+\dot{\eta}\frac{\partial\Pi}{\partial\eta}\right)F\cos\phi - gwF\cos\phi \\ &\quad +\left[\left(uS^u+vS^v+wS^w\right)F + K\left(S^{m_v}+S^{m_{cl}}+S^{m_{cf}}\right)F_y\right]\cos\phi \\ &\quad -\frac{\partial}{\partial\lambda}\left(\frac{u}{r}KF\right) - \frac{\partial}{\partial\phi}\left(\frac{v}{r}KF\cos\phi\right) - \frac{\partial}{\partial\eta}\left(\dot{\eta}KF\cos\phi\right). \end{aligned} \tag{A.16}$$

A.3.2 Potential gravitational energy evolution equation

Setting G equal to unity in (A.5) or (A.6) and multiplying bygr yields

$$\begin{aligned} \frac{\partial}{\partial t}\left[(gr)F\cos\phi\right] &= -(gr)\left[\frac{\partial}{\partial\lambda}\left(\frac{u}{r}F\right)+\frac{\partial}{\partial\phi}\left(\frac{v}{r}F\cos\phi\right)+\frac{\partial}{\partial\eta}\left(\dot{\eta}F\cos\phi\right)\right] \\ &\quad +(gr)\left(S^{m_v}+S^{m_{cl}}+S^{m_{cf}}\right)F_y\cos\phi \\ &= \left(\frac{u}{r}F\right)\frac{\partial}{\partial\lambda}(gr) + \left(\frac{v}{r}F\cos\phi\right)\frac{\partial}{\partial\phi}(gr) + \left(\dot{\eta}F\cos\phi\right)\frac{\partial}{\partial\eta}(gr) \\ &\quad +gr\left(S^{m_v}+S^{m_{cl}}+S^{m_{cf}}\right)F_y\cos\phi \\ &\quad -\frac{\partial}{\partial\lambda}(ugF) - \frac{\partial}{\partial\phi}(vgF\cos\phi) - \frac{\partial}{\partial\eta}(\dot{\eta}grF\cos\phi) \end{aligned} \tag{A.17}$$

where $F \equiv r^2\rho\partial r/\partial\eta$, $F_y \equiv r^2\rho_y\partial r/\partial\eta$ and the time independence of r has been exploited.

Using (2.61), and noting that g is constant, this simplifies to

$$\begin{aligned}\frac{\partial}{\partial t}\left[(gr)\,F\cos\phi\right] &= gwF\cos\phi + gr\left(S^{m_v}+S^{m_{cl}}+S^{m_{cf}}\right)F_y\cos\phi \\ &\quad -\frac{\partial}{\partial\lambda}\left(ugF\right)-\frac{\partial}{\partial\phi}\left(vgF\cos\phi\right)-\frac{\partial}{\partial\eta}\left(\dot{\eta}grF\cos\phi\right). \end{aligned}\tag{A.18}$$

A.3.3 Internal energy evolution equation

Using the equation of state (2.84), the rate of change of internal energy is

$$\frac{\partial}{\partial t}\left(c_{vd}\theta_v\Pi\rho\right)=\frac{p_o c_{vd}}{\kappa_d c_{pd}}\frac{\partial}{\partial t}\left(\Pi^{\frac{1}{\kappa_d}}\right). \tag{A.19}$$

Multiplying the equation of state (2.84) by $\Pi^{\frac{1-\kappa_d}{\kappa_d}}$ and then differentiating with respect to t gives

$$0=\frac{\partial}{\partial t}\left[\rho\theta_v-\frac{p_o}{\kappa_d c_{pd}}\left(\Pi^{\frac{1}{\kappa_d}}\right)^{1-\kappa_d}\right]=\frac{\partial\left(\rho\theta_v\right)}{\partial t}-\frac{p_o\left(1-\kappa_d\right)}{\kappa_d c_{pd}}\frac{1}{\Pi}\frac{\partial}{\partial t}\left(\Pi^{\frac{1}{\kappa_d}}\right), \tag{A.20}$$

which can be rewritten as

$$\frac{p_o c_{vd}}{\kappa_d c_{pd}}\frac{\partial}{\partial t}\left(\Pi^{\frac{1}{\kappa_d}}\right)=\frac{c_{vd}\Pi}{\left(1-\kappa_d\right)}\left(\rho\frac{\partial\theta_v}{\partial t}+\theta_v\frac{\partial\rho}{\partial t}\right). \tag{A.21}$$

Inserting (A.21) into (A.19), and noting that $R_d=c_{pd}-c_{vd}$ and $\kappa_d=R_d/c_{pd}$, then yields

$$\frac{\partial}{\partial t}\left(c_{vd}\theta_v\Pi\rho\right)=c_{pd}\Pi\left(\rho\frac{\partial\theta_v}{\partial t}+\theta_v\frac{\partial\rho}{\partial t}\right). \tag{A.22}$$

Multiplying by $r^2\left(\partial r/\partial\eta\right)\cos\phi$, in anticipation of integration over the domain, this can be rewritten as

$$\begin{aligned}\frac{\partial}{\partial t}\left(c_{vd}\theta_v\Pi F\cos\phi\right) &= c_{pd}\Pi\left(\frac{\partial\theta_v}{\partial t}+\theta_v\frac{1}{\rho}\frac{\partial\rho}{\partial t}\right)F\cos\phi \\ &= c_{pd}\Pi\left(\frac{D\theta_v}{Dt}-\frac{u}{r\cos\phi}\frac{\partial\theta_v}{\partial\lambda}-\frac{v}{r}\frac{\partial\theta_v}{\partial\phi}-\dot{\eta}\frac{\partial\theta_v}{\partial\eta}\right)F\cos\phi \\ &\quad +c_{pd}\Pi\theta_v\frac{\partial}{\partial t}\left(F\cos\phi\right), \end{aligned}\tag{A.23}$$

where $F\equiv r^2\rho\partial r/\partial\eta$ and the time independence of r and $\cos\phi$ has been exploited.

Setting G equal to unity in (A.5) or (A.6), (A.23) can be rewritten as

$$\begin{aligned}\frac{\partial}{\partial t}\left(c_{vd}\theta_v\Pi F\cos\phi\right) &= c_{pd}\Pi\frac{D\theta_v}{Dt}F\cos\phi-c_{pd}\Pi\left(\frac{u}{r\cos\phi}\frac{\partial\theta_v}{\partial\lambda}+\frac{v}{r}\frac{\partial\theta_v}{\partial\phi}+\dot{\eta}\frac{\partial\theta_v}{\partial\eta}\right)F\cos\phi \\ &\quad -c_{pd}\Pi\theta_v\left[\frac{\partial}{\partial\lambda}\left(\frac{u}{r}F\right)+\frac{\partial}{\partial\phi}\left(\frac{v}{r}F\cos\phi\right)+\frac{\partial}{\partial\eta}\left(\dot{\eta}F\cos\phi\right)\right]\end{aligned}$$

$$\begin{aligned}
&+c_{pd}\Pi\theta_v\left(S^{m_v}+S^{m_{cl}}+S^{m_{cf}}\right)F_y\cos\phi \\
= &-c_{pd}\Pi\left[\frac{\partial}{\partial\lambda}\left(\frac{u}{r}\theta_v F\right)+\frac{\partial}{\partial\phi}\left(\frac{v}{r}\theta_v F\cos\phi\right)+\frac{\partial}{\partial\eta}\left(\dot{\eta}\theta_v F\cos\phi\right)\right] \\
&+c_{pd}\Pi\left[\frac{D\theta_v}{Dt}F+\theta_v\left(S^{m_v}+S^{m_{cl}}+S^{m_{cf}}\right)F_y\right]\cos\phi. \qquad \text{(A.24)}
\end{aligned}$$

Rearranging and using (2.75), (2.82), (2.83) and (2.85)-(2.87), this finally yields

$$\begin{aligned}
\frac{\partial}{\partial t}\left(c_{vd}\theta_v\Pi F\cos\phi\right) = &\ c_{pd}\Pi\left[\left(1+\frac{1}{\epsilon}m_v S^{\theta}\right)+\frac{1}{\epsilon}\theta S^{m_v}\right]F_y\cos\phi \\
&-c_{pd}\left[\frac{\partial}{\partial\lambda}\left(\frac{u}{r}\theta_v\Pi F\right)+\frac{\partial}{\partial\phi}\left(\frac{v}{r}\theta_v\Pi F\cos\phi\right)+\frac{\partial}{\partial\eta}\left(\dot{\eta}\theta_v\Pi F\cos\phi\right)\right] \\
&+c_{pd}\theta_v\left(\frac{u}{r\cos\phi}\frac{\partial\Pi}{\partial\lambda}+\frac{v}{r}\frac{\partial\Pi}{\partial\phi}+\dot{\eta}\frac{\partial\Pi}{\partial\eta}\right)F\cos\phi. \qquad \text{(A.25)}
\end{aligned}$$

A.3.4 Moist energy evolution equation

Setting G equal to $\{[(L_c+L_f)\,m_v+L_f m_{cl}]\,\rho_y/\rho\}$ in (A.5) or (A.6) and using (2.85) - (2.86) then yields

$$\begin{aligned}
\frac{\partial}{\partial t}\left\{\left[(L_c+L_f)\,m_v+L_f m_{cl}\right]F_y\cos\phi\right\} = &-\frac{\partial}{\partial\lambda}\left\{\frac{u}{r}\left[(L_c+L_f)\,m_v+L_f m_{cl}\right]F_y\right\} \\
&-\frac{\partial}{\partial\phi}\left\{\frac{v}{r}\left[(L_c+L_f)\,m_v+L_f m_{cl}\right]F_y\cos\phi\right\} \\
&-\frac{\partial}{\partial\eta}\left\{\dot{\eta}\left[(L_c+L_f)\,m_v+L_f m_{cl}\right]F_y\cos\phi\right\} \\
&+\left[(L_c+L_f)\,S^{m_v}+L_f S^{m_{cl}}\right]F_y\cos\phi, \qquad \text{(A.26)}
\end{aligned}$$

where L_c and L_f are respectively the latent heats of vaporisation and fusion, assumed in the model to be constant.

A.3.5 Total energy evolution equation

Summing (A.16), (A.18), (A.25) and (A.26), integrating over λ, ϕ and η, and noting that the $\partial/\partial\lambda$, $\partial/\partial\phi$ and $\partial/\partial\eta$ flux terms do not contribute due to periodicity and the upper and lower boundary conditions $\dot{\eta}=0$ at $\eta=0,1$ of no-normal flow, yields

$$\begin{aligned}
\frac{\partial E}{\partial t} = \int_0^1\int_{-\pi/2}^{+\pi/2}\int_0^{2\pi} &\left\{\left[\rho\left(uS^u+vS^v+wS^w\right)+\rho_y K\left(S^{m_v}+S^{m_{cl}}+S^{m_{cf}}\right)\right]\right. \\
&+\rho_y\left[gr\left(S^{m_v}+S^{m_{cl}}+S^{m_{cf}}\right)\right] \\
&+\rho_y\left[c_{pd}\Pi\left\{\left(1+\frac{1}{\epsilon}m_v\right)S^{\theta}+\frac{1}{\epsilon}\theta S^{m_v}\right\}\right] \\
&\left.+\ \rho_y\left[(L_c+L_f)\,S^{m_v}+L_f S^{m_{cl}}\right]\right\}r^2\cos\phi\frac{\partial r}{\partial\eta}d\lambda d\phi d\eta, \qquad \text{(A.27)}
\end{aligned}$$

where

$$
\begin{aligned}
E &\equiv \int_0^1 \int_{-\pi/2}^{+\pi/2} \int_0^{2\pi} \left\{\rho\left[K + gr + c_{vd}\theta_v\Pi\right] + \left[\left(L_c + L_f\right)\rho_v + L_f\rho_{cl}\right]\right\} r^2 \cos\phi \frac{\partial r}{\partial \eta} d\lambda d\phi d\eta \\
&= \int_0^1 \int_{-\pi/2}^{+\pi/2} \int_0^{2\pi} \left\{\rho\left[K + gr + c_{vd}\theta_v\Pi\right] + \rho_y\left[\left(L_c + L_f\right)m_v + L_f m_{cl}\right]\right\} r^2 \cos\phi \frac{\partial r}{\partial \eta} d\lambda d\phi d\eta,
\end{aligned}
\tag{A.28}
$$

is the *total* energy. This can be decomposed into

$$
K.E. = \int_0^1 \int_{-\pi/2}^{+\pi/2} \int_0^{2\pi} \rho\left[K\right] r^2 \cos\phi \left(\partial r/\partial\eta\right) d\lambda d\phi d\eta, \tag{A.29}
$$

$$
G.P.E. = \int_0^1 \int_{-\pi/2}^{+\pi/2} \int_0^{2\pi} \rho\left[gr\right] r^2 \cos\phi \left(\partial r/\partial\eta\right) d\lambda d\phi d\eta, \tag{A.30}
$$

$$
I.E. = \int_0^1 \int_{-\pi/2}^{+\pi/2} \int_0^{2\pi} \rho\left[c_{vd}\theta_v\Pi\right] r^2 \cos\phi \left(\partial r/\partial\eta\right) d\lambda d\phi d\eta, \tag{A.31}
$$

$$
\begin{aligned}
M.E. &= \int_0^1 \int_{-\pi/2}^{+\pi/2} \int_0^{2\pi} \left[\left(L_c + L_f\right)\rho_v + L_f\rho_{cl}\right] r^2 \cos\phi \left(\partial r/\partial\eta\right) d\lambda d\phi d\eta \\
&= \int_0^1 \int_{-\pi/2}^{+\pi/2} \int_0^{2\pi} \rho_y\left[\left(L_c + L_f\right)m_v + L_f m_{cl}\right] r^2 \cos\phi \left(\partial r/\partial\eta\right) d\lambda d\phi d\eta \\
&= \int_0^1 \int_{-\pi/2}^{+\pi/2} \int_0^{2\pi} \rho\left[\frac{\left(L_c + L_f\right)m_v + L_f m_{cl}}{1 + m_v + m_{cl} + m_{cf}}\right] r^2 \cos\phi \left(\partial r/\partial\eta\right) d\lambda d\phi d\eta,
\end{aligned}
\tag{A.32}
$$

where $K.E.$, $G.P.E.$, $I.E.$ and $M.E.$ are respectively the *kinetic*, *potential gravitational*, *internal* and *moist (latent heat)* energies.

Aside :

How falling precipitation (i.e. precipitation that has not yet reached the surface) fits into the above framework needs clarification.

A.4 Conservation of dry mass

Multiply (A.1) by $G\cos\phi$ to obtain

$$\begin{aligned}\frac{\partial}{\partial t}\left(GF_y\cos\phi\right) &= -\frac{\partial}{\partial\lambda}\left(\frac{u}{r}GF_y\right)-\frac{\partial}{\partial\phi}\left(\frac{v}{r}G\cos\phi F_y\right)-\frac{\partial}{\partial\eta}\left(\dot{\eta}GF_y\cos\phi\right)\\ &\quad \frac{DG}{Dt}F_y\cos\phi,\end{aligned}\tag{A.33}$$

where $F_y\equiv r^2\rho_y\partial r/\partial\eta$ and G is any scalar. Setting G equal to unity then gives

$$\frac{\partial}{\partial t}\left(\rho_y r^2\cos\phi\frac{\partial r}{\partial\eta}\right)=-\frac{\partial}{\partial\lambda}\left(\frac{u}{r}\rho_y r^2\frac{\partial r}{\partial\eta}\right)-\frac{\partial}{\partial\phi}\left(\frac{v}{r}\rho_y r^2\cos\phi\frac{\partial r}{\partial\eta}\right)-\frac{\partial}{\partial\eta}\left(\dot{\eta}\rho_y r^2\cos\phi\frac{\partial r}{\partial\eta}\right).\tag{A.34}$$

Integrating (A.34) over λ, ϕ and η, and noting that the $\partial/\partial\lambda$, $\partial/\partial\phi$ and $\partial/\partial\eta$ flux terms do not contribute due to periodicity and the upper and lower boundary conditions $\dot{\eta}=0$ at $\eta=0,1$ of no-normal flow, then yields

$$\frac{\partial}{\partial t}\left(\int_0^1\int_{-\pi/2}^{+\pi/2}\int_0^{2\pi}\rho_y r^2\cos\phi\frac{\partial r}{\partial\eta}d\lambda d\phi d\eta\right)=0.\tag{A.35}$$

The left-hand side of (A.35) is the time rate of change of the dry mass in the atmosphere.

A.5 Conservation of moisture

Setting G equal to $(m_v+m_{cl}+m_{cf})$ in (A.33) and using (2.85)-(2.87) gives

$$\begin{aligned}\frac{\partial}{\partial t}\left[\left(\rho_v+\rho_{cl}+\rho_{cf}\right)r^2\cos\phi\frac{\partial r}{\partial\eta}\right] &\equiv \frac{\partial}{\partial t}\left[\left(m_v+m_{cl}+m_{cf}\right)F_y\cos\phi\right]\\ &= \left(S^{m_v}+S^{m_{cl}}+S^{m_{cf}}\right)F_y\cos\phi\\ &\quad -\frac{\partial}{\partial\lambda}\left[\frac{u}{r}\left(m_v+m_{cl}+m_{cf}\right)F_y\right]\\ &\quad -\frac{\partial}{\partial\phi}\left[\frac{v}{r}\left(m_v+m_{cl}+m_{cf}\right)F_y\cos\phi\right]\\ &\quad -\frac{\partial}{\partial\eta}\left[\dot{\eta}\left(m_v+m_{cl}+m_{cf}\right)F_y\cos\phi\right],\end{aligned}\tag{A.36}$$

Integrating (A.36) over λ, ϕ and η, and noting that the $\partial/\partial\lambda$, $\partial/\partial\phi$ and $\partial/\partial\eta$ flux terms do not contribute due to periodicity and the upper and lower boundary conditions $\dot{\eta}=0$ at $\eta=0,1$ of no-normal flow, then yields

$$\frac{\partial}{\partial t}\left\{\int_0^1\int_{-\pi/2}^{+\pi/2}\int_0^{2\pi}\left(\rho_v+\rho_{cl}+\rho_{cf}\right)r^2\cos\phi\frac{\partial r}{\partial\eta}d\lambda d\phi d\eta\right\}$$

$$\equiv \frac{\partial}{\partial t}\left\{\int_0^1 \int_{-\pi/2}^{+\pi/2} \int_0^{2\pi} \left[\rho_y \left(m_v + m_{cl} + m_{cf}\right)\right] r^2 \cos\phi \frac{\partial r}{\partial \eta} d\lambda d\phi d\eta\right\}$$
$$= \int_0^1 \int_{-\pi/2}^{+\pi/2} \int_0^{2\pi} \left[\rho_y \left(S^{m_v} + S^{m_{cl}} + S^{m_{cf}}\right)\right] r^2 \cos\phi \frac{\partial r}{\partial \eta} d\lambda d\phi d\eta. \tag{A.37}$$

The left-hand side of (A.37) is the time rate of change of the sum of the total water vapour, cloud liquid water and cloud frozen water in the atmosphere. To obtain the time rate of change of the total water content of the atmosphere, any falling precipitation (i.e. precipitation that has not yet reached the surface) must also be included.

Aside :

Using mixing ratios instead of specific humidities has the advantage, as noted in Section 10.4, of facilitating the numerical imposition of moisture conservation for a semi-Lagrangian treatment of moisture advection.

A.6 Conservation of tracers

Let T_i be the i'th tracer, and let

$$m_{T_i} \equiv \rho_{T_i}/\rho_y, \tag{A.38}$$

be the associated "specific tracer" quantity such that

$$\frac{Dm_{T_i}}{Dt} = S^{m_{T_i}}. \tag{A.39}$$

Setting G equal to m_{T_i} in (A.5) or (A.6), and using (A.39), gives

$$\begin{aligned}
\frac{\partial}{\partial t}\left(\rho_{T_i} r^2 \cos\phi \frac{\partial r}{\partial \eta}\right) &\equiv \frac{\partial}{\partial t}\left(m_{T_i} F_y \cos\phi\right) \\
&= -\frac{\partial}{\partial \lambda}\left(\frac{u}{r} m_{T_i} F_y\right) - \frac{\partial}{\partial \phi}\left(\frac{v}{r} m_{T_i} F_y \cos\phi\right) - \frac{\partial}{\partial \eta}\left(\dot{\eta} m_{T_i} F_y \cos\phi\right) \\
&\quad + \left(S^{m_{T_i}}\right) F_y \cos\phi,
\end{aligned} \tag{A.40}$$

where $F_y \equiv r^2 \rho_y \partial r/\partial \eta$. Integrating (A.40) over λ, ϕ and η, and noting that the $\partial/\partial\lambda$, $\partial/\partial\phi$ and $\partial/\partial\eta$ flux terms do not contribute due to periodicity and the upper and lower boundary conditions $\dot{\eta} = 0$ at $\eta = 0, 1$ of no-normal flow, then yields

$$\begin{aligned}
&\frac{\partial}{\partial t}\left[\int_0^1 \int_{-\pi/2}^{+\pi/2} \int_0^{2\pi} \rho_{T_i} r^2 \cos\phi \frac{\partial r}{\partial \eta} d\lambda d\phi d\eta\right] \\
&\equiv \frac{\partial}{\partial t}\left[\int_0^1 \int_{-\pi/2}^{+\pi/2} \int_0^{2\pi} \left(\rho_y m_{T_i}\right) r^2 \cos\phi \frac{\partial r}{\partial \eta} d\lambda d\phi d\eta\right] \\
&= \int_0^1 \int_{-\pi/2}^{+\pi/2} \int_0^{2\pi} \left[\rho_y \left(S^{m_{T_i}}\right)\right] r^2 \cos\phi \frac{\partial r}{\partial \eta} d\lambda d\phi d\eta.
\end{aligned} \tag{A.41}$$

The left-hand side of (A.41) is the time rate of change of the total amount of tracer T_i in the atmosphere.

Aside :

The true definition of ρ, the total density, is (cf. eq. 1.53) $\rho \equiv \rho_y + \rho_v + \rho_{cl} + \rho_{cf} + \sum \rho_{T_i}$. However, this is approximated in the model by 1.53, viz. $\rho \approx \rho_y + \rho_v + \rho_{cl} + \rho_{cf}$. For some chemical species, such as trace gases, it may be possible to neglect their contribution to the definition of total density because of their smallness (this is the current state-of-play and needs reviewing), but care must be exercised to do this consistently throughout the model and its parametrisations. However carbon dioxide is arguably present in the atmosphere *in sufficient quantity to be explicitly included in the definition of total density. This would presumably mean that it would not be included in the dry density.*

Aside :

Using mixing ratios instead of specific quantities has the advantage, as noted in Section 10.4, of facilitating the numerical imposition of moisture and tracer conservation for a semi-Lagrangian treatment of moisture / tracer advection.

APPENDIX B

Designer vertical grids - defining the terrain-following coordinate transformation

B.1 Introduction

The model uses a terrain-following coordinate

$$\eta = \eta\left(r, r_S, r_T\right), \tag{B.1}$$

where $\eta = 0$ corresponds to the bottom orography $r = r_S\left(\lambda, \phi\right)$, and $\eta = 1$ corresponds to the (rigid) model top at $r = r_T$ =constant. In η coordinates the integration domain is $0 \leq \eta \leq 1$. Since r_T is a constant and $r_S = r_S\left(\lambda, \phi\right)$, $\eta = \eta\left(\lambda, \phi, r\right)$. The inverse transformation can therefore be formally written as

$$r = r\left(\lambda, \phi, \eta\right). \tag{B.2}$$

Aside :

In the model code the three independent spatial co-ordinates are (λ, ϕ, η)*. Therefore, as* (B.2) *indicates, the value of* r *depends on all three spatial co-ordinates. For example, for fixed* η*, its value will in general vary with* λ *and* ϕ*. Thus, in the code the variable* r *is stored as a three-dimensional array .*

So how does one go about defining the precise functional form of the vertical coordinate? The terrain-following coordinate transformation (from r to η) should have certain attributes for the transformation to be both mathematically valid and well behaved. The transformation should be:

- monotonic (i.e. η is a monotonic function of r and vice versa);
- continuous (i.e. η is a continuous function of r and vice versa);
- continuously differentiable everywhere within the domain (i.e. the first partial derivative of r with respect to η should be continuous within the domain).

Even with the above constraints there are an infinite number of possible transformations. Further desirable attributes are:

- simplicity;
- smoothness;
- slow vertical variation of fields in the transformed coordinate.

Not only should the coordinate transformation be nice and smooth etc, the placement of levels in the transformed coordinate η should also be done in a smooth manner to maximise accuracy, and to minimise problems such as spurious numerical dispersion. All other things being equal, it is desirable to design the transformation so that a uniform, or quasi-uniform, placement of levels in the transformed coordinate η well corresponds to an optimal sampling. This is because numerical approximations, e.g. of vertical derivatives and vertical interpolation, are generally more accurate the more uniform is the computational grid - simple centred vertical derivatives (as for e.g. vertical temperature advection) are second-order accurate on a uniform grid but only first-order accurate on a too-rapidly-varying non-uniform grid (if the mesh varies sufficiently slowly, then second-order accuracy is recovered due to the slow variation).

Some possible coordinate transformations are now given, ordered according to their polynomial order.

B.2 A linear coordinate transformation

The simplest possible terrain-following transformation is the linear one

$$\eta = \frac{r - r_S(\lambda, \phi)}{r_T - r_S(\lambda, \phi)}, \tag{B.3}$$

where, recall, r_T is a constant because of the rigid lid boundary condition. For this transformation

$$\frac{\partial r}{\partial \eta} = r_T - r_S(\lambda, \phi), \tag{B.4}$$

and the inverse transformation, obtained by solving (B.3) for r, is

$$r = \eta r_T + (1 - \eta) r_S(\lambda, \phi). \tag{B.5}$$

This transformation has the virtues of monotonicity, simplicity, and good continuity and differentiability. Its principal weaknesses (and arguably important ones) are:

1. the functional dependance of η on $r_S(\lambda, \phi)$ in the upper atmosphere is much stronger than one would wish for data-assimilation and middle-atmosphere modelling purposes, i.e. constant-η surfaces do not "flatten" fast enough as a function of increasing η and are overly influenced by the underlying orography; and

2. adequate capture of the vertical variation of fields in the troposphere (and particularly in the boundary layer) results in a far from uniform sampling for the level placement (current thinking has it that this should vary approximately quadratically in r as a function of the integer level index), with the consequence of sub-optimal accuracy of the discrete vertical operators in the transformed domain.

So how would one implement this linear coordinate transformation algorithmically?

Given

- $r_S(\lambda, \phi)$, the specification of the bottom orography;
- r_T (a constant), the location of the rigid lid; and
- a sampling set $\{\eta_0 \equiv 0, \eta_1, \eta_2, ..., \eta_{N-1}, \eta_N \equiv 1\}$ for the vertical placement of levels in the terrain-following coordinate η.

To determine

- $r(\lambda, \phi, \eta_k), k = 0, 1, 2, ..., N.$

Algorithm

Evaluate

$$r(\lambda, \phi, \eta_k) = \eta_k r_T + (1 - \eta_k) r_S(\lambda, \phi), \quad k = 0, 1, 2, ..., N. \tag{B.6}$$

Aside :

Strictly speaking this coordinate transformation is not currently possible in the model. This is because $r(\lambda, \phi, \eta_{N-1/2})$ is constrained to be constant (this is assumed in the discretisation of the pressure-gradient term of the horizontal momentum equation). One could however apply this transformation everywhere except at the level $\eta = \eta_{N-1/2}$, where $r(\lambda, \phi, \eta_{N-1/2})$ would be held constant. This would *result in a small distortion of the linear coordinate transformation adjacent to the model's top.*

B.3 A composite linear/ quadratic transformation

To address the coordinate flattening and level placement/ sampling issues of the linear transformation (B.3) and its inverse (B.5), a composite transformation is now defined. This has a quadratic variation in the lower part of the domain coupled with a smooth match to a linear variation in the upper part, where the coordinate surfaces are perfect concentric spheres.

B.3.1 Functional form in the lower sub-domain $\eta_0 \equiv 0 \leq \eta \leq \eta_I$

The lower sub-domain is defined to be the region $\eta_0 \equiv 0 \leq \eta \leq \eta_I$, where $\eta = \eta_I$ is the interfacial surface and I is its integer index. Let this interfacial surface correspond to a *constant-r* surface $r = r_I =$ constant (see Fig. B.1). Also let r vary quadratically as a function of η in this lower subdomain, i.e.

$$r(\lambda, \phi, \eta) = \left(\frac{\eta}{\eta_I}\right) r_I + \left(1 - \frac{\eta}{\eta_I}\right) r_S(\lambda, \phi) - \left(1 - \frac{\eta}{\eta_I}\right)\left(\frac{\eta}{\eta_I}\right) A(\lambda, \phi), \quad \eta_0 \equiv 0 \leq \eta \leq \eta_I, \tag{B.7}$$

where, reiterating, r_I is constant. By construction the bottom topography $r = r_S(\lambda, \phi)$ corresponds to the surface $\eta_0 \equiv 0$, and the interfacial surface $\eta = \eta_I$ defines the upper bound of the lower subdomain. The introduction of the last term raises the order of the polynomial from being linear in η to being quadratic, and it must have this form for the $\eta = 0$ and $\eta = \eta_I$ surfaces to respectively correspond to the bounding $r = r_S(\lambda, \phi)$ and $r = r_I$ ones. The associated function $A(\lambda, \phi)$ is used to obtain continuity of $\partial r/\partial \eta$ across the interfacial surface $\eta = \eta_I$. Differentiating (B.7) gives

$$\frac{\partial r}{\partial \eta} = \frac{1}{\eta_I}\left[r_I - r_S(\lambda, \phi) - \left(1 - 2\frac{\eta}{\eta_I}\right) A(\lambda, \phi)\right], \quad \eta_0 \equiv 0 \leq \eta \leq \eta_I. \tag{B.8}$$

B.3.2 Functional form in the upper sub-domain $\eta_I \leq \eta \leq \eta_N \equiv 1$

The upper sub-domain is defined to be the region $\eta_I \leq \eta \leq \eta_N \equiv 1$, where $\eta = \eta_I$ is the interfacial surface and I is its integer index. Both this interfacial surface $\eta = \eta_I$ and the top

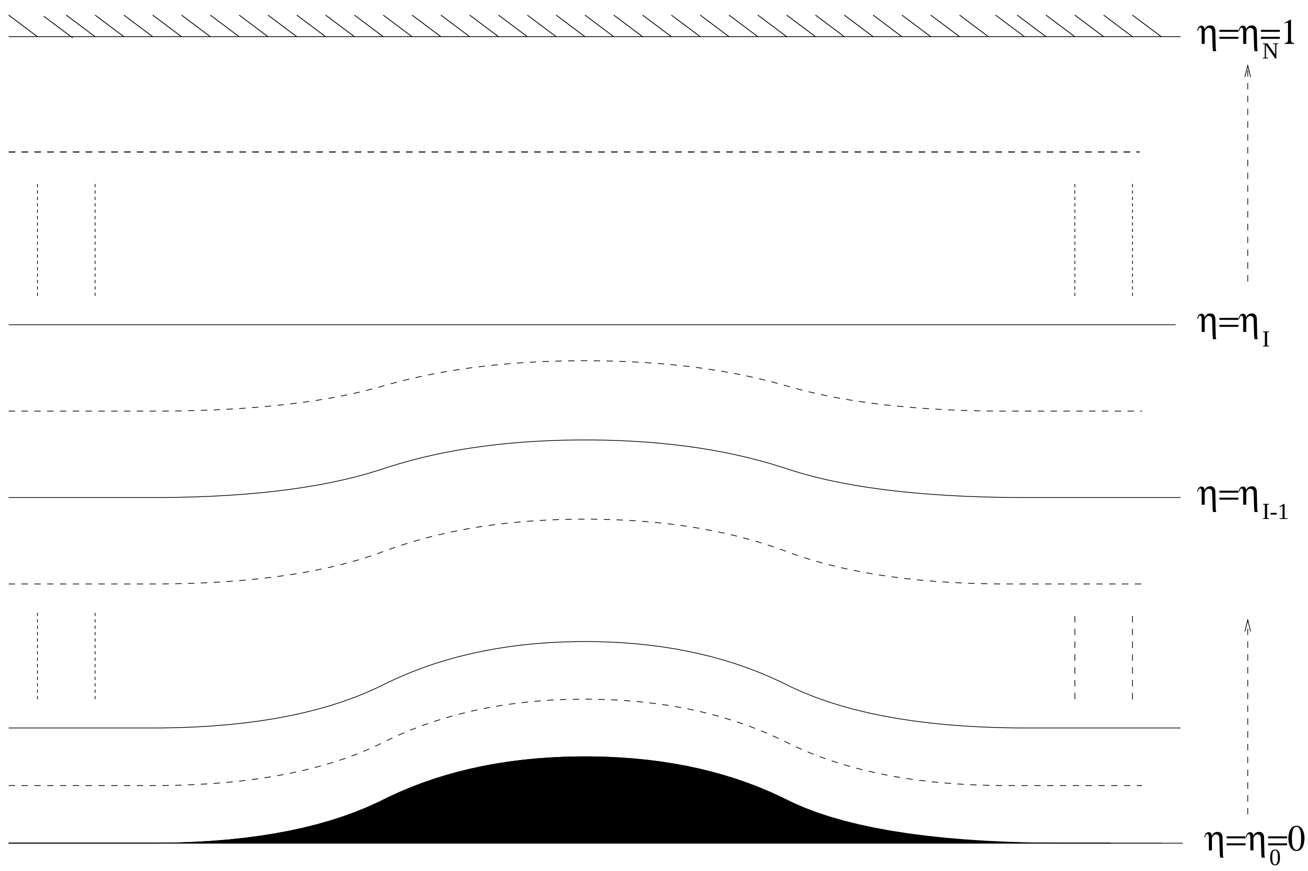

Figure B.1: Schematic of surfaces of constant η for the composite linear/ quadratic transformation. The domain is split into two subdomains separated by the interface surface $\eta = \eta_I$, corresponding to the surface of the sphere $r = r_I =$ constant. In the lower sub-domain (defined by $0 \le \eta \le \eta_I$) r varies quadratically as a function of η as described in the text, whereas in the upper subdomain (defined by $\eta_I \le \eta \le 1$) it varies linearly.

surface $\eta_N \equiv 1$ correspond to *constant-r* surfaces (see Fig. B.1), i.e to $r = r_I$ = constant and $r = r_T$ = constant respectively. Indeed all constant η surfaces in the upper sub-domain are also, by design, constant-r surfaces. Let r vary linearly as a function of η in this upper subdomain, i.e.

$$r(\lambda,\phi,\eta) = \left(\frac{1-\eta}{1-\eta_I}\right) r_I + \left(\frac{\eta-\eta_I}{1-\eta_I}\right) r_T, \quad \eta_I \le \eta \le \eta_N \equiv 1, \tag{B.9}$$

and so differentiating gives

$$\frac{\partial r}{\partial \eta} = \frac{r_T - r_I}{1-\eta_I}, \quad \eta_I \le \eta \le \eta_N \equiv 1. \tag{B.10}$$

B.3.3 Matching $\partial r/\partial\eta$ across the interface level

By construction (B.7) and (B.9) make the transformation continuous, but they do not ensure the continuity of $\partial r/\partial\eta$. This is achieved by matching $\partial r/\partial\eta$ across the mutual interface level $\eta = \eta_I$ using (B.8) and (B.10), thereby determining $A(\lambda,\phi)$. Thus

$$A(\lambda,\phi) = \left(\frac{\eta_I r_T - r_I}{1-\eta_I}\right) + r_S(\lambda,\phi). \tag{B.11}$$

Substituting this into (B.7) then yields the following definition for $r(\lambda,\phi,\eta)$ in the lower subdomain:

$$r(\lambda,\phi,\eta) = \left(\frac{\eta}{\eta_I}\right) r_I + \left(1-\frac{\eta}{\eta_I}\right)^2 r_S(\lambda,\phi) - \left(1-\frac{\eta}{\eta_I}\right)\left(\frac{\eta}{\eta_I}\right)\left(\frac{\eta_I r_T - r_I}{1-\eta_I}\right), \quad \eta_0 \equiv 0 \le \eta \le \eta_I. \tag{B.12}$$

<u>Aside :</u>

A particularly simple form for (B.12) *is obtained by defining the interface level* η_I *such that* $(\eta_I r_T - r_I)/(1-\eta_I) = -a$*, where* a *is the mean radius of the Earth, i.e. such that* $\eta_I = (r_I - a)/(r_T - a)$ *. Eq.* (B.12) *can then be rewritten as*

$$r(\lambda,\phi,\eta) - a = \left(\frac{\eta}{\eta_I}\right)(r_I - a) + \left(1-\frac{\eta}{\eta_I}\right)^2 \left[r_S(\lambda,\phi) - a\right], \quad \eta_0 \equiv 0 \le \eta \le \eta_I. \tag{B.13}$$

This simplification is examined further in Section B.4.

B.3.4 Monotonicity and constraints

The function $r(\lambda,\phi,\eta)$ defined by (B.12) is a quadratic function of η. It is monotonic increasing in the interval $[0,\eta_I]$ provided its first derivative (for all possible values of λ and

ϕ) is positive at both $\eta = 0$ and $\eta = \eta_I$. Differentiating (B.12) gives

$$\frac{\partial r}{\partial \eta} = \frac{1}{\eta_I}\left[r_I - \left(1 - 2\frac{\eta}{\eta_I}\right)\left(\frac{\eta_I r_T - r_I}{1-\eta_I}\right) - 2\left(1 - \frac{\eta}{\eta_I}\right) r_S(\lambda,\phi)\right], \quad \eta_0 \equiv 0 \le \eta \le \eta_I. \tag{B.14}$$

Evaluating (B.14) at the endpoint η_I shows that $\left.(\partial r/\partial\eta)\right|_{\eta_I} > 0$ provided that

$$r_I < r_T, \tag{B.15}$$

a condition that is straightforward to satisfy. Evaluating it at $\eta = 0$ gives

$$\eta_I < \frac{2\left[r_I - r_S(\lambda,\phi)\right]}{r_I + r_T - 2r_S(\lambda,\phi)}. \tag{B.16}$$

For this to be true for all possible values of λ and ϕ requires

$$\eta_I < \frac{r_I - \max r_S(\lambda,\phi)}{(r_I + r_T)/2 - \max r_S(\lambda,\phi)}. \tag{B.17}$$

Inequality (B.17) bounds η_I from above. A bound from below is now derived by requiring that the curvature $\partial^2 r/\partial\eta^2$ be everywhere positive in the lower subdomain in order to better capture the variation of fields in the planetary boundary layer. Differentiating (B.14) gives

$$\frac{\partial^2 r}{\partial \eta^2} = \frac{2}{\eta_I^2}\left[\left(\frac{\eta_I r_T - r_I}{1-\eta_I}\right) + r_S(\lambda,\phi)\right], \quad \eta_0 \equiv 0 \le \eta \le \eta_I. \tag{B.18}$$

Since $\partial^2 r/\partial\eta^2$ is required to be everywhere positive in the lower subdomain, so

$$\eta_I \ge \frac{r_I - \min r_S(\lambda,\phi)}{r_T - \min r_S(\lambda,\phi)}. \tag{B.19}$$

Thus putting (B.17) and (B.19) together yields

$$\frac{r_I - \min r_S(\lambda,\phi)}{r_T - \min r_S(\lambda,\phi)} \le \eta_I < \frac{r_I - \max r_S(\lambda,\phi)}{(r_I + r_T)/2 - \max r_S(\lambda,\phi)}. \tag{B.20}$$

For such an η_I to exist requires the left-hand-side of this inequality to be less than the right-hand side, which means that r_I must satisfy

$$r_I > 2\max r_S(\lambda,\phi) - \min r_S(\lambda,\phi). \tag{B.21}$$

B.3.5 Inverse transformation

The inverse of the transformation (B.12) in the lower sub-domain is now derived. Assume that $r_k \equiv r(\lambda,\phi,\eta_k)$ is known and that the corresponding value η_k is needed. Evaluating (B.12) at $\eta = \eta_k$ gives

$$r_k = \left(\frac{\eta_k}{\eta_I}\right) r_I + \left(1 - \frac{\eta_k}{\eta_I}\right)^2 r_S(\lambda,\phi) - \left(1 - \frac{\eta_k}{\eta_I}\right)\left(\frac{\eta_k}{\eta_I}\right)\left(\frac{\eta_I r_T - r_I}{1-\eta_I}\right), \quad k = 0, 1, ..., I. \tag{B.22}$$

Provided that $\eta_I r_T - r_I + (1-\eta_I) r_S \neq 0$ everywhere (the special case where the quadratic form in η of (B.22) degenerates to a linear one over oceans, is detailed in Section B.4), this may be rewritten as

$$\left(\frac{\eta_k}{\eta_I}\right)^2 - (1-c_I)\left(\frac{\eta_k}{\eta_I}\right) - c_k = 0, \quad k = 0, 1, ..., I, \tag{B.23}$$

where

$$c_k = (1-\eta_I)\left[\frac{r_k - r_S}{\eta_I r_T - r_I + (1-\eta_I) r_S}\right), \tag{B.24}$$

with solution

$$\eta_k = \left[\frac{(1-c_I) \pm \sqrt{(1-c_I)^2 + 4c_k}}{2}\right]\eta_I, \quad k = 0, 1, 2, ..., I. \tag{B.25}$$

For the transformation to hold both at the surface, where $\eta_0 \equiv 0$ and $c_0 = 0$, and at $\eta = \eta_I$, where $c_k = c_I$, requires the positive root. Note that $(1-c_I)$ is negative, because of inequality (B.17), and this has been used to deduce the choice of root. Thus the inverse transformation is

$$\eta_k = \left[\frac{(1-c_I) + \sqrt{(1-c_I)^2 + 4c_k}}{2}\right]\eta_I, \quad k = 0, 1, 2, ..., I. \tag{B.26}$$

In the upper sub-domain, the inverse transformation is straightforwardly obtained by solving (B.9) for η. Thus

$$\eta_k = \frac{(1-\eta_I) r_k + (\eta_I r_T - r_I)}{r_T - r_I}, \quad k = I, I+1, ..., N.$$

B.3.6 Algorithm for the composite linear/ quadratic coordinate and grid - Method A

The above relations may be put together in more than one way to define the vertical coordinate transformation and grid, depending upon which parameters are specified and which ones are then determined as an algebraic consequence. Two such ways are given here. The simplest, "Method A", is given in this subsection and an alternative, "Method B" (designed expressly for New Dynamics history buffs), in the following subsection (Section B.3.7).

Given

- $r_S(\lambda, \phi)$, the specification of the bottom orography;

- r_I (a constant), the location of the interfacial surface between the two subdomains, that satisfies (B.21);
- r_T (a constant), the location of the rigid lid;
- a sampling set $\{\eta_0 \equiv 0, \eta_1, \eta_2, ..., \eta_{N-1}, \eta_N \equiv 1\}$ for the vertical placement of levels in the terrain-following coordinate η; and
- I, the integer level index that determines which η_k of the sampling set defines the location of the interfacial surface between the two subdomains, chosen such that (B.20) is satisfied.

To determine

- $r(\lambda, \phi, \eta_k), \quad k = 0, 1, 2, ..., N.$

Algorithm

- Evaluate, for $k = 0, 1, 2, ..., I$,

$$r(\lambda, \phi, \eta_k) = \left(\frac{\eta_k}{\eta_I}\right) r_I + \left(1 - \frac{\eta_k}{\eta_I}\right)^2 r_S(\lambda, \phi) - \left(1 - \frac{\eta_k}{\eta_I}\right)\left(\frac{\eta_k}{\eta_I}\right)\left(\frac{\eta_I r_T - r_I}{1 - \eta_I}\right). \quad \text{(B.27)}$$

- Evaluate, for $k = I, I+1, ..., N$,

$$r(\lambda, \phi, \eta_k) = \left(\frac{1 - \eta_k}{1 - \eta_I}\right) r_I + \left(\frac{\eta_k - \eta_I}{1 - \eta_I}\right) r_T. \quad \text{(B.28)}$$

Aside :

In the above algorithm it is assumed that I, the integer level index that defines the location of the interfacial surface in the transformed coordinate η, is given. For a specified r_I (a constant, the location of the interfacial surface in the original r coordinate), varying I determines in a relative way how many levels are placed (i.e. how much resolution there is) above and below the interfacial surface (defined as $r = r_I$ in r coordinates and as $\eta = \eta_I$ in η coordinates). Thus increasing (decreasing) the value of I (but remember that it is bounded by the total number of levels, N) increases the resolution in the lower (upper) subdomain at the expense of resolution in the upper (lower) subdomain.

So how should one set this value? There is a certain arbitrariness in this, but a simple starting point is to set η_I *to a little less than the limiting value given by* (B.17)*, see what this gives, and to then decrement* η_I *from this value whilst respecting* (B.19)*. An alternative is to go close to the other extreme and set* $\eta_I = (r_I - a) / (r_T - a)$*, where* a *is the Earth's mean radius - when* $\min r_S (\lambda, \phi) = a$*, this is exactly the limiting value of inequality* (B.19)*. It corresponds to the special case detailed in Section B.4 for which the quadratic dependence of* r *on* η *degenerates into a linear one over the oceans. The disadvantage of this alternative is that the level placement in the transformed* η *coordinate will be less uniform, since the vertical variation of variables in the planetary boundary layer is generally better captured by a quadratically-varying coordinate than a linearly-varying one.*

B.3.7 Algorithm for the composite linear/ quadratic coordinate and grid - Method B

Method B assumes that the sampling set is specified as a function of r rather than of η as in Method A. This means that additional steps are required in order to specify the equivalent sampling set in the η coordinate, and this involves inverting the transformations (B.9) and (B.12) from r to η over the ocean where $r_S^{ocean} \equiv a$, the mean radius of the Earth.

Given

- $r_S (\lambda, \phi)$, the specification of the bottom orography;
- r_I (a constant), the location of the interfacial surface between the two subdomains, that satisfies (B.21);
- r_T (a constant), the location of the rigid lid;
- a sampling set $\left\{ r_0^{ocean} \equiv r_S^{ocean} \equiv a, r_1^{ocean}, r_2^{ocean}, ..., r_{N-1}^{ocean}, r_N^{ocean} \equiv r_T \right\}$ for the vertical placement of levels over the ocean; and
- I, the integer level index that determines which r_k of the sampling set defines the location of the interfacial surface between the two subdomains;

- η_I, the location in the transformed coordinate of the interfacial surface between the two subdomains, chosen such that (B.20) is satisfied.

To determine

- $\eta_k, \quad k = 0, 1, 2, ..., N.$
- $r(\lambda, \phi, \eta_k), \quad k = 0, 1, 2, ..., N.$

Algorithm

- Evaluate, for $k = 0, 1, 2, ..., I$,

$$\eta_k = \left[\frac{(1 - c_I) + \sqrt{(1 - c_I)^2 + 4c_k}}{2} \right] \eta_I, \tag{B.29}$$

  where

$$c_k = (1 - \eta_I) \left[\frac{r_k^{ocean} - r_S^{ocean}}{\eta_I r_T - r_I + (1 - \eta_I)\, r_S^{ocean}} \right]. \tag{B.30}$$

- Evaluate, for $k = I, I + 1, ..., N$,

$$\eta_k = \frac{(r_k^{ocean} - r_I) + \eta_I (r_T - r_k^{ocean})}{(r_T - r_I)}. \tag{B.31}$$

- Evaluate, for $k = 0, 1, 2, ..., I$,

$$r(\lambda, \phi, \eta_k) = \left(\frac{\eta_k}{\eta_I} \right) r_I + \left(1 - \frac{\eta_k}{\eta_I} \right)^2 r_S(\lambda, \phi) - \left(1 - \frac{\eta_k}{\eta_I} \right) \left(\frac{\eta_k}{\eta_I} \right) \left(\frac{\eta_I r_T - r_I}{1 - \eta_I} \right). \tag{B.32}$$

- Evaluate, for $k = I, I + 1, ..., N$,

$$r(\lambda, \phi, \eta_k) = \left(\frac{1 - \eta_k}{1 - \eta_I} \right) r_I + \left(\frac{\eta_k - \eta_I}{1 - \eta_I} \right) r_T. \tag{B.33}$$

B.4 The "QUADn levels" - the current preferred choice - a simple special case of the composite linear/ quadratic transformation

As already mentioned in asides in the immediately preceding sub-section (Sections B.3.3 and B.3.6), by choosing η_I such that

$$\eta_I = \frac{r_I - a}{r_T - a} = \frac{z_I}{z_T}, \tag{B.34}$$

where a is the mean radius of the Earth, and

$$z = r - a, \tag{B.35}$$

the composite linear/ quadratic transformation for Method B simplifies somewhat. This transformation is the one that has been adopted in the current version of the model since it significantly improves the flow over, around, and downstream of the Himalayas with respect to the one previously used, which failed to fully respect the continuity of $\partial r/\partial \eta$ over orography. It has the advantage of simplicity and of addressing the coordinate flattening issue (see weakness 1., early in Section B.2). However it has the disadvantage of not addressing the level placement/ sampling issue (see weakness 2., *ibid,* and the aside in Section B.3.6), and consequently the level placement in the transformed η coordinate is far from uniform in the planetary boundary layer with possible sub-optimal accuracy there. This transformation and its associated placement of levels are known in ND parlance as the "QUADn levels" where $n = I$, the integer level number of the interface surface $r = r_I$.

Using (B.34), the algorithm for Method B of the composite linear quadratic transformation simplifies to the following:

Given

- $r_S(\lambda, \phi)$, the specification of the bottom orography;
- r_I (a constant), the location of the interfacial surface between the two subdomains, that satisfies (B.21);
- r_T (a constant), the location of the rigid lid;
- a sampling set $\left\{r_0^{ocean} \equiv r_S^{ocean} \equiv a, r_1^{ocean}, r_2^{ocean}, ..., r_{N-1}^{ocean}, r_N^{ocean} \equiv r_T\right\}$ for the vertical placement of levels over the ocean; and
- I, the integer level index that determines which r_k of the sampling set defines the location of the interfacial surface between the two subdomains.

To determine

- $\eta_k, \quad k = 0, 1, 2, ..., N.$
- $r(\lambda, \phi, \eta_k), \quad k = 0, 1, 2, ..., N.$

Algorithm

- Evaluate, for $k = 0, 1, 2, ..., N$,

$$\eta_k = \frac{r_k^{ocean} - a}{r_T^{ocean} - a} = \frac{z_k^{ocean}}{z_T^{ocean}}, \tag{B.36}$$

- Evaluate, for $k = 0, 1, 2, ..., I$,

$$\begin{aligned} r(\lambda, \phi, \eta_k) &= a + \eta_k (r_T - a) + \left(1 - \frac{\eta_k}{\eta_I}\right)^2 [r_S(\lambda, \phi) - a] \\ &= a + \eta_k z_T + \left(1 - \frac{\eta_k}{\eta_I}\right)^2 z_S(\lambda, \phi). \end{aligned} \tag{B.37}$$

- Evaluate, for $k = I, I+1, ..., N$,

$$\begin{aligned} r(\lambda, \phi, \eta_k) &= a + \eta_k (r_T - a) \\ &= a + \eta_k z_T. \end{aligned} \tag{B.38}$$

__Aside :__

> *Comparison of* (B.38) *with* (B.37) *shows that the transformation between r and η over oceans is a linear one, with the two subdomains using the identical linear transformation. It is only over orography, and in the lower sub-domain, that r varies quadratically as a function of η. This can be contrasted with the general case where, from* (B.12)*, it is seen that r is a quadratic function of η* everywhere *in the lower sub-domain, including over oceans.*

B.5 Quadratic spline transformations

Whilst the composite linear/ quadratic transformation, discussed in Section B.3 above, addresses in principle the coordinate flattening and level placement/ sampling issues of the linear transformation (B.3), for uniform and quasi-uniform samplings (in η) it may not result in sufficient resolution in the planetary boundary layer. It is therefore postulated that a multi- layer (three or more) quadratic spline transformation might achieve this since there are more parameters to control its behaviour. However the parameters have to be chosen judiciously in order to satisfy all the transformation constraints, e.g. on monotonicity. A possible advantage of a quadratic spline is that since $\partial r/\partial\eta$ is then linear, so linear averaging of its values at the half-integer levels $\eta_{k+1/2}$ from those at the integer levels η_k is exact.

Let the domain $\eta_0 \equiv 0 \leq \eta \leq \eta_N \equiv 1$ be decomposed into M $(\leq N)$ subdomains $\xi_{m-1} \leq \eta \leq \xi_m$, $m = 1, 2, ..., M$. Also let $r(\lambda, \phi, \eta)$ be approximated by a quadratic spline, i.e. by a continuous function which is piecewise quadratic with continuous first derivatives at the knot points $\{\xi_1, \xi_2, ..., \xi_{M-1}\}$. Note that $\xi_0 \equiv \eta_0 \equiv 0$, $\xi_M \equiv \eta_N \equiv 1$, and that a knot point ξ_m is also a meshpoint η_k, but the converse is not necessarily true since, in general, there will be more meshpoints than there are knot points.

B.5.1 Functional form in the sub-domain $\xi_{m-1} \leq \eta \leq \xi_m$, $m = 1, 2, ..., M$.

Let r vary quadratically as a function of η in each subdomain $\xi_{m-1} \leq \eta \leq \xi_m$, i.e.

$$\begin{aligned} r(\lambda, \phi, \eta) &= \left(\frac{\xi_m - \eta}{\xi_m - \xi_{m-1}}\right) r_{m-1} + \left(\frac{\eta - \xi_{m-1}}{\xi_m - \xi_{m-1}}\right) r_m \\ &\quad - \left(\frac{\xi_m - \eta}{\xi_m - \xi_{m-1}}\right)\left(\frac{\eta - \xi_{m-1}}{\xi_m - \xi_{m-1}}\right) A_m(\lambda, \phi), \quad \xi_{m-1} \leq \eta \leq \xi_m. \end{aligned} \tag{B.39}$$

Successively differentiating (B.39) gives

$$\begin{aligned} \frac{\partial r}{\partial \eta} &= \left(\frac{r_m - r_{m-1}}{\xi_m - \xi_{m-1}}\right) - \left(\frac{1}{\xi_m - \xi_{m-1}}\right)\left[\left(\frac{\xi_m - \eta}{\xi_m - \xi_{m-1}}\right) - \left(\frac{\eta - \xi_{m-1}}{\xi_m - \xi_{m-1}}\right)\right] A_m(\lambda, \phi), \\ &\qquad \xi_{m-1} \leq \eta \leq \xi_m, \end{aligned} \tag{B.40}$$

$$\frac{\partial^2 r}{\partial \eta^2} = \frac{2A_m(\lambda, \phi)}{(\xi_m - \xi_{m-1})^2}, \quad \xi_{m-1} \leq \eta \leq \xi_m. \tag{B.41}$$

B.5.2 Matching $\partial r/\partial \eta$ across the interface levels

By construction (B.39) makes the transformation $r = r(\lambda, \phi, \eta)$ continuous, but it does not ensure the continuity of $\partial r/\partial \eta$. This is achieved by using (B.40) to match $\partial r/\partial \eta$ across the knots (interface levels) $\eta = \xi_m$, $m = 1, 2, ..., M - 1$. Thus

$$\begin{aligned} \left(\frac{1}{\xi_{m+1} - \xi_m}\right) A_{m+1}(\lambda, \phi) + \left(\frac{1}{\xi_m - \xi_{m-1}}\right) A_m(\lambda, \phi) &= \left(\frac{r_{m+1} - r_m}{\xi_{m+1} - \xi_m}\right) - \left(\frac{r_m - r_{m-1}}{\xi_m - \xi_{m-1}}\right), \\ m = 1, 2, ..., M - 1. \end{aligned} \tag{B.42}$$

Eq. (B.42) represents a bidiagonal set of $M - 1$ linear equations for the M unknowns $A_m(\lambda, \phi)$, $m = 1, 2, ..., M$. To close the problem an additional condition is required.

One way of achieving this is to "fully tension" the spline in the last interval $\xi_{M-1} \leq \eta \leq \xi_M$, such that the quadratic degenerates there into a linear function. This gives

$$A_M(\lambda, \phi) = 0, \tag{B.43}$$

and

$$r(\lambda,\phi,\eta) = \left(\frac{1-\eta}{1-\xi_{M-1}}\right) r_{M-1} + \left(\frac{\eta-\xi_{M-1}}{1-\xi_{M-1}}\right) r_M. \tag{B.44}$$

The remaining $A_m(\lambda,\phi)$, $m = M-1, M-2, ..., 2, 1$ are then obtained by recursive application of (B.42). Thus

$$A_m(\lambda,\phi) = (\xi_m - \xi_{m-1}) \left[\left(\frac{r_{m+1}-r_m}{\xi_{m+1}-\xi_m}\right) - \left(\frac{r_m - r_{m-1}}{\xi_m - \xi_{m-1}}\right) - \left(\frac{1}{\xi_{m+1}-\xi_m}\right) A_{m+1}(\lambda,\phi)\right],$$
$$m = M-1, M-2, ..., 2, 1. \tag{B.45}$$

B.5.3 Monotonicity and constraints

The function $r(\lambda,\phi,\eta)$, $m = 1, 2, ..., M-1$ defined by (B.39) is a quadratic function of η. It is monotonic increasing in the interval $[\xi_{m-1}, \xi_m]$ provided its first derivative (for all possible values of λ and ϕ) is positive at both endpoints, i.e. at $\eta = \xi_{m-1}$ and $\eta = \xi_m$.

Evaluating (B.40) at $\eta = \xi_{m-1}$ and $\eta = \xi_m$ leads to

$$A_m(\lambda,\phi) < r_m - r_{m-1}, \tag{B.46}$$

$$-A_m(\lambda,\phi) < r_m - r_{m-1}. \tag{B.47}$$

Depending upon the sign of $A_m(\lambda,\phi)$, one of (B.46) and (B.47) will be automatically satisfied.

B.5.4 The two-layer quadratic spline ($M = 2$)

If the quadratic spline is "fully tensioned" in the uppermost sub-domain, as described above, then the two-layer quadratic spline (i.e. $M = 2$) is equivalent to the composite linear/quadratic transformation discussed in Sections B.3 and B.4.

B.5.5 The three-layer quadratic spline ($M = 3$)

For the special case $M = 3$ let the interfacial surfaces be defined by $\eta = \eta_{I_1} \equiv \xi_1 =$ constant and $\eta = \eta_{I_2} \equiv \xi_2$, and note that $\xi_0 \equiv \eta_S \equiv 0$ and $\xi_3 \equiv \eta_T \equiv 1$. From (B.43) and (B.45),

$$A_3(\lambda,\phi) = 0, \tag{B.48}$$

$$A_2(\lambda,\phi) = \left(\frac{\eta_{I_2}-\eta_{I_1}}{1-\eta_{I_2}}\right) r_T - \left(\frac{1-\eta_{I_1}}{1-\eta_{I_2}}\right) r_{I_2} + r_{I_1}(\lambda,\phi), \tag{B.49}$$

$$A_1(\lambda,\phi) = \frac{1}{(\eta_{I_2}-\eta_{I_1})}\left\{\eta_{I_1}\left[(2-\eta_{I_1}-\eta_{I_2})r_{I_2}-(\eta_{I_2}-\eta_{I_1})r_T\right]/(1-\eta_{I_2}) - \left[(\eta_{I_1}+\eta_{I_2})r_{I_1}(\lambda,\phi)-(\eta_{I_2}-\eta_{I_1})r_S(\lambda,\phi)\right]\right\}. \tag{B.50}$$

It is desirable that the curvature $\partial^2 r/\partial\eta^2$ be positive in the planetary boundary layer in order to better capture the variation of fields therein. From (B.41) and (B.50), this then leads to the condition

$$\frac{\eta_{I_1}}{1-\eta_{I_2}} > \frac{(\eta_{I_1}+\eta_{I_2})r_{I_1}(\lambda,\phi)-(\eta_{I_2}-\eta_{I_1})r_S(\lambda,\phi)}{(2-\eta_{I_2}-\eta_{I_1})r_{I_2}-(\eta_{I_2}-\eta_{I_1})r_T} \tag{B.51}$$

This must hold for all (λ,ϕ), and so

$$\frac{\eta_{I_1}}{1-\eta_{I_2}} > \max\left[\frac{(\eta_{I_1}+\eta_{I_2})r_{I_1}(\lambda,\phi)-(\eta_{I_2}-\eta_{I_1})r_S(\lambda,\phi)}{(2-\eta_{I_2}-\eta_{I_1})r_{I_2}-(\eta_{I_2}-\eta_{I_1})r_T}\right]. \tag{B.52}$$

Applying (B.46) with $m=1$ leads to the condition

$$\left(\frac{\eta_{I_1}}{1-\eta_{I_2}}\right)\left[(2-\eta_{I_1}-\eta_{I_2})r_{I_2}-(\eta_{I_2}-\eta_{I_1})r_T\right] - \left[(\eta_{I_1}+\eta_{I_2})r_{I_1}(\lambda,\phi)-(\eta_{I_2}-\eta_{I_1})r_S(\lambda,\phi)\right] < (\eta_{I_2}-\eta_{I_1})\left[r_{I_1}(\lambda,\phi)-r_S(\lambda,\phi)\right] \tag{B.53}$$

for all (λ,ϕ), and so

$$\left(\frac{\eta_{I_1}}{1-\eta_{I_2}}\right) < \frac{2\min\left[\eta_{I_2}r_{I_1}(\lambda,\phi)-(\eta_{I_2}-\eta_{I_1})r_S(\lambda,\phi)\right]}{(2-\eta_{I_1}-\eta_{I_2})r_{I_2}-(\eta_{I_2}-\eta_{I_1})r_T}. \tag{B.54}$$

Thus putting (B.50) and (B.51) together yields

$$\max\left[\frac{(\eta_{I_1}+\eta_{I_2})r_{I_1}(\lambda,\phi)-(\eta_{I_2}-\eta_{I_1})r_S(\lambda,\phi)}{(2-\eta_{I_1}-\eta_{I_2})r_{I_2}-(\eta_{I_2}-\eta_{I_1})r_T}\right] < \frac{\eta_{I_1}}{(1-\eta_{I_2})} < \frac{2\min\left[\eta_{I_2}r_{I_1}(\lambda,\phi)-(\eta_{I_2}-\eta_{I_1})r_S(\lambda,\phi)\right]}{(2-\eta_{I_1}-\eta_{I_2})r_{I_2}-(\eta_{I_2}-\eta_{I_1})r_T}. \tag{B.55}$$

For the middle layer the bounds depend upon whether $A_2(\lambda,\phi)$ is positive or negative. Whilst both cases are possible, the case of $A_2(\lambda,\phi)$ being positive is the one that corresponds to the most likely practical applications since this means that the gradient of $\partial r/\partial\eta$ is positive and therefore that the resolution continues to degrade in r coordinates as a function of increasing r. Assuming that this is the case then, from (B.46) and (B.49), this gives that

$$0 < \left(\frac{\eta_{I_2}-\eta_{I_1}}{1-\eta_{I_2}}\right)r_T - \left(\frac{1-\eta_{I_1}}{1-\eta_{I_2}}\right)r_{I_2} + r_{I_1}(\lambda,\phi) < r_{I_2} - r_{I_1}(\lambda,\phi), \tag{B.56}$$

for all $r_{I_2} - r_{I_1}(\lambda,\phi)$, i.e.

$$-\min r_{I_1}(\lambda,\phi) < \left(\frac{\eta_{I_2}-\eta_{I_1}}{1-\eta_{I_2}}\right)r_T - \left(\frac{1-\eta_{I_1}}{1-\eta_{I_2}}\right)r_{I_2} < r_{I_2} - 2\max r_{I_1}(\lambda,\phi). \tag{B.57}$$

In particular, for this to be true requires the left-hand-side of this inequality to be less than the right-hand side, i.e.

$$r_{I_2} > 2\max r_{I_1}(\lambda,\phi) - \min r_{I_1}(\lambda,\phi)\,. \tag{B.58}$$

To close the problem, $r_{I_1}(\lambda,\phi)$ needs to be somehow specified. One way of doing this is to specify

$$r_{I_1}(\lambda,\phi) = \left(\frac{r_{I_1}^{ocean} - r_S^{ocean}}{r_{I_2} - r_S^{ocean}}\right) r_{I_2} + \left(\frac{r_{I_2} - r_{I_1}^{ocean}}{r_{I_2} - r_S^{ocean}}\right) r_S(\lambda,\phi)\,, \tag{B.59}$$

where $r_{I_1}^{ocean}$ is a specified oceanic value (a constant) , and r_S^{ocean} is the Earth's radius a.

The above can be put into algorithmic form as follows:

Given

- $r_S(\lambda,\phi)$, the specification of the bottom orography;
- r_{I_2} (a constant), the location of the interfacial surface between the uppermost two subdomains, that satisfies (B.57);
- $r_{I_1}^{ocean}$, the location over the ocean of the interfacial surface between the lowermost two subdomains;
- r_T (a constant), the location of the rigid lid;
- a sampling set $\{\eta_0 \equiv 0, \eta_1, \eta_2, ..., \eta_{N-1}, \eta_N \equiv 1\}$ for the vertical placement of levels in the terrain-following coordinate η; and
- I_1 and I_1, the integer level indices that determine which η_k of the sampling set define the location of the interfacial surface between the three subdomains, chosen such that (B.55) and (B.57) are satisfied.

To determine

- $r(\lambda,\phi,\eta_k)\,,\quad k = 0,1,2,...,N.$

Algorithm

- Evaluate

$$r_{I_1}(\lambda,\phi) = \left(\frac{r_{I_1}^{ocean} - r_S^{ocean}}{r_{I_2} - r_S^{ocean}}\right) r_{I_2} + \left(\frac{r_{I_2} - r_{I_1}^{ocean}}{r_{I_2} - r_S^{ocean}}\right) r_S(\lambda,\phi)\,. \tag{B.60}$$

- Evaluate, for $k = 0, 1, 2, ..., I_1$,

$$r(\lambda, \phi, \eta_k) = \left(1 - \frac{\eta_k}{\eta_{I_1}}\right) r_S + \left(\frac{\eta_k}{\eta_{I_1}}\right) r_{I_1}(\lambda, \phi) - \left(\frac{\eta_k}{\eta_{I_1}}\right)\left(1 - \frac{\eta_k}{\eta_{I_1}}\right) A_1(\lambda, \phi), \quad \text{(B.61)}$$

where

$$\begin{aligned} A_1(\lambda, \phi) &= \frac{1}{(\eta_{I_2} - \eta_{I_1})} \{\eta_{I_1} [(2 - \eta_{I_1} - \eta_{I_2}) r_{I_2} - (\eta_{I_2} - \eta_{I_1}) r_T] / (1 - \eta_{I_2}) \\ &\quad - [(\eta_{I_1} + \eta_{I_2}) r_{I_1}(\lambda, \phi) - (\eta_{I_2} - \eta_{I_1}) r_S(\lambda, \phi)]\}. \end{aligned} \quad \text{(B.62)}$$

- Evaluate, for $k = I_1, I_1 + 1, ..., I_2 - 1, I_2$,

$$r(\lambda, \phi, \eta_k) = \left(\frac{\eta_{I_2} - \eta_k}{\eta_{I_2} - \eta_{I_1}}\right) r_{I_1}(\lambda, \phi) + \left(\frac{\eta_k - \eta_{I_1}}{\eta_{I_2} - \eta_{I_1}}\right) r_{I_2} - \left(\frac{\eta_{I_2} - \eta_k}{\eta_{I_2} - \eta_{I_1}}\right)\left(\frac{\eta_k - \eta_{I_1}}{\eta_{I_2} - \eta_{I_1}}\right) A_2(\lambda, \phi), \quad \text{(B.63)}$$

where

$$A_2(\lambda, \phi) = \left(\frac{\eta_{I_2} - \eta_{I_1}}{1 - \eta_{I_2}}\right) r_T - \left(\frac{1 - \eta_{I_1}}{1 - \eta_{I_2}}\right) r_{I_2} + r_{I_1}(\lambda, \phi). \quad \text{(B.64)}$$

- Evaluate, for $k = I_2, I + 1, ..., N$,

$$r(\lambda, \phi, \eta_k) = \left(\frac{1 - \eta_k}{1 - \eta_{I_2}}\right) r_{I_2} + \left(\frac{\eta_k - \eta_{I_2}}{1 - \eta_{I_2}}\right) r_T. \quad \text{(B.65)}$$

Aside :

The algorithm above is analogous to Method A for the composite linear/ quadratic transformation. An algorithm analogous to Method B is also possible in principle.

Aside :

Instead of setting r_I to a constant, a specified latitudinal dependence could in principle be introduced to reflect the generally higher location of the tropopause as one moves equatorward.

B.6 Cubic spline transformations

The potential advantage of a cubic- spline transformation over a quadratic- spline one is that it is smoother - its second derivative is also continuous at knots. A two- layer cubic spline also offers the potential to put more resolution in the planetary boundary layer than a two-layer quadratic spline can under similar circumstances and might be preferred to a three- layer quadratic spline.

Let the domain $\eta_0 \equiv 0 \leq \eta \leq \eta_N \equiv 1$ be decomposed into M $(\leq N)$ subdomains $\xi_{m-1} \leq \eta \leq \xi_m$, $m = 1, 2, ..., M$. Also let $r(\lambda, \phi, \eta)$ be approximated by a cubic spline, i.e. by a continuous function which is piecewise cubic with continuous first and second derivatives at the knot points $\{\xi_1, \xi_2, ..., \xi_{M-1}\}$. Note that $\xi_0 \equiv \eta_0 \equiv 0$, $\xi_M \equiv \eta_N \equiv 1$, and that a knot point ξ_m is also a meshpoint η_k, but the converse is not necessarily true since, in general, there will be more meshpoints than there are knot points.

B.6.1 Functional form in the sub-domain $\xi_{m-1} \leq \eta \leq \xi_m$, $m = 1, 2, ..., M$.

Let r vary cubically as a function of η in each subdomain $\xi_{m-1} \leq \eta \leq \xi_m$, i.e.

$$\begin{aligned} r(\lambda, \phi, \eta) &= \left(\frac{\xi_m - \eta}{\xi_m - \xi_{m-1}}\right) r_{m-1} + \left(\frac{\eta - \xi_{m-1}}{\xi_m - \xi_{m-1}}\right) r_m \\ &+ \frac{1}{6}\left[(\xi_m - \eta)^2 - (\xi_m - \xi_{m-1})^2\right]\left(\frac{\xi_m - \eta}{\xi_m - \xi_{m-1}}\right) E_{m-1} \\ &+ \frac{1}{6}\left[(\eta - \xi_{m-1})^2 - (\xi_m - \xi_{m-1})^2\right]\left(\frac{\eta - \xi_{m-1}}{\xi_m - \xi_{m-1}}\right) E_m, \\ &\qquad \xi_{m-1} \leq \eta \leq \xi_m, \end{aligned} \tag{B.66}$$

where

$$E_m(\lambda, \phi) \equiv \left.\frac{\partial^2 r}{\partial \eta^2}\right|_{\eta = \xi_m}, \quad m = 0, 1, 2, ...M. \tag{B.67}$$

Successively differentiating (B.66) gives

$$\begin{aligned} \frac{\partial r}{\partial \eta} &= \left(\frac{r_m - r_{m-1}}{\xi_m - \xi_{m-1}}\right) + \frac{1}{6}\left[1 - 3\left(\frac{\xi_m - \eta}{\xi_m - \xi_{m-1}}\right)^2\right](\xi_m - \xi_{m-1}) E_{m-1} \\ &+ \frac{1}{6}\left[3\left(\frac{\eta - \xi_{m-1}}{\xi_m - \xi_{m-1}}\right)^2 - 1\right](\xi_m - \xi_{m-1}) E_m, \quad \xi_{m-1} \leq \eta \leq \xi_m, \end{aligned} \tag{B.68}$$

$$\frac{\partial^2 r}{\partial \eta^2} = \left(\frac{\xi_m - \eta}{\xi_m - \xi_{m-1}}\right) E_{m-1} + \left(\frac{\eta - \xi_{m-1}}{\xi_m - \xi_{m-1}}\right) E_m, \;\; \xi_{m-1} \leq \eta \leq \xi_m. \tag{B.69}$$

B.6.2 Matching $\partial r/\partial \eta$ across the interface levels

By construction (B.66) makes the transformation $r = r(\lambda, \phi, \eta)$ and its second derivative $\partial^2 r/\partial \eta^2$ continuous, but it does not ensure the continuity of $\partial r/\partial \eta$. This is achieved by using (B.68) to match $\partial r/\partial \eta$ across the knots (interface levels) $\eta = \xi_m$, $m = 1, 2, ..., M-1$. Thus

$$\begin{aligned}\left(\frac{\xi_m - \xi_{m-1}}{6}\right) E_{m-1} + \left(\frac{\xi_{m+1} - \xi_{m-1}}{3}\right) E_m + \left(\frac{\xi_{m+1} - \xi_m}{6}\right) E_{m+1} \\ = \left(\frac{r_{m+1} - r_m}{\xi_{m+1} - \xi_m}\right) - \left(\frac{r_m - r_{m-1}}{\xi_m - \xi_{m-1}}\right), \quad m = 1, 2, ..., M-1. \end{aligned} \tag{B.70}$$

Eq. (B.70) represents a tridiagonal set of $M-1$ linear equations for the $M+1$ unknown curvatures E_m, $m = 0, 1, ..., M$. To close the problem two additional conditions are required.

One way of achieving this is to "fully tension" the spline in the last interval $\xi_{M-1} \leq \eta \leq \xi_M$, such that the cubic degenerates there into a linear function. This gives

$$E_{M-1} = E_M = 0, \tag{B.71}$$

and

$$r(\lambda, \phi, \eta) = \left(\frac{1-\eta}{1-\xi_{M-1}}\right) r_{M-1} + \left(\frac{\eta - \xi_{M-1}}{1-\xi_{M-1}}\right) r_M. \tag{B.72}$$

The remaining E_m, $m = M-2, M-3, ..., 1, 0$ are then obtained by recursive application of (B.70). Thus

$$\begin{aligned}\left(\frac{\xi_{m+1} - \xi_m}{6}\right) E_m &= -\left(\frac{\xi_{m+2} - \xi_{m+1}}{6}\right) E_{m+2} - \left(\frac{\xi_{m+2} - \xi_m}{3}\right) E_{m+1} + \left(\frac{r_{m+2} - r_{m+1}}{\xi_{m+2} - \xi_{m+1}}\right) \\ &\quad - \left(\frac{r_{m+1} - r_m}{\xi_{m+1} - \xi_m}\right), \quad m = M-2, M-1, ..., 1, 0. \end{aligned} \tag{B.73}$$

B.6.3 Monotonicity and constraints

The function $r(\lambda, \phi, \eta)$, $m = 1, 2, ..., M-1$ defined by (B.66) is a cubic function of η. It is monotonic increasing in the interval $[\xi_{m-1}, \xi_m]$ provided its first derivative (for all possible values of λ and ϕ) is positive at both $\eta = \xi_{m-1}$ and $\eta = \xi_m$, and provided the curvature $\partial^2 r/\partial \eta^2$ is everywhere of the same sign within this interval.

From (B.69) $\partial^2 r/\partial \eta^2$ is everywhere of the same sign within the interval $[\xi_{m-1}, \xi_m]$ provided both E_{m-1} and E_m are of the same sign.

Evaluating (B.68) at the two endpoints $\eta = \xi_{m-1}$ and $\eta = \xi_m$ leads to

$$r_m - r_{m-1} \geq \frac{1}{6} \left(\xi_m - \xi_{m-1}\right)^2 \left(2E_{m-1} + E_m\right), \tag{B.74}$$

$$r_m - r_{m-1} \geq -\frac{1}{6}\left(\xi_m - \xi_{m-1}\right)^2\left(E_{m-1} + 2E_m\right). \tag{B.75}$$

Depending upon the sign of E_{m-1} and E_m (recall that they must both have the same sign for monotonicity), one of (B.74) and (B.75) will be automatically satisfied since $(\xi_m - \xi_{m-1})$ is a positive quantity.

B.6.4 The two-layer cubic spline ($M = 2$)

For the special case $M = 2$ let the interfacial surface be defined by $\eta = \eta_I \equiv \xi_1 =$ constant and note that $\xi_0 \equiv \eta_S = 0$ and $\xi_2 \equiv \eta_T = 1$. From (B.71) and (B.73),

$$E_T = E_I = 0, \tag{B.76}$$

$$E_S = \left(\frac{6}{\eta_I}\right)\left[\left(\frac{r_T - r_I}{1-\eta_I}\right) - \left(\frac{r_I - r_S}{\eta_I}\right)\right]. \tag{B.77}$$

Eq. (B.77) does not directly impose a constraint on monotonicity for this case since the curvature is everywhere of the same sign in the lower layer. However it is desirable that the curvature be positive here in order to better capture the variation of the planetary boundary layer, and this then leads to the condition

$$\eta_I > \frac{r_I - \min r_S(\lambda,\phi)}{r_T - \min r_S(\lambda,\phi)}. \tag{B.78}$$

Applying (B.74) leads to the condition

$$\eta_I \leq \frac{r_I - \max r_S(\lambda,\phi)}{(r_I + r_T)/2 - \max r_S(\lambda,\phi)}. \tag{B.79}$$

Thus putting (B.78) and (B.79) together yields

$$\frac{r_I - \min r_S(\lambda,\phi)}{r_T - \min r_S(\lambda,\phi)} < \eta_I \leq \frac{r_I - \max r_S(\lambda,\phi)}{(r_I + r_T)/2 - \max r_S(\lambda,\phi)}. \tag{B.80}$$

For such an η_I to exist requires the left-hand-side of this inequality to be less than the right-hand side, which means that r_I is constrained to satisfy

$$r_I > 2\max r_S(\lambda,\phi) - \min r_S(\lambda,\phi). \tag{B.81}$$

Substituting (B.77) into (B.66) with $M = 2$ then gives for the lowest layer that

$$\begin{aligned} r(\lambda,\phi,\eta) &= \left(1 - \frac{\eta}{\eta_I}\right) r_S + \left(\frac{\eta}{\eta_I}\right) r_I - \left(2 - \frac{\eta}{\eta_I}\right)\left(\frac{\eta}{\eta_I}\right)\left(1 - \frac{\eta}{\eta_I}\right)\left[\frac{\eta_I(r_T - r_S) - (r_I - r_S)}{1-\eta_I}\right], \\ & \quad 0 \leq \eta \leq \eta_I. \end{aligned} \tag{B.82}$$

The above can be put into algorithmic form as follows:

Given

- $r_S(\lambda, \phi)$, the specification of the bottom orography;
- r_I (a constant), the location of the interfacial surface between the two subdomains, that satisfies (B.81);
- r_T (a constant), the location of the rigid lid;
- a sampling set $\{\eta_0 \equiv 0, \eta_1, \eta_2, ..., \eta_{N-1}, \eta_N \equiv 1\}$ for the vertical placement of levels in the terrain-following coordinate η; and
- I, the integer level index that determines which η_k of the sampling set defines the location of the interfacial surface between the two subdomains, chosen such that (B.80) is satisfied.

To determine

- $r(\lambda, \phi, \eta_k)\,, \quad k = 0, 1, 2, ..., N.$

Algorithm

- Evaluate, for $k = 0, 1, 2, ..., I$,

$$r(\lambda, \phi, \eta_k) = \left(1 - \frac{\eta_k}{\eta_I}\right) r_S + \left(\frac{\eta_k}{\eta_I}\right) r_I - \left(2 - \frac{\eta_k}{\eta_I}\right)\left(\frac{\eta_k}{\eta_I}\right)\left(1 - \frac{\eta_k}{\eta_I}\right)\left[\frac{\eta_I(r_T - r_S) - (r_I - r_S)}{1 - \eta_I}\right]. \tag{B.83}$$

- Evaluate, for $k = I, I+1, ..., N$,

$$r(\lambda, \phi, \eta_k) = \left(\frac{1 - \eta_k}{1 - \eta_I}\right) r_I + \left(\frac{\eta_k - \eta_I}{1 - \eta_I}\right) r_T. \tag{B.84}$$

Aside :

The algorithm above is analogous to Method A for the composite linear/ quadratic transformation. An algorithm analogous to Method B is also possible.

APPENDIX C

Definitions of averaging and difference operators

- Horizontal averaging operators $\overline{()}^{\lambda}$, $\overline{()}^{\phi}$ and $\overline{()}^{\lambda\phi}$:

$$\overline{F(\lambda_i,\phi_j)}^{\lambda} \equiv \overline{F_{i,j}}^{\lambda} = \frac{1}{2}\left[F(\lambda_{i-1/2},\phi_j) + F(\lambda_{i+1/2},\phi_j)\right] \equiv \frac{1}{2}\left[F_{i-1/2,j} + F_{i+1/2,j}\right], \quad \text{(C.1)}$$

$$\overline{F(\lambda_i,\phi_j)}^{\phi} \equiv \overline{F_{i,j}}^{\phi} = \frac{1}{2}\left[F(\lambda_i,\phi_{j-1/2}) + F(\lambda_i,\phi_{j+1/2})\right] \equiv \frac{1}{2}\left[F_{i,j-1/2} + F_{i,j+1/2}\right], \quad \text{(C.2)}$$

$$\begin{aligned}\overline{F(\lambda_i,\phi_j)}^{\lambda\phi} \equiv \overline{F_{i,j}}^{\lambda\phi} &= \frac{1}{4}\left[F(\lambda_{i-1/2},\phi_{j-1/2}) + F(\lambda_{i+1/2},\phi_{j-1/2})\right. \\ &\quad \left. + F(\lambda_{i+1/2},\phi_{j+1/2}) + F(\lambda_{i-1/2},\phi_{j+1/2})\right] \\ &\equiv \frac{1}{4}\left[F_{i-1/2,j-1/2} + F_{i+1/2,j-1/2} + F_{i+1/2,j+1/2} + F_{i-1/2,j+1/2}\right], \end{aligned} \quad \text{(C.3)}$$

where i and j are the horizontal grid indices in the λ- and ϕ-directions respectively. i and j are both positive, integral multiples of $1/2$ (for further details of the grid structure see Section 4). λ_i denotes the value of λ at the ith grid point in the λ-direction and ϕ_j denotes the value of ϕ at the jth grid point in the ϕ-direction. For the general variable, F, $F_{i,j}$ here denotes evaluation of F at the (i,j,k) grid point where, for clarity, the k subscript has been dropped from all the horizontal operators since for these operators it does not vary.

- Vertical averaging operators $\overline{()}^{r}$ and $\overline{()}^{\eta}$:

$$\begin{aligned}\overline{F(r_{i,j,k})}^{r} \equiv \overline{F_k}^{r} &= \frac{(r_{i,j,k} - r_{i,j,k-1/2})F(r_{i,j,k+1/2}) + (r_{i,j,k+1/2} - r_{i,j,k})F(r_{i,j,k-1/2})}{r_{i,j,k+1/2} - r_{i,j,k-1/2}} \\ &\equiv \frac{(r_{i,j,k} - r_{i,j,k-1/2})F_{k+1/2} + (r_{i,j,k+1/2} - r_{i,j,k})F_{k-1/2}}{r_{i,j,k+1/2} - r_{i,j,k-1/2}}, \end{aligned} \quad \text{(C.4)}$$

$$\begin{aligned}\overline{F(\eta_k)}^{\eta} \equiv \overline{F_k}^{\eta} &= \frac{(\eta_k - \eta_{k-1/2})F(\eta_{k+1/2}) + (\eta_{k+1/2} - \eta_k)F(\eta_{k-1/2})}{\eta_{k+1/2} - \eta_{k-1/2}} \\ &\equiv \frac{(\eta_k - \eta_{k-1/2})F_{k+1/2} + (\eta_{k+1/2} - \eta_k)F_{k-1/2}}{\eta_{k+1/2} - \eta_{k-1/2}}, \end{aligned} \quad \text{(C.5)}$$

where k is the vertical grid index and is a positive, integral multiple of $1/2$ (for further details of the grid structure see Section 4). For the general variable, F, F_k here denotes evaluation of F at the (i,j,k) grid point. For clarity, the i,j subscripts have been dropped from F in the definition of the vertical operators since they remain unchanged for these operators. However, they have been retained for the variable r to emphasise that r is in fact a function of i and j in addition to k. This is in contrast to η which, being the vertical co-ordinate variable, is only a function of k.

- Horizontal differencing operators $\delta_\lambda()$, $\delta_\phi()$, $\delta_{\lambda 1}()$ and $\delta_{\phi 1}()$:

$$\delta_\lambda F(\lambda_i, \phi_j) \equiv \delta_\lambda F_{i,j} = \frac{F(\lambda_{i+1/2}, \phi_j) - F(\lambda_{i-1/2}, \phi_j)}{\Delta\lambda} \equiv \frac{F_{i+1/2,j} - F_{i-1/2,j}}{\Delta\lambda}, \tag{C.6}$$

$$\delta_\phi F(\lambda_i, \phi_j) \equiv \delta_\phi F_{i,j} = \frac{F(\lambda_i, \phi_{j+1/2}) - F(\lambda_i, \phi_{j-1/2})}{\Delta\phi} \equiv \frac{F_{i,j+1/2} - F_{i,j-1/2}}{\Delta\phi}, \tag{C.7}$$

$$\delta_{\lambda 1} F(\lambda_i, \phi_j) \equiv \delta_{\lambda 1} F_{i,j} = \Delta\lambda\delta_\lambda F_{i,j} = F(\lambda_{i+1/2}, \phi_j) - F(\lambda_{i-1/2}, \phi_j) \equiv F_{i+1/2,j} - F_{i-1/2,j}, \tag{C.8}$$

$$\delta_{\phi 1} F(\lambda_i, \phi_j) \equiv \delta_{\phi 1} F_{i,j} = \Delta\phi\delta_\phi F_{i,j} = F(\lambda_i, \phi_{j+1/2}) - F(\lambda_i, \phi_{j-1/2}) \equiv F_{i,j+1/2} - F_{i,j-1/2}. \tag{C.9}$$

Note that here, as elsewhere, a uniform grid in both λ and ϕ has been assumed so that $\lambda_{i+1/2} - \lambda_{i-1/2} \equiv \Delta\lambda$, for all i, and $\phi_{j+1/2} - \phi_{j-1/2} \equiv \Delta\phi$, for all j.

- Vertical differencing operators $\delta_r()$, $\delta_{2r}()$, $\delta_\eta()$ and $\delta_{2\eta}()$:

$$\delta_r F(r_{i,j,k}) \equiv \delta_r F_k = \frac{F(r_{i,j,k+1/2}) - F(r_{i,j,k-1/2})}{r_{i,j,k+1/2} - r_{i,j,k-1/2}} \equiv \frac{F_{k+1/2} - F_{k-1/2}}{r_{i,j,k+1/2} - r_{i,j,k-1/2}}, \tag{C.10}$$

$$\delta_{2r} F(r_{i,j,k}) \equiv \delta_{2r} F_k = \frac{F(r_{i,j,k+1}) - F(r_{i,j,k-1})}{r_{i,j,k+1} - r_{i,j,k-1}} \equiv \frac{F_{k+1} - F_{k-1}}{r_{i,j,k+1} - r_{i,j,k-1}}, \tag{C.11}$$

$$\delta_\eta F(\eta_k) \equiv \delta_\eta F_k = \frac{F(\eta_{k+1/2}) - F(\eta_{k-1/2})}{\eta_{k+1/2} - \eta_{k-1/2}} \equiv \frac{F_{k+1/2} - F_{k-1/2}}{\eta_{k+1/2} - \eta_{k-1/2}}, \tag{C.12}$$

$$\delta_{2\eta} F(\eta_k) \equiv \delta_{2\eta} F_k = \frac{F(\eta_{k+1}) - F(\eta_{k-1})}{\eta_{k+1} - \eta_{k-1}} \equiv \frac{F_{k+1} - F_{k-1}}{\eta_{k+1} - \eta_{k-1}}. \tag{C.13}$$

Aside :

It is important to note that at present the model is coded in terms of a mix of the two vertical variables η and $r(\lambda, \phi, \eta)$. Since r is itself a function of λ and ϕ, the operation of averaging in the vertical over r does not commute with horizontal averaging in either the λ- or ϕ-directions. As, in the model, r is only stored on Π- and w-points, where mixed horizontal and vertical (in r) averages are required, the vertical averaging is performed first if the variable lies on a Π-or w-point followed *by the horizontal average. But, for variables stored elsewhere, the horizontal averaging is performed first in order to obtain an estimate of the variable on either a* Π*-or* w*-point where the vertical averaging can be straightforwardly performed. For example, if we wish to evaluate the vertical (in* r*) and horizontal (in the* λ*-direction for example) average of* Π*, we first average* Π *in the vertical direction to obtain an estimate of* Π *on a* w*-point and then we perform the horizontal average in the* λ*-direction, i.e. as* $\overline{\overline{\Pi}^{r}}^{\lambda}$*. In contrast, if we wish to evaluate the vertical (in* r*) and horizontal average of* u*, we first perform the horizontal average in the* λ*-direction to obtain an estimate of* u *on a* Π*-point and then perform the average in the vertical, i.e. as* $\overline{\overline{u}^{\lambda}}^{r}$*. In the documentation the order of the averaging operators has been given in the same order as it appears in the model code. Note, that this complication does not arise with vertical averaging over* η *as this operation does commute with averages in both the horizontal directions.*

APPENDIX D

Proof of equality of the matrices M and N [(5.74) and (5.75)]

Outline derivations of nine spherical triangle formulae dominate this proof. The final step is simple substitution into the formulae to show equality of each element M_{ij} of $\mathbf{M}$ to the corresponding element N_{ij} of $\mathbf{N}$. The nine formulae are distinguished from other equations by $\star\star$ labels.

The *sides* of a spherical triangle are the great circle arcs which define it. They are conveniently specified by the angles they subtend at the centre of the sphere in whose surface they lie. The *angles* of a spherical triangle are those subtended by the great circle arcs at their points of intersection. See Heading (1970).

Consider a spherical triangle ABC having angles A, B, C and sides a, b, c as shown in Fig. D.1. Let O be the centre of the sphere, and take Cartesian axes with associated (geocentric) unit vectors $\mathbf{I}$, $\mathbf{J}$, $\mathbf{K}$; moreover, place these unit vectors so that $\mathbf{K}$ is aligned with OB, and so that $\mathbf{I}$ lies in the plane containing $\mathbf{K}$ and OC. For further convenience, choose the unit of distance to be the radius of the sphere. Then the position vectors of A, B and C relative to O are simply

$$\mathbf{r}_A = \mathbf{I}\sin c\cos B + \mathbf{J}\sin c\sin B + \mathbf{K}\cos c\,, \tag{D.1}$$

$$\mathbf{r}_B = \mathbf{K}\,, \tag{D.2}$$

$$\mathbf{r}_C = \mathbf{I}\sin a + \mathbf{K}\cos a\,. \tag{D.3}$$

[The reason for the choice of alignment of $\mathbf{K}$ with OB rather than OA is purely mnemonic: point A will correspond to the arrival point when we come to apply the formulae. Also, point C will correspond to the departure point, which involves a small alphabetical shift of association, but not the confusion of a transposition.]

Forming the scalar product $\mathbf{r}_A \cdot \mathbf{r}_C = \cos b$ from (D.1) and (D.3) gives

$$\star\star \quad \cos b = \cos c\cos a + \sin c\sin a\cos B\,. \tag{D.4}$$

The $\star\star$ label indicates that (D.4) is one of thenine formulae to be applied in the final stage of the proof. Eq. (D.4) is sometimes called the *cosine rule for sides* - a potentially misleading

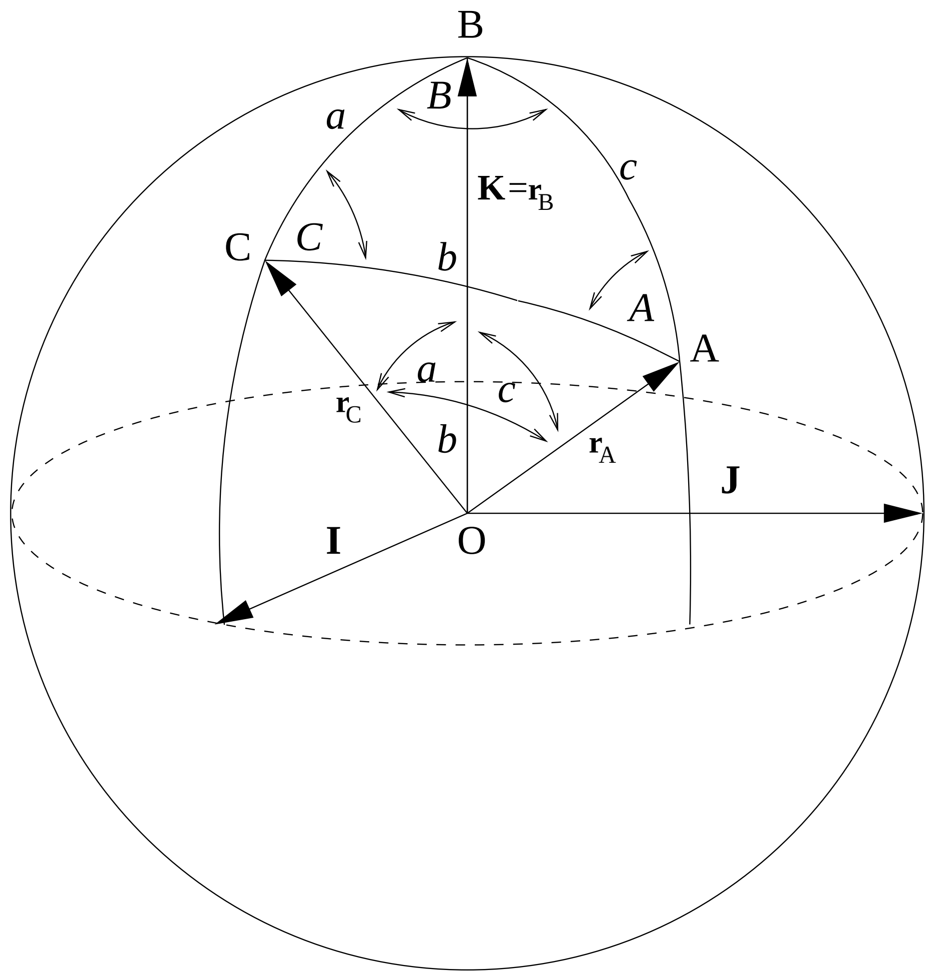

Figure D.1: A spherical triangle ABC on the unit sphere, centre O. Sides a, b, c and angles A, B, C are as indicated. The (unit) position vectors of A, B, C relative to O are $\mathbf{r}_A$, $\mathbf{r}_B$, $\mathbf{r}_C$. Geocentric unit vectors **I**, **J**, **K** are aligned so as to simplify the derivation of the formulae given in the text.

name, since one of its most important roles is to provide an expression for the cosine of the angle B:

$$\cos B = \frac{(\cos b - \cos c \cos a)}{\sin c \sin a}. \tag{D.5}$$

Expressions similar to (D.4) must exist for $\cos c$ and $\cos a$, and by cyclic change of sides and angle they must be

$$\cos c = \cos a \cos b + \sin a \sin b \cos C \,, \tag{D.6}$$

$$\cos a = \cos b \cos c + \sin b \sin c \cos A \,. \tag{D.7}$$

The implied expressions for $\cos C$ and $\cos A$ are cyclic modifications of (D.5):

$$\cos C = (\cos c - \cos a \cos b) \,/\, \sin a \sin b \,, \tag{D.8}$$

$$\cos A = (\cos a - \cos b \cos c) \,/\, \sin b \sin c \,. \tag{D.9}$$

From (D.5),

$$\sin B = \left[1 - \frac{(\cos b - \cos c \cos a)^2}{\sin^2 c \sin^2 a} \right]^{1/2} . \tag{D.10}$$

Hence (by use of basic trig identities):

$$\frac{\sin B}{\sin b} = \frac{\left[1 - \cos^2 a - \cos^2 b - \cos^2 c + 2 \cos a \cos b \cos c\right]^{1/2}}{\sin a \sin b \sin c} . \tag{D.11}$$

The right side of (D.11) is symmetric in a, b and c, so it must be equal to both $\sin C / \sin c$ and $\sin A / \sin a$ (as sceptics may verify by using (D.8) and (D.9)). Thus:

$$\frac{\sin B}{\sin b} = \frac{\sin C}{\sin c} = \frac{\sin A}{\sin a} = \frac{\left[1 - \cos^2 a - \cos^2 b - \cos^2 c + 2 \cos a \cos b \cos c\right]^{1/2}}{\sin a \sin b \sin c} . \tag{D.12}$$

This is the *sine rule* for spherical triangles. As particular cases we have

$$\star\star \quad \sin b \sin A = \sin a \sin B \,, \tag{D.13}$$

$$\star\star \quad \sin b \sin C = \sin c \sin B \,. \tag{D.14}$$

The quantity

$$\Im \equiv \left[1 - \cos^2 a - \cos^2 b - \cos^2 c + 2 \cos a \cos b \cos c\right]^{1/2} , \tag{D.15}$$

which appears in (D.12) and arises frequently (see below), can be shown to be $6\times$ the volume of the *tetrahedron* $OABC$.

Direct use of (D.5), (D.8) and (D.9) shows that

$$\cos B + \cos C \cos A = \frac{\cos b}{\sin b}\left[\frac{\Im^2}{\sin a \sin b \sin c}\right] . \tag{D.16}$$

By applying (D.12) and (D.15) to the right side of (D.16) and re-arranging, one obtains

$$\star\star \quad \cos B = \cos b \sin C \sin A - \cos C \cos A \, , \tag{D.17}$$

which is sometimes called the *cosine rule for angles.*

In addition to the well-known and named relations (D.4), (D.12) and (D.17), several subsidiary formulae are also needed to show equality of $\mathbf{M}$ and $\mathbf{N}$.

By using (D.9), (D.5) and (D.8) for $\cos A$, $\cos B$ and $\cos C$ it is straightforward to show that

$$\star\star \quad \sin b \cos A = \sin c \cos a - \cos c \sin a \cos B, \tag{D.18}$$

$$\star\star \quad \sin b \cos C = \cos c \sin a - \sin c \cos a \cos B \, . \tag{D.19}$$

Repeated application of the sine rule (D.12) to (D.18) leads to

$$\sin B \cos A = \sin C \cos a - \cos c \sin A \cos B \, , \tag{D.20}$$

and rearrangement of a cyclic counterpart of (D.20) then gives

$$\star\star \quad \cos c \sin B = \sin A \cos C + \cos b \sin C \cos A \, . \tag{D.21}$$

Similar treatment of (D.19) produces

$$\star\star \quad \cos a \sin B = \sin C \cos A + \cos b \sin A \cos C \, . \tag{D.22}$$

Use of (D.9), (D.5) and (D.8) for $\cos A$, $\cos B$ and $\cos C$, together with definition (D.15), shows that

$$\sin c \sin a + \cos c \cos a \cos B + \cos b \cos c \cos A = \frac{\Im^2}{\sin a \sin^2 b \sin c} = \sin C \sin A \, , \tag{D.23}$$

where the second equality depends on the sine rule (D.12).Rearrangement of (D.23) gives

$$\star\star \quad \sin c \sin a + \cos c \cos a \cos B = \sin C \sin A - \cos b \cos C \cos A \, . \tag{D.24}$$

All the required formulae (labeled $\star\star$ above) have now been developed. In each we put

$$a = \frac{\pi}{2} - \phi_d \, , \qquad b = \alpha \, , \qquad c = \frac{\pi}{2} - \phi_a \, , \tag{D.25}$$

$$A = \frac{\pi}{2} + \gamma_a \ , \quad B = \delta \equiv (\lambda_a - \lambda_d) \ , \quad C = \frac{\pi}{2} - \gamma_d \ . \tag{D.26}$$

By treating successively (D.17), (D.22), (D.13), (D.21), (D.24), (D.18), (D.14), (D.19), and (D.4), we find:

$$\cos\delta = \cos\alpha\cos\gamma_a\cos\gamma_d + \sin\gamma_a\sin\gamma_d \ , \tag{D.27}$$

$$\sin\phi_d\sin\delta = \cos\alpha\cos\gamma_a\sin\gamma_d - \sin\gamma_a\cos\gamma_d \ , \tag{D.28}$$

$$-\cos\phi_d\sin\delta = -\sin\alpha\cos\gamma_a \ , \tag{D.29}$$

$$-\sin\phi_a\sin\delta = \cos\alpha\sin\gamma_a\cos\gamma_d - \cos\gamma_a\sin\gamma_d \ , \tag{D.30}$$

$$\cos\phi_a\cos\phi_d + \sin\phi_a\sin\phi_d\cos\delta = \cos\alpha\sin\gamma_a\sin\gamma_d + \cos\gamma_a\cos\gamma_d \ . \tag{D.31}$$

$$\cos\phi_a\sin\phi_d - \sin\phi_a\cos\phi_d\cos\delta = -\sin\alpha\sin\gamma_a \ , \tag{D.32}$$

$$\cos\phi_a\sin\delta = \sin\alpha\cos\gamma_d \ , \tag{D.33}$$

$$\sin\phi_a\cos\phi_d - \cos\phi_a\sin\phi_d\cos\delta = \sin\alpha\sin\gamma_d \ , \tag{D.34}$$

$$\sin\phi_a\sin\phi_d + \cos\phi_a\cos\phi_d\cos\delta = \cos\alpha \ . \tag{D.35}$$

The left sides of these relations, taken in order, are the elements of $\mathbf{M}$ row by row from M_{11} to M_{33} (see (5.75)); the right sides are the elements of $\mathbf{N}$ row by row from N_{11} to N_{33} (see (5.74)). Hence equality of $\mathbf{M}$ and $\mathbf{N}$ is proved.

From (D.29), (D.32), (D.33) and (D.34), an expression for $\sin^2\alpha\sin(\gamma_d - \gamma_a)$ may be constructed, which - after use of elementary trig identitiesand of (D.35) - reduces to

$$\sin(\gamma_d - \gamma_a) = \frac{(\sin\phi_a + \sin\phi_d)\sin\delta}{(1 + \cos\alpha)} \ . \tag{D.36}$$

From (D.36), further manipulation shows that

$$\cos(\gamma_d - \gamma_a) = \frac{\cos\phi_a\cos\phi_d + (1 + \sin\phi_a\sin\phi_d)\cos\delta}{(1 + \cos\alpha)} \ . \tag{D.37}$$

Eqs. (D.36) and (D.37) define the elements of the shallow-atmosphere, HPE rotation matrix **HF** (see (5.76)).

APPENDIX E

Outline derivation of the spherical polar departure-point formulae (5.151)-(5.156)

As in the main text, consider the great circle which passes through the departure point (λ_d, ϕ_d) and the arrival point (λ_a, ϕ_a), and the midpoint (λ_0, ϕ_0) which bisects the minor arc between them. Let u_0 and v_0 be the velocity components at (λ_0, ϕ_0) at time $t^{n+1/2}$ and V_0 be the horizontal speed, i.e.

$$V_0 = \left(u_0^2 + v_0^2\right)^{1/2} . \tag{E.1}$$

If γ_0 is the angle between the latitude circle λ_0 and the great circle (see Fig. 5.9), then

$$\tan \gamma_0 = \frac{v_0}{u_0}, \quad \sin \gamma_0 = \frac{v_0}{V_0}, \quad \cos \gamma_0 = \frac{u_0}{V_0}. \tag{E.2}$$

Finally, let α_0 be *half* the angle subtended at the centre of the great circle by the radii to the departure point and the arrival point. To the usual accuracy of the departure-point calculation,

$$\alpha_0 \equiv \frac{V_0 \Delta t}{2a} . \tag{E.3}$$

The angle α_0 will nearly always be very much less than unity, and plays a key role in the analysis.

Ritchie & Beaudoin (1994) derive equations (E.6) and (E.9) - (E.15), below, by using results on the differential geometry of great circles derived in the Appendix of Ritchie (1988). The four independent relations (E.12) - (E.15) may be obtained more directly by applying some of the spherical triangle formulae developed here. The North Pole N, the arrival point A and the midpoint M define a spherical triangle bounded by two meridians and the (great circle) arc AM; see Fig. E.1. Applying the cosine rule (D.4) and the sine rule (D.12) to this spherical triangle gives immediately:

$$\sin \phi_a = \sin \phi_0 \cos \alpha_0 + \frac{v_0}{V_0} \cos \phi_0 \sin \alpha_0 \ , \tag{E.4}$$

$$\cos \phi_a \sin (\lambda_a - \lambda_0) = \cos \gamma_0 \sin \alpha_0 = \frac{u_0}{V_0} \sin \alpha_0 \ . \tag{E.5}$$

Use of (E.5) to construct an expression for $\cos^2 \phi_a \cos^2 (\lambda_a - \lambda_0)$, application of (E.4) and use of basic trig identities leads to

$$\cos \phi_a \cos (\lambda_a - \lambda_0) = \cos \phi_0 \cos \alpha_0 - \frac{v_0}{V_0} \sin \phi_0 \sin \alpha_0 \ , \tag{E.6}$$

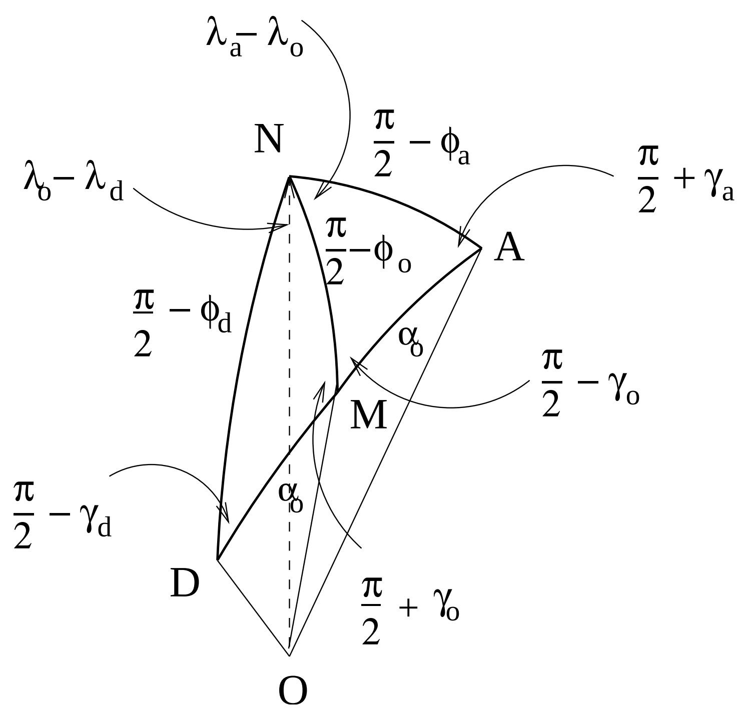

Figure E.1: The spherical triangles AMN and NMD formed by the meridians through the arrival point A, the midpoint M and the departure point D, and the great circle arc DMA. The radii to A, M, D and N are also shown. The sides NA, NM and ND are simply the co-latitudes of A, M and D. Sides DM and MA are both equal to α_0, $2\alpha_0$ being the angle subtended by A and D at the centre O of the unit sphere. The 6 angles of the spherical triangles are indicated by the 6 curved arrows.

By considering the spherical triangle defined by the North Pole N, the midpoint M and the departure point D, expressions involving $(\lambda_d,\ \phi_d)$ rather than $(\lambda_a,\ \phi_a)$ may be derived:

$$\sin\phi_d = \sin\phi_0\cos\alpha_0 - \frac{v_0}{V_0}\cos\phi_0\sin\alpha_0\ , \tag{E.7}$$

$$\cos\phi_d\sin\left(\lambda_d - \lambda_0\right) = -\frac{u_0}{V_0}\sin\alpha_0\ , \tag{E.8}$$

$$\cos\phi_d\cos\left(\lambda_d - \lambda_0\right) = \cos\phi_0\cos\alpha_0 + \frac{v_0}{V_0}\sin\phi_0\sin\alpha_0\ . \tag{E.9}$$

The departure point equations (E.7) - (E.9) differ formally from the arrival point equations (E.4) - (E.6) only in the signs of the terms involving $\sin\alpha_0$. Eqs. (E.5) and (E.8) are (5.153) and (5.156) of Section 5.5.1. With amplitude A_0 and phase δ_0 defined by

$$A_0^2 = \cos^2\alpha_0 + \frac{v_0^2}{V_0^2}\sin^2\alpha_0 = 1 - \frac{u_0^2}{V_0^2}\sin^2\alpha_0 \tag{E.10}$$

and

$$\delta_0 = \arctan\left[\frac{v_0}{V_0}\tan\alpha_0\right], \tag{E.11}$$

equations (E.4), (E.6), (E.7), (E.9) assume much more compact forms:

$$\sin\phi_a = A_0\sin\left(\phi_0 + \delta_0\right)\ , \tag{E.12}$$

$$\cos\phi_a\cos\left(\lambda_a - \lambda_0\right) = A_0\cos\left(\phi_0 + \delta_0\right)\ , \tag{E.13}$$

$$\sin\phi_d = A_0\sin\left(\phi_0 - \delta_0\right)\ , \tag{E.14}$$

$$\cos\phi_d\cos\left(\lambda_d - \lambda_0\right) = A_0\cos\left(\phi_0 - \delta_0\right)\ . \tag{E.15}$$

Eqs. (E.12) - (E.15) are (5.151) - (5.155) of Section 5.5.1.

APPENDIX F

Outline derivation of the Ritchie-Beaudoin formulae (5.157)-(5.160)

Various power series are relevant. As well as the binomial expansion of $(1+x)^p$;

$$(1+x)^p = 1 + px + p(p-1)\frac{x^2}{2!} + p(p-1)(p-2)\frac{x^3}{3!} + O(x^4), \tag{F.1}$$

the series for $\sin x$;

$$\sin x = x - \frac{x^3}{3!} + \frac{x^5}{5!} + O(x^7)\,, \tag{F.2}$$

the series for $\arcsin x$;

$$\arcsin x = x + \frac{x^3}{6} + \frac{3x^5}{40} + O(x^7)\,, \tag{F.3}$$

the series for $\tan x$;

$$\tan x = x + \frac{x^3}{3} + \frac{2x^5}{15} + O(x^7)\,, \tag{F.4}$$

and Gregory's series for $\arctan x$;

$$\arctan x = x - \frac{x^3}{3} + \frac{x^5}{5} + O(x^7)\,, \tag{F.5}$$

it is convenient to deploy some less well known expansions. From (F.2) and (F.3) it follows that, for a constant β such that $|\beta \sin x| < 1$,

$$\arcsin\left[\beta \sin x\right] = \beta x - \beta\left(1-\beta^2\right)\frac{x^3}{3!} + \beta\left(1-\beta^2\right)\left(1-9\beta^2\right)\frac{x^5}{5!} + O(x^7)\,, \tag{F.6}$$

and use of (F.4) and (F.5) shows that

$$\arctan\left[\beta \tan x\right] = \beta x + \beta\left(1-\beta^2\right)\frac{x^3}{3!} + O(x^5)\,. \tag{F.7}$$

Direct Taylor/Maclaurin expansion leads to the series

$$\arcsin\left[\frac{\sin\beta}{\sqrt{1-x}}\right] = \beta + \frac{x}{2}\tan\beta\left\{1 + \frac{x}{2}\left[1 + \frac{1}{2}\sec^2\beta\right] + \frac{x^2}{3}\left[1 + \frac{1}{2}\sec^2\beta + \frac{3}{8}\sec^4\beta\right]\right\} + O(x^4), \tag{F.8}$$

$$\arcsin\left[\sqrt{1-x}\,\sin\beta\right] = \beta - \frac{x}{2}\tan\beta\left\{1 - \frac{x}{4}\left[1-\tan^2\beta\right] + \frac{x^2}{8}\left[1 - \tan^2\beta + \tan^4\beta\right]\right\} + O(x^4). \tag{F.9}$$

Aside :

The less familiar expansions (F.6) - (F.9) *are also less well explored than* (F.1) - (F.5). *They are guaranteed only to the order quoted. A pattern in the coefficients seems to be emerging in each case, but that seen in* (F.6) *is known to be illusory, and those seen in* (F.8) *and* (F.9) *have not been tested. The number of terms given explicitly in* (F.6) - (F.9) *is ample for our purpose.*

We also need

$$\tan(\beta + x) = \tan\beta + x\sec^2\beta + x^2\sec^2\beta\tan\beta + O(x^3) \tag{F.10}$$

and

$$\sec(\beta + x) = \sec\beta\left[1 + x\tan\beta + \frac{x^2}{2}\left(1 + 2\tan^2\beta\right)\right] + O(x^3)\,. \tag{F.11}$$

In (F.10) and (F.11), as in (F.6) - (F.9), β is a constant.

Immediately from (5.153),

$$\lambda_0 = \lambda_a - \arcsin\left[\frac{u_0}{V_0\cos\phi_a}\sin\alpha_0\right]. \tag{F.12}$$

Use of (F.6) with $\beta = (u_0/V_0\cos\phi_a)$ and $x = \alpha_0 = (V_0\Delta t/2a)$ allows (F.12) to be expanded as

$$\lambda_0 = \lambda_a - \left(\frac{u_0}{V_0\cos\phi_a}\right)\left(\frac{V_0\Delta t}{2a}\right)\left\{1 + \frac{1}{6}\left[\frac{u_0^2}{V_0^2\cos^2\phi_a} - 1\right]\left(\frac{V_0\Delta t}{2a}\right)^2\right\} + O\left(\left(\frac{V_0\Delta t}{2a}\right)^5\right). \tag{F.13}$$

Eq. (F.13) is equivalent to (5.157). It is correct to $O(\Delta t^5)$ because the term in Δt^4 vanishes. Eqs. (5.158) - (5.160), which we derive next, are correct to $O(\Delta t^4)$.

Aside :

Expansion (F.6) *is valid for constant* β. *We set* $x = \alpha_0 = (V_0\Delta t/2a)$ *and* $\beta = (u_0/V_0\cos\phi_a)$ *to derive* (F.13). *In so far as* $u_0 = u_0(\lambda_0, \phi_0)$ *and* $V_0 = V_0(\lambda_0, \phi_0)$, *and* λ_0, ϕ_0 *depend palpably on* Δt, $\beta = (u_0/V_0\cos\phi_a)$ *is also a function of* Δt *and hence of* α_0. *We have assumed, it seems, that* $(u_0/V_0\cos\phi_a)$ *is a sufficiently slow function of* Δt *that* (F.6) *is correct to the order we have applied it. All that is immediately clear is that* $x = \alpha_0 = (V_0\Delta t/2a)$ *is a small quantity, and that* $\beta = (u_0/V_0\cos\phi_a)$ *is typically of order unity. This issue could be further explored numerically as well as analytically. It should be re-emphasised that* (F.13) *is equivalent to the form given by Ritchie & Beaudoin (1994).*

Immediately from (5.151),

$$\phi_0 = \arcsin\left[\frac{\sin\phi_a}{A_0}\right] - \delta_0\,. \tag{F.14}$$

Consider the arcsin term first. From (5.149) we have

$$A_0 = \left[1 - \frac{u_0^2}{V_0^2}\sin^2\left(\frac{V_0\Delta t}{2a}\right)\right]^{1/2}\,. \tag{F.15}$$

Setting $x = (u_0^2/V_0^2)\sin^2(V_0\Delta t/2a)$ and $\beta = \phi_a$ in the expansion (F.8) of $\arcsin\left[(1-x)^{-1/2}\sin\beta\right]$, and use of the sine expansion (F.2), shows that

$$\arcsin\left[\frac{\sin\phi_a}{A_0}\right] = \phi_a + \frac{1}{2}\tan\phi_a\left\{\frac{u_0^2\Delta t^2}{4a^2}\right\} + O\left(\Delta t^4\right)\,. \tag{F.16}$$

Putting $\beta = v_0/V_0$, $x = \alpha_0 = (V_0\Delta t/2a)$ in the expansion (F.7) of $\arctan[\beta\tan x]$ gives

$$\delta_0 = \left(\frac{v_0\Delta t}{2a}\right)\left[1 + \frac{1}{3}\left(1 - \frac{v_0^2}{V_0^2}\right)\left(\frac{V_0\Delta t}{2a}\right)^2\right] + O(\Delta t^4). \tag{F.17}$$

Upon noting that $V_0^2 = u_0^2 + v_0^2$, use of (F.16) and (F.17) in (F.14) gives

$$\phi_0 = \phi_a - \frac{v_0\Delta t}{2a} + \frac{1}{2}\left(\frac{u_0\Delta t}{2a}\right)^2\tan\phi_a - \frac{1}{3}\left(\frac{v_0\Delta t}{2a}\right)\left(\frac{u_0\Delta t}{2a}\right)^2 + O\left(\Delta t^4\right)\,, \tag{F.18}$$

which is (5.158).

Aside :

Although (F.16) *is beyond reproach ($\beta = \phi_a$ indeed qualifies as a constant), setting $\beta = v_0/V_0$ and $x = \alpha_0 = (V_0\Delta t/2a)$ in* (F.7) *isopen to the same reservations as we noted regarding use of* (F.6) *to derive* (F.13). *We have tacitly assumed that $\beta = v_0/V_0$ is a sufficiently slow function of Δt that* (F.7) *is correct to the order we have applied it. All that is immediately clear is that $x = \alpha_0 = (V_0\Delta t/2a)$ is a small quantity, and that $\beta = v_0/V_0$ is typically of order unity. Similar reservations may be held, on broadly similar grounds, regarding* (F.23) *and* (F.28) *below. These expressions, and* (F.18)*,are the forms obtained by Ritchie & Beaudoin (1994).*

Having found λ_0 and ϕ_0 from (F.13) and (F.18), and during the iterative calculation also u_0 and v_0, we can find the departure point coordinates λ_d and ϕ_d from (5.157) and (5.160) (for example) without further iteration. Immediately from (5.160),

$$\phi_d = \arcsin\left[A_0\sin\left(\phi_0 - \delta_0\right)\right]\,. \tag{F.19}$$

Noting (F.2) and (F.15), apply the expansion (F.9) of $\arcsin\left[(1-x)^{1/2}\sin\beta\right]$ with $x = (u_0^2/V_0^2)\sin^2(V_0\Delta t/2a)$ and $\beta = \phi_0 - \delta_0$, to obtain

$$\phi_d = \phi_0 - \delta_0 - \frac{1}{2}\left(\frac{u_0\Delta t}{2a}\right)^2 \tan(\phi_0 - \delta_0) + O\left(\Delta t^4\right) . \tag{F.20}$$

From (F.17) and (F.18) we have

$$\phi_0 - \delta_0 = \phi_a - \frac{v_0\Delta t}{a} + \frac{1}{2}\left(\frac{u_0\Delta t}{2a}\right)^2 \tan\phi_a - \frac{2}{3}\left(\frac{v_0\Delta t}{2a}\right)\left(\frac{u_0\Delta t}{2a}\right)^2 + O\left(\Delta t^4\right) . \tag{F.21}$$

To the required accuracy $[O(\Delta t^2)]$,

$$\tan(\phi_0 - \delta_0) = \tan\left(\phi_a - \frac{v_0\Delta t}{a}\right) = \tan\phi_a - \left(\frac{v_0\Delta t}{2a}\right)\sec^2\phi_a , \tag{F.22}$$

(from (F.10)). Some cancellation occurs upon use of (F.21) and (F.22) in (F.20); we obtain

$$\phi_d = \phi_a - \frac{v_0\Delta t}{a} + \left(\tan^2\phi_a + \frac{1}{3}\right)\left(\frac{v_0\Delta t}{2a}\right)\left(\frac{u_0\Delta t}{2a}\right)^2 + O\left(\Delta t^4\right) . \tag{F.23}$$

This is equivalent to (5.164).

Immediately from (5.156),

$$\lambda_0 = \lambda_d + \arcsin\left[\frac{u_0}{V_0\cos\phi_d}\sin\alpha_0\right] , \tag{F.24}$$

which, except for a sign change, is of the same form as (F.12) (with λ_d and ϕ_d replacing λ_a and ϕ_a). Thus, as well as (F.13), we have

$$\lambda_0 = \lambda_a + \left(\frac{u_0}{V_0\cos\phi_d}\right)\left(\frac{V_0\Delta t}{2a}\right)\left\{1 + \frac{1}{6}\left[\frac{u_0^2}{V_0^2\cos^2\phi_d} - 1\right]\left(\frac{V_0\Delta t}{2a}\right)^2\right\} + O\left(\left(\frac{V_0\Delta t}{2a}\right)^5\right) . \tag{F.25}$$

Elimination of λ_0 between (F.13) and (F.23), and some re-arrangement, leads to

$$\lambda_d = \lambda_a - \frac{u_0\Delta t}{2a}\left[1 - \frac{1}{6}\left(\frac{V_0\Delta t}{2a}\right)^2\right][\sec\phi_a + \sec\phi_d] - \frac{1}{6}\left(\frac{u_0\Delta t}{2a}\right)^3\left[\sec^3\phi_a + \sec^3\phi_d\right] + O(\Delta t^4). \tag{F.26}$$

By using (F.11), an expression for $\sec\phi_d$ of sufficient accuracy is readily derived:

$$\sec\phi_d = \sec\phi_a\left[1 - \left(\frac{v_0\Delta t}{a}\right)\tan\phi_a\right] + \frac{1}{2}\left(\frac{v_0\Delta t}{a}\right)^2\left[\sec^2\phi_a + \tan^2\phi_a\right] + O(\Delta t^3). \tag{F.27}$$

Use of (F.27) in (F.26) gives

$$\lambda_d = \lambda_a - \frac{u_0\Delta t}{a\cos\phi_a}\left[1 - \left(\frac{v_0\Delta t}{2a}\right)\tan\phi_a + \left(\frac{v_0\Delta t}{2a}\right)^2\left(2\tan^2\phi_a + \frac{5}{6}\right) + \left(\frac{u_0\Delta t}{2a}\right)^2\frac{\tan^2\phi_a}{6}\right] + O\left(\Delta t^4\right) , \tag{F.28}$$

which is (5.163).

APPENDIX G

Analysis of the partially- implicit/ partially- explicit discretisation of the momentum equations when simplified to only treat the Coriolis terms

G.1 Continuous equations

Consider the following linear constant-coefficient set of equations for inertial oscillations:

$$u_t - f_3 v + f_2 w = 0, \tag{G.1}$$

$$v_t + f_3 u = 0, \tag{G.2}$$

$$w_t - f_2 u = 0, \tag{G.3}$$

where

$$f_2 = 2\Omega \cos\phi, \tag{G.4}$$

$$f_3 = -2\Omega \sin\phi. \tag{G.5}$$

G.2 Discretised equations

Discretising the usual Coriolis terms in a weighted semi-implicit manner, and the additional ones explicitly (this is what is done in the New Dynamics) gives

$$\frac{u^{n+1} - u^n}{\Delta t} - f_3 \left[\alpha v^{n+1} + (1-\alpha) v^n\right] + f_2 w^n = 0, \tag{G.6}$$

$$\frac{v^{n+1} - v^n}{\Delta t} + f_3 \left[\alpha u^{n+1} + (1-\alpha) u^n\right] = 0, \tag{G.7}$$

$$\frac{w^{n+1} - w^n}{\Delta t} - f_2 u^n = 0. \tag{G.8}$$

G.3 Analytic dispersion relation

Letting

$$u = u_0 e^{i\omega t}, \quad v = v_0 e^{i\omega t}, \quad w = w_0 e^{i\omega t}, \tag{G.9}$$

and substituting into (G.1)-(G.3) leads to the dispersion relation

$$\omega = 0, \ \pm 2\Omega. \tag{G.10}$$

G.4 Numerical dispersion relation and stability

Substituting (G.9) into (G.6)-(G.8) gives

$$\begin{bmatrix} (E-1) & 0 & (f_3\Delta t)\left[\alpha E+(1-\alpha)\right] \\ 0 & (E-1) & -(f_2\Delta t) \\ -(f_3\Delta t)\left[\alpha E+(1-\alpha)\right] & (f_2\Delta t) & (E-1) \end{bmatrix} \begin{bmatrix} v_0 \\ w_0 \\ u_0 \end{bmatrix} = 0, \tag{G.11}$$

where $E=\exp(i\omega\Delta t)$. Taking the determinant of the matrix gives the numerical dispersion relation

$$(E-1)\left\{(E-1)^2+(f_2\Delta t)^2+(f_3\Delta t)^2\left[\alpha E+(1-\alpha)\right]^2\right\}=0, \tag{G.12}$$

i.e.

$$(E-1)\left\{E^2-2\left[\frac{1-\alpha(1-\alpha)(f_3\Delta t)^2}{1+(f_3\Delta t)^2\alpha^2}\right]E+\frac{1+(f_3\Delta t)^2(1-\alpha)^2+(f_2\Delta t)^2}{1+(f_3\Delta t)^2\alpha^2}\right\}=0, \tag{G.13}$$

i.e.

$$(E-1)\left(E^2+2BE+C\right)=0, \tag{G.14}$$

where

$$B=-\left[\frac{1-\alpha(1-\alpha)(f_3\Delta t)^2}{1+(f_3\Delta t)^2\alpha^2}\right], \quad C=\frac{1+(f_3\Delta t)^2(1-\alpha)^2+(f_2\Delta t)^2}{1+(f_3\Delta t)^2\alpha^2}. \tag{G.15}$$

To demonstrate instability, evaluate the Coriolis terms at the equator. Eq. (G.12) then simplifies to

$$E=1, \quad 1\pm 2i\Omega\Delta t, \tag{G.16}$$

and $|E|>1$ for the complex conjugate pair of roots. **Thus the discretisation is unconditionally unstable at the equator for inertial oscillations.**

More generally, this discretisation is guaranteed to be unstable if the absolute value of the product of the roots exceeds unity, i.e. if $|C|>1$. Consider the family of schemes such that $1/2\le\alpha\le 1$, i.e. a family that varies from Crank-Nicolson to backward implicit for the treatment of the traditionally-retained Coriolis terms. From (G.15), (G.4) and (G.5), **unconditional instability occurs in a latitudinal belt** such that

$$\tan^2\phi<\frac{1}{2\alpha-1}. \tag{G.17}$$

Increasing the off-centring parameter α from $1/2$ (Crank-Nicolson) towards unity (backward implicit) reduces the polarward extent of this equatorial belt of instability.

APPENDIX H

Stability analysis of vertical temperature advection

From (9.17), (9.21) and (9.36), the predictor-corrector equations are

$$\frac{\tilde{\theta}^{(1)} - \theta^n_{dl}}{\Delta t} = -\alpha_2 \left[(w - w^*) \, \delta_{2r} \theta \right]^n - (1 - \alpha_2) \left[(w - w^*) \, \delta_{2r} \theta \right]^n_{dl}, \tag{H.1}$$

$$\frac{\tilde{\theta}^{(2)} - \tilde{\theta}^{(1)}}{\Delta t} = -\alpha_2 \left(w^n - w^* \right) \delta_{2r} \left(\tilde{\theta}^{(1)} - \theta^n \right), \tag{H.2}$$

$$\frac{\theta^{n+1} - \tilde{\theta}^{(2)}}{\Delta t} = -\alpha_2 \left(w^{n+1} - w^n \right) \delta_{2r} \tilde{\theta}^{(2)}. \tag{H.3}$$

For uniform vertical advection W and a Fourier component $\exp(ikr)$ of θ, these equations reduce to

$$\begin{aligned} \frac{\tilde{\theta}^{(1)} - e^{-i\gamma}\theta^n}{\Delta t} &= -i\alpha_2 \frac{\sin(k\Delta r)}{\Delta r} W' \theta^n - i(1 - \alpha_2) \frac{\sin(k\Delta r)}{\Delta r} W' e^{-i\gamma} \theta^n \\ &= -i \left[\alpha_2 + (1 - \alpha_2) e^{-i\gamma} \right] \frac{\sin(k\Delta r)}{\Delta r} W' \theta^n, \end{aligned} \tag{H.4}$$

$$\frac{\tilde{\theta}^{(2)} - \tilde{\theta}^{(1)}}{\Delta t} = -i\alpha_2 \frac{\sin(k\Delta r)}{\Delta r} W' \left(\tilde{\theta}^{(1)} - \theta^n \right), \tag{H.5}$$

$$\frac{\theta^{n+1} - \tilde{\theta}^{(2)}}{\Delta t} = 0, \tag{H.6}$$

where

$$W = W^* + W' \text{ such that } \left| \frac{W'\Delta t}{\Delta r} \right| \leq \frac{1}{2}, \tag{H.7}$$

both the "residual vertical velocity" W' and W^* are constant, and

$$\gamma = kW^*\Delta t, \tag{H.8}$$

is k times the integral number of vertical meshlengths a particle is displaced when going from r_{dl} to r_a.

Eliminating $\tilde{\theta}^{(1)}$ and $\tilde{\theta}^{(2)}$ from (H.4)-(H.6) and expanding θ as $\exp(i\omega t)$ then gives

$$\theta^{n+1} = \left\{ e^{-i\gamma} - ie^{-i\gamma} \sin(k\Delta r) C' - \alpha_2 \left[\alpha_2 + (1 - \alpha_2) e^{-i\gamma} \right] \sin^2(k\Delta r) C'^2 \right\} \theta^n = E\theta^n, \tag{H.9}$$

where

$$E = \exp(i\omega\Delta t) = e^{-i\gamma} \left\{ 1 - i\sin(k\Delta r) C' - \alpha_2 \left[\alpha_2 e^{i\gamma} + (1 - \alpha_2) \right] \sin^2(k\Delta r) C'^2 \right\}, \tag{H.10}$$

is the amplification factor per timestep, and for stability $|E| \leq 1$. Thus for stability

$$
\begin{aligned}
|E|^2 &= \left\{1 - \alpha_2 \left[1 - (1 - \cos\gamma)\,\alpha_2\right] \sin^2(k\Delta r)\, C'^2\right\}^2 \\
&\quad + \sin^2(k\Delta r)\, C'^2 \left[1 + \alpha_2^2 \sin\gamma \sin(k\Delta r)\, C'\right]^2 \\
&\leq 1,
\end{aligned} \tag{H.11}
$$

where

$$C' \equiv \frac{W'\Delta t}{\Delta r}, \quad |C'| \leq 1/2\,, \tag{H.12}$$

is the "residual Courant number".

For the special case where $W^* = 0$ ($\Rightarrow \gamma = 0$) and $|C'| = |C| \equiv |W\Delta t/\Delta r| \leq 1/2$, inequality (H.11) leads to the stability condition

$$C'^2 \leq \frac{2\alpha_2 - 1}{\alpha_2^2}, \tag{H.13}$$

since $\sin^2(k\Delta r) \leq 1$. Because $|C'|^2$ can be as large as $1/4$, from (H.13) this means that a necessary condition for stability is that

$$\alpha_2 \geq 4 - 2\sqrt{3} \approx 0.54. \tag{H.14}$$

This condition is violated for $\alpha_2 = 0.5$, but a modest increase in α_2 to 0.54 addresses this.

The stability of the alternative discretisation proposed in Section 9.6 is now examined. For uniform vertical advection W and a Fourier component $\exp(ikr)$ of θ, the predictor-corrector equations from (9.17), (9.21), (9.48) and (9.51) are:

$$
\begin{aligned}
\frac{\tilde{\theta}^{(1)} - e^{-i\gamma}\theta^n}{\Delta t} &= -i\alpha_2 \frac{\sin(k\Delta r)}{\Delta r} W'\theta^n - i(1-\alpha_2)\frac{\sin(k\Delta r)}{\Delta r} W' e^{-i\gamma}\theta^n \\
&= -i\left[\alpha_2 + (1-\alpha_2)\, e^{-i\gamma}\right] \frac{\sin(k\Delta r)}{\Delta r} W'\theta^n,
\end{aligned} \tag{H.15}
$$

$$\frac{\tilde{\theta}^{(2)} - \tilde{\theta}^{(1)}}{\Delta t} = -i\alpha_2 \frac{\sin(k\Delta r)}{\Delta r} W' \left(\tilde{\theta}^{(1)} - \theta^n\right), \tag{H.16}$$

$$\frac{\theta^{n+1} - \tilde{\theta}^{(2)}}{\Delta t} = -i\alpha_2 \frac{\sin(k\Delta r)}{\Delta r} W' \left(\tilde{\theta}^{(2)} - \tilde{\theta}^{(1)}\right). \tag{H.17}$$

Eliminating $\tilde{\theta}^{(1)}$ and $\tilde{\theta}^{(2)}$ from (H.15)-(H.17) and expanding θ as $\exp(i\omega t)$ then gives

$$\theta^{n+1} = e^{-i\gamma}\left\{1 - iSC' - \alpha_2 S^2 C'^2 + i\alpha_2^2\left[\alpha_2 e^{i\gamma} + (1-\alpha_2)\right] S^3 C'^3\right\}\theta^n = E\theta^n, \tag{H.18}$$

where

$$S = \sin(k\Delta r)\,, \tag{H.19}$$

$$\begin{aligned} E &= e^{-i\gamma}\left\{1 - iSC' - \alpha_2 S^2 C'^2 + i\alpha_2^2\left[\alpha_2 e^{i\gamma} + (1-\alpha_2)\right] S^3 C'^3\right\} \\ &= e^{-i\gamma}\left\{1 - \alpha_2 S^2 C'^2 - \alpha_2^3 \sin\gamma S^3 C'^3 \right. \\ &\qquad \left. + iSC'\left[-1 + \alpha_2^3\cos\gamma S^2 C'^2 + \alpha_2^2(1-\alpha_2) S^2 C'^2\right]\right\}, \end{aligned} \tag{H.20}$$

is the amplification factor per timestep, and for stability $|E| \leq 1$. Thus for stability

$$\begin{aligned} |E|^2 &= \left(1 - \alpha_2 S^2 C'^2 - \alpha_2^3 \sin\gamma S^3 C'^3\right)^2 \\ &\quad + \left[-1 + \alpha_2^3\cos\gamma S^2 C'^2 + \alpha_2^2(1-\alpha_2) S^2 C'^2\right]^2 S^2 C'^2 \\ &\leq 1. \end{aligned} \tag{H.21}$$

For the special case where $W^* = 0$ ($\Rightarrow \gamma = 0$) and $|C'| = |C| \equiv |W\Delta t/\Delta r| \leq 1/2$, inequality (H.21) simplifies to

$$\alpha_2^4 \sin^4(k\Delta r) C'^4 - \alpha_2^2 \sin^2(k\Delta r) C'^2 \leq 2\alpha_2 - 1, \tag{H.22}$$

from which it is found that

$$\frac{\frac{1}{2} - \sqrt{2\alpha_2 - \frac{3}{4}}}{\alpha_2^2} \leq \sin^2(k\Delta r) C'^2 \leq \frac{\frac{1}{2} + \sqrt{2\alpha_2 - \frac{3}{4}}}{\alpha_2^2}. \tag{H.23}$$

From the left-hand inequality it follows that a necessary condition for stability is that

$$\alpha_2 \geq \frac{1}{2}. \tag{H.24}$$

However α_2 cannot be indefinitely large, and must also satisfy the right-hand inequality of (H.23). Because $\sin^2(k\Delta r)$ can be as large as unity and $|C'|^2$ can be as large as $1/4$, this means that

$$\frac{\frac{1}{2} + \sqrt{2\alpha_2 - \frac{3}{4}}}{\alpha_2^2} \geq \frac{1}{4}. \tag{H.25}$$

This is not very restrictive since it is satisfied for values of α_2 as large as a little more than 3.

Putting these results together, the alternative discretisation proposed in Section 9.6 should be stable for $|C| \leq 1/2$ provided

$$\frac{1}{2} \leq \alpha_2 \leq 3, \tag{H.26}$$

so this discretisation addresses the instability of the present scheme when $1/2 \leq \alpha_2 \leq 4 - 2\sqrt{3} \approx 0.54$.

APPENDIX I

Definitions for Helmholtz solver

$$X|_{1/2} = \overline{(C_{xx2})|_{1/2}\left[(\delta_{\lambda 1}\Pi')|_{1/2} - (C_{xp})|_{1/2}\overline{\left(\frac{r|_{1/2}-r|_0}{r|_1-r|_0}\right)(C_2\delta_r\Pi')|_1}^{\lambda}\right] + (C_{xy1})|_{1/2}\,(C_{xy2})|_{1/2}\left[(\delta_{\phi 1}\Pi')|_{1/2} - (C_{yp})|_{1/2}\overline{\left(\frac{r|_{1/2}-r|_0}{r|_1-r|_0}\right)(C_2\delta_r\Pi')|_1}^{\phi}\right]}^{\lambda\phi}, \tag{I.1}$$

$$X|_k = \left[C_{xx2}\left(\delta_{\lambda 1}\Pi' - C_{xp}\overline{C_2\delta_r\Pi'}^{r\lambda}\right) + C_{xy1}\overline{C_{xy2}\left(\delta_{\phi 1}\Pi' - C_{yp}\overline{C_2\delta_r\Pi'}^{r\phi}\right)}^{\lambda\phi}\right]\Bigg|_k, \tag{I.2}$$

for $k = 3/2, 5/2, ..., N-3/2$,

$$X|_{N-1/2} = \overline{(C_{xx2})|_{N-1/2}\left[(\delta_{\lambda 1}\Pi')|_{N-1/2} - (C_{xp})|_{N-1/2}\overline{\left(\frac{r|_N-r|_{N-1/2}}{r|_N-r|_{N-1}}\right)(C_2\delta_r\Pi')|_{N-1}}^{\lambda}\right] + (C_{xy1})|_{N-1/2}\,(C_{xy2})|_{N-1/2}\left[(\delta_{\phi 1}\Pi')|_{N-1/2} - (C_{yp})|_{N-1/2}\overline{\left(\frac{r|_N-r|_{N-1/2}}{r|_N-r|_{N-1}}\right)(C_2\delta_r\Pi')|_{N-1}}^{\phi}\right]}^{\lambda\phi}, \tag{I.3}$$

$$Y|_{1/2} = \overline{(C_{yy2})|_{1/2}\left[(\delta_{\phi 1}\Pi')|_{1/2} - (C_{yp})|_{1/2}\overline{\left(\frac{r|_{1/2}-r|_0}{r|_1-r|_0}\right)(C_2\delta_r\Pi')|_1}^{\phi}\right] - (C_{yx1})|_{1/2}\,(C_{yx2})|_{1/2}\left[(\delta_{\lambda 1}\Pi')|_{1/2} - (C_{xp})|_{1/2}\overline{\left(\frac{r|_{1/2}-r|_0}{r|_1-r|_0}\right)(C_2\delta_r\Pi')|_1}^{\lambda}\right]}^{\lambda\phi}, \tag{I.4}$$

$$Y|_k = \left[C_{yy2}\left(\delta_{\phi 1}\Pi' - C_{yp}\overline{C_2\delta_r\Pi'}^{r\phi}\right) - C_{yx1}\overline{C_{yx2}\left(\delta_{\lambda 1}\Pi' - C_{xp}\overline{C_2\delta_r\Pi'}^{r\lambda}\right)}^{\lambda\phi}\right]\Bigg|_k, \tag{I.5}$$

for $k = 3/2, 5/2, ..., N-3/2$,

$$Y|_{N-1/2} = \overline{(C_{yy2})|_{N-1/2}\left[(\delta_{\phi 1}\Pi')|_{N-1/2} - (C_{yp})|_{N-1/2}\overline{\left(\frac{r|_N-r|_{N-1/2}}{r|_N-r|_{N-1}}\right)(C_2\delta_r\Pi')\Big|_{N-1}}^{\phi}\right] - (C_{yx1})|_{N-1/2}\,(C_{yx2})|_{N-1/2}\left[(\delta_{\lambda 1}\Pi')|_{N-1/2} - (C_{xp})|_{N-1/2}\overline{\left(\frac{r|_N-r|_{N-1/2}}{r|_N-r|_{N-1}}\right)(C_2\delta_r\Pi')|_{N-1}}^{\lambda}\right]}^{\lambda\phi}, \tag{I.6}$$

$$(C_{xx1})|_k = \left(\frac{\overline{r^2\rho_y^n\delta_\eta r}^{\lambda}}{\overline{r}^{\lambda}\Delta\lambda}\right)\Bigg|_k, \tag{I.7}$$

for $k = 1/2, 3/2, ..., N-1/2$,

$$(C_{xx2})|_k = \left(\frac{\alpha_1\alpha_3 A_u\Delta t c_{pd}\overline{\theta_v^*}^{r\lambda}}{\overline{r}^{\lambda}\cos\phi\Delta\lambda}\right)\Bigg|_k, \tag{I.8}$$

for $k = 1/2, 3/2, ..., N-1/2$,

$$(C_{yy1})|_k = \left(\frac{\cos\phi \overline{r^2 \rho_y^n \delta_\eta r}^{\phi}}{\overline{r}^{\phi} \Delta\phi} \right)\Bigg|_k, \tag{I.9}$$

for $k = 1/2, 3/2, ..., N-1/2$,

$$(C_{yy2})|_k = \left(\frac{\alpha_1 \alpha_3 A_v \Delta t c_{pd} \overline{\theta_v^*}^{r\phi}}{\overline{r}^{\phi} \Delta\phi} \right)\Bigg|_k, \tag{I.10}$$

for $k = 1/2, 3/2, ..., N-1/2$,

$$(C_{zz})|_k = \left(\frac{\alpha_2 K \overline{r^2 \rho_y^n}^{r}}{\delta_\eta r} \right)\Bigg|_k, \tag{I.11}$$

for $k = 1, 2, ..., N-1$,

$$(C_z)|_k = \left[\frac{\alpha_2 K \delta_{2r} \theta_{ref}}{\delta_\eta r} \left(\frac{1 + \frac{1}{\varepsilon} m_v^*}{1 + \sum_{X=(v,cl,cf)} m_X^*} \right) \right]\Bigg|_k, \tag{I.12}$$

for $k = 1, 2, ..., N-1$,

$$(C_{xz})|_k = \left(\frac{\delta_\lambda r}{\overline{r}^{\lambda} \cos\phi} \right)\Bigg|_k, \tag{I.13}$$

for $k = 1, 2, ..., N-1$,

$$(C_{yz})|_k = \left(\frac{\delta_\phi r}{\overline{r}^{\phi}} \right)\Bigg|_k, \tag{I.14}$$

for $k = 1, 2, ..., N-1$,

$$(C_{xp})|_k = \left(\frac{\delta_{\lambda 1} r}{\overline{\theta_v^*}^{r\lambda}} \right)\Bigg|_k, \tag{I.15}$$

for $k = 1/2, 3/2, ..., N-3/2$,

$$(C_{xp})|_{N-1/2} = \left(\frac{\delta_{\lambda 1} r}{\overline{\theta_v^*}^{r\lambda}} \right)\Bigg|_{N-1/2} = 0, \tag{I.16}$$

$$(C_{yp})|_k = \left(\frac{\delta_{\phi 1} r}{\overline{\theta_v^*}^{r\phi}} \right)\Bigg|_k, \tag{I.17}$$

for $k = 1/2, 3/2, ..., N-3/2$,

$$(C_{yp})|_{N-1/2} = \left(\frac{\delta_{\phi 1} r}{\overline{\theta_v^*}^{r\phi}} \right)\Bigg|_{N-1/2} = 0, \tag{I.18}$$

$$(C_{xy1})|_k = (\alpha_1\alpha_3\Delta t F_u)|_k\,, \tag{I.19}$$

for $k = 1/2, 3/2, ..., N-1/2$,

$$(C_{xy2})|_k = \left.\left(\frac{c_{pd}\overline{\theta_v^*}^{r\phi}}{\overline{r}^{\phi}\Delta\phi}\right)\right|_k, \tag{I.20}$$

for $k = 1/2, 3/2, ..., N-1/2$,

$$(C_{yx1})|_k = (\alpha_1\alpha_3\Delta t F_v)|_k\,, \tag{I.21}$$

for $k = 1/2, 3/2, ..., N-1/2$,

$$(C_{yx2})|_k = \left.\left(\frac{c_{pd}\overline{\theta_v^*}^{r\lambda}}{\overline{r}^{\lambda}\cos\phi\Delta\lambda}\right)\right|_k, \tag{I.22}$$

for $k = 1/2, 3/2, ..., N-1/2$,

$$(C_2)|_k = (\theta_v^*)|_k\,, \tag{I.23}$$

for $k = 1, 2, ..., N-1$,

$$(C_3)|_k = \left.\left[\frac{r^2\rho^n\delta_\eta r}{\overline{\theta_v^n}^r\left(1+\sum_{X=(v,cl,cf)}\overline{m_X^*}^r\right)}\right]\right|_k, \tag{I.24}$$

for $k = 1/2, 3/2, ..., N-1/2$,

$$(C_4)|_k = \left.\left[\frac{\delta_\eta r\left(\frac{r^2p^n}{R_d\Pi^n} - \kappa_d r^2\rho^n\overline{\theta_v^n}^r\right)}{\kappa_d\Delta t\Pi^n\overline{\theta_v^n}^r\left(1+\sum_{X=(v,cl,cf)}\overline{m_X^*}^r\right)}\right]\right|_k, \tag{I.25}$$

for $k = 1/2, 3/2, ..., N-1/2$,

$$(C_5)|_k = \left.\left(\overline{r^2\rho_y^n}^r\right)\right|_k, \tag{I.26}$$

for $k = 1, 2, ..., N-1$,

$$\delta_{\lambda 1} \equiv \Delta\lambda\delta_\lambda, \tag{I.27}$$

$$\delta_{\phi 1} \equiv \Delta\phi\delta_\phi, \tag{I.28}$$

$$
\begin{aligned}
(RHS)|_{1/2} \;=\; & -\left[\frac{\delta_\eta r\left(\kappa_d r^2\rho^n\Pi^n\overline{\theta_v^*}^r-\frac{r^2p^n}{c_{pd}}\right)}{\Delta t\kappa_d\Pi^n\overline{\theta_v^n}^r\left(1+\sum_{X=(v,cl,cf)}\overline{m_X^*}^r\right)}\right]\Bigg|_{1/2} \\
& -\left[\frac{r^2\rho^n\delta_\eta r}{\Delta t\left(1+\sum_{X=(v,cl,cf)}\overline{m_X^n}^r\right)}\left(\frac{\sum_{X=(v,cl,cf)}\overline{(m_X^*-m_X^n)}^r}{1+\sum_{X=(v,cl,cf)}\overline{m_X^*}^r}\right)\right]\Bigg|_{1/2} \\
& +\left[\frac{1}{\cos\phi}\delta_{\lambda 1}\left(C_{xx1}u_*\right)+\frac{1}{\cos\phi}\delta_{\phi 1}\left(C_{yy1}v_*\right)\right]\Bigg|_{1/2} \\
& +\left(\frac{1}{\Delta\eta}\right)\Bigg|_{1/2}\left[C_5\left(\dot\eta^n\delta_\eta r+\alpha_2G^{-1}R_w^+-\overline{C_{xz}\overline{(u_*-u^n)}^\eta}^\lambda-\overline{C_{yz}\overline{(v_*-v^n)}^\eta}^\phi\right)\right]\Bigg|_1 \\
& +\left(C_3\right)|_{1/2}\left[\left(\frac{1+\frac{1}{\varepsilon}m_v^*}{1+\sum_{X=(v,cl,cf)}m_X^*}\right)\left(\alpha_2\delta_{2r}\theta_{ref}G^{-1}R_w^+\right)\right]\Bigg|_1 , \qquad \text{(I.29)}
\end{aligned}
$$

$$
\begin{aligned}
(RHS)|_k \;=\; & -\frac{\delta_\eta r\left(\kappa_d r^2\rho^n\Pi^n\overline{\theta_v^*}^r-\frac{r^2p^n}{c_{pd}}\right)}{\Delta t\kappa_d\Pi^n\overline{\theta_v^n}^r\left(1+\sum_{X=(v,cl,cf)}\overline{m_X^*}^r\right)} \\
& -\frac{r^2\rho^n\delta_\eta r}{\Delta t\left(1+\sum_{X=(v,cl,cf)}\overline{m_X^n}^r\right)}\left(\frac{\sum_{X=(v,cl,cf)}\overline{(m_X^*-m_X^n)}^r}{1+\sum_{X=(v,cl,cf)}\overline{m_X^*}^r}\right) \\
& +\frac{1}{\cos\phi}\delta_{\lambda 1}\left(C_{xx1}u_*\right)+\frac{1}{\cos\phi}\delta_{\phi 1}\left(C_{yy1}v_*\right) \\
& +\delta_\eta\left[C_5\left(\dot\eta^n\delta_\eta r+\alpha_2G^{-1}R_w^+-\overline{C_{xz}\overline{(u_*-u^n)}^\eta}^\lambda-\overline{C_{yz}\overline{(v_*-v^n)}^\eta}^\phi\right)\right] \\
& +\overline{C_3\left(\frac{1+\frac{1}{\varepsilon}m_v^*}{1+\sum_{X=(v,cl,cf)}m_X^*}\right)\left(\alpha_2\delta_{2r}\theta_{ref}G^{-1}R_w^+\right)}^r , \qquad \text{(I.30)}
\end{aligned}
$$

for $k=3/2,5/2,...,N-3/2$,

$$
\begin{aligned}
(RHS)|_{N-1/2} \;=\; & -\left[\frac{\delta_\eta r\left(\kappa_d r^2\rho^n\Pi^n\overline{\theta_v^*}^r-\frac{r^2p^n}{c_{pd}}\right)}{\Delta t\kappa_d\Pi^n\overline{\theta_v^n}^r\left(1+\sum_{X=(v,cl,cf)}\overline{m_X^*}^r\right)}\right]\Bigg|_{N-1/2} \\
& -\left[\frac{r^2\rho^n\delta_\eta r}{\Delta t\left(1+\sum_{X=(v,cl,cf)}\overline{m_X^n}^r\right)}\left(\frac{\sum_{X=(v,cl,cf)}\overline{(m_X^*-m_X^n)}^r}{1+\sum_{X=(v,cl,cf)}\overline{m_X^*}^r}\right)\right]\Bigg|_{N-1/2} \\
& +\left[\frac{1}{\cos\phi}\delta_{\lambda 1}\left(C_{xx1}u_*\right)+\frac{1}{\cos\phi}\delta_{\phi 1}\left(C_{yy1}v_*\right)\right]\Bigg|_{N-1/2} \\
& -\left(\frac{1}{\Delta\eta}\right)\Bigg|_{N-1/2}\left[C_5\left(\dot\eta^n\delta_\eta r+\alpha_2G^{-1}R_w^+-\overline{C_{xz}\overline{(u_*-u^n)}^\eta}^\lambda-\overline{C_{yz}\overline{(v_*-v^n)}^\eta}^\phi\right)\right]\Bigg|_{N-1} \\
& +\left(\frac{r_N-r_{N-1/2}}{r_N-r_{N-1}}\right)\left(C_3\right)|_{N-1/2}\left[\left(\frac{1+\frac{1}{\varepsilon}m_v^*}{1+\sum_{X=(v,cl,cf)}m_X^*}\right)\left(\alpha_2\delta_{2r}\theta_{ref}G^{-1}R_w^+\right)\right]\Bigg|_{N-1} , \qquad \text{(I.31)}
\end{aligned}
$$

$$(u_*)|_k = \left[u^n + \alpha_1 \left(A_u R_u^+ + F_u \overline{R_v^+}^{\lambda\phi}\right)\right]\Big|_k, \tag{I.32}$$

for $k = 1/2, 3/2, ..., N - 1/2$,

$$(v_*)|_k = \left[v^n + \alpha_1 \left(A_v R_v^+ - F_v \overline{R_u^+}^{\lambda\phi}\right)\right]\Big|_k, \tag{I.33}$$

for $k = 1/2, 3/2, ..., N - 1/2$,

where A_u, A_v, F_u, F_v, R_u^+, R_v^+ and R_w^+ are given, respectively, by: (6.65), (6.66), (6.67), (6.68), (6.34), (6.54) and (7.27).

APPENDIX J

Iterative methods for the solution of discrete Helmholtz problems

This appendix gives the necessary mathematical background and algorithmic details of various iterative solvers for discrete, elliptic Helmholtz problems. In particular, details are given of the GCR(k) solver used in the New Dynamics and discussed in Section 15.

J.1 Background

In the last decade, iterative methods for solving large sparse linear systems of equations have been gaining ground in many areas of scientific computing (Saad & van der Vorst 1999) and in particular atmospheric applications (Navara 1987, Kao & Auer 1990, Kadioglu & Mudrick 1992, Smolarkiewicz & Margolin 1994, Skamarock, Smolarkiewicz & Kemp 1997). In the past, direct solvers and in particular special purpose sparse direct solvers were often, and still are to a certain extent, the preferred choice in many applications due to their robustness and predictable behaviour. However, as the size of problems kept increasing, the need to find alternative and cost-effective ways of solving huge systems of equations shifted the balance towards iterative methods. This together with many developments in preconditioned methods resulted in many efficient algorithms that can solve large systems at a fraction of the cost of direct solvers (Brussino & Sonnad 1989).

Iterative solvers can be seen as minimisation algorithms. They are based on the idea that the solution to a linear system of equations $Ax = b$ is also the minimum of a certain functional or a surface $F(y)$ that spans all possible y's. For convenience and consistency with the widely used nomenclature in the literature, A is assumed to be a *positive definite* matrix or operator (i.e. $y^T Ay > 0, \forall y \neq 0$). In other words the search space (or the functional $F(y)$) is a convex surface and the solution of the problem coincides with the bottom of the surface. However, when A is *negative definite*, the search space is a concave one and the problem becomes one of maximisation instead of minimisation. If A is negative definite then the use of the $-A$ operator, which is positive definite, is often preferred. The terminology of negative definite is avoided deliberately as it creates unnecessary confusion and it is not consistent with the more universal (almost agreed) terminology. The algorithms are similar for both negative and positive definite matrices except for a few minor sign differences.

This area of linear algebra is huge and it is beyond the scope of these notes to cover it substantially. The aim of these notes is to give the reader, through a succession of a few related algorithms, the necessary mathematical background and the underlying mechanisms of the algorithm used in the New Dynamics. It also gives a few references as pointers for those who may wish to pursue the subject further (Saad & van der Vorst 1999, Saad 1996, Axelsson 1996).

J.2 Steepest Descent method (SD)

Consider the following system of equations

$$Ax = b, \tag{J.1}$$

where A is a symmetric positive definite matrix and x and b are the unknown and right-hand side vectors, respectively. The symmetry property is added here as it simplifies the algebra since the purpose here is simply to illustrate the mechanical details of the algorithms rather than solving a real problem with a complicated A. Define a functional $F(y)$ as:

$$F(y) = \frac{1}{2} y^T A y - b^T y + c. \tag{J.2}$$

Eq .(J.2) is known as the *quadratic form* or simply a quadratic function of y where c is a constant. It is trivial to show that actually the solution to (J.1) minimises the functional $F(y)$ given by (J.2). The minimum of any function is at $dF/dy = 0$, i.e.

$$\frac{dF}{dy}(x) = \frac{1}{2} A^T x + \frac{1}{2} A x - b = 0. \tag{J.3}$$

If A is symmetric (i.e. $A = A^T$), then (J.3) becomes

$$\frac{dF}{dy}(x) = 0 \equiv Ax - b = 0. \tag{J.4}$$

(Note that when A is non-symmetric, the minimum of (J.4) is a solution to the system $0.5(A^T + A)x = b$). Although equation (J.4) shows that the solution, x, minimises F, it does not determine whether $F(x)$ is a global minimum or not. This is where the positive definiteness property is useful. If y is any arbitrary vector and x satisfies (J.4) (i.e. x minimises F), then it follows that

$$F(y) = \frac{1}{2} y^T A y - b^T y + c = F(x) + \frac{1}{2}(y - x)^T A (y - x). \tag{J.5}$$

If A is positive definite (i.e. $v^T Av > 0$, $\forall v \neq 0$ so that $(y-x)^T A(y-x) > 0$, $\forall x \neq y$), then $F(y) > F(x)$, $\forall x \neq y$, hence $F(x)$ is a *global minimum* of F.

The *steepest descent* algorithm is similar to releasing a ball at an arbitrary point x_0 of the surface F and allowing it to slide along the direction in which F decreases most rapidly (the steepest descent), i.e. from a position x_i the ball goes in the direction of $-dF(x_i)/dy$,

$$R_i = -\frac{dF}{dy}(x_i) = b - Ax_i, \tag{J.6}$$

where R_i is usually referred to as the *residual* at the i-th iteration. If the error is defined as $e_i = x_i - x$, it is easy to see also that $R_i = -Ae_i$ (this is just to emphasise the fact that the residual can also be seen as the transformation (projection) of the error using the operator A). At each iteration $(i+1)$ the solution x_{i+1} proceeds by moving from the previous position x_i by a distance in the direction R_i, viz:

$$x_{i+1} = x_i + \alpha_i R_i, \tag{J.7}$$

where α_i measures the length of the stride along the search direction, which is also the residual for this case. One question is how long should this stride be? Since it is the minimum which is being sought, there is no need to increase F along a search path. This motivates the need to take an optimal value of α_i that minimises F along the search direction, then change to another direction. α_i is optimal when the directional derivative $dF/d\alpha_i = 0$,

$$\frac{dF}{d\alpha_i} = \frac{dF}{dy}(x_{i+1})\frac{dx_{i+1}}{d\alpha_i} = -R_{i+1}^T R_i = 0. \tag{J.8}$$

Eq .(J.8) is also equivalent to saying that the *inner-product of the two residuals (directions) is zero or the two residual vectors are orthogonal*, i.e.

$$\langle R_{i+1}, R_i \rangle = 0, \tag{J.9}$$

where for any real vectors x and y, the inner-product $\langle x, y \rangle = x^T y$. The result (J.9) is due to the fact that the component of the projection of the slope of F along the search line vanishes at the minimum before changing sign afterwards. Multiplying (J.7) by $-A$ and adding b on each side, gives

$$b - Ax_{i+1} = b - Ax_i - \alpha_i AR_{i,} \tag{J.10}$$

or simply

$$R_{i+1} = R_i - \alpha_i AR_i. \tag{J.11}$$

Aside :

Note for positive or negative definite matrices the projection of the gradient of F has only one component that vanishes at some point along a direction. If more than one vanishes, this coincides with a saddle point and the matrix is indefinite which makes the solution non-unique. The case of indefinite matrices will not be treated here as it is not relevant to our problem.

Using the constraint (J.9) and the definition (J.11) gives

$$\langle R_{i+1}, R_i \rangle = \langle R_i - \alpha_i A R_i, R_i \rangle = \langle R_i, R_i \rangle - \alpha_i \langle R_i, A R_i \rangle = 0, \tag{J.12}$$

which leads to:

$$\alpha_i = \frac{\langle R_i, R_i \rangle}{\langle R_i, A R_i \rangle}. \tag{J.13}$$

Finally, the steepest descent algorithm can be summarised as:

Algorithm 1: **SD Algorithm**

1-Given an initial guess x_0, compute $R_0 = b - Ax_0$
2-**Do** $i = 1, 2, ...,$ until convergence
3- $\alpha_i = \langle R_{i-1}, R_{i-1} \rangle / \langle R_{i-1}, AR_{i-1} \rangle$
4- $x_i = x_{i-1} + \alpha_{i-1} R_{i-1}$
5- $R_i = b - Ax_i$
6- **EndDo**

Most iterative algorithms follow a similar approach and can be seen as SD algorithms. However, the way in which the search directions are computed makes all the difference. In the above SD algorithm the same direction may be used again and again. This motivates imposing further constraints on these directions. This can be done using *conjugacy* and this is treated in the next section.

J.3 Conjugate Gradient method (CG)

Assume again that A is a symmetric positive definite matrix. If at each iteration $(i+1)$, x_{i+1} is updated using a linear combination of the previous iterate x_i and a search direction

p_i, then:

$$x_{i+1} = x_i + \alpha_i p_i, \tag{J.14}$$

from which it follows as in (J.11), that

$$R_{i+1} = R_i - \alpha_i A p_i. \tag{J.15}$$

The residuals in CG are orthogonal, i.e. $\langle R_i, R_j \rangle = 0$ for $i \neq j$ and in particular $\langle R_{i+1}, R_i \rangle = 0$,

$$\langle R_{i+1}, R_i \rangle = \langle R_i - \alpha_i A p_i, R_i \rangle = \langle R_i, R_i \rangle - \alpha_i \langle A p_i, R_i \rangle = 0, \tag{J.16}$$

which gives

$$\alpha_i = \frac{\langle R_i, R_i \rangle}{\langle A p_i, R_i \rangle}. \tag{J.17}$$

However, instead of taking the search direction as the residual as in SD, the search direction p_{i+1} is taken as a linear combination of the previous direction p_i and the present residual R_{i+1}, viz:

$$p_{i+1} = R_{i+1} + \beta_i p_i. \tag{J.18}$$

Here, it is also imposed that these search directions, p_i, are *A-conjugate or A-orthogonal* ($\langle p_i, A p_j \rangle = 0$ for $i \neq j$) and in particular that p_{i+1} is orthogonal to $A p_i$,

$$\langle p_{i+1}, A p_i \rangle = \langle R_{i+1} + \beta_i p_i, A p_i \rangle = \langle R_{i+1}, A p_i \rangle + \beta_i \langle p_i, A p_i \rangle = 0,$$

which gives:

$$\beta_i = -\frac{\langle R_{i+1}, A p_i \rangle}{\langle p_i, A p_i \rangle}. \tag{J.19}$$

Aside :

> *Eq.* (J.18) *is equivalent to saying that the basis of the Krylov subspace is constructed from the residuals. The Gram-Schmidt conjugation algorithm (see Appendix J.8) can be used to generate an A-orthogonal basis* $\{p_0, p_1, ..., p_m\}$ *from a given set* $\{v_0, v_1, ..., v_m\}$ *viz:*
>
> $$p_i = v_i + \sum_{k=0}^{i-1} \beta_{ik} p_k, \; p_0 = v_0, \tag{J.20}$$
>
> *where* $\langle p_i, A p_j \rangle = 0, \; i \neq j$*, i.e.*
>
> $$\langle p_i, A p_j \rangle = \langle v_i, A p_j \rangle + \sum_{k=0}^{i-1} \beta_{ik} \langle p_k, A p_j \rangle = \langle v_i, A p_j \rangle + \beta_{ij} \langle p_j, A p_j \rangle = 0, \tag{J.21}$$

from which it follows that:

$$\beta_{ij} = -\frac{\langle v_i, Ap_j\rangle}{\langle p_j, Ap_j\rangle}. \tag{J.22}$$

Now, for the choice $\{v_0, v_1, ..., v_m\} = \{R_0, R_1, ..., R_m\}$, (J.22) *becomes* $\beta_{ij} = -\langle R_i, Ap_j\rangle / \langle p_j, Ap_j\rangle$. *Making use of* (J.15), *the numerator of* β_{ij} *can be rewritten as:*

$$\langle R_i, Ap_j\rangle = \frac{1}{\alpha_j}\left(\langle R_i, R_j\rangle - \langle R_i, R_{j+1}\rangle\right) = \begin{cases} \langle R_i, R_i\rangle / \alpha_i & j = i, \\ -\langle R_i, R_i\rangle / \alpha_{i-1} & j = i-1, \\ 0 & j < i-1. \end{cases} \tag{J.23}$$

Notice that $\beta_{ij} = 0$ *for* $j < i-1$. *This is what makes the CG an elegant algorithm. By virtue of this construction of coupling* p*'s and* R*'s, it is sufficient to just orthogonalise* R_i *to* R_{i-1} *and* A*-orthogonalise* p_i *to* Ap_{i-1} *to produce all orthogonal* R_j*, for* $j \leq i$*, and a complete* A*-orthogonal basis* p_j*, for* $j \leq i$*. The search directions in the CG algorithm are obtained simply by the conjugation of the residuals.*

Note that the conjugacy here is equivalent to minimising the error along the direction p_i. Further simplifications of α_i and β_i to minimise operations can be obtained. Taking into account the fact that all p_i's are A-conjugate (also $\langle Ap_i, p_{i-1}\rangle = 0$) and making use of (J.18), the denominator in (J.17) can also be rewritten as:

$$\begin{aligned} \langle Ap_i, R_i\rangle &= \langle Ap_i, p_i - \beta_{i-1}p_{i-1}\rangle \\ &= \langle Ap_i, p_i\rangle - \beta_{i-1}\langle Ap_i, p_{i-1}\rangle \\ &= \langle Ap_i, p_i\rangle . \end{aligned} \tag{J.24}$$

Then (J.17) becomes:

$$\alpha_i = \frac{\langle R_i, R_i\rangle}{\langle Ap_i, p_i\rangle}. \tag{J.25}$$

Making use of (J.15) and the symmetry of A ($\langle p_i, Ap_j\rangle = \langle Ap_i, p_j\rangle$), (J.19) can be rewritten as:

$$\begin{aligned} \beta_i &= -\langle R_{i+1}, Ap_i\rangle / \langle p_i, Ap_i\rangle \\ &= -\left\langle R_{i+1}, \frac{1}{\alpha_i}(R_i - R_{i+1})\right\rangle / \langle p_i, Ap_i\rangle \end{aligned}$$

$$
\begin{aligned}
&= -\frac{1}{\alpha_i}\langle R_{i+1}, R_i\rangle / \langle p_i, Ap_i\rangle + \frac{1}{\alpha_i}\langle R_{i+1}, R_{i+1}\rangle / \langle p_i, Ap_i\rangle \\
&= \langle R_{i+1}, R_{i+1}\rangle / \langle R_i, R_i\rangle . \qquad \text{(J.26)}
\end{aligned}
$$

The CG method is based on (i) *orthogonal residuals* R_i's and (ii) *A-conjugate search directions* p_i's. The search directions in CG are related to the *gradient* of F and are *conjugated,* hence the name of *Conjugate Gradient.* (The name of conjugate gradient is (just) a bit misleading but it was maintained through historic reasons due to early algorithms, such as SD, where the directions are the gradient of F. A more accurate description would be conjugate directions.) The CG algorithm can be summarised as follows (Saad 1996):

Algorithm 2: **CGAlgorithm**

1- Compute $R_0 = b - Ax_0$, $p_0 = R_0$
2- **Do** $i = 1, 2, ...,$ until convergence
3- $\quad\alpha_{i-1} = \langle R_{i-1}, R_{i-1}\rangle / \langle Ap_{i-1}, p_{i-1}\rangle$
4- $\quad x_i = x_{i-1} + \alpha_{i-1}p_{i-1}$
5- $\quad R_i = R_{i-1} - \alpha_{i-1}Ap_{i-1}$
6- $\quad\beta_i = \langle R_i, R_i\rangle / \langle R_{i-1}, R_{i-1}\rangle$
7- $\quad p_i = R_i + \beta_i p_{i-1}$
8- **EndDo**

J.4 Conjugate Residual method (CR)

The conjugate residual method is similar to CG but (i) the residuals, R_i, are A-conjugate or A-orthogonal (hence the name of *Conjugate Residual*) and (ii) Ap_i's are orthogonal (or the search directions, p_i, are A^TA-orthogonal). Note that hereafter F refers to the general functional defined as the l_2-norm of the residual $F(x) = \|b - Ax\|_2$ and that the conjugate residual type algorithms minimise the residual norm. Using the two constraints (i) and (ii), i.e.

$$\langle R_{i+1}, AR_i\rangle = 0, \qquad \text{(J.27)}$$

$$\langle Ap_{i+1}, Ap_i\rangle = 0, \qquad \text{(J.28)}$$

and the definitions (J.14), (J.15) and (J.18), after some manipulation, α_i and β_i are given by:

$$\alpha_i = \frac{\langle R_i, AR_i \rangle}{\langle Ap_i, Ap_i \rangle}, \tag{J.29}$$

$$\beta_i = \frac{\langle R_{i+1}, AR_{i+1} \rangle}{\langle R_i, AR_i \rangle}. \tag{J.30}$$

Finally, the CR algorithm can be summarised as follows (Saad 1996):

Algorithm 3: **CRAlgorithm**

1- Compute $R_0 = b - Ax_0$, $p_0 = R_0$

2- **Do** $i = 1, 2, ...,$ until convergence

3- $\alpha_{i-1} = \langle R_{i-1}, AR_{i-1} \rangle \,/\, \langle Ap_{i-1}, Ap_{i-1} \rangle$

4- $x_i = x_{i-1} + \alpha_{i-1} p_{i-1}$

5- $R_i = R_{i-1} - \alpha_{i-1} Ap_{i-1}$

6- $\beta_i = \langle R_i, AR_i \rangle \,/\, \langle R_{i-1}, AR_{i-1} \rangle$

7- $p_i = R_i + \beta_i p_{i-1}$

8- $Ap_i = AR_i + \beta_i Ap_{i-1}$

9- **EndDo**

Note that both CG and CR are developed for symmetric A. They can also be derived from the Full Orthogonalisation Method (FOM) and the Generalised Minimal Residual (GMRES), or the GCR for that matter, respectively, for the special case of a symmetric A (see page 183 of Saad (1996)). Although several CG-type algorithms for non-symmetric systems were developed in the literature, their use in real applications has been minimal due to stability problems and lack of robustness. Most of these algorithms can be seen as a CG algorithm applied to an augmented, or transformed, symmetric system which has the same solution as the original one. This often increases the operation count as well as the condition number, resulting in slower convergence. Amongst these algorithms one can mention the CGNR (CG for Normal equation with a minimal Residual constraint, solves $A^T Ax = A^T b$), CGNE (CG for Normal equation with a minimal Error constraint, solves $A^T Ax^* = b$ where $x = A^T x^*$), BiCG (BiConjugate Gradient, solves two systems $Ax = b$ and $A^T x^* = b^*$) (Fletcher

1975), BiCGSTAB (BiCG Stabilised) (van der Vorst 1992), QMR (Quasi-Minimal Residual) (Freund & Nachtigal 1991), TFQMR (Transpose-Free QMR), and CGS (Conjugate Gradient Square) (Sonneveld 1989). For details of these algorithms and many related variants, see Barrett, Berry, Chan, Demmel, Donato, Dongarra, Eijkhout, Pozo, Romine & van der Vorst (1994) and Saad (1996).

In general, detailed convergence analysis of iterative solvers is difficult but finding an upper bound of the rate by which the energy norm of the error $\|e\|_A = \langle e, Ae\rangle^{1/2}$ is reduced at each iteration is quite useful (i.e. $\|e_i\|_A \leq \omega_i \|e_0\|_A$). This norm is usually used in the convergence analysis instead of the Euclidean one for simplicity and without loss of validity of the result. ω_i is usually a function of the *spectral condition number* $\kappa(A) = \lambda_{max}(A)/\lambda_{min}(A)$ of the matrix A, where $\lambda_{max}(A) = \max\{\lambda_i\}$, $\lambda_{min}(A) = \min\{\lambda_i\}$ and λ_i are the eigenvalues of A. For instance, $\omega_i = (\kappa - 1/\kappa + 1)^i$ for SD while $\omega_i = 2(\sqrt{\kappa} - 1/\sqrt{\kappa} + 1)^i$ for CG. In general, for CG-type algorithms, the iteration count is usually proportional to $\sqrt{\kappa}$. This, for instance, makes the iteration count for second-order elliptic PDEs of the order $O(h^{-1})$ since $\kappa = O(h^{-2})$, where h is the mesh-size (Barrett et al. 1994).

J.5 Generalised Conjugate Residual method (GCR)

Most iterative algorithms are strongly related to, or defined by, the choice of the basis of the Krylov subspace (or simply the search directions, p_i). The GMRES uses a generalised l_2-orthonormal (orthogonal with a unity l_2-norm) basis constructed using the Arnoldi process (see Appendix J.8) (Saad & Schultz 1986). In CG they are A-orthogonal, whereas A^TA-orthogonal for CR. A number of algorithms are developed on a similar basis for non-symmetric systems. Unlike CG-type methods, non-symmetric algorithms such as GMRES, ORTHOMIN, ORTHODIR, and GCR (Saad 1996) solve the original non-symmetric system. These algorithms are based on the fact that a solution x that has the smallest residual norm $\|b - Ax\|_2$ can be computed using a linear combination of the original guess x_0 and the basis $\{p_0, p_1, ..., p_i, ...\}$ of the search (Krylov) space provided that they are A^TA-orthogonal. For details see the lemma given below in Appendix J.8, also see page 184 of Saad (1996).

The GCR is based on (i) the residual is A-orthogonal to the search direction ($\langle R_i, Ap_{i-1}\rangle = 0$), and (ii) the search directions are A^TA-orthogonal ($\langle Ap_i, Ap_j\rangle = 0,\ i \neq j$). Condition (i) is also equivalent to saying that, in a similar way to CR, the residuals are A-orthogonal (i.e. $\langle R_i, AR_{i-1}\rangle = 0$, which can be easily verified by taking $\langle R_i, Ap_{i-1}\rangle = 0$ andmaking use of (J.31) below). Using the same definition (J.15), it can be easily verified that in order to satisfy the constraint (i), it suffices to take:

$$\alpha_i = \langle R_i, Ap_i\rangle \,/\, \langle Ap_i, Ap_i\rangle \,. \tag{J.31}$$

One of the simplest ways to compute the basis vector p_i is as a linear combination of the current residual R_i and all the previous directions p_j, $j = 0, i-1$, viz:

$$p_i = R_i + \sum_{j=0}^{i-1} \beta_{ij} p_j, \tag{J.32}$$

and update the solution and the residual using (J.14) and (J.15), respectively. This results in the well known *Generalised Conjugate Residual* (GCR) algorithm. Multiplying (J.32) by A gives:

$$Ap_i = AR_i + \beta_{i0}Ap_0 + \beta_{i1}Ap_1 + ... + \beta_{i,i-2}Ap_{i-2} + \beta_{i,i-1}Ap_{i-1}, \tag{J.33}$$

and taking into account the fact that the p_i's are A^TA-orthogonal ($\left\langle A^TAp_i, p_j\right\rangle = \langle Ap_i, Ap_j\rangle = 0$), i.e. that the Ap_i's are orthogonal, and in particular that $\langle Ap_i, Ap_j\rangle = 0$ for $j < i$, gives:

$$\begin{aligned}
\langle Ap_i, Ap_0\rangle \;&= \langle AR_i, Ap_0\rangle + \beta_{i0}\langle Ap_0, Ap_0\rangle = 0 \;\Rightarrow\; \beta_{i0} = -\langle AR_i, Ap_0\rangle \,/\, \langle Ap_0, Ap_0\rangle \,,\\
\langle Ap_i, Ap_1\rangle \;&= \langle AR_i, Ap_1\rangle + \beta_{i1}\langle Ap_1, Ap_1\rangle = 0 \;\Rightarrow\; \beta_{i1} = -\langle AR_i, Ap_1\rangle \,/\, \langle Ap_1, Ap_1\rangle \,,\\
\vdots \qquad & \qquad\qquad \vdots \qquad\qquad\qquad\qquad \vdots\\
\langle Ap_i, Ap_j\rangle \;&= \langle AR_i, Ap_j\rangle + \beta_{ij}\langle Ap_j, Ap_j\rangle = 0 \;\Rightarrow\; \beta_{ij} = -\langle AR_i, Ap_j\rangle \,/\, \langle Ap_j, Ap_j\rangle \,.
\end{aligned} \tag{J.34}$$

The process given by (J.34) is simply the Arnoldi or Gram-Schmidt conjugation process which generates an A^TA-orthogonal basis for the Krylov subspace from the residuals (see Appendix J.8 for details). Finally, putting all these pieces together, the GCR algorithm can be summarised as follows (Eisentat, Elman & Schultz 1983):

Algorithm 4: **GCRAlgorithm**

Compute $R_0 = b - Ax_0$, and $p_0 = R_0$

Do $i = 1, 2, ...,$ until convergence

  $\alpha_{i-1} = \langle R_{i-1}, Ap_{i-1} \rangle / \langle Ap_{i-1}, Ap_{i-1} \rangle$

  $x_i = x_{i-1} + \alpha_{i-1} p_{i-1}$

  $R_i = R_{i-1} - \alpha_{i-1} Ap_{i-1}$

  Do $j = 0, ..., i-1$

    $\beta_{ij} = - \langle AR_i, Ap_j \rangle / \langle Ap_j, Ap_j \rangle$

  EndDo

  $p_i = R_i + \sum_{j=0}^{i-1} \beta_{ij} p_j$

  $Ap_i = AR_i + \sum_{j=0}^{i-1} \beta_{ij} Ap_j$

EndDo

Note that in the above algorithm all the p_i's and Ap_i's have to be saved for future iterations and their number increases linearly with the iteration count. This dynamically increases the memory requirements, which may become computationally prohibitive if the solver does not converge in a few iterations. A variant of the above algorithm can be derived in which the algorithm is restarted with a new initial guess x_k after every k iterations. This is known as the *restarted GCR* or, using the widely used nomenclature, as GCR(k). In this algorithm, the search directions, p_i, are $A^T A$-orthogonal to at most k previous ones. This relaxes the convergence criteria in favour of computational efficiency. In theory, restarting GCR (or GMRES for that matter) means that the convergence, starting from any given initial guess, is not guaranteed, but in practice, and especially for time-dependent problems, it is not very crucial as most initial solutions are already close to the real solution in the first place. This algorithm can be summarised as (Saad 1996):

Algorithm 5: **GCR(k)Algorithm**

01- Compute $R_0 = b - Ax_0$, and $p_0 = R_0$

02- **Do** $i = 1, 2, ...,$ until convergence

03- $\quad \alpha_{i-1} = \langle R_{i-1}, Ap_{i-1}\rangle \,/\, \langle Ap_{i-1}, Ap_{i-1}\rangle$

04- $\quad x_i = x_{i-1} + \alpha_{i-1} p_{i-1}$

05- $\quad R_i = R_{i-1} - \alpha_{i-1} Ap_{i-1}$

06- $\quad$ **Do** $j = int[(i-1)/k]k, ..., i-1$

07- $\qquad \beta_{ij} = -\langle AR_i, Ap_j\rangle \,/\, \langle Ap_j, Ap_j\rangle$

08- $\quad$ **EndDo**

09- $\quad p_i = R_i + \sum_{j=int[(i-1)/k]k}^{i-1} \beta_{ij} p_j$

10- $\quad Ap_i = AR_i + \sum_{j=int[(i-1)/k]k}^{i-1} \beta_{ij} Ap_j$

11- **EndDo**

where $int[x]$ refers to the integer part of x. Note also that in algorithm 5, the direction p at the end of each restart is used as a first guess for the next restart and this is what is adopted in the New Dynamics implementation. The reason for this is that the p's are already computed using the relatively cheap reccursive relations at line 9 and 10. In contrast, a standard restart would be equivalent to repeating line 1 at each restart, and this would involve either extra storage (since $\widehat{R}$ in line 6 of algorithm 7 is not stored in the present implementation) or extra computations involving the preconditioner ($p_0 = M^{-1}R_0$) when the algorithm is preconditioned.

Aside :

Most iterative methods for non-symmetric systems are based on the lemma given below in Appendix J.8. Provided that all the search direction p's are A^TA*-orthogonal* ($\langle Ap_i, Ap_j\rangle = 0,\ \forall i \neq j$)*, the convergence to the solution with the smallest residual is guaranteed. However, restarting these algorithms violates the condition* ($\langle Ap_i, Ap_j\rangle = 0,\ \forall i \neq j$) *and therefore convergence to the minimum residual is no longer guaranteed (see page 13 of Saad & van der Vorst (1999)). Restarting can also cause stagnation (the reduction of the original norm stagnates* *at a higher value than that specified for the stopping criteria) if A is not definite (Saad 1996). Furthermore, usually after restarting, the convergence rate of a GCR(k) or GMRES(k) may also become slower than that obtained just before restarting, where the search direction is A^TA-orthogonal to more than just the previous one (Saad & van der Vorst 1999). In practice and in many applications, a suitably tuned truncation k for a GCR(k) or a GMRES(k) is sufficient to achieve an acceptable convergence over all possible situations for the application at hand.*

Aside :

One may ask the question "what is the best iterative method?". When A is symmetric the answer is almost universally agreed to be CG. However, when A is non-symmetric, it is very hard to find a definite answer. Several surveys and comparative studies of iterative methods are available to shed some light in this regard (Brussino & Sonnad 1989, Freund, Golub & Nachtigal 1992, Tong 1992). From the literature, it is clear that there is no ultimate overall winner. Many studies show that for any given method there is a class of problems for which the given algorithm performs best and less so in other classes. However, GMRES seems to be more widely used as it is the most numerically stable and robust for many scientific applications (Brussino & Sonnad 1989). CG-based algorithms are also the subject of intensive research to improve their convergence behaviour and robustness, which may increase their use in real applications. There is also increased interest in hybrid methods to combine the best features of two or more methods. Among these one can mention QMR-CGSTAB and GCRO (combining GCR and GMRES optimality). For detailed discussion of these issues, the reader is referred to pages 35-37 of Barrett et al. (1994) and the review paper of Saad & van der Vorst (1999). Almost all iterative methods are efficient for some problems and not so for others, but it is not clear a priori which method performs better for a given application. Therefore, recourse is often made to a heuristic approach by comparing the relative performances of all possible methods. This is not usually a major task as most of these iterative algorithms are freely available from a number of Internet sites for research purposes.

J.6 Preconditioning

Although iterative methods are based on sound mathematical theories, in practice they suffer from the syndrome of slow convergence, especially for *ill-conditioned* problems (large $\kappa \gg 1$), since the rate of convergence is dependent on κ. The ideal situation would be a matrix A with a condition number $\kappa(A) = 1$ (this is possible only when $A = I$, where I is the identity matrix). Therefore, instead of solving the original system $Ax = b$, it is more efficient to seek a solution to a, hopefully better, *preconditioned* system of equations, for instance:

$$(M^{-1}A)x = M^{-1}b, \tag{J.35}$$

where M is the *preconditioning matrix*. M should be as close to A as possible and relatively cheap to invert (as $M \to A$, $\kappa(M^{-1}A) \to 1$). This is a delicate balance between the cost of M^{-1} and improving the convergence rate of the solver. This is usually problem-dependent and a matter of practical experimentation. Eq. (J.35) is also known as *left preconditioning*. There are other preconditioning strategies such as *right preconditioning, split preconditioning* and *flexible*. *Right preconditioning* basically solves the following:

$$A(M^{-1}M)x = b, \tag{J.36}$$

or

$$(AM^{-1})y = b, \quad y = Mx, \tag{J.37}$$

whereas the *split preconditioning* solves:

$$L^{-1}A(U^{-1}U)x = L^{-1}b, \tag{J.38}$$

or

$$(L^{-1}AU^{-1})y = L^{-1}b, \quad x = U^{-1}y, \tag{J.39}$$

where $M = LU$ and L and U are respectively lower and upper triangular matrices. The *flexible* strategy simply allows the preconditioner M to vary from one iteration to the other, instead of keeping it fixed as in the previous strategies. Apart from a few situations such as when A is almost symmetric or when M is very ill-conditioned, there is little difference between these strategies from a practical point of view. For detailed discussions of these issues and substantial coverage of the subject see chapters 9 and 10 of Saad (1996).

Consider a right-preconditioning strategy, such as that currently adopted for the New Dynamics, and consider how the introduction of a preconditioner M into the original system of equations affects a non-preconditioned algorithm. For every algorithm a preconditioned version can be derived straightforwardly. However, here only the effect of preconditioning by M on the non-preconditioned GCR(k) is considered. A right-preconditioned GCR(k) basically solves the two systems of equations given by (J.37). From equation (J.37) it can be seen that the transformed operator is $\overline{A} = AM^{-1}$, and the solution is given by $x = M^{-1}y$, where y is the solution to the system $\overline{A}y = b$. An unsimplified preconditioned GCR(k) can be derived by simply applying the GCR(k), i.e. algorithm 5, to the two transformed systems $\overline{A}y = b$ and $x = M^{-1}y$. This results in the following algorithm:

Algorithm 6: **Unsimplified Preconditioned GCR(k)Algorithm**

01- Compute $\overline{R}_0 = b - \overline{A}y_0 = b - AM^{-1}Mx_0 = b - Ax_0$, $\overline{p}_0 = \overline{R}_0$

02- **Do** $i = 1, 2, ...,$ until convergence

03- $\overline{\alpha}_{i-1} = \langle \overline{R}_{i-1}, \overline{A}\overline{p}_{i-1} \rangle / \langle \overline{A}\overline{p}_{i-1}, \overline{A}\overline{p}_{i-1} \rangle$

or $\overline{\alpha}_{i-1} = \langle \overline{R}_{i-1}, AM^{-1}\overline{p}_{i-1} \rangle / \langle AM^{-1}\overline{p}_{i-1}, AM^{-1}\overline{p}_{i-1} \rangle$

04- $y_i = y_{i-1} + \overline{\alpha}_{i-1}\overline{p}_{i-1}$ **Then** ($x_i = M^{-1}y_i$)

05- $\overline{R}_i = \overline{R}_{i-1} - \overline{\alpha}_{i-1}\overline{A}\overline{p}_{i-1}$ also ($\overline{R}_i = b - \overline{A}y_i$)

or $\overline{R}_i = \overline{R}_{i-1} - \overline{\alpha}_{i-1}AM^{-1}\overline{p}_{i-1}$

06- **Do** $j = int[(i-1)/k]k, ..., i-1$

07- $\overline{\beta}_{ij} = -\langle \overline{A\overline{R}_i}, \overline{A}\overline{p}_j \rangle / \langle \overline{A}\overline{p}_j, \overline{A}\overline{p}_j \rangle$

or $\overline{\beta}_{ij} = -\langle AM^{-1}\overline{R}_i, AM^{-1}\overline{p}_j \rangle / \langle AM^{-1}\overline{p}_j, AM^{-1}\overline{p}_j \rangle$

08- **EndDo**

09- $\overline{p}_i = \overline{R}_i + \sum_{j=int[(i-1)/k]k}^{i-1} \overline{\beta}_{ij}\overline{p}_j$

10- $\overline{A}\overline{p}_i = \overline{A\overline{R}_i} + \sum_{j=int[(i-1)/k]k}^{i-1} \overline{\beta}_{ij}\overline{A}\overline{p}_j$

or $AM^{-1}\overline{p}_i = AM^{-1}\overline{R}_i + \sum_{j=int[(i-1)/k]k}^{i-1} \overline{\beta}_{ij}AM^{-1}\overline{p}_j$

11- **EndDo**

In practice, it is not necessary to use the above raw algorithm as it requires knowing explicitly $\overline{A} = AM^{-1}$. A much simpler and equivalent algorithm can be derived by defining the new variables α, β, R, $\widehat{R}$ and p such that $\alpha = \overline{\alpha}$, $\beta = \overline{\beta}$, $R = \overline{R}$, $\widehat{R} = M^{-1}R$ and $p = M^{-1}\overline{p}$, respectively. Furthermore, there is no need to explicitly compute the vector y since $\overline{R}_i = b - \overline{A}y_i = b - Ax_i$, which results in the following:

$$\begin{cases} \overline{R}_i & = \overline{R}_{i-1} - \overline{\alpha}_{i-1}\overline{A}\overline{p}_{i-1}, \\ b - Ax_i & = b - Ax_{i-1} - \overline{\alpha}_{i-1}AM^{-1}Mp_{i-1}, \\ x_i & = x_{i-1} + \alpha_{i-1}p_{i-1}. \end{cases} \tag{J.40}$$

Hence, the algorithm 6 can be simplified as follows (Wong, Zang & Hussaini 1986):

Algorithm 7:**Preconditioned GCR(k)Algorithm**

01- Compute $R_0 = b - Ax_0$, $\widehat{R}_0 = M^{-1}R_0$, $p_0 = \widehat{R}_0$
02- **Do** $i = 1, 2, ...,$ until convergence
03- $\quad \alpha_{i-1} = \langle R_{i-1}, Ap_{i-1}\rangle \,/\, \langle Ap_{i-1}, Ap_{i-1}\rangle$
04- $\quad x_i = x_{i-1} + \alpha_{i-1}p_{i-1}$
05- $\quad R_i = R_{i-1} - \alpha_{i-1}Ap_{i-1}$
06- $\quad \widehat{R}_i = M^{-1}R_i$
07- $\quad$ **Do** $j = int[(i-1)/k]k, ..., i-1$
08- $\qquad \beta_{ij} = -\left\langle A\widehat{R}_i, Ap_j\right\rangle \,/\, \langle Ap_j, Ap_j\rangle$
09- $\quad$ **EndDo**
10- $\quad p_i = \widehat{R}_i + \sum_{j=int[(i-1)/k]k}^{i-1} \beta_{ij}p_j$
11- $\quad Ap_i = A\widehat{R}_i + \sum_{j=int[(i-1)/k]k}^{i-1} \beta_{ij}Ap_j$
12- **EndDo**

J.7 Alternating Direction Implicit (ADI) method

Since the ADI method is used as a preconditioner for the New Dynamics GCR(k) solver, brief details of the method are outlined in this section. The ADI method was first used by Peaceman and Rachford to solve parabolic PDEs (Peaceman & Rachford 1955). It is based on splitting the operator into 2 or 3 directional operators. In matrix notation, this is similar to an additive decomposition. If the original matrix, or operator, A can be split into 2 operators, $A = A_x + A_y$ in the case of 2D (or two sub-step iterations), or 3 operators,

$A = A_x + A_y + A_z$ in the case of 3D (or 3 sub-steps iterations), then 2D and 3D ADI can be derived as follows.

The 2D-ADI *Peaceman-Rachford* scheme is simply a two stage iteration of the system:

$$Ax = b \quad \text{or} \quad \mu x + (A_x + A_y)x = b + \mu x, \tag{J.41}$$

where μ is an acceleration parameter. Using 2 sub-step iterations, (J.41) can be split into:

$$\begin{aligned} (\mu_i I + A_x)x_{i+1/2} &= b + (\mu_i I - A_y)x_i, \\ (\mu_i I + A_y)x_{i+1} &= b + (\mu_i I - A_x)x_{i+1/2}. \end{aligned} \tag{J.42}$$

The extension of the above scheme to higher dimensions, for instance to the 3D case (or 3 sub-step iterations) is a little subtle and raises some stability issues (Roache 1976). However, the ADI scheme is used here as a preconditioner to give an *approximate solution* and therefore the issue of stability is not crucial unless the scheme is used as a complete solution procedure to the system of equations at hand, though of course it may affect robustness and the rate of convergence. Using a similar equation to (J.41) but with 3 directional operators, the following 3 sub-step iterations can be obtained:

$$\begin{aligned} \mu x_{i+1/3} + A_x[\xi x_{i+1/3} + (1-\xi)x_i] &= b + \mu x_i - A_y x_i - A_z x_i, \\ \mu x_{i+2/3} + A_y[\xi x_{i+2/3} + (1-\xi)x_i] &= b + \mu x_i - A_x[\xi x_{i+1/3} + (1-\xi)x_i] - A_z x_i, \\ \mu x_{i+1} + A_z[\xi x_{i+1} + (1-\xi)x_i] &= b + \mu x_i - A_x[\xi x_{i+1/3} + (1-\xi)x_i] \\ &\quad - A_y[\xi x_{i+2/3} + (1-\xi)x_i], \end{aligned} \tag{J.43}$$

where $0 \le \xi \le 1$ is a weighting average coefficient. Eq. (J.43) can be rearranged to give:

$$\begin{aligned} (\mu_i I + \xi A_x)(x_{i+1/3} - x_i) &= b - Ax_i, \\ (\mu_i I + \xi A_y)(x_{i+2/3} - x_i) &= b - Ax_i - \xi A_x(x_{i+1/3} - x_i), \\ (\mu_i I + \xi A_z)(x_{i+1} - x_i) &= b - Ax_i - \xi A_x(x_{i+1/3} - x_i) - \xi A_y(x_{i+2/3} - x_i). \end{aligned} \tag{J.44}$$

The *3D Douglas-Rachford* scheme (Douglas & Rachford 1956) is simply the system (J.44) with $\xi = 1/2$, whereas the scheme used in the New Dynamics corresponds to $\xi = 1$.

Finding an optimal value of μ_i in general cases is not an easy task as there is no general theory as such, except for a few simplified cases (Ma & Saad 1992). Therefore, recourse is often made to a heuristic approach. When A is the result of the discretisation of an elliptic

PDE, the above iterative process can be seen to be analogous to searching for a *steady state solution* to the following pseudo-time dependent parabolic PDE:

$$\frac{1}{\psi}\frac{\partial x}{\partial \tau} = b - (A_x + A_y + A_z)x, \tag{J.45}$$

where τ is the dimensionless pseudo-time variable and ψ is a damping coefficient. It can be easily shown that the discretisation of (J.45) would give the same system as (J.44) with $\mu = 1/(\psi\delta\tau)$, where $\delta\tau$ is the pseudo-time step. (μ and $\delta\tau$ can be generalised to $\mu_i = 1/(\psi\delta\tau_i)$ and $\delta\tau_i$, respectively). Note also that most iterative methods are analogous to finding a steady state solution to a parabolic type PDE similar to (J.45) (Smolarkiewicz & Margolin 1994).

J.8 Lemmas and Algorithms

Finally, in this section some useful results and algorithms are presented.

J.8.1 Lemma

Let $\{p_0, p_1, ..., p_{m-1}\}$ *be a basis for the m-dimensional Krylov subspace* $K_m(R_0, A) = span\{R_0 = b - Ax_0, AR_0, A^2R_0, ..., A^{m-1}R_0\}$ *which is* A^TA*-orthogonal, i.e.* $\langle Ap_i, Ap_j\rangle = 0$, $\forall i \neq j$, *then the vector* x_m *which has the smallest residual norm in the affine space* $x_0 + K_m(R_0, A)$ *is given by:*

$$x_m = x_0 + \sum_{i=0}^{m-1} \frac{\langle R_0, Ap_i\rangle}{\langle Ap_i, Ap_i\rangle} p_i, \tag{J.46}$$

or recursively as

$$x_m = x_{m-1} + \frac{\langle R_{m-1}, Ap_{m-1}\rangle}{\langle Ap_{m-1}, Ap_{m-1}\rangle} p_{m-1}. \tag{J.47}$$

For details of the proof of the above lemma see page 184 of Saad (1996). The above lemma can be interpreted in simple terms as: given an initial vector x_0 on the surface $S(x_0, A)$ constructed by the sequence of the residual l_2-norms $\{||R_0 = b - Ax_0||\,,\ ||R_1 = b - Ax_1||\,, ...,\ ||R_i = b - Ax_i||\ , ...\}$, then the vector x_m that has the smallest Euclidean norm $||R_m||$ $= ||b - Ax_m||$ is given by (J.46). In other words x_m corresponds to the coordinates of the minima of the surface $S(x_0, A)$.

J.8.2 Gram-Schmidtalgorithm

The Gram-Schmidt algorithm is the process of generating an orthogonal set of vectors $\{b_1, ..., b_m\}$ from a given linearly independent set $\{v_1, ..., v_m\}$. It consists of series of rotations in the planes $\{v_1, ..., v_m\}$ until the resulting vectors are orthogonal. First $b_1 = v_1$, then take v_2 and add/subtract from it a multiple of b_1 such that the resulting vector is orthogonal to b_1 (i.e. mathematically $(b_2 = v_2 + hb_1) \perp b_1$ where h is such that $\langle b_1, b_2 \rangle = 0$). Then take v_3 and add/subtract a multiple of b_1 and b_2 so that the resulting vector $b_3 \perp b_2 \perp b_1$ (i.e. $b_3 = v_3 + h_1 b_1 + h_2 b_2$ where $\{h_1, h_2\}$ are chosen so $\langle b_1, b_3 \rangle = \langle b_2, b_3 \rangle = 0$). This process is continued in a similar fashion until the complete set is generated. The algorithm can be summarised as:

Algorithm 8: **Standard Gram-Schmidt(SGS)**

1- Choose $b_1 = v_1$

2- **Do** $i = 2, m$

3-   **Do** $j = 1, i-1$

4- $h_{ij} = -\langle v_i, b_j \rangle / \langle b_j, b_j \rangle$

5-   **EndDo**

6- $b_i = v_i + \sum_{j=1}^{i-1} h_{ij} b_j$

7- **EndDo**

In practice, the modified Gram-Schmidt algorithm, which is numerically more elegant, is more widely used:

Algorithm 9: **Modified Gram-Schmidt(MGS)**

1- Choose $b_1 = v_1$
2- **Do** $i = 2, m$
3- $b_i = v_i$
3- **Do** $j = 1, i-1$
4- $h_{ij} = -\langle b_i, b_j \rangle \, / \, \langle b_j, b_j \rangle$
6- $b_i \leftarrow b_i + h_{ij} b_j$
5- **EndDo**
7- **EndDo**

J.8.3 Arnoldi algorithm

The Arnoldi algorithm (Arnoldi 1951) is the process of generating or computing a set of m vectors $\{b_1, ..., b_m\}$ which forms a basis for the m-dimensional Krylov subspace $K_m(v_1, A)$ $= Span\{ \ v_1, Av_1, A^2v_1, ..., A^{m-2}v_1, A^{m-1}v_1\}$, which are A-orthogonal (or A-orthonormal, $\|b_i\|_2 = 1$). This algorithm is sometimes referred to as simply *Gram-Schmidt conjugation* because they are basically similar except that the given vectors are of Krylov sequences $v_i = Av_{i-1}, \ i = 1, m$. Similarly to SGS and MGS, an Arnoldi based SGS or MGS can be straightforwardly derived from the two previous algorithms. Here only the Arnoldi-MGS algorithm is given:

Algorithm 10: **Arnoldi Modified Gram-Schmidt**

1- Choose a vector $b_1 = v_1 / \|v_1\|$

2- **Do** $i = 2, m$

3- $\quad w_i = Av_{i-1}$

4- $\quad$ **Do** $j = 1, i-1$

5- $\qquad h_{ij} = -\langle w_i, b_j \rangle / \langle b_j, b_j \rangle$

6- $\qquad w_i \leftarrow w_i + h_{ij} b_j$

7- $\quad$ **EndDo**

8- $\quad b_i = w_i / \|w_i\|$(**If** $\|w_i\| = 0$ **Exit**)

9- **EndDo**

APPENDIX K

Stability and resonance analysis of the discretisation when applied to the shallow-water equations

K.1 Continuous equations

Consider the following linear constant-coefficient set of shallow-water equations:

$$\frac{Du}{Dt}+\frac{\partial\phi}{\partial x}-f_0v=-\frac{\partial\phi^s}{\partial x}, \tag{K.1}$$

$$\frac{Dv}{Dt}+f_0u=0, \tag{K.2}$$

$$\frac{D\phi}{Dt}+\Phi_0\frac{\partial u}{\partial x}=0, \tag{K.3}$$

where

$$\frac{D}{Dt}=\frac{\partial}{\partial t}+U_0\frac{\partial}{\partial x}, \tag{K.4}$$

f_0, U_0 and Φ_0 are all constant, and $u\left(x,t\right)$, $v\left(x,t\right)$ and $\phi\left(x,t\right)$ are small-amplitude perturbations about the basic state $\left(u=U_0\neq 0, v=0, \Phi=\Phi_0\right)$, and $\phi^s\left(x\right)/g$ is a small-amplitude perturbation to the basic-state orography. The basic state has uniform velocity $\left(U_0,0\right)$, with a linear (in y) bottom orographic slope to exactly balance f_0U_0 in the v- momentum equation, and constant fluid depth Φ_0/g.

K.2 Discretised momentum equations

Applying the discretisation of Section 6 to (K.1)- (K.2) gives the following discretisation of the horizontal components of the momentum equation:

$$\begin{aligned}\frac{u^{n+1}-u^n_d}{\Delta t}+\alpha_3\frac{\partial\phi^{n+1}}{\partial x}+\left(1-\alpha_3\right)\left(\frac{\partial\phi}{\partial x}\right)^n_d-\alpha_3f_0v^{n+1}-\left(1-\alpha_3\right)f_0v^n_d\\=-\alpha_3\left(\frac{\partial\phi^s}{\partial x}\right)^{n+1}-\left(1-\alpha_3\right)\left(\frac{\partial\phi^s}{\partial x}\right)^n_d,\end{aligned} \tag{K.5}$$

$$\frac{v^{n+1}-v^n_d}{\Delta t}+\alpha_3f_0u^{n+1}+\left(1-\alpha_3\right)f_0u^n_d=0. \tag{K.6}$$

K.3 Discretised continuity equation

Applying the discretisation of Section 8 to (K.3) gives the following the discretisation of the continuity equation

$$\frac{\phi^{n+1}-\phi^{n}}{\Delta t}+U_0\frac{\partial\phi^n}{\partial x}+\Phi_0\left[\alpha_1\frac{\partial u^{n+1}}{\partial x}+\left(1-\alpha_1\right)\frac{\partial u^n}{\partial x}\right]=0. \tag{K.7}$$

K.4 Decomposition of the solution into free and forced modes

The complete solution to the above linear system of discretised equations can be written as the sum of transient free modes and stationary orographically forced modes:

$$\begin{bmatrix}\phi\left(x,t\right)\\ v\left(x,t\right)\\ u\left(x,t\right)\end{bmatrix}=\begin{bmatrix}\phi^{free}\left(x,t\right)\\ v^{free}\left(x,t\right)\\ u^{free}\left(x,t\right)\end{bmatrix}+\begin{bmatrix}\phi^{forced}\left(x\right)\\ v^{forced}\left(x\right)\\ u^{forced}\left(x\right)\end{bmatrix}. \tag{K.8}$$

K.4.1 Transient free modes

The *free* solutions satisfy the discretised equations with the forcing $\phi^s\left(x\right)$ set identically to zero. Letting

$$\begin{bmatrix}\phi^{free}\left(x,t\right)\\ v^{free}\left(x,t\right)\\ u^{free}\left(x,t\right)\end{bmatrix}=\begin{bmatrix}\phi_k^{free}\\ v_k^{free}\\ u_k^{free}\end{bmatrix}e^{i(kx+\omega t)}, \tag{K.9}$$

each free mode (there are three for each wavenumber) then satisfies

$$\mathbf{A}\left(\omega\right)\begin{bmatrix}\phi_k^{free}\\ v_k^{free}\\ u_k^{free}\end{bmatrix}=0, \tag{K.10}$$

where

$$\mathbf{A}\left(\omega\right)=\begin{bmatrix}\Omega_{cty}\left(\omega\right) & 0 & ik\Phi_0\Gamma_{cty}\left(\omega\right)\\ 0 & \Omega_{mom}\left(\omega\right) & f_0\Gamma_{mom}\left(\omega\right)\\ ik\Gamma_{mom}\left(\omega\right) & -f_0\Gamma_{mom}\left(\omega\right) & \Omega_{mom}\left(\omega\right)\end{bmatrix}, \tag{K.11}$$

$$\Omega_{cty}\left(\omega\right)=\frac{\left(E-1\right)+ikU_0\Delta t}{\Delta t}, \tag{K.12}$$

$$\Omega_{mom}\left(\omega\right)=\frac{E-P}{\Delta t}, \tag{K.13}$$

$$\Gamma_{cty}\left(\omega\right)=\alpha_1E+\left(1-\alpha_1\right), \tag{K.14}$$

$$\Gamma_{mom}(\omega) = \alpha_3 E + (1-\alpha_3) P, \tag{K.15}$$

$$E(\omega) = \exp[i\omega\Delta t], P = \exp[-ikU_0\Delta t], \tag{K.16}$$

and "exact" interpolation has been assumed. This corresponds to expanding the dependent variables in a Fourier series and evaluating the series representation at upstream points. Although this would be prohibitively expensive in practice, it provides a convenient simplification for analysis purposes rather than adopting the more efficient polynomial interpolation which would lead to added complexity.

To obtain (K.11) the following relations have been used

$$\begin{aligned} \frac{\left(u^{free}\right)^{n+1} - \left(u^{free}\right)_d^n}{\Delta t} &= \frac{u^{free}(x, t^n + \Delta t) - u^{free}(x - U_0\Delta t, t^n)}{\Delta t} \\ &= \left(\frac{E-P}{\Delta t}\right) u_k^{free} e^{i(kx+\omega t^n)} = \Omega_{mom}(\omega)\, u_k^{free} e^{i(kx+\omega t^n)}, \end{aligned} \tag{K.17}$$

$$\begin{aligned} \alpha_3 r^{n+1} + (1-\alpha_3) r_d^n &= \alpha_3 \left.(r)\right|_{(x,t^n+\Delta t)} + (1-\alpha_3) \left.(r)\right|_{(x-U_0\Delta t, t^n)} \\ &= [\alpha_3 E + (1-\alpha_3) P]\, r_k e^{i(kx+\omega t^n)} = \Gamma_{mom}(\omega)\, r_k e^{i(kx+\omega t^n)}, \end{aligned} \tag{K.18}$$

$$\begin{aligned} \frac{\left(\phi^{free}\right)^{n+1} - \left(\phi^{free}\right)^n}{\Delta t} + U_0 \left(\frac{\partial \phi^{free}}{\partial x}\right)^n &= \frac{\phi^{free}(x, t^n + \Delta t) - \phi^{free}(x, t^n)}{\Delta t} + U_0 \frac{\partial \phi^{free}}{\partial x}(x, t^n) \\ &= \left[\frac{(E-1) + ikU_0\Delta t}{\Delta t}\right] \phi_k^{free} e^{i(kx+\omega t^n)} \\ &= \Omega_{cty}(\omega)\, \phi_k^{free} e^{i(kx+\omega t^n)}, \end{aligned} \tag{K.19}$$

$$\begin{aligned} \alpha_1 \left(\frac{\partial u^{free}}{\partial x}\right)^{n+1} + (1-\alpha_1)\left(\frac{\partial u^{free}}{\partial x}\right)^n &= \alpha_1 \left.\left(\frac{\partial u^{free}}{\partial x}\right)\right|_{(x,t^n+\Delta t)} + (1-\alpha_1) \left.\left(\frac{\partial u^{free}}{\partial x}\right)\right|_{(x,t^n)} \\ &= ik\left[\alpha_1 E + (1-\alpha_1)\right] u_k^{free} e^{i(kx+\omega t^n)} \\ &= ik\Gamma_{cty}(\omega)\, u_k^{free} e^{i(kx+\omega t^n)}, \end{aligned} \tag{K.20}$$

where r is $f_0 u^{free}$, $f_0 v^{free}$ or $\partial\phi^{free}/\partial x$.

Setting

$$\det[\mathbf{A}(\omega)] = 0, \tag{K.21}$$

the condition for non-trivial solutions $\left(\phi_k^{free}, v_k^{free}, u_k^{free}\right)$ to exist, then gives the dispersion relation for ω.

The exact solution for the free modes of the linearised equations (with no discretisation) can be obtained by substituting (K.9) into the continuous equations (K.1) - (K.3) to obtain

$$\begin{aligned} \omega_{exact} &= -kU_0, & (Rossby) \\ &= -kU_0 \pm k\sqrt{\Phi_0 + f_0^2/k^2}. & (gravity) \end{aligned} \tag{K.22}$$

By taking the limit $\Delta t \to 0$, (K.12)-(K.15) may be replaced by the definitions

$$\Omega_{exact}(\omega) = i(\omega + kU_0), \tag{K.23}$$

$$\Gamma_{exact}(\omega) = 1, \tag{K.24}$$

and the (free) Rossby and gravity-wave dispersion relations (K.22) then result from (K.21), This demonstrates that the solution of the discrete dispersion relation (reassuringly) converges to the exact one as $\Delta t \to 0$.

K.4.2 Stationary orographically forced modes

The *force*d (steady-state) solutions satisfy the discretised equations in the absence of any time variation ($\partial/\partial t \equiv 0$), and may be Fourier decomposed as

$$\begin{bmatrix} \phi^{forced}(x) \\ v^{forced}(x) \\ u^{forced}(x) \end{bmatrix} = \begin{bmatrix} \phi_k^{forced} \\ v_k^{forced} \\ u_k^{forced} \end{bmatrix} e^{ikx}. \tag{K.25}$$

They then satisfy

$$\mathbf{A}(\omega \equiv 0) \begin{bmatrix} \phi_k^{forced} \\ v_k^{forced} \\ u_k^{forced} \end{bmatrix} = \begin{bmatrix} 0 \\ 0 \\ -ik\Gamma_{mom}(\omega = 0)\,\phi_k^s \end{bmatrix}, \tag{K.26}$$

where $\phi^s(x)$ has also been Fourier decomposed. Note that for the *exact* solution for the forced modes of the linearised equations (with no discretisation), $\mathbf{A}(\omega \equiv 0)$ simplifies to

$$\mathbf{A}_{exact}(\omega \equiv 0) = \begin{bmatrix} ikU_0 & 0 & ik\Phi_0 \\ 0 & ikU_0 & f_0 \\ ik & -f_0 & ikU_0 \end{bmatrix}. \tag{K.27}$$

When the determinant of $\mathbf{A}_{exact}(\omega \equiv 0)$ vanishes, i.e. when

$$U_0 = \pm\sqrt{\Phi_0 + \frac{f_0^2}{k^2}}, \tag{K.28}$$

(K.26) becomes singular in the presence of non-zero orographic forcing.

Since the inverse of $\mathbf{A}_{exact}(\omega \equiv 0)$ no longer exists when (K.28) is satisfied, nor does a steady-state solution exist of the form (K.25), and the above-described solution procedure for the forced component of the flow breaks down. It can however be shown (e.g. via a singular eigenfunction analysis and decomposition) that the forced solution grows linearly as a function of time. Thus *physical* resonance occurs whenever the parameters U_0, Φ_0, f_0 and k are such that (K.28) holds. It is undesirable for a numerical scheme to give rise to spurious *computational* resonance for values of the parameters for which physical resonance does not occur.

K.4.3 Determination of computational stability and resonance properties

A scheme's *computational stability* is determined from the solutions of the dispersion relation (K.21), i.e. by solving $\det[\mathbf{A}(\omega)] = 0$ for ω and ensuring $|\exp[(i\omega\Delta t)]| \leq 1$, whereas the existence or not of *spurious computational resonance* is determined from $\det[\mathbf{A}(\omega = 0)] = 0$, leading to a constraint on the parameters U_0 and Φ_0 for resonance to occur. Note that the matrix $\mathbf{A}$ defined by (K.11) plays a determining role for both, and both are respectively discussed in the following two sub-sections.

K.5 Analysis of computational stability

K.5.1 Numerical dispersion relation

Solving (K.21) gives the numerical dispersion relation

$$\begin{aligned}[t] &[(E-1) + ikU_0\Delta t]\left\{(E-P)^2 + (f_0\Delta t)^2[\alpha_3 E + (1-\alpha_3)P]^2\right\} \\ &\quad + k^2\Phi_0\Delta t^2(E-P)[\alpha_1 E + (1-\alpha_1)][\alpha_3 E + (1-\alpha_3)P] = 0, \end{aligned} \tag{K.29}$$

which may be written more succinctly as

$$\begin{aligned}[t] &[(E-1) + iC']\left\{(E-P)^2 + F^2[\alpha_3 E + (1-\alpha_3)P]^2\right\} \\ &\quad + G'^2(E-P)[\alpha_1 E + (1-\alpha_1)][\alpha_3 E + (1-\alpha_3)P] = 0, \end{aligned} \tag{K.30}$$

where

$$C' = kU_0\Delta t,\ F = f_0\Delta t,\ G'^2 = k^2\Phi_0\Delta t^2. \tag{K.31}$$

This is a very messy expression which would, in general, need to be solved numerically, as in Section 17, and the parameter space explored. We can however gain some useful insight by using various inequalities to obtain a condition that guarantees instability will occur for the general case, and also by examining the dispersion relation for the special case of non-divergent flow.

K.5.2 Instability for the general case

Let us rewrite (K.30) in the form

$$a_3 E^3 + a_2 E^2 + a_1 E + a_0 = 0, \tag{K.32}$$

where

$$a_3 = \left(1 + \alpha_1 \alpha_3 G'^2 + \alpha_3^2 F^2\right), \tag{K.33}$$

$$a_0 = P^2 \left\{ - \left[1 + (1-\alpha_1)(1-\alpha_3) G'^2 + (1-\alpha_3)^2 F^2\right] + iC' \left[1 + (1-\alpha_3)^2 F^2\right]\right\}. \tag{K.34}$$

Eq. (K.32) may be rewritten as

$$E^3 + \frac{a_2}{a_3} E^2 + \frac{a_1}{a_3} E + \frac{a_0}{a_3} = 0. \tag{K.35}$$

Letting E_1, E_2, E_3 be the three roots of (K.35), we have

$$(E - E_1)(E - E_2)(E - E_3) = 0, \tag{K.36}$$

$$E_1 E_2 E_3 = -\frac{a_0}{a_3}. \tag{K.37}$$

Thus

$$|E_1|\,|E_2|\,|E_3| = \frac{|a_0|}{|a_3|}. \tag{K.38}$$

So instability is guaranteed whenever

$$|a_0| > |a_3|, \tag{K.39}$$

since for (K.39) to hold, at least one of the roots must exceed unity in magnitude and therefore be unstable. The converse however is not true: i.e. $|a_0| < |a_3|$ does not guarantee stability since one of the roots could still exceed unity in magnitude without the product of the three roots doing so.

With this preparation we are now ready to examine the stability/ instability of the discretisation. Plugging (K.33) - (K.34) into (K.39) tells us that instability will occur whenever

$$\left[1 + (1-\alpha_1)(1-\alpha_3)\, G'^2 + (1-\alpha_3)^2 F^2\right]^2 + C'^2 \left[1 + (1-\alpha_3)^2 F^2\right]^2$$
$$> \left(1 + \alpha_1\alpha_3 G'^2 + \alpha_3^2 F^2\right)^2 . \qquad \text{(K.40)}$$

Assuming that we constrain the time weightings such that $1/2 \le \alpha \le 1$, i.e. somewhere between the two limiting cases of Crank-Nicolson and backward implicit, then $\alpha_1 = \alpha_3 = 1$ simultaneously minimises the left-hand side of (K.40) while maximising the right-hand side. The backward-implicit weightings represents the best one can do by varying the weighting parameters within the given range to enhance stability. So if (K.40) with backward-implicit weightings is still satisfied, then the discretisation is guaranteed to be unstable for *any* choice of weighting parameters in the interval $1/2 \le \alpha \le 1$.

K.5.3 Instability for Crank-Nicolson weightings ($\alpha_1 = \alpha_3 = 1/2$)

From (K.40) instability is guaranteed for Crank-Nicolson weightings if

$$C'^2 > 0, \qquad \text{(K.41)}$$

i.e. *the scheme is unconditionally unstable with Crank-Nicolson weightings.* This is really not a good thing.

K.5.4 Instability for backward-implicit weightings ($\alpha_1 = \alpha_3 = 1$)

From (K.40) instability is guaranteed for backward-implicit weightings if

$$C'^2 + 1 > \left(1 + G'^2 + F^2\right)^2 . \qquad \text{(K.42)}$$

This will certainly be so if

$$|C'| > 1 + G'^2 + F^2, \qquad \text{(K.43)}$$

i.e. if

$$|kU_0\Delta t| > 1 + k^2\Phi_0\Delta t^2 + f_0^2\Delta t^2. \qquad \text{(K.44)}$$

Thus instability is guaranteed for backward-implicit weightings for large enough Courant number and small enough equivalent depth (Φ_0/g). For the external mode the values of the parameters ($\sqrt{\Phi_0} \sim 320\,\mathrm{ms}^{-1}$, $U_0 \sim 120\,\mathrm{ms}^{-1}$, $f_0 \sim 10^{-4}\,\mathrm{s}^{-1}$, $\Delta t \sim 10^3\,\mathrm{s}$) are such that

(K.44) is not satisfied. However, and as confirmed by the analysis of Section 17, instability is possible for higher-order internal modes - these have decreasingly- small equivalent depth as a function of increasing vertical wave number.

K.5.5 Instability for non-divergent flow

For the special case of non-divergent flow, for which $G' = 0$, the dispersion relation (K.30) reduces to

$$[(E-1)+iC']\left\{(E-P)^2+F^2\left[\alpha_3 E+(1-\alpha_3)P\right]^2\right\}=0. \tag{K.45}$$

The first root is

$$E = 1 - iC', \tag{K.46}$$

and $|E| > 1$. This means that the scheme is *unconditionally unstable for non-divergent flow.*

K.5.6 Damping of the solution by a backward-implicit scheme ($\alpha_1 = \alpha_3 = 1$)

To illustrate and quantify the damping of a backward-implicit scheme (where $\alpha_1 = \alpha_3 = 1$) set $U_0 = 0$. The dispersion relation (K.30) then reduces to

$$(E-1)\left[(E-1)^2+\left(G'^2+F^2\right)E^2\right]=0. \tag{K.47}$$

This has solutions

$$E = 1,\ \frac{1}{1 \pm i\sqrt{G'^2+F^2}}, \tag{K.48}$$

and

$$|E| = 1,\ \frac{1}{\sqrt{1+G'^2+F^2}}, \tag{K.49}$$

i.e.

$$E = 1,\ \frac{1}{1 \pm i\sqrt{(k^2\Phi_0+f_0^2)}\Delta t}, \tag{K.50}$$

and

$$|E| = 1,\ \frac{1}{\sqrt{1+(k^2\Phi_0+f_0^2)\,\Delta t^2}}. \tag{K.51}$$

The slow solution is thus neutrally stable (setting $U_0 = 0$ removes the advective instability examined above). However the gravity modes are heavily damped. This is particularly so for external gravity modes (because of the large equivalent depth) in polar regions (because the convergence of the meridians makes $\Delta\lambda$ very small and consequently G' very large).

This means that a backward-implicit treatment of the gravity-wave terms acts to (at least partially) control the instability of the forward Euler treatment of advection in the continuity equation. This damping mechanism is particularly effective for the external mode, but is inefficient for the high-order internal modes.

K.5.7 Incorporating the effects of spatial discretisation of derivatives into the analysis

The above analysis can be refined to include the effect of the spatial discretisation, by simply redefining C', F and G'^2 to be

$$C' = \left(\frac{\sin k\Delta x}{\Delta x}\right) U_0 \Delta t,\ F = \left(\cos \frac{k\Delta x}{2}\right) f_0 \Delta t,\ G'^2 = \left[\frac{\sin\left(k\Delta x/2\right)}{\Delta x/2}\right]^2 \Phi_0 \Delta t^2. \tag{K.52}$$

The condition (K.44) that guarantees instability for backward-implicit weightings then becomes

$$\left|\frac{U_0 \Delta t}{\Delta x} \sin\left(k\Delta x\right)\right| > 1 + 4\Phi_0 \frac{\Delta t^2}{\Delta x^2} \sin^2\left(\frac{k\Delta x}{2}\right) + \left(f_0 \Delta t\right)^2 \cos^2\left(\frac{k\Delta x}{2}\right). \tag{K.53}$$

This only modifies the analysis and conclusions in a minor way.

K.5.8 Summary of the stability analysis

Based on the above analysis, we might expect that a shallow-water model run with a large equivalent depth (e.g. 5-10 kms), and with a forward Euler treatment of advection in the continuity equation but a backward-implicit treatment of non-advective terms, would be computationally stable. However the same model but with a Crank-Nicolson treatment of non-advective terms, would be unstable. Ditto if run at small enough equivalent depth with a forward Euler treatment of advection in the continuity equation but a backward-implicit treatment of non-advective terms. Instability, when it occurs, is enhanced by large windspeed, large timestep, small meshlength (i.e. around the poles), and small equivalent depth (i.e. high vertical resolution).

K.5.9 Discussion of the analysed instability

The diagnosed instability can be expected to be particularly severe in polar regions where $\Delta\lambda$ is very small and the local Courant number is consequently very large, and at high vertical resolution (e.g. for stratospheric studies). It could conceivably contribute to convergence problems of the elliptic-boundary-value solver near the poles and the need for latitudinal filtering.

The source of the instability is the replacement of Φ^{n+1} by Φ^n in the time level $n+1$ flux term $\alpha_1 \partial \left(\Phi^{n+1} U^{n+1}\right) / \partial x$ of the continuity equation

$$\frac{\Phi^{n+1} - \Phi^n}{\Delta t} + \alpha_1 \frac{\partial}{\partial x} \left(\Phi^{n+1} U^{n+1}\right) + (1 - \alpha_1) \frac{\partial}{\partial x} \left(\Phi^n U^n\right) = 0, \tag{K.54}$$

where

$$U = U_0 + u, \ \Phi = \Phi_0 + \phi. \tag{K.55}$$

This is motivated by the laudable desire to avoid products of (unknown) time level $n+1$ quantities, but it unfortunately leads to a forward Euler treatment of both horizontal and vertical advection. This, as noted above, is particularly serious for horizontal advection in polar regions, but also for the jets.

The motivation for writing the continuity equation in Eulerian flux form is that doing so guarantees mass conservation, an important consideration for climate integrations. This suggests that one might wish to keep the Eulerian flux form of the equations, but find a way to handle the flux term $\alpha_1 \partial \left(\Phi^{n+1} U^{n+1}\right) / \partial x$ without replacing Φ^{n+1} by Φ^n, which would then yield a stable scheme. This could probably (with some effort!) be done but is likely to have some undesirable side effects. With the discretisation as written, it would result in horizontal advection along a polar latitude circle being spuriously and dramatically slowed down to no more than one E-W meshlength per timestep. It would also probably still create noise in polar regions and result in the need for filters to be devised and tuned, something best avoided if possible. Even if this were done, it would still result in a discretisation of advection in the continuity equation which would be inconsistent with the semi-Lagrangian discretisation of advection elsewhere, another undesirable side effect.

The above suggests that it would probably be best to discretise the continuity equation in the usual semi-Lagrangian way as other centres do for their semi-implicit semi-Lagrangian models. The downside of this approach is that mass would no longer be formally conserved. Note here though that most, and possibly all, spectral Eulerian GCM's do not formally conserve mass either (because the continuity equation is usually written in logarithmic form, and the logarithm of mass is not a conserved quantity of the governing equations). To address this conservation concern, several alternatives (there may be others) come to mind. The simplest of these is the "mass fix" approach (as e.g. used in the NCAR GCM), whereby every timestep, or every several timesteps, the mass deficiency is computed and added back with a uniform distribution. The second is the ad hoc Priestley conservation procedure, which couples conservation with monotonicity. A third way forward, and arguably the most promising, is the Purser and Leslie conservation approach based on cascade interpolation.

K.6 Analysis of computational resonance

For the discretised linear equations, whenever

$$\det\left[\mathbf{A}\left(\omega\equiv 0\right)\right]=0, \tag{K.56}$$

the stationary forced gravity modes determined by (K.26) are resonant and, as discussed above, these resonances may be a spurious artifact of discretisation. Here

$$\mathbf{A}\left(\omega\equiv 0\right)=\begin{bmatrix}\Omega_{cty}\left(\omega\equiv 0\right) & 0 & ik\Phi_0\Gamma_{cty}\left(\omega\equiv 0\right)\\ 0 & \Omega_{mom}\left(\omega\equiv 0\right) & f_0\Gamma_{mom}\left(\omega\equiv 0\right)\\ ik\Gamma_{mom}\left(\omega\equiv 0\right) & -f_0\Gamma_{mom}\left(\omega\equiv 0\right) & \Omega_{mom}\left(\omega\equiv 0\right)\end{bmatrix}, \tag{K.57}$$

where

$$\Omega_{cty}\left(\omega\equiv 0\right)=ikU_0, \tag{K.58}$$

$$\Omega_{mom}\left(\omega\equiv 0\right)=\frac{1-P}{\Delta t}, \tag{K.59}$$

$$\Gamma_{cty}\left(\omega\equiv 0\right)=1, \tag{K.60}$$

$$\Gamma_{mom}\left(\omega\equiv 0\right)=\alpha_3+\left(1-\alpha_3\right)P, \tag{K.61}$$

$$P=\exp\left[-ikU_0\Delta t\right], \tag{K.62}$$

Solution of (K.56) then leads to a quadratic equation, with complex coefficients, for $P\equiv\exp\left[-ikU_0\Delta t\right]$. Since $kU_0\Delta t$ is real, resonance is only possible for values P_{res} satisfying (K.56) and they must lie on the unit circle. Explicitly, this quadratic is

$$C'\left(1-P_{res}\right)^2+CF^2\left[\alpha_3+\left(1-\alpha_3\right)P_{res}\right]^2-iG'^2\left(1-P_{res}\right)\left[\alpha_3+\left(1-\alpha_3\right)P_{res}\right]=0, \tag{K.63}$$

where

$$C'=kU_0\Delta t,\ F=f_0\Delta t,\ G'^2=k^2\Phi_0\Delta t^2. \tag{K.64}$$

This is a very messy expression. Before tackling it in its full glory we can however gain some useful insight by examining the special case $f_0 = 0$ $(\Rightarrow F = 0)$.

Aside :

The reason (K.63) *is a quadratic in* P_{res}*, rather than the cubic it would be if one were to discretise the continuity equation in the usual semi-implicit semi-Lagrangian manner, is because the Eulerian treatment of the continuity equation no longer averages the horizontal divergence along the trajectory, thereby eliminating the appearance of the response function* P *in the continuity equation.*

K.6.1 The special case $f_0 = 0$ $(\Rightarrow F = 0)$

For this special case, (K.63) has solutions

$$P_{res} = 1, \tag{K.65}$$

$$P_{res} = \frac{C' - i\alpha_3 G'^2}{C' + i\left(1-\alpha_3\right) G'^2}. \tag{K.66}$$

The first root corresponds to the decoupled Rossby mode, which satisfies $v^{n+1} - v^n_d = (E - P)\, v^n = 0$, and it cannot resonate since it is completely decoupled from the orographic forcing.

Aside :

Note that setting $f_0 \neq 0$ *reintroduces the coupling between* v *and the other two dependent variables (see following two subsections), and the first mode then does become a candidate for resonance.*

The second root has magnitude

$$\left|P_{res}\right|^2 = \frac{C'^2 + G'^4\alpha_3^2}{C'^2 + G'^4\left(1-\alpha_3\right)^2}, \tag{K.67}$$

and for non-zero values of G', this is equal to unity (i.e. P_{res} lies on the unit circle) if and only if $\alpha_3 = 1/2$.

Thus when $f_0 = 0$, resonance can only occur if $\alpha_3 = 1/2$, and off-centering the time scheme (i.e. setting $\alpha_3 \neq 1/2$) eliminates spurious semi-Lagrangian resonance.

Now we know that resonance can only occur if $\alpha_3 = 1/2$, the question is, what further circumstance does it take to make it actually happen? This is determined from the phase of

P (the amplitude determines whether P is on the unit circle, the first of the two necessary conditions that must be met for resonance to occur). Substituting the definitions (K.62) and (K.64) into (K.66) with $\alpha_3 = 1/2$ yields the transcendental equation

$$e^{-iC'} = \frac{C' - i\frac{G'^2}{2}}{C' + i\frac{G'^2}{2}} = \frac{C'^2 - \frac{G'^4}{4} - iC'G'^2}{C'^2 + \frac{G'^4}{4}}, \tag{K.68}$$

and thus leads to the condition

$$\tan\left(\frac{C'}{2}\right) \equiv \frac{1 - \cos C'}{\sin C'} = \frac{G'^2}{2C'}. \tag{K.69}$$

It is convenient to rewrite condition (K.69) as

$$\tan\left(\frac{KC}{2}\right) = \frac{KG^2}{2C} = \frac{\Phi_0}{U_0^2}\left(\frac{KC}{2}\right), \tag{K.70}$$

where

$$C' \equiv KC,\ G'^2 \equiv K^2G^2,\ K \equiv k\Delta x,\ C \equiv \frac{U_0\Delta t}{\Delta x},\ G^2 \equiv \Phi_0\left(\frac{\Delta t}{\Delta x}\right)^2, \tag{K.71}$$

in order to separate out its dependence on waveumber whilst still writing it in terms of non-dimensional quantities.

Taking the limit $\Delta t \to 0$ in (K.70) reassuringly converges to the continuous result (K.28) (with f_0 set to zero) for physical resonance to occur. Condition (K.70) can also be compared, when f_0 is set to zero, with condition (10) of Rivest et al. (1994), viz. with

$$\tan\left(\frac{KC}{2}\right) = \pm\frac{KG}{2} = \pm\frac{\sqrt{\Phi_0}}{U_0}\left(\frac{KC}{2}\right), \tag{K.72}$$

which corresponds to a *semi-Lagrangian*, rather than Eulerian, discretisation of the continuity equation. There are two points to note here. First, the minus sign of (K.72) is absent in (K.70). This is because the Eulerian discretisation of the continuity equation filters out the appearance of the response P from the analogues of (K.58) and (K.60), thereby reducing the order of the polynomial resonance condition for P_{res} by one. Second, condition (K.70) herein corresponds to multiplying the right-hand side of (10) of Rivest et al. (1994) (i.e. of (K.72)), with the positive sign, by the inverse Froude number $G/C \equiv \sqrt{\Phi_0}/U_0$.

Setting $\Phi_0 = 5.5 \times 10^4 m^2 s^{-2}$ and $U_0 = 50 ms^{-1}$, as in Rivest et al. (1994) and which gives an inverse Froude number $G/C \equiv \sqrt{\Phi_0}/U_0 \approx 4.6$, the left and right-hand sides of (K.70) are plotted in Fig. K.1 as functions of the composite parameter $KC/2$, and the intersection of

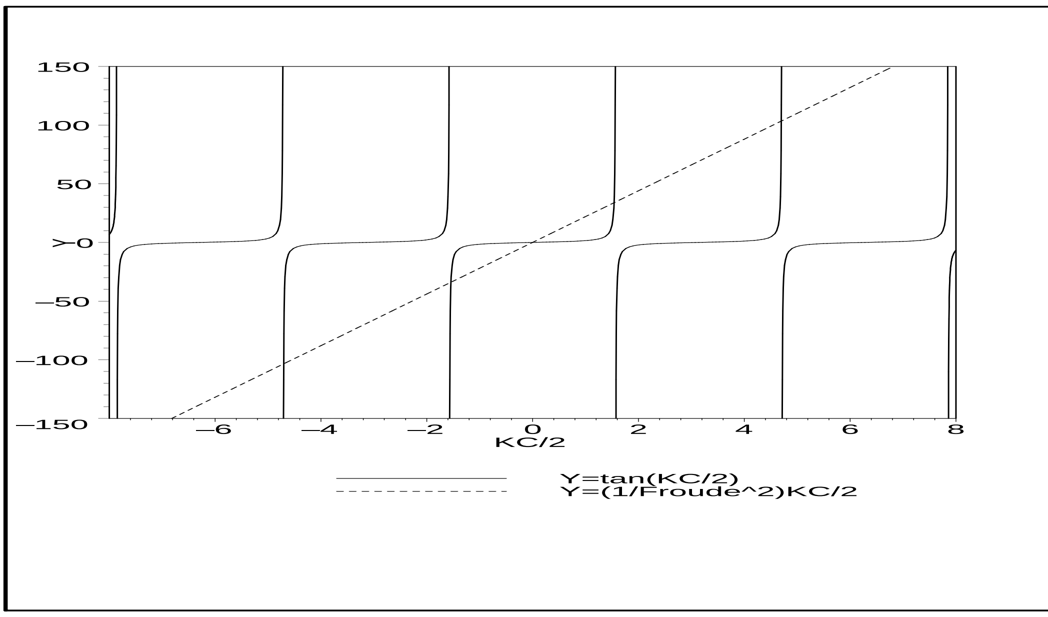

Figure K.1: The left- and right- hand sides of eq. (K.70) plotted as a function of the composite parameter $KC/2$, where C is the Courant number, $K \equiv k\Delta x$ is nondimensional wavenumber, and the values of the parameters are $U_0 = 50ms^{-1}$ and $\Phi_0 = 5.5 \times 10^4 m^2 s^{-2}$. Resonance occurs at the points of intersection of these curves.

curves are therefore the solutions to (K.70). This may be compared with the corresponding plots for the left and right-hand sides of (K.72) displayed in Fig. K.2 for the semi-Lagrangian discretisation of the continuity equation examined in Rivest et al. (1994). It is found that:

- whilst the semi-Lagrangian discretisation of the continuity equation gives rise to pairs of resonance of almost equal value of $KC/2$, one of the two solution sets is filtered out by the Eulerian discretisation;
- noting that the maximum attainable value of $K \equiv k\Delta x$ is π, associated with the smallest-resolvable space scale, it is possible for both discretisations of the continuity equation to avoid resonance by using a sufficiently small value (approximately less than unity) of the Courant number C, i.e. by using a sufficiently small timestep; and
- a slightly larger value of the composite parameter $KC/2$ may be used without encountering resonance when using an Eulerian discretisation of the continuity equation instead of a semi-Lagrangian one.

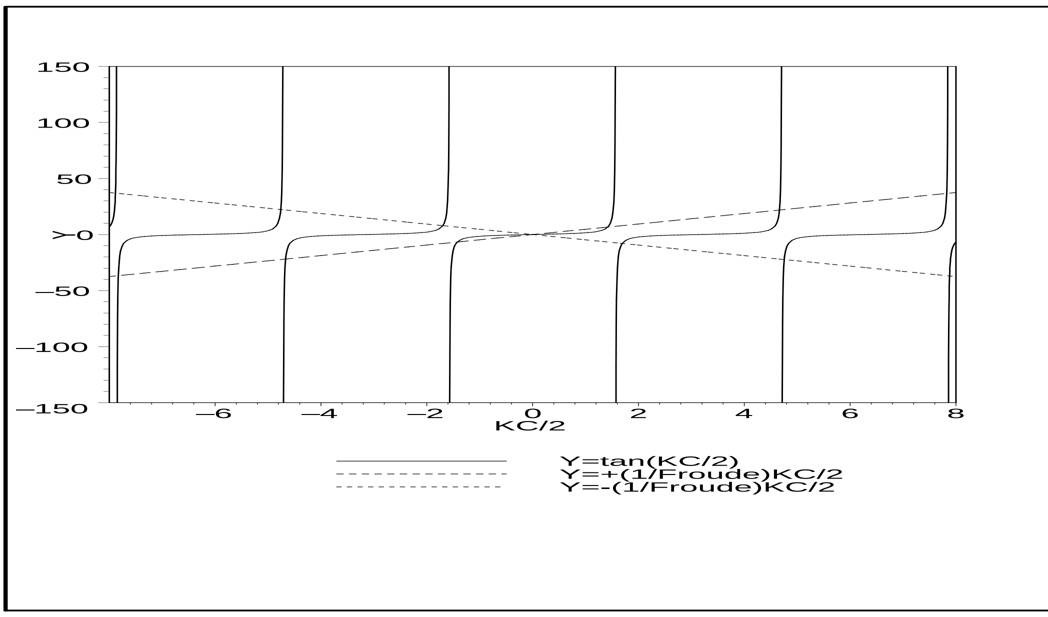

Figure K.2: The left- and right- hand sides of eq. (K.72) plotted as a function of the composite parameter $KC/2$, where C is the Courant number, $K \equiv k\Delta x$ is nondimensional wavenumber, and the values of the parameters are $U_0 = 50ms^{-1}$ and $\Phi_0 = 5.5 \times 10^4 m^2 s^{-2}$. Resonance occurs at the points of intersection of these curves.

Curves of resonance for C (Courant number) vs. K (nondimensional wavenumber) are displayed in Fig. K.3 using the same values for the parameters Φ_0 and U_0 given above and used in Rivest et al. (1994). The corresponding figure for a semi-Lagrangian discretisation of the continuity equation, again with f_0 set to zero, is Fig. K.4.

Summarising the above analysis, where $f_0 = 0$:

- *resonance can only occur if $\alpha_3 = 1/2$ and then only for values of the parameters C and G that satisfy* (K.70)*,*
- *it can be avoided at the (possibly-substantial) cost of choosing a sufficiently small timestep such that C is less than unity; and*
- *off-centering the time scheme (i.e. setting $\alpha_3 \neq 1/2$) is a more efficient way of eliminating spurious semi-Lagrangian resonance.*

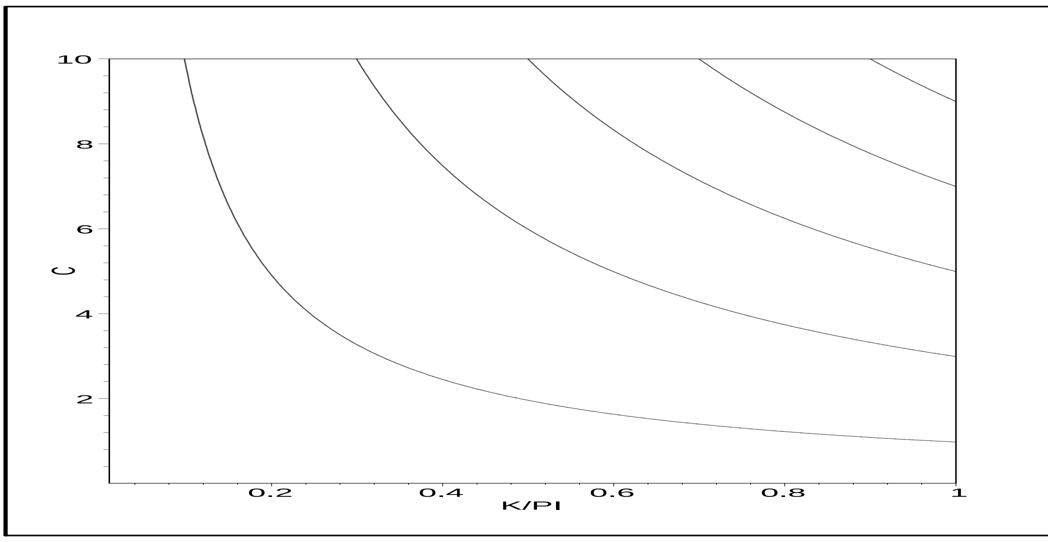

Figure K.3: Curves of resonances of eq. (K.70) as a function of Courant number C and of nondimensional wavenumber K. The values of the parameters are $U_0 = 50ms^{-1}$ and $\Phi_0 = 5.5 \times 10^4 m^2 s^{-2}$.

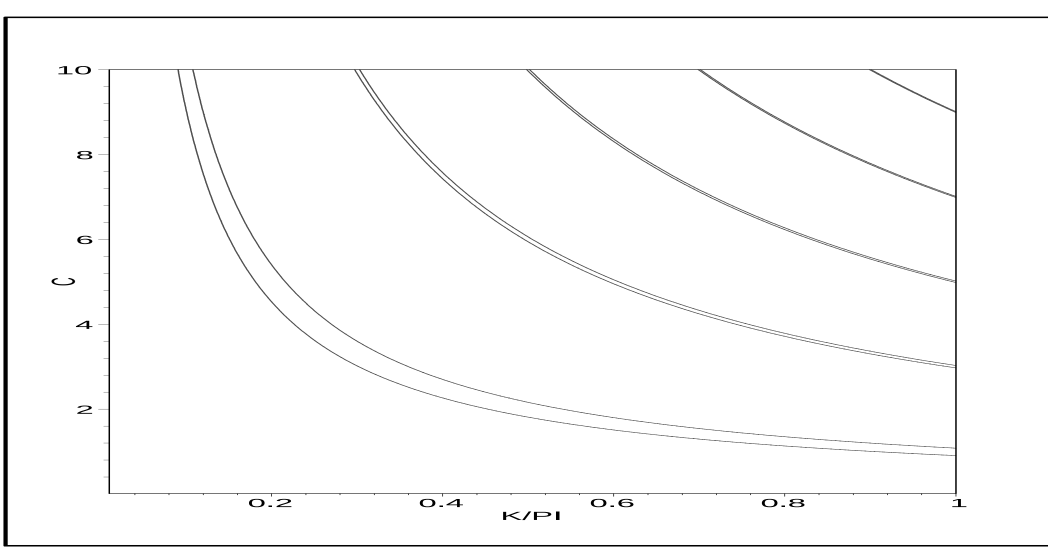

Figure K.4: Curves of resonances of eq. (K.72) as a function of Courant number C and of nondimensional wavenumber K. The values of the parameters are $U_0 = 50ms^{-1}$ and $\Phi_0 = 5.5 \times 10^4 m^2 s^{-2}$.

K.6.2 Return to the general case $f_0 \neq 0$ ($\Rightarrow F \neq 0$)

Returning now to the general case of $F \neq 0$, (K.63) implies that

$$\begin{aligned} \left\{C'\left[\left(1+(1-\alpha_3)^2 F^2\right)\right] + i\,(1-\alpha_3)\,G'^2\right\} P_{res}^2 \\ -\left\{2C'\left[1-\alpha_3\,(1-\alpha_3)\,F^2\right] + i\,(1-2\alpha_3)\,G'^2\right\} P_{res} \\ +\left[C'\left(1+\alpha_3^2 F^2\right) - i\alpha_3 G'^2\right] &= 0. \end{aligned} \tag{K.73}$$

For resonance to occur, from the definitions (K.62) and (K.64) at least one of the solutions of (K.73) must be of the form $P_{res} = \cos C' - i \sin C'$, where $C' \equiv kU_0 \Delta t$ is real, and so $P_{res} P_{res}^* = 1$ where P_{res}^* is the complex conjugate of P_{res}. Therefore, a resonant solution of (K.73) must also satisfy

$$\begin{aligned} \left\{C'\left[\left(1+(1-\alpha_3)^2 F^2\right)\right] + i\,(1-\alpha_3)\,G'^2\right\} P_{res} \\ -\left\{2C'\left[1-\alpha_3\,(1-\alpha_3)\,F^2\right] + i\,(1-2\alpha_3)\,G'^2\right\} \\ +\left[C'\left(1+F^2\alpha_3^2\right) - iG'^2\alpha_3\right] P_{res}^* &= 0, \end{aligned} \tag{K.74}$$

- this is obtained by multiplying (K.73) by P_{res}^* and setting $P_{res} P_{res}^* = 1$. Requiring both the real and imaginary components of this equation to vanish gives two linear simultaneous equations for the real and imaginary parts of $P_{res} \equiv P_{res}^R + iP_{res}^I$, viz.

$$C'\left\{2 + \left[\alpha_3^2 + (1-\alpha_3)^2\right] F^2\right\} P_{res}^R - G'^2 P_{res}^I - 2C'\left[1-\alpha_3\,(1-\alpha_3)\,F^2\right] = 0, \tag{K.75}$$

$$(1-2\alpha_3)\left(G'^2 P_{res}^R + C' F^2 P_{res}^I - G'^2\right) = 0. \tag{K.76}$$

Eq. (K.76) can be satisfied in one of two ways, depending upon whether $\alpha_3 = 1/2$ or not, so these two cases are examined in turn.

K.6.3 The case $\alpha_3 = 1/2$

Setting $\alpha_3 = 1/2$ in (K.73) gives

$$\left[C'\left(1+\frac{F^2}{4}\right) + i\frac{G'^2}{2}\right] P_{res}^2 - 2C'\left(1-\frac{F^2}{4}\right) P_{res} + \left[C'\left(1+\frac{F^2}{4}\right) - i\frac{G'^2}{2}\right] = 0, \tag{K.77}$$

so that

$$P_{res} \equiv e^{-iC'} = \frac{C'\left(1-\frac{F^2}{4}\right) \pm i\sqrt{C'^2 F^2 + \frac{G'^4}{4}}}{\left[C'\left(1+\frac{F^2}{4}\right) + i\frac{G'^2}{2}\right]}, \tag{K.78}$$

and therefore

$$|P_{res}|^2 = \frac{C'^2\left(1-\frac{F^2}{4}\right)^2 + C'^2F^2 + \frac{G'^4}{4}}{C'^2\left(1+\frac{F^2}{4}\right)^2 + \frac{G'^4}{4}} = 1. \tag{K.79}$$

So for $\alpha_3 = 1/2$ resonance can only occur for values of C', F and G' that satisfy the transcendental equation

$$e^{-iC'} = \frac{C'\left(1-\frac{F^2}{4}\right) \pm i\sqrt{C'^2F^2 + \frac{G'^4}{4}}}{\left[C'\left(1+\frac{F^2}{4}\right) + i\frac{G'^2}{2}\right]}, \tag{K.80}$$

where C', F and G' are defined by (K.64), and this leads to the condition

$$\tan\left(\frac{C'}{2}\right) \equiv \frac{1-\cos C'}{\sin C'} = \frac{C'^2\frac{F^2}{2}\left(1+\frac{F^2}{4}\right) + \frac{G'^4}{4} \mp \frac{G'^2}{2}\sqrt{C'^2F^2 + \frac{G'^4}{4}}}{C'\left[\left(1-\frac{F^2}{4}\right)\frac{G'^2}{2} \mp \left(1+\frac{F^2}{4}\right)\sqrt{C'^2F^2 + \frac{G'^4}{4}}\right]}. \tag{K.81}$$

Rewriting this as

$$\tan\left(\frac{C'}{2}\right) = \frac{\frac{F^2}{2}\left(1+\frac{F^2}{4}\right) + \frac{G'^4}{4C'^2} \mp \frac{G'^2}{2C'}\sqrt{F^2 + \frac{G'^4}{4C'^2}}}{\left(1-\frac{F^2}{4}\right)\frac{G'^2}{2C'} \mp \left(1+\frac{F^2}{4}\right)\sqrt{F^2 + \frac{G'^4}{4C'^2}}}, \tag{K.82}$$

and then multiplying by $\left(1-\frac{F^2}{4}\right)\frac{G'^2}{2C'} \pm \left(1+\frac{F^2}{4}\right)\sqrt{F^2 + \frac{G'^4}{4C'^2}}$ yields

$$\tan\left(\frac{C'}{2}\right) = \frac{1}{2}\left(\frac{G'^2}{2C'} \mp \sqrt{F^2 + \frac{G'^4}{4C'^2}}\right). \tag{K.83}$$

Using the definitions (K.71) and $F \equiv f_0\Delta t$, it is convenient to further rewrite this as

$$\tan\left(\frac{KC}{2}\right) = \frac{1}{2}\left[\left(\frac{\Phi_0}{U_0^2}\right)\left(\frac{KC}{2}\right) \mp \sqrt{\left(\frac{f_0\Delta x}{U_0}\right)^2 C^2 + \left(\frac{\Phi_0}{U_0^2}\right)^2\left(\frac{KC}{2}\right)^2}\right]. \tag{K.84}$$

Taking the limit $\Delta t \to 0$ in (K.84) reassuringly converges to the continuous result (K.28) for physical resonance to occur: by instead taking the limit $f_0 \to 0$, it leads to agreement with the results given in Section K.6.1. Contrary to the result found in Section K.6.1 when $f_0 \equiv 0$, there are now two families of resonances (one for each of the signs in (K.84)) which is also true for a semi-Lagrangian discretisation of the continuity equation. Condition (K.84) can also be compared with condition (10) of Rivest et al. (1994) for a semi-Lagrangian discretisation of the continuity equation which, when rewritten in the present notation, is

$$\tan\left(\frac{KC}{2}\right) = \pm\sqrt{\left(\frac{f_0\Delta x}{U_0}\right)^2\left(\frac{C}{2}\right)^2 + \left(\frac{\Phi_0}{U_0^2}\right)\left(\frac{KC}{2}\right)^2}. \tag{K.85}$$

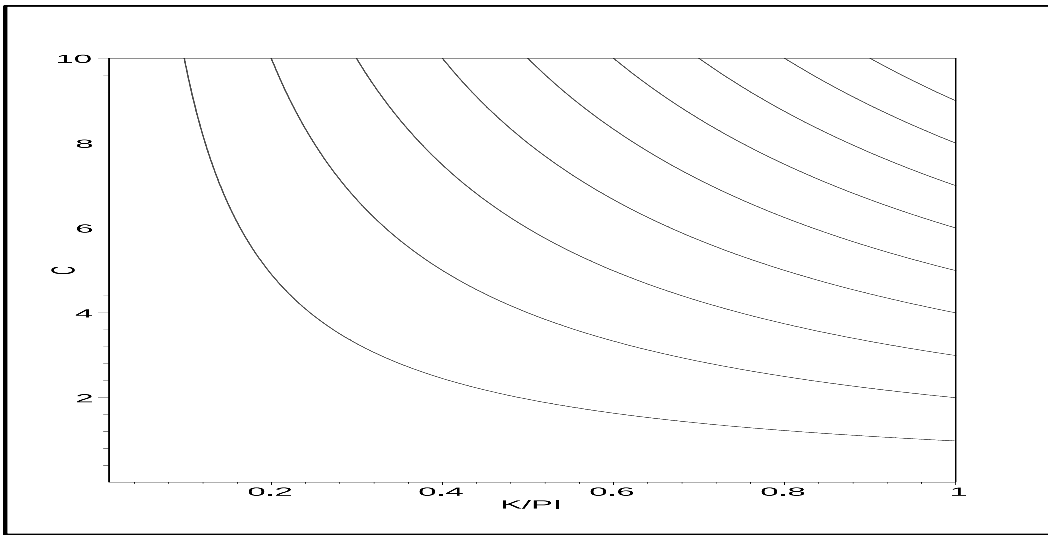

Figure K.5: Curves of resonances of eq. (K.84) as a function of Courant number C and of nondimensional wavenumber K. The values of the parameters are $U_0 = 50ms^{-1}$, $\Phi_0 = 5.5 \times 10^4 m^2 s^{-2}$, $f_0 = 10^{-4} s^{-1}$ and $\Delta x = 50\ km$.

For given Δx, the solutions of (K.84) depend upon both K and C when $f_0 \neq 0$, rather than upon the single composite parameter $KC/2$ when $f_0 = 0$. Setting $\Phi_0 = 5.5 \times 10^4 m^2 s^{-2}$, $U_0 = 50ms^{-1}$, $f_0 = 10^{-4} s^{-1}$ and $\Delta x = 50$ km, as in Rivest et al. (1994), curves of resonance for C (Courant number) vs. K (nondimensional wavenumber) are displayed in Fig. K.5. The corresponding figure for a semi-Lagrangian discretisation of the continuity equation is Fig. K.6.

It is found that

- for $f_0 \neq 0$ both the Eulerian and semi-Lagrangian discretisations of the continuity equation now give rise to pairs of resonance of almost equal value of $KC/2$; and
- for both discretisations of the continuity equation it is again possible to avoid resonance by using a sufficiently small value (approximately less than unity) of the Courant number C, i.e. by using a sufficiently small timestep.

Aside :

Eqs. (K.84) - (K.85) *can alternatively be respectively rewritten as*

$$\tan\left(\frac{KC}{2}\right) = \left(\frac{KC}{2}\right)\left[\frac{1}{2}\left(\frac{\Phi_0}{U_0^2}\right) \mp \sqrt{\left(\frac{f_0}{kU_0}\right)^2 + \frac{1}{4}\left(\frac{\Phi_0}{U_0^2}\right)^2}\,\right], \qquad \text{(K.86)}$$

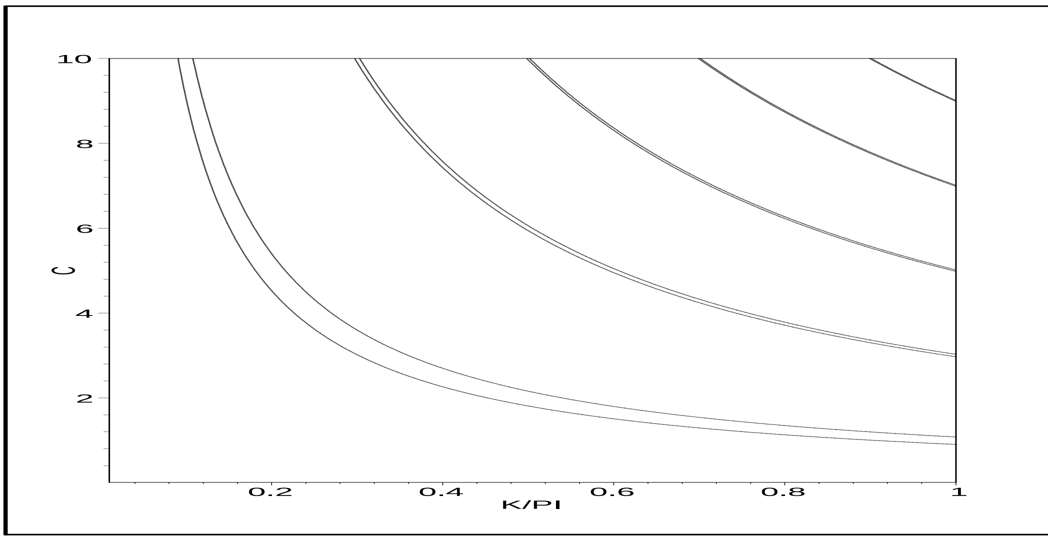

Figure K.6: Curves of resonances of eq. (K.85) as a function of Courant number C and of nondimensional wavenumber K. The values of the parameters are $U_0 = 50ms^{-1}$, $\Phi_0 = 5.5 \times 10^4 m^2 s^{-2}$, $f_0 = 10^{-4} s^{-1}$ and $\Delta x = 50\ km$.

$$\tan\left(\frac{KC}{2}\right) = \pm\left(\frac{KC}{2}\right)\sqrt{\left(\frac{f_0}{kU_0}\right)^2 + \left(\frac{\Phi_0}{U_0^2}\right)^2}, \tag{K.87}$$

where $f_0/(kU_0)$ is the inverse Rossby number.

In the above and in Rivest et al. (1994), the parameters Φ_0, U_0, f_0 and Δx are fixed. This amounts to asking the question, if we fix the spatial resolution and the data fixes the values of Φ_0, U_0, and f_0, what combinations of timestep (or equivalently Courant number) and wavelength of the orographic forcing field will give rise to resonance? However, if instead of Δx, k is specified, then (K.86) *and* (K.87) ***both*** *have the same form,* $\tan X = \gamma X$ *with γ independent of both C and K, just with different values of γ. This amounts to asking the question, if we fix the wavenumber of the orographic forcing and the data fixes the values of Φ_0, U_0, and f_0, what value of the timestep Δt, as measured by the composite parameter $KC \equiv kU_0\Delta t$, where k and U_0 are specified, will give rise to resonance?*

K.6.4 The case $\alpha_3 \neq 1/2$

Since $\alpha_3 \neq 1/2$ for this case and G'^2 is positive definite by definition, (K.76) can be simplified to

$$P^R_{res} = 1 - \frac{C'F^2}{G'^2} P^I_{res}. \tag{K.88}$$

Substitution into (K.75) then gives

$$P^I_{res} = \frac{C'F^2G'^2}{\left\{2 + \left[\alpha_3^2 + (1-\alpha_3)^2\right] F^2\right\} C'^2F^2 + G'^4}. \tag{K.89}$$

However, a necessary condition for resonance to occur is that

$$\left(P^R_{res}\right)^2 + \left(P^I_{res}\right)^2 = 1. \tag{K.90}$$

Using this in the square of (K.88), and noting from (K.89) that $P^I_{res} \neq 0$ for non-zero values of C' and F,it is found that (K.88) and (K.89) can only satisfy (K.90) if

$$G'^4 = C'^2F^2\left(\left\{1 - 2\left[\alpha_3^2 + (1-\alpha_3)^2\right]\right\} F^2 - 4\right). \tag{K.91}$$

But $\alpha_3^2 + (1-\alpha_3)^2$ has a global minimum of $1/2$ at $\alpha_3 = 1/2$ and therefore the right-hand side of (K.91) is negative definite whilst the left-hand side is positive definite. Thus when $\alpha_3 \neq 1/2$, the solution (K.89) is inconsistent with the requirement that (K.90) be satisfied, and so the values of P^R_{res} and P^I_{res} satisfying (K.75) and (K.76) cannot be written as $P^R_{res} + iP^I_{res} = \cos C' - i \sin C'$ for any real value of C'.

Thus for $\alpha_3 \neq 1/2$, there are no solutions to (K.63) *of the form $P_{res} = \exp\left[-ikU_0\Delta t\right]$ for $kU_0\Delta t$ real, and so resonance is not possible for $\alpha_3 > 1/2$ ($\alpha_3 < 1/2$ has already been excluded for stability reasons).*

It is interesting to examine the extent to which the off-centred family of schemes can correctly reproduce the amplitude of the analytic stationary solution by evaluating the ratio of the stationary discretised solution to the analytic one for the geopotential height. Fig. K.7 displays this ratio as a function of the decentring parameter α_3 ($\alpha_3 = 1/2$ corresponds to the centred scheme), and the corresponding figure (cf. Fig. 2 of RSR94) for a semi-Lagrangian discretisation of the continuity equation is shown in Fig. K.8. For both the Eulerian and semi-Lagrangian discretisations of the continuity equation there is a very strong amplification for values of α_3 close to $1/2$, which corresponds to the perfectly-centred scheme, but α_3 does not have to deviate that much from $1/2$ to significantly reduce this amplification.

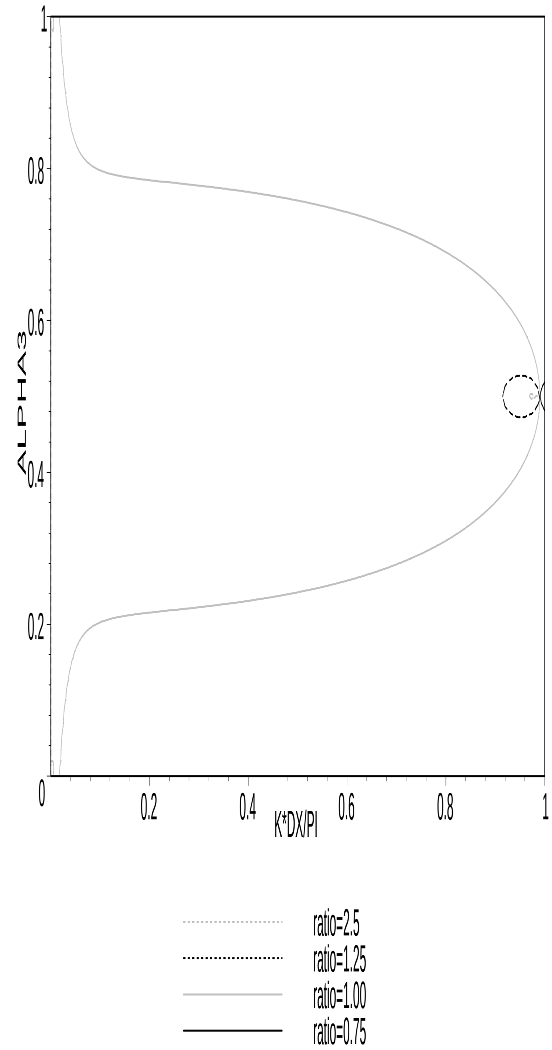

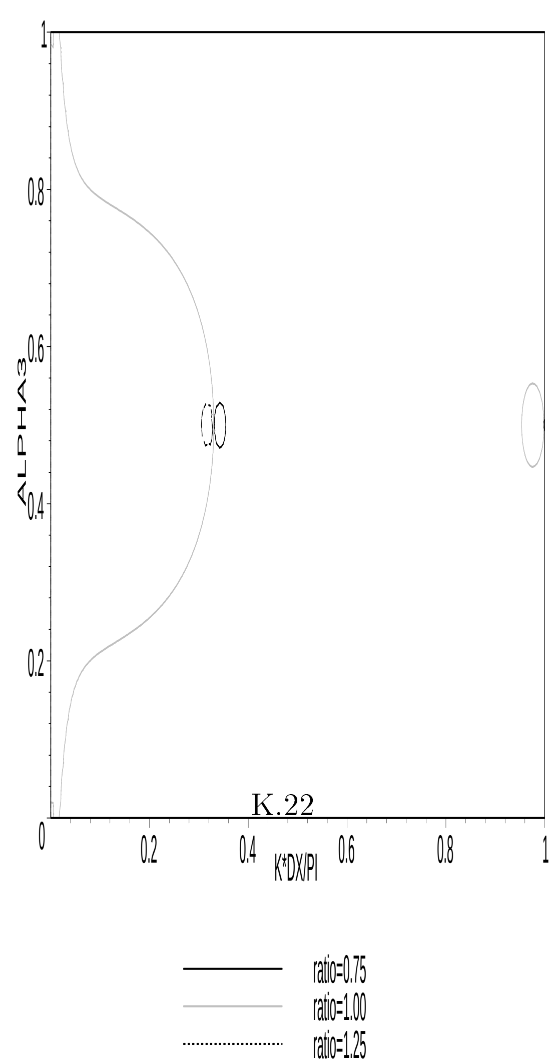

Figure K.7: Ratio of the amplitude of the numerical geopotential to that of the analytic one, with an Eulerian discretisation of the continuity equation, as a function of the decentring parameter α_3 and the non-dimensional wavenumber K, for (a) $C = 1$, and (b) $C = 3$. Other parameters are as in Fig. K.5.

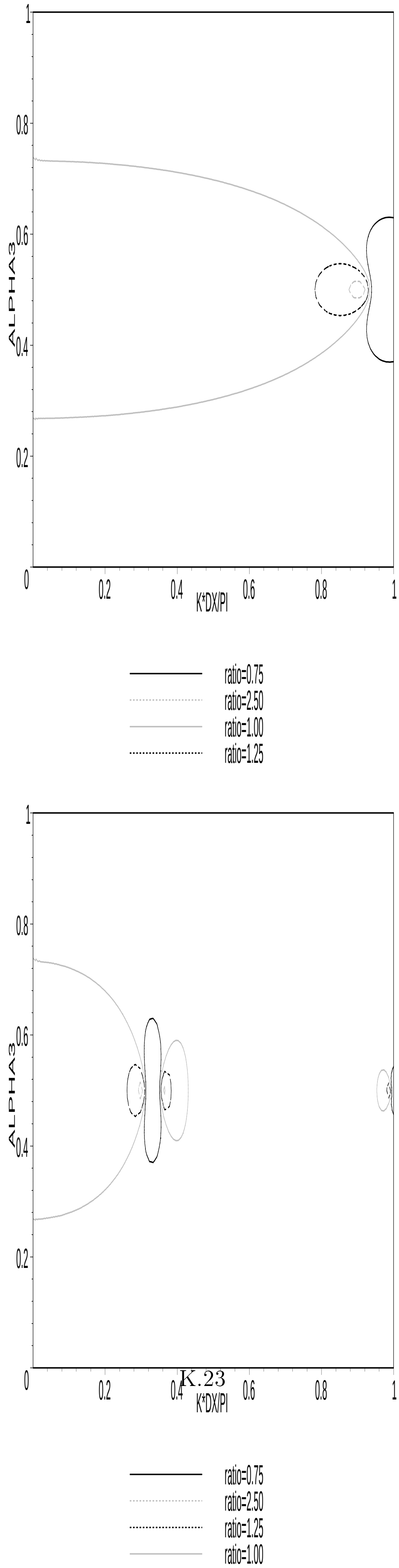

Figure K.8: Ratio of the amplitude of the numerical geopotential to that of the analytic one, with a semi-Lagrangian discretisation of the continuity equation, as a function of the decentring parameter α_3 and the non-dimensional wavenumber K, for (a) $C = 1$, and (b) $C = 3$. Other parameters are as in Fig. K.5.

Summarising, the conclusions of the above analysis when $f_0 \neq 0$ *are broadly the same as for the simpler case* $f_0 = 0$*, viz:*

- *resonance can only occur if* $\alpha_3 = 1/2$ *and then only for values of the parameters* C *and* G *that satisfy* (K.84)*,*
- *it can be avoided at the (possibly-substantial) cost of choosing a sufficiently small timestep such that* C *is less than unity; and*
- *off-centering the time scheme (i.e. setting* $\alpha_3 \neq 1/2$*) is a more efficient way of eliminating spurious semi-Lagrangian resonance.*